National Aeronautics and Space Administration

Biennial Research and Technology Development Report

Johnson Space Center







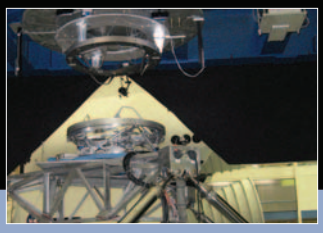
















Johnson Space Center
External Relations Office
University Research, Collaboration and Partnership Office

Kamlesh Lulla, Ph.D.
Editor

TM-2011-216163/December 2011

Biennial Research and Technology Development Report

Johnson Space Center

Human Health, Life Support and Habitation Systems, and Space Medicine

Human Exploration Systems, Technologies for Extravehicular Activity and Harsh Environments

Environmental Technologies

Materials, Structures, Development and Testing

Space Power, Energy Storage, and Propulsion

Robotics, Tele-Robotics, Autonomous Systems, and Software

Exploration, Planetary Science, and Sensor Systems

Flammability and Explosive Technologies

Space and Ground Operations

Inspiring Future Generations: Education and Outreach

Johnson Space Center
External Relations Office
University Research, Collaboration and Partnership Office

Kamlesh Lulla, Ph.D.
Editor

TM-2011-216163/December 2011

Cover background image:
This image illustrates the near-Earth satellite population. Each dot represents a man-made object (typically larger than 10 cm [4 in.] in diameter) orbiting about the Earth. These objects include operational spacecraft (~5%), non-functional spacecraft, launch vehicle stages, mission-related debris, and fragmentation debris. The size of each satellite is not to the same scale as that of the Earth. Courtesy of Nicholas Johnson, NASA Orbital Debris Program Office, Johnson Space Center.

Biennial Research and Technology Development Report 2011

NASA TM-2011-216163
Published by the Johnson Space Center External Relations Office
Michael Kincaid, Director
Kamlesh Lulla Ph.D., Project Manager and Chief Editor
Humberto Sanchez, Project Lead and Assistant Editor

Contents

Foreword
Michael L. Coats . . . . . **xv**

Introduction
Kamlesh Lulla . . . . . **xvi**

Strategic Opportunities and Partnership Development Office
Yolanda Marshall, Douglas A. Terrier, David C. Leestma, John E. James . . . . . **xviii**

Technology and Innovation at Johnson Space Center
John Saiz . . . . . **xx**

Space Life Sciences Directorate Innovation and Collaboration Success Stories
Jeffrey R. Davis, Jennifer A. Fogarty, Cynthia M. Rando, Elizabeth E. Richard . . . . . **xxiv**

Acronyms and Abbreviations . . . . . **xxvi**

Human Health, Life Support and Habitation Systems, and Space Medicine

NASA Human Health and Performance Center
Jan Fogarty **3**

Human Research Program
Dennis Grounds, Barbara Corbin, Katherine Daues, John Charles, Charles Lloyd **5**

No Drill Dentistry: Improved Composites and In Vivo Studies
Diane Byerly, George D. Arndt, Marguerite A. Sognier, John Dusl, Ivan Stangel **7**

Vitamin D: From the Antarctic to the International Space Station to North America
Sara R. Zwart, Scott M. Smith, James Locke **8**

The Value of Human Engineering in Designing Exploration Spacecraft
Jennifer Boyer, Harry Litaker **9**

Development of Usability Requirements at NASA
Anikó Sándor, Kritina L. Holden **12**

Virtual Guidance for Medical Ultrasound Procedures on Exploration Class Missions
David S. Martin, Timothy L. Caine, Timothy Matz, Michael B. Stenger, Steven H. Platts **14**

Next-Generation Anti-Gravity Suits
Michael B. Stenger, Stuart M.C. Lee, Christian M. Westby, Steven H. Platts **16**

Adjustable Mock-up for Integrated Vehicle, Seat, and Suit Evaluations
Sudhakar Rajulu, Matt Cowley, Lynn Pickett **18**

Advanced Photoluminescence Technology as an Emergency Guidance System on the International Space Station
James C. Maida, Laura E. Duvall, Kim A. Tran, Lynn K. Pickett **21**

Microwave-Based Water Decontamination System
Diane Byerly, George Arndt, Marguerite A. Sognier, John Dusl **23**

Contents

continued

In-flight Water Quality Monitoring on the International Space Station: Measuring Biocide Concentrations with Colorimetric Solid Phase Extraction
Daniel B. Gazda, Johanna Goforth, Stephanie M. Flint, Mickie Benoit, Jeff A. Rutz, Robert J. Lipert, Lorraine M. Siperko, Marc D. Porter, John R. Schultz, J. Torin McCoy **24**

Consolidation of Flight Food Provisioning for Human Space Flight
Kimberly Glaus Läte **27**

Development and Implementation of the Bulk Overwrap Bag for Food Stowage on the International Space Station
Vickie L. Kloeris **30**

Flight Crew Integration International Space Station Life Sciences Crew Comments Database: A Tool for International Space Station Post-mission Debrief Data
Susan Schuh, Krista Bagian, Abbe Barr, Laura Duvall **32**

Orion Crew Exploration Vehicle Internal and External Lighting Analyses
James C. Maida, Charles Bowen **34**

Orion Interior Acoustic Environment Modeling with a Mock-up
S. R. Chu, C. S. Allen **36**

Design and Evaluation of Displays for the Crew Exploration Vehicle
Neta Ezer, Kara Pohlkamp, Stephen Gauvain, Lee Morin, Neil Woodbury, Anna Fisher, Patrick Laport, Tim Verborgh, Patrick Henry **38**

Development of a Lunar Dust Reactivity Sensor
William T. Wallace, Antony S. Jeevarajan, Sridhar Madala **41**

Human Exploration Systems, Technologies for Extravehicular Activity and Harsh Environments

Extravehicular Activity Technology Development—Suit Technologies
Amy Ross, Lindsay Aitchison, Kate Mitchell, Richard Rhodes **47**

Extravehicular Activity Technology Development—Suit Port Technologies
Rob Boyle, Barbara Romig, Charles Allton, Peggy Guirgis, Mike Gernhardt **49**

A Cabin Air Separator for Extravehicular Activity Oxygen
John Graf, Derek Neumeyer, Angie Lenius **51**

Extravehicular Activity Technology Development—Oxygen Subsystem
Colin Campbell, Mallory Jennings, Gregg Weaver **54**

Extravehicular Activity Technology Development—Portable Life Support System Integrated Testing
Colin Campbell, Gretchen Thomas, Carly Watts **57**

Extravehicular Activity Technology Development—Thermal Subsystem
Grant Bue, Colin Campbell, Gregg Weaver **60**

Extravehicular Activity Technology Development—Ventilation Subsystem
Heather Paul, Mallory Jennings, Colin Campbell, Molly Anderson, Michael Swickrath, Summer McMillin, Gregg Weaver, Craig Broerman **62**

Contents
continued

Environmental Technologies

Environmental Sustainability at Johnson Space Center
Michael K. Ewert **67**

Greening the Johnson Space Center Aaron Cohen Child Care Center
Jerry Rowlands **69**

Leadership in Energy and Environmental Design at Johnson Space Center
Charles Noel **72**

Materials, Structures, Development and Testing

Lightweight Materials Development for Parachutes
Mary Jane E. O'Rourke **79**

Using Rotor Technology to Land a Spacecraft
Jeffrey D. Hagen, Brent A. Evernden, Adam L. Gilmore **82**

Martian Entry Simulation Using a Carbon Dioxide Test Gas in the Johnson Space Center Arc Jet Facility
Steven V. Del Papa, Brian C. Shafer, Leonard E. Suess **83**

Thermal and Structural Testing of Repaired Orbiter Thermal Protection Tiles
Priscilla A. Kelly, Louise Shivers, Kelly Carney, Cooper Snapp **85**

Functional Cargo Block Structural Life Extension
James J. McMahon **87**

Dynamic Requirements for Foam Replacement
Otto Crenwelge **89**

Vibration Attenuation Effectiveness of Foam Sandwich Enclosure
Otto Crenwelge, Paul Caradec, Brian Rhone, Vincent Fogt, Alan McDougal **91**

Space Power, Energy Storage, and Propulsion

Future Robotic Lander Attitude Control and Descent Thruster Testing
Asher Lieberman, Jeremy Bruggemann, Huu Trinh, Kimberly Newton **97**

Advanced Battery Technology Programs
Judith A. Jeevarajan, Pranav Patel **99**

Safety Advancements in Lithium-ion for the Exploration Technology Development Program Battery Program
Judith A. Jeevarajan, Pranav Patel **101**

Simulated Internal Short Standard with Underwriter's Laboratory for Lithium-ion Cells Under a Space Act Agreement
Judith A. Jeevarajan **103**

Contents

continued

Research, Experimental Development, and Application of Alpha-Ketoglutaric Acid as a Decontaminant for Hazardous Fluids
Benjamin Greene, Dion Mast **105**

Ionic Monopropellant Product Characterization
Benjamin Greene, Mark B. McClure **108**

Material Compatibility Assessment with Hypergolic Propellants and Anhydrous Ammonia
J. Clay Cantrell, Mark McClure **109**

Reference Document for Assessing and Managing Risks of Hydrazine, Monomethylhydrazine, Nitrogen Tetroxide, and Ammonia on Spacecraft
Benjamin Greene **111**

Effects of Liquid Propellants on Mechanical Properties of Nonmetals
Michelle H. Barragan, Mike Shoffstall, Darren M. Cone, Mark McClure, Miguel Maes **113**

Low Corrosion Rate Determination in Hydrazine, Monomethylhydrazine, and MON1 Propellants
Anna H. DeArmond, Dion J. Mast, Darren M. Cone **115**

Liquid Methane/Liquid Oxygen Cryogenic Monopropellant and Explosive Literature
Benjamin Greene, Stephen Taylor **116**

Robotics, Tele-Robotics, Autonomous Systems, and Software

NASGRO®—Fracture Mechanics and Fatigue Crack Growth Analysis Software
Joachim Beek, Royce Forman **121**

Progress in Space Flight Environment Effects: Predicting Spacecraft Single Event Environments with the FLUKA Monte Carlo Nuclear Reaction and Transport Code
Steven L. Koontz, Brandon D. Reddell, Paul Boeder **123**

Analysis Tool for Monte Carlo Data
Carolina I. Restrepo **126**

The Sensor Test for Orion Multi-Purpose Crew Vehicle Relative-Navigation Risk Mitigation Development Test Objective
John A. Christian, Heather Hinkel **128**

Boundary Layer Transition Flight Experiment Overview
Brian Anderson, Charles Campbell **130**

Error Bars for Computational Simulation
Benjamin Kirk, Adam Amar **133**

Copernicus Trajectory Design and Optimization System
Gerald L. Condon **135**

Habitat Demonstration Unit Core Avionics Software
Dennis Lawler, Lui Wang, Tam Ngo, Linda Moreland, Danny Carrejo, Aaron Schram, Thomas Matthews, Craig Russell, Emmy Alex, Ayman Qaddumi **138**

Supersonic Retropropulsion
Guy Schauerhamer, Kerry Trumble, William Kleb, Karl Edquist, Scott Berry, Matt Rhode **140**

Contents
continued

Exploration, Planetary Science, and Sensor Systems

Orion Multi-Purpose Crew Vehicle
Orion Team **147**

Advancing Technologies: The Morpheus Project
Morpheus Team **150**

Wassonite: The Discovery of a New Meteoritic Mineral
Keiko Nakamura-Messenger, Lindsay Keller, Simon Clemett, Zia Rahman **152**

Hayabusa—The First Asteroid Sample Return Mission
Mike Zolensky **153**

Analysis of the First Direct Samples of Early Solar System Water
Mike Zolensky **154**

Windows in the Ancient Martian Atmosphere
Paul Niles **156**

Early Life on Earth and the Search for Extraterrestrial Biosignatures
Dorothy Z. Oehler, Everett K. Gibson **158**

How Tiny Amounts of Water in the Deep Earth Saved Continents
Anne Peslier, Alan Woodland, David Bell, Marina Lazarov **159**

New Research on Purported Martian Biosignatures in Meteorite Allan Hills 84001: 1996 to 2011
Everett Gibson, Kathie Thomas-Keprta, Simon J. Clemett, David S. McKay **160**

Probing Life History of Meteorite From Early Solar System
Justin Simon **162**

The History of Mars Revisited via the Petrological and Geochemical Study of Martian Meteorites
Anne Peslier, Dan Hnatyshin, Chris Herd, Erin Walton, Alan D. Brandon, Thomas Lapen, John Shafer, Minako Righter, Vinciane Debaille, Brian Beard **164**

Magnetic Dynamo Action in Magnetohydrodynamic Turbulence
John V. Shebalin **165**

Stardust—Searching for Contemporary Interstellar Dust
David Frank, Mike Zolensky, Bradley De Gregorio, Ron Bastien, Jack Warren **166**

Mars Habitability, Biosignature Preservation, and Mission Support
Dorothy Z. Oehler, Carlton C. Allen **168**

Fluids and Their Effect on Measurements of Lunar Soil Particle Size Distribution
Bonnie. L. Cooper, David. S. McKay, William T. Wallace, Carla. P. Gonzalez **170**

Nanometer-Scale Anatomy of Entire Stardust Tracks
Keiko Nakamura-Messenger, Lindsay Keller, Simon Clemett, Scott Messenger **172**

Development of the Brine Residual in Containment Concept
Michael R. Callahan, Michael R. Casteel, David A. Glock, Karen D. Pickering **174**

Small Satellite Development
Robert S. Provence, Tim Runkle **176**

Contents

continued

Mission Operations Involvement in the Desert Research and Technology Studies Analog Mission
Ernest R. Bell, Jr., Megan Rosenbaum, Daren Welsh, Dave Coan, Randall McDaniel **178**

GeoLab
Cynthia Evans, Michael Calaway, Mary Sue Bell **180**

Managing Science Operations During Planetary Surface Missions: The 2010 Desert Research and Technology Studies Test
Dean. B. Eppler, Douglas W. Ming **183**

Forward-looking Infrared Cameras: A Potential Crew Tool for Geological Site Assessments
William L. Stefanov, Cynthia A. Evans, Kei Shimizu **186**

Microprobe Two-step Laser Mass Spectrometry Using Extreme Ultraviolet Photoionization: Analysis of Astromaterials
Simon J. Clemett, Scott Messenger **188**

Recovery After Mishap—Salvaging Genesis Solar Wind Sample Science
Judith Allton **191**

Advanced Cockpit Evaluation System—Display and Control Testing Using Small Radio-Controlled Based Analogs
Jeff Fox, Mathew Hart, Mike Goza, Patrick Laport, Jim Secor, Christie Sauers, Ray Heineman, Chip Litaker, John Crofford **194**

Unmanned Microgravity Flight Program
Mathew Hart, Mike Liable, Jeff Fox, Dave Bacque, Lee Morin, Dom Del Rosso **197**

Flammability and Explosive Technologies

New Ignition Mechanism in Oxygen-enriched Environment: Spontaneous Combustion
Joel M. Stoltzfus, Timothy D. Gallus **203**

Novel Ignition Promoter for Investigation of the High-pressure Oxygen Generator Assembly Fire-containment Capability
Timothy D. Gallus, Dax L. Rios **205**

Three-dimensional Modeling Assists in Investigation of Fires in Oxygen-enriched Environments
Dax L. Rios, Kyle M. Sparks, Stephen F. Peralta **207**

Spectroscopic Determination of Trace Contaminants in High-purity Oxygen
Steven D. Hornung **209**

Particle Impact Test Results on Stainless-Steel, High-Pressure Manual Valve
Keisa Rosales, Stephen F. Peralta, Joel M. Stoltzfus **211**

Space and Ground Operations

The Rapid Prototyping Laboratory: The Shortest Space-Time Between Dream and Reality
Lee Morin, Patrick Henry, Tim Verborgh, Patrick Laport, George Scheuch **217**

Reengineering the Mission Operations Directorate Flight Production Process
James Ruszkowski **220**

Contents

continued

Mission Evaluation Room Concept of Operations Evolution: Successful Merging of Technologies and Techniques
Thomas E. Diegelman, Tony Sang **222**

Next-Generation Spaceflight Training for Mission Operations
Valerie Gordon, Leslie Court **224**

Mission Systems Test Bed Project: The 21st Century Mission Control Center Environment
Lindolfo Martinez, Anthony C. Bruins I, Thomas E. Diegelman **227**

MCCx Convergent Technologies: Bringing the Mission Control Center to Your Personal Computer
Keith Martin, Jennifer Morehead, Karun Sen-Roy, Thomas E. Diegelman **229**

Next-Generation Mission Control Center Voice System: Extended Voice System
Eric R. Gallagher, Thomas E. Diegelman **231**

Motion Imagery and Robotics Application Project: Standards Based Protocol
Thomas Diegelman, Steve Lucord, Lindolfo Martinez **233**

Display Sharing Technology
Michael A. Brown **235**

ISS*Live!* Translator: From NASA Operations Nomenclature to Everyday Language
Matthew D. Healy, Philip D. Harris, Jesse B. Ehlinger, Katharine M. West, Ahmed Khan, Jennifer B. Price **237**

Push Technology Approach to Information Streaming: ISS*Live!*
Bruce W. Hochstetler **239**

International Space Station Power Planning and Analysis Tool
Molly Meyer-Allyn, Dan Jackson, Michael Genest, Thomas Miller, Benjamin Chisholm, Aaron Allcorn **241**

Space Weather Monitoring Improves International Space Station Extravehicular Activity Safety and Operations
Steven L. Koontz, Drew Hartman, Leonard Kramer, Danny Schmidl **243**

Mission Control Technologies Project
Alan R. Crocker **246**

Development of the International Docking System Standard
Joe Anderson, Tim Briscoe, Monty Carroll, Stan Donahoe, Steve Gaylor, Robert Grady, Skip Hatfield, Sean Kelly, Thang Le, James Lewis, George Parma, Ben Quasius, Alexander Tabakman **248**

Integrated Ultra-Wideband Tracking and Communication System
Jianjun (David) Ni, Dickey Arndt, Phong Ngo, Chau Phan, Kent Dekome, John Dusl **251**

Ultra-Wideband Tracking System Design for Relative Navigation
Jianjun (David) Ni, Dickey Arndt, Phong Ngo, Kent Dekome, John Dusl, Jodi Graf **253**

Ultra-Wideband Time-Difference-Of-Arrival Two-Point-Tracking System
Jianjun (David) Ni, Dickey Arndt, Phong Ngo, Chau Phan, Kent Dekome, John Dusl **255**

Variable Bragg Peak Methodology for Testing Electronic Parts
Charles R. Bailey, Patrick M. Oneill **257**

Standards-Based Wireless Sensor Networks and Modular Instrumentation for Space Flight Applications
Raymond S. Wagner, Richard J. Barton, Patrick Fink, Phong Ngo **258**

Contents

continued

Effect of Space Vehicle Structure Vibration on Control Moment Gyroscope Dynamics
Tatiana Dobrinskaya **260**

Transfer Impedance Measurement of Flexible Printed Wiring Board Cable Shields for Use in Crewed Space Flight
Robert C. Scully, Charles W. Roberts, Xiang Ni **262**

Shuttle Radiator Protection Helps Prevent Mission Loss from Micrometeoroid and Orbital Debris
Eric Christiansen, Dana Lear, Eugene Stansbery **265**

Shielding Against Micrometeoroid and Orbital Debris Impact with Metallic Foams
Shannon Ryan, Eric Christiansen, Dana Lear **267**

International Space Station Solar Array Guide Wire Micrometeoroid and Orbital Debris Damage
Daniel Kent Ross, Eric Christiansen, Dana Lear **270**

Low-Earth Orbit Environment Remediation with Active Debris Removal
J.-C. Liou **273**

Habitat Particle Impact Monitoring System
J.-C. Liou, John Opiela **275**

Orion On-Orbit Inspection Capability Study
Michael Rollins **277**

Development and Application of Space Flight Performance Shaping Factors for Human Reliability Analysis
Roger Boyer, Teri Hamlin, Richard Heydorn, Jennifer Mindock **279**

Development of a Cursor Control Device for Space Flight Operations
Kritina L. Holden, Shelby G. Thompson, Anikó Sándor, John W. Pace **280**

Development of a Composite Overwrapped Pressure Vessel Profilometry and Eddy Current Scanning System to Meet Manufacturing and Analytical Needs
Regor L. Saulsberry, Charles T. Nichols **282**

High-Speed Measurements Provide Key Information on Events Inside a Pyrovalve
Stephen H. McDougle, Regor L. Saulsberry **284**

Stress Rupture Nondestructive Evaluation of Composite Overwrapped Pressure Vessels
Regor L. Saulsberry, Nathanael J. Greene, Luis Hernandez **287**

Acoustic Emission and Development of Accept-Reject Criteria for Assessing Progressive Damage in Composite Materials
Jess M. Waller, Charles T. Nichols, Regor L. Saulsberry **290**

Optimized Software Approaches to Predict Rupture in Fracture-critical Composites and Implications for Structural Health Monitoring
Charles T. Nichols, Jess M. Waller, Regor L. Saulsberry, Kenneth L. Johnson, Douglas E. Weathers, Jonathan M. Tylka **293**

Space Environments and Thermal Vacuum Effects on Composite Overwrapped Pressure Vessels
Nathanael Greene, Christopher Keddy, Ralph E. Lucero, Joshua D. Tamminga **296**

Correlating Composite Vessel Shearography Nondestructive Evaluation Response to Impact Damage and Associated Burst Pressure Reductions
Charles T. Nichols, Regor L. Saulsberry, Tommy B. Yoder, Ralph E. Lucero **298**

Contents

continued

NASA White Sands Test Facility Valve Repair Facility Helps Resolve Relief Valve Issues
Christina Y. Piña Arpin, Richard McCarson **300**

Hardware Odor Containment Validation Methodology Development Using Gas Analysis and Controlled Human Evaluation Methods
Thomas B. Handley, Susana A. Harper **302**

Image Science Support to Commercial Development
Tracy Calhoun **305**

Spacecraft Flight Operability Assessment Technique
Alan R. Crocker **307**

Inspiring Future Generations: Education and Outreach

Systems Engineering Education Discovery Program: NASA Utilization of Undergraduates to Conduct Reduced Gravity Flight Research
Sara W. Malloy **313**

Successful Recruitment Strategy for Student Programs: Using the Example of the Undergraduate Student Research Program
J. Anthony Zippay **315**

Undergraduate Student Research Project Social Networking and Student Stories Initiative
Heather L. Ogletree **317**

ISS*Live!* A Rich Internet Application Development for International Space Station Educational Outreach
Ahmed Khan, Jennifer B. Price, Matthew D. Healy, Philip D. Harris, Katharine M. West, Jesse B. Ehlinger **319**

Astronaut Earth Observations—Earth's Dynamic Events and Twitpics
Justin Wilkinson, Sue Runco, Kim Willis, William L. Stefanov, Mike Trenchard **322**

Capturing Immediate Learning Outcomes of Undergraduate Internships
Bryan E. Dansberry **325**

Space Life Sciences Directorate Innovation and Collaboration for Education and Outreach
Tacey Baker **327**

Space Life Sciences Academy and the NASA Science and Technology Institute
Pamela Denkins, Karla S. Marriott, Alamelu Sundaresan, Jinghe Mao, Shakhawat Bhuiyan, Jacqueline Madry-Taylor **328**

Research for Space Colonization: NASA Ralph Steckler/Space Grant Space Colonization Research and Technology Development Opportunity
Frank Prochaska **330**

Minority University Research and Education Program at Johnson Space Center
Jennifer Scott Williams **333**

International Humans in Space Symposium Youth Art Competition
Jancy C. McPhee, S. Douglas Holland **335**

Foreword

A Look Ahead to the Future

The Space Shuttle, the most capable spacecraft ever flown, has accomplished its mission of completing the International Space Station (ISS) and expanding its scientific capabilities. The Shuttle has been retired and the International Space Station is now a national laboratory—opening up opportunities for researchers across the nation to conduct science onboard the ISS. Johnson Space Center is proud of the role we played in these major programs.



We at NASA Johnson Space Center are now poised to take the next bold steps in our nation's journey of human exploration of space. Our talented engineers and scientists are conducting research and developing technologies that will allow humans to explore farther reaches of our universe. New technologies and new scientific understanding remain the foundations for expanding our reach into deep space for exploration of the unknown.

This report highlights Johnson Space Center's scientific and technological research and engineering innovations. I believe this information will spark new ideas, encourage research, and inspire scientific communities from universities, industry, nonprofit organizations, and federal agencies to engage in discussions with us for future collaborations and partnerships. I encourage you to contact Dr. Kamlesh Lulla at *kamlesh.p.lulla@ nasa.gov* for opportunities to collaborate with us.

As we take these bold steps, it is my hope that we will build strong and long-term relationships with diverse research and engineering organizations that will enable us to meet the nation's goals in space exploration. I invite you to join us in our journey to the stars as we look ahead to the future.

Michael L. Coats
Center Director

Introduction

For almost 50 years, Johnson Space Center (JSC) has played a vital role in our nation's space exploration initiatives. JSC has been NASA's lead center for human space flight for over 4 decades. From Mercury, Gemini, and Apollo to Skylab, space shuttle, and the International Space Station, JSC has achieved excellence in engineering, mission operations, space life sciences and astromaterials, and sample return science. With the completion of the spectacular last mission of the space shuttle and new direction for NASA, JSC is in the process of inventing a new future for our nation's next bold steps in space exploration. We are transforming our center to meet the exciting challenges of the future exploration missions, and to keep the core capabilities of our center functional to accomplish the next generation of human space flight. With this focus in mind, JSC's leadership is fostering a new, open collaboration and partnership environment at the center. As a first step, the center has established a "Strategic Opportunities and Partnership Development" office (page xxii).

This office enables NASA's missions toward Human Space Exploration by successfully pursuing and maintaining strategic collaboration opportunities and partnerships for JSC that maintain, enhance, or develop key competencies and technologies required for future space exploration. It also plans to leverage other resources to maintain NASA's objectives for space exploration, and to strategically position JSC for future opportunities. These steps include establishing JSC as a global innovation leader in Human Space Exploration by bringing the best minds from universities to collaborate with the best minds of JSC to conduct research, and by reaching out to new partners to ensure that we take advantage of the best fresh ideas and viewpoints. The office provides a clear entry point for external aerospace, non-aerospace, international and academic entities, and other government agencies, and seeks to establish new partnerships, collaborations, and alliances that achieve the center's business objectives.

JSC's Robonaut 2 is an excellent example of our collaboration with industry, academia, and other federal agencies. It is a human-safe robotic assistant endowed with triple redundant-force control software. Early development included collaboration with the Defense Advanced Research Projects Agency, and later with automotive industry. Robonaut 2 was launched on STS-133 with the intravehicular activity task board. The desired outcome is to support extravehicular activities and minimize the risks to human flight crews. The center will continue to seek those technical collaborations that advance technologies for our mission while providing societal benefits.

JSC is fully engaged with universities in both research and educational endeavors. From fabricating cubesats and modeling orbital debris to developing engineering curriculum to teach systems engineering to undergraduate students, we work with our academic partners on wide range of challenges.

The purpose of this *Biennial Research and Technology Development Report* is to highlight the diverse technical, scientific, and engineering research and technology developments under way at our center. To make this report relevant to our readers, we have organized the contents into the categories listed here. These categories are also related to the NASA "Space Technology Roadmaps," developed by the Office of the Chief Technologist at NASA (page xxii).

- *Human Health, Life Support and Habitation Systems, and Space Medicine*
- *Human Exploration Systems, Technologies for Extravehicular Activity and Harsh Environments*
- *Environmental Technologies*
- *Materials, Structures, Development and Testing*
- *Space Power, Energy Storage, and Propulsion*
- *Robotics, Tele-Robotics, Autonomous Systems, and Software*

• *Exploration, Planetary Science, and Sensor Systems*

• *Flammability and Explosive Technologies*

• *Space and Ground Operations*

• *Inspiring Future Generations: Education and Outreach*

At JSC, we are interested in partnering in research and technology development areas of mutual interest and benefit. Our engineers and scientists are well positioned to collaborate in a wide array of technical disciplines. We believe our skills, facilities, and research and technology expertise will allow us to make significant contributions to non-aerospace and aerospace sectors.

Let us invent our futures together.

Kamlesh Lulla, Ph.D.
University Research, Collaboration and Partnership Office
External Relations Office

Collaborating with Johnson Space Center

NASA and JSC have a long history of working with colleges and universities, industry, federal laboratories, and other research and technology development organizations. Several vehicles are available to accomplish the collaboration and partnership objectives. Collaborative agreements, both reimbursable and non-reimbursable, can be used to provide mutual leverage of government, university, and industry resources in the cooperative pursuit of joint-interest research and technology development efforts. We look forward to hearing from you.

The electronic version of the 2011 *Biennial Research and Technology Development Report* can be found at *http://research.jsc.nasa.gov.*

Strategic Opportunities and Partnership Development Office

Yolanda Marshall, *Johnson Space Center*
Douglas A. Terrier, *Johnson Space Center*
David C. Leestma, *Johnson Space Center*
John E. James, *Johnson Space Center*

Building Alliances to Shape Our Future

The Strategic Opportunities and Partnership Development Office (SOPDO) at Johnson Space Center (JSC) uses partnerships to drive the infusion of technology, creative partnerships to develop technology, and traditional business partnerships to license and transfer NASA-developed technologies to the U.S. marketplace, each with the goal of enabling NASA's missions toward human space exploration. By successfully pursuing and maintaining strategic business opportunities and partnerships for JSC that maintain, enhance, or develop key competencies and technologies required for future space exploration, and leveraging other resources to maintain NASA's objectives for space exploration, JSC is establishing itself as a global innovation leader in human space exploration.

For decades, the space agency has triggered U.S. innovations and inventions, while nurturing partnerships to facilitate the transfer of NASA-developed technologies to the private marketplace. JSC is now increasing its efforts to partner with outside partners to drive innovation and foster collaboration, in addition to traditional technology transfer efforts.

The newly established SOPDO provides a clear entry point for external aerospace and non-aerospace entities interested in partnering with JSC, and seeks to establish new partnerships and integrate partnership efforts across JSC's directorates, including international and academic partnerships. The office also manages processes and policies associated with establishing external partnerships. For more information about JSC's capabilities and partnership opportunities, visit: *http://www.nasa.gov/centers/johnson/partnerships/index.html*.

Technology Partnerships

The SOPDO assists in the coordination of alliances, partnerships, and new business opportunities to grow future competencies and to leverage the capabilities outside of JSC. The SOPDO serves as the Office of Prime Responsibility for the JSC Procedural Requirement 1050.1, Space Act Agreement (SAA) process. In this role, SOPDO serves as the facilitator for the development of all institutional SAAs for JSC and the White Sands Test Facility, as well as the official repository of all executed JSC SAAs. SAAs are used primarily to collaborate with entities other than NASA for everything from lending personnel and expertise to equipment and other facilities and resources. The SOPDO also sponsors initiatives to encourage cross-discipline innovation that benefit human exploration and life on Earth.

The Technology Transfer & Commercialization Office at JSC, part of the SOPDO, is working on innovative partnership models to enhance and to initiate technology research and development for infusion into the agency as well as to allow access for industry, commercial space, and academic partners, to world-renowned subject matter experts, as well as to testing, laboratory and research facilities.

The methods and tools used by the SOPDO to infuse technology, spin out technology, and to partner with business and universities include SAAs, Memorandums of Understanding, and Patent Licensing Agreements.

Technology Transfer and Intellectual Property Portfolio Management

SOPDO is also the interface for NASA headquarters' Innovation Partnerships Office. As a part of NASA's statutory charter, the SOPDO facilitates the transfer and commercialization of NASA-sponsored research and technology development including industrial use of unique NASA capabilities and facilities. This includes managing JSC's Intellectual Property Portfolio from new technology reporting, to licensing patented JSC technologies, to public outreach, to educating the American taxpayer about the benefits of space.

For more than 50 years, NASA has developed technologies to orbit the Earth, to land on the moon, and to explore the stars and galaxies. This human need to explore and its attendant curiosity create new ideas and innovations that benefit everyone on Earth through spin-offs. Spin-offs are the resulting commercial products whose inventions originate with NASA funding, research, licensing, facilities, and assistance. The founders of the U.S. space program, through the Space Act Agreement of 1958, required NASA to transfer its technologies to the

marketplace so that the U.S. taxpayer can benefit from the advancements. For more information about JSC's Technology Transfer and Commercialization office, visit: *http://technology.jsc.nasa.gov*.

Strategic Technology Investments

The SOPDO oversees the Small Business Innovative Research/Small Business Technology Transfer (SBIR/STTR) projects. The SBIR/STTR programs, established by law, exist to stimulate technological innovation in the private sector by increasing participation by small business in federal research and technology development. A competitive proposal process is launched annually via a solicitation of proposals with the focus of the NASA technology program needs coupled with the potential for commercialization. Since January 2010, JSC's SBIR/STTR awards have totaled 117 with a value of $22.4 million. For more information on the SBIR/STTR programs, visit: *www.sbir.nasa.gov*.

The SOPDO also interfaces with NASA's headquarters Office of Chief Technologist. JSC's chief technologist, who is a part of JSC's management team, identifies the technology priorities for the center's Independent Research & Development activities and manages the center's investment funds for selected advanced technology projects.

Another NASA program is the Inventions and Contributions Board (ICB). Also established by the Space Act of 1958, the ICB Space Act Awards rewards and promotes outstanding scientific and technical contributions sponsored, adopted, supported, or used by NASA that are significant to aeronautics and space exploration. ICB is authorized to approve awards up to $100,000 without congressional notification. With the help of its staff and legal counsel, the ICB reviews and evaluates contributions to the government and the nation. Many of these inventions and contributions will help humanity explore the universe and improve life on Earth. The ICB approved more than 3,319 individual cash awards totaling nearly $1.8 million in 2010. For more information on ICB awards, visit: *https://nen.nasa.gov/web/oce/icb*.



Human health and performance technology development.

Contact Us

General Inquiry:
Strategic Opportunities and
Partnership Development Office
Phone: 281.483.3000
Email: *JSC-Partnerships@mail.nasa.gov*

Mailing Address:
National Aeronautics and Space Administration
Johnson Space Center
Mail Code: AO
2101 NASA Parkway
Houston, Texas 77058

Technology and Innovation at Johnson Space Center

John Saiz, *Johnson Space Center*

NASA is committed to keeping the United States at the forefront of human space exploration. In 2011, the agency released its strategic plan. One of the strategic goals calls for the creation of innovative new space technologies for exploration, science, and economic security.

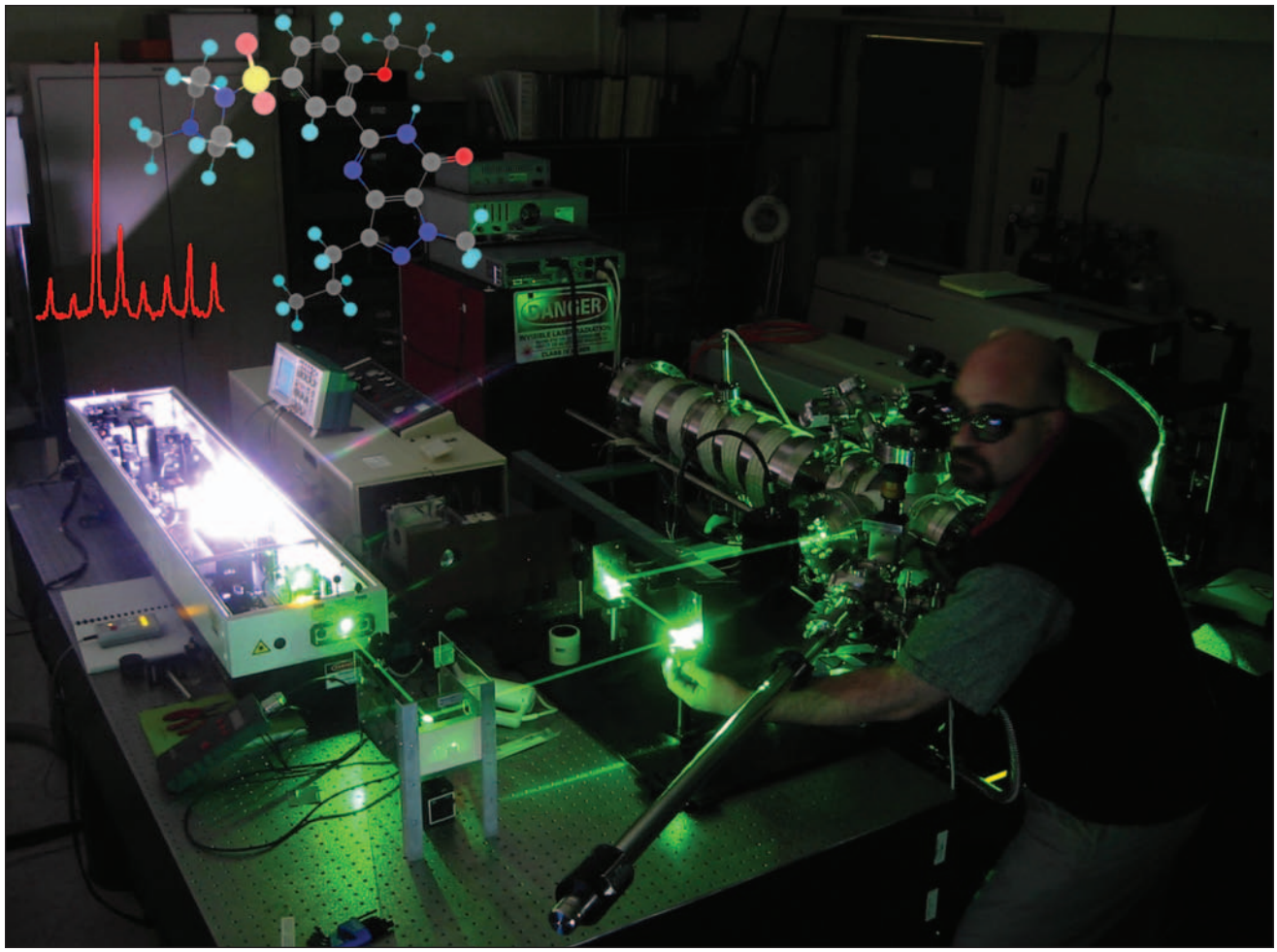
NASA's chief technologist serves as the NASA administrator's principal advisor and advocate on matters concerning agency-wide technology policy and programs. The Office of the Chief Technologist is responsible for direct management of NASA's Space Technology programs and for coordination and tracking of all technology investments across the agency. The office also serves as the NASA technology point of entry and contact with other government agencies, academia, and the commercial aerospace community. The office is responsible for developing and executing innovative technology partnerships, technology transfer, and commercial activities, and for the development of collaboration models for NASA. This office has also developed NASA's integrated technology roadmap to show how these technologies can contribute to NASA's missions and significant national needs (page xx). The keystone of that vision is effective and coordinated management technology development and innovation from Headquarters through each NASA field center resulting in leading-edge missions of the future. The field centers have been charged with providing technologies that support both national needs and human space exploration.

The chief technologist at Johnson Space Center (JSC) works closely with JSC's senior scientists, technologists, and managers to optimize available resources, select appropriate technologies, and manage a portfolio of innovation and technology projects. Center technology portfolio management efforts are coordinated according to a strategy for center innovation and technology that is based on the following innovation and technology strategic themes:

1. Develop the human space flight workforce of tomorrow.
2. Invest and nurture core capabilities needed for the future.
3. Establish a consistent approach to guide future commitments.
4. Foster "integrative thinking."

With these strategic themes in mind, the JSC chief technologist has established a set of initiatives that represent JSC's commitment to develop new technologies related to NASA Strategic Goals. These initiatives include:

- Technology and Innovation *Projects*
  - *Center-Level Independent Research and Development* – Multi-year technology project fund series supports collaborations that assure silo-smashing integration needed for cross-cutting technologies in five priority topic areas including: 1. Technologies for Space Environment Protection; 2. Technology Enabling Planetary Science; 3. Space Healthcare Innovations; 4. Planetary Surface Operations; and 5. Energy and Propulsion Technologies.
  - *Directorate-Level Independent Research and Development* – Annual fund assigned directly to JSC's major research and development-producing organizations to maintain key technology area proficiencies needed to support future missions.
  - *Innovative Charge Account* – Provides numerous small dollar value awards for individuals to pursue ideas. More importantly, the intent for Innovative Charge Account is to create the innovation time recognized as vital to a center-wide environment of ingenuity and creativity.
- Technology and Innovation *Infrastructure*
  - *Innovation Facilities, Tools and Symposia* – There are a number of facilities (e.g., the Innovation Design Center) at JSC where the community can gather to develop ideas and plan. In addition, the chief technologist is working with a number of organizations to pilot test and deploy open innovation tools (e.g., NASA@Work) to leverage an empowered workforce with the creative energies in academia and industry. Their calendar includes a continuum of events (e.g., Innovation 2011, TEDx [Technology, Entertainment, Design] events, etc.) throughout the year with the



Johnson Space Center laser mass spectrometer being used for microscopic organic analysis.

intention of fostering creativity, and moving personnel outside of normal circles to expose the workforce to new ideas, issues, and perspectives.

- *Cadre of Innovators Pilot* – Induction of candidates for membership into an elite cadre that would be supported with additional resources to continue creating. The cadre would "give back" to the community by mentoring the younger talent at JSC and sharing their experiences at public schools and universities to encourage young minds to consider careers in science, technology, engineering, and mathematics.
- *Research and Technology Ambassador Assignments* – Provides a unique opportunity for JSC employees to benefit from "immersion experiences" to gain a full appreciation of innovative cultures outside of JSC, and for JSC to develop and maintain strategic partnerships, collaborations, and alliances that achieve our business objectives.

Technology and Innovation at Johnson Space Center

continued

Successful achievement of these initiatives provides the catalyst for continued excellence in those capabilities that are the hallmark of JSC. Continued vigilance in maintenance of these competencies, capabilities, and the workforce skilled in their application is essential to remaining a world-class center for human space exploration.

JSC is committed to bringing the excitement and reward of innovation and technology to a growing community—ways that inspire new ideas, enthusiasm, and a desire to be part of a new era of human space exploration.

Relating the Johnson Space Center Innovation and Technology Initiatives to NASA Technology Roadmaps

JSC engineers and scientists are fully engaged in NASA's significant technology development efforts, and their contributions have relevance to the agency's goals. JSC has active research and technology initiatives (highlighted in red) in almost all of the areas depicted on the Space Technology Roadmap (right).

Space Technology Roadmaps—Technology Area Breakdown Structure

TA01 Launch Propulsion Systems

Solid Rocket Propulsion Systems
- Propellants
- Case Materials
- Nozzle Systems
- **Hybrid Rocket Propulsion Systems**
- Fundamental Solid Propulsion Technologies

Liquid Rocket Propulsion Systems
- LH_2/LOX Based
- RP/LOX Based
- **CH_4/LOX Based**
- Detonation Wave Engines (Closed Cycle)
- **Propellants**
- **Fundamental Liquid Propulsion Technologies**

Air Breathing Propulsion Systems
- TBCC
- RBCC
- Detonation Wave Engines (Open Cycle)
- Turbine Based Jet Engines (Flyback Boosters)
- Ramjet/ Scramjet Engines (Accelerators)
- Deeply-cooled Air Cycles
- Air Collection & Enrichment System
- Fundamental Air Breathing Propulsion Technologies

Ancillary Propulsion Systems
- **Auxiliary Control Systems**
- **Main Propulsion Systems (Excluding Engines)**
- **Launch Abort Systems**
- **Thrust Vector Control Systems**
- **Health Management & Sensors**
- **Pyro & Separation Systems**
- **Fundamental Ancillary Propulsion Technologies**

Unconventional / Other Propulsion Systems
- Ground Launch Assist
- Air Launch / Drop Systems
- Space Tether Assist
- Beamed Energy / Energy Addition
- Nuclear
- High Energy Density Materials/Propellants

TA02 In-Space Propulsion Technologies

Chemical Propulsion
- **Liquid Storable**
- **Liquid Cryogenic**
- Gels
- Solid
- Hybrid
- **Cold Gas/ Warm Gas**
- **Micro-propulsion**

Non-Chemical Propulsion
- Electric Propulsion
- Solar Sail Propulsion
- Thermal Propulsion
- Tether Propulsion

Advanced (TRL <3) Propulsion Technologies
- Beamed Energy Propulsion
- Electric Sail Propulsion
- Fusion Propulsion
- High Energy Density Materials
- Antimatter Propulsion
- Advanced Fission
- **Breakthrough Propulsion**

Supporting Technologies
- **Engine Health Monitoring & Safety**
- **Propellant Storage & Transfer**
- Materials & Manufacturing Technologies
- Heat Rejection
- **Power**

TA03 Space Power & Energy Storage

Power Generation
- Energy Harvesting
- **Chemical (Fuel Cells, Heat Engines)**
- Solar (Photo-Voltaic & Thermal)
- Radioisotope
- Fission
- Fusion

Energy Storage
- **Batteries**
- Flywheels
- **Regenerative Fuel Cells**

Power Management & Distribution
- **FDIR**
- **Management & Control**
- **Distribution & Transmission**
- Wireless Power Transmission
- **Conversion & Regulation**

Cross Cutting Technology
- **Analytical Tools**
- Green Energy Impact
- Multi-functional Structures
- Alternative Fuels

TA04 Robotics, TeleRobotics & Autonomous Systems

Sensing & Perception
- Stereo Vision
- LIDAR
- Proximity Sensing
- Sensing Non-Geometric Terrain Properties
- Estimating Terrain Mechanical Properties
- Tactile Sensing Arrays
- Gravity Sensors & Celestial Nav.
- **Terrain Relative Navigation**
- Real-time Self-calibrating of Hand-eye Systems

Mobility
- Simultaneous Localiz. & Mapping
- Hazard Detection Algorithms
- Active Illumination
- 3-D Path Planning w/ Uncertainty
- Long-life Extr. Enviro. Mechanisms
- **Robotic Jet Backpacks**
- Smart Tethers
- Robot Swarms
- Walking in Micro-g

Manipulation
- **Motion Planning Alg., High DOF**
- Sensing & Control
- Robot Arms (light, high strength)
- Dexterous Manipul., Robot Hands
- Sensor Fusion for Grasping
- Grasp Planning Algorithms Robotic Drilling Mechanisms
- Multi-arm / Finger Manipulation
- **Planning with Uncertainty**

Human-Systems Integration
- **Crew Decision Support Systems**
- **Immersive Visualization**
- **Distributed Collaboration**
- **Multi Agent Coordination**
- Haptic Displays
- Displaying Range Data to Humans

Autonomy
- Spacecraft Control Systems
- Vehicle Health, Prog/ Diag Systems
- Human Life Support Systems
- Planning/Scheduling Resources
- Operations
- **Integrated Systems Health Management**
- FDIR & Diagnosis
- System Monitoring & Prognosis
- V&V of Complex Adaptive Systems
- **Automated Software Generation**
- **Software Reliability**
- Semi Automatic Systems

Autonomous Rendezvous & Docking
- Rendezvous and Capture
- Low impact & Androgenous Docking Systems & Interfaces
- Relative Navigation Sensors
- Robust AR&D GN&C Algorithms & FSW
- Onboard Mission Manager
- AR&D Integration & Standardization

RTA Systems Engineering
- Human safety
- Refueling Interfaces & Assoc. Tools
- Modular/Serviceable Interfaces
- High Perf., Low Power Onboard Computers
- Environment Tolerance
- Thermal Control
- Robot-to-Suit Interfaces
- **Common Human-Robot Interfaces**
- Crew Self Sufficiency

TA05 Communication & Navigation

Optical Comm. & Navigation
- Detector Development
- Large Apertures
- Lasers
- Acquisition & Tracking
- Atmospheric Mitigation

Radio Frequency Communications
- **Spectrum Efficient Technologies**
- Power Efficient Technologies
- **Propagation**
- **Flight & Ground Systems**
- Earth Launch & Reentry Comm.
- **Antennas**

Internetworking
- Disruptive Tolerant Networking
- Adaptive Network Topology
- Information Assurance
- Integrated Network Management

Position, Navigation, and Timing
- Timekeeping
- Time Distribution
- Onboard Auto Navigation & Maneuver
- Sensors & Vision Processing Systems
- **Relative & Proximity Navigation**
- Auto Precision Formation Flying
- **Auto Approach & Landing**

Integrated Technologies
- **Radio Systems**
- Ultra Wideband
- Cognitive Networks
- Science from the Comm. System
- Hybrid Optical Comm. & Nav. Sensors
- RF/Optical Hybrid Technology

Revolutionary Concepts
- X-Ray Navigation
- X-Ray Communications
- Neutrino-Based Navigation & Tracking
- Quantum Key Distribution
- Quantum Communications
- SQIF Microwave Amplifier
- Reconfigurable Large Apertures

TA06 Human Health, Life Support & Habitation Systems

Environmental Control & Life Support Systems & Habitation Systems
- **Air Revitalization**
- **Water Recovery & Management**
- Waste Management
- **Habitation**

Extravehicular Activity Systems
- **Pressure Garment**
- **Portable Life Support System**
- **Power, Avionics and Software**

Human Health & Performance
- **Medical Diagnosis/ Prognosis**
- **Long-Duration Health**
- **Behavioral Health & Performance**
- **Human Factors & Performance**

Environmental Monitoring, Safety & Emergency Response
- Sensors: Air, Water, Microbial, etc.
- Fire: Detection, Suppression
- Protective Clothing / Breathing
- **Remediation**

Radiation
- Risk Assessment Modeling
- Radiation Mitigation
- Protection Systems
- Space Weather Prediction
- Monitoring Technology

TA07 Human Exploration Destination Systems

In-Situ Resource Utilization
- **Destination Reconnaissance, Prospecting, & Mapping**
- Resource Acquisition
- Consumables Production
- Manufacturing & Infrastructure Emplacement

Sustainability & Supportability
- Logistics Systems
- Maintenance Systems
- Repair Systems

"Advanced" Human Mobility Systems
- **EVA Mobility**
- Surface Mobility
- Off-Surface Mobility

"Advanced" Habitat Systems
- Integrated Habitat Systems
- **Habitat Evolution**

Mission Operations & Safety
- Crew Training
- Environmental Protection
- Remote Mission Operations
- Planetary Safety

Cross-Cutting Systems
- Modeling, Simulations & Destination Characterization
- Construction & Assembly
- Dust Prevention & Mitigation

TA08 Science Instruments, Observatories and Sensor Systems

Remote Sensing Instruments / Sensors
- Detectors & Focal Planes
- Electronics
- Optical Components
- Microwave / Radio
- Lasers
- Cryogenic / Thermal

Observatories
- Mirror Systems
- Structures & Antennas
- Distributed Aperture

In-Situ Instruments / Sensor
- Particles: Charged & Neutral
- Fields & Waves
- In-Situ

TA09 Entry, Descent & Landing Systems

Aeroassist & Atmospheric Entry
- **Rigid Thermal Protection Systems**
- Flexible Thermal Protection Systems
- Rigid Hypersonic Decelerators
- Deployable Hypersonic Decelerators
- **Instrumentation & Health Monitoring**
- **Entry Modeling & Simulation**

Descent
- Attached Deployable Decelerators
- Trailing Deployable Decelerators
- Supersonic Retropropulsion
- **GN&C Sensors**
- Descent Modeling & Simulation

Landing
- Touchdown Systems
- **Egress & Deployment Systems**
- Propulsion Systems
- **Large Body GN&C**
- Small Body Systems
- Landing Modeling & Simulation

Vehicle Systems Technology
- **Architecture Analyses**
- Separation Systems
- **System Integration & Analyses**
- Atmosphere & Surface Characterization

TA10 Nanotechnology

Engineered Materials & Structures
- Lightweight Structures
- Damage Tolerant Systems
- Coatings
- Adhesives
- Thermal Protection & Control

Energy Generation & Storage
- Energy Storage
- Energy Generation
- Energy Distribution

Propulsion
- **Propellants**
- Propulsion Components
- In-Space Propulsion

Sensors, Electronics & Devices
- Sensors & Actuators
- Nanoelectronics
- Miniature Instruments

TA11 Modeling, Simulation, Information Technology & Processing

Computing
- **Flight Computing**
- **Ground Computing**

Modeling
- **Software Modeling & Model-Checking**
- **Integrated Hardware & Software Modeling**
- **Human-System Performance Modeling**
- Science & Engineering Modeling
- **Frameworks, Languages, Tools & Standards**

Simulation
- **Distributed Simulation**
- **Integrated System Lifecycle Simulation**
- **Simulation-Based Systems Engineering**
- Simulation-Based Training & Decision Support Systems

Information Processing
- **Science, Engineering & Mission Data Lifecycle**
- Intelligent Data Understanding
- **Semantic Technologies**
- Collaborative Science & Engineering
- Advanced Mission Systems

TA12 Materials, Structures, Mechanical Systems & Manufacturing

Materials
- **Lightweight Structure**
- Computational Design
- Flexible Material Systems
- Environment
- Special Materials

Structures
- Lightweight Concepts
- Design & Certification Methods
- Reliability & Sustainment
- **Test Tools & Methods**
- **Innovative, Multifunctional Concepts**

Mechanical Systems
- Deployables, Docking and Interfaces
- Mechanism Life Extension Systems
- Electro-mechanical, Mechanical & Micromechanisms
- **Design & Analysis Tools and Methods**
- Reliability / Life Assessment / Health Monitoring
- Certification Methods

Manufacturing
- **Manufacturing Processes**
- Intelligent Integrated Manufacturing and Cyber Physical Systems
- **Electronics & Optics Manufacturing Process**
- Sustainable Manufacturing

Cross-Cutting
- **Nondestructive Evaluation & Sensors**
- **Model-Based Certification & Sustainment Methods**
- **Loads and Environments**

TA13 Ground & Launch Systems Processing

Technologies to Optimize the Operational Life-Cycle
- Storage, Distribution & Conservation of Fluids
- Automated Alignment, Coupling, & Assembly Systems
- Autonomous Command & Control for Ground and Integrated Vehicle/ Ground Systems

Environmental and Green Technologies
- Corrosion Prevention, Detection, & Mitigation
- Environmental Remediation & Site Restoration
- Preservation of Natural Ecosystems
- Alternate Energy Prototypes

Technologies to Increase Reliability and Mission Availability
- Advanced Launch Technologies
- Environment-Hardened Materials and Structures
- Inspection, Anomaly Detection & Identification
- Fault Isolation and Diagnostics
- Prognostics Technologies
- Repair, Mitigation, and Recovery Technologies
- Communications, Networking, Timing & Telemetry

Technologies to Improve Mission Safety/Mission Risk
- Range Tracking, Surveillance & Flight Safety Technologies
- Landing & Recovery Systems & Components
- Weather Prediction and Mitigation
- Robotics / Telerobotics
- Safety Systems

TA14 Thermal Management Systems

Cryogenic Systems
- Passive Thermal Control
- Active Thermal Control
- Integration & Modeling

Thermal Control Systems
- Heat Acquisition
- Heat Transfer
- Heat Rejection & Energy Storage

Thermal Protection Systems
- **Entry / Ascent TPS**
- Plume Shielding (Convective & Radiative)
- Sensor Systems & Measurement Technologies

TA15 Aeronautics

Aerosciences
- Propulsion Airframe Integration
- Drag Reduction
- Novel Configurations
- Propulsion Airframe Aeroacoustics
- Computational Methods
- Robust Aero
- Formation Flight
- Wake Vortex
- VSTOL/ESTOL
- Reduce/Mitigate Sonic Boom
- Multidisciplinary Design & Analysis Tools
- **Efficient Hypersonic Aero**

Propulsion and Power
- Quiet Propulsion
- Ultra-clean Propulsion & Alternative Fuels
- Fuel Efficiency
- Propulsion for STOL/ VTOL
- Supersonic Propulsion
- Combined Cycle Hypersonic
- Aero-Propulsion-Servo-Elasticity
- Robust Propulsion
- Hybrid Propulsion and Power
- Variable Cycle
- Alternative Engine Cycles
- Intelligent Engines
- Integrated Power Management

Dynamics, Control, Navigation, Guidance, and Avionics
- **Advanced Guidance**
- Distributed Decision, Uncertainty, & Flight Path
- Distrib Flow Contr. of Veh. Dyn.
- **Intelligent & Adaptive Control**
- Fault-Tolerant IVHM
- On-Board Weather
- **Pilot Vehicle Integration**
- Synthetic & Enhanced Vision
- UAV in the NAS
- Advanced V&V
- Load, Vibr. & Stability Control
- **Advanced Comm.**

Intelligent & Human Integrated Systems
- Complex Interactive Systems
- Separation Assurance
- Wake Vortex Systems
- Architecture Vulnerability Analysis for Air Traffic Control
- Air Traffic Control for Adverse Weather
- Collaborative Decision Systems
- Operational Maintenance Data
- Task & Attention Management
- Environmentally Friendly Aviation
- Super Density Operations

Space Life Sciences Directorate Innovation and Collaboration Success Stories

Jeffrey R. Davis, *Johnson Space Center*
Jennifer A. Fogarty, *Johnson Space Center*
Cynthia M. Rando, *Wyle Integrated Science and Engineering Group*
Elizabeth E. Richard, *Wyle Integrated Science and Engineering Group*

During 2010, the Space Life Sciences Directorate (SLSD) at Johnson Space Center embarked on a series of pilot activities that would test the utility of open innovation service provider (OISP) with respect to their ability to acquire solutions to human health and performance challenges associated with space flight. SLSD engaged the services of two OISPs—InnoCentive and yet2.com—to test this novel approach to problem solving and its feasibility for solving NASA's space flight challenges. The OISPs were chosen based on multiple factors including: network size and knowledge area span; established process; methodology; experience base; and cost.

InnoCentive and yet2.com each met the desired criteria; however, each company's approach to open innovation services is distinctly different. InnoCentive focuses on posting individual challenges to an established Web-based network of approximately 225,000 solvers; viable solutions are sought and granted a financial award, if found. Based on a specific technological need, yet2.com acts as a "technology scout," providing a broad external network of experts as potential collaborators for NASA. A relationship can be established with these contacts to develop technologies and/or maintained as an established network of future collaborators.

The challenges posted with the InnoCentive pilot have yielded 11 awarded solutions out of the seven challenges posted. A total of two proposals were granted a full award and nine proposals were granted a partial award. The six technical needs posted for the yet2.com pilot have yielded a substantial number of leads (235), some of which were not previously known to NASA. A total of 24 leads continue to be of great interest as potential collaborators for solving SLSD technology needs. The OISP methodology allows NASA to publicly issue challenges to seek innovative solutions and build awareness and collaboration with a global public. OISPs also represent a cost-effective and efficient way to seek solutions to NASA's challenges.

In addition to the success of the external open innovation efforts, SLSD made great strides in 2011 with establishing an internal NASA crowdsourcing pilot program entitled NASA@work. NASA@work was supported by the InnoCentive@work software platform. The objective of the NASA@work pilot was to connect the collective knowledge of individuals from all areas within the NASA organization via an internal Web-based platform. The platform provided a venue for NASA challenge owners (those looking for solutions or new ideas) to pose challenges to internal solvers (those, within NASA, who have the skill and desire to create solutions). The pilot was launched in 57 days—a record for InnoCentive and NASA—and ran for 3 months, with a total of 20 challenges posted agency wide. The NASA@work pilot attracted more than 6,000 participants throughout NASA with a total of 183 contributing solvers for the 20 challenges posted. At the time of the pilot's closure, solvers provided viable solutions and ideas for 17 of the 20 posted challenges. The solver community provided feedback on the pilot, describing it as a barrier-breaking activity, conveying that there was a satisfaction associated with helping co-workers, that it was "fun" to think about problems outside normal work boundaries, and that it was nice to learn what challenges others were facing across the agency.

The results of the external open innovation pilot efforts have promoted public involvement and awareness of the U.S. space program, and created an environment where one person can make a substantial difference. Similarly, the results of NASA@work—the internal collaboration platform—have demonstrated the power of leveraging internal expertise and personnel across a large and distributed agency, such as NASA.

Challenges and Lessons Learned

External Crowdsourcing Platform (InnoCentive Pilot)

1. Clear solver agreements and communication regarding NASA contractor or related civil servant participation is required.
2. Additional evaluation process training and support was required for challenge owners.

3. Scheduling difficulty between the challenge owner and InnoCentive's client services to coordinate the initial scope of challenge. The timing and schedules for challenge owners and InnoCentive's client services proved difficult at times during tight deadlines and schedules.
4. Process standards for approval to notify solvers of NASA challenge awards. The NASA Pilot Program team established an effective review panel as a process gate for the challenge owners to receive final approval of their award and rejection decisions.
5. Similar challenges posted concurrently can compete for solvers. Additionally, disparate award amounts can cause lower solver submissions. It is important to de-conflict competition between challenges to ensure success.

External Consortium Platform (yet2.com Pilot)

1. Preparing for the open innovation activity is an important step that contributes to the success of the approach. It is important to identify search areas that can benefit the most from technically developed solutions:
   - "Solvability" of the technology need
   - Urgency of the technology need
   - Internal capacity to finalize the development of a solution
   - Potential for solutions outside the main area of technical needs
   - New technologies vs. optimizing technologies
2. Much of the success in technical need selection can be attributed to the training conducted at the NASA locations.
3. Project teams that own technical needs within NASA are key stakeholders in the process of searching, selecting, and implementing solutions to the technical needs. Based on the results from the pilot search, one recommendation is to invite technical evaluators of the solution to be part of the project team.
4. The implementation of external solutions identified under this pilot would require broad organizational support across NASA centers.
5. It is important to conduct intellectual property due diligence of all external solutions.

Internal Crowdsourcing Platform (NASA@work Pilot)

1. The NASA community was receptive to the NASA@work platform and found it to be a worthwhile tool. The platform included the capability to do the following key tasks:
   - Promote and encourage collaboration
   - Assist challenge owners in the development of problem statements into challenges
   - Allow the organization to openly collaborate and evolve solutions
   - Permit owners to recognize contributions from solvers in a variety of ways
   - Provide feedback to the solver community and share success stories
2. It was found that certain challenges were more successful in attracting solvers and potential solutions than others.
   - Technical challenges generated 25% of the discussion posts of the theoretical challenges
3. It was found that the solver solutions could be placed into three categories:
   - Random Solutions—the group of solutions provided by solvers without background in the challenge area who were posting low value solutions
   - Repeat Solutions—the old and tired solutions that have been seen and tried before, but this provided a spark conversation in the group
   - Revealing Solutions—collaborative sparks where the dialogue was valuable in advancing the challenge
4. The rewards and recognition program requires refinement. Approximately 75% of the challenge owners and center champions felt that the awards offered were not sufficient for the problems posted.
5. A new innovation model often requires employees to do things in a new way, and that can be uncomfortable and adjustments need to be made to fit the culture of the NASA community.

Acronyms and Abbreviations

1Ah	1-Ampere-Hour
ABET	Accrediting Body for Engineering and Technology
ABF	Anthropometry and Biomechanics Facility
AE	acoustic emission
AFT	Advanced Food Technology
Al	aluminum
AIAA	American Institute of Aeronautics and Astronautics
AKGA	alpha-ketoglutaric acid
AMS	Asynchronous Message Service
ANSI	American National Standards Institute
ANTARES	Advanced NASA Technology Architecture for Exploration Studies
AOA	Angle of Arrival
APAS	Androgynous Peripheral Assembly System
ARES	Astromaterials Research and Exploration Science
ASHRAE	American Society of Heating, Refrigerating and Air-conditioning Engineers
ASTM	American Society for Testing and Materials
BLSS	Bioregenerative Life Support Systems
BLT	boundary layer transition
BNL	Brookhaven National Laboratory
BOB	Bulk Overwrap Bag
BRINE	brine residual in-containment
C2V2	Common Communication for Visiting Vehicle
CAD	Computer Aided Drawing
CAI	calcium-, aluminum-rich inclusion
CASEO	Cabin Air Separator for Extravehicular Activity Oxygen
CCD	cursor control device
CCSDS	Consultative Committee for Space Data Standards
CEV	Crew Exploration Vehicle
C/Ep	carbon-epoxy
CFD	Computational Fluid Dynamics
CiPAIR	Curriculum Improvements Partnership Award for the Integration of Research
CMG	Control Moment Gyroscope
CMUS	Command Module Uprighting System
CO_2	carbon dioxide
COPV	composite overwrapped pressure vessels
COTS	Commercial Orbital Transportation Services
CPAS	Capsule Parachute Assembly System
CPVWG	Composite Pressure Vessel Working Group
CSPE	Colorimetric Solid Phase Extraction
CSRTS	Carbon Stress Rupture Test System
CTS™	composite thermal switch
CWQMK	Colorimetric Water Quality Monitoring Kit
DACS	Divert and Attitude Control System
dB	decibels
DRATS	Desert Research and Technology Studies
DTN	Delay Tolerant Networking
DTO	Development Test Objective
DWC	Digital Wave Corp.
EC	eddy current
ECLSS	Environmental Control and Life Support System
EDOCS	Expeditionary Deployable Oxygen Concentration System
EEGS	Emergency Egress System
EELS	emergency egress lighting strips
ETP	Electrolytic Tough Pitch
eV	electron volt
EVA	extravehicular activity
FCI/OpsHab	Flight Crew Integration Operational Habitability
FEA	finite element analysis
FeCrNi	iron-chromium-nickel
FFP	flight production processes
FFT	Fast Fourier transform
FGB	functional cargo block
FLIR	forward-looking infrared
FLUKA	FLUktuierende KAskade
FOM	Figure of Merit
FP	floating potential
FPMU	Floating Potential Measurement Unit
Fr	Felicity ratio

FRCS	Forward Reaction Control System
FY	Fiscal Year
GPS	Global Positioning System
GRAF	Graphics Research and Analysis Facility
GRC	Glenn Research Center
H_2O	water
HCD	human-centered design
HDU	Habitat Demonstration Unit
HESTEC	Hispanic Engineering, Science, and Technology
HIMS	Habitat Particle Impact Monitoring System
HITL	human-in-the-loop
HoFi	hollow-fiber
HPH	high purity hydrazine
HPOGA	high-pressure oxygen generator assembly
HRA	Human Reliability Analysis
HRP	Human Research Program
HSWL	Hamilton Sundstrand (Windsor Locks)
HVAC	Heating, Ventilation, and Air Conditioning
Hz	Hertz
IAA	International Academy of Astronautics
I&A	integration & test
ICB	Inventions and Contributions Board
IDD	Interface Definition Document
IDSS	International Docking System Standard
IEC	International Electrotechnical Commission
IEEE	Institute of Electrical and Electronics Engineers
ILH	intermittent load hold
iLIDS	International Low Impact Docking System
IOM	Institute of Medicine
IP	Internet Protocol
IPTV	Internet Protocol Television
IR	ionizing radiation
ISA	International Society of Automation
ISAL	Image Science and Analysis Laboratory
ISO	International Standards Organization
ISP	Information Sharing Protocol
ISS	International Space Station
IT	Information Technology
Jenkins	Harriet B. Jenkins Pre-doctoral Fellowship Program
JSC	Johnson Space Center
kHz	kilohertz
kPa	kilopascals
KSC	Kennedy Space Center
ksi	kilopound per square inch
LED	light-emitting diode
LEED	Leadership in Energy and Environmental Design
LEO	low-Earth orbit
LER	Lunar Electric Rover
LET	linear energy transfer
LETF	Lighting Evaluation and Test Facility
LGH	Lunar Greenhouse
LIDAR	Light Detection and Ranging
LIDS	Low Impact Docking System
Li-ion	lithium-ion
LNG	liquefied natural gas
LONESTAR	Low-earth Orbiting Navigation Experiment for Spacecraft Testing Autonomous Rendezvous
LOX	liquid oxygen
LS	laser shearography
mAh	milliampere-hours
MCC	Mission Control Center
MCC-21	Mission Control Center 21st Century
MCCS	Mission Control Center System
MCCx	Mission Control Center Experimental
MCT	Mission Control Technologies
MER	Mission Evaluation Room
MHz	megahertz
MIRA	Motion Imagery and Robotics Application
mL/min	milliliters per minute
mMCC	mobile Mission Control Center
MMH	monomethylhydrazine
MMOD	micrometeoroid and orbital debris

Acronyms and Abbreviations

continued

MOD	Mission Operations Directorate
MOS	Mission Operations System
MOX	liquid methane/liquid oxygen
MPRES	Multi-Platform Renewable Energy System
mpy	mil per year
MSL	Mars Science Laboratory
MSP	Minority University Research and Education Program (MUREP) Small Projects
MSTB	Mission Systems Test Bed
MUREP	Minority University Research and Education Program
MUST	Motivating Undergraduates in Science and Technology
mV	millivolts
N	nitrogen
NanoSIMS	nanometer-scale, secondary ion mass spectrometry
NBIC	National Board Inspection Code
NBL	Nutritional Biochemistry Laboratory
NDE	nondestructive evaluation
Nd: YAG	neodymium: yttrium-aluminum-garnet
N_e	plasma density
NESC	NASA Engineering & Safety Center
NHHPC	NASA Human Health and Performance Center
Ni	nickel
NICE	NASA Innovations in Climate Education
nm	nanometer
nmol/L	nanomoles per liter
NNSA	National Nuclear Security Administration
NNWG	NASA Nondestructive Evaluation Working Group
ns	nanosecond
NSBRI	National Space Biomedical Research Institute
NSI	NASA Standard Initiator
NSTI	NASA Science and Technology Institute
NTO	nitrogen tetroxide
O	oxygen
OCA	Oxygen Compatibility Assessment
OISP	open innovation service provider
OSTPV	Onboard Short-Term Plan Viewer
P6	Port 6
PC	personal computer
PCA	primer chamber assembly
PCU	plasma contactor unit
PECOS	Predictive Engineering and Computational Sciences
PEM	Pressurized Excursion Module
PICA	phenolic impregnated carbon ablator
PLATO	Power Planning and Analysis Tool
PLSS	Portable Life Support System
PPI	pores per linear inch
PSAAP	Predictive Science Academic Alliance Program
PSI	Physical Sciences Inc.
psi	pounds per square inch
psig	pounds per square inch gauge
PSTI	Pre-Service Teacher Institute
PTFE	polytetrafluoroethylene
PV	photovoltaic
PWB	printed wiring board
REMPI	Resonance Enhanced Multi-Photon Ionization
RF	radio frequency
RFTA	Recycle Filter Tank Assembly
RIA	Rich Internet Application
RLLD	Robotic Lunar Lander Development
RPL	Rapid Prototyping Lab
SA	spectrum analyzer
SAA	Space Act Agreement
SAW	solar array wings
SBIR	Small Business Innovative Research
SDTO	Station Development Test Objective
SEE	single event effect
SEED	Systems Engineering Education Discovery
SEU	single event upset
SFRF	Space Food Research Facility
SFSL	Space Food Systems Laboratory
SG	signal generator
SHM	structural health monitoring

SIMS	secondary ion mass spectrometry
SLSD	Space Life Sciences Directorate
SM	Service Module
SMART/L	Spacecraft Morphing to Auto Rotation Targeted Landing
SM&C	Spacecraft Monitor and Control
SoC	states of charge
SOPDO	Strategic Opportunities and Partnerships Development Office
SQL	Structured Query Language
SRAM	static random access memory
SRP	Supersonic Retropropulsion
SS	stainless steel
SSI	Student Stories Initiative
SSOT	Strategic Science Operations Team
STA-54	Shuttle Tile Ablator 54
STEM	science, technology, engineering, and math
STOMP	Student Teacher Outreach Mentorship Program
STORRM	Sensor Test for Orion Relative-Navigation Risk Mitigation
STS	Space Transportation System
STTR	Small Business Technology Transfer
SWME	suit water membrane evaporators
TCS	Trajectory Control Sensor
TCUP	Tribal Colleges and Universities Project
TDOA	Time-Difference-of-Arrival
T_e	electron
TNT	trinitrotoluene
TSOT	Tactical Science Operations Team
UA	University of Arizona
UCLA	University of California Los Angeles
UL	Underwriter's Laboratory
µ-L2MS	unique microprobe two-step laser mass spectrometer
µm	micrometers
UNIMET	United Negro College Fund-Special Programs Mission Enabling Technology
ULF	Utilization and Logistics Flight
UPW	ultrapure water
URC	University Research Center
USAF	United States Air Force
USA FCE	United Space Alliance Flight Crew Equipment
USRA	Universities Space Research Association
USRP	Undergraduate Student Research Project
UT	ultrasonic testing
UWB	Ultra-Wideband
3-D	three-dimensional
TPS	thermal protection system
2-D	two-dimensional
UV	ultraviolet
VNA	vector network analyzer
VNS	Vision Navigation Sensor
VoIP	Voice over Internet Protocol
VR	valve repair
VRAM	Variable Bragg Peak Method
Wh/kg	Watt-hours per kilogram
WSN	wireless sensor network
WSTF	White Sands Test Facility
XRF	x-ray fluorescence

Note: the use of commercial product names in this publication does not constitute any endorsement by NASA, its staff, or its management.

Human Health, Life Support and Habitation Systems, and Space Medicine



NASA Human Health and Performance Center

Jan Fogarty, *Johnson Space Center*

The NASA Human Health and Performance Center (NHHPC) provides a collaborative, virtual forum to integrate all disciplines of the human system to address health and performance topics and issues related to space flight, aviation, and extreme Earth environments. The NHHPC serves a vital role as integrator, convening members to share information and capture a diverse knowledge base while allowing parties to collaborate on the most important human health and performance topics of interest to members. The center and its member organizations address high-priority risk reduction strategies, including research and technology development, improved medical and environmental health diagnostics and therapeutics, and state-of-the-art design approaches for human factors and habitability. The NHHPC focuses on a number of collaborative projects on human health and performance including workshops, education and outreach, information sharing and knowledge management, and research and technology development projects to advance the study of the human system in extreme environments.

Goals

The goals of the NHHPC are to:

- integrate relevant human health and performance efforts across NASA and with member organizations;
- develop and advance human system research and technology, process, and practice innovations;
- foster development of collaborative projects to enable human space flight capabilities and to address broader national human health and performance needs;
- serve as a focal point for information sharing and knowledge management through in-person and virtual forums.

Themes

The NHHPC develops and implements innovative projects and initiatives that address human health and performance themes.

Topics in health include development of novel and improved health care for humans during space flight, for crew and passengers in civilian and commercial aviation, and for workers in many aspects of occupational medicine. Collaborative projects in global medicine and general preventive health will also be pursued.

Topics in performance address development of innovative and advance human performance technologies to improve the safety and efficiency of humans living and working in space and on Earth—including the performance of all human interactions with systems such as flight crews, ground controllers, and ground maintenance personnel; development of dual-use space flight and global performance technologies.

Topics in habitability, environment, and human systems engineering include the development of information, technologies, and processes aimed at making the habitable environment safe and conducive to productive work and healthy living.

Topics include those that enhance the coordination of education and outreach initiatives that address grades K-12, the university level, professional training, and public outreach. A particular emphasis will be placed on K-12 science, technology, engineering, and mathematics education. New initiatives will be based on established local, national, and international member organization programs, and may be offered through the NASA Space Life Sciences Academy or from member organizations.

Topics in research and development include fundamental biology for space and global applications, mechanistic research such as biomarkers and common signaling pathways, and breakthrough research such as synthetic biology projects. These efforts will be evidence-based, using a standards-to-deliverables process that results in solutions aimed at mitigating the highest priority human system risks.

Various platforms will be used for NHHPC human health and performance projects including ground-based facilities of NHHPC members; government spacecraft, including the International Space Station National Laboratory; commercial spacecraft; and commercial aviation.

The NHHPC collects, integrates, and disseminates knowledge, best practices, and advancements among all elements of the human system to advance research,

NASA Human Health and Performance Center

continued

technology development, requirements development, and innovative human health and performance solutions, including the areas of fundamental biology and space cell science.

Website and Collaborative Tools

The NHHPC is primarily "virtual." Development and administration of an interactive website along with other supporting collaborative tools are critical to integration of information and leveraging human system efforts across its member organizations. The NHHPC website serves as the official gateway to a combination of collaborative tools and repositories to facilitate member recruitment, knowledge collection and dissemination, collaboration, and strategic communications.

The NHHPC website and collaborative tools supporting operations enable knowledge and information sharing among member organizations; provide the appropriate level of security yet still provide flexibility to support NHHPC operations and information release processes; provide a user-friendly mechanism to enhance traditional forms of communications and partnerships; and provide dynamic resources to support effective virtual and in-person forums. It also facilitates secure integration and coordination of NASA center business functions (such as responses to agency budget calls); provides virtual collaborative partnership capabilities that enhance the visibility of all NHHPC member organizations where possible; and supports future enhancements such as multilingual capability and user profiling to present information specific to user needs and preferences (*http://www.nasa.gov/offices/NHHPC/index.html*).

Expectations are that the majority of information exchanged as part of NHHPC operations will be public information with no sensitive or business proprietary governing requirements. All data and information on the public website will be screened and released or protected according to existing NASA protocols. Where data/information require specific protection, the appropriate processes and tools will be identified to ensure secure information exchange and appropriate markings and release.

Summary

The NHHPC convenes members from diverse organizations that share a common interest in developing collaborative and innovative approaches to enable human health and performance in many uniquely stressful environments on Earth, and in many aerospace realms from aviation, to suborbital, to orbital and planetary flights. Lessons learned in any one environment can be rapidly shared with members to enable more efficient development of research and technology proposals as well as effective mitigation applications for human health and performance risks. Members benefit by participating in the sharing of a diverse and integrated knowledge base, as well as developing collaborative projects that make maximum use of the resources of all participating members.

Human Research Program

Dennis Grounds, *Johnson Space Center*
Barbara Corbin, *Johnson Space Center*
Katherine Daues, *Johnson Space Center*
John Charles, *Johnson Space Center*
Charles Lloyd, *Johnson Space Center*

Crew health and performance is critical to successful human exploration beyond low-Earth orbit. Risks include physiologic effects from radiation, hypo-gravity, and planetary environments, as well as unique challenges in medical treatment, human factors, and behavioral health support. The goal of the Human Research Program (HRP) is to provide human health and performance countermeasures, knowledge, technologies, and tools to enable safe, reliable, and productive human space exploration.

In its fifth year of operation, the HRP continued to establish its management architecture of evidence, risks, gaps, tasks, and deliverables. Products were delivered to support the preliminary design of the Constellation Program vehicles. Experiments continued on the International Space Station (ISS), on the ground in analog environments that have features similar to those of space flight, and in laboratory environments. Data from these experiments furthered NASA's understanding of how the space environment affects the human system. These research results contributed to scientific knowledge and technology developments that address the human health and performance risks.

Objectives

These are the specific objectives of the HRP:

1. Develop capabilities, necessary countermeasures, and technologies in support of human space exploration, focusing on mitigating the highest risks to crew health and performance. Enable the definition and improvement of human space flight medical, environmental, and human factors standards.
2. Develop technologies that serve to reduce medical and environmental risks, reduce human systems resource requirements (mass, volume, power, data, etc.), and ensure effective human-system integration across exploration mission systems.
3. Ensure maintenance of agency core competencies necessary to enable risk reduction in the following areas: space medicine; physiological and behavioral effects of long-duration space flight on the human body; space environmental effects, including radiation, on human health and performance; and space human factors.

The program is comprised of six major elements that are focused to accomplish specific goals for investigating and mitigating the highest risks to astronaut health and performance. These six elements are: ISS Medical Project, Space Radiation, Human Health Countermeasures, Exploration Medical Capability, Space Human Factors and Habitability, and Behavioral Health and Performance. These elements provide the program's knowledge and capabilities to conduct research to address the human health and performance risks as well as advance the readiness levels of technology and countermeasures to the point of transfer to the customer programs and organizations.

Partnerships and Collaborations

The HRP works with universities, hospitals, and federal and international agencies for the purpose of sharing research facilities and multiuser hardware, and for collaboration on research tasks of mutual interest. The HRP uses bed rest facilities at the University of Texas Medical Branch in Galveston, Texas, to study changes in physiologic function associated with weightlessness. Many of these changes occur in people subjected to bed rest with the head tilted downward at a 6-degree angle.

Facilities at the General Clinical Research Center in Stony Brook, New York, and the Lerner Research Institute at the Cleveland Clinic/University of Washington support the HRP. These facilities provide bed rest and 6-degree head-down-tilt simulation along with a zero-gravity locomotion simulator, which is a treadmill used by a person lying down such as during bed rest.

The NASA Space Radiation Laboratory at the Department of Energy's Brookhaven National Laboratory in Upton, New York, is used to conduct research using accelerator-based simulation of space radiation. The HRP also uses radiation research facilities at the Loma Linda University Medical Center in Loma Linda, California.

The National Space Biomedical Research Institute (NSBRI)—an academic institute funded by the HRP—investigates the physical and psychological challenges of long-duration human space flight. Founded in 1997 through a NASA competition, the NSBRI is a nonprofit research consortium that connects the research, technical,

Human Research Program

continued

and clinical expertise of the biomedical community with the scientific, engineering, and operational expertise of NASA. Additional information about the NSBRI can be found at: *www.nsbri.org*.

The HRP also maintains collaborative relationships with the ISS International Partners through various working groups. These relationships enhance the research capabilities of all partners and provide synergism of research efforts. Some of the working groups HRP participates in include:

- International Space Life Sciences Working Group (Canada, Japan, Germany, Ukraine, France, and the European Space Agency)
- U.S.-Russian Joint Working Group
- European Union in Radiobiology Research Program
- International Council of Radiation Protection

The HRP organizes and participates in international collaborative meetings and coordinates research and technology workshops. The workshops are conducted to inform researchers outside of NASA about the HRP's research and to obtain information about research going on outside of NASA. Some of the workshops include:

- International Space Life Sciences Working Group *http://www.nasa.gov/exploration/about/islswg.html*
- Meeting of the U.S.-Russian Joint Working Group
- Human Research Program Investigators' Workshop *http://www.dsls.usra.edu/meetings/hrp2010/*
- 61st International Astronautical Congress *http://www.iafastro.com/?title=IAC2010/*
- 21st Annual NASA Space Radiation Investigators' Workshop *http://www.dsls.usra.edu/meetings/radiation2010/*
- 18th International Academy of Astronautics Humans in Space Symposium *http://www.dsls.usra.edu/meetings/IAA/*

Education and Outreach

The Human Research Program Education and Outreach Project is committed to using NASA's space research and exploration to educate the nation in science, technology, engineering, and mathematics. Project activities and materials target educational communities, the general public, policymakers, and the media using formal and informal venues. The project has made notable strides in their K-12 programs and outreach efforts. Their primary grade programs include the 21st Century Explorer, Fit Explorer, and Sports and Exploration, while their secondary programs include Math and Science @ Work and Exploring Space through Math.

Each year, the HRP compiles and publishes an annual report highlighting major programmatic and technical accomplishments. These reports can be found at: *http://www.nasa.gov/exploration/humanresearch/research_info/overview/program_docs_detail.html.*

To learn more about the Human Research Program Education and Outreach Project, please visit: *http://www.nasa.gov/exploration/humanresearch/education/index.html.*

No Drill Dentistry: Improved Composites and In Vivo Studies

Diane Byerly, *Johnson Space Center*
George D. Arndt, *Johnson Space Center*
Marguerite A. Sognier,
Universities Space Research Association
John Dusl, *Jacobs Technology*
Ivan Stangel, *Biomat Sciences*

Currently, limited options exist for treating dental emergencies during space flight. The longer the mission duration, the greater the probability of spontaneous dental problems occurring. The pain and discomfort arising from lost fillings, broken or cracked teeth, and infections can affect mission success. The standard treatment for caries (tooth decay) requires the use of a local anesthetic, drilling to remove the decayed areas of a tooth, and tooth reconstruction. Such procedures are not practical for space flight and future exploration. To address these issues and optimize crew health, innovative technology is under development to enable emergency caries treatment and tooth repair to be performed in flight by astronauts who are not experts in dentistry.

The Biomedical Engineering Technology Development Team at Johnson Space Center previously developed a lightweight handheld microwave system consisting of a sharply focused antenna, signal source, and power amplifier for dental applications. Using unique test beds, the team demonstrated that microwave energy could effectively eradicate the caries-causing bacteria—Streptococcus mutans. To further advance this innovative technology for future human application, small-animal studies were performed. The objective was to determine the effects of microwave energy on rat incisors and the immediate surrounding tissues. Incisors were treated with microwave energy for 0, 30, or 60 seconds, and were compared to untreated incisors after different time intervals. Microscopic evaluation, performed by an independent veterinary histopathology expert, focused on gingival tissues, dental pulp, and alveolar bone housing of incisors. Under the conditions of this study, no microwave-associated harmful effects were detected involving incisors, pulpal tissue, gums or bone exposed for 30 or 60 seconds at 1, 7, or 56 days following treatment in this rodent model. These results demonstrate the feasibility of using microwave energy for dental treatments.

In parallel studies, the microwave system was evaluated for its effectiveness in curing new, proprietary composite materials for tooth reconstruction and repair. These tests involved exposing the materials to various curing protocols. Researchers performed a series of crush tests to assess the hardness and quality of the cured composite materials. These tests included composite samples that were: exposed to microwave energy (no pre-curing); pre-cured using microwave energy; or pre-cured with a commonly used dental blue-light instrument. Researchers obtained significantly improved composite results when pre- and post-hardening was performed using microwave energy; i.e., composites were harder and more durable. Future studies are planned to test the in vivo performance of these composites in rodents.

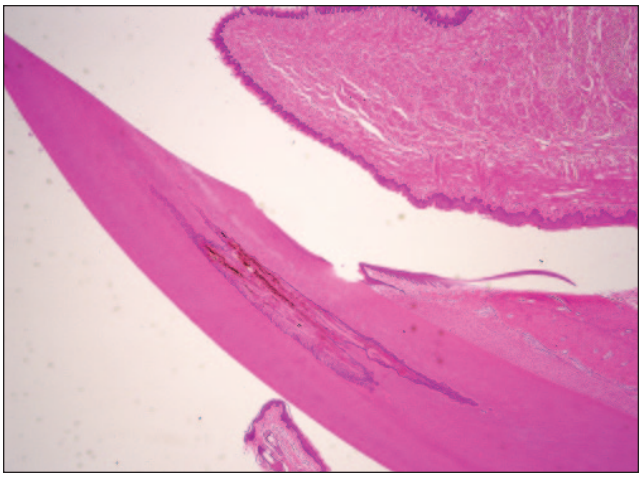


Fig. 1. *Cross section of lower rat incisor stained with H&E showing no damage from radio frequency exposure.*

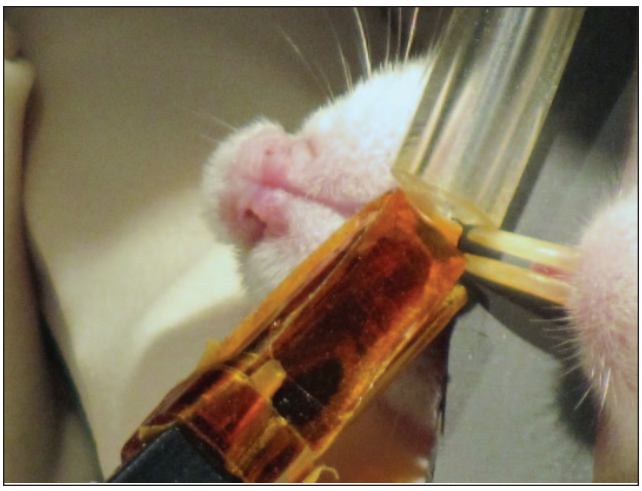


Fig. 2. *Rat incisor being exposed to radio frequency energy.*

Upon completion of additional animal-based studies, further development of this technology will ultimately involve human clinical trials before it can become available for common use. This new technology will revolutionize current dental practices by making it less expensive, simpler, faster, and less invasive with more durable, longer-lasting tooth repairs.

Vitamin D: From the Antarctic to the International Space Station to North America

Sara R. Zwart, *Universities Space Research Association*
Scott M. Smith, *Johnson Space Center*
James Locke, *Johnson Space Center*

Vitamin D is unique in that exposure to ultraviolet light allows the body to synthesize the vitamin from a precursor in the skin. Because the diet of most individuals includes few good natural sources of vitamin D, many people depend on sun exposure or supplements to fulfill the majority of their vitamin D requirement.

The most recognized role of vitamin D is its involvement in calcium metabolism. Classic target organs include bone, intestine, and kidney. Deficiency of vitamin D will lead to bone diseases, such as rickets in children and osteomalacia in adults. In both cases, the vitamin D deficiency renders the body unable to absorb calcium from the diet—a process that depends on vitamin D. The body depletes bone calcium content to make calcium available to other parts of the body. Vitamin D is critical for space travelers because they lack exposure to ultraviolet light and have an insufficient dietary supply of vitamin D. Astronauts are provided 800 international units per day (IU/d) of vitamin D in supplements to make up for the deficiency; the dose is based on ground analog research.

A good model for studying vitamin D metabolism is Antarctica because of the limited sunlight exposure during the winter period, which lasts about 6 months. The Antarctic science station model has been used successfully as a ground-based analog for space flight in studies of behavior, immune response, and reactivation of latent viruses. The Nutritional Biochemistry Laboratory's (NBL's) experience conducting studies in Antarctica has shown that ground-based models of insufficient sun exposure are a valuable asset for clear determination of the optimal dose of vitamin D required to maintain optimal blood levels of 25-hydroxyvitamin D.

The NBL collaborated with the National Science Foundation to use the Antarctic winter as an analog for two investigations in recent years. In the first study, conducted in 2007, scientists evaluated the effectiveness of three different daily doses of vitamin D in maintaining serum 25-hydroxyvitamin D at 80 nanomoles per liter (nmol/L). Results revealed that 2,000 IU/d increased vitamin D status from baseline levels to about 70 nmol/L, but researchers also discovered that some of the study participants had difficulty complying with the instructions to take the supplement every day.

The NBL conducted the second study during the Antarctic winter in 2009 and found that a weekly dose (10,000 IU, once a week) of vitamin D supplement could be used as effectively as a daily dose. The researchers also found that the effects of stress, viral reactivation, and vitamin D status interact. That is, when biochemical markers of stress levels were high, a higher vitamin D status protected against reactivation of latent virus. Latent virus reactivation is also known to occur during space flight. Both studies revealed that body mass index had a significant effect on a person's response to vitamin D supplementation. A person with a higher body mass index requires more vitamin D to achieve the same blood concentration of vitamin D as someone with a lower body mass index.

In 2011, the Institute of Medicine (IOM) released a report on the reevaluation of vitamin D requirements for North Americans. The 2009 Antarctic publication was featured in the report, specifically in the area of studies that had minimal ultraviolet light—a confounding issue when considering vitamin D requirements. The IOM developed a dose-response curve using data from studies conducted in environments with minimal ultraviolet light, and based the new vitamin D recommendation on the lower confidence interval of that curve. The 2009 Antarctic study contributed three data points to that dose-response curve, and influenced the IOM's calculations and ultimate recommendation. Because the IOM panel had only the initial 2009 publication from which to work, NBL scientists went back to the full data set (and added the data from the second study) to determine whether the same curve could be generated. When all individual subject data were combined, the scientists found that, indeed, the IOM model held up well. However, as mentioned, body mass index affects vitamin D status and the response to intake of vitamin D. These data were published in a letter to the journal editor in 2011 in support of including more information to evaluate the dietary recommendations for Americans.

The data from these ground-based experiments will enable NASA to provide space crews with evidence-based recommendations for vitamin D supplementation. The space agency often points to the broader implications of its research, and this is a perfect example of how work done to better understand space flight literally played a part in establishing dietary recommendations for people across North America.

The Value of Human Engineering in Designing Exploration Spacecraft

Jennifer Boyer, *Johnson Space Center*
Harry Litaker, *Johnson Space Center*

The role of a human engineering team on a major design and development project such as the Orion spacecraft, Space Exploration Vehicle, or Lander is to ensure the design follows a human-centered design (HCD) process. An HCD process supports development of an effective, efficient, productive, and safe design by linking task, crew, and design requirements.

Three major human engineering activities are conducted to ensure human safety and performance when following an HCD process. These activities include:

- ***Task analysis:*** Definition of the tasks that crew members will perform both nominally and off-nominally, the hardware they will use, and the context of how they will perform the tasks (mission phase, vehicle configuration, time constraints, number of crew members, etc.)
- ***Modeling:*** Use of Computer Aided Drawing (CAD) models to represent concepts and static physical volumes, and to assess static crew body positions for the various tasks identified in the task analysis. Modeling should be driven by anthropometric and biomechanical requirements.
- ***Human-in-the-loop (HITL) evaluation:*** Use of physical mock-ups with crew and non-crew subjects to simulate tasks and evaluate the design under mission-like conditions.

Task analyses, modeling, and HITL evaluations each provides unique information about the tasks that the crew members need to perform, potential crew postures for a range of anthropometric sizes, and the acceptability of the design in performing identified tasks. Each activity within the process informs the other. For example, tasks and scenarios identified in a task analysis may be modeled using CAD software to provide guidance on what is needed per task (such as volume, equipment, and cabin configuration), and this may then be validated with crew subjects in an HITL evaluation. Physical testing in mock-ups of increasing fidelity allows for evaluations of crew performance involving dynamic tasks, translations, and coordination between crew members. HITL evaluations are critical for providing information on how a design impacts crew task efficiency, effectiveness, and satisfaction.

Thus, it is crucial that all three activities—task analysis, modeling, and HITL evaluations—be used throughout the vehicle design process.

Impact on Design

Early and iterative HITL evaluations are used to identify design and integration problems, improve usability, and reduce cost and schedule impacts. Throughout the Orion design life cycle, numerous focused HITL evaluations have assessed and improved vehicle design. For example, from 2008-2010, human engineering facilitated at least 39 formal evaluations and 49 human factors hardware consultations.

Evaluation of vehicle designs progresses in stages/phases. Early evaluations focus on individual components, and ensure the design supports the concepts of operation. Work then continues to integrate the components within a subsystem, such as evaluating cursor control device operability using a notional procedure and display. With continued refinement of the design, evaluations are integrated at the system level. For example, a vehicle egress evaluation provides data on seat design, strut design, interior volume, and mobility aids. The data collected during each evaluation vary depending on the objectives of the particular evaluation. Human engineering uses quantitative measures (e.g., error rates) and qualitative measures (e.g., subjective workload scales) to provide a complete picture as to how the design impacts human safety and performance.



Fig. 1*. Suited subject egressing through the Orion side hatch.*

The Value of Human Engineering in Designing Exploration Spacecraft

continued



Fig. 2. *Photos from left to right: Computer Aided Design model of the Orion cabin, suited subjects inside the Orion cabin, and suited subject inside the Orion cockpit.*

Several human engineering evaluations have resulted in significant design impacts, either by saving cost or improving usability.

Example A. By conducting an early seat egress evaluation for Orion, NASA identified an impediment to egress caused by the location of a support beam, allowing for early rework of the design and thereby saving cost and schedule.

Example B. Evaluation of the Orion side hatch height showed that the crew could effectively egress at varying heights in various suit types, allowing the project to make a needed design change to the bulkhead height without an impact to crew safety or performance.

Example C. Iterative task analysis, CAD modeling, and evaluation of the Orion crew net habitable volume facilitated requirements progression from a number derived from analysis, to task-driven functional volume assessed through HITL evaluation.

Example D. A series of viewability studies identified the need to angle the outer displays, increasing cross-cockpit viewability and crew situation awareness.

Example E. Evaluation of the Orion window size and shape early in the design cycle allowed the Orion project to determine the inner and outer mold line without costly adjustments.



Fig. 3. *Interior configuration of the Altair Lander before and after human factors input.*

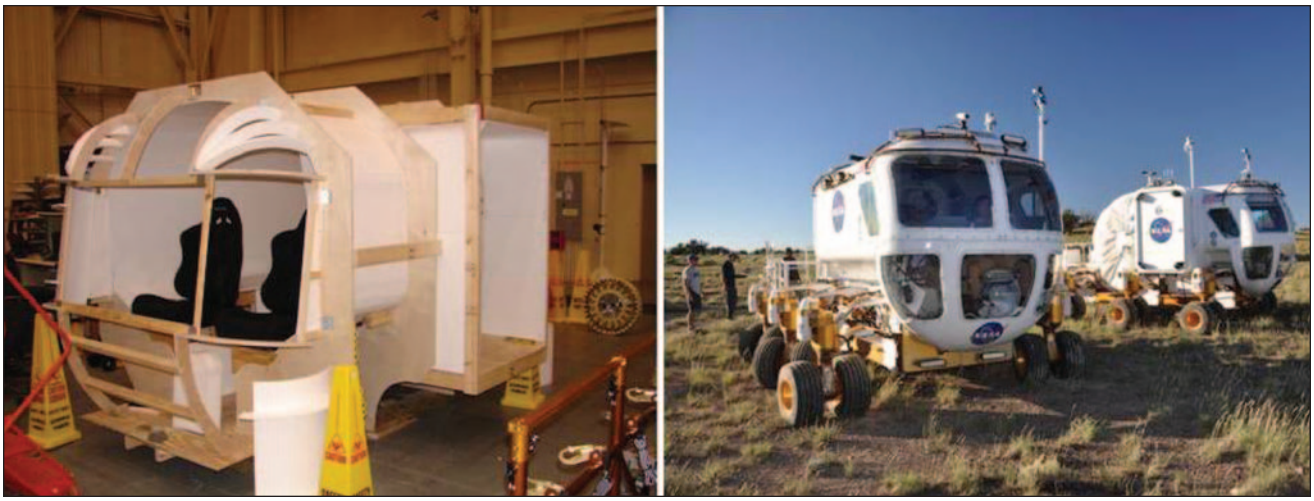


Fig. 4. *Progression of the Space Exploration Vehicle from initial to current design.*

Example F. A seat egress evaluation using various suit types and a range of anthropometric crew sizes identified the need to relocate the Translational Hand Controller from the lower console to the upper console, preventing a snag hazard for the crew.

Example G. An HITL evaluation revealed that vehicle stowage for the Altair Lander was inadequate for an extravehicular activity task, impacting performance and increasing crew's workload (left photo). Human factors engineers and vehicle designers improved the stowage by designing suit stowage bags and a hoist system to maximize the upper vertical volume of the vehicle. A follow-up HITL evaluation revealed that crew workload decreased and volume was vastly improved (right photo).

Example H. Using data and lessons learned from a functional volume HITL evaluation of 16 dynamic tasks on the Space Exploration Vehicle, vehicle designers updated the cabin configuration—including adding an environment enclosure for spacesuits—and made modifications to window design/placement.

Example I. HITL data gathered while a crew of two worked and lived in the functional mock-up of the Space Exploration Vehicle for 3 days proved to be invaluable to vehicle designers. Lessons learned from these simulated missions resulted in a redesign of the cockpit, updated seat adjustment mechanisms, redesigned stowage capacity, and a redesigned trash management system.

Conclusion

Early, iterative human factors analyses and HITL evaluations provide design and management teams with an enhanced ability to make informed decisions during design and development. Informed decisions reduce costs, and help ensure effectiveness and efficiency for crewed missions.

Development of Usability Requirements at NASA

Anikó Sándor, Johnson Space Center
Kritina L. Holden, Johnson Space Center

The International Organization for Standardization [ISO] published a number of standards for the operational evaluation of usability. The ISO 9241-11 standard defines usability as "the extent to which a product can be used by specified users to achieve specified goals," and recommends evaluating usability in terms of measures of effectiveness, efficiency, and satisfaction. Measures of effectiveness relate the goals or sub-goals of the user to the accuracy and completeness with which these goals can be achieved. Measures of efficiency relate the level of effectiveness achieved to the expenditure of resources. Finally, satisfaction measures the extent to which users are free from discomfort as well as their attitudes toward the use of the system. All three factors are important in evaluating the usability of a system.

Usability is a key element of the human-centered design approach. Human-centered design is a design philosophy and a process that takes into account human capabilities and limitations at each stage of the design process. Applying a human-centered design process to system development contributes to crew health and safety by increasing system usability. Insufficient integration of human concerns with the vehicle design may result in inadequate interfaces and deficiencies in commonality, consistency, and usability that translate into less-than-optimal operations, higher training costs, and an increased risk to mission objectives. A usable system will provide increased effectiveness, efficiency, and satisfaction. Furthermore, good usability reduces errors, training time, and overall life cycle costs, and it is essential to ensure crew safety and mission success.

The Need for a Usability Requirement at NASA

At NASA, the development of space vehicles and related hardware and software are driven by verifiable requirements. In spite of the need for requirements and the recognized importance of usability, it has taken many years to add a usability requirement to NASA program documentation. First, writing a usability requirement is difficult because the requirement must be easy to operationalize. For example, how can usability be measured and, therefore, verified? Furthermore, can usability be represented by a single, simple metric? Second, the verification methodology needs to be achievable with the time and cost limitations typically encountered in the space industry. For example, the number of interfaces tested, number of test sessions, and number of participants tested must be limited to maintain reasonable cost. Third, the requirement must be broadly applicable to system, subsystem, and component levels. Finally, the requirement should encourage a process approach. Good usability cannot be accomplished with a one-time evaluation but only with iterative usability evaluations from the beginning to the end of the life cycle of a system.

General Practices in the Area of Usability

NASA reviewed the documentation of a number of companies and agencies such as the Department of Defense and the Federal Aviation Administration to understand their approach to usability. NASA found that the common practice is to follow human factors guidelines and standards, such as the Military Standards, MIL-STD-1472; include human factors and usability professionals in the system development life cycle; and evaluate designs through expert evaluations and user testing. However, NASA did not find any practice among those agencies that includes objective, verifiable usability requirements and criterion of verification. Furthermore, industry often has multiple criteria for its products. For example, a voice recognition system should have a 98% accuracy rate to be usable, but a cell phone may have 85% success rates on expert tasks, and 95% on common tasks. The space agency concluded that these practices and approaches were not appropriate for the safety-critical space industry.

Development of the Usability Requirement at NASA

In developing a usability requirement for NASA, the metric of choice was errors. Obviously, there are many other metrics for usability. However, errors are objective, easy to understand by all stakeholders, and highly related to all factors of usability. Virtually all tasks in the space domain are driven by procedures, and NASA's approach was to put the emphasis on identification of usability problems by calculating error rates per procedure ***step*** and

Table 1. *An Example Scenario Illustrating the Error Count on a Procedure with 10 Steps Completed by a Group of 10 Participants*

	Step 1	Step 2	Step 3	Step 4	Step 5	Step 6	Step 7	Step 8	Step 9	Step 10
Participant 1	0	1	0	0	0	0	0	1	0	0
Participant 2	0	1	0	0	0	0	0	0	1	0
Participant 3	0	1	0	0	1	0	0	0	0	0
Participant 4	0	1	0	1	0	0	0	0	0	0
Participant 5	1	1	0	0	0	0	0	0	0	0
Participant 6	0	1	0	0	0	0	1	0	0	1
Participant 7	0	1	0	0	0	0	0	0	0	0
Participant 8	0	0	0	0	0	0	0	0	0	0
Participant 9	0	1	1	1	1	1	1	1	1	1
Participant 10	0	1	0	0	0	0	0	0	0	0

per ***participant***, rather than calculating an overall error rate. Furthermore, NASA focused on errors that were design-induced to ensure the space agency captured errors that are design-related, and not necessarily caused by other factors, such as the variability of the human. Because NASA wanted to reduce the complexity and subjectivity of the method, it decided not to focus on the severity of the errors. Early experiences during development of the usability requirement showed that using severity ratings increases the subjectivity of the decisions, and there are already many other documented requirements that mitigate severe errors.

In a usability test it is important to detect steps with many errors. High error rates on a step suggest usability issues related to the execution of that step (e.g., design problem with the hardware, software, or instructions). On the other hand, it is equally important to detect participants who commit many errors. These participants may be outliers due to things such as different training background. Table 1 shows an example of the error counts for a sample of 10 participants executing a procedure composed of 10 steps. Note that on Step 2, most participants committed errors, and Participant 9 committed errors on most of the steps. This is a situation in which Step 2 merits human factors attention and potential design changes. Participant 9's background and test circumstances should be investigated further to identify any differences that resulted in the high error rate.

In developing the usability requirement, NASA took into account both of these aspects, and thus developed criteria for both (5% and 10%, respectively), based on testing and computer simulations. As a result, the requirement ensures that the number of design-induced errors is minimized for every task step and every participant. With proper error definition, analyses indicate that this type of requirement is very stringent for the types of tasks anticipated for spacecraft verification. The final approved requirement wording documented in the Human-Systems Integration Requirements document is as follows:

"The system shall provide crew interfaces that result in a maximum of 5% erroneous task steps per participant, where each erroneous task step is committed by 10% or fewer participants."

Achieving a community-approved usability requirement in a NASA document is a significant accomplishment because this indicates a first step toward full inclusion of usability in the NASA system development life cycle. NASA is at the forefront of evolving the usability practice by having a verifiable usability requirement using objective measures for usability verification.

Virtual Guidance for Medical Ultrasound Procedures on Exploration Class Missions

David S. Martin,
Wyle Integrated Science and Engineering Group
Timothy L. Caine,
Wyle Integrated Science and Engineering Group
Timothy Matz, *MEI Technologies*
Michael B. Stenger,
Wyle Integrated Science and Engineering Group
Steven H. Platts, *Johnson Space Center*

Ultrasound can be used to image nearly every part of the body, making it a useful, noninvasive tool for both research and diagnostic studies. Hardware advances have resulted in compact designs, making ultrasound an ideal imaging modality for use on the International Space Station (ISS) and future manned space vehicles. The size and up-mass requirements of other medical imaging equipment make their deployment in space vehicles problematic. However, ultrasound imaging is traditionally a highly operator-dependent modality, and requires lengthy training to perfect. To obtain quality ultrasound images on the ISS, much of the expertise has been shifted to the ground in the form of remote guidance. This technique involves minimal astronaut training coupled with real-time remote guidance from an expert on the ground. The technique has been used successfully with several research projects requiring ultrasound on the ISS and has been validated in diagnostic clinical scenarios, as well. With plans for missions of greater duration and distance from Earth, the time delay in communication from Earth to a spacecraft can increase substantially, projected to be as long as 40 minutes on a Mars mission. In this setting, remote guidance will not be a realistic possibility, and astronauts will be forced to operate more autonomously ("just in time training"). Virtual Guidance ultrasound is designed to fill this gap. Virtual Guidance is a comprehensive audio/video tutorial designed to guide an untrained operator through a detailed ultrasound study without the need for extensive training or remote guidance. The purpose of this study was to demonstrate the feasibility (on the ground) of Virtual Guidance to obtain clinically relevant measures of the carotid artery including intima-media thickness.

Methods

In a step-by-step manner, the Virtual Guidance tutorial demonstrates equipment setup, patient/subject positioning, ergonomics of scanning, study protocol, location and when to use controls, as well as scanning guidance. Intended operators are likely to initially produce less than adequate images; therefore, a series of typical scanning errors are demonstrated along with strategies to recover. This tutorial is viewed in real time using commercially available virtual reality video glasses, while the operator performs the ultrasound scan. The video glasses allow hands-free, full screen viewing of the tutorial while maintaining an unobstructed view below the glasses of the ultrasound screen, keyboard, and patient. The audio/video tutorial program can reside on any video source including—but not limited to—iPod, laptop computers, and DVD players. For the current study, the tutorial was stored on, and played back through, an Apple iPod.

Researchers recruited 10 untrained subjects to operate an ultrasound system, acquiring images and Doppler from a carotid artery of a subject using only Virtual Guidance for instruction. Commercially available ultrasound equipment was used (Philips CX50, Philips Medical, Andover, Mass.). Images selected by the scanner, with advice from only the Virtual Guidance tutorial, were stored digitally. Additionally, two trained sonographers scanned the same subject for comparison purposes.

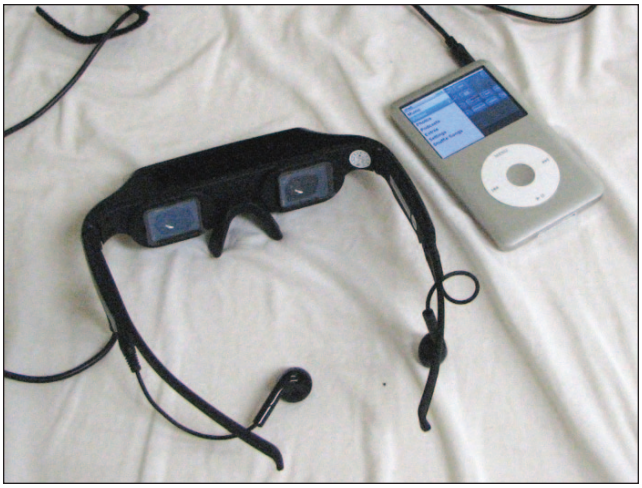


Fig. 1. *Video glasses and iPod.*

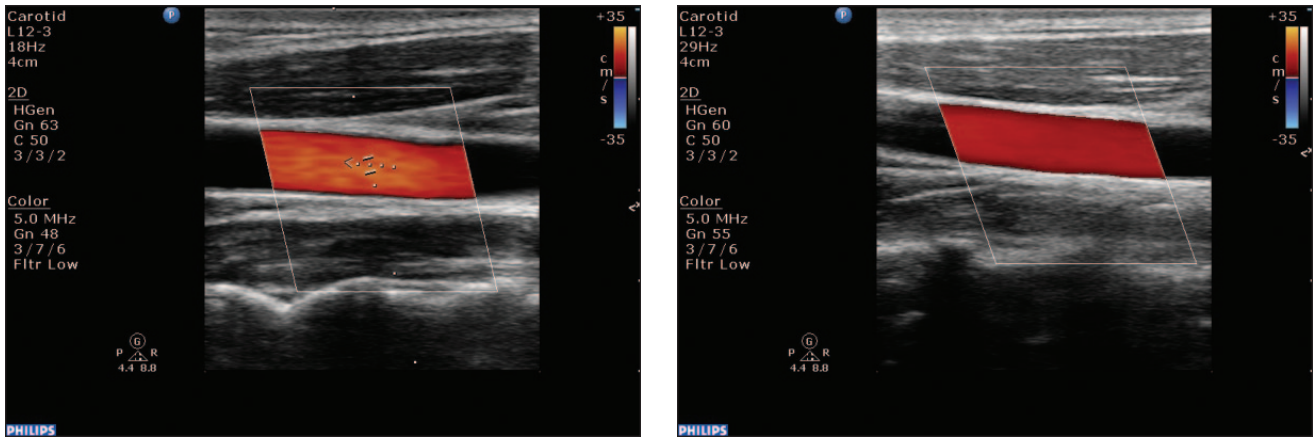


Fig. 2. *Color Doppler of the carotid artery from: a) an untrained scanner; and b) an experienced sonographer.*

Results

A cardiologist who was experienced in interpreting cardiovascular ultrasound images evaluated and scored the images. Eight of the 10 untrained operators achieved scores that were considered to be diagnostically adequate.

Conclusions

This study demonstrated the ability of untrained operators to acquire diagnostically adequate images of a carotid artery with guidance from only Virtual Guidance. The untrained operators in this study were at somewhat of a disadvantage when compared to crew members on ISS, who typically have introductory ultrasound training preflight when participating in a research study that involves remote guidance ultrasound. Additionally, greater success would be anticipated if time and budget allowed for further refinement of the tutorial video. While this tutorial was specifically developed for carotid artery, it is possible that tutorials could be developed for any of the many terrestrial clinical or research ultrasound applications.

Next-Generation Anti-Gravity Suits

Michael B. Stenger,
Wyle Integrated Science and Engineering Group
Stuart M.C. Lee,
Wyle Integrated Science and Engineering Group
Christian M. Westby,
Universities Space Research Association
Steven H. Platts, *Johnson Space Center*

Orthostatic intolerance after space flight is still an issue for astronaut health. No in-flight countermeasure has been 100% effective, to date. NASA currently uses an inflatable anti-gravity suit during reentry; however, this device can be uncomfortable when inflated, and loses effectiveness upon egress from the shuttle. The Russian Space Agency currently uses a mechanical counterpressure garment (Kentavr) that is difficult to adjust without the aid of a medical specialist, and prolonged use may result in painful swelling at points where the garment coverage is not continuous (i.e., feet, knees, and groin). To improve comfort, reduce upmass and stowage requirements, and control fabrication and maintenance costs, the Johnson Space Center research team has been evaluating a variety of gradient-compression, mechanical counterpressure garments, constructed from spandex and nylon, as a possible replacement for the current anti-gravity suit. Researchers examined comfort and cardiovascular responses to knee-high garments in normovolemic (normal volume of blood) subjects; thigh-high garments in hypovolemic (low volume of blood) subjects (a basic model for plasma volume losses in space) and in astronauts after space flight; and one-piece breast-high garments in hypovolemic subjects. These gradient compression garments provide 55 mmHg of compression over the ankle, decreasing linearly to approximately 35 mmHg at the knee. In thigh-high versions, the compression continues to decrease to approximately 20 mmHg at the top of the leg, and for breast-high versions, to approximately 15 mmHg over the abdomen. Measures of efficacy include increased tilt survival time, elevated blood pressure and stroke volume, and lower heart-rate response to orthostatic stress compared to control subjects without a countermeasure. Results from these studies suggest that the greater the magnitude of compression and the greater the area of coverage, the more effective the compression garment becomes. Researchers are currently testing a three-piece breast-high compression garment on astronauts after space shuttle missions. The team chose a three-piece garment consisting of thigh-high stockings and shorts because it is easy to don and comfortable to wear, and the garment should provide the same level of protection as the one-piece breast-high garments evaluated in hypovolemic test subjects.



Fig. 1. *Compression garments consist of thigh-high stockings with overlapping shorts that provide continuous, gradient compression from the feet to the bottom of the ribcage.*

Methods

Eight astronauts have enrolled in this study to determine the comfort and effectiveness of breast-high gradient-compression garments to prevent post-space flight orthostatic intolerance. These garments have a compression gradient similar to previous designs, with maximum (55 mmHg) compression at the ankles, decreasing to approximately 15 mmHg over the abdomen. To date, three astronauts completed all test sessions, which included testing 60 (L-60) and 30 (L-30) days preflight, followed by testing on landing day (R+0) and 1 day after landing (R+1). Sixty days before flight, subjects were measured for the custom-fit garments depicted in figure 1. Baseline orthostatic tolerance was assessed during a stand test without garments on L-30, and garment effectiveness was tested with a similar stand test after space flight on R+0 and R+1. Orthostatic tolerance was determined by upright responses of continuous heart rate, blood pressure, and stroke volume. Cardiac output, total peripheral resistance, and measures of autonomic function were calculated offline. These treatment subjects were compared to a control cohort who underwent an identical orthostatic challenge before and after space flight, although without stroke volume measurements.

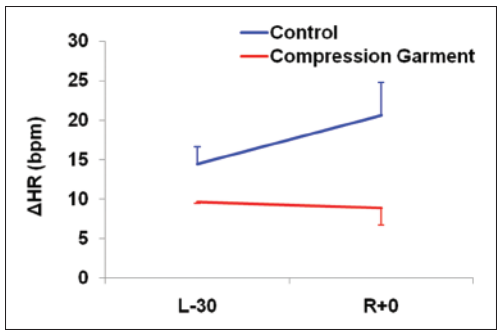


Fig. 2. *Control subjects (n=6) exhibit an elevated heart rate response to standing after space flight compared to compression garment subjects (n=3).*

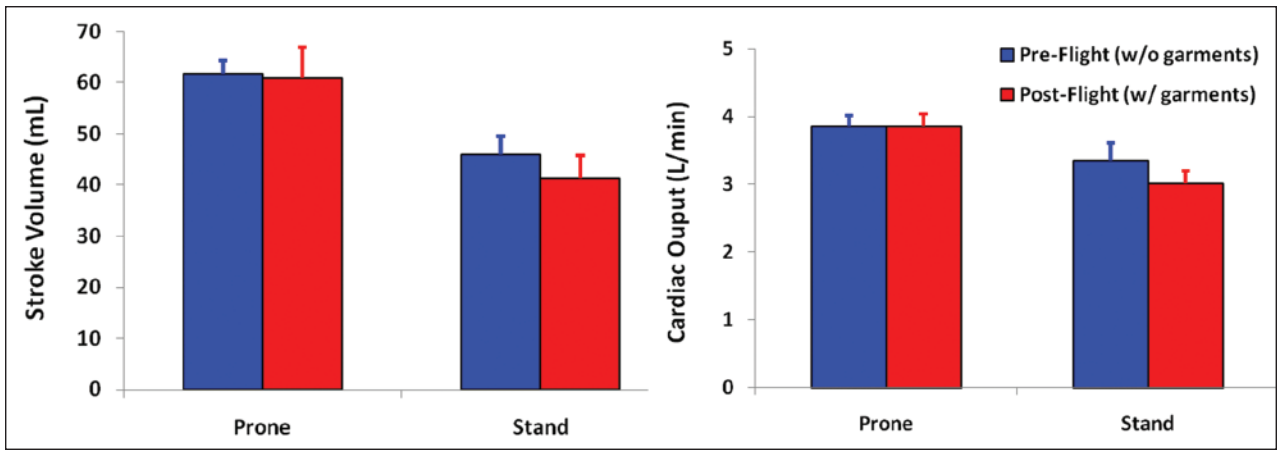


Fig. 3. *Prone and upright stroke volume (left) and cardiac output (right) before (blue) and after (red) a space shuttle mission (n=3).*

Results

Preliminary results (n=3 treatment, n=6 control) suggest that this new compression garment prevented the increase in heart rate that is commonly observed on R+0 in control subjects after space flight (figure 2).

Furthermore, in this small group of subjects, the expected decrease in post-flight stroke volume and cardiac output appears to have been prevented (figure 3).

Summary

This study is in progress, and final results are not yet available from which to make specific recommendations. However, preliminary data suggest that these garments are comfortable to wear and may be a viable replacement for the current anti-gravity suits used during reentry, landing, and immediately post-flight. If these garments are shown to be effective and comfortable in astronauts following these space shuttle missions, they may be appropriate for use by pilots and passengers participating in commercial space flight ventures and in astronauts following long-duration space flight.

Adjustable Mock-up for Integrated Vehicle, Seat, and Suit Evaluations

Sudhakar Rajulu, *Johnson Space Center*
Matt Cowley, *Lockheed Martin*
Lynn K. Pickett, *Lockheed Martin*

Vehicle accommodation requirements are difficult to test and verify. Activities such as ingressing the seat in a vehicle require adequately capturing and analyzing the entire ingress motion to ensure that crew members can deal with limited and restrictive ingress volume space without being stopped or bumping into any surrounding hardware interfaces and protrusions. Having an accurate mock-up is critical because the vehicle, seats, hatch, suits, and other surrounding, necessary hardware all affect motions and postures adopted by the crew member to perform tasks. Postures and movement strategies will also change depending on the occupant's size, age, and gender. The culminating effect of all these factors on subject performance is something that is not easily understood and captured with just simulation software such as digital human modeling. Often, the multifactorial aspects of specific vehicle-seat-suit interfaces and how they would affect (collectively and singularly) pressure-suited humans of different shapes and sizes have yet to be captured in such a simulation software. Most importantly, to simulate such realistic conditions is simply not possible. To see the full picture, some human-in-the-loop testing is required.

Human-in-the-loop testing was previously carried out in standard mock-ups to address design performance and verify requirements are being met. However, standard mock-ups have opaque walls that limit the ability to use motion-capture technology, still and video cameras, and visual observations. Ordinarily these mock-ups also rely on hardware permanently fixed in place to a specific design iteration. Extensive changes to the mock-up design (shape and volume) often would result in the need to build an entirely new mock-up. This may prove to be costly and time consuming. Most importantly, engineers do not get an adequate amount of relevant engineering specific data, which they need to mitigate potential crew-hardware interface accommodation issues.

In the automobile and aerospace industry, it is common practice to design and evaluate vehicle cockpits using transparent and adjustable mock-ups along with state-of-the-art motion-capture technologies (figure 1). Collecting motion-capture data during ingress/egress and other types of tasks in an open mock-up greatly increases the ability to understand and quantify the ergonomic issues associated with various-sized humans interacting with tasks to be carried out in confined work areas. However, nothing of this nature existed at NASA for testing designs for space vehicle cockpits.

The Anthropometry and Biomechanics Facility (ABF) at Johnson Space Center (JSC) developed an adjustable, transparent mock-up of the Orion crew module to fill this void in the design verification abilities of NASA and allow designers to use the latest technologies for human-in-the-loop hardware evaluation. The new mock-up is designed to reduce the amount of visual occlusions to the still, video, and motion-capture cameras and test observers; be adjustable to multiple crew module configurations; and maintain a high level of realism for the test subjects. Figure 2 depicts an assembly of the module structure, netting, display panel, seat pallet, and high-fidelity Orion seats.

Nylon mesh is used for the walls and other hardware in the crew module to give the subject the perception of solid objects, while allowing the cameras and observers to see through the structure. The netting was chosen over glass and transparent plastics because it did not refract light, which would render motion-capture cameras useless. The netting is retractable and enables safety personnel quick and easy access to suited test subjects from any location should a problem arise.

The mock-up is designed with an extruded aluminum frame for easy assembly/disassembly and portability, while maintaining the ability to support loads incurred during testing. The structural configuration for the Orion crew module (fig, 2) frame components can support the weight of a suited crew member during evaluations, allowing that crew member to perform tasks in a realistic manner. The structure can support the full weight of the largest suited crew member when catching a fall on one of the several handholds (not shown).

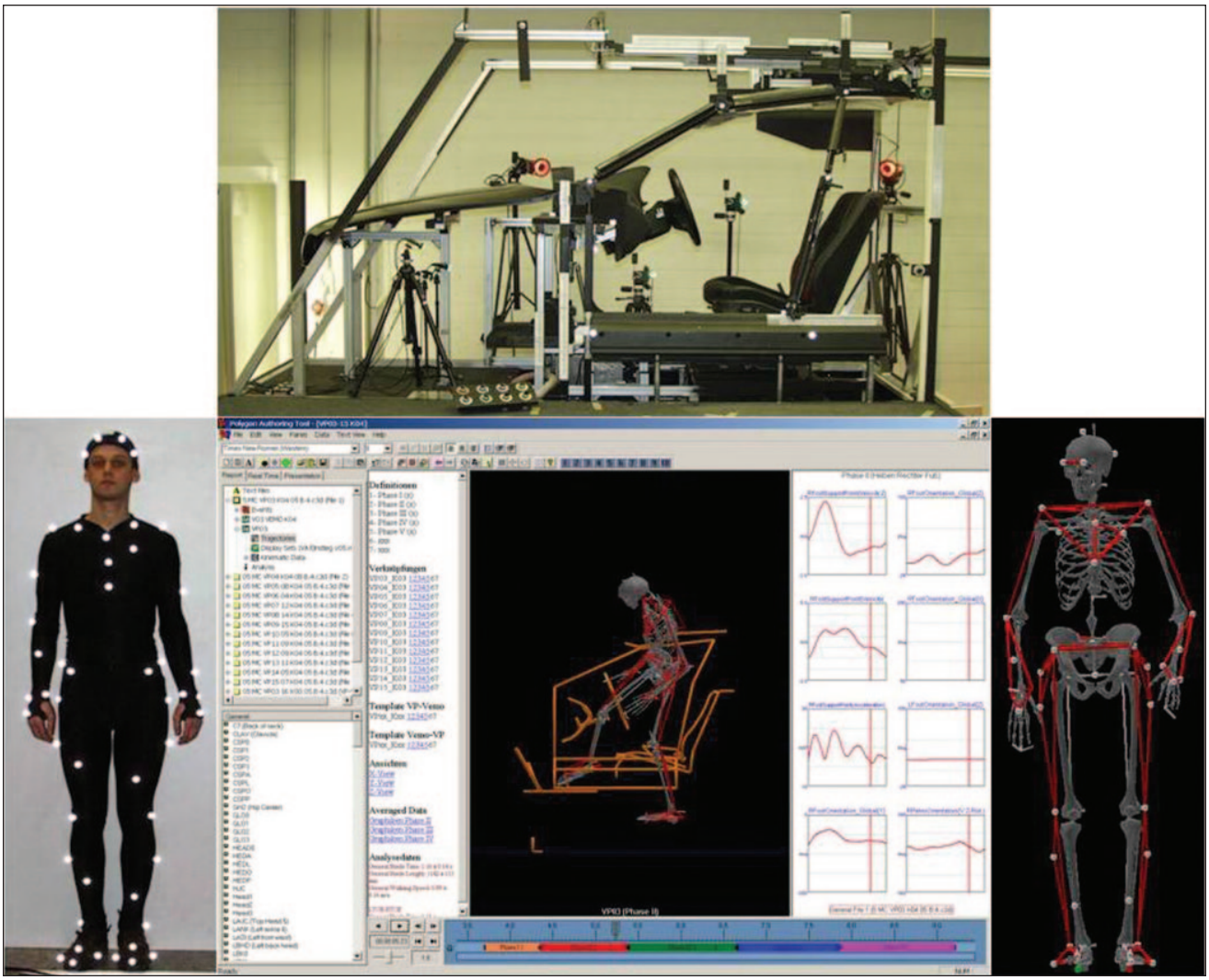


Fig. 1. *Human ingress movements for optimization of vehicle accessibility. (Courtesy of Technical University of Munich and BMW)*

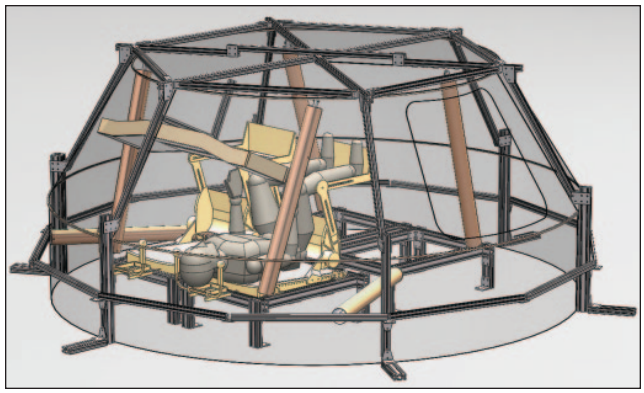


Fig. 2. *Computer-aided design depiction of the adjustable mock-up set to Orion crew module dimensions.*

The pallet and frame can be easily changed to simulate a variety of crew module designs and volumes. The structural members of the frame can be shortened, lengthened, or changed in angle. Interior hardware—such as seats, pallets, control panels, struts, and other additional hardware—can also be easily changed to fit new dimensions or new crew modules designs. This ability to change the mock-up shape and its hardware content allows for quick turnaround times for verification testing on design changes. For example, the Orion crew module could be swapped out for a commercial design quickly. Dimension verification is simplified with the ability to use the motion-capture equipment. Markers are placed on numerous critical landmarks, and the entire mock-up is

Adjustable Mock-up for Integrated Vehicle, Seat, and Suit Evaluations

continued

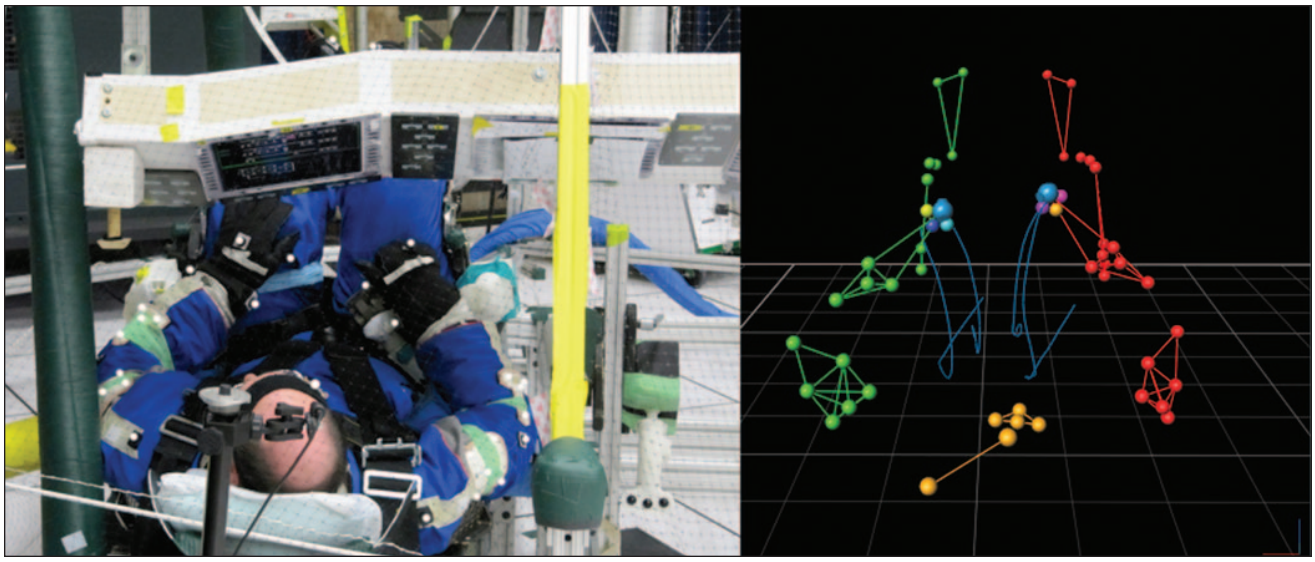


Fig. 3. *A subject in a prototype suit performing Orion launch-and-entry tasks (left) with traces of hand movements in the motion-capture software (right).*

measured in just a few seconds down to the millimeter. The use of Faro Arm (a 6-degrees-of-freedom, 3-dimensional measurement device; not shown) during mock-up testing also enhances the ability to compare and contrast human dimensions to hardware dimensions and clearances.

With the mock-up completed, the JSC ABF team is performing a series of evaluations to test several extravehicular activity prototype suits in the Orion crew module vehicle/seat environment (figure 3). Suited subjects perform planned ingress, egress, and flight tasks while motion-capture data, video data, subjective comment data, dimensional clearances, and observational data are collected. Data that the ABF team will be able to gather using this approach will include, but are not limited to: functional range of motion, motion paths, identification of keep-out zones, collision detection, seated comfort, joint stress, task time to completion, and general observer functionality comments. Performance of the suits, updates to requirements based on actual required task motions, and identification of what is causing certain issues (vehicle, seat and/or suit) are determined.

The mock-up is being used to evaluate the performance of new prototype extravehicular activity suits. An additional benefit of this type of testing is the ability to capture much of the task performance data and then project the individual person's data to a range of subjects to study the impact of vehicle accessibility for a wide range of the population. NASA engineers often have to contend with making important decisions based on only a few subjects' data or comments due to a limited number of suits and suit sizes, or to limited subject availability. While it is true that individual subjects may exhibit different mobility and postural patterns, it is now possible to make a calculated prediction and assessment of a specific vehicle-seat-suit interface for a wide range of population. One additional advantage of this method of using transparent mock-ups with advanced motion-capture technology is that NASA engineers will be able to graphically view and analyze the 3-dimensional human and hardware interference data in a computer-generated replica of the conceptual crew vehicle design and make moderate changes—e.g., to the display control panel—to arrive at a better design without needing to redo the expensive evaluations.

Advanced Photoluminescence Technology as an Emergency Guidance System on the International Space Station

James C. Maida, *Johnson Space Center*
Laura E. Duvall, *Johnson Space Center*
Kim A. Tran, *Lockheed Martin*
Lynn K. Pickett, *Lockheed Martin*

The Graphics Research and Analysis Facility (GRAF), Lighting Evaluation and Test Facility, and Flight Crew Integration team in the Habitability and Human Factors Branch at the NASA Johnson Space Center worked closely with the International Space Station (ISS) Program Office to find an innovative and low-cost solution to a crew egress concern. During the assembly phases of the ISS when the electrical system was being deployed in stages, a battery backup system was used to power light-emitting diode (LED) light strips around designated hatch areas in the event of a power failure for general illumination in a module. This system, known jointly as the Emergency Lighting Power System (ELPS) and emergency egress lighting strips (EELS), required regular battery testing of the deployed system on orbit and replacement units on the ground. As the ISS electrical system matured, its reliability and redundancy increased to the point that the ELPS and EELS became less critical and its cost benefit became questionable. To reduce the costly maintenance of testing batteries and flying replacements in efforts to provide emergency egress guidance, a photoluminescent solution was investigated and implemented.

Photoluminescent materials ("glow-in-the-dark" or afterglow capabilities) have been used for decades. For safety applications, they first appeared in the marine industry for ships and oil rigs and were later approved by the Federal Aviation Administration for airplane cabins and aisle pathways. The technology has improved significantly in the past 10 years, and Underwriters Laboratories has begun certifying high-performance formulations for use as exit signs in buildings. The grading system used to rate performance of photoluminescent materials was developed by the ASTM [American Society for Testing and Materials] International. The standard minimum luminance properties of manufactured components (manufacturing quality control) is rated at 20/2.8 or 20 milli-candelas (1/1000 of a candela) at 10 minutes and 2.8 milli-candelas at 60 minutes in the dark after exposure to 1000 lux for 5 minutes (E2072-04). The standard minimum luminance of installed components is rated at 15/2.0 (ISO 16069). These standards also require a minimum target area of 25.6 mm.

NASA has been using photoluminescent markers to label emergency egress path, but only in conjunction with its ELPS as a complete emergency lighting system because the photoluminescent materials used did not provide sufficient luminance for extended periods of time in darkness. The goal was to find a product that would provide the extended visibility needed to cover long periods of possible darkness to support crew activity. All of the products offered low cost and low maintenance. Figure 1 shows the results of a trade study between the two most competitive products. Product B, in its rigid form, is the material used previously. Product A, in a rigid form, is used for the photoluminescent-based Emergency Egress System (EEGS) being deployed on the ISS for future use. It is rated at 600/90. Additional evaluations have shown that if exposed to 108 lux of illumination for 10 minutes, EEGS will be visible in total darkness for as many as 14 hours. In the case of a short exposure time, EEGS will be visible for as many as 3 minutes after 10 seconds of 108 lux of illumination.

Luminance decay rates comparisons after illumination for 8 hours @ 100 lux (ISS minimum is 108 lux)	Initial mcd	mcd @ 3 min. (mininum evacuation time)	mcd @ 10 min	mcd @ 60 min	mcd @ 8 hrs (interpolated) (minimum crew sleep period)	Nominal Shelf Life (yrs)
Vendor A (Rigid)	435.0	79.0	46.0	29.0	15.0	10.0
Vendor B (Flexible)	236.0	65.0	37.0	20.9	9.8	3.0
Vendor A (Flexible)	250.0	76.0	40.0	21.4	9.5	10.0
Vendor B (Rigid)	63.0	17.0	4.0	2.0	0.5	3.0

Fig. 1. *Product comparison.*

The human factors team assessed the ISS hatch areas, looking at available real estate and nearby light fixtures. All of the EEGS potential hatch locations, with their respective ISS general lighting systems illuminating them, were modeled using Radiance (a validated light-modeling system used in the GRAF). The more advantageous locations were evaluated to see whether they received the appropriate illumination for charging the photoluminescent material. These locations were then documented for use in the installation kits developed for the crew. Figure 2 provides an example of the on-orbit ISS U.S. Laboratory installation. The other module bulkheads have similar patterns in place.

Advanced Photoluminescence Technology as an Emergency Guidance System on the International Space Station

continued

A circular shape was chosen because it requires no orientation, is highly detectable to the human eye, and has no corners for reduced peeling. The EEGS targets are mounted by adhesive (966 acrylic) to metal surfaces, with a maximum target size of 57.15 mm and a minimum target size of 25.4 mm (figure 3). The maximum size is determined by provisions of flammability testing for on-board ISS hardware, and the minimum is determined by ASTM standards.

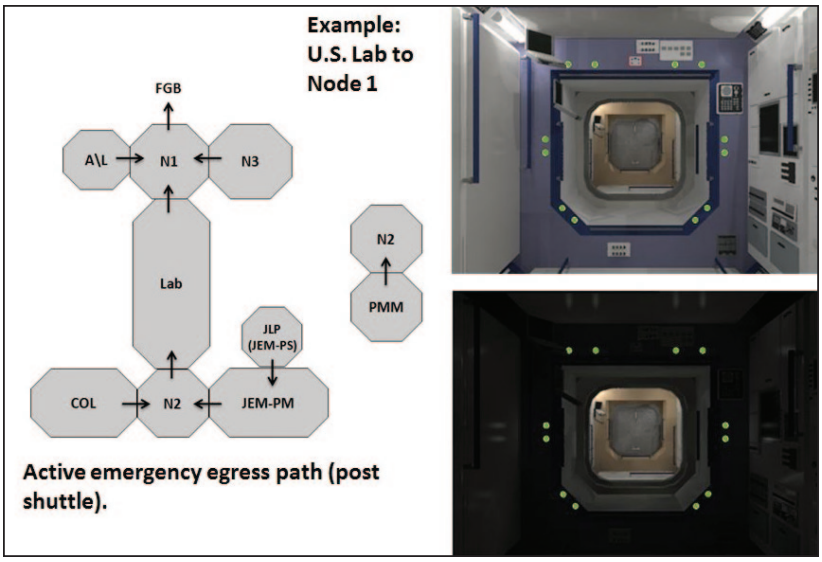


Fig. 2. *Marked hatchways and example hatch layout for the Emergency Egress System.*

The planned EEGS deployment for the designated emergency egress paths within ISS was approved to end at the Node 1 to FGB [functional cargo block] hatch (i.e., does not include Russian segments). At the time of this report, the EEGS has been installed on all hatch area segments except those of the international partners. Installation for the international partners is expected in the near future. The plans for deployment and the actual installations matched very closely, demonstrating the effectiveness of the installation kits and the choice of circular markers. At the time of reporting, stowage rules are being developed to protect the markers from blockage by future stowage. Redundancy was designed into the system (additional markers were installed) to help minimize this problem.



Fig. 3. *Circular markers with adhesive backing.*

In conclusion, the EEGS has been installed in U.S. ISS modules and is functioning as a successful guidance system for ISS during this transitional time period. The current Japan Aerospace Exploration Agency H-II Transfer Vehicle cargo transfer vehicles are using this application of photoluminescent technology, and it is anticipated that future cargo transfer and crewed vehicles will do so as well. As the ISS ages, it is expected that EEGS will provide adequate emergency egress functionality for some time. However, as the reliability of the on-board power system lessens, the need for a more active emergency light system may increase. Emergency egress systems that are hybrids of LED technology and photoluminescent technology are being developed that can enhance the charge of the photoluminescent material directly (i.e., no battery in the loop) with long extended durations as well as a low-power and -maintenance light source.

Microwave-Based Water Decontamination System

Diane Byerly, *Johnson Space Center*
George Arndt, *Johnson Space Center*
Marguerite A. Sognier,
Universities Space Research Association
John Dusl, *Jacobs Technology*

One challenge for the International Space Station (ISS) and future crewed space exploration is to produce sufficient quantities of potable water to meet mission requirements. Current ISS water treatment includes the use of iodine, which produces undesirable health effects and does not eliminate issues related to bacterial contamination of water systems. In addition, research performed on the ISS has shown that bacteria in space can mutate into strains that are more resistant and difficult to eradicate. Alternate approaches are needed—approaches that can effectively eliminate bacteria, are chemical free, and require minimal or no consumables.

The Biomedical Engineering Technology Development Team at Johnson Space Center developed an innovative water purification method that uses selected frequencies of microwave energy to effectively kill bacteria in water. This prototype system is based on a modified version of a small, lightweight, handheld microwave system that was previously developed and tested for medical and dental applications.

Preliminary testing identified specific microwave frequencies and exposure times for killing Burkholderia cepacia—a bacteria known to be present in the ISS water system. Waterborne bacteria was intermittently and randomly circulated for 4 weeks in a growth chamber to simulate a water filtration system. Bacteria adhered to and grew on the flat surfaces of the chamber, forming biofilms. These bacterial biofilms were irradiated with high-frequency microwave energy for various time intervals in static (non-circulating) water. The test results showed that exposure to microwave energy for 1.5 minutes could effectively kill waterborne bacteria within the chamber and also bacterial biofilms.

The next series of tests involved the assessment of bacterial kill in a circulating water test bed. The system was configured so that the water flowed through a series of hairpin loops during microwave exposure. Using this system, the waterborne bacteria could be effectively eradicated in 30 seconds.

This microwave-based technology could be used for different space applications including generation of purified water using an in-situ system in which circulating water is continuously subjected to microwave energy. The specific frequency of the microwave energy used allows the bacteria in circulating water to selectively absorb the energy, thereby killing the bacteria. Other applications include a modified version of this system, which could be used to eliminate bacteria accumulation in existing water cooling loops and heat exchangers. Since this system is portable, it could extend the life of existing water filters, prevent the growth of bacteria entering a water storage system at the inlet, and add a level of redundancy to currently existing purification systems.

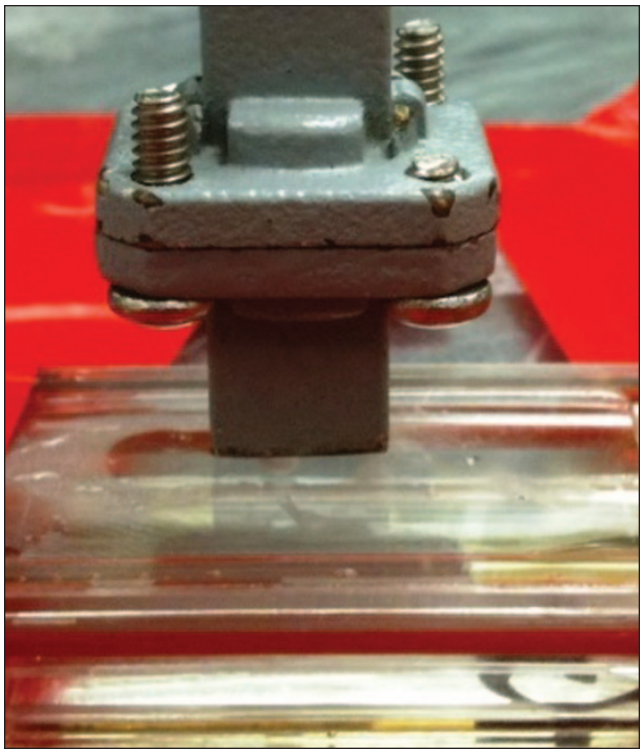


Fig. 1. *Radio frequency exposure of water borne bacteria and bacterial biofilms in test chamber.*

Once fully developed, this technology could be used for space exploration as well as commercial space flight including spacecraft, habitats, spacesuits, and rovers. It would also have a broad range of applications on Earth such as battlefield/field treatments for the military, isolated geographical areas, and hospital/research environments.

In-flight Water Quality Monitoring on the International Space Station: Measuring Biocide Concentrations with Colorimetric Solid Phase Extraction

Daniel B. Gazda,
Wyle Integrated Science and Engineering Group
Johanna Goforth, *Lockheed Martin*
Stephanie M. Flint, *Johnson Space Center*
Mickie Benoit,
Wyle Integrated Science and Engineering Group
Jeff A. Rutz,
Wyle Integrated Science and Engineering Group
Robert J. Lipert, *Iowa State University*
Lorraine M. Siperko, *University of Utah*
Marc D. Porter, *University of Utah*
John R. Schultz,
Wyle Integrated Science and Engineering Group
J. Torin McCoy, *Johnson Space Center*

Access to representative water quality data is critical to ensuring that a safe supply of potable water is available to the crew on the International Space Station (ISS). At the present time, the vast majority of the water quality data from the environmental control and life support systems on the ISS are obtained by analyzing archive water samples that are collected in flight and returned to the ground. There are several limitations inherent in this archival approach to water quality monitoring, most notably the time lapse between sample collection and ground analysis. Samples collected on orbit must be stored until they can be returned to the ground for analysis. Typical on-orbit storage times for water samples can range from 1 to 4 months, but in certain circumstances storage times can be much longer due to launch delays and limited return payload capacity. This time lapse between sampling and analysis precludes implementation of real-time adjustments or corrective actions when water does not meet specifications.

After the final space shuttle mission, there will be a sharp decrease in available return-payload mass. Inevitably, this will limit both the volume and total number of environmental samples that can be returned to the ground for analysis. At that point, it will no longer be feasible to rely on archive water samples for detailed water quality data. New hardware systems capable of monitoring multiple water quality parameters in flight on the ISS will need to be developed to ensure representative water quality data can be collected.

The unique operational environment on the ISS and the rigorous safety regulations applied to hardware deployed on the ISS dictate that any water quality monitoring system developed for use in flight possess several key characteristics. “Ideal” water quality monitoring systems must be small, lightweight, reliable, sensitive, provide direct real-time readout of results, minimize waste, contain no hazardous materials, meet strict storage and power guidelines, and function effectively in zero gravity. The ideal system would also be based on a platform technology that can be readily adapted to monitor multiple analytes with minimal hardware modifications. Finally, any system designed for use in flight must be rapid and easy to use so that the crew time required for training and operation on orbit is minimal. One technology that embodies many of the characteristics of the ideal water quality monitoring platform for the ISS, including the ability to add capability with minimal hardware modifications, is Colorimetric Solid Phase Extraction (CSPE).

CSPE is a sorption-spectrophotometric technique that combines colorimetric reagents, solid-phase extraction, and diffuse reflectance spectroscopy to quantify trace levels of target analytes in water samples. In CSPE, a syringe is used to meter a known volume of sample through an analysis cartridge that contains a membrane disk impregnated with an analyte-specific colorimetric reagent and any additives required to optimize the complexation of the reagent and analyte. As the sample is passed through the analysis cartridge, analytes are selectively extracted and complexed on the membrane. Formation of the analyte-reagent complex causes a detectable change in the color of the membrane disk that is proportional to the analyte concentration. The analyte is then quantified by measuring the color of the membrane disk surface using a handheld diffuse reflectance spectrophotometer. This entire process is illustrated in figure 1.

An experimental water quality monitoring kit—the Colorimetric Water Quality Monitoring Kit (CWQMK)—was designed and flown as a Station Development Test Objective (SDTO) experiment to evaluate the suitability of CSPE technology for routine use on the ISS. The experiment—SDTO #15012-U “Near Real-time Water Quality Monitoring Demonstration for ISS Biocides Using Colorimetric Solid Phase Extraction (CSPE)”—was launched on STS-128/17A and initially deployed on the ISS in September 2009. A photo of the CWQMK hardware and a photo from one of the initial in-flight analysis sessions are provided in figure 2. The primary purpose of

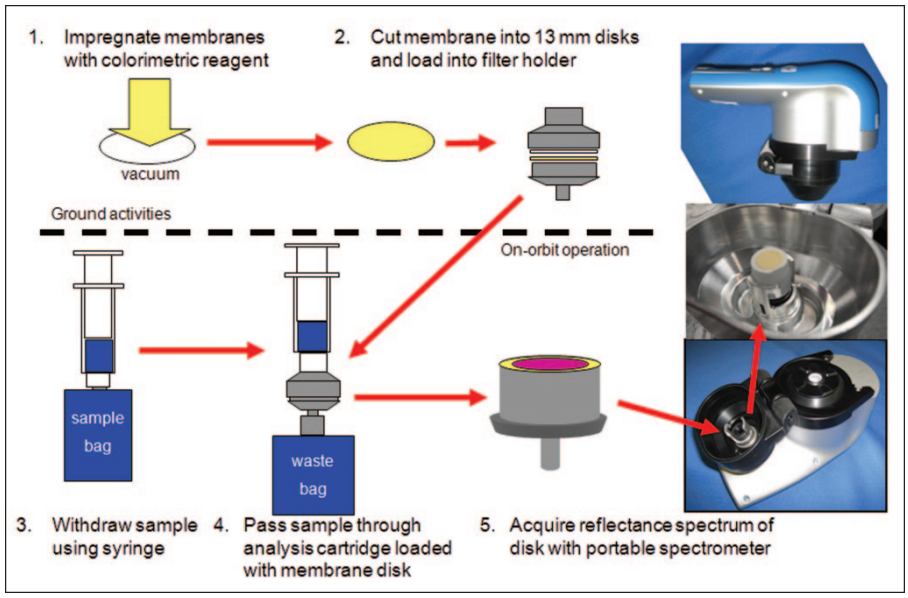


Fig. 1. *Overview of Colorimetric Solid Phase Extraction analysis.*



Fig. 2. *Colorimetric Water Quality Monitoring Kit packaged for launch (left), and International Space Station crew member conducting and in-flight analysis session (right).*

the SDTO experiment was to demonstrate the capability to collect in-flight water quality data on the ISS using CSPE technology. This was accomplished by measuring ionic silver and molecular iodine concentrations in ISS water samples on orbit with the CWQMK. Silver and iodine were selected as test analytes for the SDTO experiment because they are the biocides used in the potable water storage and distribution systems on the ISS.

Biocides are added to the potable water systems on spacecraft to inhibit microbial growth. On the U.S. segment of the ISS molecular iodine serves as the biocide, while the Russian space agency uses silver as a biocide in their systems. These biocides pose a unique challenge for water quality monitoring. For most environmental contaminants, the goal is to ensure the concentration of the contaminant does not exceed a threshold value. With biocide monitoring, the goal is twofold: the biocides must be maintained at a level sufficient to control bacterial growth, but low enough to avoid any negative effects on crew health. As such, ensuring that biocides are maintained at safe, effective levels was a perfect application to illustrate the need for in-flight water quality monitoring systems to ensure the health and safety of spaceflight crews.

In all, 13 in-flight analysis sessions were run with the CWQMK as part of the SDTO experiment. During each in-flight session, ground-supplied standard solutions and water samples collected from different points on the ISS were analyzed with the CWQMK hardware. Samples were collected from both the U.S. and Russian segments of the ISS, and were analyzed in triplicate to assess the reproducibility of the CSPE methods. Ground experiments were conducted in parallel with the in-flight analysis sessions to serve as a control for the in-flight analyses. The ground experiments were used to assess the stability of the standard solutions and analysis cartridges as well as check for any degradation in performance that may have occurred as a result of exposure to launch environments and storage conditions on the ISS.

Data collected with the CWQMK during the SDTO experiment are summarized in Table 1. Results obtained from ground analysis of archive samples collected at the same time as the sample analyzed with the kit are also included in the table. While some differences are apparent, most of these are due to an anomalous result from one of the replicate analyses. When these anomalous points are excluded from calculations, the mean results obtained in flight show excellent agreement with the results obtained using standard laboratory methods. In other instances, information contained in crew notes provides insight into difficulties encountered during the analysis sessions that could be responsible for the observed differences.

In-flight Water Quality Monitoring on the International Space Station: Measuring Biocide Concentrations with Colorimetric Solid Phase Extraction

continued

Table 1. *Results from Station Development Test Objective Experiment*

	Concentrations Measured by Session Number (mg/L)												
Solution	**1**	**2**	**3**	**4**	**5**	**6**	**7**	**8**	**9**	**10**	**11**	**12**	**13**
Silver standard	0.404	0.315	0.277	0.236	0.236	0.268	0.537	0.290	0.253	0.205	0.237	0.211	0.136
Sample from SVO-ZV[1]	<0.100	<0.100	<0.100	<0.100	0.397	0.100	0.225	<0.100	<0.100	<0.100	<0.100	<0.100	0.163
	-	<0.100	<0.100	<0.100	0.108	-	0.245	-	<0.100	<0.100	<0.100	<0.100	<0.100
	-	-	<0.100	<0.100	<0.100	-	0.250	-	<0.100	<0.100	<0.100	<0.100	<0.100
Archive from SVO-ZV	0.023	0.081	0.018	0.056	0.069	0.090	0.086	0.125	0.044	0.050	0.060	N/A	0.035
Iodine standard	2.79	1.95	1.33	1.49	0.32	1.04	1.32	0.90	1.00	0.94	0.36	N/A	N/A
Sample from PWD[2] dispensing needle	<0.20	<0.20	<0.20	-	-	-	<0.20	<0.20	-	<0.20	-	<0.20	<0.20
	-	<0.20	<0.20	-	-	-	1.44	-	-	<0.20	-	<0.20	<0.20
	-	<0.20	-	-	-	-	1.40	-	-	-	-	<0.20	<0.20
Archive from PWD dispensing needle	<0.050	<0.050	<0.050	-	-	-	<0.050	<0.050	-	<0.050	-	<0.050	<0.050
Sample from PWD aux. port	-	-	-	1.04	0.74	0.38	-	-	1.45	-	1.63	-	-
	-	-	-	0.63	0.33	-	-	-	0.74	-	1.69	-	-
	-	-	-	0.63	0.71	-	-	-	0.80	-	1.68	-	-
Archive from PWD aux. port	-	-	-	N/A	1.11	<0.050	-	-	N/A	-	2.05	-	-

N/A = not analyzed

[1] Russian system for dispensing ground supplied water

[2] Potable Water Dispenser

Based on the success of the SDTO experiment, the CWQMK was certified as operational hardware in April 2011. As part of the certification process, the kit was augmented to provide the capability to measure total iodine compounds (defined as the sum of the concentrations of molecular iodine, iodide, and triiodide). Addition of this capability required no hardware modifications; the only changes to the kit were the incorporation of total iodine reagent cartridges and a minor firmware update for the diffuse reflectance spectrophotometer that can be performed on orbit. With this added capability, the CWQMK provides a means to meet a previously unmet requirement to monitor biocidal iodine and total iodine compounds in water samples collected from the U.S. segment of the ISS.

Development of the CWQMK and the SDTO experiment were collaborative efforts that paired researchers from NASA Johnson Space Center with partners in academia and industry. Method development work is ongoing. The team is evaluating additional applications for CSPE technology in both spacecraft and terrestrial environments. Specific compounds under evaluation include nickel, acetone, acetate, ammonia, and ortho-phthalaldehyde.

Consolidation of Flight Food Provisioning for Human Space Flight

Kimberly Glaus Läte, *Lockheed Martin*

The Space Food Systems Laboratory (SFSL) is a multipurpose laboratory responsible for the production of food and related hardware for NASA space flight, as well as the research and development of space foods and space food packaging. Located on site at Johnson Space Center (JSC), this facility supports the production and development of flight food, menus, packaging, and food-related hardware for all NASA programs, including the Space Transportation System (STS) Space Shuttle Program and the International Space Station (ISS). The facility also houses the research team working on the Advanced Food Technology (AFT) Project, developing food systems for future missions beyond low-Earth orbit.

Prior to October 2010, flight food provisioning was managed by two separate organizations—the bulk of food production and stowage for STS was within the United Space Alliance Flight Crew Equipment (USA FCE) organization, while the SFSL managed both flight food provisioning for ISS and menu development for STS crews. USA FCE had multiple freeze dryers as well as the assembly equipment to manufacture septum adapter assemblies, which are critical components of all rehydratable food items and beverages. The SFSL produced most of the thermostabilized pouched food products through the Space Food Research Facility (SFRF), located on the campus of Texas A&M University. The SFRF was established through a partnership between NASA, Texas A&M University, and Wyle Integrated Sciences and Engineering Group to provide a facility dedicated to the production of foods for space flight and the advancement of food science education and research. Both USA FCE and SFSL contributed important components of the food systems for STS and ISS. With the termination of the Space Shuttle Program, the ISS Program Office had an opportunity to consolidate all food production for human space flight within one facility.

International Space Station Crew of Six

When the ISS food system took shape in the late 1990s, the SFSL was identified as the primary flight food provisioning facility. The ISS food system was developed to provide the ISS nominal crew of three with half its daily rations (the other half of the daily rations were to be provided by the Russian space program, by international agreement). The ISS food system was based on thermostabilized pouched food products, as opposed to the rehydratable food items that were the mainstay of the STS food system. STS crew member menus were designed to use primarily rehydratable food products, to take advantage of the plentiful supply of water available on the shuttle. As ISS was not designed to generate its own water supply, a food system using thermo-stabilized pouched foods that do not require the addition of water prior to consumption was planned. Over time, the two food systems blended as STS crew members requested more thermo-stabilized food products and additional rehydratable food items were provided to ISS crew members, thus increasing the variety of foods available to them. This led to an exchange of food items between the USA FCE shuttle food facility and the SFSL ISS facility, thus precluding each organization developing an additional production capability. The SFSL maintained a research focus and relied on USA FCE to produce the bulk of the freeze-dried food items and beverages for ISS. In 2008, the ISS Program Office directed the SFSL to plan for increased food provisioning to support an increase in the ISS crew size of three to six astronauts. This need to accommodate the increased production required both a significant change in SFSL operations and a paradigm shift for the SFSL team from a predominately research orientation to a production orientation.

The first hurdle the team encountered was reimagining the SFSL facility. How do you create a food production facility in an office environment? SFSL team members conducted a process improvement event that was designed to improve the flow of products and materials through the facility. The team evaluated the current work flow, created functional areas to collocate materials and equipment, and reorganized the placement of equipment and materials to best accommodate planned production. Making these changes enabled the team to successfully scale up production. In May 2010, the SFSL ISS Provisioning Team was recognized with a NASA Group Achievement Award for outstanding efforts in the initial provisioning of food to six ISS crew members.

Consolidation of Flight Food Provisioning for Human Space Flight

continued

Food Task Consolidation

By October 2009, the provisioning activities to support crew of six operations were well under way. When the decision was made to consolidate all food provisioning for human space flight within the SFSL, the SFSL Food Task Consolidation group evaluated the challenges. With the decommissioning of the USA FCE food facility, the SFSL would be required to make or procure all freeze-dried food items as well as beverages and ancillary hardware (septum adapter assemblies, straws, utensil kits). The SFSL would also be required to provide all additional STS support required for shuttle flights remaining after October 2010. While this was initially assessed to be one flight (STS-335—a "Launch on Need" rescue mission), as the launch schedule slipped, one flight turned into three after October 2010: STS-133, STS-134, and STS-135 (formerly STS-335).

The Food Task Consolidation group had to plan for the financial and staff resource challenges these opportunities presented, and to reevaluate the available facility space. What worked for provisioning a crew of six with food and hardware support from USA FCE would not work for provisioning all food and hardware required to support crew-of-six operations and the remaining shuttle flights. A facility specifically designed for food production was the ideal; however, a facility with the required floor drains, sealed floors, washable walls, and utility connections did not exist at JSC. It was thus determined to increase the size of the existing facility and modify it as needed to accommodate the NASA-owned equipment being transferred to the SFSL from the USA FCE food facility.

The Food Task Consolidation group in concert with the JSC Integrated Facility Planning Office eventually agreed to an additional 3100 ft^2 of an adjoining room for staff office space. The relocation of SFSL staff to the adjoining room made further facility modification possible (see figure 1).

One of the ideal conditions identified during the process improvement event was the creation of a "clean packaging environment." This is not a "clean room," which is not required for flight food packaging, but a packaging



Fig. 1. *Clean packaging "room within a room."*

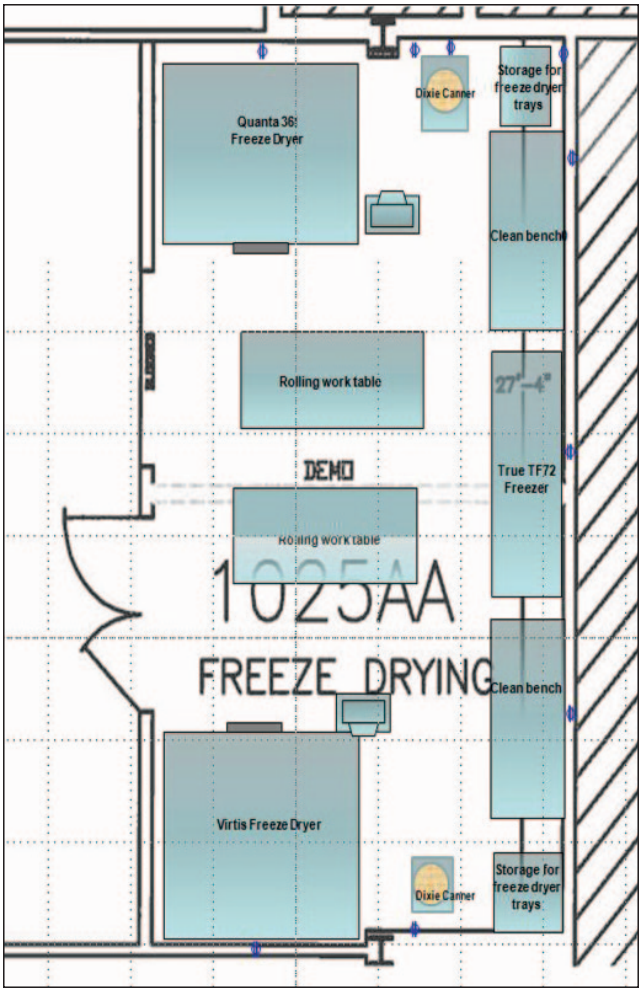


Fig. 2. *Equipment placement within freeze drying room.*

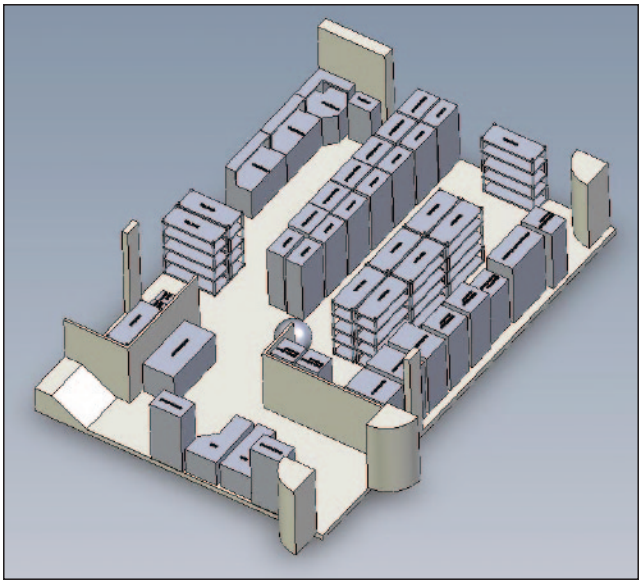


Fig. 3. *Three-dimensional layout of work room.*

environment with filtered air to ensure that packaged flight food continues to meet NASA microbiological standards for flight food. High-efficiency particulate air [HEPA] filters installed in the ceiling panels provide a positive pressure environment within the clean packaging environment. The additional space and arrangement of equipment supports multiple packaging activities occurring simultaneously in the room (see figure 2).

Prior to the food task consolidation activities, the SFSL maintained packaging equipment and one freeze dryer in two adjacent rooms. A second freeze dryer was required to continue to provide the variety of food items currently available to the crew. A dividing wall was removed and the packaging equipment was relocated to the clean packaging room, thus making space for both freeze dryers as well as for ancillary equipment.

To maintain the flight food inventory and Class I hardware required for ISS flight food provisioning, the SFSL controlled storage space was reconfigured to create separation between finished Class I hardware and Class I ingredients and hardware that was "in work." This required relocation of three environmental chambers and installation of utilities to support package integrity testing equipment. The current configuration allows flight hardware to be stowed in containers and prepared for transfer to shipping without leaving the controlled storage area (see figure 3).

The final facility modification involved creation of a "workroom"—i.e., a project work space as well as a materials storage and receiving area. The SFSL team worked together to create a room configuration that best supported all of the required uses of the space: housing for incubators and environmental chambers, and bench-top space for equipment maintenance and troubleshooting as well as for project and materials storage.

The facility modifications are complete and the facility was unveiled at JSC Innovation Day on May 4, 2011. The SFSL is currently working on reformulation of more than 80 flight food items to reduce sodium, in addition to provisioning all U.S. food for ISS and STS and conducting research for future exploration vehicles and missions. As space food systems evolve to meet changing requirements and missions, the SFSL facility is keeping pace.

Development and Implementation of the Bulk Overwrap Bag for Food Stowage on the International Space Station

Vickie L. Kloeris, *Johnson Space Center*

The Bulk Overwrap Bag (figure 1)—or BOB, as it is affectionately known in NASA Johnson Space Center's Space Food Systems Laboratory—was originally conceived as part of the Advanced Food Technology project. NASA's Constellation Program's Orion vehicle was oversubscribed on mass, so scientists had to develop a lighter-in-weight alternative to the metal food containers used on the Space Shuttle Program's Space Transportation System (STS) and on the International Space Station (ISS) for stowing food on Orion. Additionally, the container was required to be reconfigurable to fit irregularly sized stowage spaces. This requirement led to the idea of a flexible bag, which in turn led to the initial version of the BOB.

Background of Food Stowage

During the "three crew" operational period on the ISS, all food preparation and dining was done in the Russian Service Module (SM). The SM has a rehydration station for adding water to foods and beverages, as well as a dining table. In proximity to the dining table is a rack that is sized to hold the Russian food containers. In addition to fitting in the SM rack, the Progress resupply vehicle also has racks designed to accommodate these food containers. The United States reverse engineered a collapsible food container from the Russian design to ensure that the U.S.-built container would fit in the SM and Progress racks. This U.S. Collapsible Food Container (figure 2) was the principal method for stowing food to be launched to the ISS. These collapsible containers were returned via the shuttle, mostly on Multi-Purpose Logistics Module flights, and refurbished for reuse.

The ability to return and reuse containers would end with the Space Shuttle Program. The ISS Program had to make a decision regarding food containers. Should more of the collapsible food containers be built and burned up as trash after use, or should an alternative method for food stowage be found? The Space Food Systems Laboratory proposed implementation of the BOB concept for use on the ISS, and the ISS Program accepted that proposal.

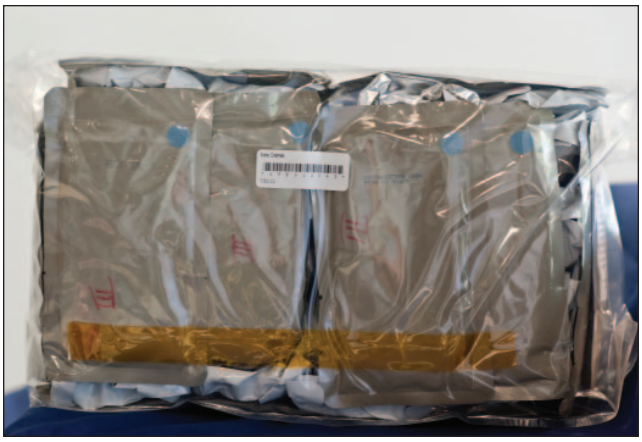


Fig. 1. *Bulk Overwrap Bag (BOB).*

Adaptation of the Bulk Overwrap Bag Concept

The BOB design had to be modified slightly for use on the ISS. The first modification was to size the BOB to hold the same amount of food as a collapsible food container. The usage rate of food on the ISS is carefully tracked. Having the quantity of food in a BOB equivalent to that of a collapsible food container would greatly facilitate that tracking process. In addition, NASA personnel developed a rigid framework to hold the empty BOB during packing to provide a template for the technicians packing food into the bags. This ensured consistent width and height of the packed BOBs. The labeling and bar coding system used on the collapsible food containers also had to be modified to work with the BOBs. Food lab personnel had to work with the ISS Stowage Team to determine a plan for stowing BOBs for launch to orbit. Finally, NASA developed an on-orbit operational scenario for the BOBs.

Implementation of Bulk Overwrap Bags

The first BOB of food arrived on the ISS with the docking of Japanese H-II Transfer Vehicle in January 2011. Since food on the ISS is used on a first-in, first-out basis, actual use of the packed BOBs of food will begin to occur



Fig. 2. *US Collapsible Food Container.*

gradually as the supply of standard menu food packed in collapsible containers is depleted. Feedback on the operational use of the BOBs will be forthcoming as ISS crew members who have used the BOBs on orbit return to Earth and participate in post-increment food debriefs. The average weight of a packed BOB of food is 5.0 kg (11 lbs) versus the 6.0 kg (13.2 lbs) average weight of a packed collapsible food container. This represents a significant savings in up mass for the ISS Program. For instance, the use of the BOB on STS-135/ULF7 (Utilization and Logistics Flight) resulted in approximately 240 kg (~529 lbs) of up mass savings on that flight alone. These up mass savings obviously allow for additional cargo to support other activities, such as science experiments, to be launched to the ISS.

Future of the Bulk Overwrap Bag

Space Food Systems Laboratory personnel view the BOB as a work in progress. Lab personnel will be listening to feedback from crew members for ideas on improving the BOB. Also, the team has some ideas in development for "continuous improvement" of the BOB concept.

Flight Crew Integration International Space Station Life Sciences Crew Comments Database: A Tool for International Space Station Post-mission Debrief Data

Susan Schuh, *MEI Technologies*
Krista Bagian, *Lockheed Martin*
Abbe Barr, *Lockheed Martin*
Laura Duvall, *Johnson Space Center*

At the completion of each International Space Station (ISS) expedition, the ISS Program office schedules a series of intensive debriefs with returning U.S. crew members and International Partner crew members (when available) to determine individual observations and concerns related to working and living on board the ISS. An estimated 20 to 25 post-mission debriefs are conducted after each expedition; these debriefs address topics related to specific disciplines and systems, including habitability and human factors, logistics and maintenance, payloads, stowage, food, procedures, etc.

The Flight Crew Integration Operational Habitability (FCI/OpsHab) team, within the NASA Johnson Space Center (JSC) Space and Life Sciences Directorate SF3 Habitability and Human Factors Division, participates in all public ISS post-mission debriefs. Team members collect, identify, and analyze data from each of the crew debriefs. Data collected during the debrief process are maintained within the FCI ISS Life Sciences Crew Comments Database in a secure and searchable SQL [structured query language] platform with a versatile SharePoint interface. The database provides advanced search capability across, and within, all ISS expeditions via an advanced "Google"-like search capability and SQL reporting capabilities. The database includes a comprehensive data set of post-mission debrief data from Expedition 1 to present (more than 38,000 crew comments). These comments are categorized and sub-categorized based on topics such as architecture, environment, habitability, human computer interaction, etc. All comments are de-identified to preserve crew privacy. As debrief data contain crew members' personal observations, opinions, and experiences, policies are in place to protect crew member privacy. These policies are established and agreed on by the FCI/OpsHab team, the NASA JSC Crew Office, and the NASA JSC Legal Office. Based on these agreements, the FCI/OpsHab team maintains strict data protection and handling policies to ensure that the data generated do not attribute comments to specific crew members and individual comments are not incorporated improperly.

Based on existing privacy and legal restrictions for crew comments data, the database can only be directly accessed by the FCI/OpsHab team; however, limited access to a controlled data SharePoint site can be granted to NASA civil servants and contractors. The SharePoint site allows these users to view existing data summary products generated from the database and also to request new data summaries tailored to their specific needs.

Gathering, trending, and analyzing the post-mission debrief data within the database allows the OpsHab team to generate products that document the trends and lessons learned observed over the life of the ISS. Advanced search functions give the team the ability to search across all comments for those related to a particular category, sub-category, keyword, mission, or debrief topic. Data summary products provide a broad perspective on topics regarding all aspects of habitability, systems, and operations on board ISS by assessing and integrating debrief data across all disciplines and expeditions. Data summaries are reviewed and approved by the crew office prior to distribution to requestors or posting to the database SharePoint site. Existing data summary topics include: habitable volume, waste and hygiene, labeling, robotics, procedures, planning, human computer interaction, extravehicular activity, hardware, and government-furnished equipment, Crew Health Care System, acoustics, training, tools, multipurpose logistics module, galley, food and dining, communications, architecture, restraints and mobility aids, water sampling, sleep stations, stowage, Soyuz, exercise, radiation, and European Space Agency operations and payloads. New data summaries are continually in development, and existing data summaries are often updated to include the most recent crew debrief data.

The FCI ISS Life Sciences Crew Comments Database provides the most complete and searchable archive of ISS crew debrief data known to exist. The data and related products provide a valuable resource for current and future space flight programs and also support design and development of vehicles, systems, hardware, requirements, standards, procedures, and processes. Debrief data content

is developed and relevant to each system, and allows system managers, hardware owners, and other interested parties a cumulative glimpse at feedback related to their systems. For example, data have been provided to support ongoing efforts with the ISS training group and the crew office to understand training lessons learned and make necessary improvements to both training protocol and the crew time necessary for training on the ground and on orbit. Data have also been applied to the design and development of the ISS crew quarters, waste and hygiene compartment, medical hardware, and flight software. This allows for the use of valuable debrief information to affect the development of requirements and standards and inform human-centered design.

It is imperative that we learn from past efforts of human space flight to improve future missions. As the most complete and searchable archive of ISS debrief data, the FCI ISS Life Sciences Crew Comments Database enables the FCI/OpsHab team to create products that support various project teams and ensure the crew member feedback and lessons learned are applied to future designs, training, operations, planning, operations nomenclature, stowage, habitability, etc. Maintaining a secure site and de-identifying comments adheres to crew member privacy and confidentiality agreements, while allowing the comprehensive products to be distributed to those teams and individuals with a need to know. The FCI ISS Life Sciences Crew Comments Database is designed to allow the FCI/OpsHab team to quickly and efficiently create useful products applicable to current ISS requirements, and to the development of future space programs.

Orion Crew Exploration Vehicle Internal and External Lighting Analyses

James C. Maida, *Johnson Space Center*
Charles Bowen, *Lockheed Martin*

Graphics Research and Analysis Facility (GRAF) and Lighting Evaluation and Test Facility (LETF) personnel used lighting and modeling expertise and tools to complete lighting analyses for both internal and external aspects of the Orion Crew Exploration Vehicle (CEV). GRAF and LETF personnel provide an integrated approach, working closely with the end customer to understand operations and constraints, and to deliver a meaningful result.

Internal CEV analyses included assessment of the egress ladder, side hatch latch, emergency locker and displays, and control console. Actual beam axial intensity data were collected from prototype CEV light-emitting diode (LED) lights. GRAF and LETF personnel were able to begin developing accurate models using the latest Pro-E model of the interior configuration of the lights and the interior configuration. In an effort to better refine the models, these workers engaged in discussions with CEV operations personnel to sufficiently understand planned operations to consider any constraints on placement and motion of the human during operations. Based on these discussions, two scenarios were run—one with nominal power configuration and one with auxiliary power settings to cover the worst-case scenario. Researchers used a 99-percentile male model for this exercise since this is the worst case for blocking and shadowing available light. Assumptions were made about surface material and color that impact reflectance and glare based on current design.

Visualizations and data were provided using Radiance software to determine actual light levels within the interior volume based on the assumptions above. A realistic picture of expected light levels (figure 1) and color-coded scaled visualizations (figure 2) were provided to illustrate the actual light-levels for each scenario. Radiance provided the predicted light levels that could then be compared against requirements and aid in design iterations.

Personnel completed an external lighting analysis to look at post-landing recovery strobe lights. A creative solution was found to establish the likelihood that the lights will be visible from all directions at a useful distance. Unlike the case in space, NASA has not established a clear-cut eye illumination threshold for operations at sea. It is expected that shadowing of the strobe lights by the structure of the spacecraft and strobe light reflections from the spacecraft surfaces will result in a complex pattern of illumination at a distance surrounding it. The analysis provides a representation of the illumination pattern and scalable values that may be compared to any desired detection threshold.

The method used for the strobe analysis involves the use of the Radiance ray-tracing program in association with other software to model the strobe lights and the reflective surfaces of the Orion spacecraft. The model also includes a hypothetical, nonreflective, black projection surface on which the illumination from the strobe lights falls. This is a spherical surface centered on and surrounding the



Fig. 1. *Realistic image of light model.*



Fig. 2. *Color-coded scaled visualization.*

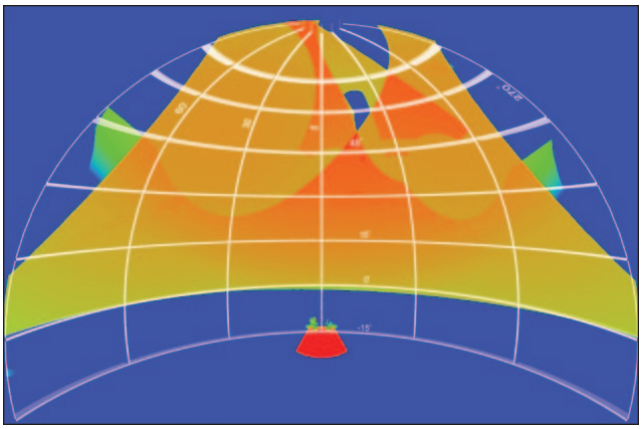


Fig. 3. *Contour maps of strobe lights reflected on projected dome.*

spacecraft at a certain radial distance. This distance is great enough, compared to the spacecraft dimensions, to allow the light from each strobe to be considered as if the light is emanating from a single (common) point. This assumption allows the effective beam intensity directed from the point source to a point on the interior surface of the sphere to be calculated from the illuminance at the point and the square of the sphere's radius. The sphere's radius was chosen such that the intensity (candela) directed toward any direction is equal to 1000 times the illuminance (lux, candela/meter^2) predicted at that point. Contour maps projected on the spherical surface reveal the patterns of intensity in all directions around the spacecraft (figure 3). These maps are presented as two views "looking" in opposite directions. The spherical surface is slightly larger than a hemisphere to allow for an anticipated list in the floating spacecraft.

The intensity for each of the strobe lights was again modeled as based on actual beam patterns. The beam axis was taken as the normal vector passing from/through the center of the LED array. The beam pattern was assumed to be symmetrical about the beam axis.

Command Module Uprighting System (CMUS) bags are anticipated to be a significant factor in determining the strobe light projection pattern. Analysis results illustrated the shadowing and reflection of the strobe light beams by the bags. Since the reflective properties of the bags are not yet defined, a "bracketing" approach was taken to bound their effect on the beam patterns. The maximally reflective case was modeled using hypothetical 100% reflective white, diffuse (Lambertian) bag material. The minimally reflective case was modeled using hypothetical, totally absorbing black diffuse bag material. Illuminance simulations for each case were presented for comparison.

The creative approach of using a dome to "shine" the light on proved to be a valuable demonstration of the current design. The beam intensities derived from the spherical projection represent the peak values produced by the strobes as steady-state levels. Since the strobe light flash patterns are synchronized, separate projections for each of the four lights are not necessary. Composite patterns for the baseline three strobes and for these in combination with a notional fourth strobe are included.

Light from the strobes is attenuated from two causes: scattering from dust, salt, and water particles; and absorption of light by gasses and water vapor in the atmosphere. In the visible range of wavelengths, these losses are each equal to about 50%, resulting in a total attenuation of at least 75%. The illuminance values in the spherical projections do not include atmospheric attenuation.

Results of the analyses showed that the intensity of the light reflected on the CMUS bags is insignnificant in comparison to direct-path strobe light. The strobe lights are much more visible from the 0-degree side than the 180-degree side, mainly due to shadowing by the CMUS bags. Intensity values given should be derated by 75% to allow for atmospheric scattering and absorption. The GRAF/LETF was also able to provide some alternative strobe light positions that will improve the results and visibility of the vehicle for recovery.

Orion Interior Acoustic Environment Modeling with a Mock-up

S. R. Chu, *Lockheed Martin*
C. S. Allen, *Johnson Space Center*

Acoustic modeling can be used to identify key noise sources, determine/analyze suballocated requirements, keep track of the accumulation of minor noise sources, and predict vehicle noise levels at various stages in vehicle development, first with estimates of noise source levels, and later with experimental data.

The Johnson Space Center (JSC) Acoustics Office constructed an Orion crew module acoustic mock-up (figure 1) and associated acoustic model (figure 2) with incrementally increased fidelity, and validated the accuracy of the model in predicting the mock-up interior sound pressure level under various noise sources and vehicle configurations. Confidence in modeling techniques has been gained through extensive model validation.

The initial configuration of the crew module acoustic mock-up contained only a 12-faced enclosure of two-layered medium-density fiberboard wall. This dense wall material was used for trapping sound inside the mock-up to simulate on-orbit operation. The volume of the mock-up interior matches the Orion pressure vessel, with the surface area of the mock-up also very close to that of the vessel's.

A reverberation time T60 measurement using a dodecahedron speaker was performed to characterize the acoustic absorption of the mock-up interior. A model of this bare mock-up was constructed. The predictions of the model under the excitation of single and two reference sound sources were compared to sound pressure level measurements inside the mock-up. Excellent agreement was found. Furthermore, patches of sound absorptive Thinsulate™ material were attached to interior surface of the mock-up. The model was used to predict the area of these patches for reaching targeted absorption level, and was verified by T60 measurement. Scientists performed Modified Rhyme Tests with various simulated noise environments inside the mock-up to develop a new requirement for Orion post-landing speech interference limit.

As an alternative method of modeling the absorption of the mock-up interior, scientists performed impedance tube testing of sound absorptive materials. They identified several acoustic material properties by curve fitting the measured absorption. The identified properties were then used to construct a single- or multi-layered noise control treatment lay-up model. The lay-up models were placed inside the mock-up system model to account for the absorption contribution of noise control treatments. The JSC Acoustics Office uses an impedance tube for acoustic absorption and transmission loss measurements. The tube can be configured with two or four microphones, and is used for absorption or transmission loss measurements, respectively.



Fig. 1. *Orion crew module acoustic mock-up exterior, wall made of two medium-density fiberboard sheets, 1 in. total thickness.*

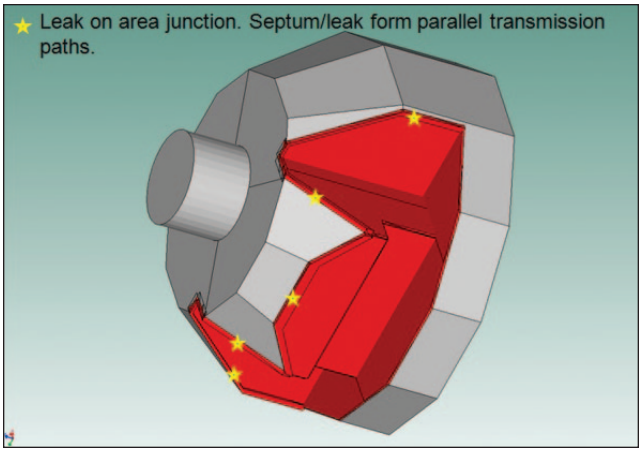


Fig. 2. *Orion crew module acoustic mock-up model with leaky gap sealing.*



Fig. 3. *Reverberation time measurement of Orion crew module acoustic mock-up with bare Environmental Control and Life Support System wall and open gap.*

The fidelity of the bare mock-up and corresponding model were then increased by including simple ventilation systems. The airborne sound powers of ventilation fans were measured by sound intensity mapping, since the sound power levels were not known beforehand. This was opposed to earlier studies where reference sound sources with known sound power levels were used. Comparisons of model predictions with measurements in the mock-up showed good agreement.

The fidelity of the mock-up and the model were further increased by including an Environmental Control and Life Support System (ECLSS) wall, and associated closeout panels with a gap between the ECLSS wall and the mock-up wall. The effect of sealing the gap and adding sound absorptive treatment to the ECLSS wall were also modeled



Fig. 4. *Orion crew module acoustic mock-up with sealed gap and Thinsulate™ covering the cabin side of the Environmental Control and Life Support System wall.*

and validated under the following configurations: bare mock-up and bare ECLSS wall with open gap; bare mock-up and bare ECLSS wall with sealed gap; bare mock-up and ECLSS wall with sealed gap and one layer of Thinsulate™ completely covering the cabin side of the ECLSS wall; and bare mock-up and ECLSS wall with sealed gap, and one layer of Thinsulate™ covering part of the ECLSS wall on the cabin side and the remaining ECLSS wall on the ECLSS bay side (figures 3 and 4). Both measured and predicted sound pressure levels show that deploying part of available Thinsulate™ treatments inside the ECLSS bay is more effective in the sound pressure level in the cabin than deploying all the treatment in the cabin.

Aluminum sheets/tapes were attached to the interior surfaces of the mock-up wall recently for increasing the interior reverberation time to a more realistic level because the medium-density fiberboard wall is more absorptive compared to a typical metallic surface of a spacecraft. Validation of the bare mock-up model showed excellent agreement between model predictions and measurements. The mock-up model with ECLSS wall, Thinsulate™ treatments, and open/sealed gaps will be validated soon.

The fidelity of the mock-up will be further increased in the near future by including a secondary structure, storage lockers, and snorkel fan.

Design and Evaluation of Displays for the Crew Exploration Vehicle

Neta Ezer, *Futron Corporation*
Kara Pohlkamp, *Johnson Space Center*
Stephen Gauvain, *United Space Alliance*
Lee Morin, *Johnson Space Center*
Neil Woodbury, *Johnson Space Center*
Anna Fisher, *Johnson Space Center*
Patrick Laport, *Aerospace Applications North America*
Tim Verborgh, *Aerospace Applications North America*
Patrick Henry,
Science Applications International Corporation

Crew members aboard NASA's Orion Crew Exploration Vehicle (CEV) are envisioned to monitor and command the vehicle primarily through graphical computer displays and electronic procedures. Not only will this make for a lighter vehicle, but this paperless "glass cockpit" concept can make crew tasks more efficient by collocating vehicle information and controls. If this paperless glass cockpit is properly designed, crew members can obtain insight into vehicle states, use electronic procedures to complete tasks effectively, and respond to off-nominal situations quickly. If it is not properly designed, however, the displays could lead to design-induced human errors, such as sending incorrect commands, high crew workload, poor situational awareness, and extensive need for training. Thus, display standards and an iterative design and evaluation process have been employed as ways to optimize display design.

Background on Displays and Electronic Procedures

The CEV commander and flight engineer will be able to monitor system states across subsystems, send vehicle commands, interact with electronic procedures, and, if needed, manually fly the vehicle from three display units. More than 50 displays have been designed for use throughout all phases of flight, including during prelaunch and post-landing activities.

Crew members have the ability to perform all display tasks manually or with electronic procedures. During manual operation, crew members can navigate to a display and use a cursor control device, cursor knob, or edge keys to traverse through and select commandable elements. Commands are sent through pop-ups. The electronic procedure system, referred to as eProc, is designed as a powerful alternative to reduce crew workload. eProc assists crew members by highlighting vehicle states on a display and cueing up appropriate displays, pop-ups, and commands. eProc is also linked to fault messages, such that crew members can quickly access procedures to any message that appears on the fault summary or log displays. Thus, eProc is a critical component of crew interaction with other displays and with the caution-and-warning system. The focus of the display development work is to ensure that crew members have accurate and easy interactions with the display, both manually and with eProc (see figure 1).

Iterative Display Design Process

A human-centered, iterative design process is used to increase efficiency, effectiveness, and satisfaction of crew members interacting with displays. The process—which is led by a small interdisciplinary team composed of members of the Mission Operations Directorate, Human Engineering, and the Crew Office, which includes the Rapid Prototyping Lab (RPL)—begins by taking early concepts developed by flight and system experts in PowerPoint and reworking them based on the needs of the task to be performed, compliance with Human System Integration Requirements (CxP 70024, Rev D.) and Orion Program Display Format Standards (CxP 72242, Rev. A). Display standards, which are used to define all common display elements (e.g., symbology, text, modes of interaction, and colors), ensure consistency in look and feel across displays and allow crew members to use their experience and knowledge about interaction with one display to facilitate their interaction with other displays. Display standards have also reduced prototype development and software coding time by creating modular and reusable display components. This translates to cost savings for both the vehicle and flight software.

Once the team is satisfied with the PowerPoint concept, RPL programmers develop an interactive prototype that can be evaluated by crew members in a human-in-the-loop evaluation. In preparation for the evaluation, the team works with the subject matter experts of each system to develop a series of representative nominal and off-nominal scenarios and procedures that allows participants to get a feel for how interaction with the display will occur.

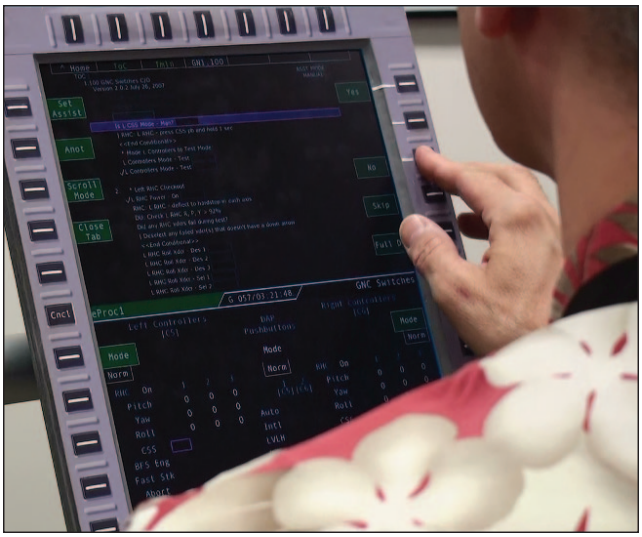


Fig. 1. *Human-in-the-loop evaluation participant interacts with eProc and system display.*

Tasks are selected that exercise frequent, critical, and unique display interactions. State files are created to model vehicle telemetry within the prototypes; these are based on commands that are sent or failures built into the scenarios. Flight displays are driven by a combination of the Advanced NASA Technology Architecture for Exploration Studies [ANTARES] simulation software and state files.

Interactive prototypes and procedures are reviewed frequently by the team and updated based on emerging issues. The team has found that design elements that seemed like good ideas in PowerPoint sometimes become glaring issues when they are viewed on the display hardware and interacted with. Additionally, the translation of paper procedures into eProc has revealed that writing electronic procedures is not as simple as placing a paper procedure into an electronic format. Electronic procedures need to be written in a unique way so that they work seamlessly with corresponding displays, are integrated within the eProc architecture, and are understandable by the user. Thus, frequent review and iteration of display designs and procedures prior to crew evaluations has proved to be an essential part of the process.

Once the team is satisfied with prototypes and procedures, Human Engineering leads the human-in-the loop evaluations of the displays with crew members and representatives. Each evaluation includes five to nine participants with a range of experience from the space shuttle, International Space Station, and Russian Soyuz capsule. They include both "experts," those individuals who are familiar with the displays, and "novices," those individuals who are seeing these displays for the first time.

Participants are provided with an overview of the displays and modes of interaction during the evaluation. They are then asked a set of questions to gauge their initial impressions of the displays as well as to prime them for thinking about layout, terminology, and other aspects of the displays. Next, these participants go through a series of procedures and simulated mission control callouts that allows them to interact with display components. During this interaction, all participant comments and any observations about behavior (e.g., errors and observed frustration or points of confusion) are captured. Interview questions and questionnaires provide additional information about whether participants are interpreting display elements correctly and are satisfied with the design of the displays. After the evaluation, the results are analyzed, and issues and recommendations for design changes are presented and reviewed by the team and system experts.

By capturing crew member inputs through this iterative design process, design issues are identified before any flight software is written. Display and cockpit operability improvements are of minimal cost at this stage of design. So far, 31 display formats have gone through at least one of the 14 total human-in-the-loop evaluations that have taken place. Through these early prototype evaluations, more than 100 usability issues, including potential critical errors, have been identified and resolved via redesign. As an example, in the propulsion display evaluation it was revealed that the indication of auxiliary (+X) jets firing after a main engine failure was not visually salient enough—*none* of the participants noticed the jets firing.

Design and Evaluation of Displays for the Crew Exploration Vehicle

continued



Fig. 2. *During an evaluation, Human Engineering records crewmembers' comments and observations. Automated data analysis software runs in the background to capture design-induced errors. The results of the evaluation are used to improve the design of the displays.*

Based on this finding, the jet icons were altered to fill in with a bright white when firing and were changed to an unfilled gray outline when unavailable. As an additional benefit, the evaluations have identified design simplifications to make crew members' tasks easier and reduce flight software costs (see figure 2).

Summary

The structured nature of the design and evaluation process has allowed CEV displays to go from paper prototypes to interactive prototypes that are evaluated and improved on in a matter of a few weeks—a very cost-effective method with significant benefits. Continuing and future work will include more integrated, phase-based evaluations, continued refinement of display designs, validation of display standards, and integration of the display suites with the vehicle flight software. Although the displays designed and evaluated thus far are specific to Orion, they could be generically applied to any vehicle. Other spacecraft will have electrical power systems, life support systems, propulsion systems, etc. Features of the design of Orion displays, the design process, lessons learned, eProc standards, and display standards could be applied to any future space vehicle that has a paperless, glass cockpit design.

Development of a Lunar Dust Reactivity Sensor

William T. Wallace,
Wyle Integrated Science and Engineering

Antony S. Jeevarajan, *Johnson Space Center*
Sridhar Madala, *Indus Instruments*

During the Apollo missions, NASA discovered that the pervasive lunar dust caused a multitude of problems for the astronauts. The dust obscured vision, coated and abraded surfaces, clogged equipment, and caused false instrument readings. As various space agencies make plans to return to the moon, one of the biggest concerns might be that of lunar dust inhalation by the astronauts upon entering a lunar habitat or landing vehicle. Astronauts described lunar dust as having a "gunpowder-like smell," and at least one astronaut complained of "lunar dust hay fever" after inadvertently inhaling some dust.

On the harsh surface of the moon, lunar soil is constantly being formed and modified by micrometeorite (< 1 millimeter [mm]) bombardment and interactions with solar-wind particles. This creates particulates with highly fractured surfaces that contain a high number of free radicals able to react with those things with which it comes into contact, such as the human respiratory system. If this occurs, reactive oxygen species, such as hydroxyl radical, superoxide, and hydrogen peroxide, may be produced. These reactive oxygen species could cause damage to cells, as seen with the effects of freshly fractured quartz.

NASA Johnson Space Center (JSC) previously developed a technique for testing the reactivity of lunar dust in solution. This method takes advantage of a change of fluorescence emission of the terephthalate anion when it is hydroxylated in solution. The fluorescence increase seen with increasing hydroxyl radical concentration is linear, allowing us to make direct comparisons of reactivity between different concentrations of an individual dust or the same concentration of different dusts. Using this procedure, the JSC team tested the reactivity of ground lunar soil and compared it to ground lunar dust simulant, ground quartz, and unground lunar dust (figure 1). The team determined that ground lunar dust was approximately three to four times more active for hydroxyl radical generation than ground lunar simulant and approximately eight times more active than ground quartz. Grinding of the lunar dust resulted in an increased reactivity of approximately 10 times as compared to unground lunar dust. Further testing showed that the increased reactivity was due to the presence of iron nanoparticles residing in the amorphous surface rims of the lunar dust.

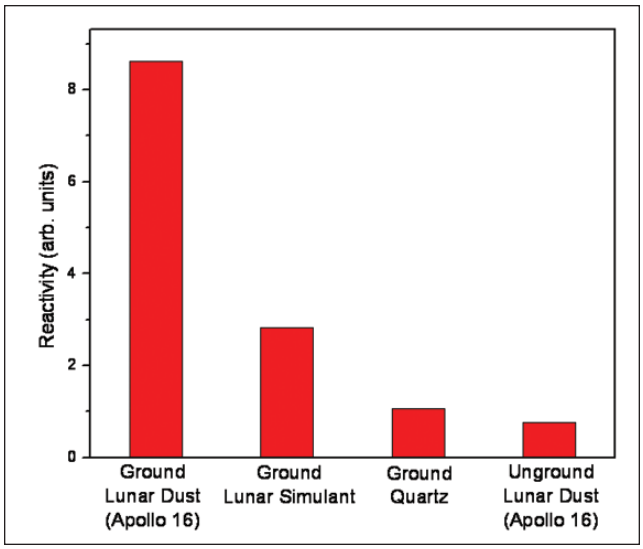


Fig. 1. *Relative changes in the production of hydroxyl radicals in aqueous solution by different dusts.*

This project was aimed at the development of a novel sensor for the determination of lunar dust reactivity in a matrix of humidified air or aqueous solution. Understanding the reactivity of lunar dust will aid in the development of mitigation techniques for lunar dust inhalation. The sensor described here was initially based on a previous NASA-designed sensor to monitor dissolved oxygen levels in solution. That system used a light-emitting diode (LED) to excite a fluorescent dye, and then measured the fluorescent emission. The presence of oxygen would quench the fluorescence, providing a sensitive monitor of the oxygen concentration. The plans for the present sensor are aimed to develop a similar platform, using JSC's novel fluorescence technique for determining the reactivity of lunar dust.

Initial work focused on the development of a sturdy optical system, capable of efficiently collecting photons emitted from the test solution while minimizing interference from stray light. The optical setup used for the current

Development of a Lunar Dust Reactivity Sensor

continued

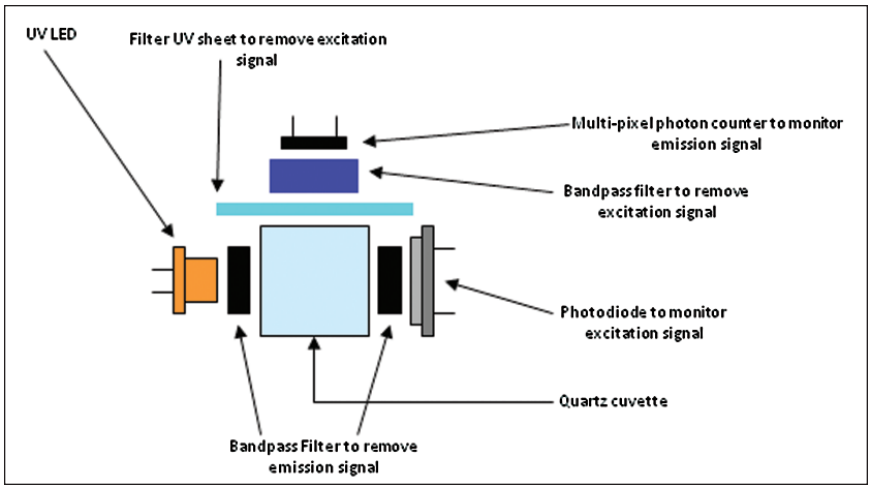


Fig. 2. *Optical schematic of lunar dust reactivity sensor.*

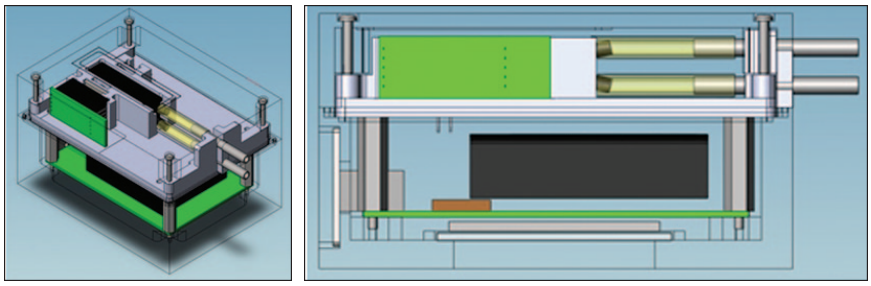


Fig. 3. *Design of the completed lunar dust reactivity sensor.*

sensor (figure 2) consists of a quartz cuvette filled with the solution to be tested, a 320 nanometer (nm) ultraviolet (UV) LED excitation source, and photodiodes to collect (individually) both excitation and emission photons. The emission is collected at a right angle to reduce the amount of excitation light reaching the emission photodiode. The emission detector is also protected by band-pass filters, which only transmit certain wavelengths of light. The power consumption of the UV LED used for testing was on the order of 100 milliwatts. This is in contrast to larger (and more powerful) UV lamps typically used for fluorescence measurements that require several watts of power. It is this low power consumption and small size that makes it possible to produce this compact sensor. The use of multiple photodiodes in the platform serves two functions. First, the emission signal can be normalized against the excitation signal to account for changes in the source output. Second, the excitation signal can be monitored to check the health of the UV LED.

The mechanical design of the sensor (figure 3) consists of three pieces: a base containing the optics assembly (cuvette, UV LED, optical filters, photodiodes); a bottom case containing electronics (shown in green), a battery compartment (shown in black) containing 3 AA batteries and a liquid crystal display panel; and a top cover that encloses the optics to provide a light sealed chamber. Removing stray light is important, as any additional photons could raise the background fluorescence. Tubes attached to the cuvette on one side protrude through the lid to permit flow through of the test fluid.

The JSC team performed a test of the capabilities of the sensor with ground lunar dust simulant and ground quartz at different concentrations, as well as background fluorescence measurements with an empty cuvette and one filled with water. The data shown in figure 4 were collected using an acquisition time of 100 seconds. As shown in the figure, the addition of water to the cuvette slightly increases the background signal. When either quartz or lunar dust simulant mixtures are introduced into the cuvette (the mixtures are filtered prior to entering the sensor), higher emission intensities are found, and the signals continue to increase with increasing dust concentration.

The dust concentrations used for the tests shown in figure 1 were 4 milligrams/milliliter (mg/mL), the lowest concentration used in the sensor testing. For the lunar dust simulant, this concentration produced an output signal

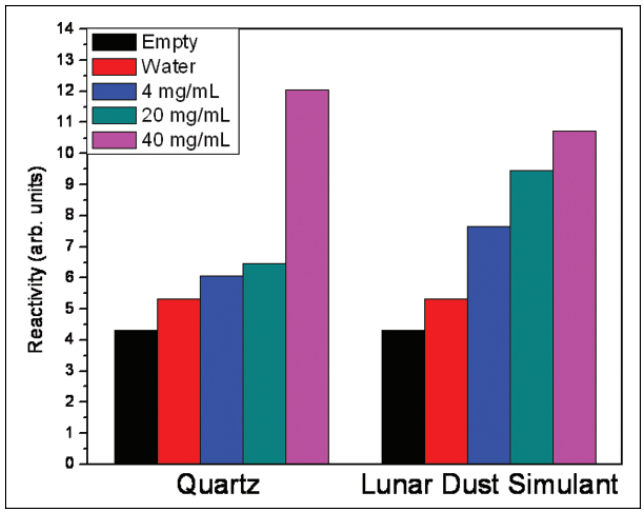


Fig. 4. *Reactivity of quartz and lunar dust simulant measured by the lunar dust reactivity sensor.*

approximately 40% higher than the water background, while the quartz produced an approximately 10% higher signal than water. The relative reactivities of these two dusts, as measured by the sensor, are similar to those measured with a standard laboratory fluorimeter. Because the fluorescence intensity produced by the quartz mixture at this concentration is so close to that of the background, the operational limit of detection would be greater than 4 mg/mL. However, if a more reactive lunar dust were tested, the platform should be capable of producing usable signal levels at this concentration.

In summary, the JSC team developed and tested a sensor platform capable of monitoring the reactivity of dust on the lunar surface during future human habitation. This sensor uses the change in fluorescence of a probe compound upon hydroxylation to determine the amount of hydroxyl radicals produced by lunar dust. While the sensor was developed for lunar dust testing, its small volume and mass would make it useful for terrestrial applications as well, such as in mining operations.

Human Exploration Systems, Technologies for Extravehicular Activity and Harsh Environments



Extravehicular Activity Technology Development—Suit Technologies

Amy Ross, *Johnson Space Center*
Lindsay Aitchison, *Johnson Space Center*
Kate Mitchell, *Johnson Space Center*
Richard Rhodes, *Johnson Space Center*

The Space Suit Assembly Group performs the functions of providing a habitable environment in hazardous conditions to enable a crew member to perform meaningful work outside of a vehicle. The Extravehicular Activity (EVA) Technology Development Team, which is within the Crew and Thermal Systems Division at NASA Johnson Space Center (JSC), is developing critical technologies and suits to enable future exploration missions.

Gloves

Gloves are the primary means by which a crew member performs EVA tasks, and thus are an area in need of continual improvement and development. Recent activities have focused on increasing the operational life of gloves and improving glove mobility. A joint cycle model, created through collaboration with the Anthropometrics and Biomechanics Facility at JSC, was generated. The model simulated a long-duration lunar mission. The team performed life tests, which used this cycle model and a busy board to simulate EVA tasks, employing Phase VI gloves to benchmark life performance of these state-of-the-art gloves (figure 1). Tasks included activities such as using a joystick, brushing the suit (to remove dust), and picking up samples from the ground. A lunar regolith simulant was deposited between the glove bladder and the thermal micrometeoroid garment to provide a more representative testing environment in an effort to provide similar abrasion to the abrasion that would be seen during a lunar mission. Areas of high wear were identified and analyzed using a digital microscope.

Suit Port Compatibility

The concept of using a suit port for rapid vehicle ingress and egress impacts the development of a spacesuit in several ways. The team undertook a number of development tasks to assess these impacts and overcome the technical challenges associated with them. First, suit port operations dictate that an exploration spacesuit be donned and doffed through a rear-entry hatch with a suit port interface plate—i.e., the surface that makes a pressure seal with the vehicle and is clamped by the mechanisms within the suit port. A rear-entry upper torso with a suit port interface plate is under development and will be completed in 2011. Donning a suit via a suitport also means that the crew member will be entering a suit that is already pressurized. This provides additional challenges associated with making sizing adjustments to the suit because all adjustments would be made in opposition to the suit pressure. NASA developed proof-of-concept designs for gloves and boots in which sizing adjustments could be made while the suit was pressurized.



Fig. 1. *Phase VI glove life testing.*

Extravehicular Activity Technology Development—Suit Technologies

continued

Bio-contamination-resistant Materials

Bacterial and fungal growth during long-duration missions is a concern for future exploration missions. Crew members sweat when performing an EVA, and the crew-worn suits must subsequently be stored for periods of time that could range from days to months. A team from NASA performed a trade study of commercially available materials that could reduce resulting biological activity. The team selected, purchased, and evaluated several materials. In addition to these new materials, materials and material layups from the space shuttle extravehicular mobility unit and the Advanced Crew Escape System were also included in the test as a benchmark. The test matrix included samples that were inoculated with specific bacteria or fungi commonly found in spacesuit applications (figure 2).

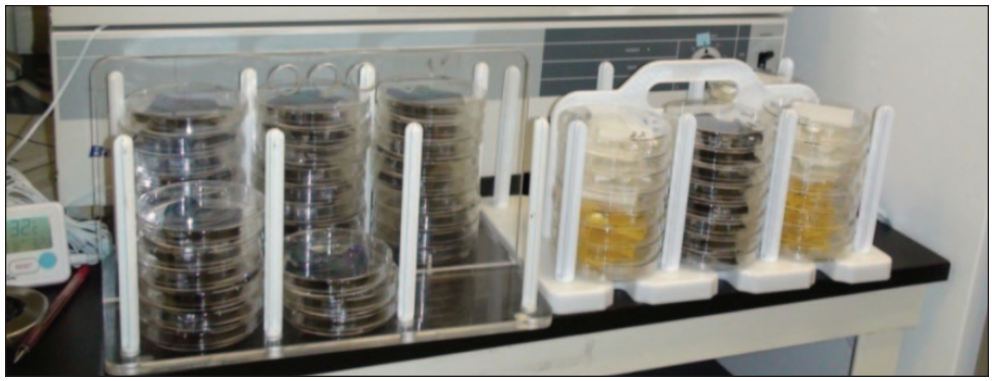


Fig. 2. *Biological testing of spacesuit materials.*

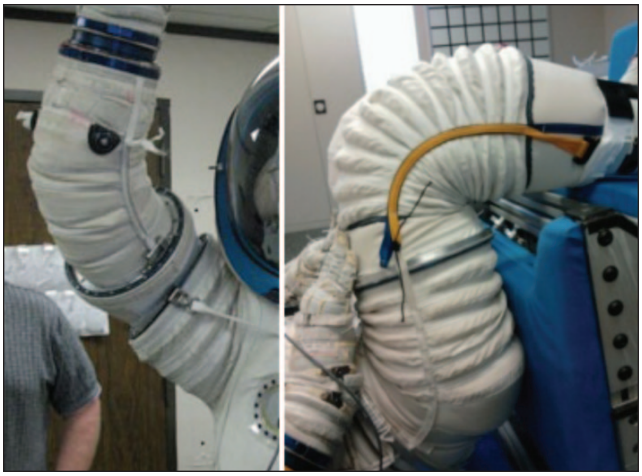


Fig. 3. *Zipper entry I-suit shoulder and hip.*

Soft Mobility Elements for Launch Entry Abort Suits

Spacesuits are needed to protect crew members from hazardous conditions that could occur within the cabin of a vehicle during specific mission phases. Crew members are at risk from mission scenarios that could include cabin depressurization or the release of toxic chemicals. Therefore, crew members primarily wear suits to provide protection from these conditions during mission phases with large accelerations such as launch, atmospheric reentry, or mission abort. These large accelerations increase the likelihood of injury to the crew member due to the potential of coming into contact with hard elements within the suit-like bearings. A zipper entry I-suit was modified with two different soft shoulder designs and a soft hip (figure 3) to minimize this injury risk. The team tested these new joints to demonstrate acceptable pressurized mobility for a launch-entry-abort-type mission.

Extravehicular Activity Technology Development—Suit Port Technologies

Rob Boyle, *Johnson Space Center*
Barbara Romig, *Johnson Space Center*
Charles Allton, *Johnson Space Center*
Peggy Guirgis, *Johnson Space Center*
Mike Gernhardt, *Johnson Space Center*

The multi-mission space exploration vehicle and extravehicular activity (EVA) development teams have jointly developed suit port technology in support of EVAs. A suit port enables rapid vehicle egress and ingress for future space exploration vehicles. It currently takes approximately 2.5 hours of preparation time to perform an EVA from the International Space Station. A further 0.5 hour is needed to depressurize the airlock, and another 1 hour (post-EVA completion) is invested in the total before the crew member finishes with his or her EVA-related duties. The goal of the suit port is to limit the amount of crew time to fewer than 30 minutes prior to the EVA and after the EVA. Several demonstrations have been performed to mature this technology.



Fig. 1. *Desert Research and Technology Studies field testing.*

Operational Assessments

The operational scenarios associated with a suit port have been assessed with the multi-mission space exploration vehicle as part of the Desert Research and Technology Studies mission analog. These evaluations have focused on demonstrating timelines and human factors associated with integrating the suit port into the multi-mission space exploration vehicle cabin and aft bulkhead. The evaluations have been used to mature and evaluate the suit port sealing and latching designs. An example of relevant Desert Research and Technology Studies field testing is shown in figure 1.

Alignment Guide Assessments

Once the basic operational scenario and suit port technology were demonstrated, additional detailed evaluations of a suit port alignment guide were performed. Multiple concepts for aligning the Portable Life Support System into the suit port hatch were developed and tested in a laboratory setting. Alignment is important and challenging because the EVA crew member is backing up into the suit port and has limited visibilty. If the Portable Life Support System and suit port interface plate do not line up properly, the latches and seal cannot be made, which would prevent the crew member from being able to return to the vehicle. Following testing (figure 2), a simplified, low-profile concept was selected out of this study and is being used in future evaluations.

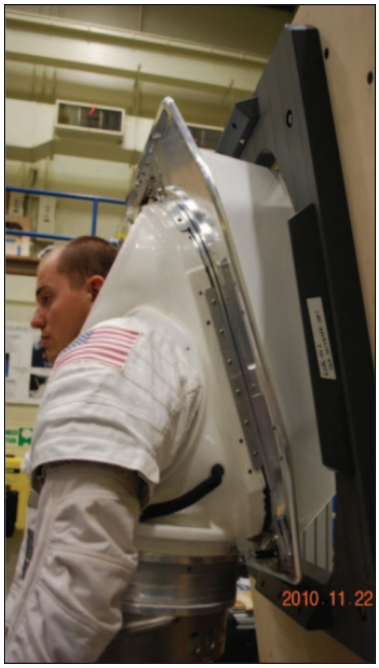


Fig. 2. *Suit port alignment testing.*

Extravehicular Activity Technology Development—Suit Port Technologies

continued

Pressurized Evaluations

The concept of using a suit port for rapid vehicle ingress and egress impacts on development of a spacesuit in several ways. The teams undertook a number of development tasks to assess these impacts and overcome the technical challenges associated with them. First, suit port operations dictate that an exploration spacesuit be donned and doffed through a rear-entry hatch with a suit port interface plate. The suit port interface plate is the surface that makes a pressure seal with the vehicle and is clamped by the mechanisms within the suit port. A rear-entry upper torso with a suit port interface plate is under development and will be completed in 2011. Donning a suit via a suit port also means that the crew member will be entering a suit that is already pressurized. This provides additional challenges associated with making sizing adjustments to the suit because all adjustments would be made in opposition to the suit pressure. The teams developed proof-of-concept designs for gloves and boots in which sizing adjustments could be made while the suit was pressurized, and performed an ambient pressure vacuum chamber demonstration (figure 3).



Fig. 3. *Ambient pressure vacuum chamber demonstration.*

A Cabin Air Separator for Extravehicular Activity Oxygen

John Graf, *Johnson Space Center*
Derek Neumeyer, *Johnson Space Center*
Angie Lenius, *Johnson Space Center*

Presently, the extravehicular activities (EVAs) conducted from the Quest Joint Airlock on the International Space Station (ISS) use high-pressure, high-purity oxygen that was delivered to the ISS by the space shuttle. With the retirement of the shuttle, a new method of delivering high-pressure, high-purity oxygen to the high-pressure gas tanks will be needed. One method is to use a cabin air separator to sweep oxygen from the cabin air, generate a low-pressure/high-purity oxygen stream, and compress the oxygen with a multistage mechanical compressor. This capability is being developed under the direction of the ISS Program Office with the project name Cabin Air Separator for EVA Oxygen (CASEO). This type of system can use the existing low-pressure oxygen supply infrastructure that is the source of cabin oxygen. The ISS has two water electrolysis systems that deliver low-pressure oxygen to the cabin, as well as chlorate candles and compressed gas tanks on cargo vehicles. Each of these systems can feed low-pressure oxygen into the cabin, and any low-pressure oxygen source can be used as an on-board source of oxygen. CASEO enables EVA-grade oxygen to be delivered to the ISS in the form of water—a dense, stable liquid that is safe to transport.

Physical Layout

CASEO will be delivered to the ISS in three modules: an oxygen separator module, an electronics module, and a boost compressor module. The modules will be connected and mounted along the same wall in the airlock where the Oxygen Recharge Compressor Assembly is presently located. A photo of a CASEO mock-up in the ISS airlock mock-up is shown in figure 1. As it appears in this figure, the compressor module is on the left, the electronics module is in the middle, and the separator module is on the right. Dimensions of the modules are also shown. The weight allocation at the time of the Preliminary Design Review is as follows: booster module—54.5 kg (120 lbs); electronics module—36.3 kg (80 lbs); separator module—68.1 kg (150 lbs); total system—159 kg (350 lbs).

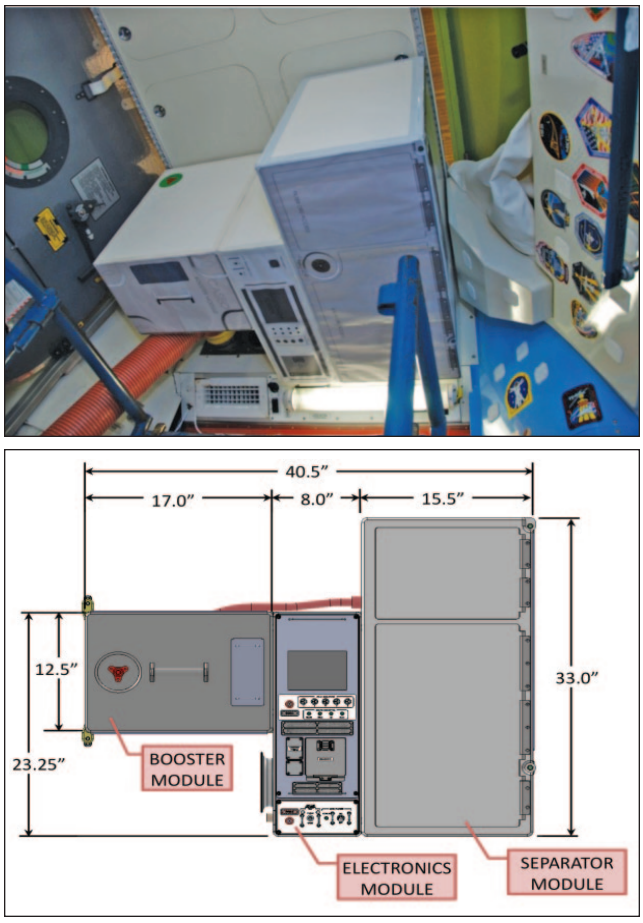


Fig. 1. *Physical layout and dimensions of modules (modules are 56 cm [22 in.] deep).*

Boost Compressor Module

The boost compressor module is a modified form of a three-stage mechanical piston compressor supplied by Cobham Life Support and Mission Equipment (Davenport, Iowa) and is shown in figure 2. It was originally designed for military medical oxygen applications. The major modifications are to use a direct-current-powered, flight-compatible motor, and to add a return spring on the first-stage inlet so the pump can receive oxygen product at low pressures, and a spring to the second and third

A Cabin Air Separator for Extravehicular Activity Oxygen

continued

stages to ensure electrical grounding. Without the first-stage spring modification, the inlet oxygen needs to have pressure of 15 psig or greater, or the first stage piston will not fully extend. Supplying oxygen at greater than 15 psig causes separator performance to suffer. The layout of the compressor module and balance of plant components is shown in figure 3, along with a detail of the first-stage inlet spring modifications.

Electronics Module

The electronics module consists of four sub-modules, as well as a cooling, data, power, and oxygen pass-through. The components are selected with a radiation hardness pedigree when possible. The Central Processing Unit is modified to include an external circuit to make it fault tolerant for single event upsets. The circuit protection is done at low voltages to allow for smaller gauge wires to be safely used. The circuit protection is done with fast-reacting devices. The CASEO circuit protection has a faster response time than the ISS vehicle power supply interface. All circuits are designed to withstand power spikes for a duration of 10 times longer than the response time of the circuit breaking devices.

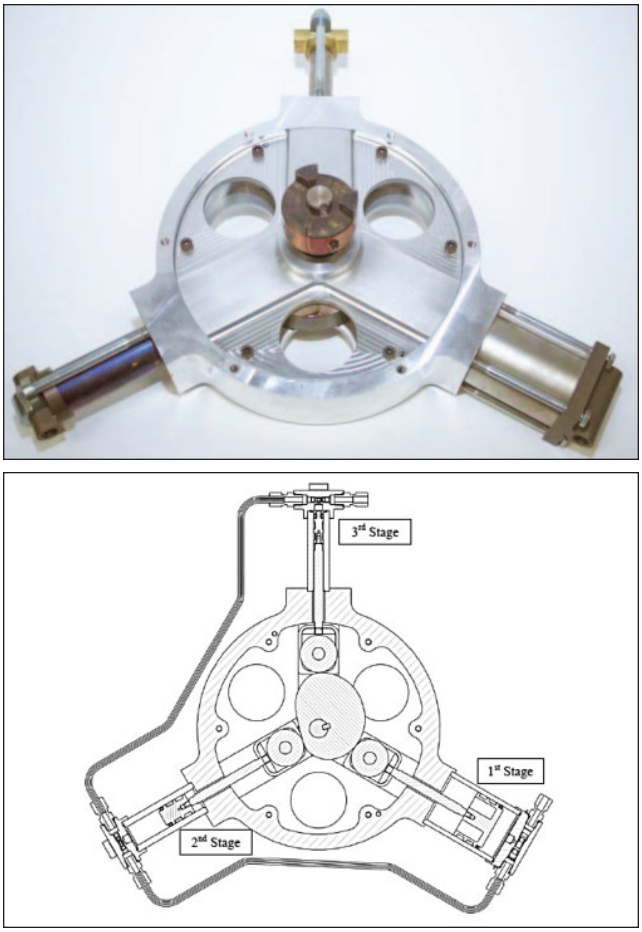


Fig. 2. *Photograph and schematic diagram of the boost compressor.*

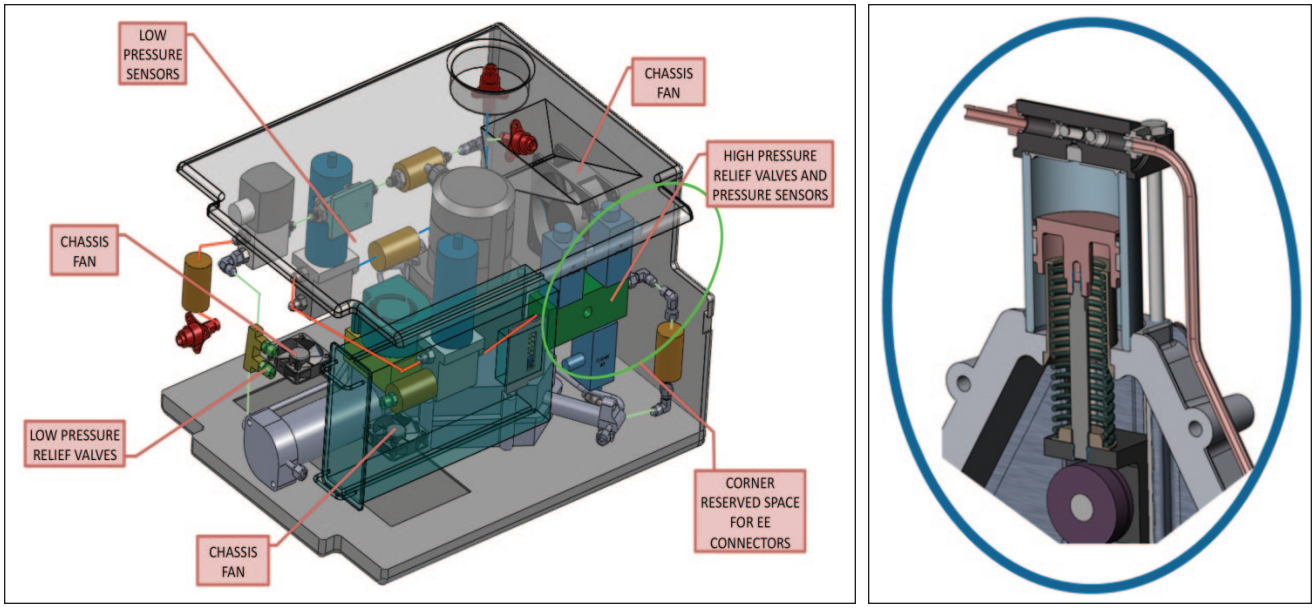


Fig. 3. *Layout of the boost compressor module with first-stage spring detail.*

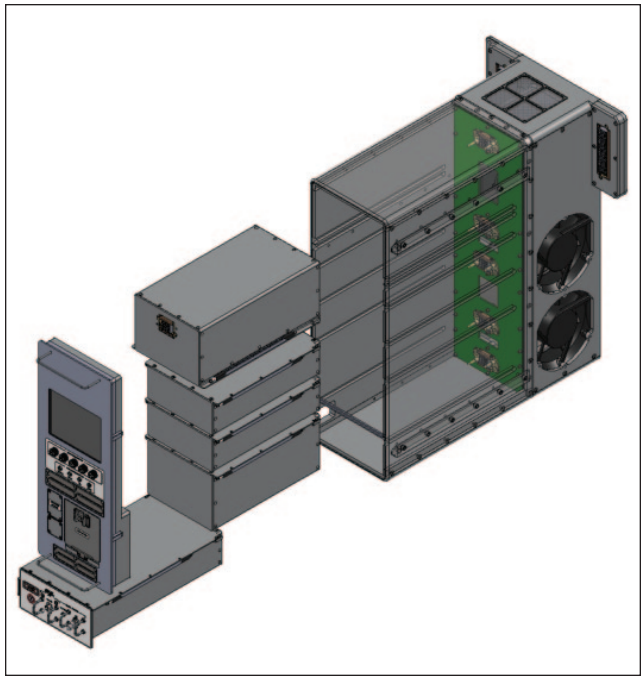


Fig. 4. *Electronics module configuration.*

CASEO can safely operate as a stand-alone device. It needs no command from the ISS, and it does not need any data from the vehicle. It has two methods of transferring data to the ground: one through a wired Ethernet, and one through a portable Universal Serial Bus device. The configuration of the electronics module is shown in figure 4.

Separator Module

The oxygen separator is a two-stage device that uses pressure swing adsorption as the method of oxygen separation. The separator module uses a compressor to compress cabin air to a pressure of 100 psig. When compressed, two different humidity control devices dry the air to -45°C (-50°F) dew point conditions. The first dryer is a membrane dryer; the second dryer is a pressure swing adsorption dryer that uses silica gel and type 13X zeolite. The first stage of the separator removes nitrogen from cabin air, and is designed to deliver a product that is nominally 95.5% oxygen, 4.3% argon, and 0.2% nitrogen. The second stage of the separator uses carbon molecular sieve material to remove the argon from the first-stage product. The calculated recovery efficiency projects a 1.5 liter per minute oxygen delivery rate. The nominal composition of the product gas is 99.6% oxygen, 0.3% argon, and 0.1% nitrogen.

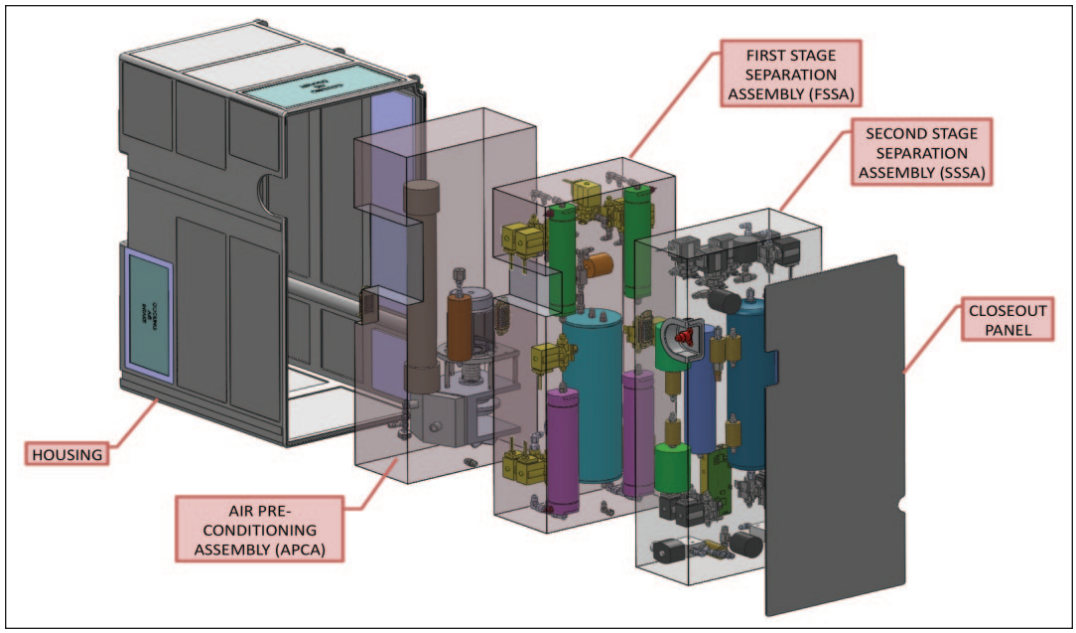


Fig. 5. *Packaging concept of the separator module.*

Extravehicular Activity Technology Development—Oxygen Subsystem

Colin Campbell, *Johnson Space Center*
Mallory Jennings, *Johnson Space Center*
Gregg Weaver, *Jacobs Technology*

The Extravehicular Activity (EVA) Technology Development Team—within the Crew and Thermal Systems Division of NASA Johnson Space Center (JSC)—is developing critical oxygen subsystem components to support the next-generation spacesuit. The oxygen subsystem of the Portable Life Support System of a spacesuit provides a crew member with gaseous oxygen for metabolic consumption, a pressurized environment, and the ability to supply open-loop purge flows for carbon dioxide washout or supplemental cooling. Primary components of the oxygen subsystem are tanks and regulators. Additional components include quick disconnects, purge valves, and relief valves.

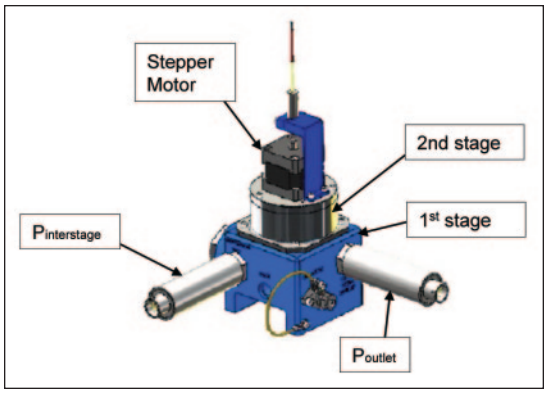




Fig. 1. *Primary variable regulator.*

Primary Variable Regulator

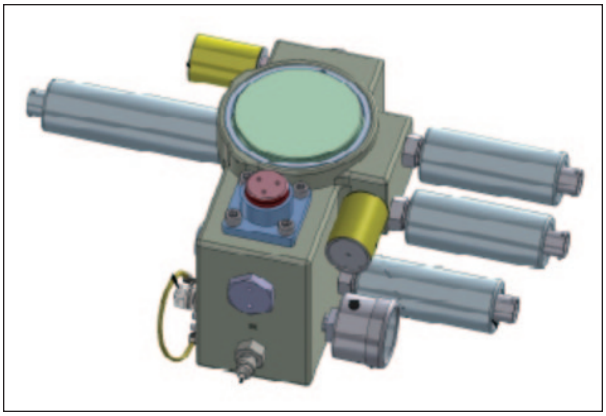
The space shuttle and International Space Station extravehicular mobility units have oxygen regulators with only two mechanically fixed set points. However, having a variable-pressure regulator in the spacesuit architecture allows for greater functionality (figure 1). The team performed work to develop a regulator to meet requirements, which stated that the regulator must decrease pressure from 20,684 kilopascals (kPa) (3000 psia) in the oxygen tank to a nominal suit pressure of approximately 33.1 kPa (4.8 psia). Making the regulator capable of varying the pressure setting provides added functionality because it can be used to regulate suit pressure to: match different vehicle pressures; perform procedures to prevent or treat decompression sickness; or minimize prebreathe durations prior to performing an EVA. An electronically driven regulator has been developed with a minimum of five set points and a goal of making the regulator continuously variable. Carleton Technologies Inc. (Orchard Park, New York), a subsidiary of Cobham plc (Wimborne, Dorset, UK), built this regulator by using a stepper motor to adjust the compression of a spring that then mechanically sets the regulator. This development effort not only includes the mechanical operations of the regulator, but also the electronics that drive both the regulator and the control logic. This regulator is being tested at JSC on a test stand (figure 2) that has been designed and built to evaluate candidate regulators for future spacesuit development.



Fig. 2. *Regulator test stand.*

Variable Electronic Regulator

The variable electronic regulator (figure 3) is an alternative concept to implement a variable-pressure regulator. The variable electronic regulator is one of the approaches currently being examined to meet improved requirements by using electronically controlled solenoid valves that are connected to high- and low-pressure supplies. The valves are controlled based on a pressure feedback to set the regulation pressure of the regulator. Key features of the variable electronic regulator include precise pressure control without droop or hysteresis.



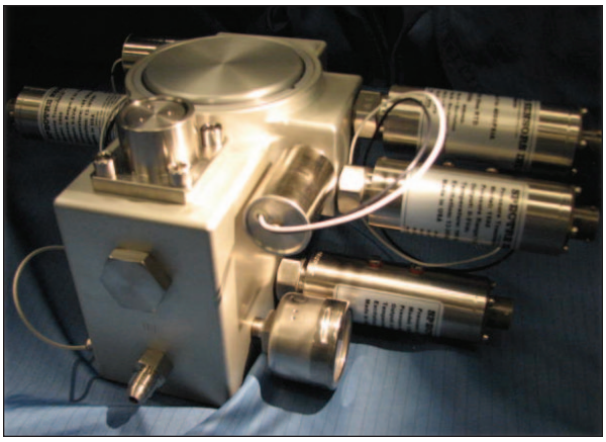
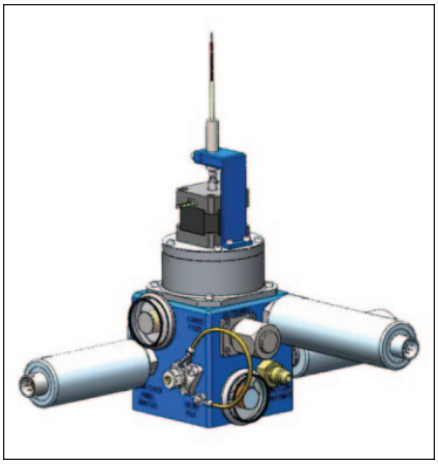


Fig. 3. *Variable electronic regulator.*

Secondary Oxygen Regulator

The secondary oxygen regulator (figure 4) is used to regulate the oxygen supply pressure coming from the secondary tank. The reliability of this regulator and the actuation mechanism that controls it is critical. A secondary oxygen regulator benchtop prototype has been built, delivered to JSC, and tested. The objective of this work is to develop a remotely operated high-pressure oxygen regulator that will function nominally in a lunar dust environment to enable doffing of the Portable Life Support System at vacuum. The space shuttle extravehicular mobility unit has experienced nine secondary oxygen regulator failures due to high actuation forces in a clean environment. The new benchtop prototype of the secondary oxygen regulator is designed for remote actuation in a lunar dust environment. Future work consists of building a functional prototype of the secondary oxygen regulator that has flight-like fluid passages and is compatible with oxygen for dust and vibration testing. Additional work includes development of a controller (modeling and testing of complex electromechanical systems) and research into



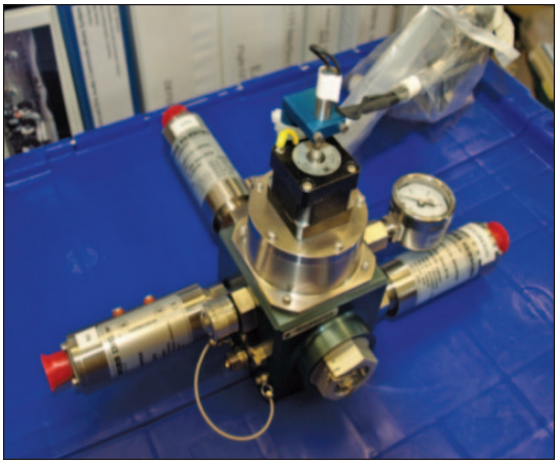


Fig. 4. *Secondary oxygen regulator.*

Extravehicular Activity Technology Development—Oxygen Subsystem

continued

oxygen-compatible materials (new lightweight oxygen materials that are safe up to 27,579 kPa [4000 psia]). Development of alternative regulator designs (e.g., a balanced dual-stage regulator that could simplify system design via integral fault tolerance) may also be needed.

Spacesuit Assembly Simulator

NASA designed a spacesuit assembly simulator to provide a transparent, ground-based test bed for studying and validating oxygen flow in a spacesuit during simulated EVA conditions. The team created the spacesuit assembly simulator hardware Pro-E model (figure 5) using two combined laser scans of a Mark III development EVA suit. To obtain these laser scans, the team first pressurized the Mark III suit, and then took one laser scan of the suit exterior to obtain the exterior surface topography. The outermost layers of the Mark III suit were removed, as it was impractical for the interior of the suit to be laser scanned. A scan of the inflated bladder was taken and assumed to be the interior surface of the suit. The team then combined these two laser scans into a single Pro-E model, which became the base spacesuit assembly simulator model.

NASA performed computational fluid dynamics analyses relating to nitrogen purge times and carbon dioxide washout. The interior of the suit model was developed from a scan of a suit and contains typical fabric ripples and folds, thus the spacesuit assembly simulator hardware can be tested to obtain realistic interior airflow data and used to validate the analyses. Having a transparent spacesuit simulator will also help researchers obtain a better visual understanding of ventilation flow paths and their interactions with and around other hardware within the suit.



Fig. 5. *The spacesuit assembly simulator Pro-E model and pressure test arm.*

Extravehicular Activity Technology Development—Portable Life Support System Integrated Testing

Colin Campbell, *Johnson Space Center*
Gretchen Thomas, *Johnson Space Center*
Carly Watts, *Johnson Space Center*

A spacesuit provides distinct protection for a single crew member who is working and operating in challenging extravehicular activity (EVA) environments. An EVA system is a key component of any plans for the future human exploration of space. The EVA system typically consists of a suit; a Portable Life Support System (PLSS); a Power, Avionics, and Software System; and suit interface hardware. The PLSS, which houses the Power, Avionics, and Software System components, consists of the oxygen subsystem, ventilation subsystem, and thermal control subsystem. As a unified system, the PLSS provides all of the functionality for breathing, pressurization, and cooling required to keep the crew member alive, comfortable, and protected during an EVA.

Since 2008, EVA technology development has focused on maturing key component technologies for each of the subsystems within the PLSS. The advancement of these technologies will improve hardware life, robustness, on-back regeneration, and mission flexibility. These advancements incorporate multiple technologies over current state-of-the-art capability and will keep the crew member alive more efficiently during an EVA. Johnson Space Center (JSC) has developed both an advanced PLSS concept design and a detailed schematic based on system analysis of each of the developmental hardware components. This promising PLSS design represents a significant state-of-the-art improvement over current extravehicular mobility unit technology. The overall PLSS schematic has been matured, and individual hardware component testing for each of the developmental subsystems has been achieved over the last several years and continues with promising results. The developmental

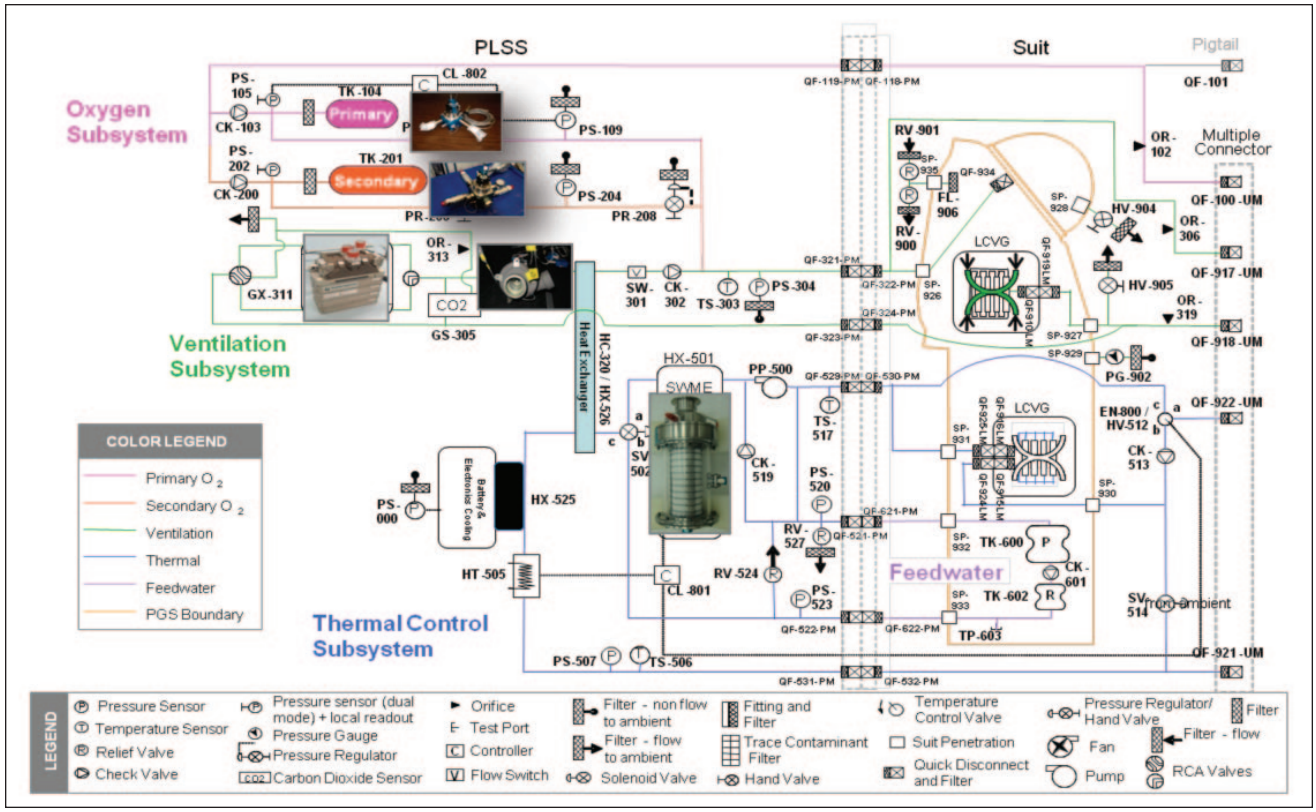


Fig. 1. *System-level baseline Portable Life Support System schematic showing the components.*

Extravehicular Activity Technology Development—Portable Life Support System Integrated Testing

continued

components include a primary oxygen regulator, a secondary oxygen regulator, a spacesuit water membrane evaporator, a rapid cycle amine, a fan, and a pump. Now that many of these technologies have been successfully demonstrated at a component level, integrated system evaluations of the entire assembled and integrated system are critical to advance the PLSS design further (figure 1). Therefore, integrated test planning has been under way, and testing will commence in fiscal year 2011 (FY11) by the EVA Technology Development Team, which is within the Crew and Thermal Systems Division of JSC.

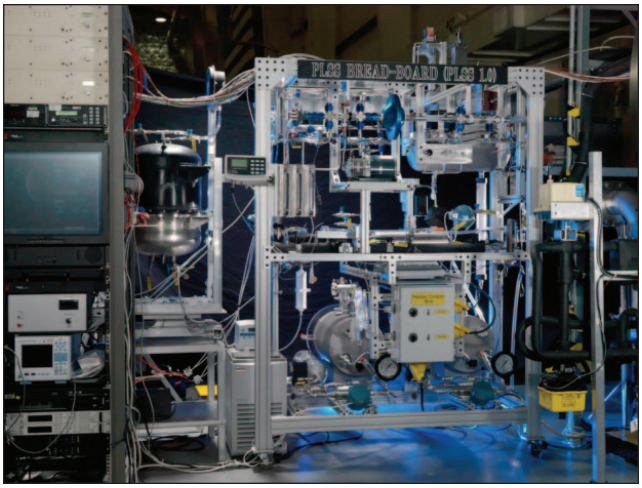


Fig. 2. *Portable Life Support System breadboard 1.0 test stand.*

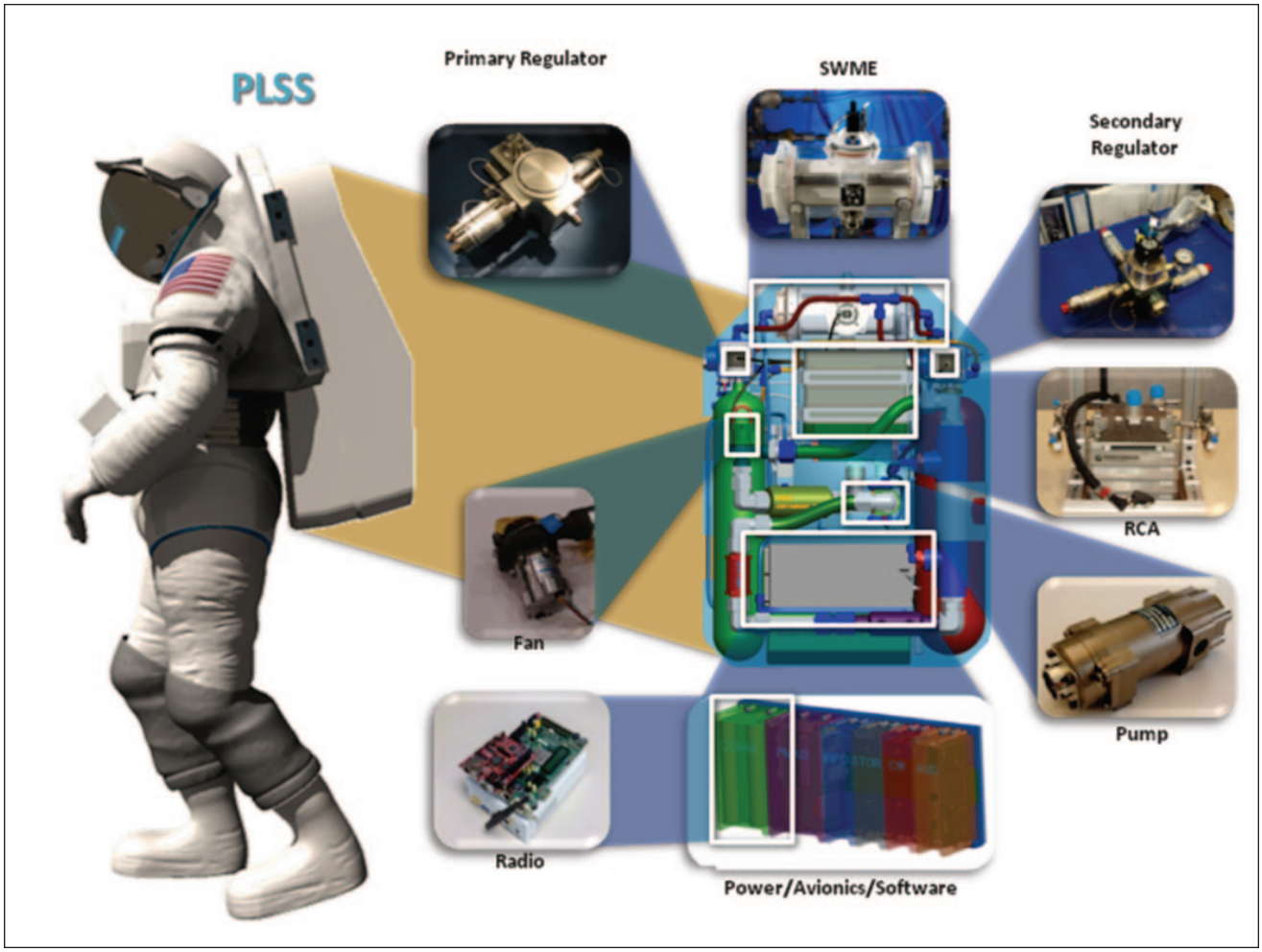


Fig. 3. *Advanced Portable Life Support System 2.0 design concept with component technologies for each subsystem.*

Portable Life Support System Integrated Breadboard Test

Integrated testing of EVA development hardware marks the first new major system-level evaluations since the development of the Space Shuttle Extravehicular Mobility Unit Program more than 3 decades ago. The first system demonstration—PLSS 1.0—will focus on integration of the next-generation PLSS. The test configuration is based on the PLSS schematic developed for integrating each subsystem component completed prior to FY11. The breadboard (figure 2) has been configured and approved for testing in FY11. Since this is the first attempt at system demonstrations, the hardware will be arranged in breadboard fashion and test objectives will focus on demonstrating primary system functions. The primary objective of the PLSS 1.0 series is to demonstrate system performance through a series of human metabolic profiles and thermal loads, and to obtain engineering data characterizing the performance of a PLSS-integrated system in a benchtop environment using simulated human and vehicle interfaces. The tests will demonstrate the operation of the benchtop PLSS in nominal intra-vehicular activity (i.e., pre- and post-EVA), EVA, and recharge configurations as well as under certain failure conditions. The tests will experimentally characterize the actions of the integrated system to define the system more precisely for modeling purposes, identify unexpected interactions and modes of operation, and build confidence in the system design. All breadboard testing will be crewless and will use nitrogen as the primary gas constituent, rather than air or pure oxygen. This is because pure nitrogen is safer than both pure oxygen and air, as pure nitrogen is nonflammable. At the same time, pure nitrogen will work well with all components of the ventilation loop and will give results comparable to a 100% oxygen system.

The PLSS 1.0 series only represents the initial system evaluations needed to develop an advanced EVA system. Follow-on system demonstrations will increase in complexity, evolving to include flight-like packaging and human test subjects. Future development activities will involve performing system trade studies and analyses; maturing system design to flight demonstration; packaging a PLSS 2.0 test article (figure 3) with the spacesuit water membrane evaporator, rapid cycle amine, primary regulator, fan, and secondary regulator; performing PLSS 2.0 testing; and ultimately carrying out human-rated testing (PLSS 3.0).

Extravehicular Activity Technology Development—Thermal Subsystem

Grant Bue, *Johnson Space Center*
Colin Campbell, *Johnson Space Center*
Gregg Weaver, *Jacobs Technology*

The thermal subsystem provides temperature control of an astronaut and associated equipment. In the latest advanced Portable Life Support System (PLSS) schematic, the thermal subsystem consists of a single-phase liquid water loop containing a pump, an evaporative cooling device, an avionics coldplate, a water bladder that serves as an accumulator, and the liquid cooling and ventilation garment that the astronaut wears. The Extravehicular Activity Technology Development Team, which is within the NASA Johnson Space Center Crew and Thermal Systems Division, is developing critical thermal subsystem components to support the development of the next-generation spacesuit. Development of suit water membrane evaporators (SWMEs) addresses PLSS heat rejection, and an advanced pump development addresses heat transport. These technologies are targeted for possible lunar, Martian, or asteroid missions that involve a human presence.

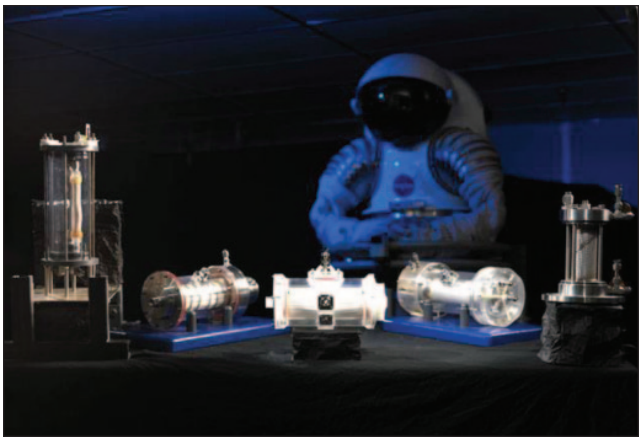


Fig. 1. *Several generations of suit water membrane evaporator test articles.*

Suit Water Membrane Evaporator

An SWME provides cooling to the spacesuit water loop by evaporating some of the water across a membrane into the vacuum of space (figure 1). As the water turns to vapor and is vented into space, it takes the energy needed to cause the phase change with it. A back-pressure control valve is used to control pressure within the evaporator assembly, which, in turn, controls the amount of water that is evaporated and, therefore, the amount of cooling that the crew member experiences. A critical aspect of the SWME is its ability to maintain acceptable performance through an entire 6-month mission of a spacesuit, as would be required on the lunar surface. Another critical aspect of this membrane-based device is its sensitivity to contamination.

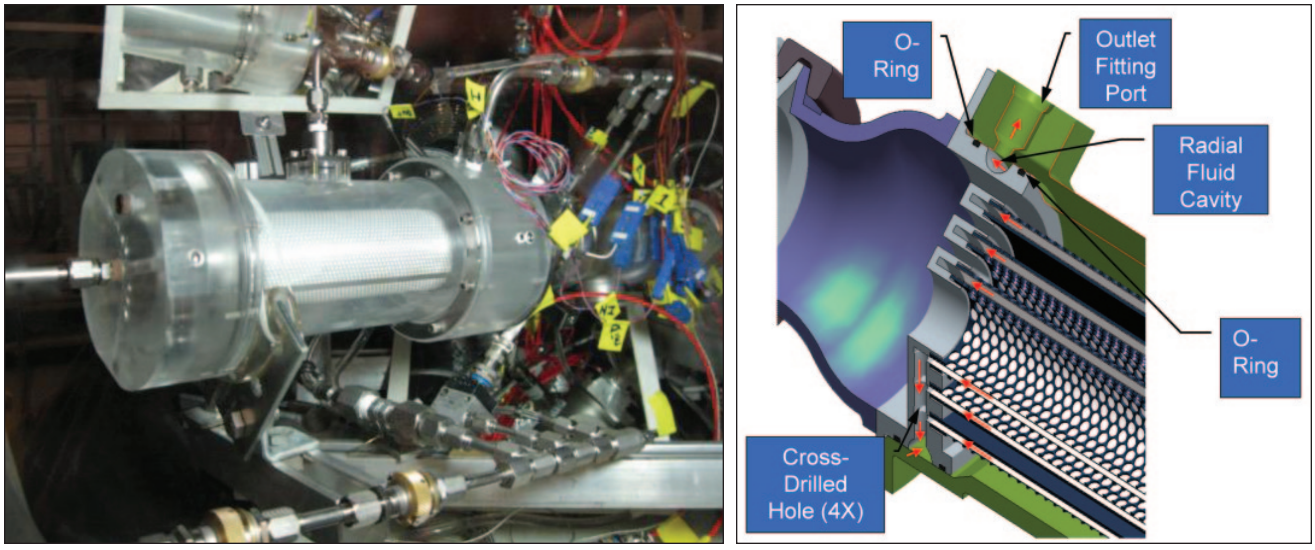


Fig. 2. *Sheet membrane suit water membrane evaporators.*

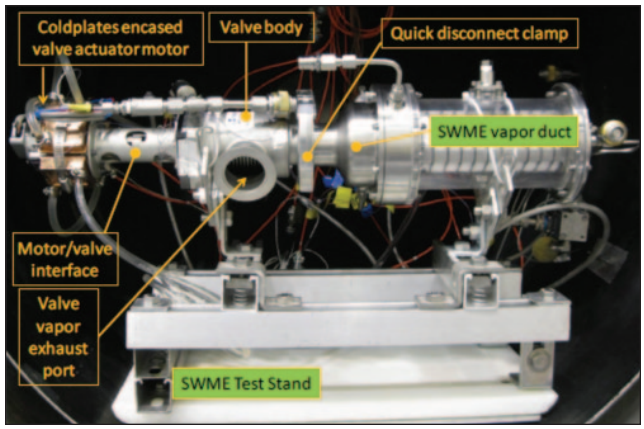


Fig. 3. *Hollow-fiber suit water membrane evaporators design.*

Two types of SWMEs have been developed and tested. The sheet membrane SWME (figure 2) uses six concentric cylindrical, porous, hydrophobic membranes to create alternating coolant water/vacuum passages. In addition to performance testing, the sheet membrane SWME was subjected to life testing and also to challenge testing in which different contaminants were present in the water. Further tests were performed to provide sizing data, demonstrate the controllability of the unit by using a back-pressure control valve, and evaluate how the unit would handle bubbles in the water.

The hollow-fiber (HoFi) SWME (figure 3) operates on the same principles as the sheet membrane SWME. However, instead of using sheet membranes arranged in concentric cylinders, the HoFi SWME uses a bundle of thousands of hollow tubes made from another porous hydrophobic material in which coolant flows through the center of the tubes and vacuum is present on the outside. The HoFi SWME was subjected to the same battery of tests as the sheet membrane SWME. The HoFi "cage" is shown in figure 4.

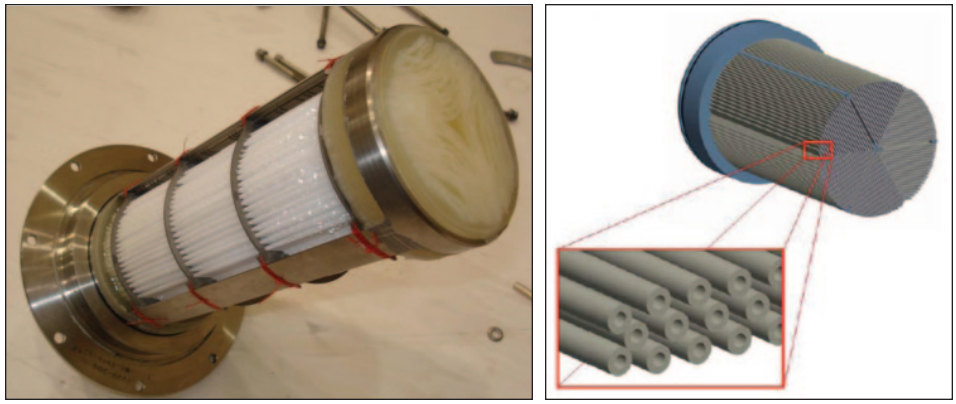


Fig. 4. *Hollow-fiber "cage."*

Following testing of the sheet membrane SWME and HoFi SWME, a down-select was performed and just the HoFi SWME was further developed. Key improvements in the next design focused on reducing mass and volume, and on developing a more flight-like back-pressure valve. This second-generation HoFi SWME (figure 5) underwent a battery of tests similar to those performed on its predecessor, with excellent results.

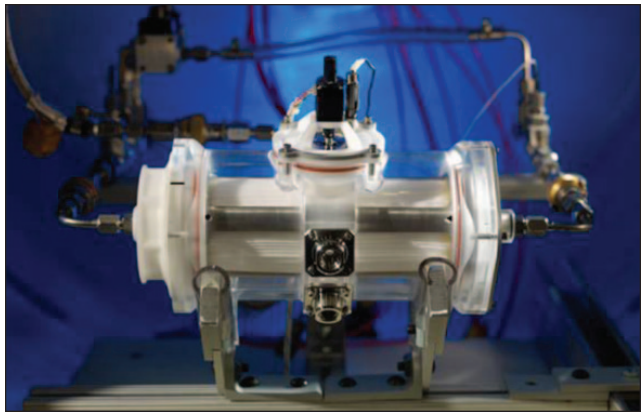


Fig. 5. *Second-generation hollow-fiber suit water membrane evaporators with improved back-pressure valve (on top).*

Extravehicular Activity Technology Development—Ventilation Subsystem

Heather Paul, *Johnson Space Center*
Mallory Jennings, *Johnson Space Center*
Colin Campbell, *Johnson Space Center*
Molly Anderson, *Johnson Space Center*
Michael Swickrath, *Johnson Space Center*
Summer McMillin, *Jacobs Technology*
Gregg Weaver, *Jacobs Technology*
Craig Broerman, *Jacobs Technology*

The ventilation subsystem provides oxygen circulation, carbon dioxide (CO_2) removal, trace contaminant removal, and humidity control. The Extravehicular Activity (EVA) Technology Development Team, which is within the Crew and Thermal Systems Division at NASA Johnson Space Center (JSC), is developing critical ventilation subsystem components to support future NASA missions.

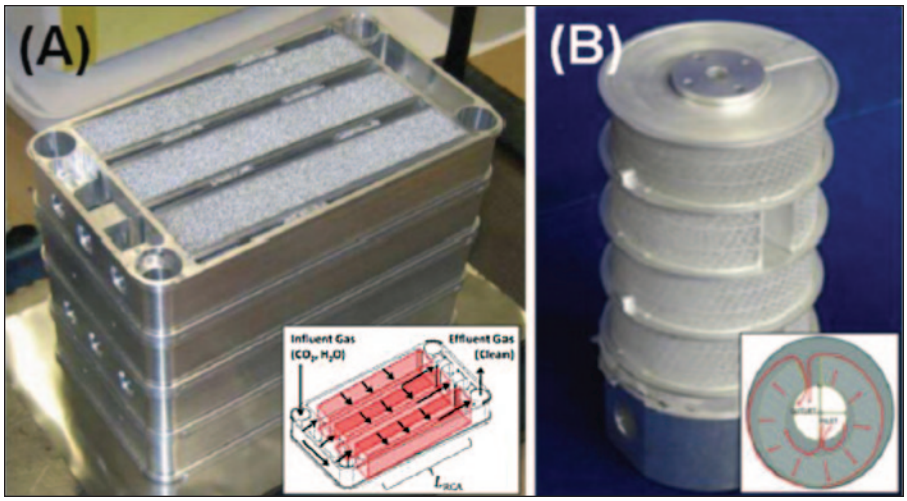


Fig. 1. *Rectangular rapid cycle amine unit (A) and cylindrical rapid cycle amine unit (B).*

Rapid Cycle Amine Swing Bed

A principal concern for EVA spacesuits is the ability to control CO_2 and water vapor (H_2O) for the suited crew member. The release of CO_2 into a confined or an unventilated area is dangerous for human health and could lead to asphyxiation. As water vapor also must be controlled to maintain crew comfort, CO_2 and H_2O control are leading factors in the design and development of advanced spacesuits. Hamilton Sundstrand (Windsor Locks, Connecticut) (HSWL) developed an amine-based CO_2 and H_2O vapor sorbent for use in pressure-swing regenerable beds. The application of solid-amine materials with vacuum-swing adsorption technology has demonstrated the capacity to manage CO_2 and H_2O levels concurrently through a regenerative cycle that eliminates mission constraints imposed by non-regenerative technologies. Two prototype solid amine-based systems (rectangular and cylindrical), known as rapid cycle amine swing beds, were designed and tested (figure 1).HSWL designed the rectangular unit (A), which is a full-scale, linear flow unit. Jacobs Technology designed the cylindrical unit (B) as an alternative rapid cycle amine design. This unit is a subscale radial flow unit. Each prototype solid amine-based system was designed to continuously remove CO_2 and H_2O from a constantly flowing ventilation stream through the use of a two-bed, amine-based, vacuum-swing adsorption system. While one set of sorbent layers was exposed to the ventilation stream to remove both CO_2 and H_2O (adsorb), the other set of beds was regenerated by exposure to vacuum (desorb). Testing was performed in a sea-level pressure environment and a reduced-pressure environment with simulated human metabolic loads in a closed-loop configuration. Both the full-scale and subscale test articles were tested. Test

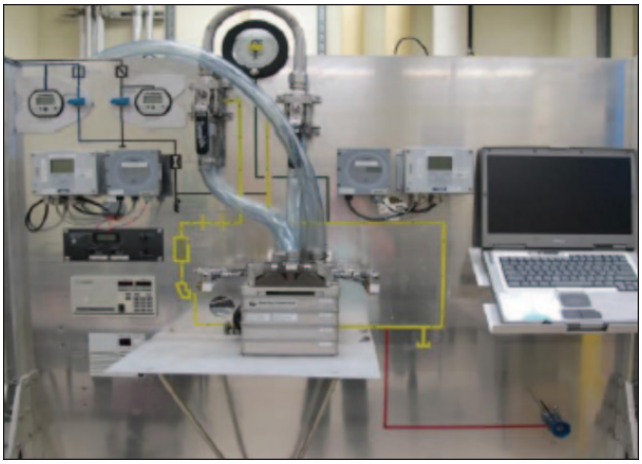


Fig. 2. *Portable Life Support System ventilation subsystem test loop with the rectangular rapid cycle amine unit.*

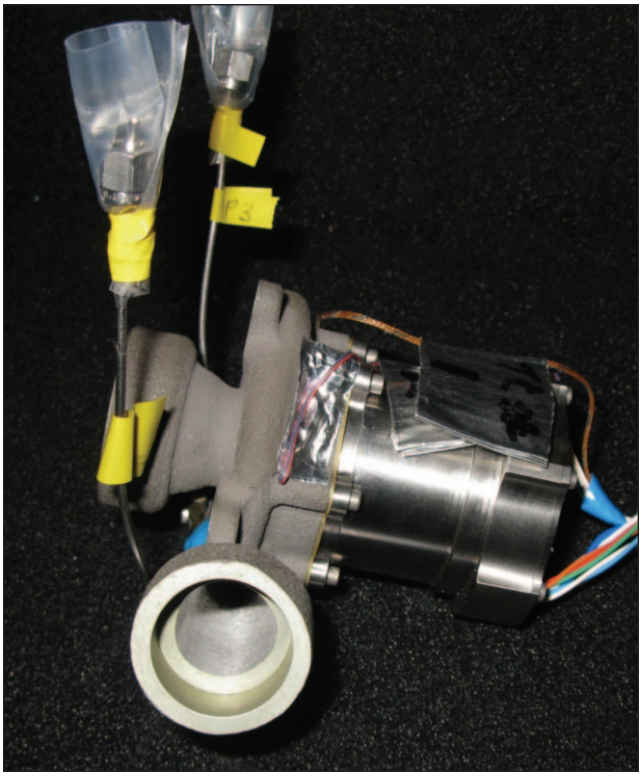


Fig. 3. *Photograph of fan assembly.*

points simulated a range of crew member metabolic rates. Experimental results demonstrated the ability of each rapid cycle amine unit to remove sufficient CO_2 and H_2O from both a closed-loop and a sub-ambient atmosphere.

Ventilation Fan

The team developed and tested a centrifugal fan to meet the expected requirements for ventilation flow modes in the next-generation Portable Life Support System (figure 2). Performance testing and life cycle testing (at atmospheric and sub-atmospheric pressures) were conducted at JSC. An oxygen compatibility assessment evaluation was also conducted at the NASA White Sands Test Facility. Fan development for the ventilation subsystem has focused on minimizing mass and power while providing adequate flow over a wider range of flow rates and pressure drops than are found in heritage spacesuit fans. A photograph of the fan assembly is shown in figure 3.

Environmental Technologies



Environmental Sustainability at Johnson Space Center

Michael K. Ewert, *Johnson Space Center*

Johnson Space Center (JSC) adopted a policy of "conducting our mission in a manner that promotes environmental stewardship, sustainability, compliance, and continual improvement." This policy is being implemented with the help of teams such as the Sustainability Partnership Team and Green Team, and through the use of Leadership in Energy and Environmental Design (LEED) standards for construction. Center leadership, organizations within JSC, contractor partners, and grassroots employee efforts all work together to make JSC "greener."

The Sustainability Partnership Team was formed in 2004 to improve environmental sustainability and increase JSC's exposure to "dual use" technologies that may be beneficial in both terrestrial and space exploration environments. NASA's work in space promotes technological advances that result in "spin-off" technologies, which are also useful on Earth. At the same time, various federal government executive orders and NASA policy directives compel the center to take action to reduce environmental impact through waste reduction, energy efficiency, and other actions. Combining these two NASA goals with JSC's technical expertise and space hardware development mission motivates the team to take advantage of the latest state-of-the-art technologies at JSC's facilities.

Sustainability is defined here as development that meets the needs of present generations without compromising the ability of future generations to meet their own needs. Since sustainability is an interconnected issue, the Sustainability Partnership Team uses systems analysis to guide its efforts. To measure progress, the team developed a set of 15 sustainability indicators for JSC. These sets are grouped into the categories of air pollution, waste/resource use, and energy. Figure 1 shows one example for municipal waste generated.

Examples of Sustainability Partnership Team projects include the investigation of solar air-conditioning and solar water heating for JSC buildings, and the retrofitting of several electric carts with solar panels for recharging (figure 2). In 2007, a Multi-Platform Renewable Energy System was constructed at the JSC Child Care Center.

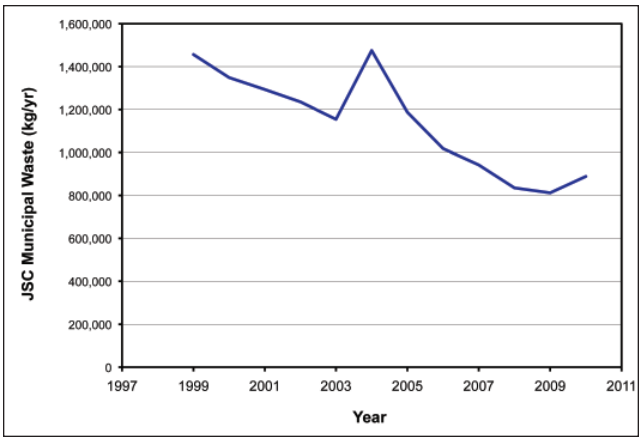


Fig. 1. *Example of a Johnson Space Center sustainability indicator.*



Fig. 2. *Electric cart powered by solar panel.*

Environmental Sustainability at Johnson Space Center

continued

(For details, see the article titled "Greening the Johnson Space Center Aaron Cohen Child Care Center.") In 2009, technicians installed solar water heating and day-lighting systems at the JSC Gilruth Recreation Center (figure 3).

The Green Team was formed in 2010 to encourage JSC employees to adopt more environmentally friendly behaviors at work and at home. This team—with representatives from across the center—has broadcast energy- and water-saving tips, and has organized contests to determine which work groups can save the most paper and energy.

JSC is striving to go beyond NASA's standard of new building and major renovation construction at the LEED Silver level or higher. LEED promotes a whole-building approach to sustainability by recognizing performance in these five key areas of human and environmental health: sustainable site development; water savings; energy efficiency; materials selection; and indoor environmental quality. In the past few years, JSC has been awarded LEED basic certification on one project, Silver on one project, Gold on three projects, and Platinum for a new office building, completed in 2010. (Detailed information is provided in the article titled "Leadership in Energy and Environmental Design at Johnson Space Center.")



Fig. 3. *Solar water heater at the Johnson Space Center Gilruth Recreation Center.*

Greening the Johnson Space Center Aaron Cohen Child Care Center

Jerry Rowlands, *Johnson Space Center*

In 2007, Johnson Space Center (JSC) took a major step in the direction of renewable energy usage by constructing a Multi-Platform Renewable Energy System (MPRES) at the Aaron Cohen Child Care Center. The MPRES was constructed at the end of fiscal year (FY) 2007 and was brought on line in FY 2008. This project had several goals:



Fig. 1. *Johnson Space Center Aaron Cohen Child Care Center Multi-Platform Renewable Energy System.*

1. To support the Engineering Directorate's mission by providing an opportunity to gain an understanding of large, surface-based photovoltaic (PV) arrays necessary for lunar surface exploration.
2. To gain the JSC-specific experience with various renewable energy technologies.
3. To collect real field data to confirm the viability of renewable energy technologies at JSC.
4. To strive to meet energy Executive Order mandates.

The child care center was selected as the site for the MPRES because the size of the facility allowed for renewable energy system flexibility, the tie into the electrical grid would not be complicated, and it provided excellent educational opportunities. Solar PV, solar thermal, and wind technologies were determined to be the best fit for JSC's initial venture. Therefore, the MPRES consists of:

a. Eight 2.8-kW PV modules with a solar tracker for a system output of 22.4 kW

b. Three 1.0-kW PV modules with a solar tracker for a system output of 3 kW

c. Three 1.0-kW fixed PV modules for a system output of 3 kW, fashioned in a decorative "lollipop" design

d. Two 33-foot-high, 1.8-kW wind turbines rated at 3.6 kW and a peak output of 4.8 kW—the total system's electrical generation is rated at 32 kW

e. Solar Thermal Glycol Hot Water Generating System with an 80-gallon hot water storage tank

Benefits of the Project

This project provided a number of benefits:

1. Supported the JSC mission by providing the Engineering Directorate with data that demonstrated:

- How to build, operate, and maintain a large, surface-based PV array to accomplish lunar surface exploration
- A focus on systems engineering and integration issues
- A future robotic assembly and maintenance, automated monitoring, and advanced regenerative fuel cells
- That the objective of the Engineering Directorate was not only to capture information that would contribute to the development of lunar surface energy systems, but also to perfect technology that could be exported to other centers for a NASA-wide benefit

2. Gave JSC valuable experience with:

- Actual costs associated with implementing a successful renewable energy project
- The best design and constructability options for future renewable energy projects
- Maintaining and operating renewable energy systems

3. Allowed JSC to confirm the viability of renewable energy technologies with the real field data collected and assisted the center in making cost-effective decisions for future renewable energy projects.

4. Allowed JSC to move forward in compliance with the Energy Policy Act of 2005 renewable energy mandate. These mandates required that by 2013, a minimum of

Greening the Johnson Space Center Aaron Cohen Child Care Center

continued

7.5% of any Federal Government Agency's electrical consumption must be from a renewable energy source. As an additional bonus in the plan, any power generated on-site is given double credit in this percentage calculation. JSC determined that its new mission with energy conservation would not only achieve both energy reduction and renewable energy requirements, but attempted to lead the way with on-site generation.

5. Saved JSC critical funding with the reduction of purchased utilities, as well as reducing JSC's greenhouse gas footprint.

Green Savings

In 3 full years of operation, MPRES has:

- Generated 153,353 kilowatt (kW) hours
- Avoided 168,030 pounds carbon dioxide, 689 pounds nitrogen oxides, and 693 pounds oxides of sulfur

This renewable generation averted the gases emitted by 19 cars in 1 year and is enough power to operate eight homes for 1 year. The MPRES provides 20% of the electrical energy needs at the Aaron Cohen Child Care Center. When the building is unoccupied during evenings and weekends, and when electrical load requirements are low, the surplus energy is fed to the site's electrical grid and made available to the remainder of JSC.

Photovoltaic Details

The MPRES consist of tracking and stationary PV arrays. A photocell, affixed at the peak of the arrays, detects the brightest object in the sky (assumed to be the sun), and sends a signal to the small, low-voltage DC motor. Through a gear drive assembly, the PV array is moved to a perpendicular position relative to the sun's rays. The dual tracking system travels horizontally to follow the sun east to west throughout the day, and vertically for the sun's height in the sky for the different seasons. By tracking the sun and capturing all the power accessible—whenever it's available, at any time of the day—the system provides maximum efficiency and generation production.

The remainder of this system encompasses three 1-kW stationary decorative lollipop PV arrays. The three lollipop PV arrays do not track the sun, but they can be manually adjusted vertically for the different seasons throughout the year. The stationary PV systems, though less efficient than the tracking systems, require less initial investment.

Wind Turbine Details

The wind's renewable energy is captured by two 1.8-kW wind turbines. The turbines are based on new technology with simplified installation for plug-and-play grid interconnection. The controls and inverters are built into the turbine's unit. This provides quiet, clean electricity at low wind speeds. Using a slip ring and passive yawing, the wind turbines are able to follow the wind and produce maximum power from any direction.

GeoExchange Heating, Ventilation, and Air Conditioning System

In keeping with JSC's commitment to implement green technologies, the center replaced the existing Heating, Ventilation, and Air Conditioning (HVAC) system at the Aaron Cohen Child Care Center with an extremely efficient GeoExchange HVAC system. This system uses the Earth for both a heat source and a heat sink. Water is pumped from a geothermal heat pump to a vertical closed-loop polyethylene piping system in the Earth where heat is either discarded from the water or absorbed by the water. On the air-conditioning side, the Earth works as a cooling tower to cool the water and heat it up on the heating side.

Forty 300-ft-deep, 4¾-in.-diameter bore holes were drilled, and two 1-in.-diameter polyethylene pipes (supply and return) connected at one end by u-bend pipe were placed in each hole. These 40 loops were then connected to a manifold at the other end using 3-in. to 1-in. polyethylene piping to create a reverse return with the water flow though the piping system. Reverse return is employed to create a constant flow and to spread out the thermal energy through the well field. A 150-ft horizontal bore was completed from the well field to a closet on the back of the child care center. Two 4-in. polyethylene pipes (supply and return)

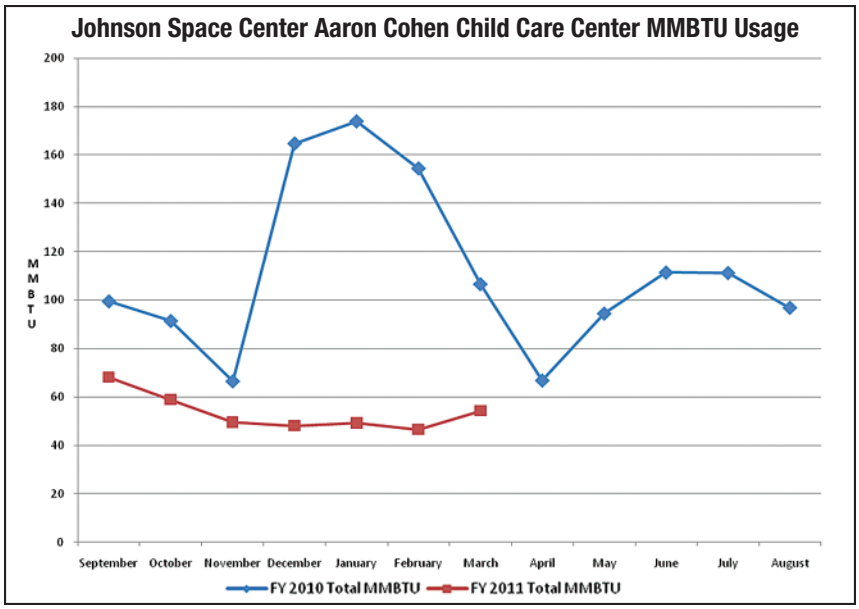


Fig. 2. *Million British Thermal Units (MMBTU) Reduction After GeoExchange HVAC System installation.*

were pulled through this horizontal bore up through the ceiling of the closet where the size decreased to 2 in., and eventually to 1 in., and through the attic to a platform where the 12 GeoExchange units were installed.

The existing HVAC system consisted of a four-zone, direct expansion air-conditioning system with natural gas duct heaters for heating. This project involved changing to a 12-zone system with complete duct replacement. The interior construction involved a great deal of coordination and flexibility. The child care center had to remain open and the air conditioning had to be maintained during the construction. With these challenges, the existing HVAC system was demolished one zone at a time and temporary air conditioning was provided until the new units and duct work was installed and operational. This work was completed at night. A Web-based thermostat system controlled the new 12-zone GeoExchange system.

The GeoExchange system has been in operation since September 2010 and has reduced the million British thermal units usage in the child care center by 44% without compromising comfort (figure Rowlands Greening 2).

System Monitoring

A Web-based metering system collects MPRES data in real time and is displayed locally and on the internet, showing performance figures on each individual system as well as historical information. This metering system impacts both research and education at JSC, as well as other NASA sites. This page is easily accessible through the website. It can be viewed by all of JSC, other NASA facilities, and educational institutions, thereby permitting the data accumulated to be used for both research and education. Additionally, a kiosk that displays the page shown below with real-time data has been placed in the lobby of the child care center for educational purposes.

Blue Marble Award

In FY 2009, the MPRES was featured in the Federal Energy Management Program Leadership poster. This project was part of the winning NASA Headquarters Environmental Management Division's 2010 Blue Marble Awards for Environmental and Energy Excellence. The award was the NASA Excellence in Energy and Water Management Award – Group: Energy Efficiency and Water Conservation Team (JSC) – Renewable Energy and Energy Conservation Program.

Other Greening Projects

JSC has completed additional efficiency projects in an effort to reduce the electrical usage in the Aaron Cohen Child Care Center and, in turn, provide the building with added renewable energy. The center added solar screens to the windows to reduce the infiltration of thermal energy from the sun. Since the child care personnel complete an abundance of laundry each day, JSC replaced the two stacked washers and dryers with a high-efficiency, front-loading washer and dryer. The center replaced refrigeration equipment in the kitchen with ENERGY STAR apparatus. JSC resolved an issue with ventilation of the attic, which was adding to the HVAC loading, by adding vents and an attic fan. In the future, JSC may look into gaining a Leadership in Energy and Environmental Design Operations and Maintenance Certification for this building.

Leadership in Energy and Environmental Design at Johnson Space Center

Charles Noel, *Johnson Space Center*

The designs of all new construction and major renovation of facilities at Johnson Space Center (JSC) meet the Leadership in Energy and Environmental Design (LEED) criteria. This criterion ensures energy and material efficiency and sustainability are inherent in all new construction.



Fig. 1. *Building 20.*

The architect-engineer firm performing a specific design, the project manager, and project team perform an LEED design charette at the pre-design stage to assure that JSC meets NASA Headquarters' minimal LEED Silver-level requirements. This charette calls for an item-by-item review of the U.S. Green Building Council's LEED Project Scorecard to determine which LEED points are reasonable to accomplish within the scope of a project and which are open possibilities.

As a project progresses through its 30%, 60%, and 90% design review, the JSC team reexamines the scorecard to determine which points must be dropped out or might be added due to the latest engineering design data. At the 30% stage, the team justifies—by a life cycle cost analysis—the design concept proposed by the architect-engineer. This analysis is adjusted and refined as the project progresses to its final stage.

This process has enabled JSC to design, construct, and certify the following LEED buildings over the past 6 years:

LEED Certified

Building 27: The Astronaut Quarantine Facility

LEED Silver Certified

Building 207A: Gilruth Recreation Center facility addition

LEED Gold Certified

Building 2 North: Office of Communications and Public Affairs
Building 26: The Center for Human Space Flight Performance and Research
Building 265: Source Evaluation Board office additions

LEED Platinum Certified

Building 20: The New Office Building

The New Office Building Description

JSC's newest facility (figure 1)—the New Office Building—is a three-story, 83,000-ft^2 office building employing numerous sustainable features. In the design, JSC originally strove for an LEED Gold rating; however, because of improvements and innovation during facility construction, the building received the agency's first Platinum LEED rating by the U.S. Green Building Council. The New Office Building was constructed to support JSC's multiyear building refurbishment program by providing "flex" space for employees who are temporarily relocated due to refurbishment of another building. The main design decisions for the new building centered on creating a highly flexible space that could be altered quickly at minimum cost. Additionally, designers meant to create a highly sustainable facility using the "less-is-more strategy" (i.e., an efficient building design reduces the programmed building area [footprint] and the amount of finishes, where applicable).

Features included in the project

The design team oriented the New Office Building to maximize daylight harvesting and installed an ENERGY-STAR-compliant, highly reflective roof. The team also selected low-flow restroom fixtures, including waterless urinals, dual-flush valves, and flow restrictors on faucets. Native plants and adapted species are seeded around the facility to reduce maintenance and water use, and condensate water is used as the primary irrigation source.

Faced with the extra challenge of optimizing building energy performance for a facility anticipated to undergo significant change over the coming years, the design team installed a high-efficiency under-floor Heating, Ventilation and Air Conditioning (HVAC) system for flexibility.

The building includes such extras as Solarban® 70 energy-efficient windows (figure 2), built-in solar shading barriers, solar hot water heating for the restrooms, ultraviolet lighting in air handlers to reduce microbial growth, and a detention pond and structural controls to manage and improve storm water runoff.

As constructed, the New Office Building will reduce potable water consumption for landscape irrigation by 54%, use 34% less water than a building that just meets baseline fixture performance requirements of the Energy Policy Act of 1992, be 55% more energy efficient than ASHRAE [American Society of Heating, Refrigerating and Air-conditioning Engineers] 90.1 specifies, and divert greater than 90% of all construction waste from disposal.

Facility occupants will benefit from a building designed to provide natural daylight to all office spaces. The design includes natural light in the stairwells, bicycle racks, and showers to encourage employee health and fitness.

LEED Under Construction

Building 29: Constellation Avionics Integration Laboratory (will be submitted for LEED Silver certification soon)
Building 12: Administrative Support Building

Administrative Support Building Description

Building 12, one of JSC's oldest original permanent buildings, is undergoing a complete refurbishment to modernize it to help serve JSC well into the 21st century. This two-story, 67,348-ft^2 office building houses JSC accounting, administrative, and training groups, and is located on the historic Central Mall of the JSC campus.

Sustainability has been at the forefront of the design process since project inception, and such features are integrated into the building. Most of the inherent obstacles that presented challenges to the refurbishment program and to sustainability goals were creatively overcome and, in some cases, were turned into assets. The project posed the daunting task of complete renovation and upgrade to meet current applicable codes and standards. These included: life safety; environmental; energy; mechanical, electrical and plumbing engineering; and structural. Two of the largest existing building systems by weight and volume, however, were retained with new engineering analysis and upgrades in the refurbished design. These building systems included the iconic JSC white-quartz-faced precast concrete exterior wall panels and the building's steel framing and concrete foundations. The majority of all materials removed and demolished were accounted for and sent to recycling entities or, in the case of hazardous materials, to environmentally certified disposal. Project design started in 2008, and construction will be completed in 2012. Building 12 uses LEED for New Construction version 2.2 to track the sustainability aspects of the project. JSC is currently projecting a LEED Gold rating.

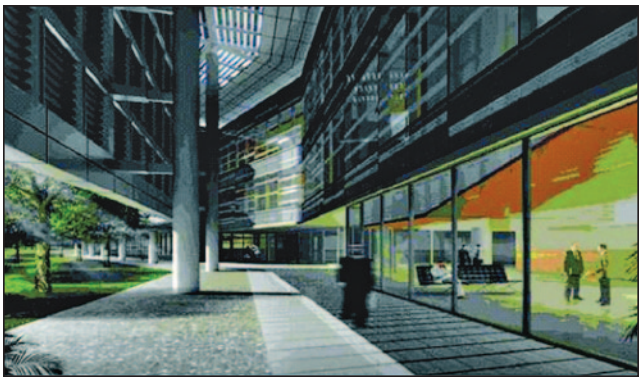


Fig. 2. *High efficiency solar shades.*

Features included in the project

The refurbishment effort involves all parts of Building 12— interiors, exterior skin, and roof. Interiors will use low-odor materials including paints and coatings, adhesives and sealants, composite wood, and carpet systems. Offices are located toward the central core of the building to enhance daylight and views to the outside.

Certified wood and durable materials will be used as well. New lighting will provide greater control to the occupants and reduce energy use. Lighting control features include occupancy sensors, daylight sensors, and low-voltage

Leadership in Energy and Environmental Design at Johnson Space Center

continued

relays. Low-flow plumbing fixtures will be installed throughout the building, with a projected water use savings of 43%. The building will use JSC's existing central utility plant, but multiple strategies have been implemented to reduce energy use. Such strategies include:

- Under-floor air distribution system that also increases building-use flexibility
- Variable speed drives on mechanical equipment
- Daylight harvesting and occupancy sensors that reduce lighting costs
- Photovoltaics integrated into shading devices
- Four highly efficient vertical axis wind turbines placed on the roof (figure 3)
- Strategically engineered sun shading devices tailored to maximum solar efficiency while enhancing indirect natural day lighting inside the space

The exterior of the building includes a new curtain wall system with dual-glazed low-emissivity windows, premium exterior envelope insulation, and sun shades. Such features reduce heat glare and heat gain into the building, which improves occupant comfort and reduces energy use. A vegetated roof will help reduce the heat-island effect for the building and site, and will assist in mitigating storm water runoff (along with the site landscaping) (figure 4). JSC is making an effort to promote alternative transportation and added conveniences; therefore, bicycle storage is provided, and shower facilities are located within the building. The center is also setting aside parking spaces for fuel-efficient and carpool vehicles.

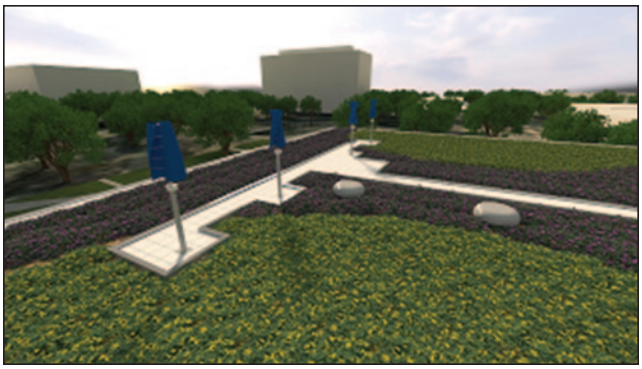


Fig. 3. *Wind turbines on roof.*

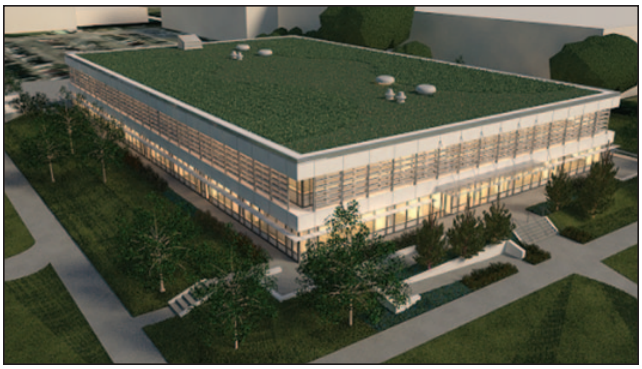


Fig. 4. *Building 12.*

Materials, Structures, Development and Testing



Lightweight Materials Development for Parachutes

Mary Jane E. O'Rourke, *Johnson Space Center*

Parachutes for the Orion Multi-Purpose Crew Vehicle must meet requirements for volume and mobility in the parachute compartment in addition to meeting constraints on launch weight. Parachute pack density must be kept low; therefore, decreasing parachute volume by increasing parachute pack density is not a solution. It is imperative that pack density be low enough to allow for complete, rapid, and damage-free deployment of the parachutes. High pack density was cited as the most difficult challenge to the main parachutes on Apollo, and must therefore be avoided for the Multi-Purpose Crew Vehicle. Development of lightweight parachute materials will help meet requirements on volume, mobility, and weight.

One material identified for development is lightweight Nylon broadcloth for the skirt-to-shoulder region of the main parachute canopies (figure 1). This technology development addresses the risk of insufficient volume for the Capsule Parachute Assembly System (CPAS) main chute pack and harness and riser routing, offering a significant reduction in parachute material volume in an already constrained parachute compartment volume. While weight savings is of secondary concern to decreased pack density, successful development of the lighter-weight fabric results in a weight savings of approximately 25 to 50 lbs. to the vehicle as well.

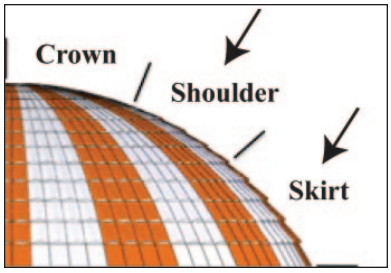


Fig. 1. *Skirt-to-shoulder region of the parachute canopy.*

The development is conducted in a phased approach, with Phase I completed in 2010. The first phase was a feasibility assessment of the fabric. Phase II will assess performance of the fabric in a parachute. A parachute using one of the newly developed lightweight Nylon broadcloths is currently in production and will be flight tested to assess performance.

Phase I was comprised of fabric builds and laboratory testing of the resultant fabrics to verify that these fabrics meet requirements, with areal density being one of the most critical requirements to this work. The baseline CPAS design uses Nylon broadcloth of 1.10 ounces per square yard (oz/yd^2) in the region identified for use of the new fabric. A goal of 0.70-0.90 oz/yd^2 was required for the areal density of the new lightweight Nylon broadcloth. Additional requirements included a permeability of 100 ± 20 cubic feet per minute (cfm) to meet the baseline CPAS design, and an elongation in both warp and fill directions of 20% minimum. Because it is expected that a reduction in areal density will come with some penalty to strength, both a goal strength to meet the baseline CPAS design and a minimum strength to meet expected loads were identified for break and tear strengths. A goal of 42 lbs. with a minimum of 38 ± 10% lbs was identified for break strength in both warp and fill directions, and a goal of 5 lbs with a minimum of 4 lbs. was identified for tear strength in both warp and fill directions. Warp and fill are defined in figure 2.

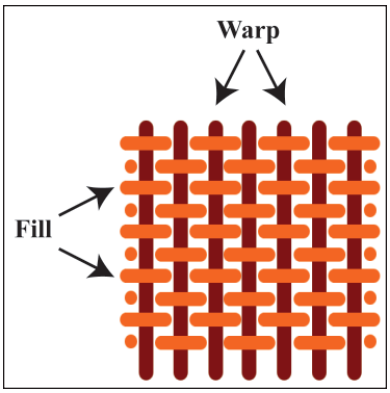


Fig. 2. *Warp and fill.*

A lighter-weight fabric presents challenges in seaming and joining. Stitches are less likely to hold the more delicate fabric in place. Thus, seam and joint design, builds, and laboratory testing of these seams and joints were also critical to Phase I. Seam and joint efficiencies are defined as the strength of the pristine material to the strength of the material over a seam or joint. While an efficiency of 80% or greater was identified as a highly desirable accomplishment, the goal of this project was not to increase seam and joint efficiency, but to match that of the baseline CPAS joints in the same region. NASA selected one standard seam—a single reinforced French fell seam, as described in American National Standards Institute/ American Institute of Aeronautics and Astronautics S-017A-2000, "Aerodynamic Decelerator and Parachute

Lightweight Materials Development for Parachutes

continued



A B C D E

Fig. 3. *Heat set and pack: A. Packing fixture; B, C. Seam and joint samples and extra packing material for filling required volume at required pressure are packed into the packing fixture using a hydraulic press; D. Packed samples and fabric are held in the heat set fixture; E. Packed samples following 8-hour heat set. Photos courtesy of Pioneer Aerospace Corporation.*

Drawings"—for evaluation and comparison across all fabrics (figure 3). The agency also evaluated alternative standard seams, as well as some original seam designs.

Performance of the seams and joints after exposure to a heat set and pack, as well as to salt fog, was also of interest. To achieve and maintain the parachute pack density, parachutes are typically packed into their deployment bags using a hydraulic press, held under pressure, and heated to set. It is vital that the parachute deploy properly and without damage after this treatment. Any effect of this process on the baseline 1.1 oz/yd^2 fabric is known to be of no consequence, but a lighter-weight fabric could be more susceptible to any unwanted adhesion between surfaces, leading to possible damage on deployment. Additionally, the heat set and pack treatment could cause deterioration of fibers and seams in the lightweight fabrics. Therefore, it was required that a heat set and pack demonstration be executed on a total of 1 lb. of fabric at a temperature of 82°C (180°F), with a pack density of 45 lbs. per cubic foot and a pack pressure minimum of 450 lbs. per square inch (figure 3). Seam and joint samples were included in this demonstration, as well as additional yardage to make up the remainder of the required 1 lb.

Parachutes are expected to encounter a salt fog environment. While it is known that the baseline 1.1 oz/yd^2 fabric can tolerate this exposure, the effect of exposure and possible formation of salt crystals within the smaller denier fibers of the lighter-weight Nylon was unknown. Thus, NASA also performed salt fog testing, with exposure in accordance with military standard MIL-STD-810G, Method 509.5. The efficiency of the seams and joints was demonstrated and documented before and after heat set and pack demonstrations, and before and after exposure to salt fog. Some seam samples were also subjected to both heat set and pack and salt fog exposure so that a predicted worst-case condition could be evaluated.

Two different parachute vendors participated in this development. The products of the Phase I work are four viable fabrics—two from each vendor. The permeability, elongation, break strength, and tear strength of each, along with the corresponding minimum requirements, are listed in Table 1. It may be easily observed that all requirements are met, with the one exception of the permeability of Fabric 4. Recall that the required permeability was 100 ± 20 cfm, or a minimum of 80 cfm. Because it is the upper bound of this requirement that is most significant to parachute performance, it was determined that the 4% deviation below the lower bound would be acceptable, allowing for inclusion of the lightest-weight fabric in the options to select from for Phase II of the work.

All seam and joint testing of seams constructed in all four fabrics resulted in efficiencies above the desired 80% efficiency. Heat set and pack did not induce any degradation in performance below this desired efficiency, while salt fog exposure did show a very small negative effect on Fabrics 2 and 4, while improved performance was observed in the case of Fabric 3. This result should be further investigated in a larger sample set for improved statistics.

Table 1. *Fabric Properties*

	Minimum Requirement	Fabric 1	Fabric 2	Fabric 3	Fabric 4
Areal weight (oz/yd²)	0.70	0.83	0.89	0.87	0.76
Permeability (cfm)	80.0	119	86.5	93.5	77.0
Elongation (%)					
Warp	20.0	33.9	31.4	37.7	36.4
Fill	20.0	26.5	27.8	37.5	37.5
Break strength (lbs.)					
Warp	34.0	45.2	42.8	41.9	41.1
Fill	34.0	37.5	43.5	43.2	41.7
Tear strength (lbs.)					
Warp	4.0	8.1	8.1	10	5.5
Fill	4.0	4.5	7.1	9.5	5.8

A single main parachute will be built and flight-tested during Phase II. A successful flight test will demonstrate mass and pack density reduction, with the parachute remaining packable and deployable without damage. Flight performance needs to be similar to the reference CPAS parachute in inflation loads, parachute stability, and parachute drag area. Timing of flight testing is intended to take advantage of existing planned CPAS tests with the agreement of all circumstances and parties.

Future development of a second lightweight fabric—an M5 fiber-based fabric for use in the structural grids of all parachutes in the system—is being pursued. M5 is a novel fiber with a tenacity, or strength-to-weight ratio, approximately twice that of Kevlar®. Development of M5 fiber-based fabrics in the form of cords, straps, and tapes could result in a weight savings to the vehicle estimated at 104 lbs. in addition to the decrease in pack density, which is so important for complete and rapid damage-free deployment of the parachutes.

Using Rotor Technology to Land a Spacecraft

Jeffrey D. Hagen, *Johnson Space Center*
Brent A. Evernden, *Johnson Space Center*
Adam L. Gilmore, *Johnson Space Center*

Two of the key challenges associated with a parachute-based landing system are poor landing accuracy and excessive touchdown velocity. Poor landing accuracy forced other parachute-based vehicles to land in remote, deserted areas (Soyuz) or in the ocean (Apollo). High touchdown velocity forced some vehicles to generate crew load attenuating solutions: stroking seats (Orion); water landing (Orion and Apollo); crushable landing struts (X-38); or retro-rockets (Soyuz). Other significant constraints exist for vehicles that land as a fixed wing glider (space shuttle). These challenges laid the groundwork for the development of a radically different landing technology called Spacecraft Morphing to Auto Rotation Targeted Landing (SMART/L).

After contributing thousands of volunteer hours over a 10-year period, the SMART/L project team received its first formal funding in Fiscal Year 2011. The original concept from 2001 proposed stowing rotor blades in a basic Apollo-shaped capsule. This concept continues to head toward a tangible reality as the Johnson Space Center (JSC) team conducted the first scaled drop test in March 2011 in Building 49. The SMART/L design team envisions developing a suite of rotor-based deceleration systems for space vehicles, thus providing a viable trade alternative to parachutes.

A reentry capsule outfitted with SMART/L technology would work as follows: after reaching the right speed and altitude, blades deploy from the capsule into the free stream, initiating rotation and telescoping of the blades. The blades are pitched in a manner to most efficiently use the free stream flow and maximize the rotational momentum of the system. Then, just as a helicopter would operate in an unpowered landing, the blades of the capsule are collectively pitched to convert the rotational inertia into vehicle lift for a soft, controlled landing (figure 1). Hover time can be extended by mounting small ramjet thrusters at the rotor blade tips.

The core SMART/L team from JSC's Structural Engineering Division continues to collaborate with the Flight Mechanics and Robotics divisions, Rice University, Ames Research Center, Defense Advanced Research Projects Agency, and local radio-controlled helicopter

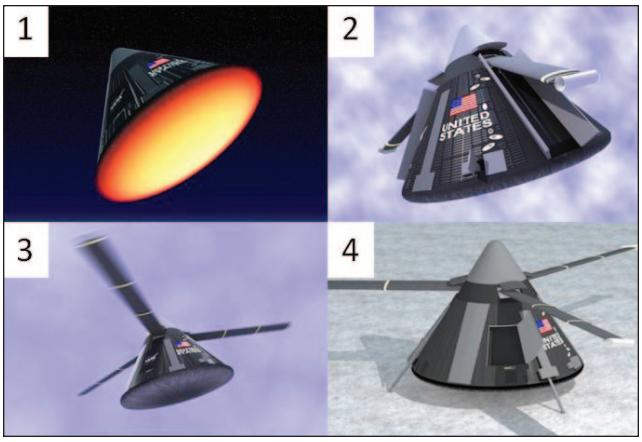


Fig. 1. *Rotor deployment sequence.*

organizations. Through these collaborations, the SMART/L team realized the following key advancements this fiscal year: scaled prototype capsule construction and drop testing from JSC Building 49's 95-ft indoor tower to test rotor spin-up and flare without motor power; retrofit of a radio-controlled helicopter into the capsule shape using ducted fans to replace the tail rotor (this enhancement enables fast turnaround, higher altitude [>1000 ft] drop testing to further assess rotor spin-up and flare using auto-rotation only); and computational flow dynamics analysis to assess loads and stability during rotor system deployment.

The SMART/L team soon plans to redirect its focus toward two of the top development risks for the system: rotor blade unfolding; and rotor blade telescoping. Specifically, these focus areas will include mechanism development and ground-based testing for the deployment systems (including wind tunnel testing), enhanced deployment and stability analyses, and demonstration of controllability in auto-rotation flight leading up to integrated demonstrations of in-flight deployment and landing.

The SMART/L team believes there is vast potential for this rotor technology in the near future, whether it be to return time-critical payloads from the International Space Station directly to JSC, or to enable an injured astronaut to reenter Earth's atmosphere and land on the helipad at the Houston Medical Center.

Martian Entry Simulation Using a Carbon Dioxide Test Gas in the Johnson Space Center Arc Jet Facility

Steven V. Del Papa, *Johnson Space Center*
Brian C. Shafer, *Jacobs Technology*
Leonard E. Suess, *Jacobs Technology*

The Atmospheric Reentry Materials Structures Evaluation Facility (figure 1) —otherwise referred to as the Arc Jet Facility—is a high-enthalpy wind tunnel that is used for simulating the extreme environment a spacecraft experiences upon reentry into Earth's atmosphere. Ground testing within the Arc Jet Facility is critical throughout all phases of a spacecraft's lifecycle, beginning at basic material screening and characterization, through analysis validation and material qualification, and through mission support involving flight anomalies and material requalification.

The Arc Jet Facility accomplishes this demanding task via electrically heating air (referred to as the test gas) using a 13-megawatt direct current power supply and supersonically accelerating the resultant plasma over a test article. The power level and the test gas flow rate are then adjusted to obtain reentry-equivalent surface conditions such as temperature, pressure, and shear on the model surface. However, perhaps the most important aspect of the arc jet test is obtaining the reentry-relevant chemical environment. At hypersonic speeds, the energy imparted on the surrounding air can disassociate the diatomic molecules (O_2 and N_2) into their atomic components: oxygen (O) and nitrogen (N). Atomic oxygen is chemically reactive; a material that would normally survive high temperatures within an inert environment can catastrophically fail. In addition, it is possible for a material to promote the recombination of these chemical bonds, resulting in an exothermic reaction that can greatly increase the heating. This is referred to as catalytic heating. Thus, arc jets are critical to understanding and properly modeling the behavior of spacecraft thermal protection systems within this environment.

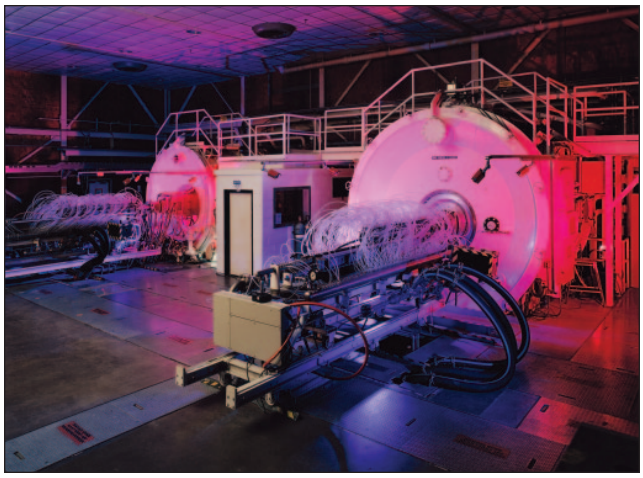


Fig. 1. *Photo shows the two test positions at Johnson Space Center's Atmospheric Reentry Materials Structures Evaluation Facility.*

The Arc Jet Facility simulates the Earth's atmosphere with individually controlled O_2 and N_2 test gas systems that deliver a 23:77 O_2:N_2 mass ratio within the arc heater. One major advantage of this configuration is the ability to dynamically adjust the O_2 ratio through the control system, from 0% up to 65%. The Mars Science Laboratory spacecraft is using a phenolic impregnated carbon ablator (PICA) as the heat shield. In 2008, engineers tested four PICA models in the Arc Jet Facility at varying O_2 ratios to better understand the impact of the atomic oxygen on the performance of this material (figure 2). All four PICA models were exposed to equivalent heating rates, impact pressures, and exposure durations, and a correlation of increased recession to increased oxygen content was evident. Since the Mars atmosphere can contain as much as 97% carbon dioxide (CO_2) by mass, a greater understanding of thermal protection system response to this radically different environment is required for accurate modeling and robust design to ensure mission success.

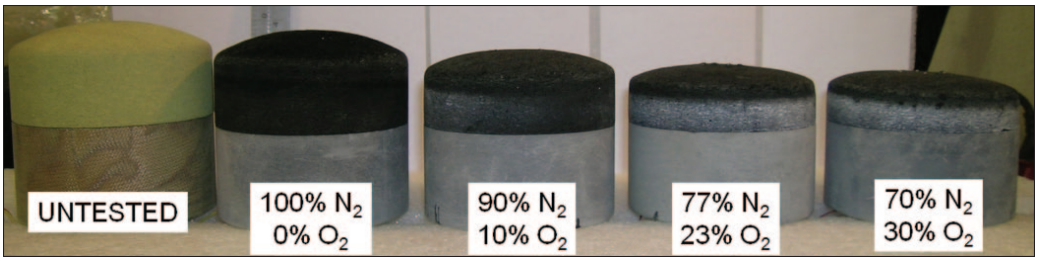


Fig. 2. *Four-inch-diameter phenolic impregnated carbon ablator models following arc jet testing at varying levels of oxygen.*

Martian Entry Simulation Using a Carbon Dioxide Test Gas in the Johnson Space Center Arc Jet Facility

continued

In the summer of 2010, a concerted effort began in the Arc Jet Facility to add a CO_2 test gas capability to simulate a Mars atmosphere. The primary obstacle to overcome was in determining the amounts, if any, of carbon monoxide, cyanide, and hydrogen cyanide being produced, and whether the amounts posed a hazard to personnel and/or equipment. Since carbon monoxide can be an explosive hazard at certain pressures and concentrations, nitrogen was injected into the vacuum system as a dilutant. A residual gas analyzer was installed downstream of the heat exchanger in the vacuum system to sample the cooled exhaust gases. Also, after each test run with CO_2, an industrial hygienist analyzed surface sample wipes of the test chamber for the presence of cyanide. A secondary obstacle to overcome was in determining whether the presence of CO_2 within the arc heater was detrimental to its performance or to the lifespan of the electrodes.

Testing began at moderate CO_2:N_2 mass ratios to gain familiarity with the resultant safety data, and subsequent tests were performed with an increasing concentration of CO_2. In February 2011, engineers performed a test run on a PICA model with a 90:10 CO_2:N_2 mass ratio and a 2.60-megawatt power level (figure 3). The next test run, scheduled for the summer of 2011, is designed to achieve the final goal of a 97% CO_2 concentration. Throughout this effort, personnel found no detectable levels of cyanide. The production rate of carbon monoxide is now understood and can be managed safely. Also, the arc heater and electrodes performed remarkably well, with no failures. An efficient process has been developed to allow rapid transitions to Earth or Mars configurations.

In parallel with the data for safety, flow field calibration data were obtained in various forms. Stagnation heating rates and pressure readings were made with calorimeter probes. Laser-induced fluorescence was used for quantifying the velocity, temperature, and species concentration of the atomic oxygen.

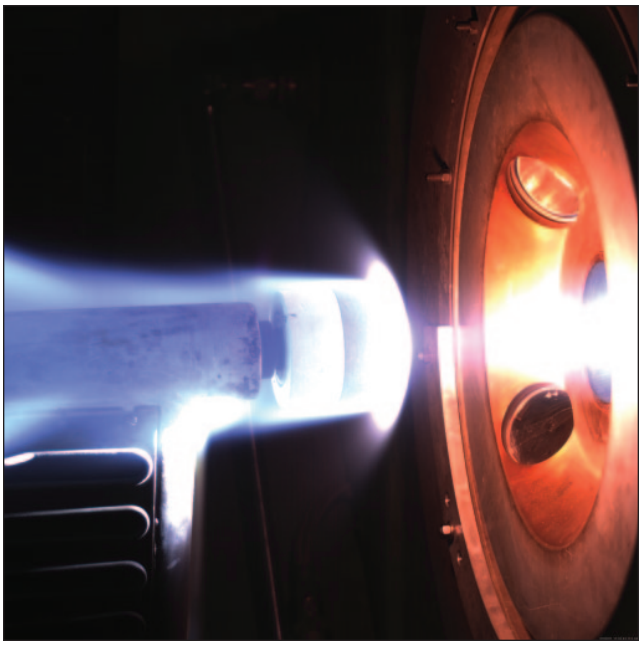


Fig. 3. *Four-inch-diameter phenolic impregnated carbon ablator model exposed to a 90% carbon dioxide environment in Johnson Space Center's Atmospheric Reentry Materials Structures Evaluation Facility.*

As a result of these efforts, engineers developed a unique capability for the agency and for the nation. No other facility worldwide has performed a successful arc jet test with 90% CO_2 at this power level and associated test gas flow rates. Future testing is planned to expand capability (up to 13-megawatt power level and higher gas flow rates), and to understand and accurately model the test environment via laser-induced fluorescence data, stagnation heat flux and pressure data, and probe sweeps of the flow field. This capability is a valuable, cost-effective tool for the thermal protection system community to screen, develop, and certify materials and systems for Mars and other CO_2-rich planetary entry environments.

Thermal and Structural Testing of Repaired Orbiter Thermal Protection Tiles

Priscilla A. Kelly, *Johnson Space Center*
Louise Shivers, *Johnson Space Center*
Kelly Carney, *Glenn Research Center*
Cooper Snapp, *Johnson Space Center*

Johnson Space Center (JSC) and The Boeing Company collaborated on thermal and structural testing and analysis of orbiter thermal protection tiles that have been repaired with Shuttle Tile Ablator 54 (STA-54). Tile repair is a new aspect of mission support since the return to flight effort following the space shuttle *Columbia* accident in 2003.

Using STA-54 to repair tile damage is one contingency option that has been developed and tested to understand the thermal and structural behavior of the ablative tile repair material and tile-ablator combination in the sequence of environments the orbiter experiences throughout its trajectory from space, reentry into the Earth's atmosphere, and landing. Analytical tools developed by Boeing are used to assess STA-54 and are correlated with ground-based STA-54 vacuum-dispensed test data. Scientists conducted a series of tests to develop and compare on-orbit-dispensed and ground-dispensed STA-54 test data to show that analytical tools are valid for assessing on-orbit dispenses.

In March 2008, orbiter tile test articles with large cavities simulating tile damage were filled with STA-54 on-orbit during STS-123. In parallel, tiles with the same configuration were filled with STA-54 in a vacuum. Upon return from flight, two of the flight test articles and a ground-filled test article were thermally tested at JSC's Arc Jet facility and subsequently structurally tested in the JSC Structures Test Laboratory.



Fig. 1. *STS-123 on-orbit STA-54 dispense (top); STA-54 on-orbit dispensed test articles post-flight (bottom).*

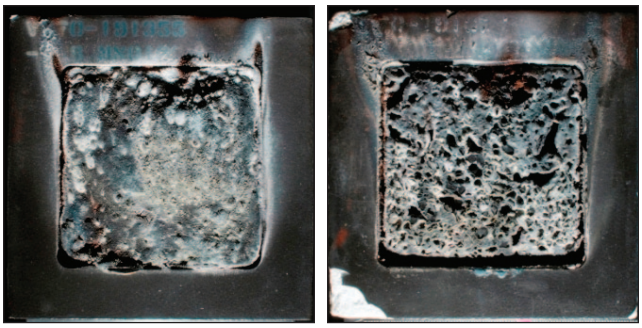


Fig. 2. *On-orbit dispensed Arc Jet test articles.*

Thermal and Structural Testing

During Arc Jet tests, which simulate the orbiter's reentry heating environment, the tiles were subjected to a 927°C (1700°F) environment for 900 seconds. Post test, the test articles were three-point flexure tested at room temperature to a deflection an order of magnitude greater than the maximum deflection expected during flight.

Thermal and Structural Testing of Repaired Orbiter Thermal Protection Tiles

continued

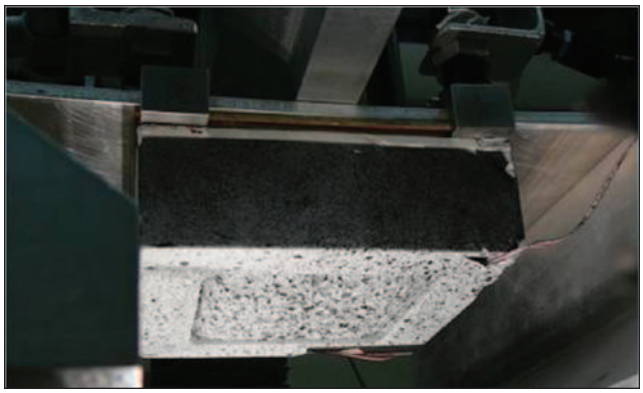


Fig. 3. *Three-point flexure test.*

Thermal test results indicate that both ground-dispensed and on-orbit-dispensed test articles performed similarly in STA-54 ablation and swell. Transient temperature profiles closely matched for ground-dispensed, on-orbit dispensed, and the baseline nominal undamaged tile. Tile strain data collected during flexure testing for STA-54 ground-dispensed and on-orbit-dispensed tile were within range of each other, exhibiting very small tile strain—200 micro-strain at most. Test data show similar thermal and structural performance of ground-dispensed and on-orbit dispensed Arc Jet tile repairs, a favorable outcome that demonstrates the analytical tools correlated with ground-dispensed STA-54 tile repairs are valid for on-orbit STA-54 tile repairs. These results build confidence in the thermal and structural performance of STA-54. Confidence is also gained in the material as a viable contingency option for tile repair that will protect the orbiter's aluminum structure from high heat during reentry—an important role in bringing the crew home safely.

Functional Cargo Block Structural Life Extension

James J. McMahon, *Johnson Space Center*

The Functional Cargo Block—usually referred to by the Russian acronym FGB—was the first module of the International Space Station (ISS) to be launched. This event took place on November 20, 1998 (figure 1).

The certified life of the FGB was originally 15 years, meaning it would reach the end of its certified life by the end of 2013. The original life expectancy for the ISS was 2016. This 3-year discrepancy drove the FGB life extension effort that began in 2004.

The ISS is truly an international collaboration involving many international partners. Two major contributors are the United States and Russia. The design and certification philosophies between these two partners, however, were not necessarily the same. To work together successfully, the partners developed an agreement stating that certification of the U.S. elements would be performed using U.S. standards, and certification of the Russian elements would be performed using Russian standards. In light of the United States' responsibility for overall ISS integration, both partners worked jointly to evaluate—not certify—Russian elements against U.S. standards. This evaluation approach was used for the FGB life extension effort.

The structural life of the FGB was certified using a dedicated fatigue test article. Three highly loaded interfaces were identified for testing. These locations were the forward end where the FGB attached to the pressurized mating adapter and the U.S. segment, the aft end where it attached to the service module, and at one of the two solar array attachment points. Engineers developed a design load spectra at each of these interfaces, which would envelop the actual load spectra to which the interfaces would be exposed. These spectra were then applied at each of the three interfaces one at a time with each set of three spectra representing a 15-year life. Since the Russians required a scatter factor of 8 on life, this procedure was repeated seven more times (figure 2).

The United States evaluates life with a different approach, and generally does an analytic determination of life. That is, the United States uses fatigue analysis, and for critical locations, a fracture mechanics analysis.

Several pieces of data were necessary to perform the fracture mechanics analysis—data not immediately



Fig. 1. *The Functional Cargo Block on orbit.*



Fig. 2. *The Functional Cargo Block.*

available for the FGB. These data included: fracture mechanics properties of the Russian materials, and non-destructive evaluation (NDE) flaw detectability of the Russian NDE techniques.

Samples of several materials were shipped from Russia to Johnson Space Center in Houston, Texas, for testing to obtain the fracture mechanics properties of the Russian materials. Two of these materials were sheets of Russian Aluminum AMg6-H and AMg6-M. These materials are commonly used by the Russians, as the FGB shell was fabricated using AMg6-H. Several technical interchange meetings were held in Houston and in Moscow to determine the materials' NDE flaw detectability. Russian

Functional Cargo Block Structural Life Extension
continued

techniques were used on standard NDE specimens. It was determined that the Russian techniques had almost identical results to the U.S. methods.

With these data, the U.S. and Russian team performed further analysis as part of the additional evaluation for the integration task. There were two areas of evaluation, the first of which was robustness of the design. Using fracture mechanics techniques, the team demonstrated that the FGB was a leak-before-burst design, meaning if a crack-like flaw occurred in the structure, the module would not rupture but would, at worst, leak. The second area of evaluation involved performing spot checks of some critical areas using fracture mechanics techniques.

Life Extension
Life extension for the FGB (and for the ISS) can be a difficult task. Since the hardware is on orbit, it can't be structurally modified to give it additional life, or be re-inspected to demonstrate additional life. Because of the difficult nature of life extension, the FGB certification included U.S. methods along with the Russian methods.

Fatigue Test Article
While the FGB was not accessible during the life extension activities, the Russian partners retained their fatigue test article to allow for additional test cycles. Additional fatigue testing was done using the design spectrum at the forward and aft interfaces, which were run to a 2028 equivalent time frame. The solar array attachments were not included in this assessment because the FGB solar arrays were refolded due to an interference with the main radiators on the U.S. segment after the solar arrays were deployed (figure 3).

Updated Spectra
Fracture mechanics methods can be more conservative than fatigue analysis or tests, therefore it was unlikely that a fracture mechanics method would demonstrate life for all components of the FGB to 2028 using existing analysis with the existing design spectrum. However, since the ISS has been in operation for the past 10 years, access to actual loads data to which the FGB has been exposed is available.



Fig. 3. *The Functional Cargo Block with solar arrays folded.*

As such, a new spectrum was developed using the history to date and new predicted spectra to 2028.

Analysis Updates
In some cases, simply modifying the loads spectra was not sufficient to demonstrate adequate life. In these cases, it was also necessary to refine the stress analysis that determined the stresses used in the fracture analysis.

Weld Fracture Data
The FGB structural shell consists of a number of machined segments that were welded together. During its initial evaluation, the material testing done to obtain fracture mechanics properties did not include welded materials. To adequately perform life analysis on the welds, these data were needed. To this end, the Russians produced weld samples for use in developing these properties. Given the FGB's original construction was 15 years ago, advances in welding process in the intervening years raised concerns. Several weld sections were cut out of the fatigue test article to account for this. These sections, along with samples that the Russians produced, were tested at Johnson Space Center to determine the fracture properties of the as welded material. These data were, in turn, forwarded to the Russians for use in their fracture assessment of the FGB.

Conclusion
Extending the life of an on-orbit vehicle can be challenging, and the FGB was no exception; however, life predictions for the FGB were increased by gathering additional data and removing conservatism from analysis. Although this work is not complete, all indications are that the FGB life certification will be extended to 2028.

Dynamic Requirements for Foam Replacement

Otto Crenwelge, *Johnson Space Center*

Foam packaging materials are used to attenuate the quasi-static and dynamic loads transmitted to orbital replacement units during launch to the International Space Station. Currently, there is a shortage of data in manufacturer's literature to describe the static and dynamic characteristics of their foam packaging materials. This paper presents a normalized approach to describe the dynamic attenuation characteristics of foam materials. The approach can also be used to describe the properties needed in a substitute or less expensive material, if one should be needed. As an example, the normalized dynamic attenuation characteristics of ZOTEK® and Minicel® are developed from data measured in foam sample tests at Johnson Space Center.

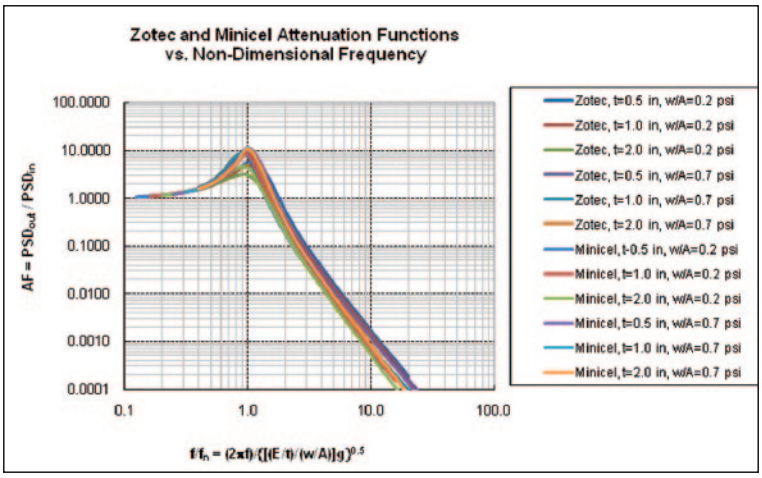


Fig. 1. *Measured non-dimensional dynamic attenuation functions of ZOTEC® and Minicel®.*

Random Vibration Attenuation Functions of ZOTEK® and Minicel® vs. Frequency

Attenuation functions vs. frequency of ZOTEK® and Minicel® foams obtained from random and sinusoidal vibration tests are presented in Appendix I of the NASA SSP 50835 and in the Excel file entitled "Cargo Tool" on the International Space Station Vehicle Office – Management Integration Office website at http://iss-www.jsc.nasa.gov/nwo/vh1/vmi/web/. The attenuation function is the square of the transmissibility function and is defined as the ratio of acceleration power spectral density (PSD) of the response to that of the excitation.

The attenuation functions are functions of frequency f, geometric properties (thickness [t], weight [w], cross-sectional area [A]) and material properties (modulus of elasticity [E] and damping [η]), and their curves vary widely with these parameters.

Attenuation Functions of ZOTEK® and Minicel® vs. Non-dimensional Frequency

The frequency scale of the attenuation functions can be scaled and made non-dimensional by dividing each curve by its measured approximate natural frequency. Figure 1 shows the curves of ZOTEK® and Minicel® from the original data of SSP 50835 and the Cargo Tool after dividing each curve by the center frequency of the 1/3-octave band that contains the peak response. As is seen, this shifts some of the curves slightly from peaking at a frequency ratio of 1.0, since the exact value of fn for each curve is unknown; i.e., it is only known that it lies somewhere in that 1/3-octave bandwidth. In simplest terms, the frequency scales of the curves have been non-dimensionalized by the natural frequency, which is defined for a single-degree-of-freedom mass/spring system.

Note that the curves of figure 1 pretty much overlap, since ZOTEK® and Minicel® are both closed-cell polyethylene foams. This makes it hard to differentiate between their material characteristics. Hence, another normalization approach is needed to separate the characteristics of the two.

Attenuation Functions of ZOTEK® and Minicel® vs. Normalized Frequency

To better separate the material characteristics of ZOTEK® and Minicel® while negating the geometric effects of the samples tested, the original data of SSP 50835 and the

Dynamic Requirements for Foam Replacement

continued

Cargo Tool were instead normalized as in figure 2 by multiplying the frequency scale (f) by 2π times the square root of the product of (t/g) times (w/A), where g is the acceleration of gravity.

This approach separates the effects of the material property E of each material while reducing the geometric effects of w, A, and t. Note that this was done with no knowledge of the values of E for each material.

Additional Simplification of Normalized Attenuation Functions of ZOTEK® and Minicel®

To make the comparison between ZOTEK® and Minicel® simpler, the multiple geometric curves were removed from figure 2 and only the maximum values at each frequency for each foam were enveloped and plotted in figure 3 to produce the envelope attenuation function for each foam. These results conservatively represent the highest amplification values obtained in the tests of these two materials.

Conclusion

The above approach using the envelopes of normalized maximum dynamic attenuation functions can be used for producing conservative estimates of random vibration requirements of foams. Hence, if needed, this approach can be used for comparing one foam's dynamic material data with those of other foams for selection of substitute foam materials.

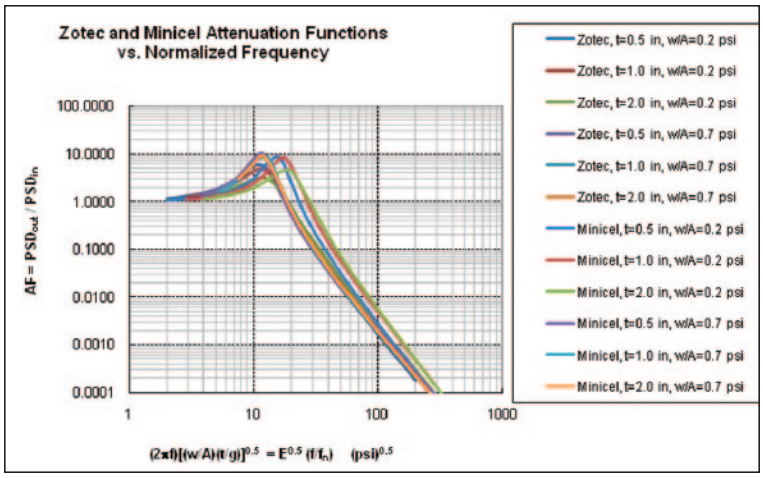


Fig. 2. *Measured normalized dynamic attenuation functions of ZOTEC® and Minicel®.*

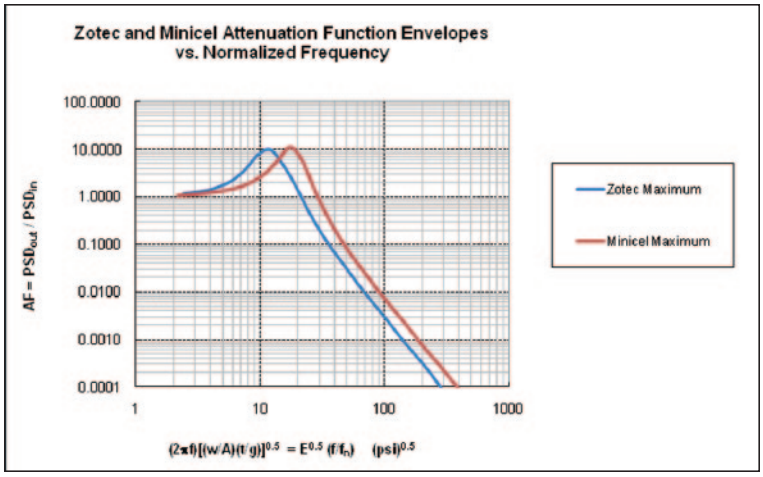


Fig. 3. *Envelopes of normalized measured dynamic attenuation functions of ZOTEC® and Minicel®.*

Vibration Attenuation Effectiveness of Foam Sandwich Enclosure

Otto Crenwelge, *Johnson Space Center*
Paul Caradec, *Johnson Space Center*
Brian Rhone, *Johnson Space Center*
Vincent Fogt, *Johnson Space Center*
Alan McDougal, *Johnson Space Center*

Various foam materials and cargo bags are used to attenuate vibration transmitted to orbital replacement units to assure that International Space Station's (ISS's) orbital replacement units can successfully sustain launch environments when they are directly attached to the spacecraft structure, as is often done for the Progress, Soyuz, and other visiting vehicle launches. One such attenuation scheme is the foam sandwich "clamshell" box (figure 1), comprising stiff-soft-stiff foam materials. This box was designed specifically to carry the Recycle Filter Tank Assembly (RFTA) orbital replacement units to the ISS.



Fig. 1. *Recycle Filter Tank Assembly trainer in foam sandwich "clamshell" box, sandwich wall comprising stiff-soft-stiff foam materials, and clamshell strapped to test plate on shaker table.*

NASA performed a number of random vibration tests on the RFTA trainer and the RFTA flight unit #5 to verify the vibration attenuation effectiveness of the clamshell enclosure design. The trainer and the flight unit were both tested to the ISS workmanship vibration environment while hard-mounted to the shaker table. The trainer was also tested to both the ISS workmanship environment and the Space Shuttle Program 50835 Common Interface Requirements Document environment while isolated inside the clamshell enclosure strapped to the shaker table. This environment envelopes the internal volume stowage vibration environments of all the currently defined visiting vehicles.

For comparison, NASA obtained measured data predictions of isolated trainer response by multiplying the hard-mounted trainer response spectra by the attenuation functions developed from foam sample vibration test data. A similar analytical approach was used to predict the isolated response of the flight unit. While it would have been desirable, for research purposes, to have tested the flight unit in the foam sandwich clamshell, this was not deemed necessary for flight certification purposes due to the reasonable agreements obtained between isolated measurements and predictions for the trainer.

Conclusions

Recycle Filter Tank Assembly Tests

- The conclusions listed below were drawn from the random vibration tests.
- Measured response levels of the hard-mounted flight unit are lower than those of the hard-mounted trainer.
- Clamshell isolated RFTA responses are considerably attenuated over the hard-mounted responses for flexible body modes above 40 Hz (figure 2).
- Amplification at low frequencies is caused by resonance of the RFTA rigid body mass on the foam spring system, and hence is not a problem.
- Attenuation functions for the foam sandwich clamshell, as developed from measured foam sample attenuation data, provide good estimates of the measured clamshell attenuation functions.
- Multiplying hard-mounted trainer test data by the predicted attenuation functions yields reasonable predictions for the foam clamshell attenuated trainer response (figure 2).
- Multiplying hard-mounted flight unit test data by the predicted attenuation functions yields reasonable estimates of foam clamshell attenuated flight unit response (figure 3).

Vibration Attenuation Effectiveness of Foam Sandwich Enclosure

continued

Comparison with Progress Vehicle Requirements

Results of random vibration tests conducted on the RFTA were compared against Progress vehicle requirements. Findings are:

- The foam-sandwich clamshell box and strap isolation system will attenuate the Progress vehicle random vibration excitation by a factor of 100 at the RFTA's 95 Hz first resonance frequency and by much greater factors at higher frequencies.
- Hence, the RFTA is verified to meet the Progress vehicle random vibration requirements. Further vibration testing of the RFTA and its foam-sandwich isolation box and strap system is not needed.

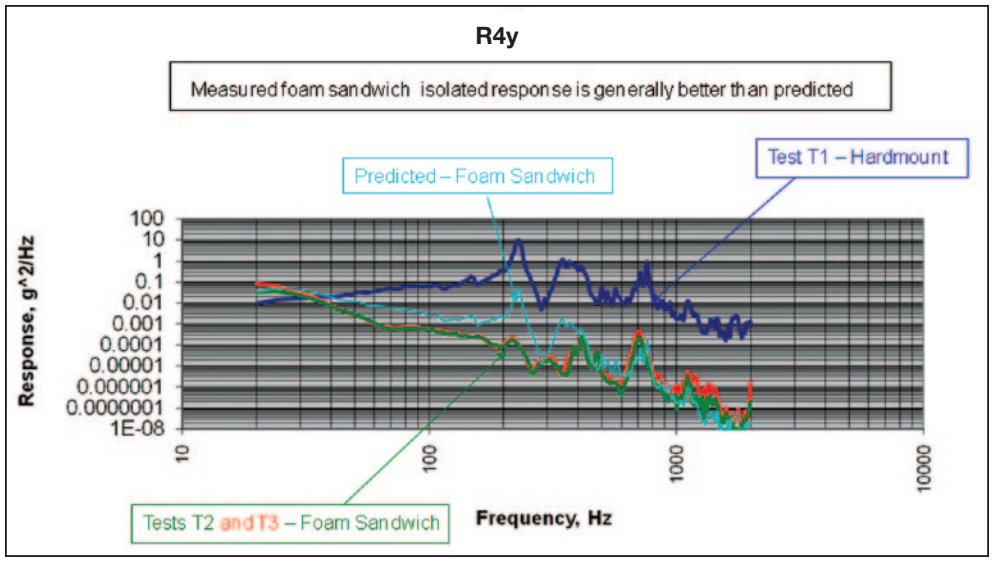


Fig. 2. *Comparison of measured hard-mounted response, measured clamshell isolated responses, and predicted clamshell isolated response (from measured foam sample attenuation data). Note: label R4Y denotes the Y direction response accelerometer at measurement location 4.*

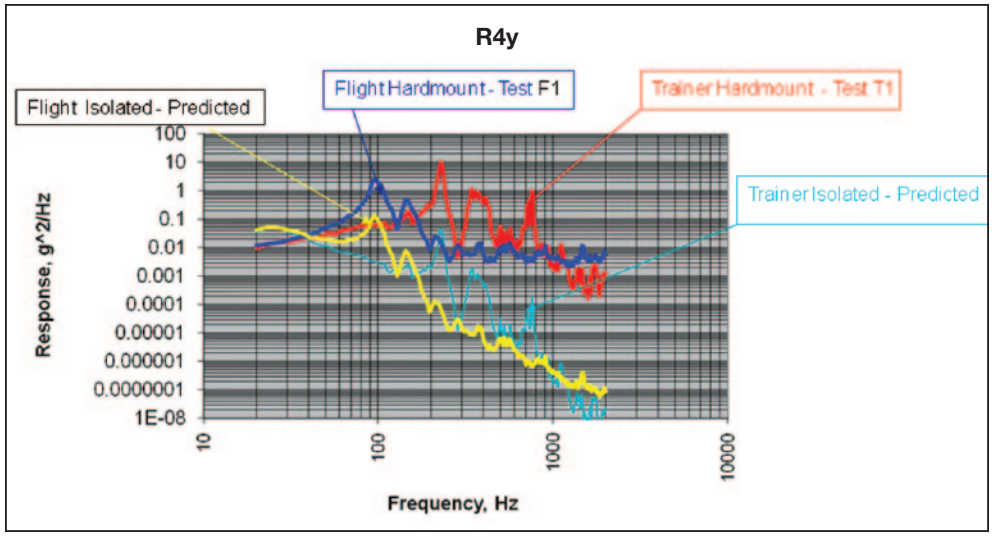


Fig. 3. *Comparison of Recycle Filter Tank Assembly trainer and flight unit responses as measured in hard-mounted configuration and predicted for foam clamshell configuration using measured foam isolation data. Note: label R4Y denotes the Y direction response accelerometer at measurement location 4.*



Space Power, Energy Storage, and Propulsion



Future Robotic Lander Attitude Control and Descent Thruster Testing

Asher Lieberman, *White Sands Test Facility*
Jeremy Bruggemann, *White Sands Test Facility*
Huu Trinh, *Marshall Space Flight Center*
Kimberly Newton, *Marshall Space Flight Center*

A series of thruster tests in support of the Robotic Lunar Lander Development (RLLD) Program were successfully completed in September 2010 at NASA Johnson Space Center's White Sands Test Facility (WSTF). The RLLD Program is a collaborative effort by NASA's Marshall Space Flight Center (MSFC), Johns Hopkins University Applied Physics Laboratory (Laurel, Md.), and Pratt & Whitney Rocketdyne (Canoga Park, Calif.). The program's objective is to develop the next generation of robotic lunar landers that NASA will use to enable future exploration of the moon's surface and the surface of other celestial bodies with little to no atmosphere. The thrusters tested will be used to maneuver and land the golf-cart-sized robotic landers.

The two thrusters tested were considered to be high thrust-to-weight ratio thrusters. One of the thrusters was a 100-pound-class thruster, which will be used for spacecraft control during descent operations. The other thruster was a 5-pound-class thruster and will be used for attitude control in the roll, pitch, and yaw degrees of freedom. These miniaturized thrusters were selected to meet the requirement of reducing overall spacecraft mass due to their light weight and ability to be integrated in a compact manner. Additionally, the requirement to reduce the mission cost was met as these thrusters were existing hardware obtained from the Divert and Attitude Control System (DACS) developed by the U.S. Missile Defense Agency of the Department of Defense.

The tests performed at WSTF were a critical step in reducing the propulsion technology risks associated with MSFC's robotic lander mission. The objective was to use the testing results to develop future plans associated with the lander's propulsion system design. Specifically, the fact that the thrusters were originally used for short-duration flights, and had not been qualified for space missions under the DACS program, made testing necessary to assess their capability for long-duration burns. The tests were also performed to evaluate thruster performance and combustion behavior in a simulated space environment with representative lunar mission profiles developed by the RLLD Program.

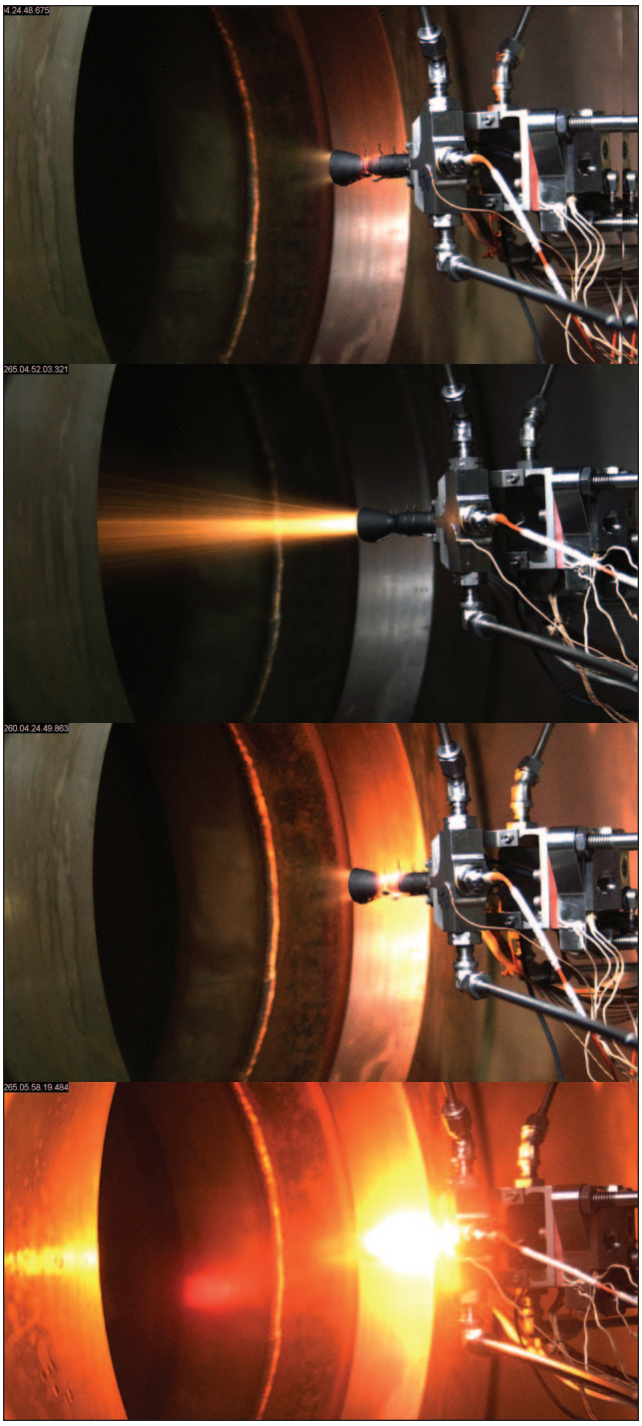


Fig. 1. *5-pound-class hot-fire test in Test Stand 406 at White Sands Test Facility.*

Future Robotic Lander Attitude Control and Descent Thruster Testing

continued

Thruster Testing

Engineers tested both thrusters in Test Stand 406 at WSTF. They selected this test stand for use due to its ability to provide an environment with little to no atmosphere through the use of the facility's vacuum pump system and Small Altitude Simulation System. The test stand's existing hypergolic propellant feed systems that were in place from the space shuttle Vernier Reaction Control System and Primary Reaction Control System fleet lead and qualification testing easily accommodated the 100-pound-class thruster testing. However, the 5-pound-class thruster testing required some modifications to the hypergolic feed systems. WSTF's expert technicians and engineers worked diligently to modify the system. The modifications involved rebuilding the interfacing system between the test article and the monomethylhydrazine (MMH) and nitrogen tetroxide mobile skids, which both have maximum allowable operating pressures of 1500 pounds per square inch (psi).

Additionally, engineers made modifications to the thrust stand to which the thruster was mounted to accommodate the 5-pound-class thruster's high-frequency pulsing mission duty cycle. They performed modal testing of the thrust stand to identify areas of the stand that required stiffening. This was done to ensure that the thruster's pulsing frequency was not near any of the thrust stand's resonant frequencies, as this situation could have led to over excitation of the thrust stand and resulted in structural damage.

Firing a pressure sweep from approximately 3.5 to 10 torr was achieved during tests of the 100-pound-class thruster using the facilities' small altitude simulation system, which strictly used the venturi effect to reduce test cell pressure. The pressure sweep in the test cell met the requirements levied by the RLLD Program, and mimicked the project's lander mission profile and operation scenarios. The test included the following: several trajectory correction maneuvers during the cruise phase; nutation control burns to maintain spacecraft orientation; thruster vector correction during the solid motor braking burn; and a terminal descent burn on approach to the lunar surface.

A simulated altitude of approximately 48,800 m (~160,000 ft) was obtained for the 5-pound-class thruster testing by using the facility's vacuum pump system (figure 1). The objective for the 5-pound-class thruster test was similar to the 100-pound-class thruster test with an additional emphasis on the thruster heating assessment due to the long-duration mission profile and operation with MMH fuel and a nitrogen tetroxide (75%)/nitrogen oxide (25%) (MON-25) oxidizer. Because the MMH/MON-25 propellant system has never been used in space, these tests allowed engineers to benchmark the test against other propellant systems.

The test program fully accomplished its objectives, including evaluation of combustion stability, engine efficiency, and the ability of the thruster to perform the mission profile and a long-duration, steady-state burn at full power. Stable combustion was exhibited in all scenarios and favorable temperature results were attained. The test results will allow the RLLD Program to move forward with robotic lander designs using advanced propulsion technology.

Advanced Battery Technology Programs

Judith A. Jeevarajan, *Johnson Space Center*
Pranav Patel, *Engineering and Science Contract Group*

The advanced battery technology programs include market research and testing of state-of-the-art, commercial off-the-shelf as well as custom-made cells for testing and inclusion in the existing NASA Johnson Space Center cell database. As in the past, this allows for the ease of selection and use of cells for quick turnaround projects requiring power for government-furnished equipment as well as payload hardware. Advanced cell technology studies were carried out under the Exploration Technology Development Program that was changed to Exploration Technology Development and Demonstration—the government-furnished equipment battery technology programs. The results from a few of the cell studies will be described in this publication.

As part of the Exploration Technology Development Program /Exploration Technology Development and Demonstration effort, commercial off-the-shelf cell studies included the Panasonic as well as AGM cell test programs. The Panasonic lithium-ion (Li-ion) cell of 2.9 ampere-hour (Ah) capacity had an energy density that was greater than 200 Watt-hours per kilogram (Wh/kg). The AGM 7.5 Ah cell had an innovative safety circuitry internal to the cell in the header area. Tests carried out included rate capability studies, performance under different temperatures, overcharge, over-discharge, external short, heat-to-vent, and simulated internal short tests.

Table 1. *Summary of the Rate Capability Studies Carried Out on the Panasonic 18650 Lithium-Ion Cell*

Charge Rate	Discharge Rate	Cycle Number	Capacity (Ah)	Energy Density (Wh/kg)	Change in Energy Density From 1 to 200 Cycles (Wh/kg)
C/5	C/10	1	2.917	241.91	
		200	2.792	231.28	10.63
C/5	C/5	1	2.899	239.06	
		200	2.676	219.69	19.37
C/5	C/2	1	2.827	228.25	
		200	2.622	210.50	17.75
C/5	C	1	2.817	221.75	
		200	2.493	194.51	27.24
C/10	C/10	1	2.914	242.34	
		200	2.781	230.88	11.46
C	C	1	2.812	222.15	
		200	1.195	88.97	133.19

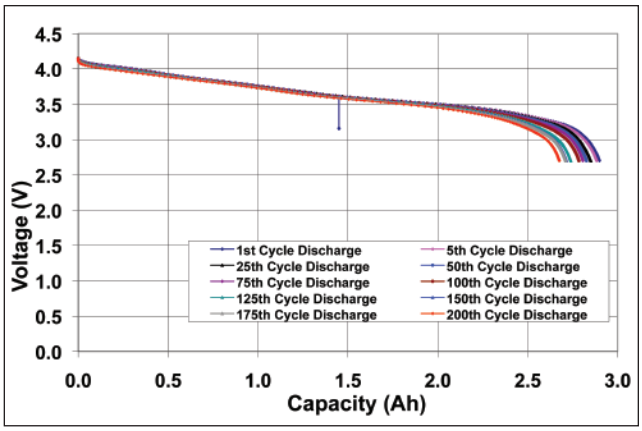


Fig. 1. *Panasonic 18650 lithium-ion cell rate capability at C/5 charge and discharge rates.*

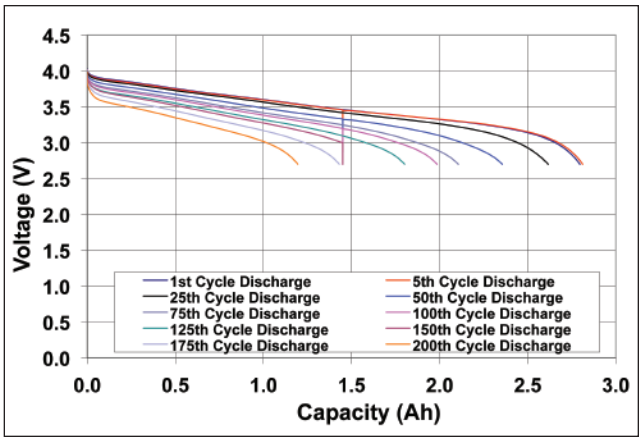


Fig. 2. *Panasonic 18650 lithium-ion cell rate capability at 1C-rate charge and discharge.*

Figures 1 and 2 show the trend for two different rate protocols. Table 1 provides a summary of the results obtained for the rate capability studies for the Panasonic 18650 Li-ion cell.

Advanced Battery Technology Programs

continued

Figures 3 and 4 show the trend for two different sample rate protocols for the AGM Li-ion cells.

The AGM Li-ion cells showed variability in performance from cell to cell and did not have a high rate capability. They performed very well at low rates of charge and discharge. It was also observed, during the overcharge test, that the circuit board inside the cell cuts off cell performance making the cell safe.

Cell studies under the government-furnished equipment advanced technology program included the performance and safety testing of the Varta Li-ion polymer cells. The Varta Li-ion polymer cells were used to power a nano-satellite flown by the University of Texas at Austin in the space shuttle payload bay and later released on orbit for Global Positioning System studies. Another test program was also carried out to determine the effect of over-discharged cells in a cell string that had one imbalanced cell. The extent of capacity imbalance was varied and characterized to determine the voltage imbalance this would induce. The performance of the cell string was studied for a maximum of 75 cycles to determine the level of imbalance that was tolerated and safe. It was determined, under the conditions studied, that if the imbalance was approximately 20 millivolts (mV), no over-discharge into reversal was observed for the 75 cycles studied. But if the imbalance was greater than or equal to 70 mV, the unbalanced cell goes into reversal during the first discharge. With imbalances in between these values, the number of cycles obtained before cell reversal occurred varied linearly. For example, with 100 milliampere-hours (mAh) removed (imbalance of 50 mV), reversal starts occurring at about 56 cycles. For the case where 125 mAh were removed (imbalance of 60 mV), cell reversal starts at 22 cycles. Figure 5 shows the charge profile for the cell that had gone into reversal on the 22nd cycle.

Destructive physical and chemical analysis of cells at over-discharged or reversed states indicated excess hydrofluoric acid is present in over-discharged cells. This could be a huge impact on cells in over-discharged conditions as they could cause corrosion of the inner walls of the metal can with age.

The authors would like to acknowledge Mobile Power Solutions (Beaverton, Ore.), Applied Power International (Athol, Idaho), and Symmetry Resources, Inc. (Arab, Ala.), for carrying out a majority of the tests. They would also like to acknowledge all the collaborators from the battery industry for giving the authors an opportunity to test their cells.

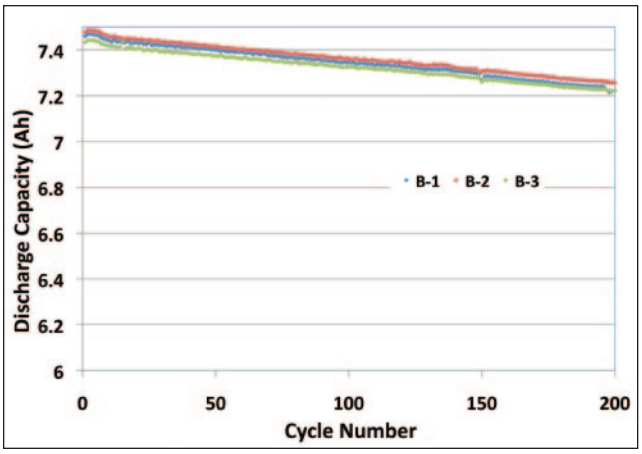


Fig. 3. *Rate capability test for the AGM 7.5 Ah lithium-ion cell at C/5 charge and discharge rates.*

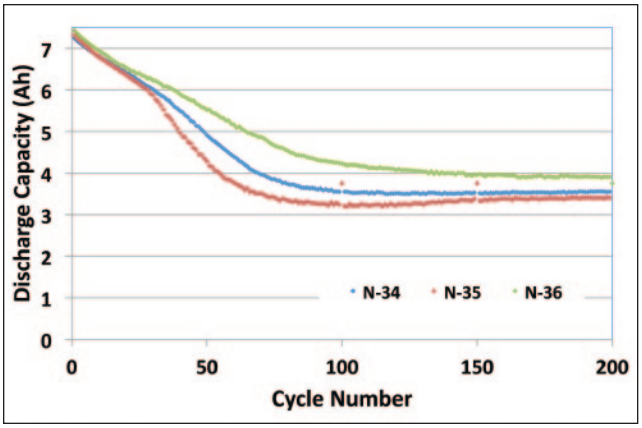


Fig. 4. *Rate capability test for the AGM 7.5 Ah lithium-ion cell at 1C-rate of charge and discharge.*

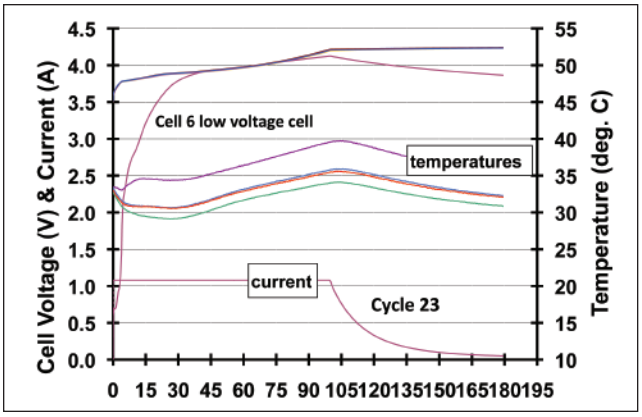


Fig. 5. *Charge profiles of cell string with an imbalanced cell that had 125 mAh capacity removed at the start of the test program.*

Safety Advancements in Lithium-ion for the Exploration Technology Development Program Battery Program

Judith A. Jeevarajan, *Johnson Space Center*
Pranav Patel, *Engineering and Science Contract Group*

The Exploration Technology Development Program that was changed to Exploration Technology Development and Demonstration had contracts awarded through NASA Research Announcements to obtain safety improvements from two companies—Physical Sciences Inc. (PSI) (Andover, Mass.) and Giner, Inc. (Newton, Mass.).

PSI worked on coating lithium-ion metal oxide cathode powders with a lithium cobalt phosphate coating to provide a safer cathode material. The advantages of using the coating included obtaining a coating that was a lithium conductor, achieving greater stability than the metal oxide counterparts, reaching higher energy density of the cathode material, and identifying common processing steps resulting in low-cost manufacturing. In the case of the coated material, the lithium metal phosphate layer remains in the reduced form even at full charge voltages, preventing the oxidation of the electrolyte. Figure 1 shows an illustration of the coating used by PSI.

In Year 1, PSI coated commercially available lithium cobalt oxide with lithium cobalt phosphate, showing a suppression of the exotherm observed due to the heating of the delithiated material, using Differential Scanning Calorimetry studies. The electrochemical performance was demonstrated to be equivalent at C/10 rates at both room temperature and 0°C (32°F). Personnel observed greater than 89% capacity retention after 200 cycles, with the coated cathodes and overcharge testing in pouch cell configurations showing that the heat generation under this abuse condition was reduced. The coating was also performed on a Jet Propulsion Laboratory synthesized cathode and shown to shift the peak exotherm to higher temperatures although the total heat generated remained unchanged.

In Year 2, the application and scale-up of the coating developed in Year 1 was carried out with a mixed metal oxide cathode (TODA NMC-9100) supplied by SAFT America, Inc. (Cockeysville, Md.), per NASA Johnson Space Center (JSC) contract. Tasks included cycle life and safety testing of the coated material in coin cell and pouch cell configurations. In Year 2, the coating procedures were also optimized and testing carried out to show that the exotherms observed on heating the delithiated cathode material were reduced, the change in discharge capacity

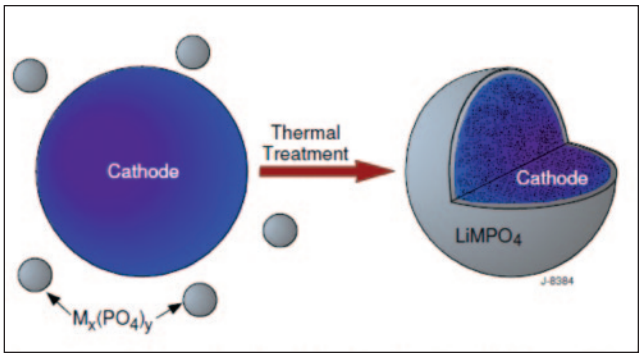


Fig. 1. *Illustration depicting coating of the cathode metal oxide powders with lithium metal phosphate.*

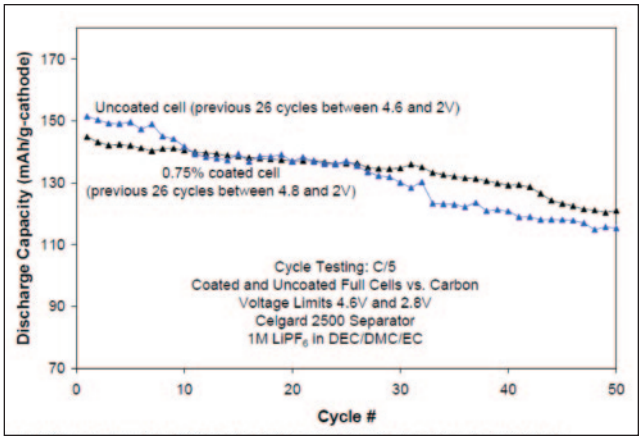


Fig. 2. *Capacity trend for Physical Sciences Inc. coin cells with and without the phosphate-coated cathodes.*

over 50 cycles at C/5 rate was less than 1 % (figure 2), and there was no reduction in discharge capacity in 1-Ampere-Hour (1Ah) pouch cells. The final optimized coating consisted of 0.75% phosphate coating of equal ratio of cobalt and phosphate.

Ten 1Ah pouch cells were delivered to JSC, and cycle life testing was carried out on these cells at the Energy Systems Test Area at JSC. The rate capability tests indicated that 77% of capacity retention was obtained after 10 cycles at C/5 discharge rate followed by 10 cycles at C/2 discharge rate.

NASA Research Announcements, with Giner, Inc., included the demonstration of a composite thermal

Safety Advancements in Lithium-ion for the Exploration Technology Development Program Battery Program

continued

switch (CTS™) material incorporated into the substrates in lithium-ion cells that would cause current flow to shut down when the cells experienced a temperature rise of over 80°C (176°F). In Year 1, feasibility was established. In Year 2, optimization of the mixing, coating, and curing conditions was carried out with delivery of coupons as well as coin cells that incorporated the CTS™. Giner, Inc. worked on optimizing the composition as well as the process for applying the CTS™ film on the cell electrode substrates. A spray method was adopted to obtain a more uniform pre-coat as well as coating of the CTS™. An orbital mixing and direct gravity feed method was used to reduce clogging of the nickel/Teflon® ink that was used to carry out the coating. The CTS™ was a mixture of nickel (Ni) nano-powders in a Teflon® solution.

Coupon testing of the CTS™ showed that with 8.4% Ni powders in 200 nanometer (nm) polytetrafluoroethylene (Teflon®) and curing at 146°C (295°F) with 500 pounds per square inch pressure used for calendaring the samples for 20 minutes, good switching characteristics were observed (figure 3). Some issues were encountered with this NASA Research Announcements contract as the source of the Ni powders seemed to be unreliable and had to be changed a few times through the course of the 2-year work period.

The authors would like to acknowledge the principal investigators—Dr. Chris Lang at Physical Sciences Inc. and Dr. Bob McDonald at Giner, Inc.—for their dedication and commitment to the contracts. The authors would like to acknowledge Jon Read for help with coordinating the PSI and Giner, Inc. sample tests carried out at JSC. They would also like to acknowledge Laura Baldwin, Tony Parish, Randall Parish, and David Dao for their efforts in getting the samples tested at JSC.

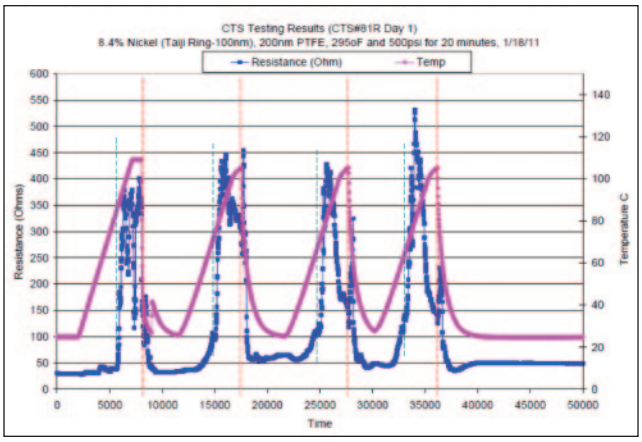


Fig. 3. *CTS™ Coupon showing successive switching behavior with increased temperatures.*

Simulated Internal Short Standard with Underwriter's Laboratory for Lithium-ion Cells Under a Space Act Agreement

Judith A. Jeevarajan, *Johnson Space Center*

Lithium-ion battery chemistry provides the state-of-the-art gravimetric energy density and highest efficiency of battery systems available in the market today. However, with several hundred lithium-ion cell manufacturers in existence, product quality is often sacrificed for cost and quantity of production. Lithium-ion cells—with their flammable electrolyte—are highly susceptible to certain impurities, especially those with metal particles as these can compromise the separator, causing internal shorts that result in fires and thermal runaway. Several research groups and standards organizations have been studying the issue of internal shorts in lithium-ion cells due to the fires encountered in the field as well as during transportation of cells and batteries of this chemistry.

A simulated internal short test method that included crushing the cells with a blunt rod has been carried out at NASA Johnson Space Center (JSC) for more than 12 years. However, the equipment used for testing was very crude and is manually operated, which prevents it from being converted into a standard that the battery industry could use. In recent years, Underwriter's Laboratory (UL) has put in a lot of effort in developing a simulated internal short test method using a blunt nail test. Although the equipment used was custom built, the team at UL had some issues with getting consistent test results without penetrating the cell can. An effort was initiated between UL and JSC to carry out testing under a Space Act Agreement to standardize a method to carry out simulated internal shorts in lithium-ion cells.

UL provided test equipment for the development of this standard to NASA (figure 1). The first set of cells used for this test were Sony 18650 lithium-ion cells due to the extensive heritage NASA has with this cell design. Cells were subjected to a variety of tests before they underwent the simulated internal short test using the UL test equipment. Each test protocol included a sample size of 10 cells. One set of cells were subjected to two cycles and labeled as fresh cells. Other test sets included 200 cycles, 500 cycles, 1000 cycles, high end-of-charge voltage cycling, high-rate cycling, and cycling at low temperatures. A set of 10 cells that was rejected from a battery manufacturer and subjected to two cycles, also underwent the same crush test.

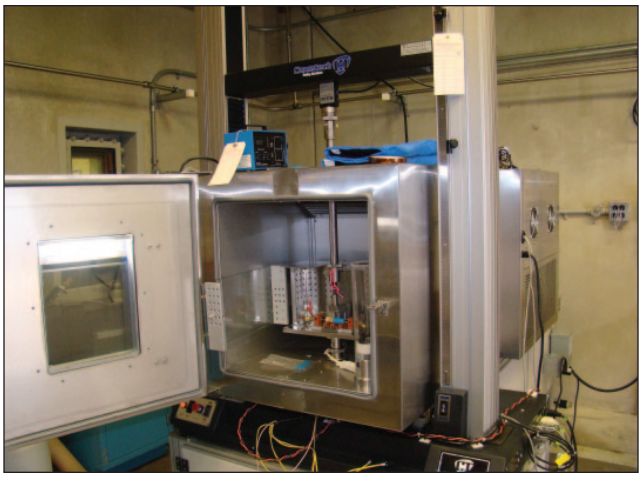


Fig. 1*. Underwriter's Laboratory test equipment at NASA Johnson Space Center for the simulated internal short test.*

At first, the team used rods of different diameters and radius of curvature to optimize the rod diameter and the rate at which the crush was carried out. A third variable that the team used as one of the test criteria was the voltage drop that indicates occurrence of the internal short. The final variable used was the location of the crush. For this last factor, all cells were x-rayed to determine the location of the aluminum (Al) tab inside the cell and marked. Literature data indicate that, in theory, thermal runaway temperatures can be produced if the internal short occurred at the location inside the cell where the Al current collector tab is in touch with the anode active material. Hence, crushes were performed at the location of the Al tab as well as 90° away from the location of the Al tab.

Cells that underwent preliminary testing with the crush test equipment, in an effort to optimize the rod diameter and the crush speed, were subjected to computed tomography (CT) scans. The CT scan data provided the extent of indentation as well as data on any damage to the cell's internal components and electrodes. Figures 2 and 3 show the CT scans depicting the indentations created by the 1/8-in. and 1/4-in. rods used under this study. The team also observed that with the 1/8-in. rod, a high speed of crush of about 0.1 millimeters per second (mm/sec) penetrated the cell can. However, with lowering the speed to about 0.01 mm/sec, a controlled internal short was obtained.

Simulated Internal Short Standard with Underwriter's Laboratory for Lithium-ion Cells Under a Space Act Agreement

continued

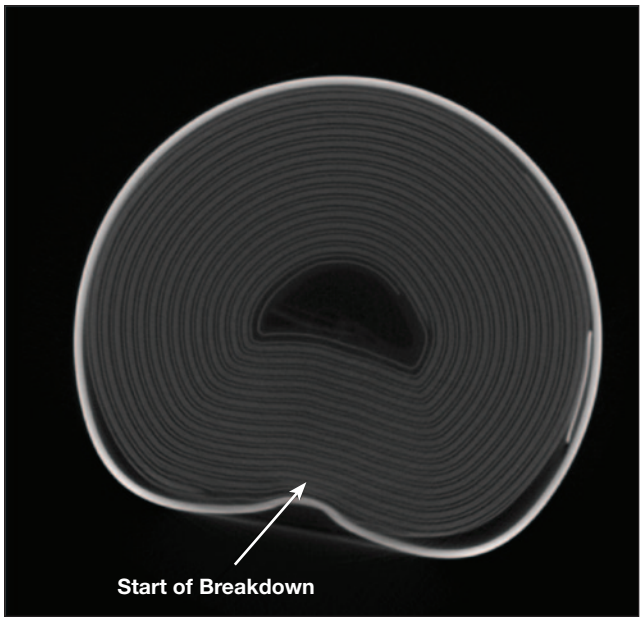


Fig. 2. *Computed tomography scan showing indentation and location of internal short with 1/8-in. crush rod.*

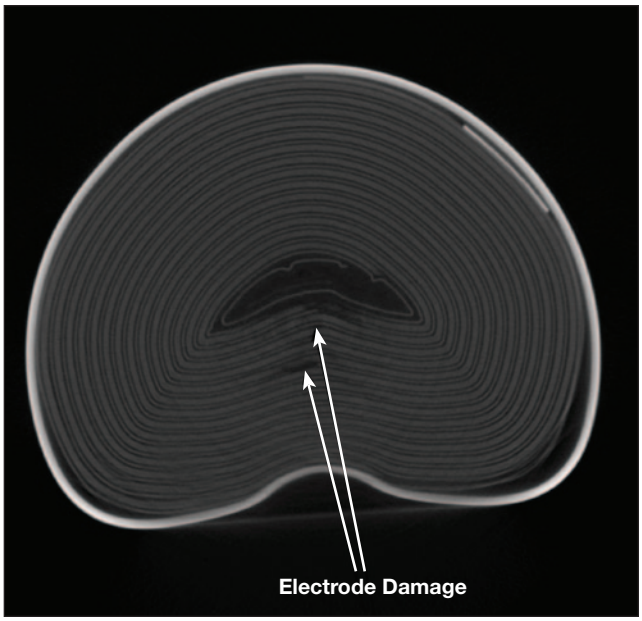


Fig. 3. *Computed tomography scan showing indentation as well as electrode damage with 1/4-in. crush rod*

The team observed that internal shorts do not result in a thermal runaway when the cell capacity is 50% the original capacity and if the cell state-of-charge was less than or equal to 50% or fully discharged. It did not matter if the cells were crushed at the location of the Al tab or away from the tab as long as the state-of-charge or capacity was as mentioned in the previous sentence.

The author would like to acknowledge Dr. Mahmood Tabador, Dr. Thomas Chepin, and Mr. Harry Jones at Underwriter's Laboratory for their commitment and collaboration in this effort, and for providing the funding and test equipment to carry out this test program. The author would also like to thank Thomas Viviano, Toby Dartez, Henry Bravo, and Nick Kidd for their efforts in carrying out the testing at JSC.

Research, Experimental Development, and Application of Alpha-Ketoglutaric Acid as a Decontaminant for Hazardous Fluids

Benjamin Greene, *White Sands Test Facility*
Dion Mast, *White Sands Test Facility*

In 2008, NASA Kennedy Space Center (KSC) became interested in alpha-ketoglutaric acid (AKGA) for monomethylhydrazine (MMH) and hydrazine decontamination because of its potential cost and operational benefits. Also, AKGA has gained attention for the potential decontamination of space shuttles for museums or other displays because of the reduced safety and health risks of its by-products. NASA Johnson Space Center's White Sands Test Facility (WSTF) collaborated with NASA Engineering and Safety Center in an assessment of AKGA use for treatment of hydrazine- and MMH-contaminated hardware, hardware decommissioning, and reduction of hydrazine and MMH waste streams. Although that assessment reported low technology readiness levels at that time, WSTF anticipated further evaluation and performed a literature survey and laboratory investigations with AKGA, hydrazine, and MMH to characterize AKGA reactions. WSTF also conducted a decontamination evaluation on a space shuttle orbiter Forward Reaction Control System (FRCS) test article.

Research and Experimental Development

The literature research yielded a limited amount of data on the reaction of AKGA with hydrazine or MMH, but provided an excellent baseline for investigative work. WSTF performed multiple experiments designed to provide a fundamental understanding of AKGA-hydrazine and AKGA-MMH reaction chemistry not found in the literature. Experiments included pH measurements, reaction characteristics and rates under stoichiometric conditions, concentration effects, open beaker screening tests, and vapor measurements on AKGA-treated hydrazine- and MMH-contaminated soft-goods material. Studies were also performed using 1.0 M (moles per liter) AKGA to determine corrosion rates of selected alloys commonly used in aerospace applications.

The reaction of AKGA with hydrazine produces 1,4,5,6-tetrahydro-6-oxo-3-pyridazinecarboxylic acid (PCA) and water, and with MMH produces 1-methyl-1,4,5,6-tetrahydro-6-oxo-3-pyridazinecarboxylic acid (MPCA) and water. Reaction rates and completeness of reactions are concentration dependent. AKGA solutions are acidic and must be handled with appropriate safety precautions. When pure hydrazine and AKGA are combined, the reaction of hydrazine evolves gas and is sufficiently exothermic that the fuel must be diluted for safety reasons. Similar precautions should be applied to MMH although no heating or gas evolution was observed.

MMH-contaminated polytetrafluoroethylene (PTFE) was not decontaminated by AKGA. Corrosion rates were obtained for stainless steel (SS) 304, SS 316, 17-4, MP35, Inconel® 718, and titanium (Ti) 6-4 in 1.0 M AKGA and were in low microinch per year (μin/yr) ranges, considered acceptable for decommissioned but not reusable hardware. If hardware is reused, the corrosive nature of AKGA must be considered during the refurbishment process to ensure that surface characteristics, compositions, and tolerances are acceptable. Corrosion rates must also be taken into account for the determination of AKGA soak times so as not to corrode hardware beyond acceptable limits. Note: During the initial investigation, no characterizations were performed at WSTF with 4.0 M AKGA, which was the most concentrated solution evaluated by KSC.

It was thought that AKGA may be well suited to the control of hydrazine and MMH spills because it is relatively nontoxic, does not ignite, does not produce volatile halogenated products, and forms stable products. When a stoichiometric excess of AKGA is used, it favors rapid and complete reactions. It was recommended that AKGA be examined as a spill control agent for hydrazine and MMH at WSTF, and that lab and field experiments be performed to establish optimum fuel dilution and AKGA concentrations and to develop written spill procedures, and the use of AKGA be considered as a potential means for eliminating hydrazine and MMH waste streams. This was one of the primary reasons for KSC interest in AKGA.

Experimental Application

When KSC took the lead to examine 4.0 M AKGA for decontamination and decommissioning of hydrazine- and MMH-contaminated flight hardware, tests at WSTF were performed using 4.0 M AKGA. Two MMH-contaminated

Research, Experimental Development, and Application of Alpha-Ketoglutaric Acid as a Decontaminant for Hazardous Fluids

continued

test articles were taken from the Fleet Leader FRCS pod at WSTF. The test articles (manifolds and lines previously decontaminated during FRCS disassembly) were modified with fittings that allowed the test articles to be readily sealed and filled with AKGA solutions. The fittings were designed to also serve as sampling ports to accept Dräger Pac III® hydrazine vapor monitors for MMH vapor measurements (figure 1). The test articles were purged with gaseous nitrogen gas for 6 and 8 days, respectively, to ensure they were free of detectable residual MMH vapor. Nitrogen gas effluent was monitored at each exit orifice using the vapor monitors. The pretest MMH vapor concentration in Test Article #1 registered 340 parts per billion (ppb) after 30 minutes; in Test Article #2, vapor concentration fluctuated between zero and 10 ppb after 24 hours.

Both test articles were filled with 4.0 M AKGA from the same source that KSC used; Test Article #1 remained filled for 125 days and Test Article #2 remained filled for 119 days. On Test Article #1, brown liquid leaked from a flange 11 days after testing was initiated, and solidified within 2 days (figure 2). The crystals were analytically determined to be AKGA.

After the AKGA was drained, the test articles were flushed with deionized water to remove residual detectable AKGA to below 1.0 part per million (ppm) as determined by liquid chromatography, then flushed with gaseous nitrogen to remove residual water. Test Article #2, however, continued to maintain residual AKGA concentrations above 1.0 ppm and therefore was not subject to subsequent steps, and no posttest vapor concentration measurements were taken. The AKGA foamed when drained, and care was taken because pressure had built up from reactions with the metals in the test articles.

Dissolved metals from the posttest fluids were determined by inductively coupled plasma mass spectrometry. To investigate the corrosion of the FRCS test article line materials (a combination of stainless steels including 304, 316, 321, and 17/7), correlating amounts of iron, chromium, and nickel powders were immersed in 4.0 M AKGA solutions and monitored visually for color change. Results are shown in figure 3. The colors of the solutions were also compared to solutions of equivalent concentrations prepared from the addition of iron(II) sulfate heptahydrate, chromium(III) nitrate nonahydrate, and nickel(II) nitrate hexahydrate dissolved in 4.0 M AKGA solution.

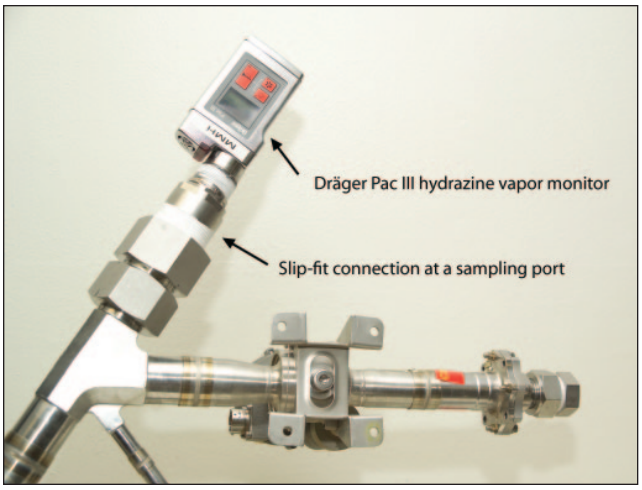


***Fig. 1**. Dräger Pac III® hydrazine vapor monitor affixed to Forward Reaction Control System test article.*



***Fig. 2**. Crystallized material on test article flange.*

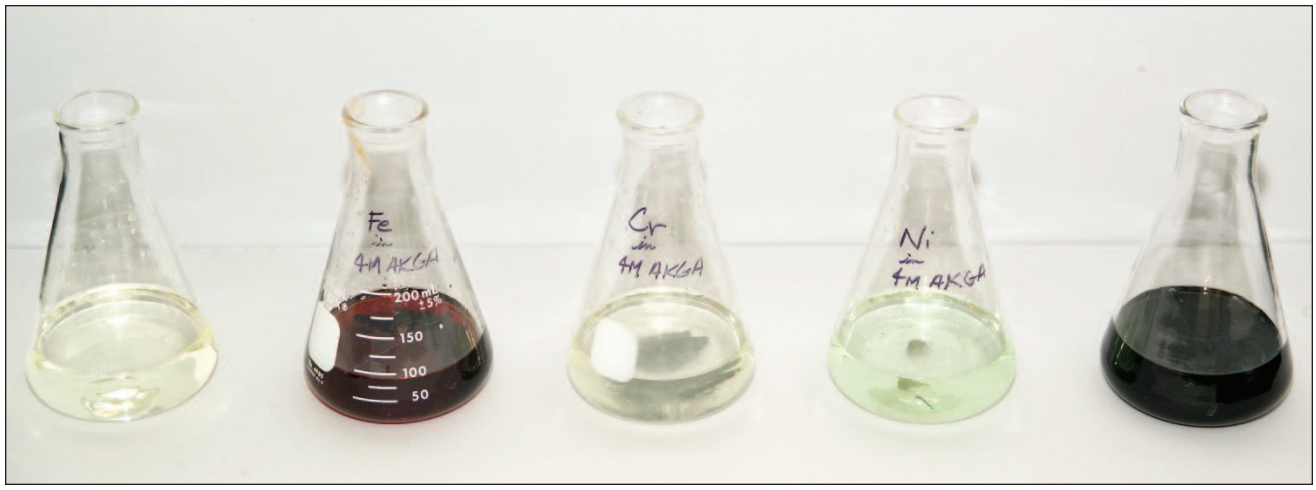


***Fig. 3**. Appearance of pretest 4.0 M alpha-ketoglutaric acid (AKGA), and iron, chromium, nickel powders in 4.0 M AKGA, and posttest 4.0 M AKGA.*

Conclusions

Laboratory investigations found that reactions of AKGA with hydrazine and MMH produce PCA and MPCA, respectively. AKGA solutions are acidic and must be handled with safety precautions. AKGA-hydrazine reaction evolves gas sufficiently exothermic that the fuel must be diluted for safety. It was also found that MMH contaminated PTFE was not decontaminated by AKGA. Corrosion rates of relevant metals in 1.0 M AKGA were low enough to use for decommissioned but not reusable hardware.

AKGA may be well suited to the control of hydrazine and MMH spills and waste streams because it is relatively nontoxic, does not ignite, does not produce volatile halogenated products, and forms stable products. When a stoichiometric excess of AKGA is used, it favors rapid and complete reactions. Further investigation is strongly recommended.

The investigation of AKGA as a decontaminant fluid for decommissioned MMH contaminated flight hardware found that 4.0 M AKGA was not successful. The reduction of MMH vapor achieved could be due to factors other than the reaction with AKGA. AKGA is known to not be effective in decontaminating soft goods, and test data show that 4.0 M AKGA is significantly corrosive toward the stainless steel alloys. The practical implications are that 4.0 M AKGA is not only corrosive to the FRCS metal components, but gas pressure can build up to the point where liquid inside the test article can be forcefully expelled. If there is no leak path, gas overpressure could result in component failure and consequential damage to hardware and potential injury to personnel.

The FRCS decontamination investigation concluded that residual MMH remains in the contaminated soft goods even after decommissioning decontamination, hardware corrosion will occur, and the use of 4.0 M AKGA could raise internal pressure due to gas evolution. Lastly, 4.0 M AKGA is a strong acid (pH 1.2) that requires appropriate safety precautions.

Ionic Monopropellant Product Characterization

Benjamin Greene, *White Sands Test Facility*
Mark B. McClure, *White Sands Test Facility*

Ionic monopropellants are an emerging technology with the potential to replace hydrazine and nitrogen tetroxide for propulsion and power. Monopropellant alternatives to hydrazine have garnered increasing interest due to their relatively safe, nontoxic, and environmentally benign properties, potential attractive propellant performance characteristics, and lower cost in handling. The United States Air Force (USAF) and other Department of Defense agencies are actively pursuing investigations into these monopropellants, and NASA has supported limited testing for these agencies in addition to its own testing. It is likely that NASA will consider ionic monopropellants as potentially viable on future spacecraft. Testing requirements are more stringent for NASA than other agencies due to crewed spacecraft considerations; therefore, testing has been proposed in NASA Johnson Space Center's White Sands Test Facility (WSTF) laboratory, propulsion areas, and larger-scale testing in the WSTF hazardous fluids test area.

Characterization of the products of liquid ionic monopropellants for spacecraft propulsion is in accordance with green propellant initiatives, and the demand for high-performance propellants has already led to increased information into the formulation, testing, and characterization of ionic monopropellants developed by the USAF such as AF-M315E, and others developed by different agencies including the Swedish Defense Agency. Some of the benefits of AF-M315E are that, as a monopropellant, it offers bipropellant performance; the system footprint would be smaller, meaning fewer parts, a reduced system risk, and increased payload; and because it would be a hydrazine replacement, the monopropellant offers reduced toxicity/carcinogenicity. An off-gassed product evaluation of AF-M315E was conducted at WSTF, and the results were reported to the USAF for evaluation.

The performance of ionic monopropellants has been compared with hydrazine, but with greatly reduced vapor toxicity. However, one area that needs study is the identification of combustion and non-combustion by-products. Combustion and non-combustion products are a concern for a variety of reasons including plume impingement on sensitive surfaces, extravehicular activity operations where contamination could occur, and vehicle health—e.g., the formation of potentially explosive products such as Fuel/Oxidizer Reaction Products (as was learned from the Space Shuttle Program) and other compounds believed in part responsible for "hard starts" in other programs.

An innovative test program is under way at WSTF to determine combustion and non-combustion products of ionic monopropellants. A gas chromatograph with a mass spectrometer detector will be configured to pack the injector inlet with selected catalyst material. Ionic monopropellant (microliter quantities) will be injected onto the catalyst bed and products swept into the detector for identification. The temperature of the catalyst in the inlet will be varied and product distribution characterized as a function of temperature. The data will be used to assess environmental and safety hazards of the ionic monopropellant products. A literature survey of work reported to date will also be performed.

Material Compatibility Assessment with Hypergolic Propellants and Anhydrous Ammonia

J. Clay Cantrell, *White Sands Test Facility*
Mark B. McClure, *White Sands Test Facility*

NASA Johnson Space Center's White Sands Test Facility (WSTF) has developed a process for analyzing the compatibility of systems, components, and materials in contact with hypergolic propellants; e.g., hydrazine fuels, nitrogen tetroxide, and anhydrous ammonia. These media are known to react with many materials, which can result in material degradation or decomposition of the propellant. In addition, these propellants are highly toxic; human exposure can occur by absorption through the skin, inhalation, or ingestion. Due to these hazards, it is important to exercise caution when selecting components and materials for use with hypergolic fluids, whether they be wetted, non-wetted, or for long- or short-term use in system design.

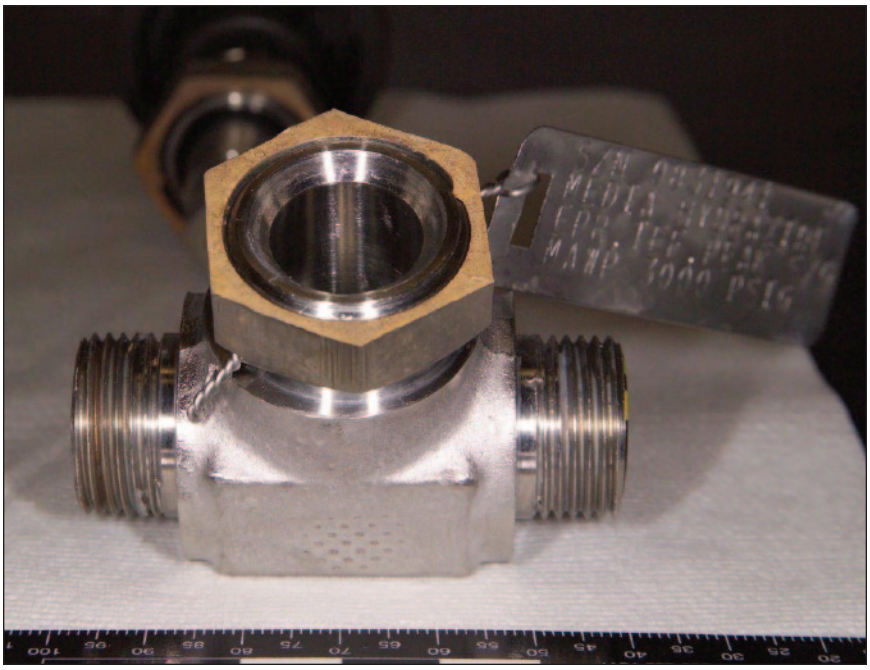


Fig. 1*. Failed CPV valve resulting from reaction with decomposed propellant.*

When selecting materials, it is also imperative to consider the materials' compatibility with decomposition products such as ammonium hydroxide produced from hydrazine and monomethylhydrazine, and nitric acid produced from nitrogen tetroxide. These products can be formed when the media comes into contact with moisture in the atmosphere. The reactivity of these by-products can sometimes be more hazardous than the original fluid. For example, figure 1 illustrates the bonnet failure of a valve after 10 years of service in hydrazine. This failure resulted from the decomposition of hydrazine, which permeated the seal and produced ammonium hydroxide, corroding the bonnet. Ultimately, the material cracked and failed.

The WSTF Hypergol Material Approval Committee has performed hypergol material compatibility assessments on many of the systems at WSTF. The goal in performing one of these assessments is to prevent these types of valve and other failures from occurring in the future. These precautions ensure systems can be operated safely without presenting undue risk to personnel or the system itself.

WSTF performs compatibility analyses for individual components as well as for entire systems for varying use conditions. A compatibility analysis consists of performing a material breakdown of each component within a system. The compatibility of each separate material with the fuel or oxidizer is then determined based on WSTF testing and available data. Parts within components that lie on the media boundary, located just beyond the soft goods sealing the media from the atmosphere, are assessed for compatibility hazards with decomposition products associated with the specified media. Based on such an analysis, the Hypergol Material Approval Committee makes recommendations concerning the incompatible part or component.

The compatibility and functionality of a soft good material may be assessed through mechanical property tests by using a screening process if the material is unknown, new, or if there are limited data on that material. The first step is to review documentation and identify incompatibilities

Material Compatibility Assessment with Hypergolic Propellants and Anhydrous Ammonia

continued

and potential reactivity the material may have with the fuel or oxidizer fluid. The next step is to verify the general class of the material through reviewing previous certifications, inspections, and specifications. In a third step, a small sample of the material is immersed in a beaker with the fuel or oxidizer fluid to determine whether the material demonstrates any adverse reactions at ambient temperature and pressure.

For samples being screened for oxidizer compatibility, the exposed material will be characterized by using Differential Scanning Calorimetry to identify potentially sensitive and reactive materials. A post-test Fourier Transform Infrared Spectroscopy is performed to look for evidence of nitration. Screening is then performed per Ambient Pressure Screening (Test 15) – NASA-STD-6001B (or latest revision). During Test 15, the sample is immersed in the fluid in which it is to be used at the vapor pressure of the medium at that temperature for 48 hours. Test 15 is performed for both fuel and oxidizer samples. For oxidizer samples, a final Differential Scanning Calorimetry and Fourier Transform Infrared Spectroscopy are performed.

Compatibility assessments are not conducted solely within WSTF systems. WSTF has performed system hazard assessments for the Ares I Reaction Control and Roll Control Systems per the protocol identified in American Institute for Aeronautics and Astronautics SP-084-1999 *Fire, Explosion, Compatibility, and Safety Hazards of Hypergols – Hydrazine*, Annex A. This assessment addresses possible failures—and their consequences—of system components. Hazards considered include possible failure modes and effects of fire, explosion, reactivity, and personnel and equipment exposure to hydrazine.

Reference Document for Assessing and Managing Risks of Hydrazine, Monomethylhydrazine, Nitrogen Tetroxide, and Ammonia on Spacecraft

Benjamin Greene, *White Sands Test Facility*

A reference document has been published by NASA Johnson Space Center's White Sands Test Facility for assessment and management of risks associated with hydrazine, monomethylhydrazine (MMH), nitrogen tetroxide (NTO), and ammonia on spacecraft. Hydrazine is used for monopropellant propulsion and power, MMH and NTO are used in bipropellant propulsion systems, and ammonia is used in spacecraft cooling systems. Because of the performance, fire, explosion, reactivity, and safety aspects of these fluids, extensive risk assessments and risk management strategies are required to assure safe and reliable mission performance (on-ground, pre-launch, launch, on-orbit, landing, and recovery). The information is compiled primarily from the Apollo, Space Shuttle, and Constellation Programs, and from uncrewed U.S. satellite exploration programs, with some information from international programs.

Definitions and references, guidelines, historical examples, and technical data are provided for assessing and managing risks associated with these hazardous materials. The content provides engineering information; lessons learned; possible options to address technical issues; classification of similar items, materials, or processes; interpretative direction and techniques; and other guidance information that may help assess and manage risks of hydrazine, MMH, NTO, and ammonia on spacecraft.

Cited and fully referenced sources of information include textbooks, journals, books, conference proceedings, reputable websites, and technical reports. Every reasonable effort has been made to present accurate information; however, users are urged to assess each situation carefully and to use the information in this document for guidance only.

The reference document—approximately 200 pages—is divided into three parts and includes appendices and an extensive reference list. It begins with an overview of risk assessment and risk management requirements and tools, and provides examples of range safety, spacecraft risks, surveys of spacecraft reliability, and failures relevant to these fluids.

Part I provides a general overview of hydrazine, MMH, NTO, and ammonia use on spacecraft. The focus is on the identification of risks associated with mission profile phases, passivation and decommissioning of spacecraft, orbital debris (including that resulting from hypergolic propellant explosions), and mission abort scenarios.

Part II addresses risk assessment and includes topics such as the aerospace environment, freeze-thaw hazards, thruster plume impingement zones, chemical reactivity, hard starts and explosion hazards, ignition hazards, auxiliary power unit hydrazine risks, and decontamination in spacecraft.

Part III focuses on risk management and acceptance including spacecraft design considerations, procedures to minimize risk, spill management, debris strikes, extravehicular activities, pressure hazards (water hammer and adiabatic compression), toxicity hazards, mitigation of hydrazine, MMH, and ammonia fires on spacecraft, personal protective equipment, and medical management of hydrazine, MMH, NTO, and ammonia exposures.

Appendices provide detailed information on case histories and summary lessons learned from mishaps, accidents, and relevant anomalies. Representative data, diagrams, graphs, and chemical equations are provided. Table 1 is a representative sample of useful chemical information provided.

The *Reference Document for Assessing and Managing Risks of Hydrazine, MMH, NTO and Ammonia on Spacecraft* may be obtained from the Laboratories Office at NASA White Sands Test Facility, Las Cruces, New Mexico (*www.nasa.gov/centers/wstf/laboratories*).

Reference Document for Assessing and Managing Risks of Hydrazine, Monomethylhydrazine, Nitrogen Tetroxide, and Ammonia on Spacecraft

continued

Table 1. *Selected Properties of Hydrazine, Monomethylhydrazine, Ammonia, and Nitrogen Tetroxide 1*

Property	Hydrazine	Monomethylhydrazine	Ammonia	Nitrogen Tetroxide
Vapor-pressure (at specified temperature)	1.89 kPa	6.60 kPa	909 kPa	(20°C) 0.95 atm
Autoignition Temperature	438-673 K (165-400°C)	457 K (184°C)	924 K (651°C)	N/A
Flammability Limits in Air	Lower Flammability Limit (LFL) 2.9% v/v Upper Flammability Limit (UFL) 100% v/v	LFL 2.5% v/v UFL 98% v/v	LFL 15.0% v/v UFL 33.5% v/v	N/A
Heat of Vaporization	43.43 kJ $mole^{-1}$	40.38 kJ $mole^{-1}$	23.33 kJ $mole^{-1}$ (351.4 K)	99 cal/g (21.2°C)
Critical States	Temperature 653 K (380°C) Pressure 14,692 kPa Density 0.231 g/mL	Temperature 585 K (312°C) Pressure 8,237 kPa Density 0.29 g/mL	Temperature 405.6 K (132.5°C) Pressure 11,370 kPa Density 0.235 g/mL	Temperature 158.2°C Pressure 100 atm Density 0.557 g/mL
Melting Point	274.63 K (1.48°C)	220.79 K (-52.36°C)	195.4 K (-77.7°C)	-11.2°C
Boiling Point	387.3 K (114.2°C)	360.81 K (87.66°C)	239.8 K (-33.3°C)	21.2°C
Liquid Density	1.004 g/mL	0.8702 g/mL	0.6819 g/mL (-33.3°C)	1.447 g/mL (-20°C)
Flash Points	Open Cup 324 K (51°C) Closed Cup 311 K (38°C)	Open Cup 294K (21°C) Closed Cup 24K (20°C)	210 K (-60°C) (approx.)	N/A
Heat Capacity of Liquid	3.077 J g^{-1} K^{-1}	2.93 J g^{-1} K^{-1}	(239.8 K) 4.39 J g^{-1} K^{-1}	33.71 cal/deg/mole (290 K)
Heat of Combustion	-577 kJ $mole^{-1}$	1304 kJ $mole^{-1}$	-383 kJ $mole^{-1}$	N/A
Heat of Formation	50.37 kJ $mole^{-1}$	54.836 kJ $mole^{-1}$	-45.6 kJ $mole^{-1}$	2.309 kcal/ $mole^{-1}$

[1] Properties are at 298 K (25°C [77°F]) and pressure of 101.3 kPa (14.7 psia) unless otherwise specified.

Effects of Liquid Propellants on Mechanical Properties of Nonmetals

Michelle H. Barragan, *White Sands Test Facility*
Mike Shoffstall, *White Sands Test Facility*
Darren M. Cone, *White Sands Test Facility*
Mark B. McClure, *White Sands Test Facility*
Miguel Maes, *White Sands Test Facility*

Aerospace fluids such as hydrazine, monomethylhydrazine, and nitrogen tetroxide (oxidizer) are primarily appraised for their performance as propellants. Unfortunately, most propellants come with a list of undesirable side effects, such as toxicity and material incompatibility, which require attention as well. If the chosen propellant has detrimental effects on its storage and delivery systems, the consequences could be a significant loss in performance and inadvertent release of propellant. For example, figure 1 depicts the effect of MON-3 (mixed oxides of nitrogen, 3% nitric oxide) on a nonmetal o-ring constructed of a material considered compatible; i.e., chemically stable, with MON-3, which has been used for decades in this capacity. The results are dramatic; however, the effects of propellant exposure on a material may not always be as obvious as figure 1 illustrates.

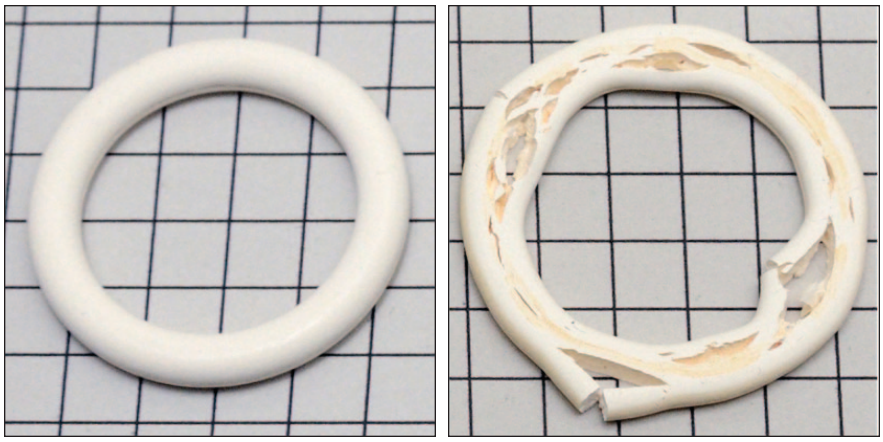


Fig. 1*. Oxidizer-compatible O-ring test sample (unexposed [left], exposed [right]).*

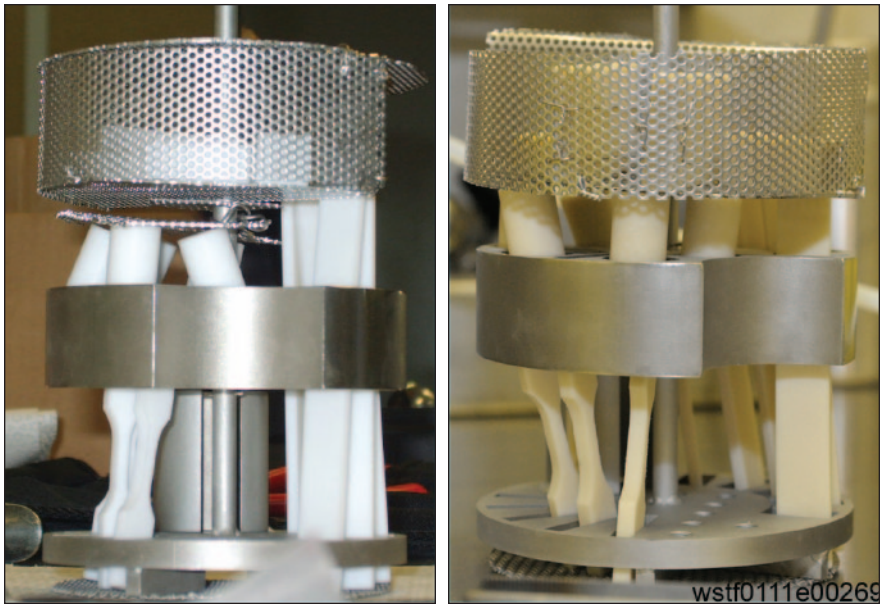
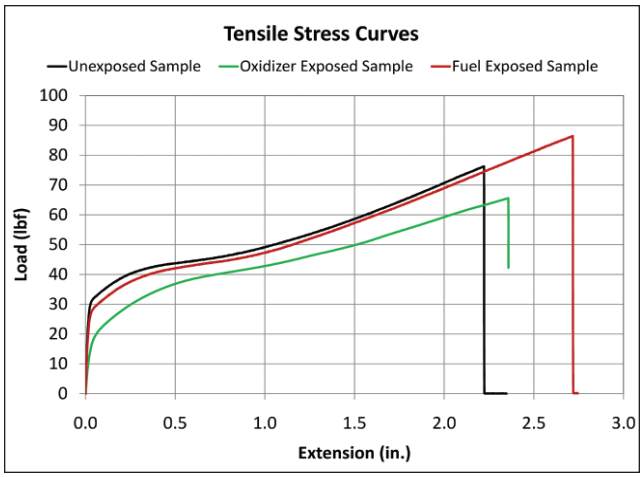


Fig. 2*. Oxidizer-compatible bar-stock fabricated test samples (unexposed [left], exposed [right]).*

The nonmetal test samples shown in figure 2 were fabricated from bar stock in accordance with the appropriate American Society for Testing and Materials standard for their respective mechanical property tests. The samples were exposed to MON-3 in a similar manner as the o-rings in figure 1; however, the samples do not show obvious signs of degradation other than a change in coloration. Material properties testing is needed to determine whether this change in color also correlates to a change in the mechanical properties of the samples. The NASA Johnson Space Center's White Sands Test Facility has the capability of performing material properties tests on samples conditioned in propellants. The mechanical property measurements commonly performed on propellant-conditioned samples are: tensile/elongation, hardness, compression set, compressive strength, flexural strength, swelling, and mass. Additional mechanical property tests may be performed per customer requirements.

Effects of Liquid Propellants on Mechanical Properties of Nonmetals

continued



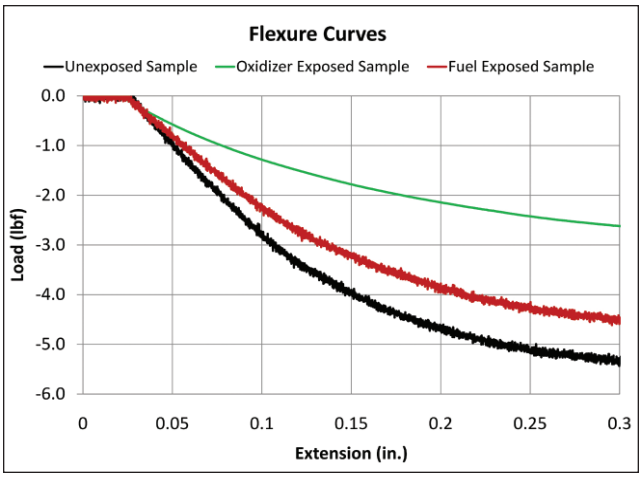


***Fig. 3**. Tensile and flexure curves for unexposed and exposed test samples*

The results of the tensile and flexure data of the samples in figure 2 are shown in figure 3, which also includes data for the same material conditioned in monomethylhydrazine. The data indicate that a change occurred in the mechanical properties of the material as a result of conditioning the sample. Qualitative data, such as visual inspection of the samples (figure 1), are sufficient for deeming a material incompatible with the propellant tested. However, the quantitative data shown in figure 3 can be used to determine whether the material is compatible in its intended use condition.

Conclusion

Previously, propellant system designers focused on materials to avoid in propellant systems because the data available were often qualitative and based on visual observations. The performance of a material after exposure to the intended use condition can be evaluated quantitatively with materials properties data. White Sands Test Facility can perform material properties testing of materials exposed to a variety of propellants. Testing data equips system designers with the information they need to confidently specify the best materials for successful use in propellant systems.

Low Corrosion Rate Determination in Hydrazine, Monomethylhydrazine, and MON1 Propellants

Anna H. DeArmond, *White Sands Test Facility*
Dion J. Mast, *White Sands Test Facility*
Darren M. Cone, *White Sands Test Facility*

Relatively high corrosion rates for 304 stainless steel (SS) are predicted in literature, and references are made to iron leaching into hydrazine and its increase with a rising concentration of carbon dioxide (CO_2) in the solutions. This would be a sign of general corrosion. The potential hazard caused by general corrosion during accidental exposure is of concern to NASA as its fuel systems age.

Although there are many different types of corrosion (localized, galvanic, crevice, etc.), the best known and most studied is uniform or general corrosion, which is the type most often encountered at NASA facilities. Damage caused by uniform corrosion is predictable. The corrosion rate gives information on the depth of surface penetration caused by uniform corrosion in the lifetime of a structure as a result of the material's exposure to the environment. Structures can be made more mechanically robust by taking uniform corrosion into account during construction design. Other types of corrosion are less predictable, and are difficult to measure.

Low corrosivity under normal operating conditions is generally tabulated as < 1 mil per year (mpy) (a mil is one-thousandth of an inch). Most alloys used by NASA have excellent corrosion resistance, and are used with fuels like monopropellant hydrazine (MPH) and monomethylhydrazine (MMH), which are not very corrosive. The Chemistry and Materials Section at NASA Johnson Space Center's White Sands Test Facility developed a technique to measure corrosion rates as low as 10^{-3} mpy. This technique consists of 6 or more days of alloy immersion and detection of the corrosion products by inductively coupled plasma-mass spectrometry. This procedure can be used to determine corrosion rates in any fluid that can be evaporated to nonvolatile residue or used directly in the inductively coupled plasma-mass spectrometry instrument, provided that corrosion products of the tested materials are soluble in the immersion fluid.

For fuel systems such as MPH, high purity hydrazine (HPH), or MMH, normal operating and storage conditions are without air and moisture. When exposed to air,

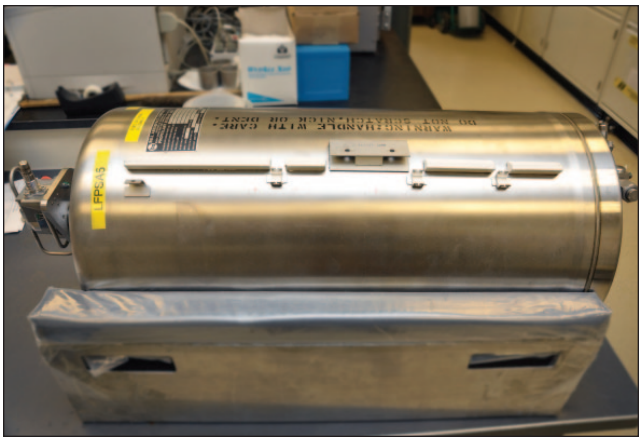


Fig. 1*. Typical fuel propellant storage assembly.*

MPH, HPH, and MMH absorb CO_2 and form carbazic and methylcarbazic acids, which are known corrosion agents. Because of the possibility of accidental exposure, a 4-year study measured the influence of CO_2 and water contamination in MMH and MPH and yielded useful information on the corrosion rates of alloys frequently used in fuel systems (304 SS, 316 SS, 17-4 SS, and Ti-6Al-4V). The objective was to study the effect of fuel contamination by CO_2 and water on the corrosion rate of the alloys when immersed in fuel while opened to nitrogen or dry air. It was found that the corrosion rates of all four alloys in MMH and MPH, contaminated to different degrees with water and CO_2, did not reach the order of 10^{-2} mpy.

Also, MMH and MON1 (nitrogen tetroxide with 1% by weight nitric oxide), stored since 1970 in Minuteman propellant storage assemblies made of alloys A 286 and 347 SS (figure 1) were analyzed for the corrosion products of their alloy components. The corrosion rates, conservatively estimated from corrosion products found in the samples, were of the order of 10^{-10} mpy for MMH and 10^{-9} mpy for MON1. These results confirm that propellants can be kept indefinitely when stored properly in containers of compatible materials.

Liquid Methane/Liquid Oxygen Cryogenic Monopropellant and Explosive Literature

Benjamin Greene, *White Sands Test Facility*
Stephen Taylor, *White Sands Test Facility*

Liquid methane/liquid oxygen (MOX) solutions have received some, but limited, attention in the literature as a propellant or as an explosive. The acronym MOX is used to refer to cryogenic monopropellant mixtures of liquid methane or liquefied natural gas and liquid oxygen. Interest in reduced-toxicity, high-performance propellants with the potential for in situ production in extraterrestrial environments has prompted a new look into the potential of a MOX propulsion system and its explosion hazards.

A literature review was performed and consolidated at NASA Johnson Space Center's White Sands Test Facility to provide a single source of information for references to MOX properties, hazards, critical diameter considerations, burning rates, combustion instability, trinitrotoluene (TNT) equivalency, shock sensitivity, and vibration tolerance, some related to spacecraft environments and others to Earth-based explosive applications. The review contains information found on MOX monopropellant evaluation and feasibility studies, detonation and burning characteristics, explosive systems, ignition and combustion characteristics, patents, and methods for preparation and storage. The review also includes some advantages and disadvantages of MOX monopropellant versus liquid oxygen (LOX)/ methane bipropellant and storage systems.

LOX/liquid methane has been examined by a number of investigators since the 1950s as a monopropellant for jet or spacecraft engines, and as a brisant (powerful and shattering) explosive. Recent testing raised concerns over the potential formation of MOX with explosive consequences. The potential for cold flows (flowing of propellants under non-ignition conditions), or inadvertent mixing of LOX and liquid methane to form a potentially detonable mixture, demonstrated the need for a better understanding of MOX. Oxygen and methane form a single-phase liquid at temperatures above the freezing point of methane; at much lower temperatures, it is still possible to prepare very concentrated single-phase mixtures. A methane-oxygen phase diagram is shown in figure 1. Research has shown that the most brisant mixture was the stoichiometric mixture (33.33 mole percent methane and 66.67 mole percent oxygen). The phase

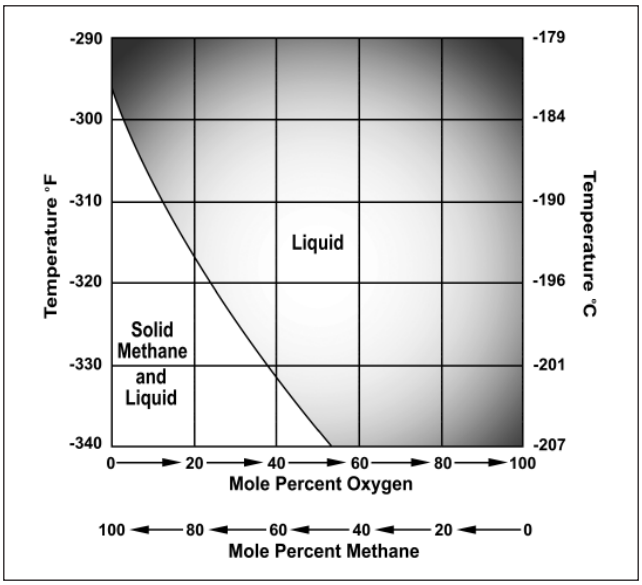


Fig. 1*. Methane-liquid oxygen phase diagram.*

diagram also illustrates the wide temperature range over which MOX is a liquid at that composition.

This work presents a summary of literature relevant to MOX and LOX/liquid methane monopropellant and explosive properties and testing. MOX made with liquefied natural gas (LNG) and LOX/LNG monopropellant and explosive are included. Patent literature was included because of the limited amount of technical publications and for the reader to appreciate the claims related to propulsion and explosive applications. In addition, some of the patents provide methods for the preparation and storage of MOX, which may be useful if this fluid gains interest in use.

Figure 2 depicts the approximate number of MOX-related publications and patents found in this survey. The most concentrated interest in MOX began around 1957 and peaked in 1966. There were limited publications between 1970 and 1978, and only one found in the 1980s. Sporadic publications and patents, including this review, appeared from 1994 to the present.

While an extensive variety of LOX/hydrocarbon bipropellant combinations, including LOX/methane, have

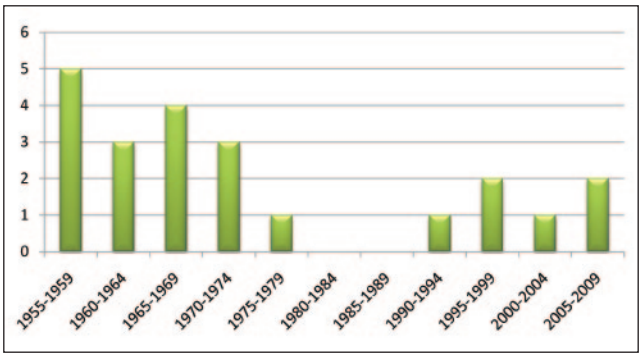


***Fig. 2**. Number of liquid methane/liquid oxygen-related papers vs. year of publication.*

been successfully used for many years in spacecraft engine applications, monopropellant blends have experienced significantly fewer applications, sometimes with explosive results. The bulk of collective experience with LOX/hydrocarbon mixtures is that shock sensitive mixtures are produced when LOX and the hydrocarbon are mixed in ratios near stoichiometric. Not only has MOX been proposed and evaluated as a cryogenic monopropellant, it has also been patented as an explosive for cracking rock in mining applications.

The literature appears limited to experimental work and calculations; no reports of known functioning spacecraft engines using MOX were found. Utility as a monopropellant is limited by the potential for detonations (including deflagration-to-detonation transition back through feed lines from a combustion chamber to the fuel tank), physical considerations such as phase changes, and non-Earth cryogenic storage challenges. However, the potential advantages of MOX as a monopropellant—with respect to the relative simplicity of high performance monopropellant engines and loss of weight penalty due to elimination of associated hardware including tanks, supply lines, and valves as compared to bipropellant engines—should be kept in mind. As LOX/liquid methane bipropellant systems continue to garner interest and increased use, and if in situ propellant production in extraterrestrial environments transitions from concept to reality, the potential for MOX monopropellant systems should also be considered.

Robotics, Tele-Robotics, Autonomous Systems, and Software



NASGRO®—Fracture Mechanics and Fatigue Crack Growth Analysis Software

Joachim Beek, *Johnson Space Center*
Royce Forman, *Johnson Space Center*

Structural failure due to the consequences of naturally occurring and service-induced flaws, damage, or cracks in a part or structure, is the primary threat to the integrity, safety, and performance of nearly all highly stressed mechanical structures. Consequences of such failures include serious injury or loss of life, severe environmental damage, and substantial economic loss. One such example is the Aloha Airlines flight 243 incident in 1988 in which a 5.5-m (18-ft) section of the fuselage separated from the aircraft during flight; the cause was found to be metal fatigue exacerbated by corrosion.

The NASA-developed NASGRO® fracture mechanics analysis computer program is the standard software tool used by NASA and its contractors for fracture analysis of space hardware and safety-critical ground systems. The importance to NASA is the ready availability of an accepted, accurate, reliable, state-of-the-art code with unmatched analytic capabilities.

Under continued active development for over 25 years, NASGRO®'s initial use was for fracture control implementation on space shuttle primary structure and was later extended to other critical spacecraft hardware. However, developments in recent years have made NASGRO® so powerful and versatile that it is now used in the wider aerospace industry as well as in areas as varied as railroad and ship-building. In 2003, NASGRO® was the recipient of NASA's "Software Of The Year" Award and R&D Magazine's "R&D100" Award.

Features that make NASGRO® unique among fracture mechanics analysis tools include:

- a large library of more than 70 crack geometry solutions
- a material property database containing data for hundreds of metallic materials
- a unique crack growth equation (and seven legacy equations) able to model onset of growth, small-crack behavior, crack growth retardation effects, and instability
- capabilities to model elastic-plastic loading, failure of glass or glass-like materials under constant loading, critical crack size



Fig. 1*. Underwriter's Laboratory test equipment at NASA Johnson Space Center for the simulated internal short test.*

Major recent developments include:

- a number of advanced weight function crack geometry solutions able to accommodate complex crack plane stresses that are nonlinear due to local geometric discontinuities such as arbitrary notches and cutouts
- an advanced interpolation scheme allowing crack growth analysis over the entire range of crack growth, even in the asymptotic threshold to instability regions, at varying operating temperatures for both tabular and NASGRO® equation representation of crack growth data
- advanced failure criteria combining the effects of material yielding and crack instability, hitherto modeled as independent mechanisms; the new criteria are important in applications such as power generation
- configuration control allowing engineering managers to lock down which features and options are available to their analysts
- a built-in link allowing two-way communications between NASGRO® and Excel® spreadsheets, or between NASGRO® and other structural analysis tools

NASGRO®—Fracture Mechanics and Fatigue Crack Growth Analysis Software

continued

Current development activities include:

- research into fatigue crack growth threshold behavior for several aerospace alloys to determine valid threshold parameter values that are independent of test method and environment; this research marries solid mechanics modeling with material science and has the potential to change the accepted fracture mechanics community's understanding of basic threshold mechanisms from mechanics-based plasticity approaches to include more metallurgy-based microstructural considerations
- research to implement modeling of damage tolerance for composites, such as fiber delaminations, by implementing a virtual crack closure technique in a two-dimensional, anisotropic, layered Boundary Element Analysis method; for verification of composite structures, such a tool could become a useful alternative to resource-intensive structural testing
- incorporation of new Finite Element Analysis-based crack geometry solutions to allow modeling of continuing damage such as interaction and linking of multiple cracks; such solutions are important since real-world damage rarely occurs as simplified independent single cracks

Progress in Space Flight Environment Effects: Predicting Spacecraft Single Event Environments with the FLUKA Monte Carlo Nuclear Reaction and Transport Code

Steven L. Koontz, *Johnson Space Center*
Brandon D. Reddell, *Johnson Space Center*
Paul Boeder, *The Boeing Company*

Abstract
The contribution of nuclear reactions and secondary particle showers, caused by cosmic ray interactions with spacecraft materials, to spacecraft avionics system single event environments is explored using the FLUKA Monte Carlo nuclear reaction and transport code and spacecraft in-flight single event upset (SEU) data.

Introduction
Natural space flight ionizing radiation (IR) environments are radically different from the IR environments, both natural and artificial, encountered on Earth's surface. The space flight IR environment is dominated by high-kinetic-energy-charged particles with relatively small contributions from x-rays and gamma rays, and essentially no contribution from the natural radioisotope decay processes that dominate the natural Earth surface IR environment. The energetic charged particles of interest consist of galactic and solar cosmic rays and energetic charge particles trapped in planetary magnetospheres (e.g., Earth's Van Allen belts), and can interact with spacecraft materials to produce both ionization along the particle track through the material and secondary particle showers following collisions with spacecraft nuclei. Energetic charged particles are the ultimate cause of spacecraft SEUs (i.e., effects caused by a single energetic charged particle), and they determine the character of the spacecraft avionics single event effect (SEE) environment and, ultimately, spacecraft safety and reliability.

Preliminary results of FLUKA Monte Carlo nuclear reaction and transport code calculations of spacecraft SEE environments and the corresponding electronic device event rates are reported in this paper.

First, **FLUKA** (i.e., **FLU**ktuierende **KA**skade)-based calculations of spacecraft avionics SEE and corresponding SEU rates are compared with in-flight data for several spacecraft avionics devices as a first step in evaluating the FLUKA code for spacecraft SEE applications.

Second, CRÈME-96 deterministic modeling of SEU rates and Petersen Figure of Merit (FOM) are also compared to FLUKA SEU rate estimates and in-flight data, to further validate the FLUKA-based methods against widely used semi-empirical methods for those cases in which all three methods are applicable.

Finally, the effects, on device SEE rates, of incorporating thin (1 micron) heavy element metallization layers into microelectronic circuits are examined using the FLUKA-based methods reported here.

Results/Discussion
Table 1 and figure 1 compare in-flight SEU rates for various complementary metal oxide semiconductor (CMOS) spacecraft micro-devices with estimates produced using the FLUKA code applied to a generic three-dimensional "spacecraft" consisting of concentric spherical shells of spacecraft shielding mass material with thin (10 micron) silicon detector shells placed at various shielding mass depths. Thin layers (1 micron) of high atomic number elements such as silver (Ag), Hafnium (Hf), tungsten (W), or lead (Pb) can be placed on the silicon detector shells. On-orbit SEU rate estimates produced with the FOM and the two-dimensional deterministic CRÈME-96 codes are shown in figure 1 and Table 1 for purposes of comparison. Rates are compared at the same estimated median spacecraft shielding mass as well as the same device cross section and device thickness parameters.

As can be seen in figure 1, the three SEU rate estimation methods provide comparable accuracy, are generally within a factor of 10 of the on-orbit rate, and often much better—an accuracy that is more than adequate for practical avionics systems design and verification purposes. The three SEU rate estimators are compared using the least squares performance metric that measures the net deviation of the various SEU rate estimates with observed in-flight SEU rates.

It is interesting to note that the accuracy of FLUKA predictions of Mercury Messenger static random access memory (SRAM) SEU rates improves dramatically when a 1-micron W film is placed in contact with the outer surface of each silicon detector shell—an expected outcome given the probable role of W in Mercury Messenger SRAM SEU sensitivity. FLUKA simulations show that the magnitude of the W film effect increases the SEU rate at higher shielding mass by as much as three orders of magnitude for high

Progress in Space Flight Environment Effects: Predicting Spacecraft Single Event Environments with the FLUKA Monte Carlo Nuclear Reaction and Transport Code

continued

linear energy transfer (LET) threshold (> 4 megaelectron volt centimeter squared per milligram [MeV cm^2]/mg) devices but was unobservable for low LET threshold devices (<4 [MeV cm^2]/mg).

Figures 2 and 3 show the results of FLUKA-based calculations demonstrating the effects of thin W layers proximal to the silicon scoring detector shells in the concentric spherical shell "spacecraft" model used in the FLUKA simulations. The 1977 solar minimum interplanetary galactic cosmic ray spectrum is the natural space radiation environment and the spacecraft shielding mass is aluminum (Al) in the subject calculations. In both figures, the total flux of charged particles with LET values greater than some threshold value X is plotted as a function of Al shielding mass for the corresponding silicon detector shell. The values of X are, in order from maximum to minimum particle flux, 0.001, 0.012, 0.120, 1.30, 4.03, 9.8, 15, and 30 MeV cm^2/mg. The model used to generate the figure 2 data contained only 10 micron silicon detector shells while for the figure 3 data, 1 micron of W was placed in contact with the outer surface of each silicon detector shell. Two statistically independent FLUKA Monte Carlo runs were averaged to produce the data in figures 2 and 3.

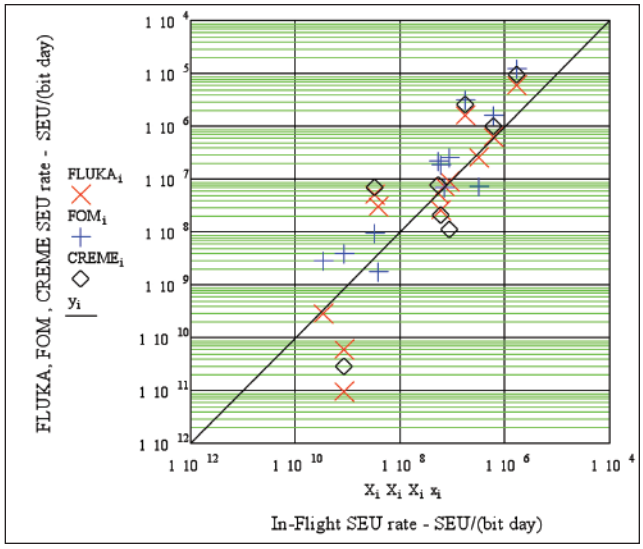


***Fig. 1**. In-flight single event upset (SEU) rates vs. predicted SEU rates.*

Comparison of the two figures shows no remarkable differences until the magnitude of particle LET is greater than 4 (MeV cm^2)/mg. As expected, both figures show a rapid increase in the total particle flux above threshold as the LET threshold is increased from 0.001 MeV cm^2/mg to 30 MeV cm^2/mg. However, substantial differences in the total particle flux are apparent for LET threshold values of 9.8, 15, and 30 MeV cm^2/mg, especially at higher shielding mass values, with the W case showing much higher fluxes than the no-W case. The flux of particles with LET > 30 MeV cm^2/mg is zero at all shielding masses for the no-W case, while in the W case the LET > 30 MeV cm^2/mg flux is between 0.1 and 1.0 per day at nearly all shielding masses. The relatively high flux of particles with LET > 10 MeV cm^2/mg in the W case implies an increased risk of both hard (destructive) and soft (recoverable) avionics

***Table 1.** Predicted vs. Observed In-flight Single Event Upset Rates for Complementary Metal Oxide Semiconductor Micro-Devices (International Space Station [ISS], Interplanetary [IP], Geosynchronous [GEO] spacecraft flight data).*

Spacecraft Identifier	Flight Environment	Device Part Number or other identifier	Median Shielding Mass g/cm^2	In-Flight SEU/bit day (X)	FLUKA Predicted SEU/bit day (FLUKA)	CRÈME-96 Predicted SEU/bit day (CRÈME)	Petersen Figure of Merit (FOM) Predicted SEU/bit day (FOM)
ISS	ISS	TMS44400	10	8.5×10^{-8}	8.9×10^{-8}	1.1×10^{-7}	2.5×10^{-7}
ISS	ISS	TMS44400	40	7.0×10^{-8}	7.2×10^{-8}	3.1×10^{-8}	6.8×10^{-8}
ISS	ISS	SMK416400	10	3.2×10^{-9}	5.1×10^{-8}	7.2×10^{-8}	9.6×10^{-9}
ISS	ISS	SMK416400	40	3.7×10^{-9}	2.8×10^{-8}	2.0×10^{-8}	2.1×10^{-9}
ISS	ISS	KM44S32030T-GL	40	3.3×10^{-10}	2.2×10^{-10}	1.9×10^{-10}	2.0×10^{-10}
Space Shuttle	ISS	IMS1601EPI	34	3.1×10^{-7}	2.5×10^{-7}	2.7×10^{-7}	7.4×10^{-8}
Thuraya	GEO	ASIC 0.25 µ static random access memory, IBM SA-12	0.7	5.3×10^{-8}	5.3×10^{-8}	7.9×10^{-8}	2.2×10^{-7}
Mercury Messenger	IP	ASIC "rad/single event effect hard" static random access memory	1.0	8.6×10^{-10}	5.8×10^{-11} (W)	2.9×10^{-11}	4.0×10^{-9}
Mercury Messenger	IP	ASIC "rad/single event effect hard" static random access memory	1.0	8.6×10^{-10}	9.3×10^{-12} (no-W)	2.9×10^{-11}	4.0×10^{-9}
Cassini	IP	OKI (4Mx1)	3.4	5.8×10^{-8}	2.5×10^{-8}	2.1×10^{-8}	1.9×10^{-7}
Solar Heliosphreic Observatory	IP	SMJ44100	1.0	5.9×10^{-7}	6.4×10^{-7}	1.2×10^{-6}	1.6×10^{-6}
Solar Heliospheric Observatory	IP	CP65656EV	1.0	1.7×10^{-7}	1.6×10^{-6}	2.5×10^{-6}	3.1×10^{-6}
ETS-V (Engineering Test Satellite V)	GEO	PD4464D-20	5.8	1.7×10^{-6}	6×10^{-6}	9.3×10^{-6}	1.2×10^{-5}

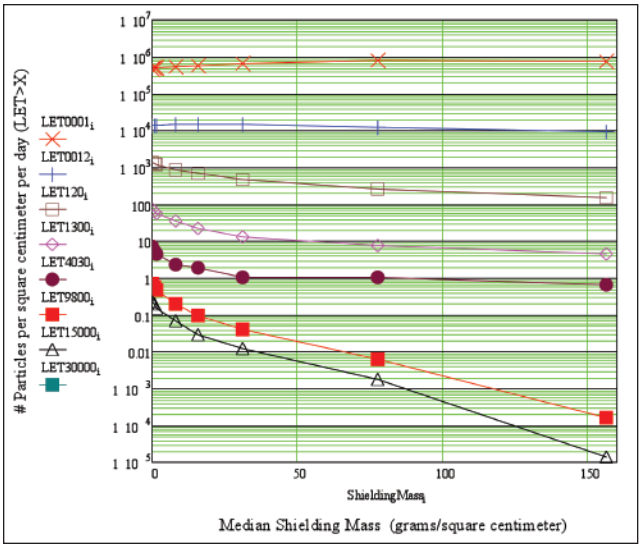


Fig. 2. Particle flux vs. shielding mass – no tungsten.

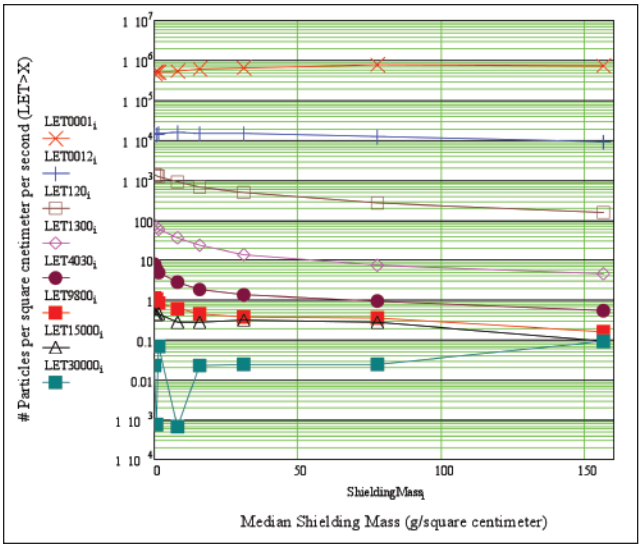


Fig. 3. Particle flux vs. shielding mass – tungsten.

SEE effects, even at high shielding mass, that would not be anticipated on the basis of experience with silicon-based microelectronic devices that do not contain W. The increasing use of high atomic number (Z) elements in modern electronic devices presents new avionics risk factor that must be addressed with innovative spacecraft avionics design, test, and verification techniques.

The fissility factor is a metric describing the relative likelihood of an energetically excited nucleus to decay by fission as opposed to other decay modes. If 1-micron films of elements other than W are placed in contact with the silicon detector shells, the relative flux of particles with LET > 10 MeV cm^2/mg into the silicon detector should increase with the fissility factor (Z^2/A) of the elements, at least for Z > 40. Figure 4 shows the fissility parameter correlation with the X > 10 MeV cm^2/mg particle flux (normalized with respect to W) entering the silicon detector shells at median shielding masses of 31 (□) and 77 (◇) grams per centimeter squared (g/cm^2) Al with the 1-micron over-layers of the elements shown in Table 2. When measured fission probabilities are plotted against the fissility parameter, the curve displays a minimum around atomic number 40 and increases rapidly as atomic number increases above 40 and decreases below 40. The fissility parameter itself only describes the relative likelihood of fission, not the LET range of the fission products. The number of high LET fragments produced by a fission event will depend on the atomic number of the parent nucleus. Low-Z nuclei simply can't produce the high-Z, high-LET fragments that high-Z nuclei can produce. Relative fission probabilities (○, also normalized with respect to W) are also plotted in figure 4 for comparison. The trend in fission probability is in reasonable agreement with the FLUKA calculations of LET > 10 MeV cm^2/mg particle flux into the silicon detector shells.

***Table 2.** Silicon Detector Shell Over-Layer Elements and Fissility Parameters for Figure 4*

Element	Aluminum (Al)	Silver (Ag)	Hafnium (Hf)	Tungsten (W)	Lead (Pb)
Fissility Factor	6.259	20.434	29.124	29.923	30.918

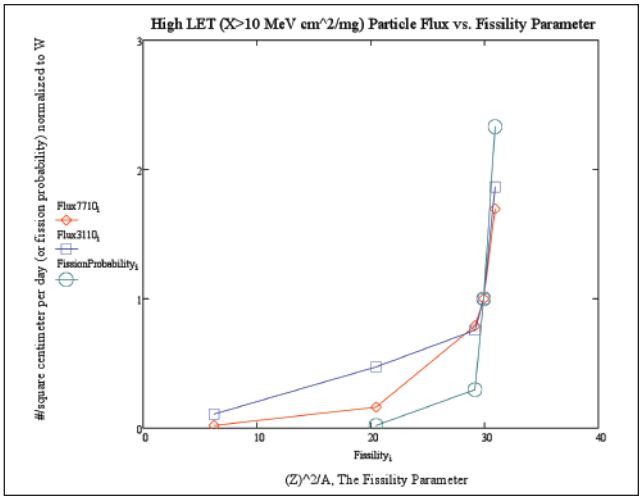


Fig. 4. One micron over-layers on silicon detector shells.

Conclusions

FLUKA can be used to calculate estimates of spacecraft SEE environments and the corresponding microelectronic device SEE upset rates. In comparable cases, FLUKA-based calculations compare favorably with CRÈME-96 and FOM estimates of in-flight SEE rates.

Finally, the FLUKA based SEU rate estimation method outlined here has been shown to be useful in evaluating the effect of incorporating heavy elements into microelectronic devices on device SEE rates—evaluations that cannot be performed with CRÈME-96 or FOM. FLUKA-based methods also enable investigations of the effects of spacecraft microelectronic elemental composition as well as spacecraft shielding mass elemental composition; i.e., cases in which CRÈME-96 and the FOM are not applicable.

Analysis Tool for Monte Carlo Data

Carolina I. Restrepo, *Johnson Space Center*

Johnson Space Center (JSC) has developed an analysis tool that engineers can use to quickly gain a better understanding of a spacecraft design solely through analysis of Monte Carlo simulation data sets, thus reducing the time required within each design and analysis cycle (figure 1). This cycle iterates during the project life, in effect multiplying the improved efficiency this tool provides.

Monte Carlo simulations, used extensively during the design and analysis cycle of spacecraft development projects, consider a wide range of design parameters to generate thousands of flight scenarios that must be analyzed in detail by flight dynamics engineers.

These simulations create results that represent test data without the high costs associated with conducting real ground and flight testing. Historically, the analysis of these types of data for a fully integrated spacecraft is mostly performed manually on a case-by-case basis, often requiring several analysts to write additional scripts to sort through large data sets to identify the driving design variables. This process alone can take months.

But now, engineers have a consistent analysis methodology by which they can study a given data set in detail and gain insight into a design, regardless of whether they created it or someone else created it. This tool provides structure to the analysis process and helps engineers focus on problem areas within the current design.

The tool uses two tractable pattern recognition algorithms to search through large data sets to identify variables and variable subsets that influence a specific performance metric. The analyst classifies each simulation run in a Monte Carlo set as either a successful run or a failed run. With this information, algorithms within the tool create mathematical models of the data in both the successful-run class and the failed-run class. Subsequently, the two data classes are compared, and the differences between each are used to then identify and rank the design parameters according to their influence on a specified performance metric.

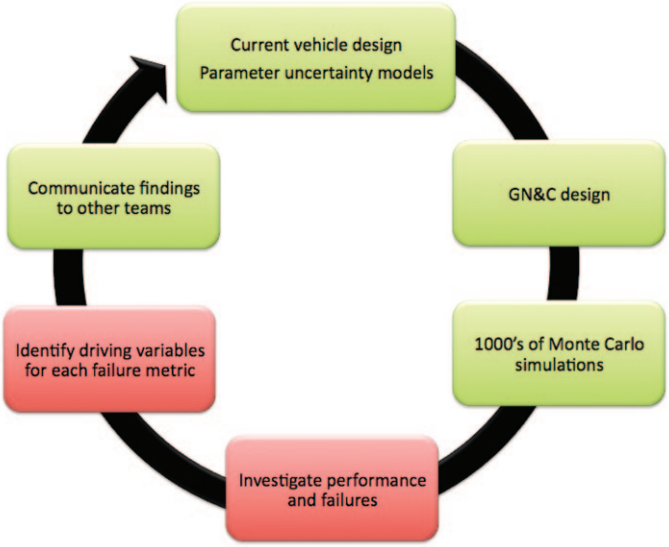


Fig. 1. *Spacecraft design and analysis cycle.*

This tool is readily applicable to a wide range of problems. It accepts the Monte Carlo data and the correlating performance metric information in a straightforward manner, so the user does not have to write problem-specific scripts. The method is 100% non-intrusive to the model equations and the simulation, and does not require running multiple Monte Carlo sets.

The only input requirement is that the Monte Carlo set must contain both successful and failed simulation runs. The inputs to the tool are three simple sets of data: the dispersed input parameters; the Monte Carlo simulation outputs, which can be saved at several discrete points in time along a trajectory; and the performance metrics information for each simulation run. The outputs of the tool are a list of ranked design variables and a list of ranked variable subspaces.

The two ranked lists provide different sets of information to an analyst (figure 2). Ranked design variables identify and prioritize which design changes should be addressed in subsequent design cycles; ranked variable combinations

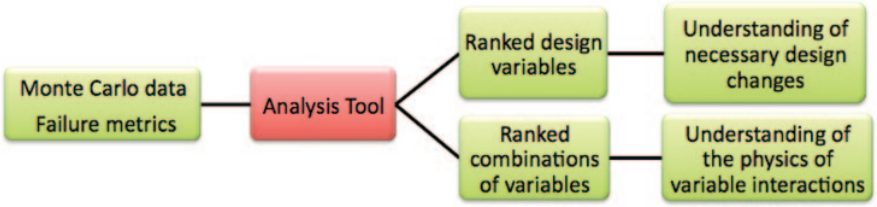


Fig. 2. *Analysis tool inputs and outputs.*

provide insight into the physics of the problem that is causing certain simulation runs to fail the specified performance metric.

The tool output does not analyze the data for the engineer, but it guides the engineer along the analysis process. In other words, it does not replace the analysts, but it does improve efficiency by identifying variables that the analysts must review in further detail.

Several of the tool's features make it readily applicable to most flight dynamics data analysis problems. One of the main benefits is the simple input data format required since most data sets can be formatted in this way. Additionally, the algorithms do not manipulate the data at any time throughout the analysis, nor do they require the analyst to do so. This means that each variable preserves its original units, and thus physical meaning. The method makes no assumptions on the uncertainty models of simulation input variables so it analyzes the dispersed inputs as they come.

Due to the tool's ease of use, an engineer who is not necessarily an expert in the fields of statistics or pattern recognition can still work with the algorithms, and understand and track how the tool analyzes the data. Of course, the engineer must possess basic problem domain knowledge to interpret the results the tool produces. Conversely, the tool is flexible enough that a system expert can introduce additional variables and modify performance metrics to drive the tool to converge on the design's most problematic issues.

The tool has recently been used to aid in the analysis of Monte Carlo data for the Orion vehicle to identify individual design variables that affect certain types of system failures. Due to the high computational cost of searching for failure regions in a problem with hundreds of variables, future versions of the analysis tool will be programmed on a graphical processing unit. In this way, engineers can explore—in detail—data sets containing hundreds of variables and thousands of variable combinations.

The Sensor Test for Orion Multi-Purpose Crew Vehicle Relative-Navigation Risk Mitigation Development Test Objective

John A. Christian, *Johnson Space Center*
Heather Hinkel, *Johnson Space Center*

The primary relative navigation sensor for the Orion Multi-Purpose Crew Vehicle (MPCV) will be the Vision Navigation Sensor (VNS). As such, the VNS will be a critical instrument in allowing Orion MPCV to perform the essential tasks of rendezvous, proximity operations, and docking with the International Space Station (ISS). The VNS—built by Ball Aerospace & Technologies Corp. (headquartered in Boulder, Colorado)—is a cutting-edge Flash Light Detection And Ranging (LIDAR) system that is expected to detect reflectors on the ISS from as far as 5 km (~3.1 miles) away. These data will be used by the Orion MPCV navigation systems to calculate the relative position and velocity of Orion MPCV during these flight phases. The VNS is also capable of simultaneously tracking enough reflectors to compute relative attitude at ranges less than 15 m (49 ft) while on an ISS approach profile.

After studying the lessons learned from relative navigation sensors on many previous flight programs and performing ground test programs, engineers at Johnson Space Center (JSC) determined it was essential to perform an on-orbit test of the VNS sensor. This was the origin of the Sensor Test for Orion MPCV Relative-Navigation Risk Mitigation (STORRM) Development Test Objective (DTO), which flew on the STS-134 space shuttle mission to the ISS in May 2011. In addition to the VNS, the STORRM DTO provided on-orbit testing of the new high-definition Orion MPCV docking camera. The VNS and the docking camera were tested on a nominal shuttle approach trajectory during docking on Flight Day 3, and on an Orion MPCV-like approach trajectory during an unprecedented re-rendezvous following undock and fly-around of the ISS. Development of the STORRM DTO sensor hardware, avionics (containing power distribution and data recording), support infrastructure, and data analysis algorithms was a 3-year collaboration between JSC, NASA Langley Research Center (Hampton, Virginia), Ball Aerospace & Technologies Corp., and Lockheed Martin (headquartered in Bethesda, Maryland).

LIDARs have a long history of use as relative navigation sensors. The space shuttle, for example, used a scanning LIDAR system called the Trajectory Control Sensor (TCS) to track a single ISS-mounted reflector at a given time. In a scanning LIDAR system, a narrow laser is scanned throughout the instrument's field of view, and it will identify a reflector and return the bearing and range to only that one reflector. Unlike scanning LIDARs that can only track one reflector at a time, a Flash LIDAR system such as the VNS has no moving parts and can track many reflectors at one time. A Flash LIDAR sends out a broad laser pulse and captures the return with a camera-like detector system. The result is two digital images of: (1) the intensity of the laser return at each pixel location; and (2) the measured range at each pixel location. Therefore, a Flash LIDAR system creates a three-dimensional map of the observed scene (from the range measurements) and a corresponding map of the intensity of the laser return. Because the reflectors were designed to be highly reflective in the VNS laser wavelength, the reflectors should be among the brightest objects in each VNS intensity image. The STORRM DTO used JSC-developed image processing algorithms to automatically detect the reflectors in the VNS images (figure 1). The VNS data will be compared to the TCS data, post-flight.

Astronauts attached specially designed reflectors built at NASA Langley Research Center to the ISS docking target and standoff cross to properly test the VNS during space shuttle mission STS-131 in April 2010. These reflectors are highly reflective at the VNS laser wavelength, but are opaque (not reflective) at the TCS laser wavelength. This reflector pattern will be used to demonstrate the ability of the VNS to track multiple reflectors and compute relative position and attitude from 15 m (49 ft) through docking on an ISS approach trajectory.

After the launch of STS-134 in May 2011, NASA performed a checkout of all the STORRM hardware and software on Flight Day 2. Then, the VNS and docking camera collected data during the rendezvous with the ISS on Flight Day 3. During this time, screenshots of the STORRM software application as well as health and status information of the STORRM hardware components were downlinked to the Mission Control Center at JSC through a near real-time TV system called Sequential Still Video. This system provided information about how well the STORRM data recorders, VNS, and docking camera functioned during the rendezvous.

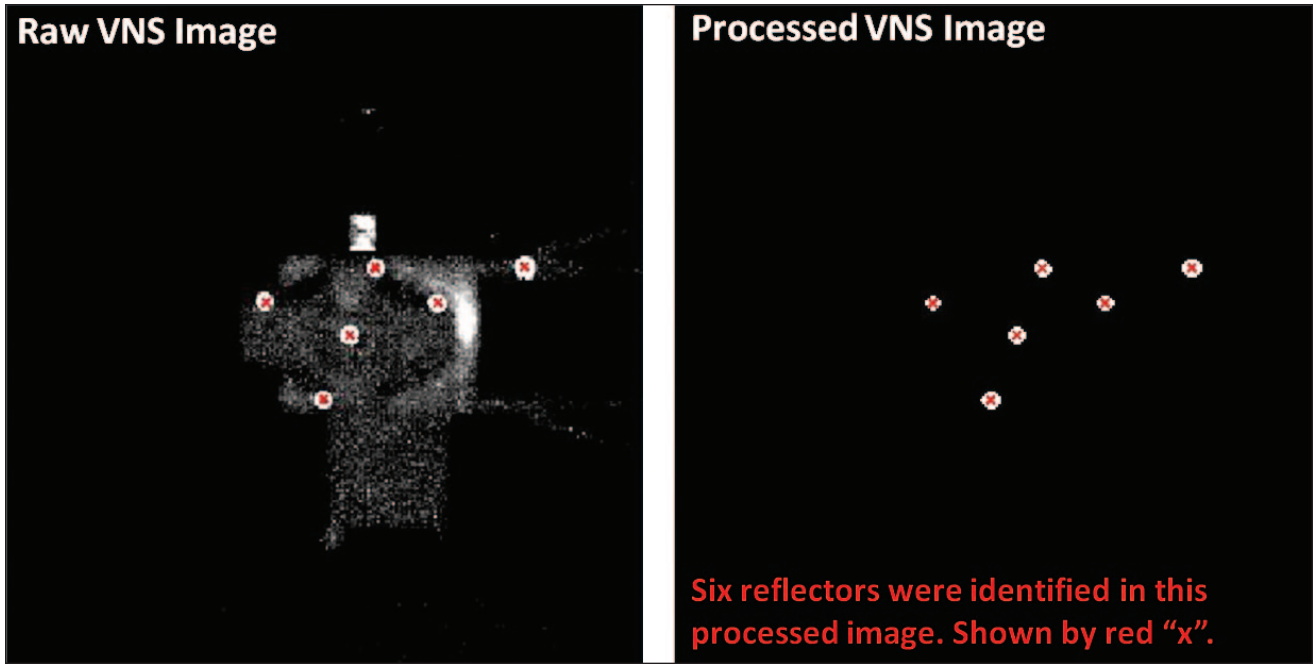


Fig. 1. *The Vision Navigation Sensor (VNS) is capable of detecting the six reflectors (five Sensor Test for Orion Multi-Purpose Crew Vehicle Relative-Navigation Risk Mitigation-like reflectors, and one 5 cm (2-in. blue street reflector) mounted on the docking target at a range of about 4.5 m (14.7 ft) in this test image from April 2010.*

After the shuttle docked with the ISS, a small set of prioritized data was retrieved from the STORRM drives and downlinked to the Mission Control Center. These data were then analyzed by STORRM analysts to determine whether the VNS and docking camera operated as expected during the Flight Day 3 rendezvous. The results of this analysis informed the STORRM team of any changes that needed to be made to the VNS or docking camera settings, which could be modified through configuration files before the re-rendezvous on the day of undocking. Additionally, before the standoff cross was removed from the docking target, the crew took a number of photographs of the target from several angles. These images were used for a photogrammetry analysis to determine the actual location of each reflector on the docking target to within 3 mm (0.12 in.).

The STORRM hardware was powered on again before undocking from the ISS. The VNS collected data throughout the ISS undocking, fly-around, and during the re-rendezvous on the Orion MPCV-like approach trajectory. These data allowed the STORRM team to assess the VNS performance along a trajectory similar to what is planned for the Orion MPCV and other future vehicles. The shuttle and Orion MPCV trajectories are different in a number of ways making this a critical part of the STORRM test. The re-rendezvous took shuttle to a targeted point 305 m (1000 ft) below and 91 m (300 ft) behind the ISS. STORRM operated and collected data through 5 km (3.1 miles) on the departing trajectory.

The experience and sensor data gained by the STORRM DTO will be of great value to the Orion MPCV Program Office and to all of the STORRM team members. In addition to benefiting the development of the VNS for Orion MPCV, the STORRM DTO is also benefiting other projects using the VNS, such as the VNS Autonomous DPP Rendezvous Experiment, which is scheduled to fly to the ISS as part of the DEXTRE Pointing Package (DEXTRE is a sophisticated dual armed robot on the ISS built by the Canadian Space Agency). The maturation of this state-of-the-art sensor will make this technology available to future NASA programs (crewed or uncrewed) for rendezvous and docking. The advancement of Flash LIDAR technology also benefits the cross-cutting application of hazard avoidance, which is required for safe landing on asteroids, the moon, and Mars. This sensing technology may also improve a variety of earthbound applications such as climate and environmental observations, robotic maneuvering, topographical surveillance, and hazard avoidance systems for cars or aircraft.

Boundary Layer Transition Flight Experiment Overview

Brian Anderson, *Johnson Space Center*
Charles Campbell, *Johnson Space Center*

A thermal protection system (TPS) is required for the safety and success of any vehicle entering a planetary atmosphere, and such a system significantly affects the vehicle's design and ultimate weight. One of the design drivers to TPS sizing is the time during entry at which the boundary layer transitions from laminar to turbulent flow. The study of boundary layer transition (BLT) has been a significant effort for many decades, but the specific physics-based mechanisms that cause hypersonic BLT are poorly understood.

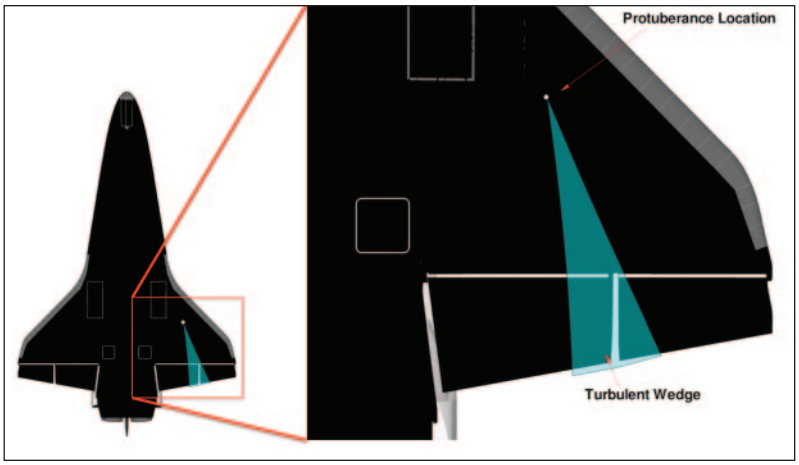


Fig. 1. *Selected protuberance location and predicted turbulent wedge.*

This lack of understanding hinders designers from accurately predicting when the boundary layer will become turbulent, and affects sizing and understanding of TPS robustness. If engineers know the geometry of a vehicle, they can obtain ground-test data from wind tunnels to develop engineering correlations.

However, one major weakness of a ground-based correlation approach is poor understanding of differences between wind tunnel and flight environments, and how those differences affect BLT. In addition to difficulties present in predicting BLT onset, hypersonic turbulent heating predictions have also proven to be challenging in many cases. A small amount of data exists to verify turbulent heating prediction models at low Reynolds numbers and hypersonic conditions.

During space shuttle mission STS-114, astronauts performed an unprecedented spacewalk to remove two protruding gap fillers because mission directors determined that the risks associated with the uncertainties concerning early BLT and resultant heating effects were higher than the risks of the spacewalk itself.

To mitigate these risks for future missions, the BLT team proposed a flight test using a protuberance on the orbiter to purposefully trip the boundary layer at a targeted Mach number. A protuberance tile and augmented instrumentation package (thermocouples) was installed on two space shuttle orbiters—*Discovery* and *Endeavour*.

The BLT flight experiment flew on five flights: STS-119, STS-128, STS-131, STS-133, and STS-134.

NASA Langley Research Center also led an activity, complementary to the BLT flight experiment, to image the orbiter during reentry using infrared detectors. The Hypersonic Thermodynamic Infrared Measurements team imaged the orbiter on each of the BLT flight experiment flights, as well as on STS-125 and STS-132.

Experiment Design Overview

Given the uncertainties in predicting BLT onset and associated TPS effects, and to ensure safety, the team decided early in the planning stages to approach the flight test program incrementally.

The team installed the protuberance on the port wing—outboard of, and downstream from, the main landing gear door (figure 1).

The flown height of the protuberance, derived using the orbiter BLT tool, was 0.64 cm (0.25 in.) for STS-119 and 0.89 cm (0.35 in.) for both STS-128 and STS-131. A height of 1.3 cm (0.5 in.) was flown for STS-133 and STS-134. These heights were designed to induce BLT at approximately Mach 15 (0.64-cm [0.25-in.] height), Mach 18 (0.89-cm [0.35-in.] height), and Mach 19 (1.3-cm [0.5-in.] height).



Fig. 2. *Final protuberance shape, installed on tile.*

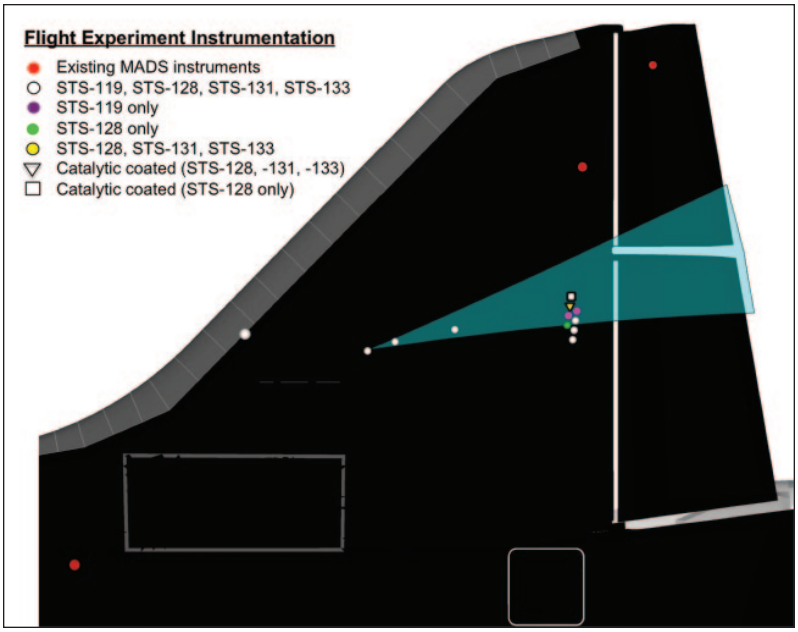


Fig. 3. *Instrumentation locations on* Discovery.

The protuberance tile was fabricated using Boeing Replacement Insulation-18 tile material; the installed length and width was 10-cm (4 in.) and approximately 1 cm (0.4 in.), respectively, for all five flights. The protuberance was machined into the tile such that the leading edge was oriented at a 45-degree angle relative to the predicted local flow streamline (figure 2).

The flight experiment instrumentation augmentation added 10 thermocouples on *Discovery* (figure 3) and four on *Endeavour*.

In addition to BLT and turbulent heating at high Mach numbers, another aerothermodynamic phenomenon not clearly understood is the potential coupling effect between turbulent flow and a catalytic material. Using expertise developed from previous flight experiments, a catalytic coating material originally formulated by NASA Ames Research Center was reconstituted and applied to study this potential effect.

Data from this aspect of the experiment could have significant impact on future capsule designs that use orbiter tiles. Technicians installed tiles downstream of the BLT protuberance with instrumentation directly below the catalytic coating for STS-128, STS-131 (figure 4), STS-133, and STS-134.

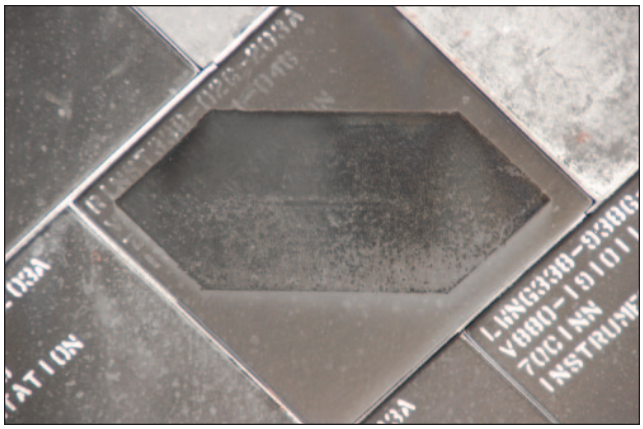


Fig. 4. *Post-flight runway photograph of catalytic coating following STS-131.*

Results and Summary

Data were obtained during reentry of STS-119, STS-128, STS-131, STS-133, and STS-134. Data from each flight thus far have proven to be useful; however, flight data from STS-128, STS-131, and STS-133 appear to be affected by an unknown temperature anomaly. At approximately 750 seconds into reentry during STS-131, instrumentation recorded a rapid drop in temperature (figure 5), which is not completely understood but seems to have been caused by environmental coupling with the orbiter instrumentation system, and initiated at roll reversal.

Boundary Layer Transition Flight Experiment Overview

continued

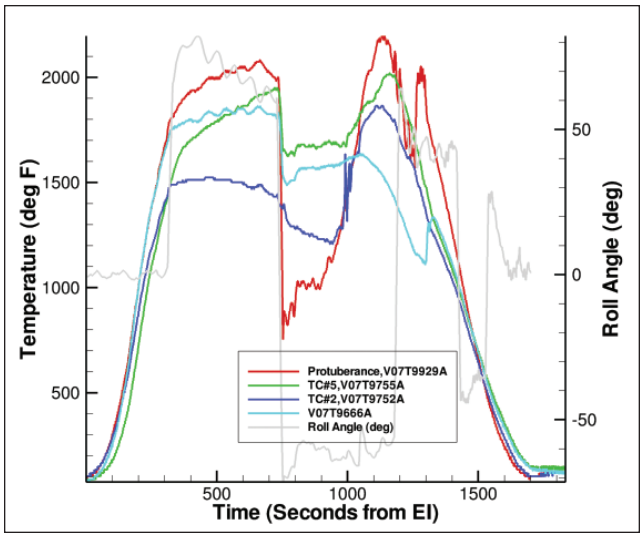


Fig. 5. *Representative thermocouple data from STS-131.*

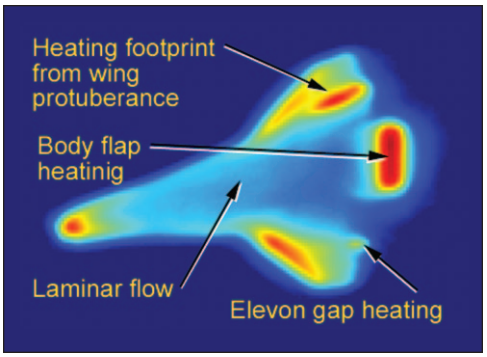


Fig. 6. *STS-128 Hypersonic Thermodynamic Infrared Measurement imagery showing the heating footprint caused by the protuberance.*

Unfortunately, this temperature anomaly has prevented significant conclusions for the catalytic coating tile experiment. The extent and magnitude of the heating footprint (figure 6) was inferred from the thermocouple data.

Conclusion

Data obtained during the flight experiment campaign have been beneficial to the technical community. Preliminary analysis indicates that the orbiter BLT tool is good at predicting BLT onset, with predictions typically within 0.5 Mach number of flight data indications. Analytical temperature predictions were much higher than the actual temperature data obtained from the flights, though analysts have not yet determined the cause for this discrepancy.

Future BLT tests will likely include experiments to determine the cause for this difference between predicted and actual flight temperatures.

Error Bars for Computational Simulation

Benjamin Kirk, *Johnson Space Center*
Adam Amar, *Johnson Space Center*

"Prediction is very difficult, especially if it's about the future." – Niels Bohr

The Crew Exploration Vehicle (CEV) Aerosciences Project at Johnson Space Center is responsible for defining the aerodynamic and aerothermodynamic environments that the Orion capsule will experience during reentry. The relevant physical processes involved during reentry from superorbital velocity are shown in figure 1. It is impossible to simultaneously reproduce all of these physical phenomena in any ground test facility because of the tremendous amounts of energy and large scales involved in reentry. Consequently, designers increasingly leverage complex computer simulations to predict what these environments will be. These predictions are then used to design the vehicle without full system-level test data. The obvious question is: how much can the designer trust these predictions? Specifically, how does one define "error bars" for computational simulation?

NASA is not the only agency struggling with this question. As it turns out, the Department of Energy's National Nuclear Security Administration (NNSA) is posed with a similar challenge. The NNSA is responsible for the stewardship of the nation's nuclear stockpile, and is banned by treaty from performing full system-level testing. This question is so vital to the NNSA mission that it created the Predictive Science Academic Alliance Program (PSAAP) to address it.

The Department of Energy awarded five PSAAP centers in 2008. Each center was awarded 5 years of funding to study advanced verification, validation, and uncertainty quantification techniques for coupled multi-physics applications relevant to the NNSA mission. The University of Texas at Austin's Center for Predictive Engineering and Computational Sciences (PECOS) is one of the five PSAAP centers.

The goal of the PECOS center is to develop the next generation of advanced computational methods for predictive simulation of multi-scale, multi-physics phenomena, and to apply these methods to the analysis of vehicles reentering the atmosphere. The Engineering Directorate at Johnson Space Center has partnered with

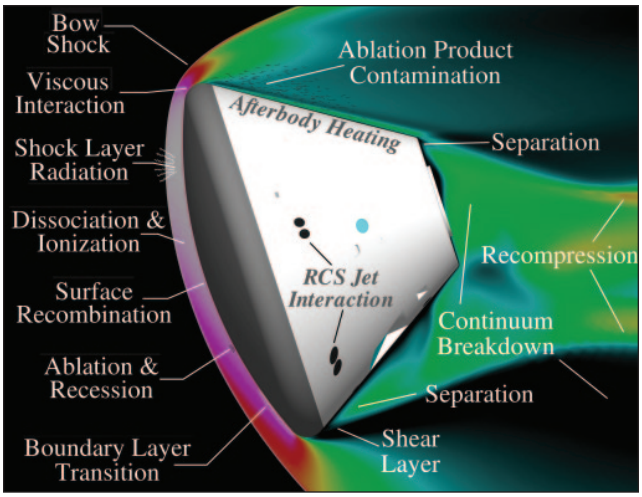


Fig. 1. *Coupled multi-physics relevant in hypersonic entry. The physical scales and energies involved in reentry preclude system-level testing, requiring engineers to increasingly rely on computational predictions in the design process. Understanding the accuracy of these simulations is a critically important and difficult aspect of design. Quantifying the uncertainty in such predications is one focus of NASA's current research.*

PECOS in this goal, and has set up a Space Act Agreement to facilitate the sharing of data and discipline expertise between the two groups.

Today's computational analysts are presented a wealth of mathematical models— each with its own strengths and weaknesses—to describe the phenomena in figure 1. Each model has certain parameters whose values are determined from either theory or experiment. Once the best models and their associated parameters are determined, predictions can be made for the flight environment. Historically, model selection and parameter determination has been somewhat ad hoc, often with single "optimal" parameter values determined for simple configurations, and reported in the literature. A central tenant of the PECOS research is *rigorously informed model selection and parameter determination*. In this approach, the model parameters are instead recast in terms of probabilities, whose most likely values are determined from experimental data. Thus, parameters are defined not by single values but rather through rigorously informed probability distribution functions. In this approach, prediction then does not yield a

Error Bars for Computational Simulation

continued

single value, but rather again a distribution function whose width defines the confidence in that prediction.

Additionally, the proliferation of computational models is often a challenge. To simulate the effects of turbulence in a fluid, for example, the analyst must first choose from no fewer than five separate turbulence models, each with its own strengths and weaknesses. Historically, selecting the "optimal" model has been ad hoc, which is unsettling because this choice can have a critical impact on design. The PECOS group introduced the concept of *model plausibility* to address this challenge. Again, the approach is to employ statistical inference techniques to determine which model(s) are most preferred by the available data.

This approach is illustrated in figure 2, where three separate models are employed to predict wall shear stress in a fluid. The result of each prediction is a probability distribution function centered about the most likely value for each model. Further, the models are ranked in terms of plausibility. In this case, Model #3 is dramatically preferred by the data, which would suggest to the analyst that it is the best model to use for prediction in the absence of data.

The project has already contributed some significant findings. As research enters its 4th year, focus is shifting from calibration and model selection to prediction of the coupled multi-physics of reentry using rigorously informed and selected physical models. This is a significant step in the research and will allow designers to use computational predictions with meaningful "error bars" applied because, after all, no computational model will ever be perfect.

"All models are wrong, some are useful." – George Box

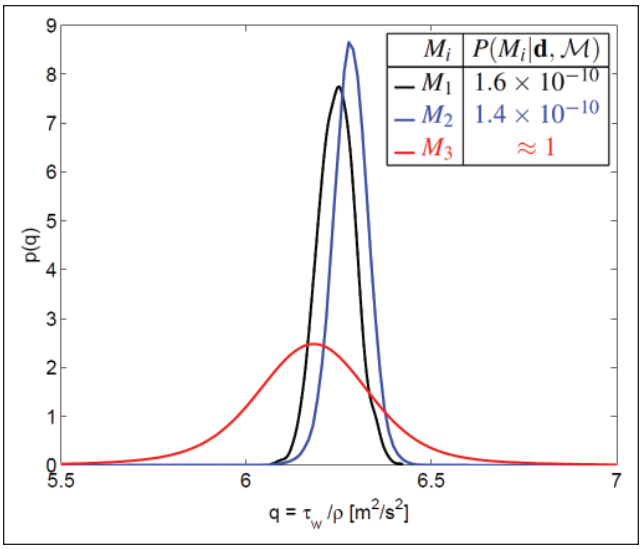


Fig. 2. *Model plausibility and quantity of interest predictions for shear stress in a turbulent flow. Model #3 has the highest uncertainty in the uncertainty in the quantity of interest, but is most likely the correct model given the set of calibration data used. Dr. Todd Oliver of Predictive Engineering and Computational Sciences provided this result.*

Copernicus Trajectory Design and Optimization System

Gerald L. Condon, *Johnson Space Center*

Future space missions can involve multiple spacecraft, multiple destinations, multiple gravity fields, and multiple or hybrid propulsion systems. These complex missions will require intricate trajectory design and optimization, fast and high-precision results, large multidimensional trade spaces, and analyses of both mission design concepts and mission operations. The Copernicus Trajectory Design and Optimization System provides a solution to these future mission design demands with a general, robust, efficient, and practical high-fidelity three-degrees-of-freedom tool to determine timely and accurate solutions for both human and robotic exploration studies.

Copernicus can generate engineering solutions for a myriad of possible planetary and interplanetary destinations including, but not limited to, lunar missions, Earth neighborhood libration point missions, interplanetary missions (including missions to satellites of the outer primary planets, asteroids, and comets), powered flight landing/ascent maneuvers, formation flying, far-field rendezvous, and weak stability boundaries.

The power of Copernicus lies in a standardized methodology used to solve problems, coupled with an integrated output that provides immediate graphical feedback to the user as to the "goodness" of the solution. This approach allows Copernicus to produce high-precision solutions for a large range of (complex) missions with faster response time.

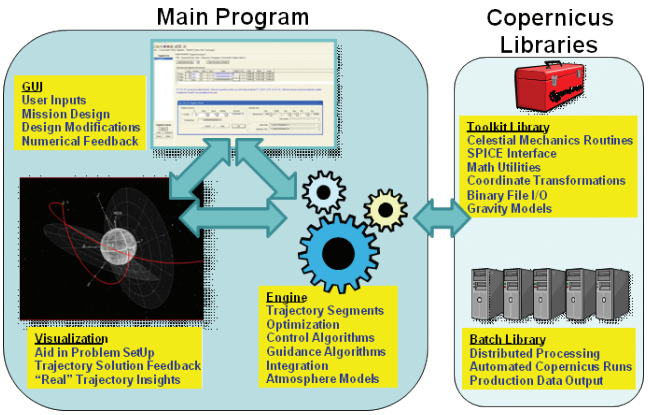


Fig. 2. *Copernicus integrated input graphical user interface, trajectory visualization, and processing engine.*

This tool can be used by mission designers, researchers, and students, and has both civil service and contractor users at several NASA centers, commercial industry, and academia locations across the country. Copernicus has been used in the trajectory design for the successful Lunar Crater Observation and Sensing Satellite mission (figure 1) as well as a plethora of architecture, mission, trajectory, and analysis studies for the Constellation Program, Orion Project, and NASA Headquarters.

A key advantage of the system is its versatility—it was specifically designed to address trajectory design and optimization issues associated with many different mission classes. Copernicus is a unique software tool because it integrates a powerful modular trajectory design and optimization engine, an easy-to-use graphical user interface, and interactive visualization. This interaction is a key component in the solution process because it helps the user to understand the construction of the solutions and to produce a convergent sequence of iterations to create a final mission trajectory.



Fig. 1. *Copernicus-based trajectory design for Lunar Crater Observation and Sensing Satellite mission.*

Copernicus Trajectory Design and Optimization System

continued

Copernicus also interfaces with a modular tool kit library of coordinate frames, environmental models, ephemerides, and utilities (figure 2).

In addition to being a key component of the tool suite, this tool kit is also a foundation for developing other programs and processors, such as the Mission Assessment Post Processor, which was used extensively in Orion propellant requirement analyses.

Copernicus can run on a Windows-based PC platform or a Unix-based computer cluster. The Unix configuration—a batch processing mode—is well suited to computationally intensive tasks and has been used extensively. For example, analysts used this batch processing mode to run Copernicus automatically, millions of times, to generate large performance matrices in support of the Constellation Program. The team then used the large amount of data in these matrices to assess the on-orbit performance requirement for landing anywhere on the lunar surface and during a metonic cycle (approximately 18.6 years). With this batch capability, analysts could better understand the statistical nature of the performance requirement, and thus the impact of changing the Orion spacecraft propellant loading.

Copernicus is a segment-based system that uses a segment object as a basic building block to construct simple to complex trajectories (see figure 3). The segment building block contains numerous parameters that model a single spacecraft. These parameters include: mass and state properties, propulsion system, and boundary conditions. Multiple segments constitute a spacecraft mission, and because users have total control over how to connect these segments, they can model single or multiple spacecraft problems.

The methods used to propagate the equations of motion and the methods used to converge and satisfy the boundary conditions are independent and selectable. This results in a highly versatile system. It is a system that evolves seamlessly as new modeling and optimization techniques are developed and introduced to the state-of-the-art suite of algorithms.

The user-friendly design of Copernicus allows the analyst to quickly translate an idea and initial drawing or

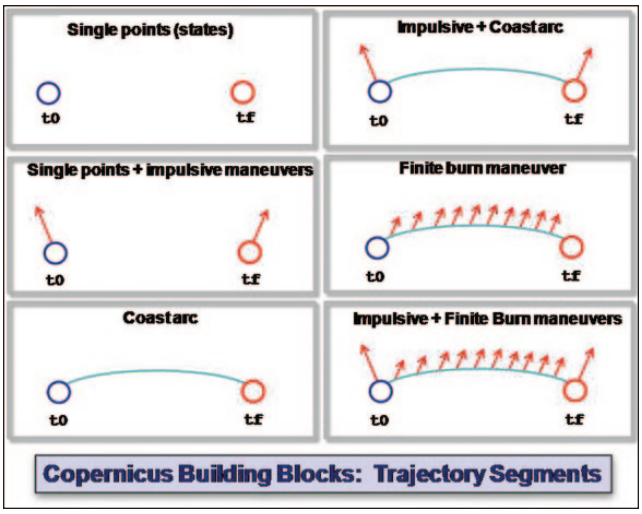


Fig. 3. *Copernicus building block trajectory segments.*

schematic into a high-fidelity powered flight trajectory. Figure 4 shows a conceptual view of the solution process for a low-thrust variable specific impulse round-trip Earth-Mars mission with constraints on stay time at Mars and overall mission duration. The analyst maps an initial schematic of the problem (upper left) by entering appropriate mission inputs (lower left) into the simple-to-use graphical user interface. A graphical output of the solution (right) includes the transfer orbit and indicators of thrust magnitude and direction during the trip.

Although Copernicus is a small project in terms of overall funding, this software's capability has allowed NASA centers to provide comprehensive performance analysis for the Orion Project and the Constellation Program, both of which identified Copernicus as a primary performance analysis tool. Copernicus has allowed engineers at the centers to obtain a deep understanding of the lunar mission design effects on vehicle performance in a short time (figure 5).

The Copernicus development work reflects a collaborative effort among civil servants and contractors in the Aeroscience and Flight Mechanics Division of Johnson Space Center and the University of Texas at Austin. This symbiotic relationship allowed the center to take advantage of research and development advancements in academia while more directly engaging the university in NASA projects.

Copernicus continues to adapt to serve user needs as NASA programs change and associated mission and trajectory design needs change with them. From mission architecture feasibility to spacecraft performance to prototyping of candidate guidance and targeting algorithms, Copernicus remains one of NASA's preeminent mission and trajectory design software tools, and promises to enhance user productivity with a powerful capability for years to come.

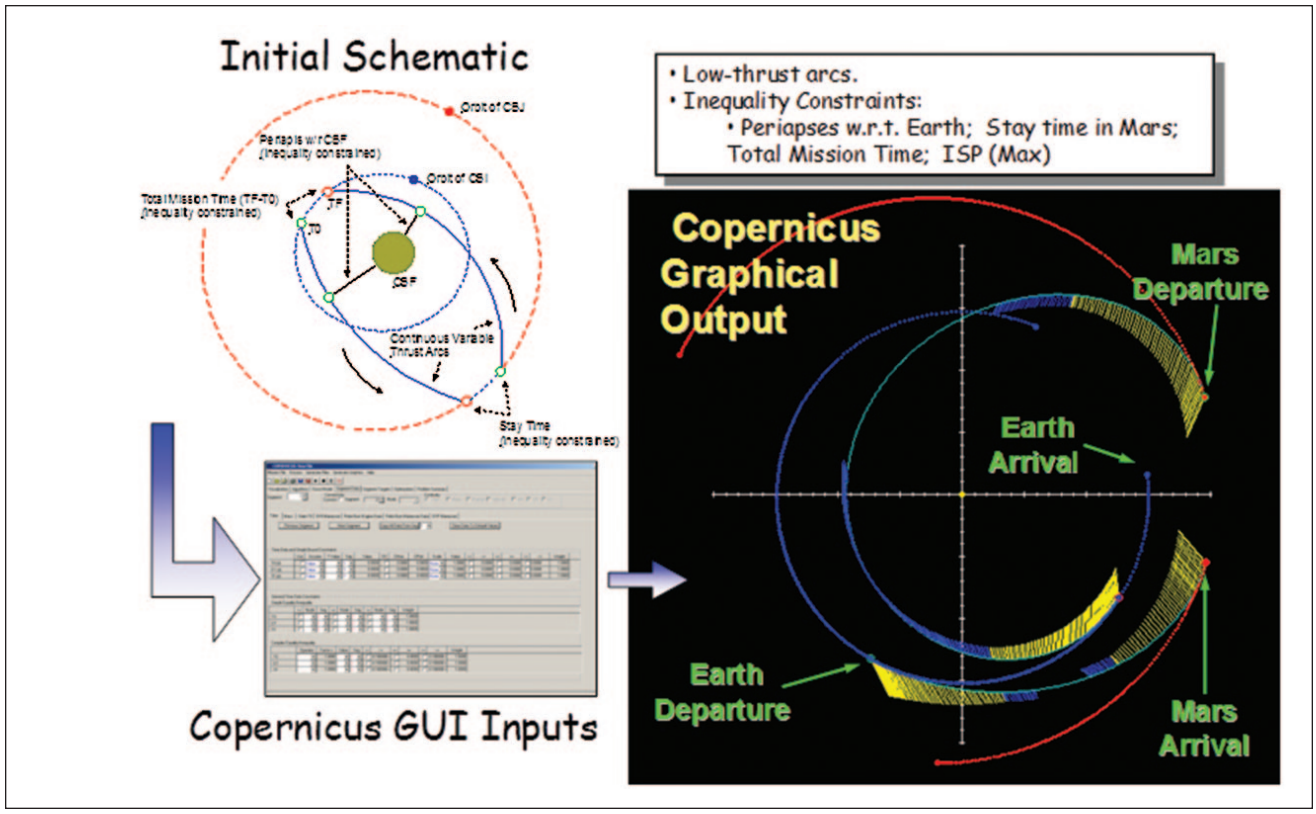


Fig. 4. Copernicus trajectory design example.

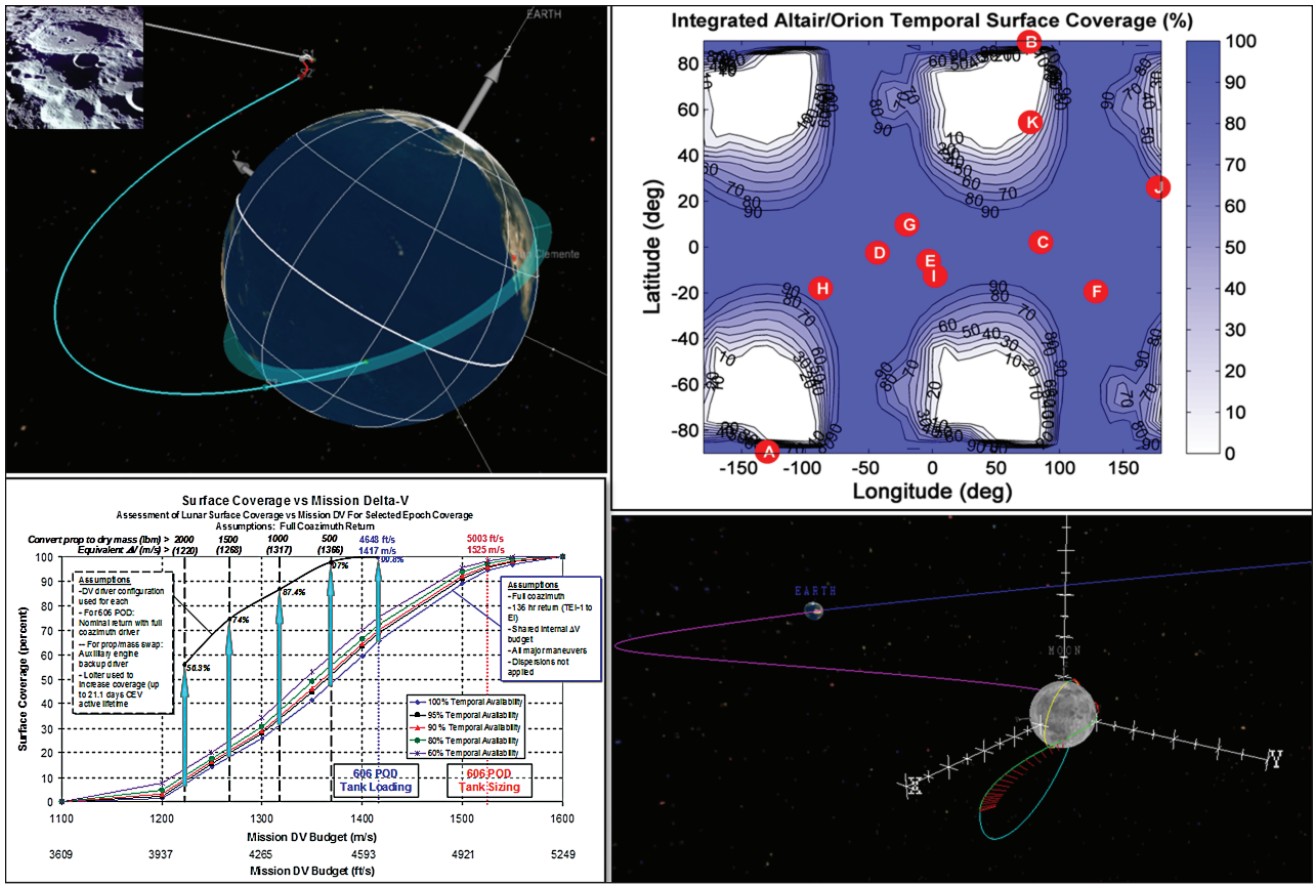


Fig. 5. Copernicus-based trajectories, lunar accessibility, and Orion propellant requirements.

Habitat Demonstration Unit Core Avionics Software

Dennis Lawler, *Johnson Space Center*
Lui Wang, *Johnson Space Center*
Tam Ngo, *Johnson Space Center*
Linda Moreland, *Johnson Space Center*
Danny Carrejo, *Johnson Space Center*
Aaron Schram, *Johnson Space Center*
Thomas Matthews, *Johnson Space Center*
Craig Russell, *Johnson Space Center*
Emmy Alex, *Johnson Space Center*
Ayman Qaddumi, *Johnson Space Center*

Increased crew autonomy will be required to support long-duration missions and missions with significant time delay. This will include capabilities such as gradual automation of routine tasks, increasing crew efficiency, the ability to revert to manual mode in the event of off-nominal behavior, and the ability to refine procedures onboard without waiting for ground inputs. A flexible software test bed that allows engineers to exploit such capabilities will be required to productively experiment with these types of advanced operational functionalities.

The multicenter Habitat Demonstration Unit (HDU) project designed and built a planetary surface analog element with a configurable, habitable volume and basic infrastructure services (i.e., power, lighting, command and data handling, thermal control, etc.), as well as a number of "workshop"-like capabilities (e.g., maintenance and repair workstations). This provides an opportunity to implement and operate just such a software test bed. For example, the onboard computer systems furnished a distributed computing environment encouraging new software design approaches, and incorporated wireless data acquisition technology that required new software interface protocols.

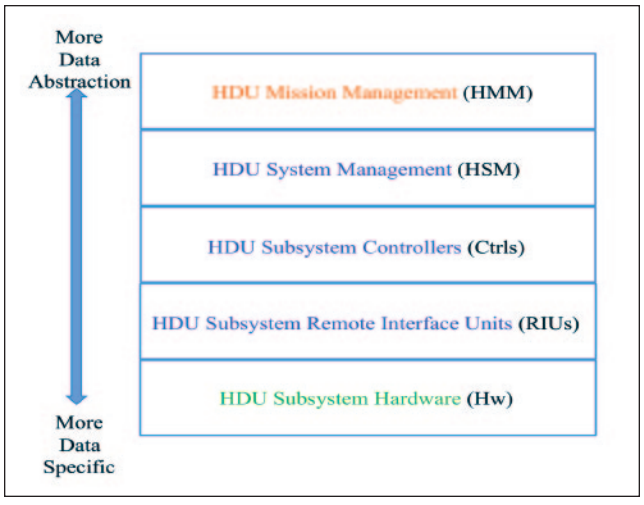


Fig 1. *Functional layers add modularity while providing hierarchical structure.*

The Habitat Demonstration Unit Core Avionics Software (HDU-CAS) is designed to provide the required functionality for an engineering prototype of a highly autonomous space habitat element, and provide an opportunity for new software technologies to be tested in an environment that provides that functionality. As such, the HDU-CAS provides complete command and data handling and intelligent autonomous operations functions to HDU subsystems in all operational circumstances (nominal and off-nominal), and it must do so in a manner that allows technologists to test prototype software for these functions.

Earlier approaches for this problem space relied on manual, one-of-a-kind designs that optimized size and computational performance, often developed unique communication interface protocols, and were deployed on centralized computer assets. Also, they were often highly constrained by the need to integrate with the legacy software environments that restricted the ability to implement new software technology. These approaches would save some time and reduce risk, but were not designed for flexible integration and could preclude any practical experimentation.

In contrast, HDU-CAS was designed and implemented using an innovative mixture of open standard communication products, commercial subsystem diagnostic modeling software, specialized procedural automation scripting software, and a hierarchical structure. It was developed over the period from September 2009 to September 2010, and deployed/evaluated during the Desert Research and Technology Studies exercise in September 2010.

The structure of the HDU-CAS consists of a hierarchical arrangement of hardware interface components (called Remote Interface Units), subsystem-specific controllers, and system management components. The overall component connectivity in the distributed computer network is provided by a message handling middleware between computer assets and a shared memory component with any particular computer (figures 1 and 2).

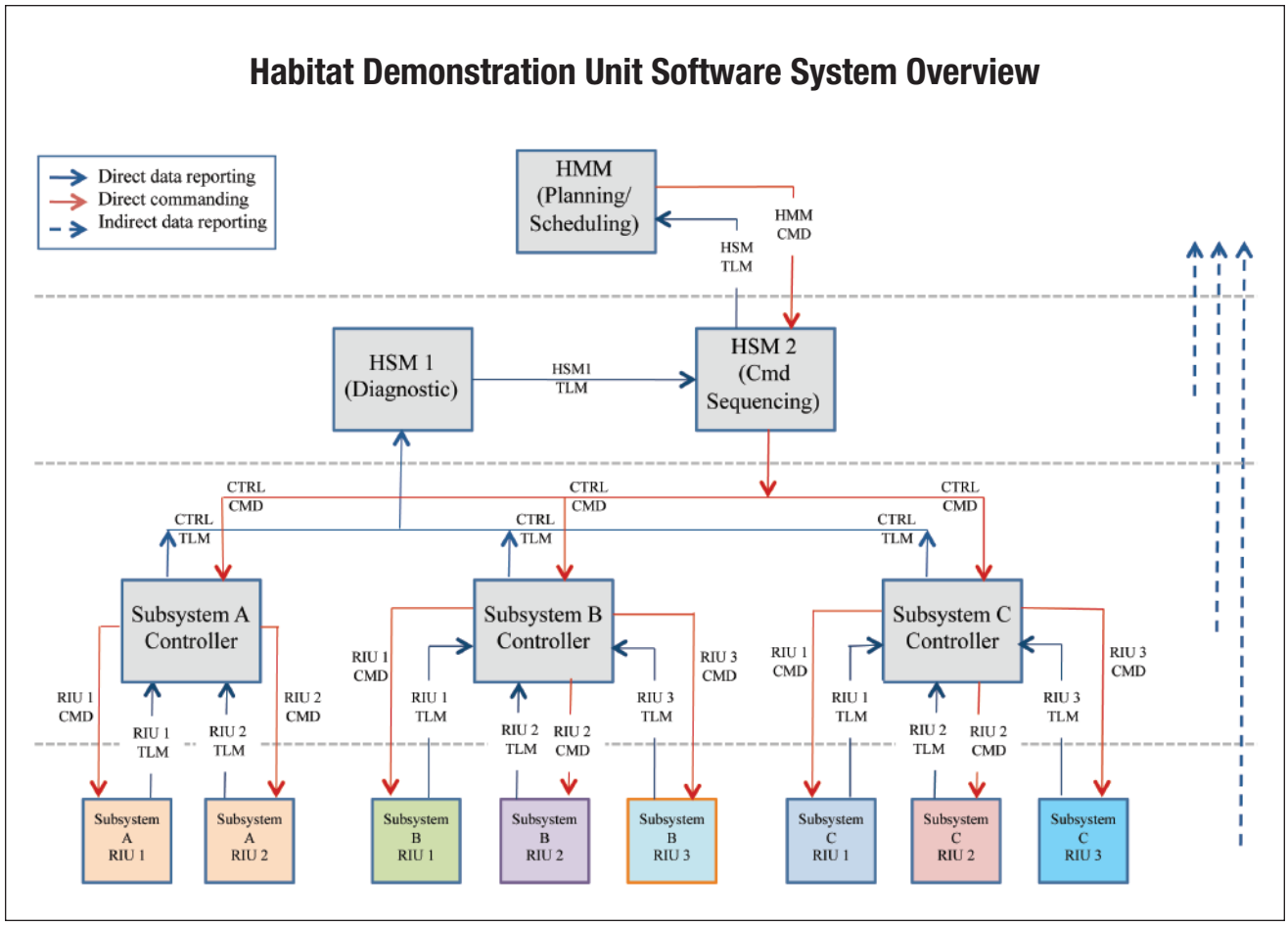


Fig. 2. *Middleware connectivity for communication between computers and processes.*

The functional operation of the HDU-CAS consists in the use of the data acquisition, logging, message handling, and controller components to monitor telemetry and provide manual and automated command paths for subsystem operations.

The system management components use the collected data and controller observations to manage habitat-wide operations involving the concurrent control of multiple subsystems. Specifically they identify subsystem faults, isolate the diagnosis to problem components, and execute recovery actions either automatically or under the direction of crew/HDU operators via the crew display and interface.

The overall design modeled a structure generally compatible with the ARINC [Avionics Application Standard Software Interface] 653 Safety Critical Software Specification to ease later integration into a deployed space vehicle compliant with that specification.

In addition, previous software environments for spacecraft habitat systems often did not consider *intelligent* automation as a high priority. The HDU-CAS was developed uniquely to integrate technologies that provide intelligent automation and other autonomous operations capabilities right from the start as a high priority.

As deployed for the HDU, this innovative integrated software design provided enormous flexibility and ease of integration that greatly facilitated the dexterity needed when working in such a prototyping environment where subsystem design and behavior can vary broadly as integration proceeds and new operational knowledge is acquired.

Supersonic Retropropulsion

Guy Schauerhamer, *Johnson Space Center*
Kerry Trumble, *Ames Research Center*
William Kleb, *Langley Research Center*
Karl Edquist, *Langley Research Center*
Scott Berry, *Langley Research Center*
Matt Rhode, *Langley Research Center*

As NASA turns its focus to space exploration beyond low-Earth orbit, one clear goal is reaching Earth's neighboring planet—Mars. To meet this goal, a spacecraft must decelerate from tens of thousands of miles per hour to a delicate, soft landing on the Mars surface, which is very challenging. To add complexity to this feat, the mass of future spacecraft is rising.

Since the current robotic missions (approximately 1 metric ton) have already reached the limit of scalability for current deceleration techniques, larger robotic- or human-scaled (10s of metric tons) missions to Mars require a new enabling technology.

Supersonic Retropropulsion (SRP) is a viable means for decelerating high-mass vehicles during Martian atmospheric entry. Retropropulsion has been used successfully in previous missions during the final stages of Martian landing, but its flow characteristics at higher (supersonic) velocities, experienced earlier in the entry trajectory, still require much research.

Ground and flight tests would provide designers with data to predict the flow field around a vehicle. But, because setting up entry conditions in wind tunnels and conducting flight tests on Mars can be difficult and cost-prohibitive, analysts use Computational Fluid Dynamics (CFD) to obtain these data and to develop the SRP method.

The SRP flow structure involves an opposing jet firing into a supersonic flow causing shocks, free shear layers, recirculation, and stagnation regions. The complexity of this interaction stretches current CFD capabilities, and mandates validation of CFD for this type of flow.

Four flow solvers across the agency have been employed to validate CFD for SRP. These codes, OVERFLOW (detailed in this report), FUN3D, DPLR, and US3D have solved SRP problems by simulating cases from historic and recent wind tunnel tests. Through code-to-code and code-to-test comparisons of surface pressure, forces and moments, and shock structure, analysts can validate the CFD and confidently use it for the complex Martian entry problem.

CFD was used to simulate historic wind tunnel experiments like Daso et al (American Institute of Aeronautics and Astronautics [AIAA] 2007-1423).

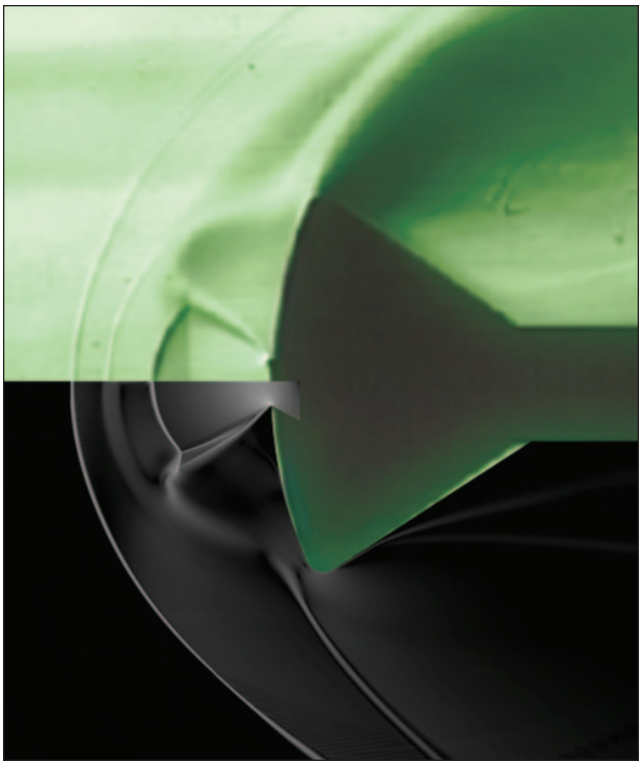


Fig. 1. *Comparison of test Schlieren from Daso et al (top) and the log of the density gradient magnitude from OVERFLOW (bottom).*

Code-to-code and code-to-test comparisons matched closely and were encouraging (figure 1).

Using historic data for SRP development does have its drawbacks—existing documentation lacks critical information needed for CFD validation, and all tested thrust levels were lower than what is desired for flight. Engineers designed a new wind tunnel test specifically for CFD validation to address these concerns.

The team used observations from pretest CFD simulations to improve the design of the test model and run conditions. In CFD results, the original model diameter caused surface pressure discrepancies due to wall effects, low temperatures in the plumes caused concern of liquefaction, possible blockage was shown at high thrust coefficients, and the plume structure contained high-frequency unsteadiness.

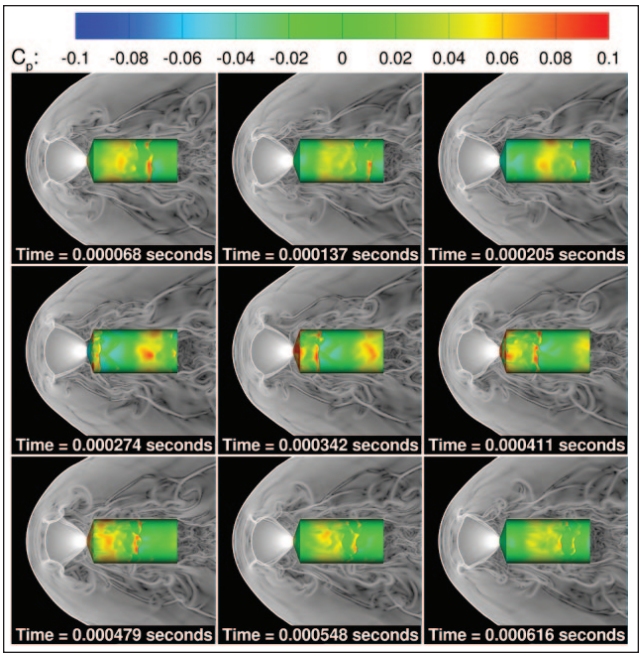


Fig. 2. *OVERFLOW time-accurate simulation of a single nozzle Langley Unitary Plan Wind Tunnel posttest case. The log of the density gradient magnitude are in grayscale and surface pressure coefficient are in color. Mach = 4.6, Reynolds/foot = 1.5E+06, and thrust coefficient = 2.*

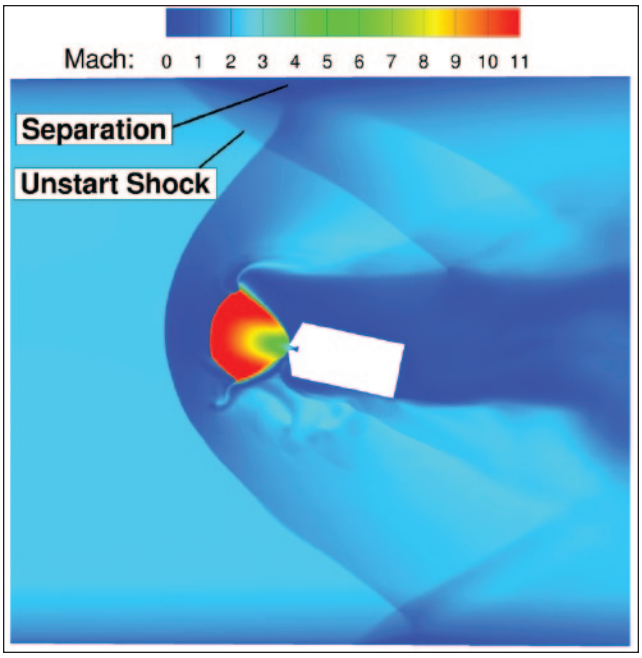


Fig. 3. *OVERFLOW simulation of tunnel unstart in the Langley Unitary Plan Wind Tunnel. Mach = 2.4, Reynolds/foot = 1E+06, thrust coefficient = 4, angle of attack = 12 degrees.*

In response to these observations, the team decreased the test model diameter, heated the plume gas before entering the model plenum, decreased the thrust levels in the run envelope, and added high-frequency pressure gauges and high-speed Schlieren (photographing the flow of air around objects) capabilities.

The team successfully completed the test in July 2010 in the 1.2 x 1.2 m (4 x 4-ft) supersonic Langley Unitary Plan Wind Tunnel. High-speed Schlieren, 165 pressure taps, and 11 high-frequency gauges were employed on a large run matrix to provide the team with the data needed to perform CFD validation.

Each code completed time-accurate sensitivity studies to compare grid refinement, numerical method choice, turbulence model, and time-step values. Once the team members established best practices, they compared final products to tunnel data. This not only supplied CFD validation, but also tested each code's predictive capability.

The test captured high-frequency—approximately 2 kilohertz—unsteadiness with enough detail to use it as a metric for CFD validation. Figure 2 shows an example of a run simulated with OVERFLOW organized in a time series to visualize the unsteady behavior of the jet plume. The flow structure, behavior, dominant frequency, and averaged surface pressures matched those of the test. Similar code-to-test comparison successes for OVERFLOW occurred across the run matrix, with variance in nozzle quantity (1, 3, or 4), angle of attack, and thrust coefficient.

Qualitatively, the code-to-code comparisons differed mostly in the level of unsteadiness, which was dampened by some of the flow solvers. These differences were most likely caused by turbulence model implementation.

At certain conditions, the Langley Unitary Plan Wind Tunnel test showed tunnel unstart—a supersonic choking reaction caused by the bow shock reflection off the wall. At the reflection, a separation region forms and increases in size, causing a new shock that propagates upstream. Unstart was predicted (figure 3) by using OVERFLOW, and modeling the settling chamber, nozzle, and full test section of the tunnel to properly form the large boundary layer on the walls around the model. This capability will help in the design of future SRP wind tunnel tests.

The Langley Unitary Plan Wind Tunnel test provided valuable information for validation of CFD for SRP. However, due to the large boundary layers in the tunnel, test runs could not simulate the high level of thrust needed for flight conditions. The lower thrust coefficients in the test created a fair amount of unsteadiness, which caused concern for vehicle stability. But when higher thrust coefficients were tested, the flow field became much

Supersonic Retropropulsion

continued

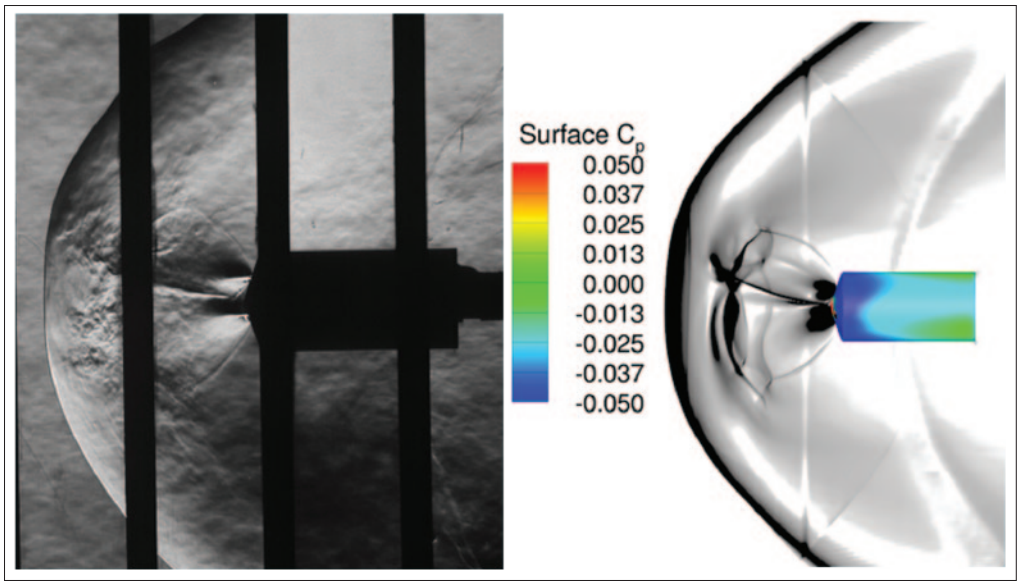


Fig. 4. *Langley Unitary Plan Wind Tunnel triple-nozzle case. Left image is the test Schlieren and the right image is an OVERFLOW simulation. Grayscale coloring displays a constructed Schlieren (in three-dimensional view) of the Computational Fluid Dynamics solution created by a program written by David Saunders; the vertical line through the plume is a grid effect. Mach=3.5, Reynolds/foot=1E+06, thrust coefficient=6.*

steadier. For example, a triple nozzle case at zero angle of attack was much steadier at a thrust coefficient of 6 (figure 4) than at 3.

SRP analysts will use the same model from the Langley Unitary Plan Wind Tunnel test for future analysis in the 2.7 x 2.1-m (9-ft x 7-ft) Ames Research Center Unitary Plan Wind Tunnel. Because the Ames tunnel is larger, which will further decrease wall effects, the team expects to test using larger, more flight-representative thrust coefficients.

CFD will continue to build validity in code-to-code and code-to-test comparisons as modeling difficulty increases. Some planned milestones include engine startup, six-degree-of-freedom simulations, chemistry effects for reacting nozzle flows, and simulating the Mars atmosphere composed mostly of carbon dioxide.

Exploration, Planetary Science, and Sensor Systems



Orion Multi-Purpose Crew Vehicle

Orion Team, *Johnson Space Center*

Drawing from more than 50 years of space flight research and development, NASA has designed the Orion Multi-Purpose Crew Vehicle (MPCV) to meet the evolving needs of our nation's beyond low-Earth orbit space exploration program for decades to come (figure 1).

The Orion MPCV features dozens of technology advancements and innovations that have been incorporated into the spacecraft's subsystem and component design. The Orion MPCV spacecraft includes both crew and service modules, a spacecraft adaptor, and a revolutionary launch abort system that will significantly increase crew safety (figure 2).

The Orion MPCV's unique life support, propulsion, thermal protection, and avionics systems in combination with other deep space elements will enable extended-duration deep space missions. These systems were developed to facilitate integration of new technical innovations as they become available in the future.

The Orion MPCV is capable of transporting astronauts on a variety of expeditions beyond low-Earth orbit, ushering in a new era of space exploration.

The past 18 months of development yielded phenomenal accomplishments by the Orion NASA-industry team. The flawless flight test of the launch abort system—one of only four ever developed and flown—was a significant achievement. The advanced technologies developed for this system enable state-of-the-art crew survivability in the event an emergency occurs during launch or ascent to orbit. In addition, the team fabricated the world's largest heat shield structure, demonstrated an inventive new navigation and docking

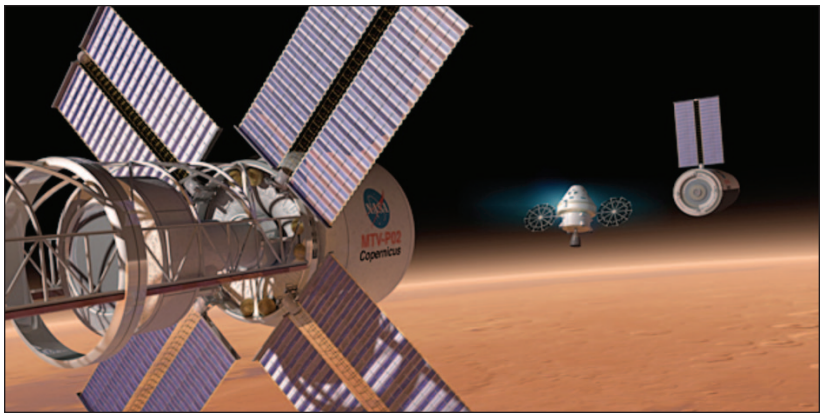


Fig. 1. *Artist concept of the Orion Multi-Purpose Crew Vehicle on a beyond low-Earth orbit mission.*

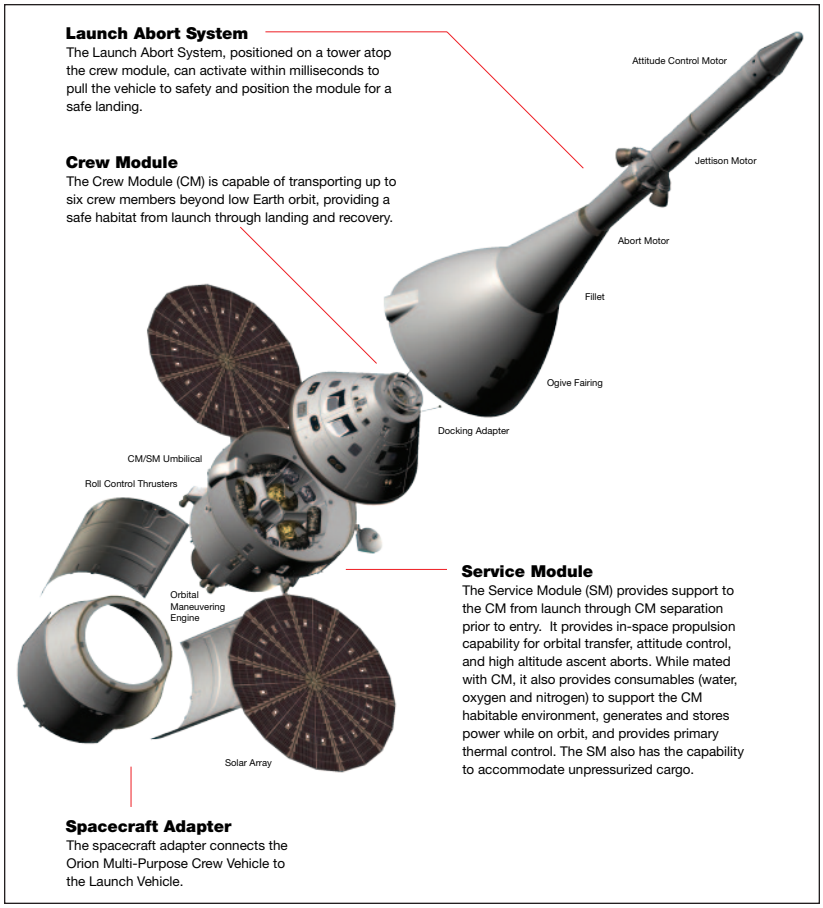


Fig. 2. *Orion Multi-Purpose Crew Vehicle systems.*

Orion Multi-Purpose Crew Vehicle

continued

system, validated Orion's assembly and production operations, completed the first space-flight-worthy Orion crew module, and made significant progress on Orion's thermal protection and software systems. All of this work will result in creating the only U.S. spacecraft for deep space exploration that meets NASA's stringent human rating requirement.



Fig. 3. *The Orion Multi-Purpose Crew Vehicle at the Lockheed Martin Vertical Test Facility in Colorado.*

A National Undertaking

Supported by a network of major and minor subcontractors and small businesses working at 88 facilities across the country, Lockheed Martin Space Systems Company serves as NASA's prime contractor for the Orion MPCV (figure 3).

In addition, the program contracts with more than 500 small businesses across the United States through an expansive supply chain network.

Lockheed Martin facilities in California, Colorado, Florida, Louisiana, and Texas help support the Orion MPCV's design and development work. Additionally, the company has independently invested in a network of Exploration Development and System Integration Labs that conduct early risk mitigation and system-level analyses to help reduce project costs, schedule, and risk.

Subcontractor facilities have been instrumental in the design, fabrication, and testing of myriad components and subsystems for the Orion MPCV.

ATK's facilities in Utah and Maryland tested the abort and attitude control motors for the Orion MPCV launch abort system. Aerojet's propulsion center in California has provided ongoing testing and verification for the Orion MPCV's powerful motors and engines, and United Space Alliance's Thermal Protection Facility in Florida has painstakingly handcrafted all of the Orion MPCV's thermal tiles. Hamilton Sundstrand's engineers in Connecticut, Illinois, and Texas have developed the Orion MPCV's intricate life-support and power systems, while Arizona-based Honeywell has developed intelligent avionics and software that support data, communications, and navigation.

In addition to large aerospace contractors, small businesses from all socioeconomic interests have provided specialized skills and engineering services critical to the Orion MPCV's development. Risk management, life-cycle cost, systems analysis, and propulsion trade studies are just a few examples of their expertise. Additionally, small businesses support all of the spacecraft's systems with design, development, and manufacturing of advanced space flight hardware.

Ready to Explore

NASA's Orion MPCV will be capable of sustaining a crew of up to six astronauts on deep space missions that could last anywhere from 6 days for a lunar flyby mission (figure 4) to as many as 900 days for a Mars exploration mission when paired with additional propulsion and habitation systems. These long-duration missions will require sophisticated life support and power systems that can endure the harsh environments of deep space

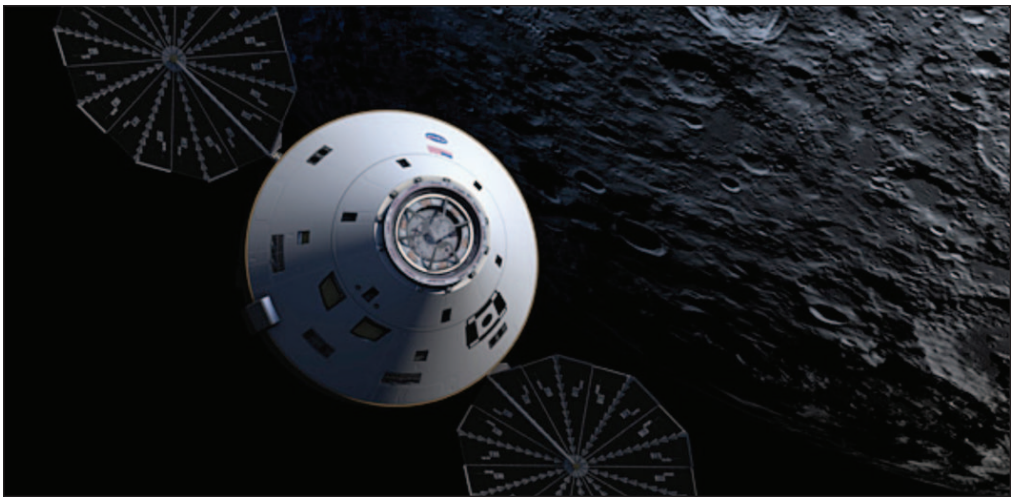


Fig. 4. *Artist rendering of Orion Multi-Purpose Crew Vehicle in lunar orbit.*

and return the crew safely to Earth. New and innovative technologies have been designed and integrated into the spacecraft to achieve such a daunting task, making the Orion MPCV the most advanced human space exploration vehicle ever built.

The advanced technologies developed for the Orion MPCV launch abort system will enable state-of-the-art crew survivability in the event of an emergency on the launch pad or during ascent to orbit. Orion MPCV's increased thrust is necessary to meet the abort needs at launch and provide the required separation distance.

The Orion MPCV's advanced communications and tracking system must ensure optimal communications for the crew. Global Positioning Systems and other tracking systems used in low-Earth orbit are not available for space-to-ground communications from deep space because of the extreme distances traveled.

The Orion MPCV long-duration deep space exploration missions require 40% more habitable space than short-duration low-Earth orbit missions, such as crew and cargo ferry flights to the International Space Station. This additional living space is needed to accommodate suit entry/egress, and exercise. These mission requirements also call for extended life support and multi-day contingency survival ability in spacesuits.

The Orion MPCV will have stringent human rating requirements to ensure optimal crew health and safety throughout the entire mission, regardless of its duration.

The Orion MPCV's deep mission trajectory will require the spacecraft to reenter the Earth's atmosphere at a velocity about 50% higher than a low-Earth orbit return. This high-speed trajectory combined with the capsule diameter determines the heating rate. The Orion MPCV advanced heat shield material, Avcoat, is designed to withstand the extreme heating rate associated with this type of reentry.

For deep space exploration missions, the change in direction/speed or delta-v is driven by the spacecraft's return from deep space. For missions in low-Earth orbit, the delta-v requirements are driven by the need to break the Earth's orbit, rendezvous, and deorbit. A typical Orion MPCV deep space mission requires three to five times more delta-v than a typical ferry mission to the International Space Station. The change in delta-v is the most important measure of "distance" in space flight. The requirements for delta-v determine the need for additional propellant tanks, structure design, and launch abort system design.

Advancing Technologies: The Morpheus Project

Morpheus Team, *Johnson Space Center*

Morpheus is a vertical test bed demonstrating new green propellant propulsion systems and autonomous landing and hazard detection technology (figure 1). Designed, developed, manufactured, and operated in-house by engineers at NASA's Johnson Space Center (JSC), the Morpheus Project represents not only a vehicle to advance technologies, but also an opportunity to try out "lean development" engineering practices.

Morpheus is a NASA-designed vehicle.



Fig. 1. *Morpheus test firing.*



Fig. 2. *Cold flow test.*

Morpheus was manufactured and assembled at JSC and Armadillo Aerospace (Heath, Texas). Morpheus is large enough to carry 499 kg (1100 lbs) of cargo—e.g., a humanoid robot, a small rover, or a small laboratory to convert moon dust into oxygen—to the moon, performing all propellant burns after the translunar injection. The primary focus of the test bed is to demonstrate an integrated propulsion and guidance, navigation, and control system that can fly a lunar descent profile to exercise the Autonomous Landing and Hazard Avoidance Technology safe landing sensors and closed-loop flight control. Additional objectives include technology demonstrations—for instance, tank material and manufacture, reaction control thrusters, main engine performance improvements, helium pressurization systems, ground operations, flight operations, range safety, software, and avionics architecture.

Morpheus is a full spacecraft, with all the associated subsystems: avionics; software; guidance, navigation and control; power; power distribution; structures; propulsion; and instrumentation. Morpheus' propellant combination—liquid oxygen and methane—is of particular interest for a number of reasons (figure 2). It can be stored for longer times in space, compared to other common propellants such as liquid hydrogen.

It is extremely cheap and safe to operate and test, and performs better—much more so than hypergols, another type of fuel often used in space flight.

In addition, the methane can also be made from ice on the moon or Mars. In fact, about 454 kg (1000 lbs) of methane are produced on International Space Station and dumped overboard as waste gas every year—enough to entirely fill the Morpheus lander.

For in-space propellant transfer, Morpheus uses the propellant of choice for future missions that would use in-space refueling and/or depots. In addition, the lander has all the systems required for automated rendezvous and docking. With modification of the propellant and pressurization system for transfer plumbing and a docking mechanism that meets the international docking standard, two landers could rendezvous in low-Earth orbit and demonstrate all the key technologies required for in-space propellant transfer and storage of mid-temperature range cryogenic propellants. For an asteroid rendezvous, the lander would need more study, but conceptually the lander may have most of the systems needed to attempt an asteroid rendezvous. The precision landing system for Project Morpheus, with some modification to the software, could be used as is to rendezvous with an asteroid.



Fig. 3. *Distances from surroundings.*

The workforce behind Project Morpheus has gained valuable experience that will provide the cornerstone for design of future missions. In addition, the project is setting mid-range performance and design requirements that will drive down the production cost of future landers. Project Morpheus is taking the lessons learned from our industry partners to facilitate this alternative design approach.

Morpheus is actually the second vertical test bed built by the project team. The first, Pixel, was literally constructed from spare parts from Armadillo Aerospace through an Innovative Partnership Agreement. NASA converted the Pixel lander to use liquid oxygen and methane as its fuel, instrumented the vehicle and conducted early guidance, navigation, and control testing. Pixel was flown last year under tether 17 times and three free flights at Armadillo's facility near Dallas.

Vertical Test Bed Flight Complex

Morpheus is being tested at the Vertical Test Bed Flight Complex at JSC. Careful consideration has been given to the surroundings when planning thrust levels and future trajectories (figure 3). While we don't expect any complications, Morpheus has multiple safety controls including onboard soft abort systems and a wireless Flight Termination System. In addition, during a free flight, spotters are being placed in multiple locations to ensure that if the vehicle goes outside of the established flight path, the engine will be immediately shut down.

The Vertical Test Bed Flight Complex has three different pads that will be used for Morpheus testing (figure 4). The single pad on the west end of the complex is used for both hot fire and tethered tests.

A crane is used during both tethered and hot fire testing. During hot fire testing, the vehicle is also strapped to the ground. This allows the vehicle to remain virtually motionless during engine firings. The other two pads are used for free flights. During a free flight, Morpheus will fly up to a height of around 30 m (98 ft), then translate over to the western pad and descend for a soft landing.


Fig. 4. *Tower view panorama.*

Wassonite: The Discovery of a New Meteoritic Mineral

Keiko Nakamura-Messenger, *Johnson Space Center*
Lindsay Keller, *Johnson Space Center*
Simon Clemett, *Johnson Space Center*
Zia Rahman, *Johnson Space Center*

Using state-of-the art instruments, researchers in the Robert M. Walker Laboratory for Space Science at Johnson Space Center (JSC) discovered a new mineral within a meteorite. The new mineral is a titanium sulfide and is named wassonite in honor of meteoriticist Professor John Wasson (University of California Los Angeles [UCLA]). The tiny grains of wassonite were found in the Yamato 691 enstatite chondrite, a rare type of meteorite that originated in the asteroid belt and later fell to Earth in Antarctica. Colleagues at UCLA recognized the wassonite grains as a potential new mineral. The team measured the chemical composition of the grains, but were unable to determine its other properties. A thin slice of one of the wassonite grains was nano-machined and extracted from the meteorite, using the focused ion beam instrument, for measurements with the JSC field-emission transmission electron microscope. The microscope analyses revealed the atomic structure of the grains, showing that wassonite has a relatively simple crystal structure consisting of alternating layers of titanium and sulphur atoms. Researchers measured the chemical composition of wassonite and the speciation of the constituent atoms using x-ray and electron spectroscopies at nearly the atomic scale. The textural relationship between wassonite and the other minerals in the meteorite (figure 1) are remarkably well-preserved in the focused ion beam section. These data were sufficient for the Committee on New Mineral Names of the International Mineralogical Association to give official approval for the name "wassonite." Titanium sulfide has been synthesized and studied by scientists for decades in the semiconductor industry, but it had never before been found in nature.

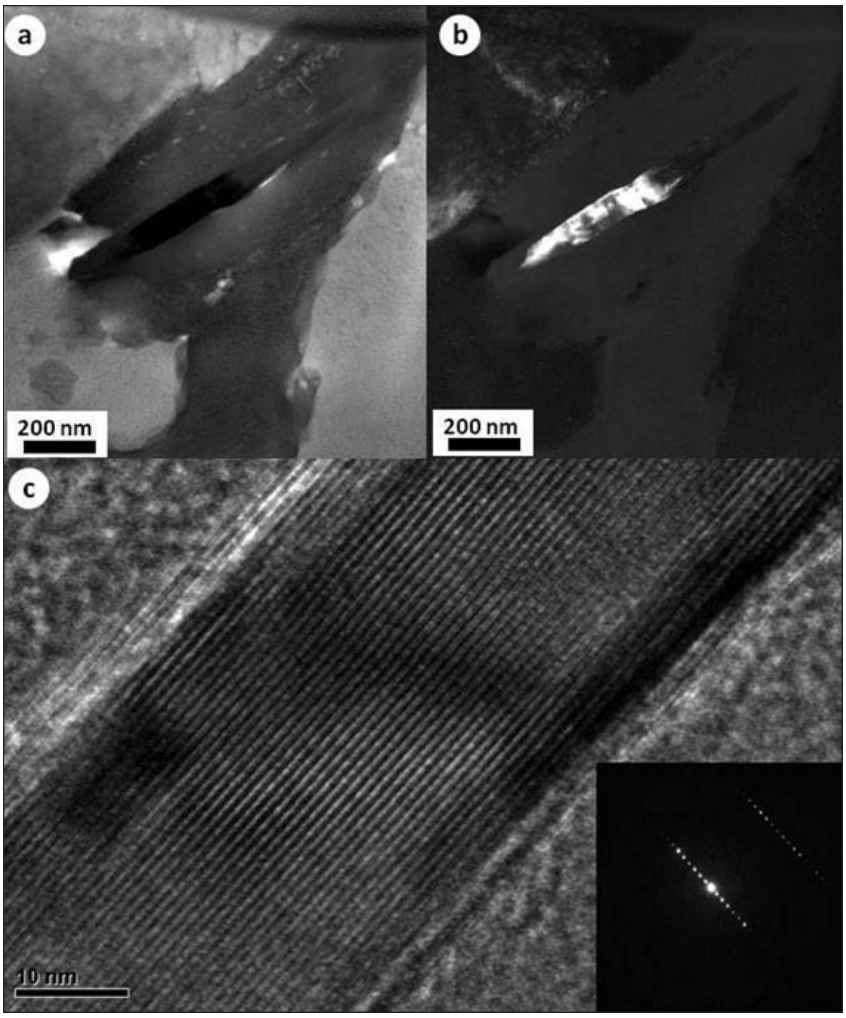


Fig. 1. *Wassonite grain in the Yamato 691 meteorite: (a) bright field transmission electron microscope image showing a wassonite grain in dark contrast; (b) high angle annular dark field transmission electron microscope image of the same grain; (c) high-resolution transmission electron microscope image of wassonite grain from the boxed area in (a). Inset is the selected area electron diffraction pattern of wassonite.*

In the vast majority of minerals, titanium is bonded to oxygen and is referred to as a lithophile element. In wassonite, the titanium is bonded to sulfur, indicating that it formed in a strongly reducing (oxygen-poor) environment at high temperatures (>1500 Kelvin). These conditions existed close to the sun in the early solar system approximately 4.5 billion years ago.

Hayabusa—The First Asteroid Sample Return Mission

Mike Zolensky, *Johnson Space Center*



Fig. 1. *The Hayabusa capsule is examined by the recovery team following reentry.*

When the Institute of Space and Astrological Science/Japan Aerospace Exploration Agency Hayabusa spacecraft parachuted into the Woomera Prohibited Area in South Australia on the evening of June 13, 2010, Johnson Space Center (JSC) scientists were there to meet it. The JSC participants were members of the science team of the Hayabusa mission, the first sample return mission to visit an asteroid and only the third sample return mission since the Apollo and Luna missions of the 1960s and 1970s. The JSC members helped coordinate ground-based observers of the atmospheric reentry fireball and served in the field on the capsule recovery team. The atmospheric reentry and landing of the spacecraft was flawless, and the capsule landed very near the center of the calculated landing ellipse—an astounding feat considering the difficulties in navigating the spacecraft and steering it into the atmosphere. Figure 1 shows the Hayabusa capsule, following reentry, under examination by the recovery team. The team was prepared to douse the spacecraft with spermicide liquid in the event the capsule had opened upon landing.

Those who have been following the mission know about the many nail-biting episodes in its flight both to and from asteroid Itokawa. But even after the safe landing back on Earth, the big question remained, "Would there be any samples inside?" The asteroid regolith sampling mechanism had failed, and all hopes centered on the possibility that stray regolith grains might have been captured during one or more of the spacecraft's forceful touch-and-go landings on the asteroid's surface. On recovery, the capsule was flown by chartered jet to a new curation laboratory at the Institute of Space And Astrological Science's Sagimihara campus for dissection.

It took weeks of work, but science team members found and removed thousands of asteroid regolith grains for detailed analysis. Every technique involved in sample removal, handling, and preliminary analyses were developed and optimized for these special samples, but the recent experience with the Stardust mission samples of comet Wild-2 were integral to the success with the Itokawa samples—all members of the Hayabusa sample analysis teams were previously involved in the Wild 2 samples. The JSC scientists—the only U.S. team members and leaders of the preliminary analysis of the Wild-2 samples in 2006—are participating in the preliminary Hayabusa analyses in Japan. At the March 2011 Lunar and Planetary Science Conference, the Hayabusa preliminary analysis teams reported the first results to packed crowds of planetary scientists. Figure 2, an excerpt from the initial reporting, is an electron backscattered image of one asteroid Itokawa grain.

After completion of the preliminary analysis, the Itokawa samples will be made available to investigators worldwide. At this time, 10% of the recovered samples will be permanently transferred to JSC, where they will be housed in a new Hayabusa Curation Laboratory, just down the hall from the comet Wild-2 samples. Together, these samples will drive new efforts into understanding the origin and early history of the solar system.

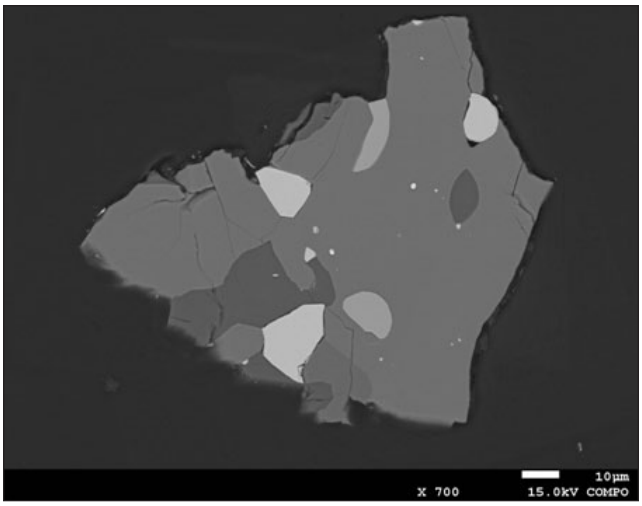


Fig. 2. *An electron backscattered image of one asteroid Itokawa grain. Bright areas are sulfide and oxide crystals, grey regions are silicates. Scale bar is 10 micrometers.*

Analysis of the First Direct Samples of Early Solar System Water

Mike Zolensky, *Johnson Space Center*

Over the past 3 decades, NASA has become increasingly aware of the fundamental importance of water, and aqueous alteration, on primitive solar system bodies. Liquid water is apparently as essential to life as is carbon. All classes of the most primitive astromaterials that the space agency has studied show some evidence of interaction with aqueous fluids. NASA can also observe cryo-volcanism of several small solar system bodies (e.g., Saturnian and Jovian moons), and so are certain of the continuing and widespread importance of aqueous processes across the solar system. Nevertheless, the space agency is still lacking fundamental information such as the location and timing of the aqueous alteration and the detailed nature of the aqueous fluid itself. A major impediment to the understanding of aqueous alteration has been the apparent absence of direct samples of aqueous fluids in meteorites.

NASA's understanding of early solar system fluids took a dramatic turn 10 years ago with the discovery of fluid inclusion-bearing halite crystals in the matrix of two freshly fallen brecciated H chondrite (meteorite) falls—Monahans and Zag. The halites were dated by potassium-argon, rubidium-strontium, and iodine-xenon systematics to be 4.5 billion years old. Johnson Space Center (JSC), in collaboration with Virginia Polytechnic Institute and State University, began examining both meteorites for the presence of aqueous fluid inclusions, which were immediately found.

Fluid inclusions are micro-samples of fluid that are trapped at the crystal/fluid interface during growth (primary) or some later time along a healed fracture (secondary) (figure 1). Both varieties of fluid inclusions are found in Monahans and Zag halite. The presence of secondary inclusions in the halite indicates that aqueous fluids were locally present following halite deposition suggesting that aqueous activity could have been episodic. In any fluid inclusion analysis, it is thus critical to separately analyze the primary and secondary inclusions, if possible, thereby yielding temporal information on fluid compositional changes. Heating/freezing measurements were made on the halite fluid inclusions for both Monahans and Zag,

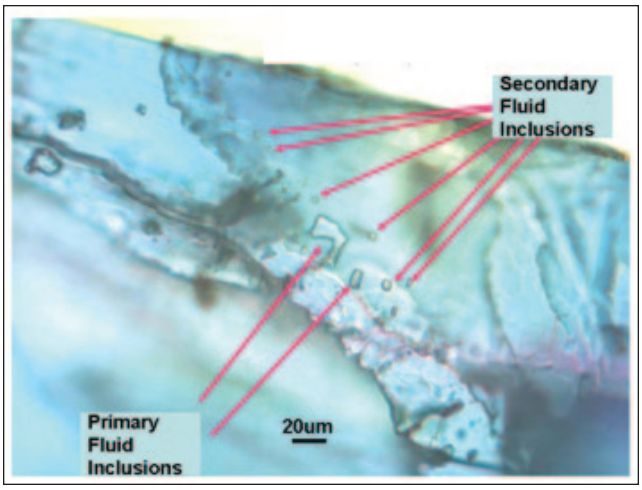


Fig. 1. *Monahans halite with target fluid inclusions indicated. Scale bar measures 20 micrometers.*

determining that the fluids were trapped at approximately 25°C (77°F). These are the first direct measurements of aqueous alteration temperature in any astromaterials, and are also important because they demonstrate unequivocally that these halites have never been subsequently heated. A disadvantage of halite is that it is so readily dissolved in the terrestrial atmosphere, unless extreme care is taken with the samples. Understanding this problem, NASA maintains the Monahans and Zag samples in curation-grade, dry nitrogen-filled cabinets waiting for technology to catch up with the samples, to finally permit chemical and isotopic analyses of the trapped water droplets and to discover their origin. This time has finally arrived.

The first step has been to measure the hydrogen and oxygen isotopic composition of the fluid inclusions' aqueous solutions to understand the origin of these fluids. The oxygen and hydrogen isotopic composition of the aqueous fluids will be compared to determine which of these bodies were the parent objects: asteroids, comets, micrometeorites, interplanetary dust particles, giant planet moons. The aqueous fluids will also be compared to the Earth's water. Testing of JSC's hypothesis is that the oxygen and hydrogen isotopic composition of the aqueous fluids in meteorites (in fluid inclusions) will be shown to

be most similar to cometary coma water, and also similar to the water being ejected from cryo-volcanoes on Jovian and Saturnian moons. The bulk composition of the fluid inclusion-bearing phases in each meteorite will be measured, as a further guide to the aqueous fluid bulk composition. This will further test the hypothesis that the water was not asteroidal in origin for the halite, at least.

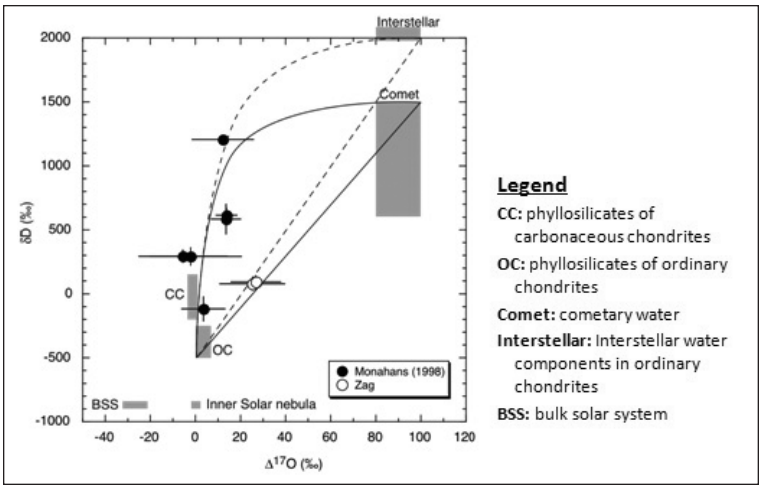


Fig. 2. *Results of the analysis of oxygen and hydrogen isotopes of several Monahans and Zag halite fluid inclusions. Lines are expected mixing lines between cometary (or interstellar) water and ordinary chondrite.*

Several Zag and Monahans halite crystals have been selected for secondary ion mass spectrometry (SIMS) analysis by a collaborator at Hokkaido University (Japan), who modified his Cameca 1270 SIMS with a special internal freezing stage. The aqueous fluid inclusions have to be frozen before being exposed (by sputtering) for analysis in the SIMS. After a great deal of effort, NASA developed the correct sample preparation and analytical techniques to obtain quality oxygen and hydrogen isotopic measurements of individual aqueous fluid inclusions in the halites. Figure 1 shows one Monahans halite crystal, indicating the fluid inclusions that were analyzed. The SIMS freezing stage holds the sample temperature to about -150°C (-238° F) (during measurements by liquid nitrogen. Fluid inclusions in the depth of approximately 50 micrometers (μm) from the halite surface have been succeeded to measure. The sizes of inclusions were about 5μm. Initial results of this work are shown in the figure 2. The observed distribution of isotopic variations of fluid inclusions seems to be results of interaction between comet-like water and meteorite silicates. These may be results of temporal information on compositional change of asteroidal fluid by episodic events. Now, techniques are being optimized to permit a reduction in the errors and to target specific individual fluid inclusions—a necessary capability to permit the measurement of temporal changes in aqueous compositions by distinguishing between preselected primary and secondary fluid inclusions. The team now has a unique sample suite that is being analyzed by a unique instrument, thus providing critical information on the activity of water in the early solar system—information that can be obtained in no other manner.

The team hypothesizes that organics being carried through the parent body of the halite have been deposited adjacent to the fluid inclusions, where they have been preserved against any thermal metamorphism. These are being analyzed using confocal Raman spectroscopy at the Carnegie Geophysical Institution (Washington, DC). These organics will be compared with those found in chondrites and Wild-2 comet coma particles to determine whether these classes of organics had an origin within aqueous solutions.

Finally, the team is locating and analyzing fluid inclusions in other meteorites. Fluid inclusions in six other meteorites have already been located to broaden the scope work and extend it to other primitive water-bearing solar system objects.

Windows in the Ancient Martian Atmosphere

Paul Niles, *Johnson Space Center*

Using data returned from NASA's Mars Reconnaissance Orbiter spacecraft and the Phoenix Lander, researchers associated with Johnson Space Center made several important discoveries that help the space agency understand the ancient climate of Mars and the fate of carbon dioxide in its atmosphere.

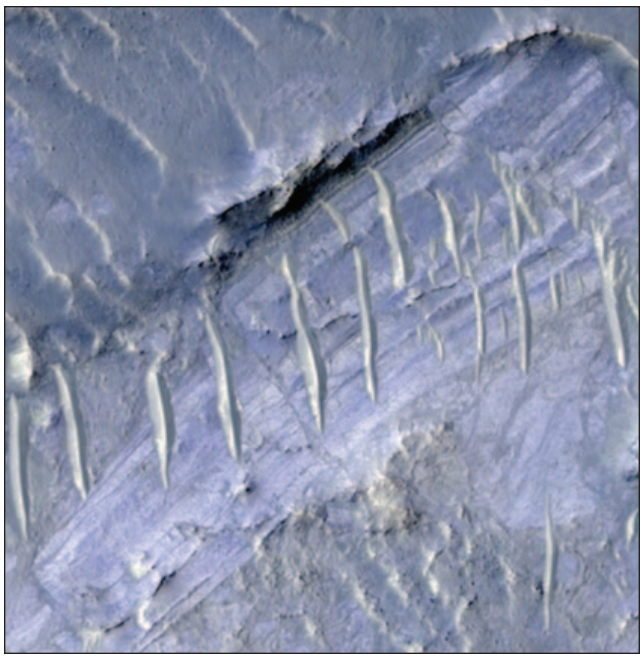


Fig. 1. *The central peak of Leighton crater—located at 57 E, 3 N—contains layered materials that have been uplifted from depth and tilted on end, displaying one of the best exposures of deep crust seen on Mars. Bedrock exposed in the uplifted central peak of the 65-kilometer crater contains clay minerals and carbonates suggesting hydrothermal alteration.*

A deposit of carbonate rocks that once existed 6 kilometers (km) below the surface of Mars was uplifted and exposed by an ancient meteor impact and has now been identified using the Compact Reconnaissance Imaging Spectrometer for Mars (figure 1). The carbonate minerals exist along with hydrated silicate minerals of a likely hydrothermal origin. Carbonate rocks have long been a Holy Grail of Mars exploration for several reasons: 1) carbonates form from liquid water on the surface and such deposits could indicate past seas that were once present on Mars; and 2) these minerals are the primary means for removing carbon dioxide (CO_2) from the atmosphere and abundant carbonates suggest that ancient Mars may have supported a denser CO_2 atmosphere with a much stronger greenhouse effect.

While this is not the first detection of carbonates on Mars, this particular detection is special because carbonates coexist along with hydrothermal silicate minerals, thereby indicating that a hydrothermal system existed in the presence of CO_2 deep in the Martian crust. This is exactly the type of environment that could be capable of sustaining microbiological life in the subsurface of Mars, which is protected from the harsh surface environment.

The Martian atmosphere is mainly composed of CO_2 and is less than 1% of the terrestrial atmosphere (figure 2). NASA's Mars Exploration Program has put a high priority on learning more about the history of the atmosphere on the planet, especially whether the modern atmosphere is a remnant of an older, thicker atmosphere or whether the modern atmosphere represents the conditions that have always been present on the planet.

Measurements of the isotope ratios in Martian CO_2 can address these questions, in addition to assisting in the discovery of ancient carbonate deposits. The Phoenix Lander made these measurements in the summer of 2008 with unprecedented precision. The measurements revealed that CO_2 on Mars has proportions of carbon and oxygen isotopes similar to CO_2 in Earth's atmosphere. This unexpected result reveals that Mars is a much more active planet than previously thought. In fact, results suggest that Mars has replenished its atmospheric CO_2 relatively recently, and that the CO_2 has reacted with liquid water present on the surface.

The low gravity and lack of a magnetic field on Mars mean that as CO_2 resides in the atmosphere, it will be lost to space—a process that favors loss of the lighter carbon-12 isotope compared to carbon-13. Although an older atmosphere on Mars should contain much more carbon-13, it doesn't. This suggests that the Martian atmosphere has been recently replenished with CO_2 emitted from volcanoes, and volcanism has been an active process in Mars' geologically recent past—within millions of years rather than billions.

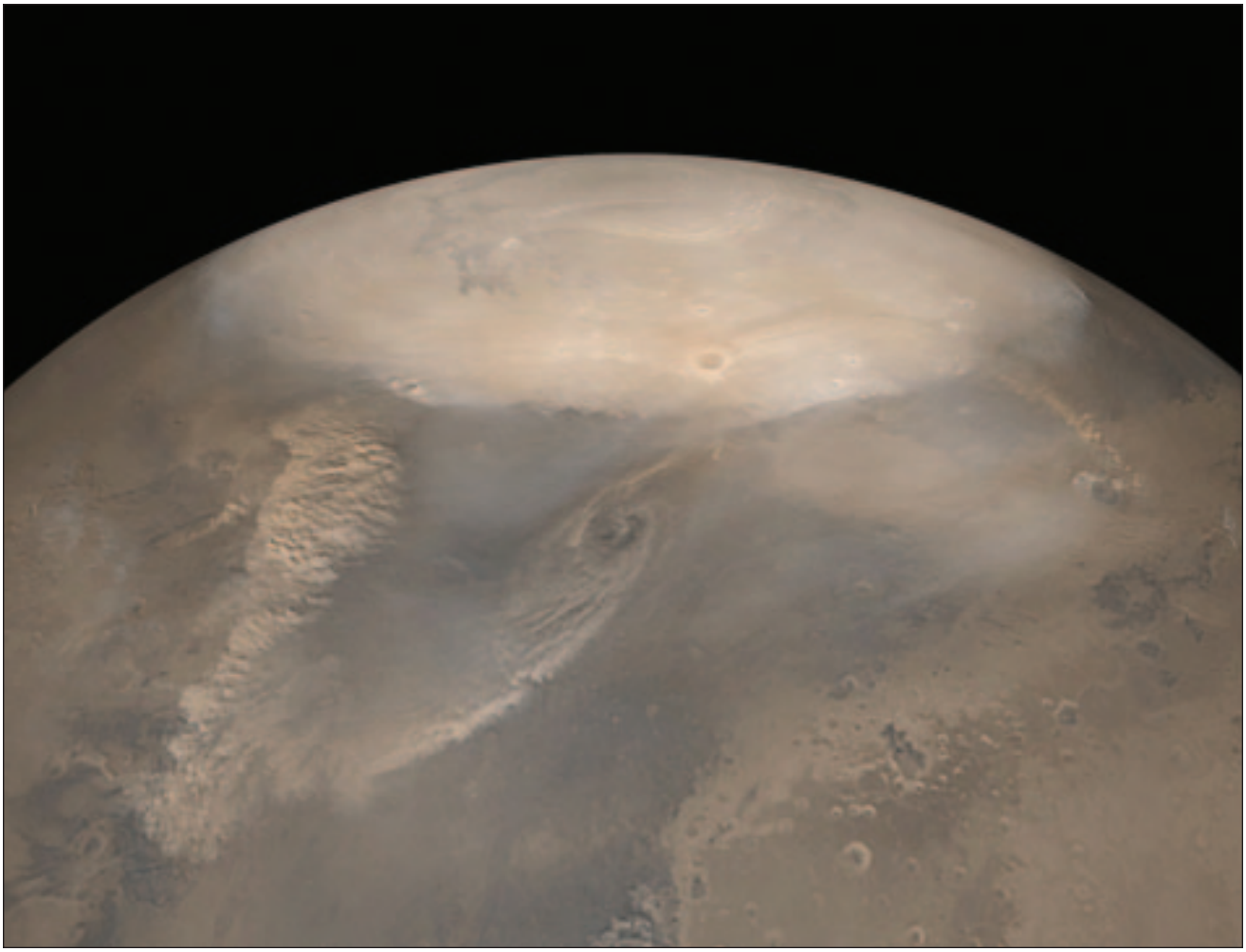


Fig. 2. *During spring on the Martian north pole, condensed carbon dioxide (CO_2) ice begins to thaw and return to the atmosphere. During Martian winter, as much as 25% of the atmospheric CO_2 can be frozen at one of the poles. This is a mosaic of images taken by the Mars Global Surveyor spacecraft in 2002. Credit: NASA/JPL/Malin Space Science Systems*

A volcanic signature is not present in the proportions of oxygen-18 and oxygen-16 in Martian CO_2, thereby suggesting that the CO_2 has reacted with liquid water, enriching the oxygen in CO_2 with heavier oxygen-18. These findings also suggest that the liquid water has primarily existed at temperatures near freezing, and that hydrothermal systems similar to Yellowstone National Park hot springs on Earth have been rare on Mars throughout its history. The findings do not reveal specific locations or dates of liquid water and volcanic vents, but geologically recent occurrences of those conditions provide the best explanations for the isotope proportions that were found.

The comparisons of the Phoenix Lander atmosphere measurements to measurements of Martian meteorites collected on Earth provide confirmation of key findings. The meteorites contain carbonate minerals similar to those detected from orbit. Certain meteorites contain carbonates with isotopic proportions that match the atmospheric measurements by the Phoenix Lander. This provides supporting evidence that the watery conditions associated with carbonate formation have continued even under Mars' current cold and dry conditions.

Early Life on Earth and the Search for Extraterrestrial Biosignatures

Dorothy Z. Oehler, *Johnson Space Center*
Everett K. Gibson, *Johnson Space Center*

An understanding of earliest terrestrial life is of astrobiological importance, as knowledge of early evolutionary processes on Earth could provide insight to development of life on other planets. Yet, the nature of early life on Earth is difficult to assess because the oldest potential biosignatures are commonly poorly preserved.

Johnson Space Center has been using the relatively new technique of nanometer-scale, secondary ion mass spectrometry (NanoSIMS) to evaluate ancient microorganisms preserved on Earth. Results from well-preserved and non-controversial microfossils have provided new criteria for assessing the origin of poorly preserved organic materials. These criteria were applied to controversial organic microstructures from a 3-billion-year-old sedimentary rock in Australia. Results suggest that the organic structures are biogenic and the same age as the rock. More importantly, results from NanoSIMS add to a growing body of data suggesting that by 3 billion years ago, life on Earth was multifaceted and diverse. This view of early terrestrial evolution may increase the likelihood that primitive life on other planets could survive and adapt to adverse or unusual conditions by ready development of diversity in form and biochemistry (figures 1 and 2).

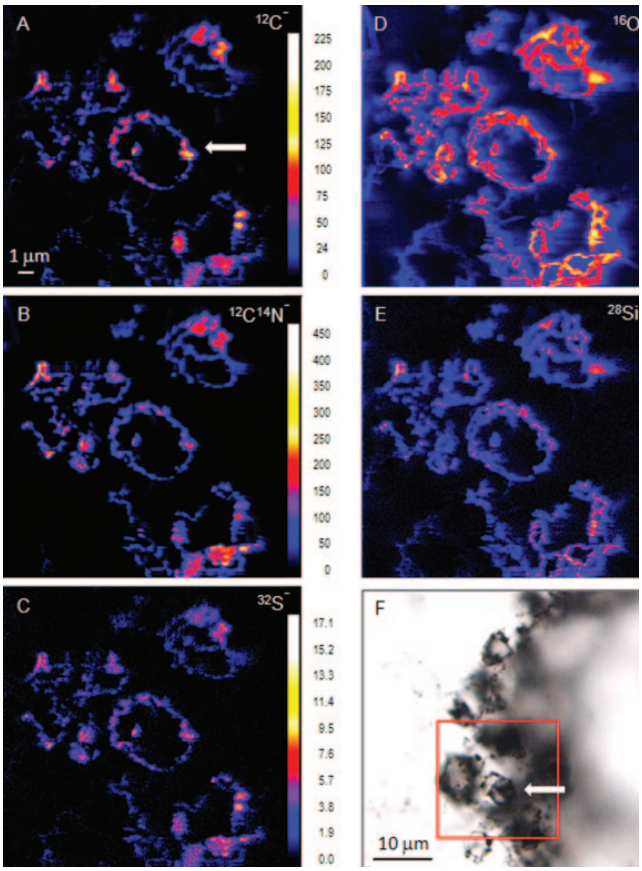


Fig. 2. *Controversial, organic microstructures in a 3-billion-year-old rock from the Pilbara of Australia: (a-e) nanometer-scale, secondary ion mass spectrometry element maps of the spheroidal structures within the red rectangle of (f); (f) optical photomicrograph in transmitted light of a thin section.*

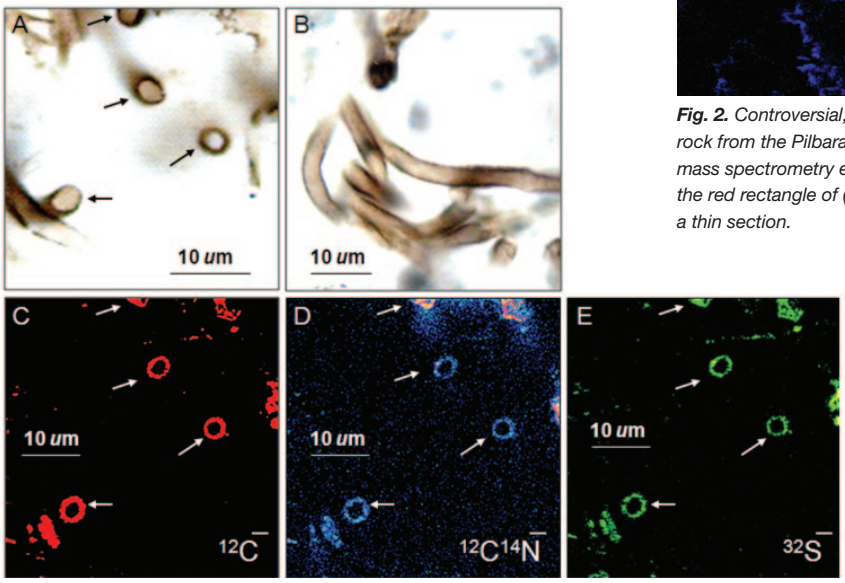


Fig. 1. *Well-preserved, 1-billion-year-old organic microfossils, Bitter Springs Formation, Australia: (a-b) optical photomicrographs in transmitted light of filamentous microfossils in a thin section; (c-e) nanometer-scale, secondary ion mass spectrometry element maps of the three filaments imaged in cross-section of (a).*

How Tiny Amounts of Water in the Deep Earth Saved Continents

Anne Peslier, *Johnson Space Center*
Alan Woodland, *University of Frankfurt*
David Bell, *Arizona State University*
Marina Lazarov, *University of Frankfurt*

The Earth is unique in our solar system not only because of its water-filled oceans and oxygen-rich atmosphere, but also because of its plate tectonic engine. The layer on which the tectonic plates float is called the asthenosphere and is made of slowly deformable rock. Huge chunks of the crust and mantle sink constantly into the asthenosphere when they become old and dense at subduction zones, while new crust is being made at mid-ocean ridges. Finally, continents break up and collide over hundreds of million-year cycles, thereby churning up even more crust at their edges. And yet, over its 4.5-billion-year history, the Earth has managed to preserve some very old rocks—some more than 3 billion years old. What prevented these rocks from being recycled into the asthenosphere?

Recent work published in the September 2, 2010, issue of *Nature* by Johnson Space Center (JSC) and colleagues at the University of Frankfurt, and Arizona State University bring answers to this puzzle. For this study, the team turned its attention to the ancient cores of continents, called cratons, where the oldest rocks can be found. Cratons are also part of tectonic plates and therefore float on the asthenosphere. The cratons resemble icebergs in an ocean with deep keels, down to 200 kilometers, protruding into the asthenosphere. Samples from these keels, brought up by magmas—called kimberlites—that traverse them, are available. The latter are incidentally famous for also bringing up diamonds. It is known that these roots are as old as the rocks found at the surface—around 3 billion years old. Scientists have long tried to explain why these keels exist, as it would be expected that they would be eroded away by the surrounding hot and dynamic asthenosphere. It has been proposed that the keels help the cratons float because they are less dense than the asthenosphere. Over their billion-years history, magmas have removed dense elements (iron, aluminum, calcium) from the keels. Geologists also think that the cold temperature, compared to that of the asthenosphere, make the keels stiff and resistant. Finally, scientists have long proposed that water—or, more exactly, the absence of it in the keel—could make the keel strong and resistant. This last hypothesis has never been proven until this study.

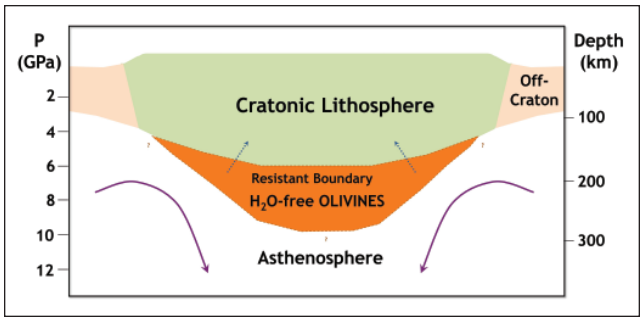


Fig. 1. *A sketch of a cross-section of a craton. A layer of resistant dry rock (orange) and the bottom of the cratonic keel prevents it from being eroded away over billions of year by the convection in the asthenophere (purple arrows).*

JSC has the capability of measuring tiny amounts of water locked up in minerals. The main mineral of the rocks from the keel of the Kaapvaal craton located in South Africa was analyzed. The more this mineral—called olivine—contains water, the softer it becomes. On the contrary, olivines from the bottom of the craton are dry, making them hard to deform and break (figure 1). So here is a mechanism for rendering the keels of cratons resistant: they have a shell of very hard, dry olivines. This work has crucial implications on our understanding of Earth plate tectonics, why continents exist, and the evolution of planetary interiors since the formation of the solar system.

New Research on Purported Martian Biosignatures in Meteorite Allan Hills 84001: 1996 to 2011

Everett Gibson, *Johnson Space Center*
Kathie Thomas-Keprta, *Johnson Space Center*
Simon J. Clemett, *Johnson Space Center*
David S. McKay, *Johnson Space Center*

Using the latest and most advanced analytical instrumentation available, a research team at Johnson Space Center (JSC) has reexamined the hypothesis about potential biosignatures in the Martian Meteorite Allan Hills 84001 (ALH84001). The team's results and conclusions present strong evidence for possible biological activity on Mars during its first 600 million years of evolution.

By reassessing the leading alternative non-biologic hypothesis that heating produced the tiny magnetites, researchers discovered that the results of this study of Martian meteorite ALH84001 reinforce the original hypothesis that biology played a role in the formation of the carbonate disks and their associated tiny magnetite crystals. The heating hypothesis for the formation of the magnetites has been favored by many researchers for about a decade, but it is now shown to be an implausible explanation not supported by either theory or by new detailed observations of the ALH84001 meteorite.

It is well known that ALH84001 preserves evidence of interaction with water while on Mars in the form of microscopic carbonate disks present in many cracks and crevices in this meteorite. These carbonate disks are believed to have precipitated 3.9 billion years ago on Mars at the beginning of the Noachian epoch—the time of the oldest, still-exposed Martian surface, and perhaps the time when Martian oceans were present. Embedded in cracks and veins throughout these carbonate disks are nanocrystal magnetites (Fe_3O_4) with unusual chemical and physical properties, whose origins have become the source of considerable scientific debate. Various research teams from around the world have suggested that these magnetites are the product of partial thermal decomposition of the host carbonate in which the iron-rich carbonate was heated by meteorite impacts and thermal events, resulting in the loss of some of its carbon dioxide. This process is theorized to leave only the iron oxide behind as magnetite crystals. Alternatively, the origins of magnetite and carbonate may be unrelated; that is, magnetite is not directly related to or formed from the carbonate, but has been washed into the carbonate disks during and after the time when the disks were formed from Martian ground or surface water.

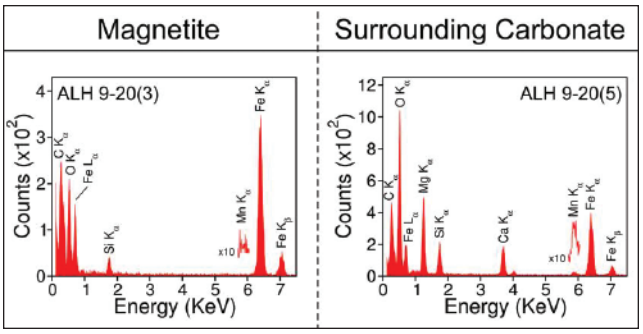


Fig. 1. *Energy-dispersive x-ray spectrometry spectra of chemically pure magnetite (left) and host carbonate (right). While the carbonate contains both manganese and magnesium, the magnetite crystal is chemically pure and contains neither element as would be expected if the magnetite was a product of carbonate decomposition.*

The team sought to resolve these hypotheses through the detailed characterization of the compositional and structural relationships of the carbonate disks and associated magnetites within the cracks and crevices of the rock in which they are embedded. Extensive use of state-of-the-art focused ion beam milling techniques, along with microanalysis by high-resolution transmission electron microscopy, have been used for sample preparation and analysis. The team then compared their observations with those from experimental thermal decomposition studies of iron carbonates under a range of plausible geological heating scenarios.

The JSC team concluded that the vast majority of the nanocrystal magnetites present in the carbonate disks could not have formed from the enclosing carbonate by any of the currently proposed thermal decomposition or shock scenarios. Instead, the team found considerable evidence in support of an alternative origin for the magnetite, unrelated to any shock or thermal processing of the carbonates. In the favored hypothesis, the magnetites were brought in from somewhere else and added to the carbonates as the carbonates crystallized.

In natural iron-rich carbonate systems, minor and trace elements such as manganese and magnesium are often associated with the carbonates. When these carbonates

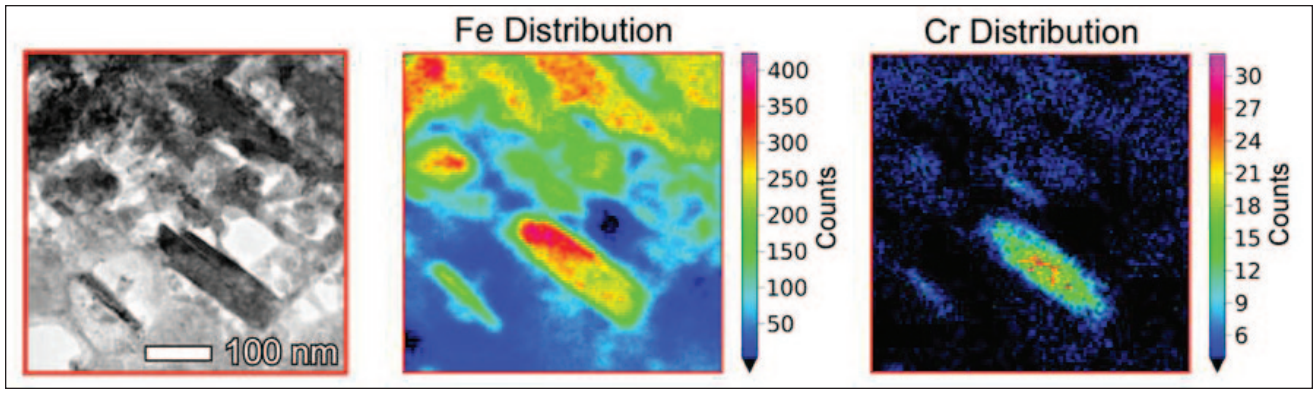


Fig. 2. *Magnetite embedded in carbonate (left); energy-dispersive x-ray spectrometry maps of region at left showing the distribution of iron and chromium (center and right). This magnetite crystal is impure, containing minor chromium.*

are decomposed by thermal processes, the resulting Fe_3O_4 will contain trace levels of the host carbonate's minor and trace elements. However, for magnetites produced from biological processes, the resulting Fe_3O_4 will contain no contaminant trace elements such as manganese and magnesium. In some kinds of Earth bacteria (magnetotactic bacteria), Darwinian-derived processes purify magnetites—even in the presence of magnesium and manganese—by excluding the contaminant elements, making these magnetites more efficient detectors of the Earth's magnetic field. Detailed analysis of selected magnetites within ALH84001 shows no trace element contaminants for the majority of the magnetites (figure 1). Most are identical to the unique population of magnetites known to be formed on Earth by biology. A few ALH84001 magnetites contain minor chromium and/or aluminum; neither element is present in the host carbonate. This indicates that these impure magnetites formed elsewhere before being incorporated into the carbonate and are not a product of thermal decomposition (figure 2). Additionally, a fraction of magnetites are present in carbonate that contains little to no iron, indicating the magnetites had to form elsewhere prior to being embedded in carbonate.

The scientific results offer strong support to the original 1996 hypothesis and show that most of the alternative arguments are invalid. The original hypothesis advanced by the JSC team was that 3.9 billion years ago, the carbonates were precipitated in cracks and hollows of a cooled Martian volcanic rock with the help of Martian microbes. These carbonates trapped or included tiny crystals of magnetite identical in specific properties to those known to be formed on Earth by specialized bacteria. The original hypothesis proposed that there could have been conditions on Mars favoring habitability for life, and which could have supported active biogenic processes.

While the new work does not prove that the biogenic hypothesis is true, it does show that the most popular alternative non-biologic hypotheses (thermal decomposition or shock decomposition of iron-rich carbonate) to explain the properties of ALH84001 simply do not fit the evidence in the meteorite. This new discovery removes the single most important obstacle to the acceptance of the original hypothesis of the JSC group—which proposed that ALH84001 contained evidence of past life on Mars—by showing that thermal decomposition models are unlikely. Evidence supporting the possibility of past life on Mars, which has been slowly building up during the past decade, include signs of past surface water such as the remains of rivers, lakes, and possibly oceans; signs of current water near or at the surface; water-derived deposits of clay minerals and carbonate outcrops in old terrain; and the identification of methane in the Martian atmosphere.

Probing Life History of Meteorite From Early Solar System

Justin Simon, *Johnson Space Center*

Scientists at Johnson Space Center (JSC) and colleagues at Lawrence Livermore National Laboratory, the University of California, Berkeley, and the University of Chicago have performed a microprobe analysis of the core and outer layers of a pea-size fragment meteorite some 4.6 billion years old to reconstruct the history of its formation, providing the first evidence that dust grains experienced wildly varying environments during the planet-forming years of our solar system. These dust grains—called calcium-, aluminum-rich inclusions (CAIs)—are understood to have formed very early in the evolution of the solar system and in contact with nebular gas, either as solid condensates or as molten droplets. On the basis of the oxygen isotope record found, the team interpreted these findings in the context of models about how matter formed in the early protoplanetary nebula and reported their implications for the formation of terrestrial planets in the March 2011 issue of the journal *Science*.

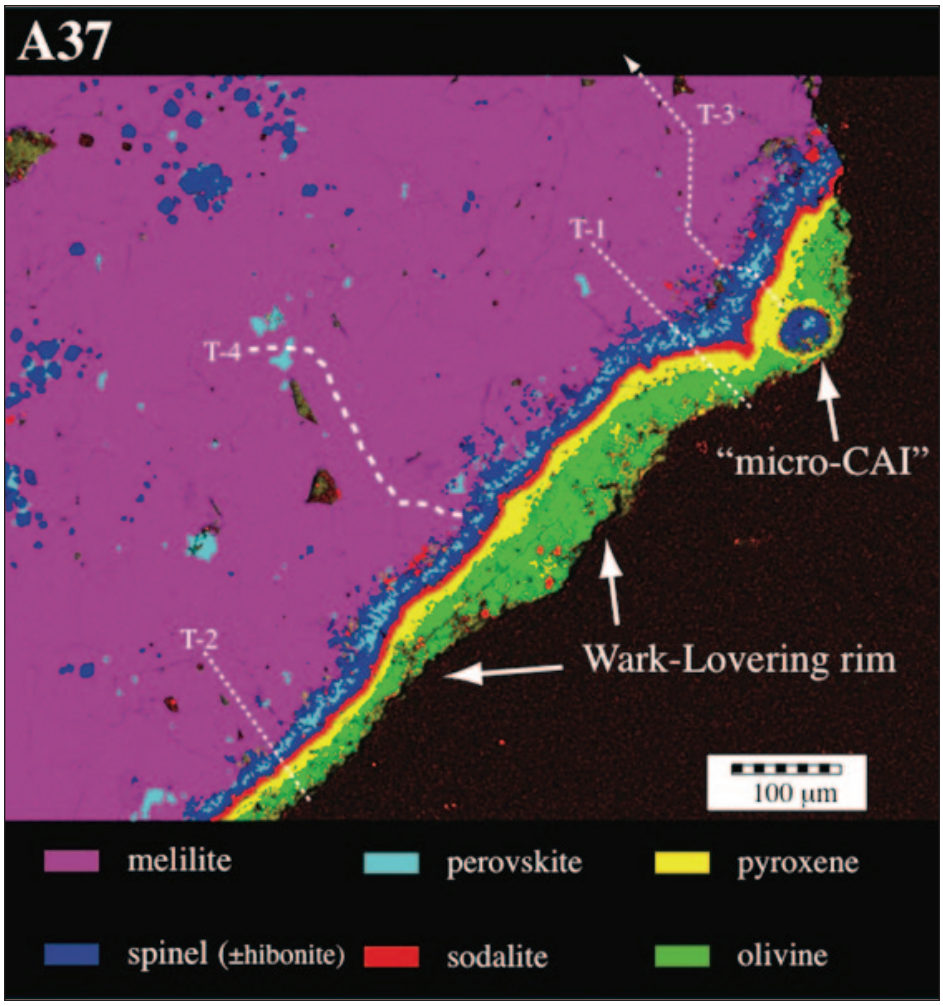


Fig 1. *Compositional x-ray image of the rim and margin of an approximately 4.6-billion-year-old calcium-, aluminum-rich refractory inclusion from the Allende carbonaceous chondrite.*

The micrometer-scale analyses of a CAI, and the characteristic mineral bands mantling the CAI, reveal that the outer parts of this primitive object have a large range of oxygen isotope compositions. The variations are systematic; the relative abundance of ^{16}O (oxygen isotope 16) first decreases toward the CAI margin, approaching a planetary-like isotopic composition, then shifts to extremely ^{16}O-rich compositions through the surrounding rim. The variability implies that CAIs formed from several oxygen reservoirs, likely located in distinct regions of the solar nebula. The observations support early and short-lived fluctuations of the environment in which CAIs formed, either because of transport of the CAIs themselves to distinct regions of the solar nebula or because of varying gas composition near the proto-sun.

Scientists measured a component of the primitive meteorite Allende (the CAI called A37) and its surrounding concentric rim by nanometer-scale, secondary ion mass spectrometry (NanoSIMS)—an ion microprobe with nanometer-scale spatial resolution—to investigate intra-CAI oxygen isotopic variations. An image of A37 can be seen in figure 1. The core of A37, extending well beyond the field of view to the upper left, consists of the minerals melilite, spinel, and perovskite. The rim consists of a sequence of monomineral layers (hibonite, perovskite, spinel, melilite/sodalite, pyroxene, and olivine) a few micrometers thick. A spinel-rich micro-inclusion appears to have been entrapped while the rim was forming. The ion microprobe measurements were obtained as approximately 2 micrometers (μm) spot analyses spaced every 7 to 10 μm across the rim and the outer approximately 150 μm of the interior. At the resolution that is accessible with the NanoSIMS, both A37 and its rim exhibit more than 20‰ (part per thousands) variation in Δ17O (the deviation of the O isotopic composition from the terrestrial fractionation line)—a range that is close to the full range thought to exist among solids formed in the entire solar system. These data imply that A37 was transported among several different nebular oxygen isotopic reservoirs, potentially as A37 passed through and/or into various regions of the protoplanetary disk.

The evidence for transport of solid matter reported by the team supports the inference from theoretical studies that outward radial transport of solid matter is a basic consequence of protoplanetary disk evolution. Large-scale radial circulation of nebular solids is also consistent with the reports of crystalline material located in the outer reaches of our solar system, and in the outer, cool regions of distant stars. The variable but largely ^{16}O-rich composition of the rim suggests that after transport out of the inner solar system, CAIs either continued to form within a region in the outer solar system that varied in composition, or they were returned back to the inner solar system.

The History of Mars Revisited via the Petrological and Geochemical Study of Martian Meteorites

Anne Peslier, *Johnson Space Center*
Dan Hnatyshin, *University of Alberta*
Chris Herd, *University of Alberta*
Erin Walton, *Grant McEwan University*
Alan D. Brandon, *University of Houston*
Thomas Lapen, *University of Houston*
John Shafer, *University of Houston*
Minako Righter, *University of Houston*
Vinciane Debaille, *Université Libre de Belgique*
Brian Beard, *University of Wisconsin*

Key advances have been made in understanding the geological history of Mars via the study of Martian meteorites—our only samples from this planet. Each time a new meteorite from this planet is found, potential huge strides in this science can be made. A team of scientists at Johnson Space Center (JSC), the University of Alberta, and the University of Houston concentrated on the petrological study of a Martian meteorite—called LAR 06319—found in Antarctica in 2006. Detailed petrological study revealed that this meteorite represents a sample from lava erupted at the surface of Mars. The importance of this meteorite is that its minerals represent an entire sequence of snapshots of the history of the magma from the time it left the depths of the Martian mantle to the time it reached the surface of the planet. By carefully determining the temperature and oxygen fugacity conditions at which these minerals formed at these various times throughout the history of this magma, the team could show that information about the chemical and physical conditions in the source of Martian magmas can be lost during the evolution of the magma after it has left the Martian mantle. However, the team could use this particular meteorite—having preserved all the information from its source to its eruption—to redefine the conditions pertaining at the source of Martian magmas. This study makes it easier to model the magmatic history of Mars by narrowing the range of oxygen fugacity of the source Martian magmas.

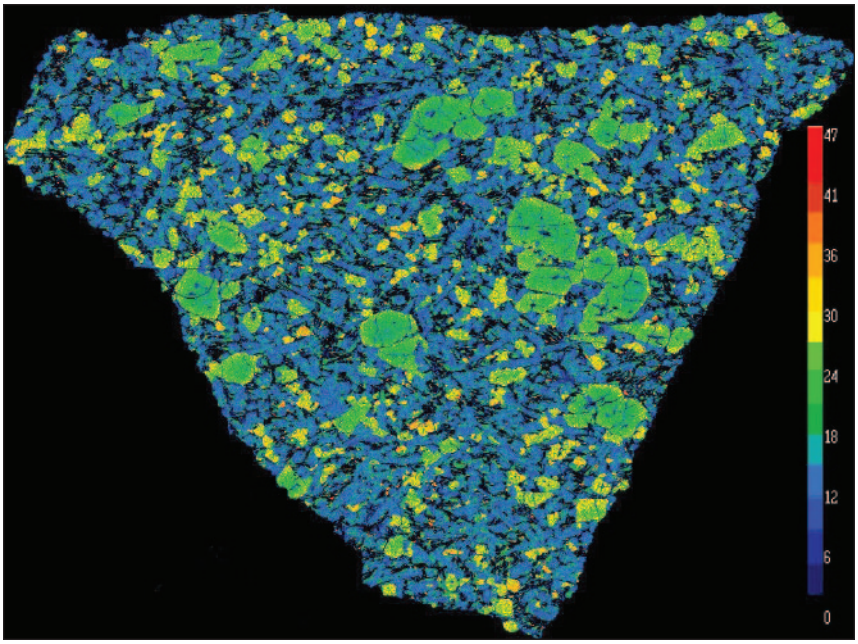


Fig 1. *The figure shows a map of the iron content of a thin slice of the Martian meteorite LAR 06319. The sample is about 2 centimeters at its widest side. The large green minerals formed first in conditions closed to that of the source of the magma deep in the Martian mantle, while the thin needle-like black ones most likely formed at eruption at the Martian surface. Blue indicates low amounts of iron, while orange–reds means large amounts of iron.*

Scientists at JSC also collaborated with University of Houston scientists in refining the timeline of volcanic activity on Mars with the precise dating of the oldest Martian meteorite ALH 94001 and the age determination of the meteorite LAR 06319. These studies affirm that only one Martian meteorite is very old (ALH 94001 is more than 4 billion years old), while all others are samples of magmas erupted on the Martian surface much later—less than 600 million years ago. All these results constrain models of planetary formation and evolution.

Magnetic Dynamo Action in Magnetohydrodynamic Turbulence

John V. Shebalin, *Johnson Space Center*

Johnson Space Center (JSC) conducted research that may help solve the "dynamo problem"—that is, the problem of explaining how the generally turbulent magnetofluids (i.e., plasmas) contained in stars and planets (and some laboratory devices) produce large-scale magnetic fields.

A number of complicated attempts have been made to solve this problem, and there have also been quite intricate numerical simulations that reproduce solar magnetic and geomagnetic phenomena. A general mechanism was found that does this in a relatively simple way and that could be applicable to more realistic cases.

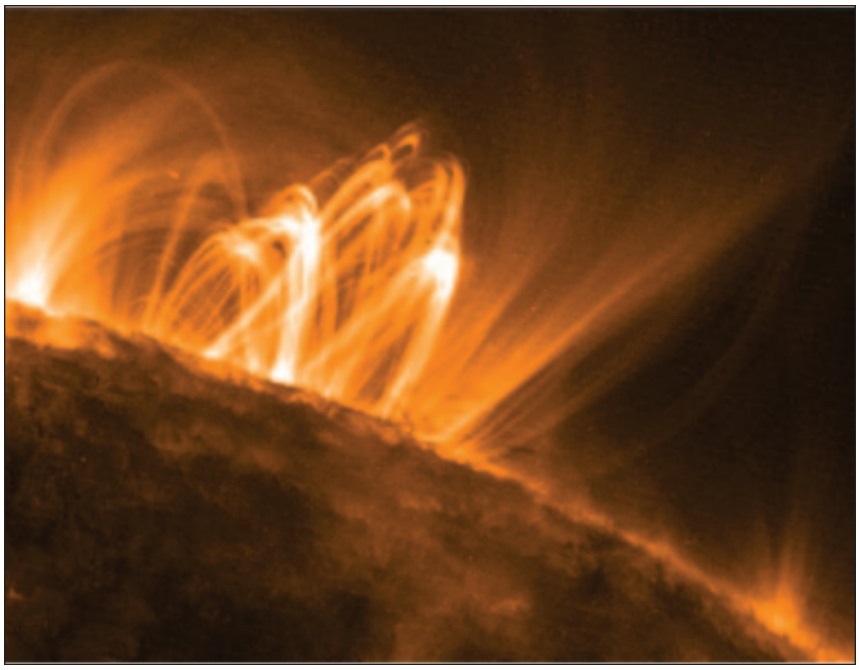


Fig. 1. *NASA Transition Region and Coronal Explorer image of the sun on September 12, 2000.*

In brief, most researchers have long believed that if you take a magnetofluid and stir it up, as it relaxes it produces turbulent magnetohydrodynamic fluctuations at all length scales, but the average direction of any of these fluctuations over a reasonably long time will be zero, which is in keeping with ensemble predicitions based on the statistical mechanics of ideal (i.e., non-dissipative) turbulence. (When time averages and ensemble averages match, the system has "ergodicity.")

JSC found a mechanism that breaks the ergodicity (hence, "broken ergodicity") and produces quasi-stationary, large-scale magnetic fields. This is a qualitatively new result and a conceptual change with regard to a long-held paradigm (the so-called mean field dynamo theory) concerning the origin of magnetism in planets and stars. The results pertain to the plasmas associated with plasma engines and some other devices that confine plasmas if these devices can maintain relatively stable plasma for a long enough period of time, as is the case for stars and planets (figure 1).

Stardust—Searching for Contemporary Interstellar Dust

David Frank, *Johnson Space Center*
Mike Zolensky, *Johnson Space Center*
Bradley De Gregorio, *Johnson Space Center*
Ron Bastien, *Johnson Space Center*
Jack Warren, *Johnson Space Center*

In 2006, the Stardust Mission returned the first samples from a primitive solar system body. This NASA discovery class mission, along with the Apollo and Genesis missions, represents NASA's third sample return from a celestial body. The Stardust spacecraft made a close encounter—at 6 kilometers per second (km/s)—with comet Wild-2, and successfully captured thousands of dust grains ejected from the comet's coma. The collector was an array of silica aerogel and aluminum foils arranged in the approximate size and shape of a tennis racket.

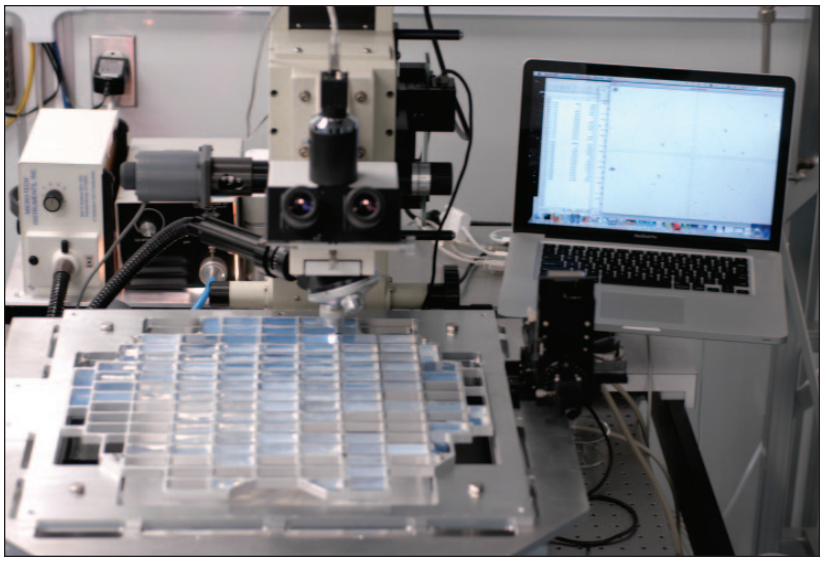


Fig. 1*. The Stardust aerogel scanning system at Johnson Space Center with the interstellar collector mounted for automated scanning.*

Although the primary (and successfully completed) objective of the mission was to capture these Wild-2 comet samples, a second similar collector was flown on the same payload and exposed to the stream of "contemporary interstellar dust": particles that originate from other stars, planetary systems, and nebulae. This very low flux of micrometer (μm) and sub-μm-sized dust grains pass through our solar system at speeds in excess of 20 km/s as the sun revolves around the center of the Milky Way Galaxy. While thousands of particles in the size range of a few μm up to approximately 150 μm were collected from comet Wild-2, it is expected that only perhaps a few dozen dust grains approximately a few μm *and less* were captured from the interstellar medium. The extremely low particle flux and tiny grain size make locating these particles a colossal challenge. To overcome this "needle in a haystack" search, the team conducts automated scanning of the aerogel at high resolution using an optical compound microscope equipped with a live video feed and computer-controlled stage. To date, the team has scanned almost one half of the collector and created roughly one quarter of a million "focus movies," each of which represents a field of view of 0.24 mm squared. These movies are distributed for inspection to volunteers around the world via the web-based Stardust@home project. With more than 29,000 volunteers, it is the largest ever collaboration in planetary science.

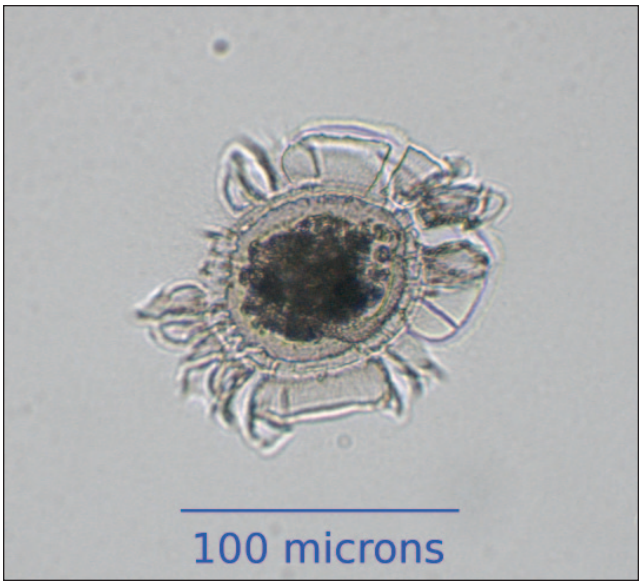


Fig. 2. *A cavity seen through the aerogel scanning system, possibly created by the hypervelocity impact of an interstellar dust grain.*

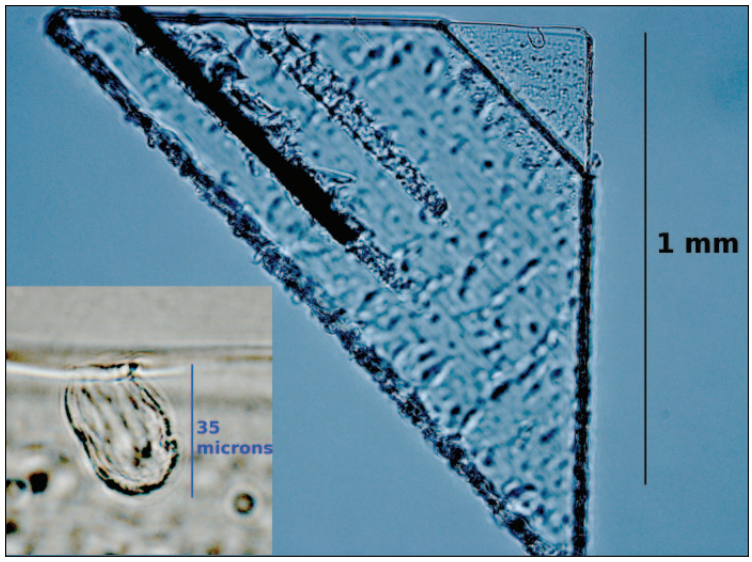


Fig. 3. *An aerogel wedge cut and mounted to a silicon "micro-fork" containing a microscopic particle impact that may be one of the first identified contemporary interstellar dust samples.*

Potential features identified by Stardust@home are closely examined. Real particle impacts are extracted from the collector in tiny wedges of aerogel less than 0.5 mm thick, using glass needles formed to a µm-sized tip. The needles are programmed to repeatedly poke into the aerogel via computer-controlled micromanipulators, eventually creating a series of precise "cuts" in the aerogel. These samples are extracted and prepared for investigators around the globe. The Stardust Laboratory at Johnson Space Center is one of two laboratories in the world with this specialized capability (figure 1).

External scientists analyze the compositions of candidate interstellar grains using synchrotron-based, x-ray spectroscopy, and attempt to determine which particles are real interstellar dust and which originate from the spacecraft, other contaminants, or from within our own solar system. At the March 2011 Lunar and Planetary Science Conference, the Stardust Interstellar Preliminary Analysis Teams reported that four of these identified, extracted, and analyzed particles may be the first of the rare and elusive interstellar dust grains (figures 2 and 3).

The team will continue to conduct automated scanning and particle extraction to identify and analyze impacts by interstellar dust. These samples will complement the highly successful and dramatic collection of Wild-2 comet dust. Taken together, they will increase our understanding of our own solar system and its early history, how it compares to other planetary systems and galactic materials, and the astrophysical environment of interstellar space in between.

Mars Habitability, Biosignature Preservation, and Mission Support

Dorothy Z. Oehler, *Johnson Space Center*
Carlton C. Allen, *Johnson Space Center*

Scientists and researchers at Johnson Space Center (JSC) have been studying the Martian surface to identify areas of past habitability with enhanced potential to preserve biosignatures. One area has been singled out in southern Acidalia Planitia/northern Chryse Planitia of the Martian lowlands. This area is predicted to have accumulated thick sequences of fine-grained sediments that could include preserved biosignatures. The area also contains tens of thousands of mud-volcano-like mounds (e.g., figure 1).

Mud volcanoes on Mars could have provided long-lived conduits for fluid movement from depth to the surface (figure 2), microhabitats for in-situ, endolithic life (figure 3), and a mechanism for transporting samples from depth to the surface where they could be accessed by future rovers. In response to a call by the Mars Program for imaging targets for future landing site candidates, JSC submitted multiple sites from the Chryse/Acidalia region of potential mud volcanism.

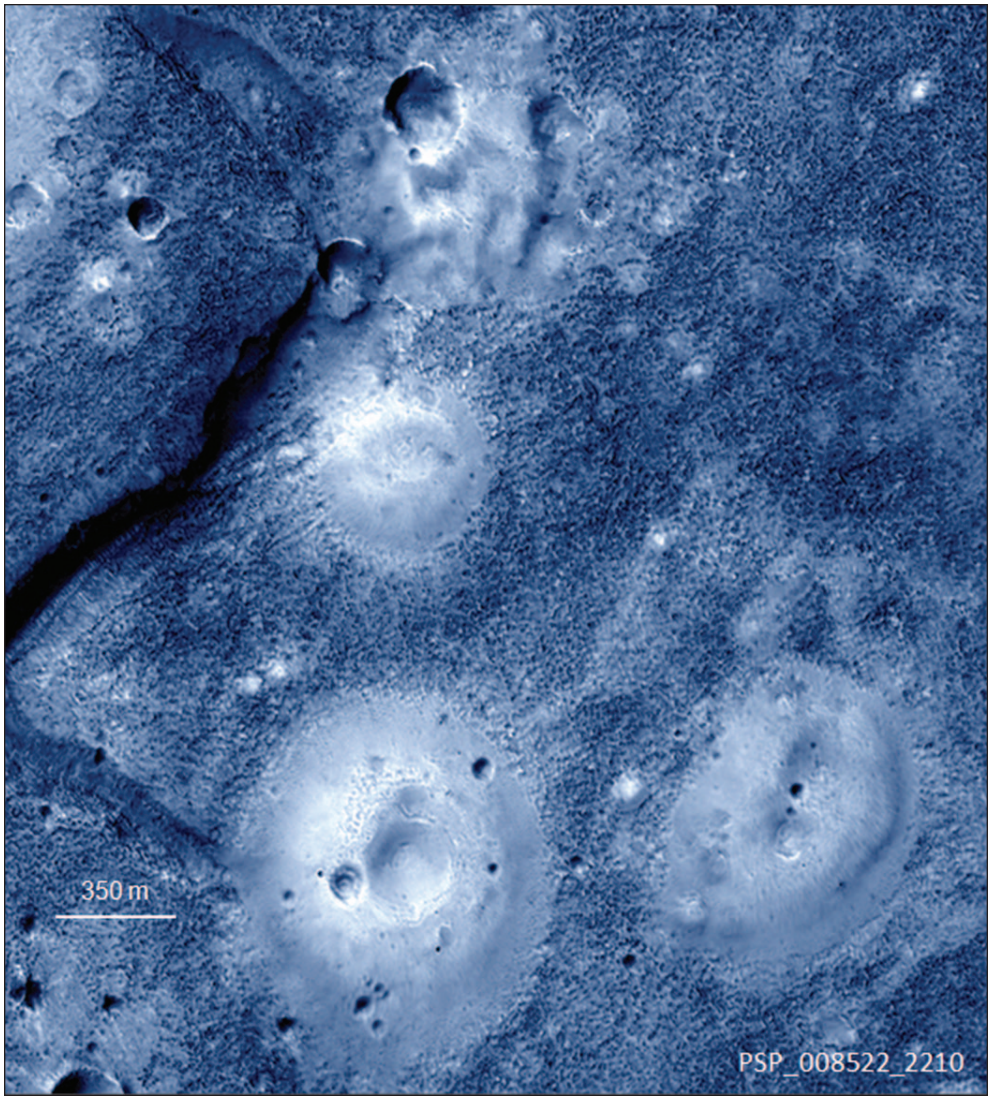


Fig. 1. *Mounds in Acidalia Planitia, Mars. These features have been compared to terrestrial mud volcanoes.*

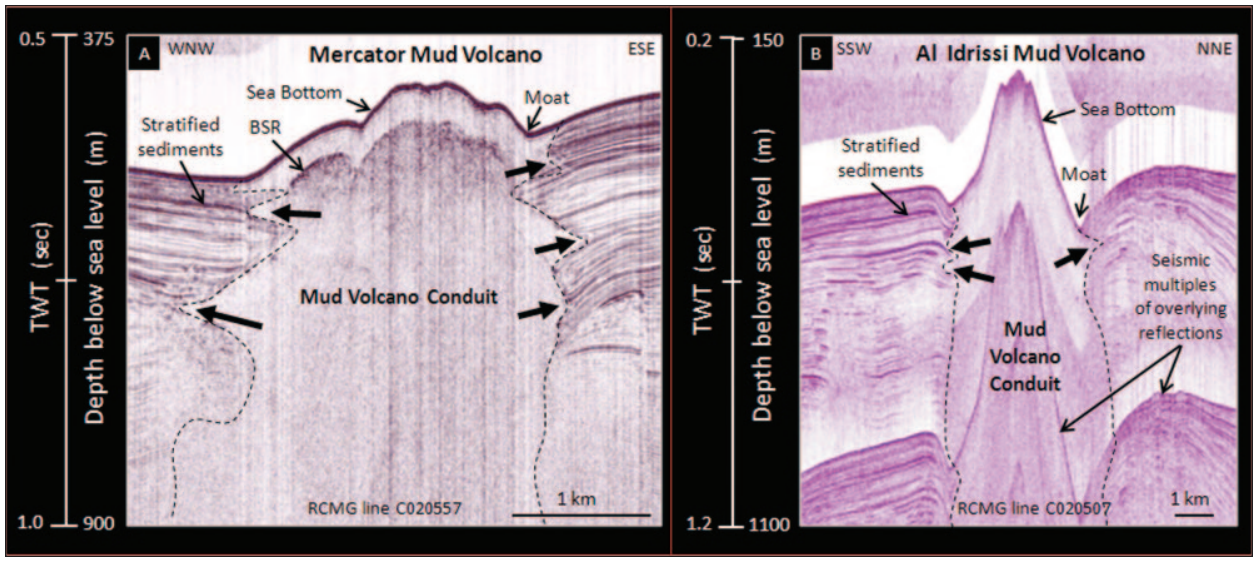


Fig. 2. *Seismic profiles of mud volcanoes in the Gulf of Cadiz, offshore Morocco, illustrating the conduits to the surface created by these types of structures. Thick arrows point to levels where mudflows interfinger with the stratified sediments in the subsurface.*

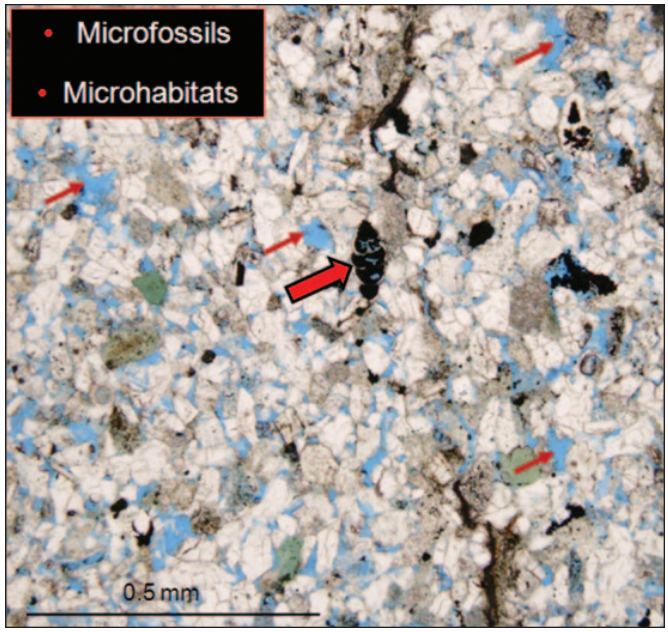


Fig. 3. *Coarse-grained sediment brought to the surface by a terrestrial mud volcano, illustrating microhabitats. Optical photomicrograph in transmitted light of a thin section. Large red arrow points to microfossil. Small red arrows illustrate potential microhabitats in porosity (shown in blue from tinted epoxy).*

Fluids and Their Effect on Measurements of Lunar Soil Particle Size Distribution

Bonnie L. Cooper, *Johnson Space Center*
David S. McKay, *Johnson Space Center*
William T. Wallace, *Johnson Space Center*
Carla P. Gonzalez, *Johnson Space Center*

From the late 1960s until now, lunar soil particle size distributions have typically been determined by sieving—sometimes dry, and at other times with fluids such as water or Freon. Laser diffraction instruments allow rapid assessment of particle size distribution, and eventually may replace sieve measurements. However, when measuring lunar soils with laser diffraction instruments, care must be taken in choosing a carrier fluid that is compatible with lunar material.

Background

Distilled water is the fluid of choice for laser diffraction measurements of substances when there is no concern about adverse effects of water on the material being measured. When scientists at Johnson Space Center began the analyses of lunar soils using laser diffraction, the first measurements were made with distilled water. Although the medians measured were comparable to earlier sieve data, the means tended to be significantly larger than expected.

The effect of water vapor on lunar soil has been studied extensively. The particles interact strongly with water vapor, and subsequent adsorptions of nitrogen showed that the specific surface area increased as much as threefold after exposure to moisture. It was observed that significant porosity had been generated by this exposure to water vapor. The possibility of other physical changes in the surfaces of the grains was not studied.

Investigation

A dispersion test showed that the use of distilled water resulted in clumping of lunar soil (figure 1). When a size-fractionated sample from lunar soil 14003,96 was measured in water, the volumetric mean was 121.1 micrometers, and the median was 98.04 micrometers (figure 2). When another sample of the same material was measured with isopropanol, the volumetric mean was 59.63 micrometers, and the median was 57.30 micrometers. Variation in aliquots could not be invoked as the cause of this difference.

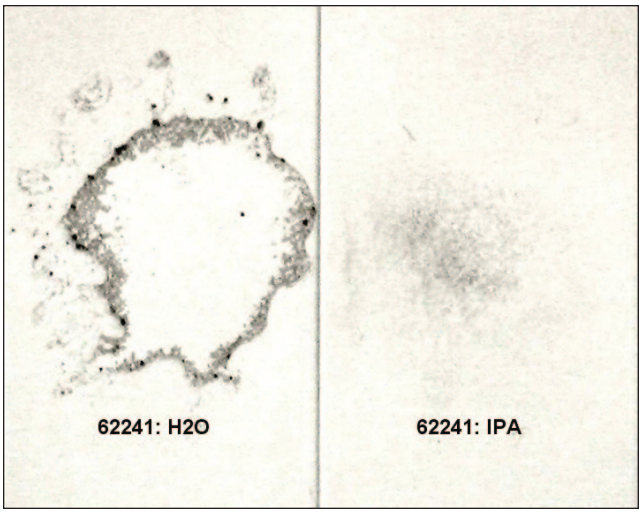


Fig. 1. *Dispersion tests with drops of water (left) and isopropanol (right) on a microscope slide, followed by application of a few milligrams of lunar soil 62241.*

A measurement of Apollo 11 soil 10084,2006 also showed significant variations related to the fluid that was used for measurement (figure 3). Moreover, when comparing three separate measurements of the sample in water, the standard error was seen to be significantly larger than the standard error produced when isopropanol was used.

It was found that the use of isopropyl alcohol resulted in little or no clumping. However, there was concern that the isopropyl alcohol might partially dissolve and disaggregate the agglutinates because of their high proportion of potentially reactive glass, and thus create smaller particles than would have occurred naturally. To address this concern, scientists at Johnson Space Center performed dissolution tests on lunar soil 14003,96 using isopropanol and water, and also using an acidic citrate phosphate buffer (pH 4). The solutions were analyzed with inductively coupled plasma mass spectroscopy. It was observed that neutral pH water had a strong tendency to dissolve the silicon, calcium, and aluminum in lunar soil, and that the isopropanol dissolved a negligible amount of these elements when corrected for the blank control (figure 4).

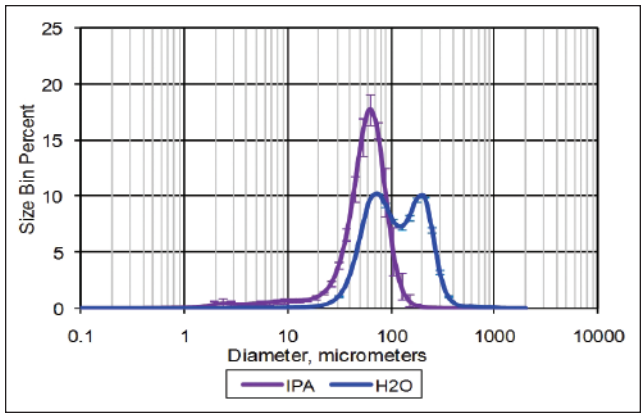


Fig 2. *Measurements of a size-fractionated sample from Apollo 14 soil 14003,96 in water (blue) and in isopropanol (purple). Note the secondary peak at large (~200 micrometers) particle size in the histogram that was measured in water, and was thought to be caused by clumping.*

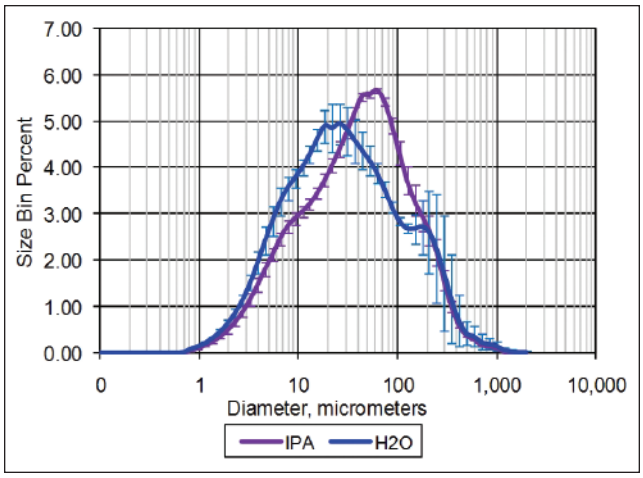


Fig. 3. *Measurements of Apollo 11 soil 10084 in water (blue) and isopropanol (purple).*

Discussion and Conclusion

During the studies of lunar soils 10084, 14003, 62241and 61141, it was found that water tends to cause clumping in the soil particles that cannot be de-agglomerated by sonication or by dispersant. Dissolution also occurs when lunar soil samples are placed in water. The finest fraction of lunar soil is known to concentrate both glass particles and plagioclase-rich particles. The dissolution studies show that the major elements of plagioclase are the elements most affected by dissolution in water at neutral pH, but are not detectibly dissolved by isopropyl alcohol. Dissolution and clumping can apparently create a spurious bimodal distribution in water-exposed lunar soil. Therefore, the use of alternative fluids of lesser polarity for particle size measurements is recommended. Isopropyl alcohol appears to have negligible chemical effect on lunar soil grains and its use avoids spurious grain size artifacts.

Element	Water	H_2O Control	Isopropanol (IPA)	IPA Control	pH 4 buffer Solution	pH 4 buffer Solution Control
Silicon	304.5	9	1280	1500	~35,000	~700
Calcium	0.53	0.14	0.1	0.2		
Aluminum	3	2	8	8	~22,500	~100
Magnesium	0.32	0.04	0.04	0.04		
Iron	5	8	20	20	~17,000	~100
Sulfur	0.7	0.7	1.6	1.6		
Titanium	1	1	4	4	~1700	~100

Fig. 4. *Dissolution of lunar soil 14003 in water, isopropanol, and in a pH 4 buffer solution. Controls were water, isopropanol, and pH 4 buffer solution without soil or other solute.*

Nanometer-Scale Anatomy of Entire Stardust Tracks

Keiko Nakamura-Messenger, *Johnson Space Center*
Lindsay Keller, *Johnson Space Center*
Simon Clemett, *Johnson Space Center*
Scott Messenger, *Johnson Space Center*

Analyses of samples returned from Comet 81P/Wild-2 by the Stardust spacecraft revealed a number of surprising findings that show the origins of comets are more complex than previously suspected. However, these samples pose new challenges for study because they are diverse and suffered fragmentation, thermal alteration, and fine scale mixing with aerogel. Consequently, fundamental questions remain about the nature of cometary materials, such as the abundances of organic matter, crystalline materials, and presolar grains. To overcome these challenges, Johnson Space Center (JSC) researchers developed new sample preparation and analytical techniques tailored for entire aerogel tracks of Wild2 sample analyses both on "carrot" and "bulbous" tracks. The team successfully sliced an entire track along its axis while preserving its original shape. The track was sliced into 510 thin sections with 70 nanometer (nm) thickness (figure 1). This innovation allowed examination of the distribution of fragments along the entire track from the entrance hole all the way to the terminal particle. Researchers used a scanning transmission electron microscope for elemental and detailed mineralogy characterization, a NanoSIMS for isotopic analyses, and an ultrafast two-step laser mass spectrometry (*ultra* L2MS) to investigate the nature and distribution of organic phases.

The JSC team's most important findings from the analysis of these two Wild2 aerogel tracks and their terminal particles include the following:

- The terminal particles are dominated by magnesium-rich crystalline silicates (forsterite and enstatite) that formed at high temperatures.
- The crystalline silicates have oxygen (O) isotopic compositions within the range of meteoritic materials, implying that the crystalline silicates originated in the inner solar system.
- The forsterite grain shows a ^{16}O-enrichment of ~40‰, and likely formed in the inner solar system. This grain may have formed together with amoeboid olivine aggregates in meteorites.
- Sub-micrometer diamond grains were identified that likely formed in the solar system
- Complex aromatic hydrocarbons are distributed along aerogel tracks and in terminal particles. These organics are likely cometary but affected by shock heating.
- Some cometary grains contain nitrogen-rich organic matter in the form of aromatic nitriles (R-C≡N). Such materials have potential astrobiological importance because it is believed that comets significantly contributed to the prebiotic chemical inventory of both the Earth and Mars.
- The Stardust organic compounds share some similarities with those of carbonaceous chondrites but are more similar to interplanetary dust particles. These findings are consistent with the notion that a fraction of interplanetary dust is cometary.

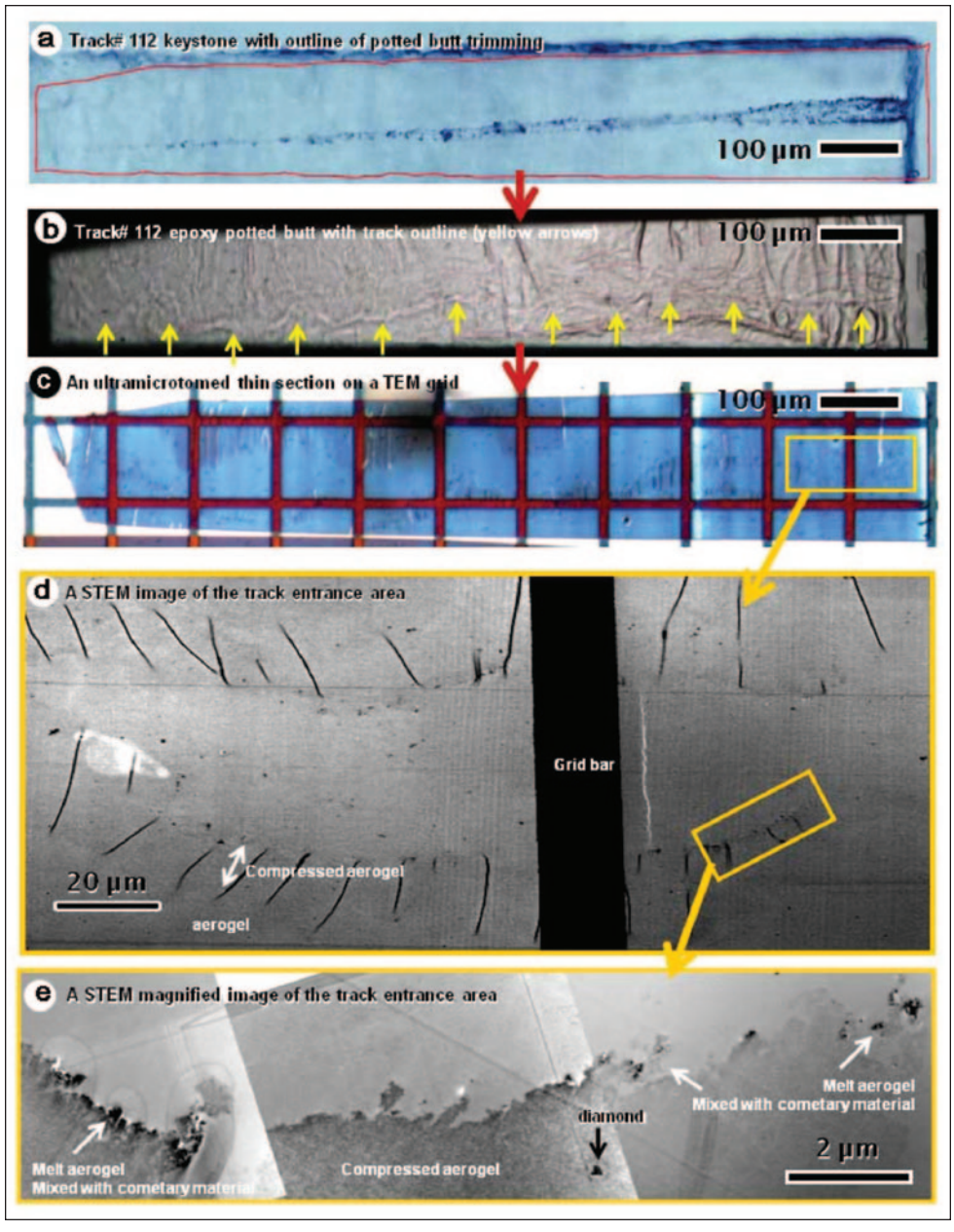


Fig. 1. *Processing flow chart for dissecting the whole track in aerogel.* ***(a)*** *Low magnification optical micrograph (under transmitted light) of the Track112 keystone after the terminal particle extraction. The red trapezoid indicates the outline of trimmed potted butt.* ***(b)*** *Top view of the epoxy potted butt of Track112 after trimming into trapezoid shape. Yellow allows indicate the track outline visible through the covering epoxy resin.* ***(c)*** *One out of 510 ultramicrotomed thin sections of Track112 mounted on amorphous carbon supported Cu transmission electron microscope grid.* ***(d)*** *A bright-field scanning transmission electron microscope micrograph of the boxed area in (c). The track morphology is well-preserved in an ultramicrotome thin section and material is intact. The aerogel within 20 µm of the track wall (darker contrast with wrinkles) was compressed by the impact.* ***(e)*** *Photo mosaic of bright-field scanning transmission electron microscope micrographs of boxed area in (d). Numerous sub-micrometer-sized grains are observed along the track wall. Many of these tiny grains consist of melt particles (cometary material intimately mixed with melted aerogel). One of the diamond grains is located in the compressed aerogel (arrowed).*

Development of the Brine Residual in Containment Concept

Michael R. Callahan, *Jacobs Technology*
Michael R. Casteel, *Jacobs Technology*
David A. Glock, *Johnson Space Center*
Karen D. Pickering, *Johnson Space Center*

Technology improvements in the recovery of water from brine are critical to establishing full-closure water recovery systems and achieving a sustained human presence in space. The NASA Exploration Life Support Project initiated a brine dewatering task to survey, develop, and test technologies for extracting water from concentrated wastewater brines. In response to this effort, the NASA Johnson Space Center Advanced Water Recovery Systems group proposed developing a novel brine dewatering concept that is referred to as brine residual in-containment (BRIC). The BRIC concept aims to address specific challenges associated with designing reliable systems that can approach 100% water recovery from brine. These issues include the buildup and removal of sticky and potentially toxic brine solids that tend to foul process equipment and reduce the overall efficiency of heat transfer and solids removal.

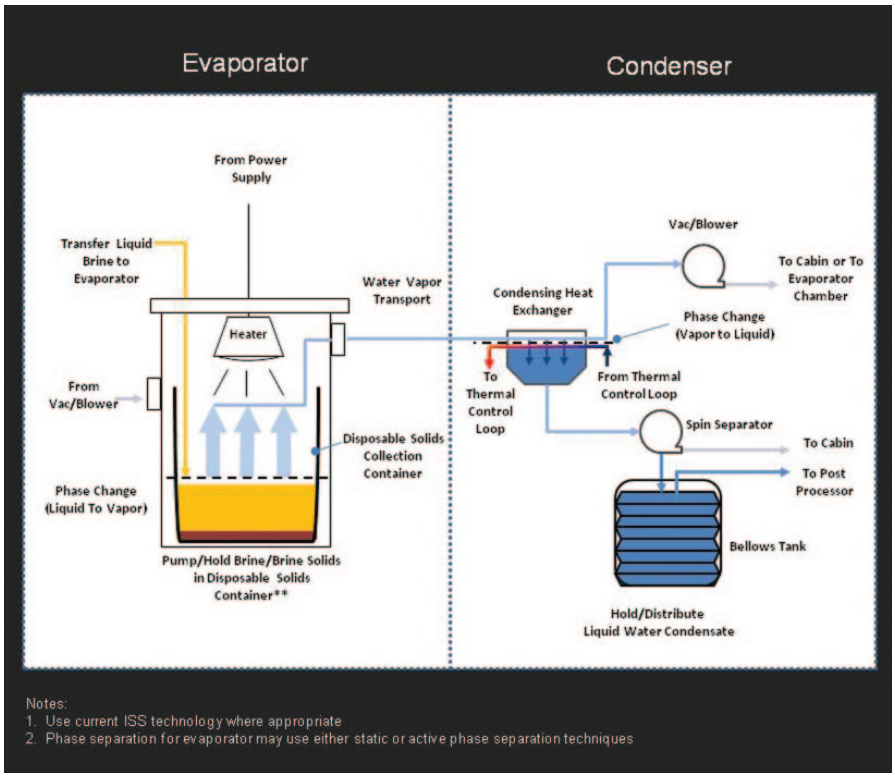


Fig. 1. *Simplified schematic of brine residual in-containment concept.*

The BRIC concept implements a technique in which brine drying is effected within the container used for final disposal of solid residual waste in an attempt to obviate some of the design complexity associated with removing and transporting brine solids. The practice of in-place drying has some precedence in the nuclear waste industry, where it has been proposed for use in minimizing disposal volumes and reducing human exposure to hazardous waste materials. The in-place drying design for BRIC is expected to allow for high water recovery without the attendant complexity associated with attempting to mechanically remove, transport, and store the residual brine solids. The BRIC design also incorporates thin-film-drying processes and vacuum- and radiative-heat-transfer methods to increase the efficiency of the drying process and to promote options for fluid/solid management under conditions of microgravity; e.g., the use of capillary- and/or rotary-based design solutions.

A simplified diagram of the BRIC concept is shown in figure 1. Liquid brine is transferred to the evaporator using a metering pump or differential pressure between the evaporator and the ambient environment. A thin layer of brine spreads across the bottom of a disposable solids collection container. Spreading is accomplished by gravity and/or surface force interactions. Variable heat control and vacuum are supplied to facilitate evaporation and maintain temperatures at the desired set point. Water vapor from evaporating brine is transferred to a condensing heat exchanger via a vapor duct. The condensing heat exchanger is used to return purified water vapor to a liquid state. The condensate is then collected in the condensate tank. An optional recirculation loop that uses the vacuum pump exhaust or an additional blower may be incorporated to transfer vapor and aid in the overall evaporation process. A baffle or demister element in the vapor duct is used to prevent brine aerosols from entering the condensing

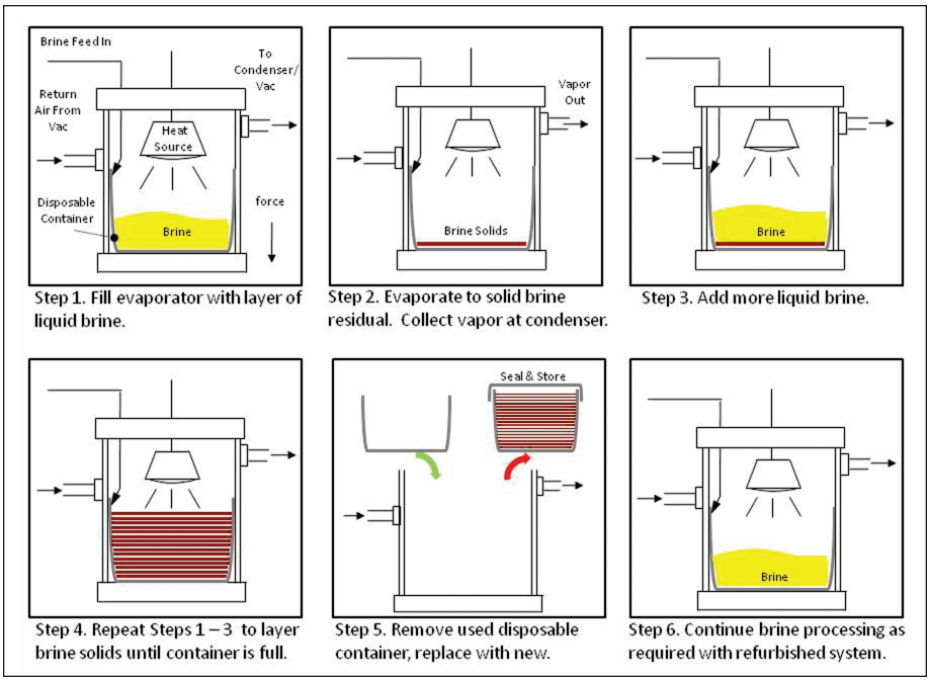


Fig. 2. *Basic concept of brine residual in-containment operation.*



Fig. 3. *Brine residual in-containment pre-prototype.*

chamber. In the current BRIC designs, direct radiative heat transfer and dielectric technologies, such as infrared and microwave systems, are currently being targeted as the evaporative heat source.

Figure 2 shows the steps involved in the basic concept of operation for the BRIC process. In Step 1, brine is introduced into the evaporator where it is contained for drying within a disposable solids collection container. In Step 2, the liquid brine is evaporated, the vapor process stream is recovered using the condenser, and the residual brine solids are held in place. More liquid brine is added to the evaporator in Step 3. In Step 4, the liquid brine injection and drying cycle is repeated until the solids collection chamber is full. In Step 5, the disposable solids collection chamber is sealed and removed, and a new solids collection chamber is installed in its place. The entire brine drying and solids collection process is repeated as noted in Step 6. A photograph of the BRIC pre-prototype is provided in figure 3.

Development of the BRIC concept has been in work for the past year. Efforts have focused on the design, buildup, and preliminary test of a pre-prototype laboratory demonstration unit. Tests conducted to date using both deionized water and as much as 16% sodium chloride solutions have demonstrated evaporation rates between 0.6 and 4.0 milliliters per minute (mL/min); as much as 95% water recovery; and the deposition, containment, and removal of a dried solid salt conglomerate. A new technology reporting disclosure for the BRIC was submitted to the NASA e-NTR system in late 2010. Current planning is under way to refine the BRIC process, establish system performance with actual brine waste streams, and develop a gravity-independent version of the dewatering system.

Small Satellite Development

Robert S. Provence, *Johnson Space Center*
Tim Runkle, *Johnson Space Center*

NASA Johnson Space Center is sponsoring collaboration between engineering students of Texas A&M University and the University of Texas at Austin. Each university has a dedicated satellite laboratory focused on NASA's Low-earth Orbiting Navigation Experiment for Spacecraft Testing Autonomous Rendezvous (LONESTAR) project.

LONESTAR's overarching mission is to design, develop, and fly small satellites (figure 1) using only the student workforce and university laboratories, though NASA oversees the project and provides technical expertise when necessary. The ultimate goal is for small spacecraft to cooperatively perform autonomous-formation flying and docking maneuvers. To increase the likelihood of mission success, the project has four separate stages, each with its own flight, mission, and objectives.

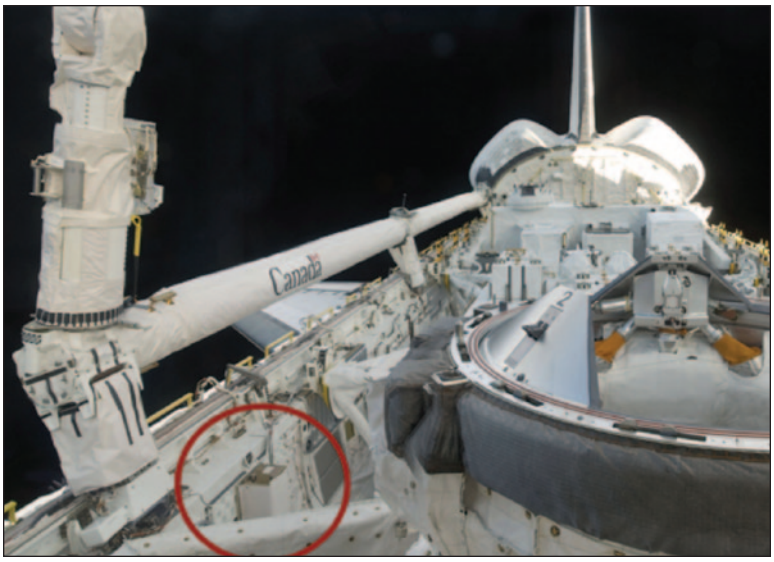


Fig. 2. *The LONESTAR satellites in Space Shuttle Picosat Launcher moments before deployment.*

The first mission's primary objective was to characterize a Global Positioning System (GPS) sensor that will be used for relative navigation in subsequent flights. The first mission also taught the students how to work as a team, and taught them the NASA process for a developmental test objective (DTO) payload.

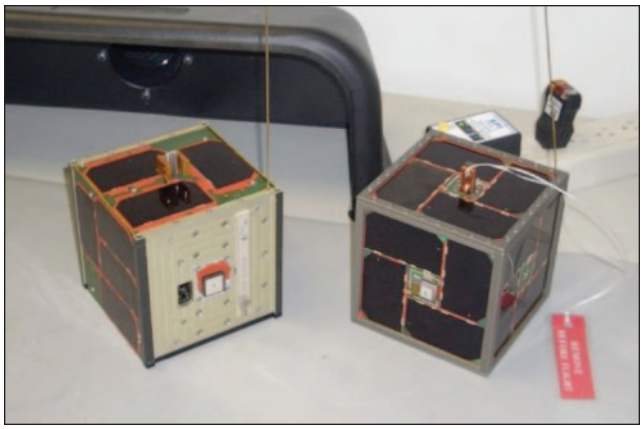


Fig. 1. *Mission 1 satellites during assembly.*

The first mission was aboard the Space Shuttle *Endeavour* during the STS-127 in the summer of 2009. Two 12.7-cm (5-in.) cube satellites were stacked and loaded into a single deployment mechanism in the payload bay (figure 2).

LONESTAR Mission 1 flew as a DTO and was deployed from Space Shuttle *Endeavour* on July 15, 2009 (figure 3).

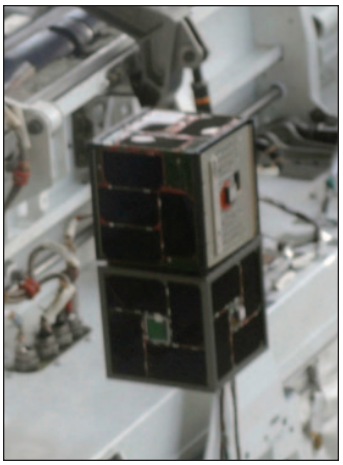


Fig. 3. *The LONESTAR satellites leaving the payload bay.*

Mission operations for this first flight lasted from deployment until March 17, 2010—just over 8 months. University students worked in their mission control centers (figure 4), first to establish a link with the satellites, then to command the satellite, and finally to download GPS data. Along with



Fig. 4. *Texas A&M University mission control center.*

the lessons learned in the development phase, the students learned to overcome real-time operational issues.

LONESTAR Mission 2 launch is scheduled for January 2013. Students are learning that the enhanced objectives of this mission are driving the physical characteristics of the satellites, which, in turn, is changing the deployment approach.

The second mission's primary objective will be to test the active attitude systems of both satellites and the thrusters on the chaser vehicle. The chaser vehicle (figure 5) will almost double in volume to accommodate the attitude and translation technology.

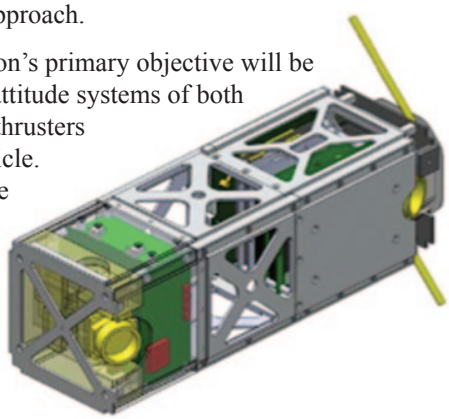


Fig. 5. *Chaser spacecraft for Mission 2.*

The target vehicle volume will be more than 100 times greater than the volume of the Mission 1 satellite. The target vehicle will house the chaser until verification and checkout of both satellites is performed. Mission Control will send the release command to deploy the chaser spacecraft that will begin relative vehicle operation.

Once the Space Shuttle Program ends, the LONESTAR project will work with the International Space Station on deployment strategies. A pressurized vehicle will transport the Mission 2 satellites to the space station, to the Japanese Experiment Module exposed facility for deployment into low-Earth orbit.

The third mission's primary objective will be to test a small satellite docking system. Since this mechanism does not yet exist, the students will be expected to design the innovative technology to allow small satellites to dock and undock, and to complete both tasks reliably.

The fourth mission's primary objective is to bring the whole system together for automated rendezvous and docking. The final test of the small satellite technology will involve a mission where both satellites perform translation maneuvers and dock autonomously.

Each incremental stage in the LONESTAR project benefits NASA by increasing the agency's knowledge of a currently emerging field where rapid development and cost-effective projects are a major focus. LONESTAR is also an educational opportunity for university students to learn about the aerospace industry under the guidance of NASA mentors, in essence developing the engineers of our future space programs.

Mission Operations Involvement in the Desert Research and Technology Studies Analog Mission

Ernest R. Bell, Jr., *United Space Alliance*
Megan Rosenbaum, *United Space Alliance*
Daren Welsh, *United Space Alliance*
Dave Coan, *United Space Alliance*
Randall McDaniel, *Johnson Space Center*

The NASA Desert Research and Technology Studies (Desert RATS) is an annual field test of advanced concepts, prototype hardware, and potential modes of operation to be used on human planetary space exploration missions. For the 2009 and 2010 NASA Desert RATS field tests, NASA incorporated various engineering concepts and operational exercises into mission timelines and executed in a simulated mission framework similar to current space shuttle and International Space Station missions.

The field test for 2009 revolved around a 2-week lunar exploration simulation using a single two-person Lunar Electric Rover (LER). In 2010, the field test again centered on planning and executing a simulated 14-day lunar surface mission, but increased the number of LERs to two, and incorporated docked operations with a pressurized excursion module. The tests were conducted in a once-active volcanic region north of Flagstaff, Arizona, where Apollo crews formerly trained in field geology.

The LERs are conceptual two-person rovers containing an enclosed cabin with extravehicular activity (EVA) access via twin aft bulkhead suit ports. Each LER carried a deployable portable utility pallet containing a communications relay system, suit port transfer module stowage, and geology tools and sample stowage. The EVA equipment for the field tests included geology tools and additionally, for the 2010 field test, an electronic cuff system capable of displaying procedures, recording field notes, and providing navigation. The pressurized excursion module was a mock-up of a design for a pressurized habitat module that contained science, maintenance, and medical workstations, as well as an airlock and multiple LER docking locations.

The field test included the crew, the mission operations team, a geological science team, a mission management team, engineering teams, and a communications and data support team. For these field tests, each LER crew consisted of one systems expert (astronaut or engineer) and one field geologist. The mission planning, team integration, crew training, and test execution were all led by the mission operations team. This team consisted of certified NASA Mission Operations Directorate flight controllers, and provided the core of the Desert RATS mission control team executing the simulated lunar missions. Their backgrounds were in the areas of EVA, mission integration and timeline development (OpsPlan), onboard mechanical systems and maintenance, and robotics. With the simulated EVA operations, mechanized operations (the rover), and need for timeline re-planning, these flight control disciplines were especially well suited for the execution of the 2009 and 2010 Desert RATS field tests.

The mission operations team pulled from their "plan, train, fly" experience in the Mission Operations Directorate to integrate test objectives from multiple organizations and NASA centers. Leading up to the actual simulation at the field test, the operations team members worked closely with the science, hardware, and research teams to produce a mission plan complete with timeline, executable procedures, flight rules, training, and reference manuals. The timelines, procedures, and flight rules all went through multi-team reviews, analogous to space shuttle and International Space Station processes. The coordination of the training of not only the crew members, but also cross-training between the teams to increase cross-disciplinary knowledge and to provide for a more integrated simulation, was also provided by the operations team. During the field test, the mission operations team then executed the mission plan in a flight-like manner, coordinating and integrating among the teams.

With respect to the simulated mission control architecture, the mission operations and science teams operated from a mobile Mission Control Center (mMCC) (figure 1) and several engineering support transport cargo containers were outfitted as science backrooms. All were located at a base camp in the area of operation. In all, approximately 30 positions were filled and set up in a mission control-type architecture. Of these positions, the mission operations team manned the traverse director, assistant traverse director, capsule communicator, and operations planning positions within the mMCC.

The operations team led the mission simulation via the role of traverse director. This position was analogous to a combination of a flight director, simulation supervisor, and Neutral Buoyancy Laboratory test director. Each rover had a traverse director in the mMCC and on the chase team



Fig. 1. *Desert RATS Mission Operations Team working inside the mobile Mission Control Center.*

who coordinated between the science and engineering teams, and the crews.

The OpsPlan position had the responsibilities of developing the daily timeline that integrated the mission operations and science team objectives, creating daily reference materials, and coordinating with the LER support position to transfer electronic files between the mMCC and the LER. Additionally, this person captured the actual execution of the activities in contrast to the pre-mission plan.

The third position filled by the mission operations team was that of capsule communicator. This position's responsibility, just as in actual spaceflight, was to be the voice of the control team to the crew for the non-science activities. During science activities, this responsibility was handed over to a SciCom position that was filled by one of the geologists supporting the simulation.

Although this was not specifically a test of operational techniques, but rather an engineering field test supported within a realistic mission scenario, the inclusion of an operations team has provided the benefit of giving NASA mission operations flight control personnel the opportunity to begin examining operational mission control techniques, team compositions, and mission scenarios for lunar exploration. It provided the mission operations team the opportunity to gain insight into functional hardware requirements via lessons learned from executing the Desert RATS field test simulated lunar missions.

This knowledge will be applied to future Desert RATS field tests to continue the evolution of manned space operations in preparation for human planetary exploration. It is important that operational knowledge for human space exploration missions be obtained during Earth-bound field tests to the greatest extent possible. This allows mission operations personnel the ability to examine various flight control and crew operations scenarios in preparation for actual space missions.

GeoLab

Cynthia A. Evans, *Johnson Space Center*
Michael Calaway, *Johnson Space Center*
Mary Sue Bell, *Johnson Space Center*

What is GeoLab?

GeoLab is a prototype geological laboratory designed for deployment and testing during NASA's analog missions. Johnson Space Center (JSC) scientists built GeoLab as part of a technology project to support the development of science operational concepts on future planetary missions. GeoLab was integrated it into NASA's Habitat Demonstration Unit-1/Pressurized Excursion Module (HDU1-PEM)—a first generation exploration habitat testbed (figure 1).

As a testbed, GeoLab (figure 2) provides a safe, contained working space for crew members to perform preliminary examination and characterization of geologic samples. The GeoLab concept builds from the hardware and protocols used in JSC's Astromaterials Sample Curation laboratories. The centerpiece of the GeoLab is a custom-built glovebox, constructed from stainless steel and polycarbonate, and built to support a positive-pressure nitrogen environment. The glovebox is mounted onto the habitat's structural ribs; the unique shape (trapezoidal prism) fits within a pie-shaped section of the cylindrical habitat. A key innovation of GeoLab is the mechanism for transferring samples into the glovebox—a mechanism composed of three antechambers (airlocks) that pass through the shell of the habitat. These antechambers allow geologic samples to enter and exit the main glovebox chamber directly from (and to) the outside, thereby minimizing potential contamination from inside the habitat. The glovebox also incorporates a state-of-the-art environmental monitoring system. The main chamber of the glovebox is equipped with sensors that monitor oxygen parts per million, pressure millibar, humidity, and temperature, and each antechamber contains pressure sensors. Four video surveillance cameras provide real-time displays of operations inside the GeoLab workstation and the area around the antechamber doors on the outside the habitat.



Fig. 1. *The Habitat Demonstration Unit-1/Pressurized Excursion Module (center) with two docked space exploration rovers. The main module volume includes several workstations. Three circular ports below "Habitat Demonstration Unit" are the antechamber doors that provide access directly into the GeoLab glovebox.*



Fig. 2. *GeoLab integrated into the Habitat Demonstration Unit-1/Pressurized Excursion Module. The suite of instruments included a handheld x-ray fluorescence analyzer (far left), stereomicroscope (center, above glovebox), network cameras, and touch screen computers.*

Configurability

The GeoLab design includes a large set of ports for rapid reconfiguration with new instruments for sample characterization. The initial setup included a stereomicroscope (Leica M80) for microscopic examination and image capture of samples, and an Innov-X handheld Delta DP6000 x-ray fluorescence (XRF) spectrometer for whole rock geochemical fingerprinting. Images and data from the instruments can be saved and "downlinked" to a remote science team. The glovebox also contains a mass balance and scale for collecting sample mass and size. All instrumentation and cameras are controlled at the workstation with two touch-screen computers (HP Touchsmart 600xt) mounted over the workstation and integrated into the HDU1-PEM avionics system. The cameras and sensor displays can be viewed and controlled in real time on the remote network, and data from the microscope and XRF can be quickly moved



Fig. 3. *Crew member collecting a geological sample during a Desert Research and Technology Studies traverse.*

across the network, thus enabling collaboration between the astronaut crew and a supporting science backroom.

Field Trials

The GeoLab and HDU1-PEM were tested for the first time as part of the 2010 Desert Research and Technology Studies (Desert RATS)—NASA's analog field exercise in Northern Arizona. The demonstration was initially conceived to guide the development of requirements for the Lunar Surface Systems Program and test initial operational concepts for an early lunar excursion habitat that would follow rovers performing geological traverses (figures 1 and 3). GeoLab objectives targeted general support of future planetary surface geoscience activities by providing an infrastructure for preliminary examination of samples, early analytical characterization of key samples, and insight into special considerations for curation, and by using data for prioritization of samples for return to Earth.

GeoLab Operations in the Field

The specific 2010 GeoLab operations included testing basic functions of the glovebox and associated instruments with a variety of operators (figure 4), and supporting the Desert RATS science team with additional data on samples that were collected during the rover traverses. When the crews examined samples in the GeoLab, they were testing these four major objectives at a high level:

1. How does the GeoLab function as a workspace, including glovebox and instrument operations?
2. How well do the crew and science team work together; what benefits are achieved by crew-scientist interactions during the integrated GeoLab tests?
3. Can the data collected in the GeoLab inform the science team about the geologic units and the geologic history of the traverse area?
4. Can the data collected in the GeoLab help the science team prioritize samples for decisions regarding future return to Earth?

Initial GeoLab Results

Results from the GeoLab 2010 operations provide a first look at both the value and the operational constraints associated with human-tended geological operations in a laboratory setting on a planetary surface. Initial assessments suggest that:

1. The GeoLab glovebox provided a high-fidelity field laboratory, and it performed well. With a trained crew, samples could be examined relatively quickly, and provide additional detailed data for further consideration by the science team.
2. GeoLab operations benefited from science team participation. The science team saved valuable crew time by performing certain tasks (e.g., camera control), and guided the crew for decisions regarding data collection.



Fig. 4. *During GeoLab operations, all data could be viewed in near-real time by a remote science team.*

GeoLab

continued

3. The detailed data collected in the GeoLab added to the body of evidence applied to understanding the regional geology. Even though initial assessments of the geochemical data include many uncertainties, the full body of data collected on each sample suggests that similar-looking rock units could be distinguished, providing data useful for geologic interpretation of the area (figure 5). Of note, data collected on alteration surfaces of samples provided additional detail and information that was difficult to obtain in the field. The team assumes these data would also be useful to the science team for decisions regarding sample handling and prioritization.

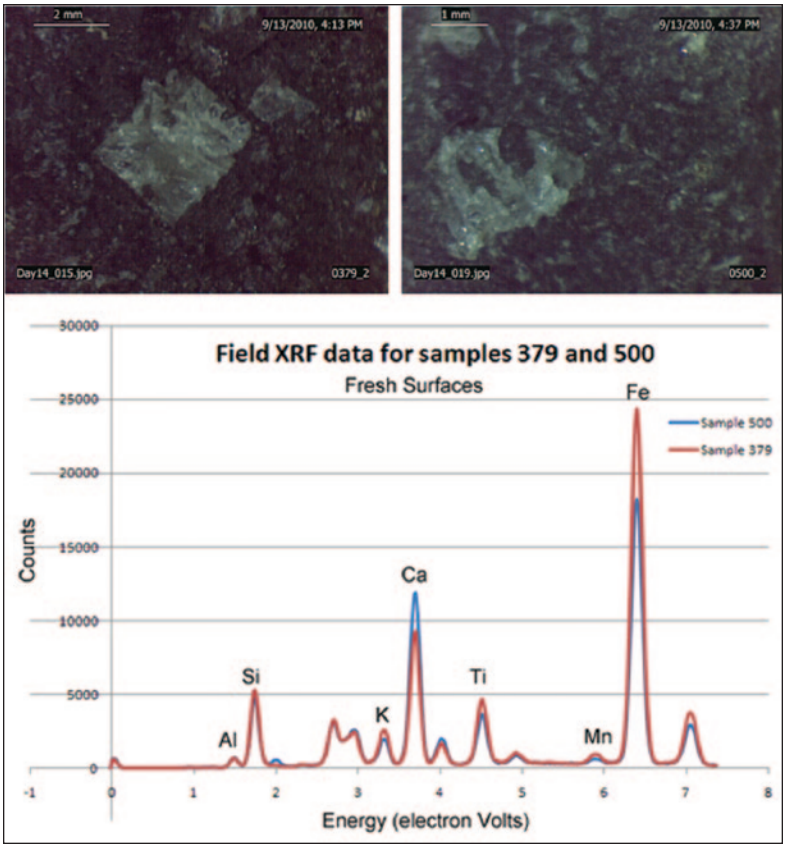


Fig. 5. *Microscopic images (texture and phenocryst assemblage) and x-ray fluorescence spectra for rapid geochemical fingerprinting of two samples from similar-looking units [Sample 379, left; Sample 500, right] suggest compositional differences between the older flow unit (500) and an older cinder cone (379).*

Future Plans for GeoLab

There are several areas of continued development for future GeoLab operations. The team is testing best operating practices for the XRF as a field/lab instrument, and assessing how to interpret XRF data for whole rock geochemical fingerprinting. Not surprisingly, the GeoLab XRF data must be interpreted within the context of the field occurrence and detailed visual descriptions (especially texture, homogeneity, surface roughness and alteration, and more), and microscopic imagery. The team is characterizing the performance of the XRF spectrometer, in parallel to analysis of Desert RATS data, by conducting tests with rocks of known composition and a variety of surfaces, and by building working calibration curves for the major rock-forming elements. The data will be used for analyzing the results of Desert RATS samples. There is also the plan to test the configurability of GeoLab in the 2011 Desert RATS field tests by integrating additional analytical instruments, and by upgrading and simplifying the instrument interfaces for remote operations. Collaboration will continue with both the science and the operations teams for integrated tests, to take full advantage of the operational environment provided by the field deployment.

Continued testing of GeoLab operations in a field environment will contribute to the development of habitat-based laboratory concepts. The scientific and operational value of additional analytical capabilities will be tested in GeoLab, and, in the future, the results will be compared to similar analyses using field instruments that are operated by crew or instruments mounted on robots. The team aims to apply its work toward defining preliminary examination and sample handling protocols required for efficient field campaigns and initial curation efforts that control contamination and preserve pristine samples collected during exploration missions. Assessment of the laboratory operations will drive the definition of requirements and support the advancement of new technologies for handling and examining extraterrestrial samples, and transporting them back to Earth.

Managing Science Operations During Planetary Surface Missions: The 2010 Desert Research and Technology Studies Test

Dean B. Eppler, *Johnson Space Center*
Douglas W. Ming, *Johnson Space Center*

Desert Research and Technology Studies (Desert RATS) is a multi-year series of hardware and operations tests carried out annually in the high desert of Arizona on the San Francisco Volcanic Field. Conducted since 1997, these activities are designed to exercise planetary surface hardware and operations in conditions where long-distance, multi-day roving is achievable. Such activities not only test vehicle subsystems through extended rough-terrain driving, they also stress communications and operations systems and allow testing of science operations approaches to advance human and robotic surface capabilities. Desert RATS is a venue where new ideas can be tested, both individually and as part of an operation with multiple elements. By conducting operations over multiple yearly cycles, ideas that "make the cut" can be iterated and tested during follow-on years. This ultimately gives both the hardware and the personnel experience in the kind of multi-element integrated operations that will be necessary in future human planetary exploration.

Desert RATS 2010 tested two crewed rovers designed as first generation prototypes of small pressurized vehicles. Each rover provided the internal volume necessary for crew members to live and work for periods up to 14 days, as well as allowing for extravehicular activities (EVAs) through the use of rear-mounted suit ports. The 2010 test was designed to simulate geologic science exploration traverses over a 14-day period through a terrain of volcanoes, lava flows, and underlying sedimentary rocks. Prior to the test, a series of traverses was planned using techniques that were first developed during the Apollo missions. These activities were based on a photogeologic interpretation of air photo and satellite images conducted by the U.S. Geological Survey in Flagstaff, Arizona, and they were designed to simulate a reconnaissance investigation by two rover crews of a planetary surface operating under a variety of communications constraints such as intermittent connectivity. Predicted areas of good radio reception were overlaid on the planned traverses, and locations of geological interest were adjusted to ensure communications supported the planned test conditions during each day of the test. The resulting set of traverses and stations was then field checked by the test team leads to ensure the set matched the planned test conditions.



Fig. 1. *Crew members acquire a basalt sample at a stop during a 2010 Desert Research and Technology Studies geologic traverse.*

Conduct of the actual test took place between August 31 and September 13, 2010. Two crew members lived in and drove each rover for a single week with a "shift change" on day 7, resulting in a total of eight test subjects for the 2-week period. Each crew consisted of an engineer/commander and an experienced field geologist. Three of the engineer/commanders were experienced astronauts with at least one space shuttle flight each. The field geologists were drawn from the academic community (figure 1).

Operations were tested with different communication states and rover deployment conditions. Three days of each week operated under conditions were the crew could always talk with mission operations team (called continuous communications), and 3 days the crew could only talk to mission control for approximately 1 hour in the morning and approximately 1 hour at the end of the traverse day (called 2-A-Day communications). In addition, portions of the traverses were conducted with the two rovers working together as a combined crew; during other periods, the rovers operated out of line-of-site of each other, pursuing independent science objectives.

Science Operations Management Approach

In previous Desert RATS operations, the science support room operated largely in an advisory role to the mission test team. This approach was driven by the need to provide a loose science mission framework that would underpin the engineering tests, rather than be an element of the operations that was conducting science-discipline-specific test operations. However, the extensive nature of the traverse operations for 2010 drove the decision to expand the role of the science operations and test specific operational approaches as part of the science support for the test. The success of the Apollo mission science support team as well as the science operations approach used by the Mars Exploration Rover missions became the baseline for the science test.

Past experience has shown that overseeing crewed operations of multiple vehicles requires a separate control room for each (e.g., space shuttle and International Space Station operations prior to docking of the orbiter to space station or after undocking). Consequently, each rover worked directly with a Tactical Science Operations Team (TSOT) responsible for managing real-time science operations while each crew conducted "boots on the ground" geologic field operations. The TSOT operated during normal duty days, between approximately 7:30 a.m. and 5:30 p.m. In addition to the TSOT, independent test operations with two rovers required an integration team, termed the Strategic Science Operations Team (SSOT). The SSOT analyzed the results of daily sciences operations from each rover crew and evaluated those operations within the larger objectives of the field traverse plans. In particular, a major function of the SSOT was to evaluate the completion status of a particular day's objectives and, if necessary, recommend to the mission manager variations in the following days' operations in response to missed objectives or important, unexpected discoveries. The SSOT operated during the night shift, between approximately 8:00 p.m. and 4:00 a.m. Both the SSOT and TSOT were crewed by scientists with a range of experience levels in both field geology and planetary mission operations.

Each TSOT was housed in a separate trailer in the field that had seven console positions (figure 2). The TSOTs were managed by a team lead who was responsible for the overall conduct of a particular rover's science operations during an EVA. Communications with the rover crew were conducted by a science communicator—the only person on the TSOT who communicated directly with the crew. A documentarian assisted the TSOT lead with a real-time, running "war diary" of field operations, describing the operations, identifying specific issues to be resolved downstream, and providing the overall daily reference document for science operations. Two of the remaining console positions were responsible for managing the operation of a variety of still, panoramic, and video cameras, and downlinking image products to be used in real time for situational awareness and management of the science operations at a particular station. Lastly, two TSOT members were responsible for overseeing the science activities of a single crew member. This activity included downlinking image data from backpack cameras, listening to and conducting real-time science analysis of crew members' verbal descriptions, and providing advice to the TSOT lead on operations. In addition, each TSOT maintained a team member (OPSLINK) in the primary operations control trailer to act as the liaison between each science team and the overall mission operations team. In particular, OPSLINK managed the control hand off between mission operations team, which controlled the rovers when they were driving between stations, and the TSOT, which took over when the crew members stepped off the rover to begin geologic work.

The SSOT was conducted in a hotel conference room in Flagstaff, Arizona, separate from the field operations site. Like the TSOT, there were a number of standing positions on the team held by a variety of scientists. The SSOT was managed by a team lead responsible for management and completion of all activities of the SSOT, including replanning of traverses for the following day's science operations. In addition, the team lead was responsible for presenting any changes to the day's plan to the Mission Management Team following the SSOT's daily operations.



Fig. 2. *Science operations control room located near the 2010 Desert Research and Technology Studies field test site.*

The team also included a documentarian whose role was similar to the counterpart on the TSOT. An SSOT strategic operations lead was responsible for managing long-term constraints that affected the daily re-planning process (e.g., communications constraints), and any items that may affect the mission in light of re-planned science operations. The activity planners were responsible for taking the recommendations of the SSOT team lead for changes to future tactical plans and preparing the revised daily plan for each rover crew. The long-term planning lead was responsible for coordinating the science teams that worked on datasets critical to planning the next day's tactical activities, determining whether there were discoveries or issues that warranted traverse replanning, and revising traverse plans in accordance with new directions. Various geosciences teams were responsible for analyzing data sets produced by the crew rover imaging and science teams (e.g., crew field notes, panoramic or backpack imaging data), making specific recommendations to the strategic operations lead on revising the following day's geologic traverses, and identifying key samples collected that were candidates for further study.

The 2010 RATS Science Operations Test was extremely successful, testing a variety of old and new operations approaches to managing science data and crew operations on planetary surfaces. In addition to providing substantive lessons learned about how to do extended planetary science operations, the test served to begin training a new generation of scientists in the demands of planetary surface science operations.

Forward-looking Infrared Cameras: A Potential Crew Tool for Geological Site Assessments

William L. Stefanov, *Johnson Space Center*
Cynthia A. Evans, *Johnson Space Center*
Kei Shimizu, *Brown University*

Plans for future crewed missions to the lunar or Martian surface, or near-Earth objects such as asteroids or comets, will include field traverses to assess site geological character and potential geohazards, and to identify potential in-situ resources. While much of this information—e.g., mineralogy, chemical composition, and surface particle size distributions—can be obtained from multispectral or hyperspectral instruments located on orbiters, the very high spatial resolution of field validation data obtainable by crews "on the ground" is desirable prior to establishment of site infrastructure and habitats.

A handheld forward-looking infrared (FLIR) camera was investigated as a field assessment tool for rapid estimation of rock abundance and discrimination of geological materials using both laboratory and field analog site approaches. NASA selected the FLIR Systems, Inc. (headquartered in Wilsonville, Oregon) FLIR SC660 640 x 480 pixel array, uncooled microbolometer thermal infrared camera, as it includes a co-registered digital camera for simultaneous acquisition of visible wavelength (red, green, and blue bands) data. A typical experimental setup of the camera in the laboratory is shown in figure 1.

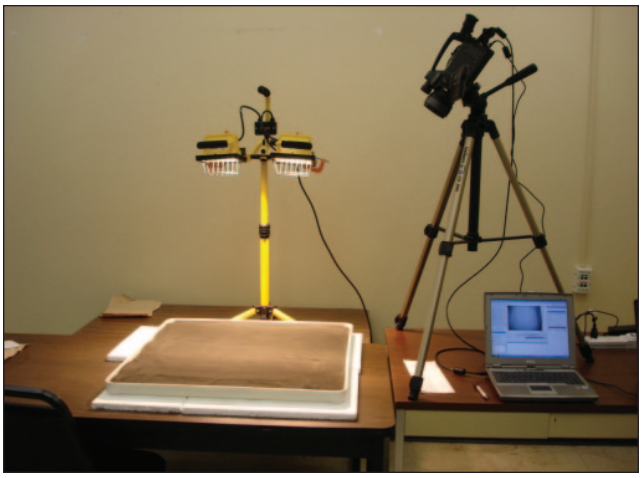


Fig. 1. *Typical forward-looking infrared experimental setup.*

The camera signatures and thermal response of a laboratory analog of a lunar mare surface were characterized. The analog surface used lunar soil simulant, basalt "gravel" (including vesicular scoria and dense lava fragments), and included depressions to represent impact craters. Figure 2 (left) shows the visible wavelength (true color) image of the laboratory lunar analog surface; the lunar soil simulant substrate is gray, basalt scoria is red to pink, and lava fragments are gray to black. A diurnal cycle was simulated with two 500-watt halogen lamps to illuminate and heat the analog surface over periods ranging from 1 to 8 hours (sunrise, lunar "day"), followed by lamp switch-off and 3 to 16 hours of darkness (sunset, lunar "night"). The percent area of basalt gravel, number of impact craters, and illumination angle were also varied over different data collection runs.

The FLIR camera recorded thermal infrared and co-registered visible wavelength imagery at 1-minute intervals during each data collection run. This allowed the team to observe qualitative variations in apparent thermal inertia—generally speaking, a measure of how quickly a given material heats up and subsequently cools down—related to the different analog materials, particle sizes, and illumination conditions, and provided confidence that the team could obtain similar data in the field. Figure 2 (right) shows a false-color thermal infrared image of the analog surface during heating. Relatively hot, low apparent thermal inertial surfaces appear bright yellow and cooler; high apparent thermal inertial surfaces appear dark orange to violet.

NASA conducted a field assessment with the FLIR camera at Colton Crater—located north of Flagstaff, Arizona—

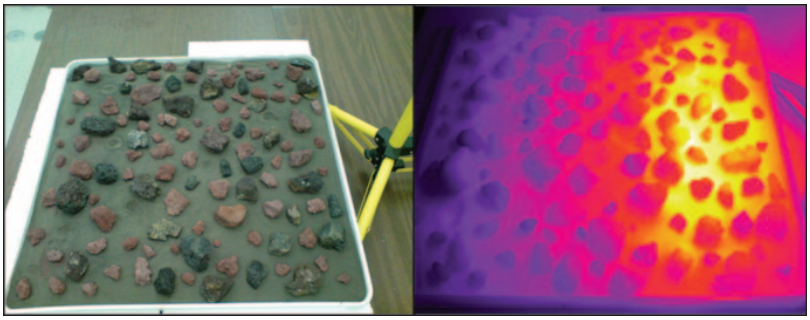


Fig. 2. *Visible image compared to simultaneous thermal infrared image in laboratory environment.*

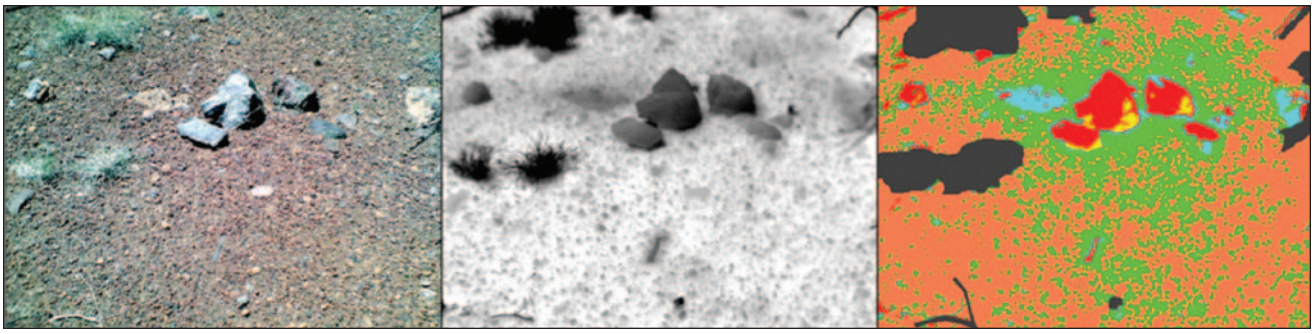


Fig. 3. *Forward-looking infrared field data comparison.*

following initial trials at Johnson Space Center's Planetary Analog Test Site or "rock yard." While this crater was formed from explosive volcanic processes rather than a meteor impact, its basaltic character, geomorphology, and ease of access made it an ideal lunar (and Martian) analog site for the study. Data collection occurred at, or shortly following, sunrise at several sites around and within the crater during the field assessment to maximize apparent thermal inertia contrast between different materials and surfaces—e.g., fine sediments on the crater floor and basaltic gravels and boulders; basaltic agglutinate (hot spatter deposits subsequently welded together) outcrop and surrounding soil, etc. The field data collection methodology was informed by the results of the laboratory analog study, resulting in approximately 4-hour collection runs with thermal infrared and visible imagery collected at 5-minute intervals.

Scientists then performed principal component analysis to extract the most correlated information from the field data, and to reduce noise. By applying both unsupervised and supervised image classification algorithms to the visible wavelength data, thermal infrared data, and fused visible + thermal infrared data, the team assessed the performance of these relatively simple classification approaches for different geological materials and surfaces in the field to simulate "on the fly" operations by crew members—i.e., without significant science backroom support and analysis.

Figure 3 illustrates imagery obtained in the field at Colton Crater. The left image shows a visible wavelength (true color) image and the center image shows the corresponding thermal infrared image. Relatively hot surfaces (indicating low apparent thermal inertia) are bright, and relatively cool surfaces (indicating high apparent thermal inertia) are dark in the center image. The right image shows a supervised classification of fused visible and thermal infrared data: red—basalt boulders; pink—basalt gravel; yellow—shadows; green—basalt agglutinate; blue—high albedo (high reflectance) materials; gray—masked vegetation, not classified.

The team anticipated mixed results from these initial tests. Performance with regard to discrimination of different types of geological materials at Colton Crater was generally poor, with a large variance in overall accuracy obtained using both unsupervised and supervised approaches (35% to 80%); the range of variance for individual class accuracy was similar. This is largely a result of the relatively limited spectral sampling obtained by the FLIR camera—red, green, and blue visible wavelengths, and a single broad thermal infrared band. In contrast, the classified FLIR camera data performed satisfactorily for determination of rock abundance compared with visual estimation in the field. These results suggest that current FLIR cameras would be a useful addition to a crew "tool kit" for geohazard and site suitability assessment, and suggest that further development of multispectral, microbolometer-based thermal infrared and visible wavelength imagers would produce a highly useful tool for crew field geology activities.

Microprobe Two-step Laser Mass Spectrometry Using Extreme Ultraviolet Photoionization: Analysis of Astromaterials

Simon J. Clemett, *Johnson Space Center*
Scott Messenger, *Johnson Space Center*

The human race has only just begun to take the first tentative steps toward interplanetary travel. Nevertheless, it is already possible to directly study, in the laboratory, fragments of the asteroid belt, the stuff from which comets are made, rocks from the surface of Mars, the wind from the sun, and—perhaps most remarkable of all—the dust that fills the void between the stars. These samples are brought by meteorites and interplanetary dust particles accreted by the Earth, and by the recent sample return missions—Genesis, Stardust, and Hayabusa. The laboratory study of these materials gives us a means of exploring the origin and evolution of the galaxy and the solar system.

Johnson Space Center's research in the Astromaterials Research and Exploration Science (ARES) Directorate focuses on the analysis of organic species in astromaterials. Organic matter is pervasive throughout the galaxy and solar system. Hundreds of organic molecules have been identified in interstellar clouds, primitive meteorites, and comets, and are formed by complex chemical processes in diverse environments.

Carbon is unique in its capacity to form hybridized molecular bonding orbitals and, thus, self-catenate. As a consequence, organic molecules take a staggering variety of forms; the number of organic compounds exceed those from all other elements combined. By virtue of this diverse chemistry, organic matter preserves a detailed record of its physical and chemical formation and subsequent alteration processes. By deciphering this record, light can be shed on interstellar chemical processes and conditions in the early solar system. However, these analyses present a number of significant challenges:

- Certain organic species may only be present in trace concentrations, parts per million or less.
- Organic matter may consist of complex mixtures containing hundreds or thousands of species.
- Samples are limited and/or extremely heterogeneous.
- Samples are unique and hence precious.

The ARES team has designed and constructed a unique microprobe two-step laser mass spectrometer (μ-L^{2}MS) to measure organic compounds with great sensitivity, selectivity, and spatial resolution (figure 1). A key feature of this instrument is that molecules are vaporized and ionized in two separate steps with independent laser sources. In the first step, a pulsed infrared laser is focused on the sample to cause rapid, localized heating. In the second step, a pulsed ultraviolet (UV) laser ionizes some of the molecules desorbed by the first laser. Which molecules

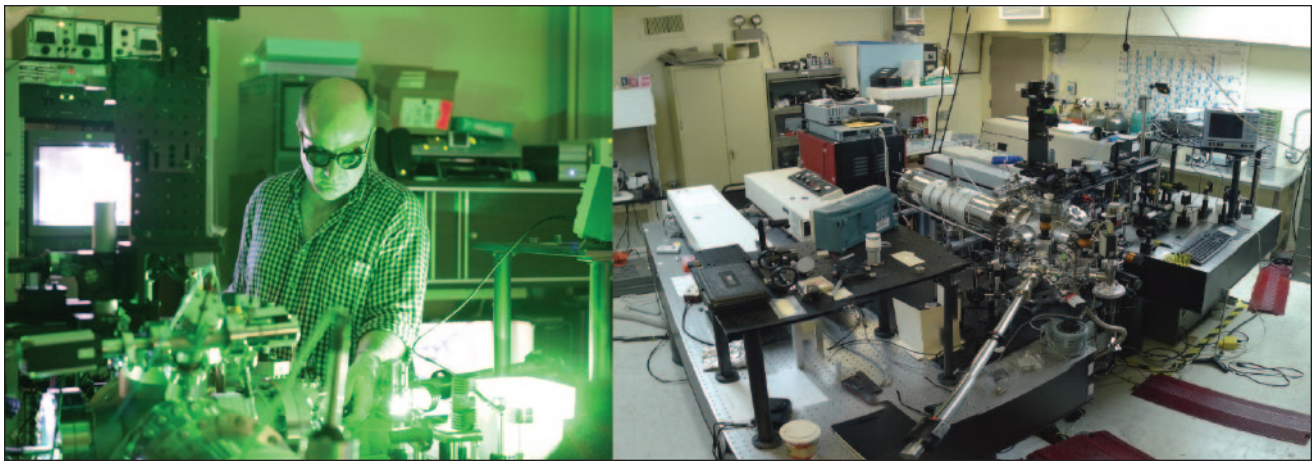


Fig. 1. *Astromaterials Research and Exploration Science microprobe two-step laser mass spectrometer (μ-L^{2}MS) laboratory.*

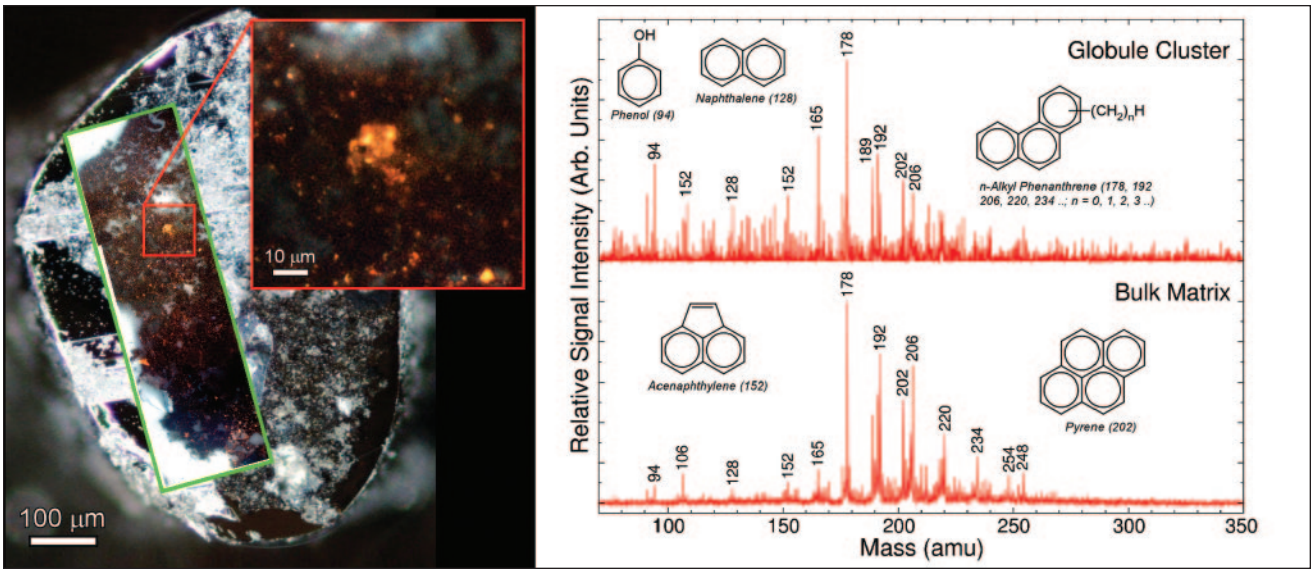


Fig. 2. *Microprobe two-step laser mass spectrometer (µ-L²MS) of a nanoglobules cluster in the Bells (CM2) chondrite. The left panel shows the optical image of the microtomed surface on which is overlaid a native fluorescence image in which a globule cluster is identified and shown magnified. In the right panel, the µ-L²MS spectra obtained on the globule cluster is compared to that of the averaged surface. While both globules and bulk organic composition share a similar distribution of multiply alkylated 3-4 ring polycyclic aromatic hydrocarbons, there is a distinct difference in their distributions of lower molecular weight (< 178 atomic mass unit) species.*

are ionized depends on their spectroscopic properties and the wavelength of the UV laser light. The resulting ions are then mass analyzed in a reflectron time-of-flight apparatus. The design of the instrument makes it possible to measure organic molecules intact, avoiding fragmentation in both the vaporization and ionization steps. Consequently, the µ-L²MS instrument can be used to analyze mixtures of molecules in complex materials without extraction, purification, or other complex sample preparation. Moreover, it is capable of micrometer spatial resolution so that the organic measurements can be correlated to mineralogical features of the sample.

The ARES team has analyzed organic matter in a wide range of astromaterials with the µ-L²MS instrument, including carbonaceous and ordinary chondrite meteorites, Martian meteorites, Antarctic micrometeorites, interplanetary dust particles, interstellar graphite grains, interstellar ice analogs, and Stardust cometary dust particles. For example, figure 2 illustrates the analysis of a cluster of organic nanoglobules embedded within the matrix of the Bells (CM2) chondrite. In work published by lead author Keiko Nakamura-Messenger, also of ARES, the work showed that these organic globules are older than the Earth and may have originated in a cold interstellar cloud.

A limitation of the µ-L²MS instrument has been that the range of organic compounds that could be studied has been restricted to species containing aromatic and/or conjugated functionalities. This is a consequence of the 1+1 Resonance Enhanced Multi-Photon Ionization (REMPI) process that was used. In this scheme, photoionization occurs through the successive absorption of two UV photons; absorption of the first photon causes excitation into a rovibrational manifold of the first electronic excited state, resonant adsorption of a second photon then leads to ionization. Using a 266 nanometer (nm) (~4.3 electron volt/photon [eV/photon]) UV laser source, the only

Microprobe Two-step Laser Mass Spectrometry Using Extreme Ultraviolet Photoionization: Analysis of Astromaterials

continued

accessible intermediate excited electronic state in organic molecules corresponds to a π-π* transition, hence the restriction to aromatic and/or conjugated species.

To expand the range of compounds that can be detected, the ARES team has developed and is currently incorporating a coherent vacuum ultraviolet, single-photon ionization source that will complement the team's existing μ-L^{2}MS capabilities (figure 3). The generation of coherent vacuum ultraviolet radiation is achieved by the nonlinear frequency tripling of the 3rd harmonic (λ 355 nm) of a mode-locked Q-switched picosecond neodymium: yttrium-aluminum-garnet (Nd:YAG) laser in a xenon-argon gas cell to produce 118.2 nm (~10.5 eV/photon) radiation. Efficient phase matching of 118.2 and 355 nm photons is possible due to the negative dispersion of xenon in the region 117.2 to 119.2 nm due to the 5p-5d electronic transition, allowing conversion efficiencies of approximately 0.01%. Since the first ionization potential for nearly all organic molecules lie in the range of 5 to 10 eV, effectively all organic species can be photoionized by such vacuum ultraviolet photons. Furthermore, this provides both an efficient and a "soft" ionization process comparable to that currently achievable with the team's (1+1) REMPI source. The team hopes that its new μ-L^{2}MS and its future successors will become another powerful instrument in the arsenal that astrochemists have for exploring and understanding the universe.

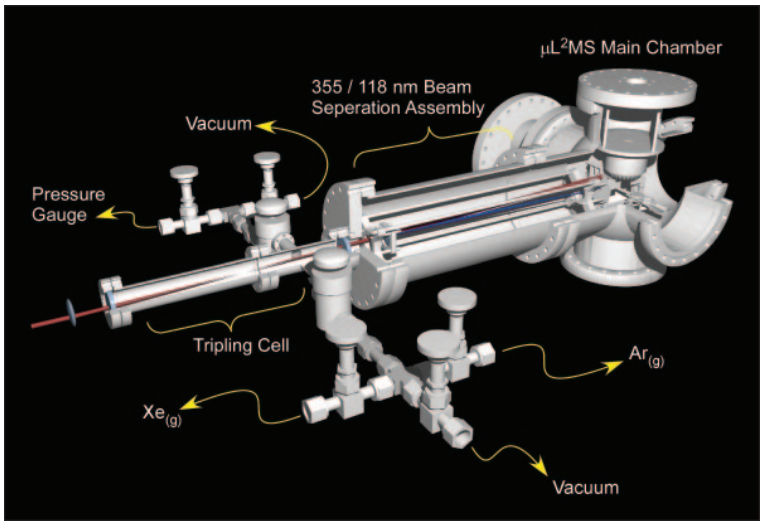


Fig. 3. *Ray-traced illustration of 3rd harmonic generator for production of 118.2 nm coherent radiation. Frequency tripling occurs within a low pressure xenon-argon gas cell at the beam waist of a focused 355 nm laser pulse. Separation of the 3rd harmonic from the fundamental is done in vacuo within the μ-L^{2}MS chamber using an off-axis plano-convex magnesium fluoride focusing lens.*

Recovery After Mishap—Salvaging Genesis Solar Wind Sample Science

Judith Allton, *Johnson Space Center*

The collectors returned by the Genesis mission contain solar wind atoms that can be analyzed in sophisticated laboratory instruments to measure, very precisely, the composition of the sun. Since the sun contains more than 99% of the mass in the solar system, knowing its elemental and isotopic composition is a good average measure of the composition of the solar nebula at the time when the planets were forming. Scientists already have rocks from the moon, Mars, and the asteroids and dust particles from comets. Genesis' solar data allow new insights into tracing the chemical evolution of diverse planetary samples, most of which came from a common starting material—the solar nebula. Separate collections were made of high-speed solar wind, coronal mass ejection solar wind, and interstream low-speed solar wind. Information from these different solar regimes adds to the understanding of solar physics (figure 1).

Genesis solar wind collectors are highly polished surfaces into which solar wind nuclei are implanted, typically 40 to 100 nanometers below the surface (figures 2 and 3).

The advantages of returning samples to the laboratory are many. State-of-the-art instrumentation can be used for analysis to very high precision, different techniques can be used to verify the same measurement, multiple teams can confirm or dispute the results, and evolving science questions can be addressed through new types of analyses. To this list of advantages of returned samples, add one more: recovery from mishaps is greatly enhanced.

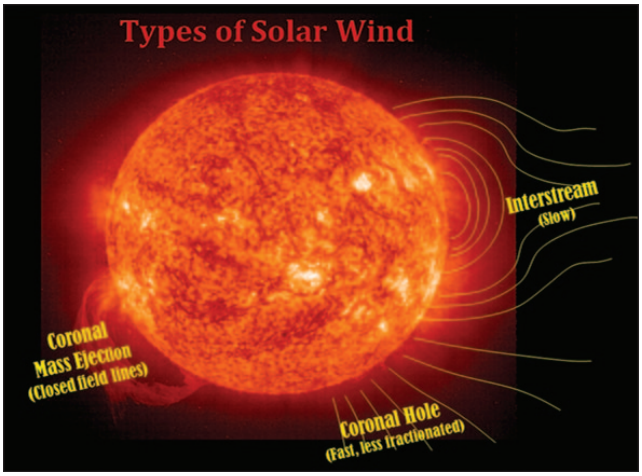


Fig. 1. *Genesis mission collected separately three regimes of the solar wind: interstream slow solar wind, coronal hole high-speed solar wind, and coronal mass ejection solar wind.*

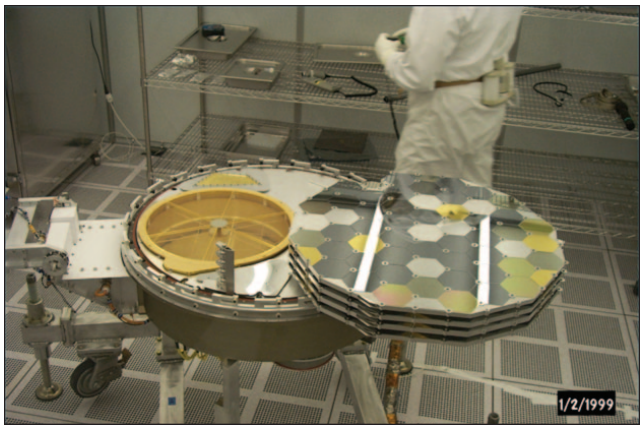


Fig. 2. *Hexagonal polished collectors of pure materials accumulated solar wind from three regimes over a 28-month period at the Earth-Sun L1 location.*

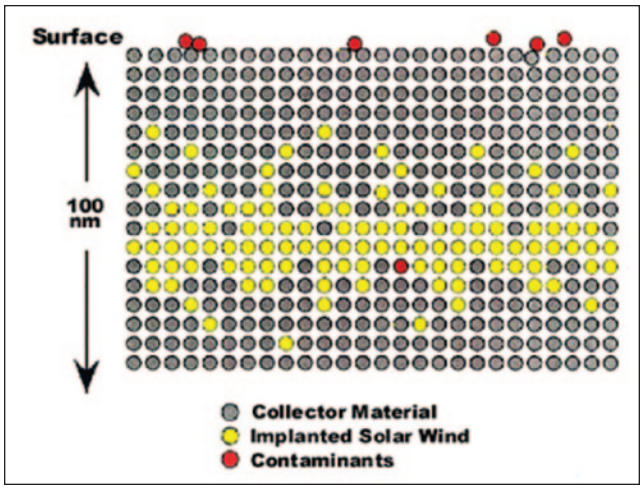


Fig. 3. *Solar wind nuclei are implanted just below the surface of the polished collectors.*

The Genesis mission was launched in August 2001, collected solar wind at the Earth-Sun L1 location for

28 months, and returned to Earth in September 2004. The parachute did not deploy, and the return capsule hit the ground at an estimated 300 kilometers per hour, which resulted in the collector canister breaking open and exposing the collectors to the environment. Many of the collectors were fragmented and contaminated with particulate debris and a molecular film.

Early Design Choices Proved Useful During Recovery

Because the analytical goals were challenging, the solar collectors were comprised of very pure, very clean materials, and assembled under International Organization for Standardization Class 4 conditions. Fifteen distinct materials were used for collectors, allowing overlap in analysis for specific elements on a variety of materials. Some materials survived the hard landing better than others. Sapphire-based collectors survived in larger pieces. Diamond surfaces were more resistant to scratching.

A variety of collector cleaning processes were tested to remove the contaminant particles and molecular film after return. Some collector materials proved more easily cleaned than others. Thus, the variety of collector materials not only provided an analytical redundancy, but also more options for cleaning the surface without disturbing the solar wind.

Flight-like collector reference materials were preserved. These specimens proved crucial as "blanks" for subtracting background components of measured parameters. These reference materials were also used in development of cleaning processes.

The thickness of the hexagonal solar collectors was unique for each solar wind regime: 700 micrometers (μm) for bulk solar wind, 650 μm for coronal mass ejection, 600 μm for high speed, and 550 μm for low speed. Since collectors were dislodged and fragmented on the hard landing, collector thickness is the only direct way to determine solar wind regime.

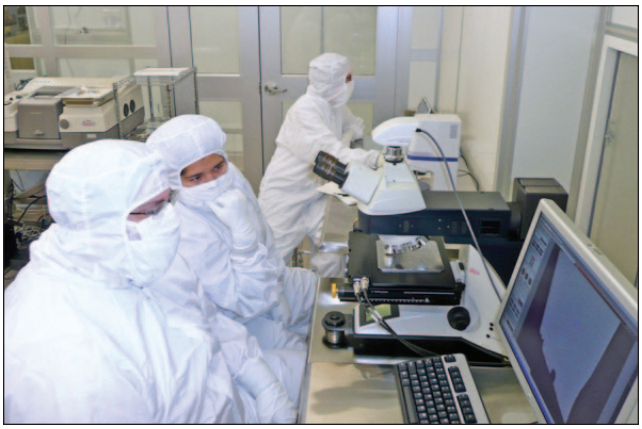


Fig. 4. *Recovered collector fragments are imaged and measured for the online catalog.*

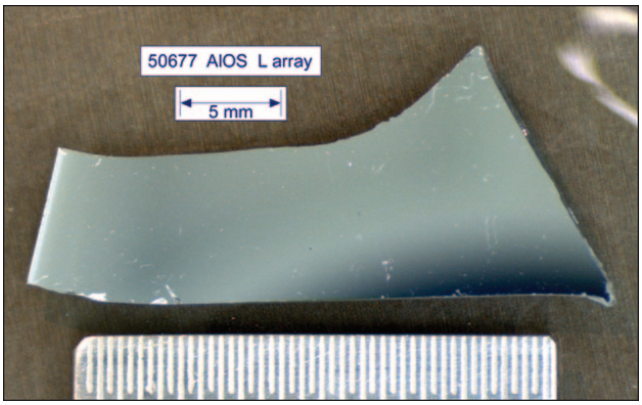


Fig. 5. *An example from the online catalog is this aluminum-on-sapphire sample.*

Characterization of Collector Fragments

Collector fragments can be easily identified by optical observation, except for silicon. The two types of silicon are crystals grown by different methods. They are distinguished by use of Fourier transform infrared spectroscopy to observe a carbon-oxygen bond, present only in silicon crystals grown by one method. A catalog of the collector fragments is available on the internet. The catalog contains an image, the material, the dimensions and

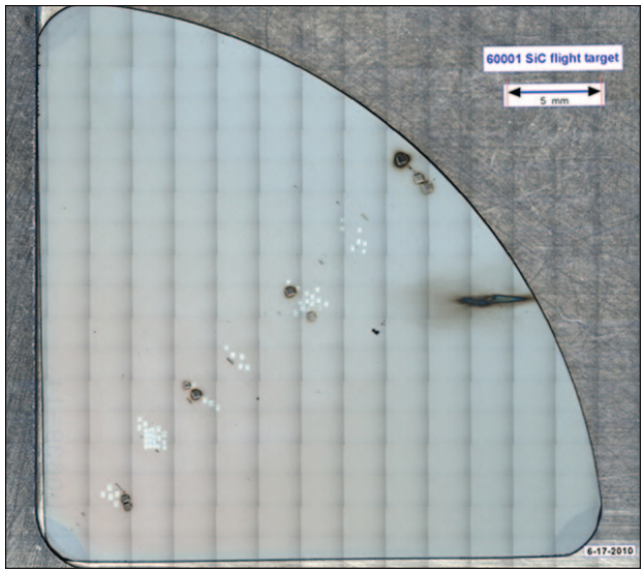


Fig. 6. *This mosaic image of a Genesis silicon carbide collector shows the effects of ion beam analyses by two science groups.*

area, the solar wind regime, and a qualitative assessment of surface condition (figures 4 and 5). Cataloging is an ongoing process with 1600 samples displayed as of 2011.

Cleaning of Collectors Fragments

Megasonically energized ultrapure water (UPW), which was successfully used to clean the payload prior to launch, was adapted to remove particulate contamination from solar wind collectors. The continuous flow process produces water of 18 megohm/centimeter resistivity (ionic concentrations in the low parts per trillion). A megasonic cleaning head was mounted to a single wafer spin processor to apply UPW cleaning to small, irregular collector fragments. In this configuration, a small collector fragment held by a vacuum chuck is spun up to 3000 rpm. Megasonically energized UPW is applied for 30 seconds to 15 minutes, depending on material. Extra spin time effectively dries the collector fragment. Particles greater than 5 µm are efficiently removed, leaving no solvent residue.

A commercial ultraviolet (UV) lamp device creates a UV ozone-cleaning atmosphere, which effectively removes the 5 nm film found on some collector fragments. Typical UV exposure times are 30 minutes.

Cleaning performed at Johnson Space Center (JSC) Genesis curation facility is first-order cleaning. Members of the science team have developed second-round cleaning with strong acids, such as hydrofluoric and aqua regia. JSC curation assists with documentation and logistics for this iterative process with the science community.

Science Results

Important science results are emerging from analysis of the Genesis solar wind samples. The science community is doing this challenging work on the 400 Genesis solar wind samples allocated for research purposes. Investigators have the capability to choose a measurement site on a given collector sample to avoid damaged areas and to make multiple analyses. Figure 6 shows a silicon carbide collector, which has been analyzed for two different elements by two different research groups. The number one and two science goals of determining the solar oxygen isotope and nitrogen isotope compositions have been published.

Advanced Cockpit Evaluation System—Display and Control Testing Using Small Radio-Controlled Based Analogs

Jeff Fox, *Johnson Space Center*
Mathew Hart, *Johnson Space Center*
Mike Goza, *Johnson Space Center*
Patrick Laport, *Johnson Space Center*
Jim Secor, *Johnson Space Center*
Christie Sauers, *Johnson Space Center*
Ray Heineman, *Johnson Space Center*
Chip Litaker, *Johnson Space Center*
John Crofford, *Johnson Space Center*

How can one test real-time commanded augmented reality display and control (D&C) concepts on the ground and in three-dimensional space quickly, routinely, and at low cost and risk? Use low-cost analogs such as small radio-controlled (RC) vehicles to move video and position sensors around, and to downlink the data to a wide-field-of-view mobile cockpit generating an "out-the-window" view. Also, control these vehicles in the RC realm, as any object controlled remotely from a closed cockpit could be 1.5 m (5 ft) away, and mimic one many thousands of miles away.

These concepts can obviously be tested on full-scale aircraft, but the cost and scheduling for such platforms do not allow for a rapid testing and turnaround of various D&C concepts. Using small, low-cost platforms operating in the RC realm make this rapid prototyping model much simpler.

Creative Resourcing

Other nontechnical—though no less important—aspect of the project's success was the partnering and reuse of assets. The team was able to compete for small innovation funding to construct an RC helicopter and associated sensor pallet; build a rover with education funds in exchange for doing student outreach; borrow and use the central processing units that drive Orion displays in a lab to drive the software in the Advanced Cockpit Evaluation System (ACES) remote cockpit; and to reuse the X-38 Remote Cockpit van and convert it to the ACES configuration. All of these methods represent creative ways to team across different organizations to achieve mutual goals through the sharing of assets.

Test Platform Overview

Basic elements of the ACES system were built/integrated over a 6-week period in the summer of 2011. The hardware includes a remote cockpit built into the back of a 15-passenger van, an RC helicopter, and a rover (RC rock crawler). The helicopter is flown in typical RC fashion using a standard transmitter. The outside line-of-sight safety/backup pilot performs the takeoffs and landings, and hands over control to the inside van operator who flies it to preselected points in the same way a shared "buddy" box transmitter is used to train a new RC pilot where the safety pilot can always assume control with the release of a single spring-loaded switch. The rover is controlled from inside the van using a standard RC controller. Both air and ground configurations are able to view video and navigation downlink from the sensor pallet. Video camera and attitude/position data are also downlinked to the van where it creates a natural out-the-window view in a multi-paneled wide-field-of-view cockpit. Although quite challenging, special attention was paid to deconflict and keep all frequencies in the unlicensed "free" band.

Additional details:

Van: GSA Ford E-350 15 Passenger Van (figure 1) with tow-behind trailer housing a 4-kilowatt generator, pilot seat, five wraparound liquid crystal display (LCD) displays, one downward-looking LCD display, joystick/



Fig. 1. *Advanced Cockpit Evaluation System Van (top), 5 panel wraparound displays (bottom).*

pedals, intercom, blacked-out windows, video receivers for four onboard video signals, telemetry receiver, and network of seven computers.

Sensor Pallet: A small carbon fiber pallet was built to house three forward-looking and one downward-looking low-cost color cameras that are linked to four video transmitters and downlinked to the van. A second set of low lux black-and-white cameras can be used for night flying. An attitude/position sensor is downlinked to the van, as well. The flexible mounting system allows for transfer of the pallet from the helicopter (air/three-dimensional based) to rover (ground/two-dimensional based) in just a couple minutes.

Helicopter: An electric T-REX 600 class helicopter (figure 2) was selected to keep vibration and noise to a minimum while keeping the operation simple by merely charging batteries. Typical flight times with up to a 3.6-kg (8-lb) payload are 6 to 7 minutes with a single battery and marginally longer with dual batteries. The helicopter is also equipped with a spare receiver to perform several other operations such as gimballing of the camera mount and activation of the subscale article release mechanism. A custom landing gear was built to accommodate the sensor platform.

Rover: A 1:5 scale rock crawler (rover) platform was selected to allow for sensor information to be downlinked to the van in times where testing is required, but the helicopter cannot be flown due to weather, pilot availability, etc. High-torque motors were selected to accommodate the sensor pallet and additional payloads in the 9- to 11-kg (20- to 25-lb) range, such as a robotic arm or additional sensors.

Planned and Potential Uses

Initial use of the ACES system included the test of augmented reality software through the blending of live images with synthetic obstructions and navigation information to help identify hazards in a pilot's flight path (figure 3). The other planned use was to fly the helicopter in such a way as to emulate a planetary lander. Integration of a processor and sensor hardware aboard the helicopter is in work to test automated rendezvous and docking



Fig. 2. *Helicopter (top), landing gear with dual-use sensor pallet (center), rover (bottom).*

Advanced Cockpit Evaluation System—Display and Control Testing Using Small Radio-Controlled Based Analogs

continued

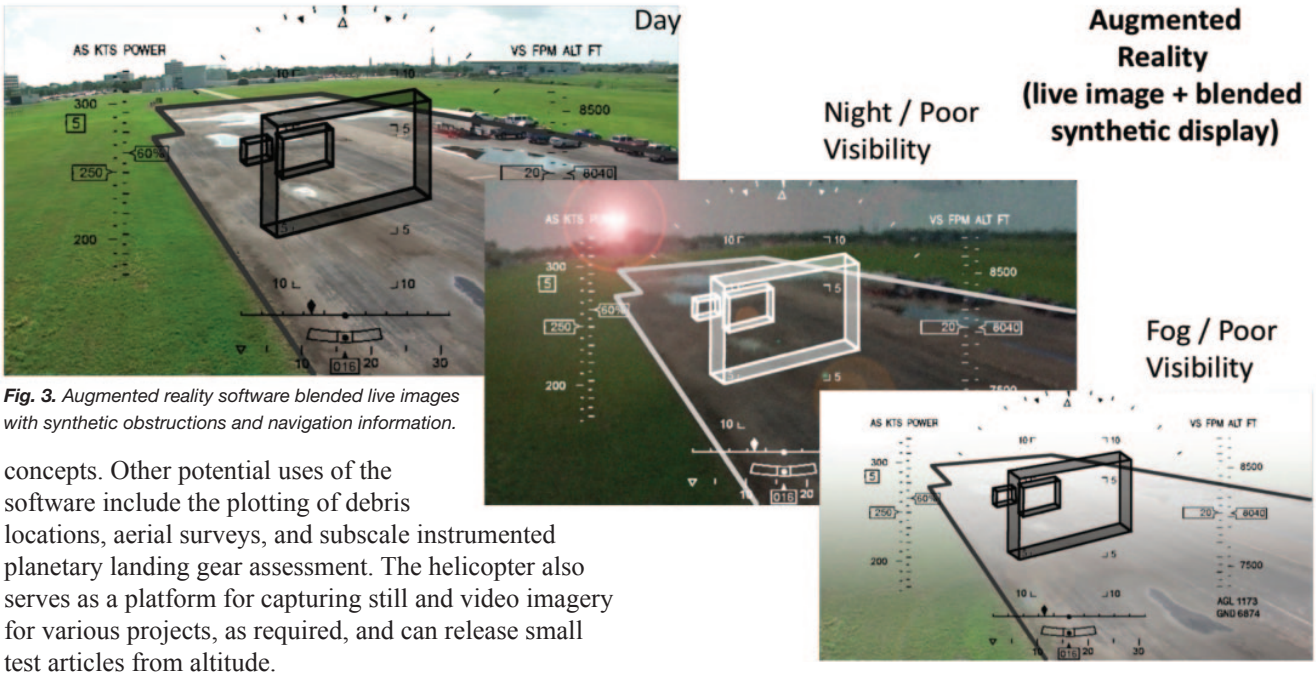


Fig. 3. *Augmented reality software blended live images with synthetic obstructions and navigation information.*

concepts. Other potential uses of the software include the plotting of debris locations, aerial surveys, and subscale instrumented planetary landing gear assessment. The helicopter also serves as a platform for capturing still and video imagery for various projects, as required, and can release small test articles from altitude.

Summary

This system represents a robust, flexible, hands-on D&C test platform. Engineers are encouraged to use its capabilities to supplement office design with "in-the-field" testing. Low-cost, rapid prototyping test platforms such as this provide another opportunity for risk mitigation and requirements refinement by identifying issues in the field with real hardware and software in the loop, which raises the "reality and criticality" factor, thus creating increased awareness of a system's operation.

The team purchased the helicopter and sensor system, and the team built, tested, and flew the system in just 6 weeks. Rapid flight tests at the rate of up to twice weekly followed. The low dollar and risk factor made this aggressive test program possible. All this was accomplished for approximately $5,500, roughly the cost of "1" hour of typical jet aircraft flight time.

The ACES assets are expanding to include an additional RC helicopter and RC fixed-wing aircraft, which will create new innovative test platforms and partnering opportunities. Work continues to complete integration of the augmented reality software.

Unmanned Microgravity Flight Program

Mathew Hart, *Johnson Space Center*
Mike Liable, *Johnson Space Center*
Jeff Fox, *Johnson Space Center*
Dave Bacque, *Johnson Space Center*
Lee Morin, *Johnson Space Center*
Dom Del Rosso, *Johnson Space Center*

Current microgravity facilities are limited to a maximum of 5 seconds, except for the full-scale microgravity aircraft. Envisioned here is a small, unmanned aircraft that could fly 3.6- to 4.5-kg (8- to 10-lb) payloads in reduced-gravity trajectories for 12 to 15 seconds at a cost competitive to operating a drop tower. Lunar or Martian gravity profiles would also be targeted.

Initial Testing

Existing small, radio-controlled planes were equipped with accelerometers as an initial feasibility test and to identify areas of development (figure 1). The test data showed that even without telemetry, the pilot was able to fly parabolas "blind" and achieve +/- 0.1 g. The data also confirmed the need for an onboard computer and sensors to smooth out the remaining vibration.

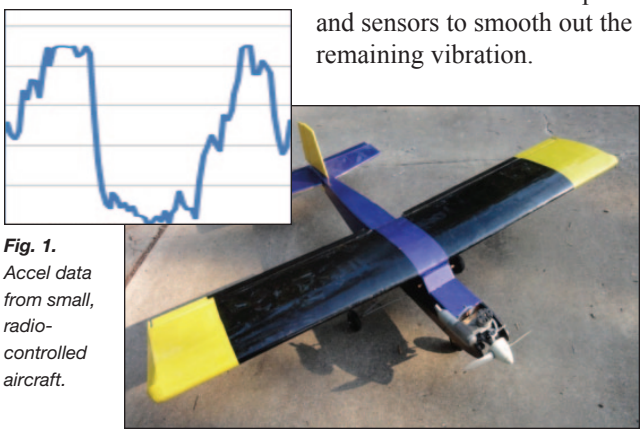


Fig. 1. *Accel data from small, radio-controlled aircraft.*

Airframe and Powerplant Selection

A study conducted by the European Space Agency (ESA) in 1995 provided useful recommendations and concluded that improved autopilots and powerplants, particularly a gas turbine, would be best suited for this type of mission, but were not readily available and/or cost-effective at that time. Fast forward 16 years, and a range of sensors and powerplants to test the feasibility have surfaced. To achieve the desired time in microgravity, projectile motion equations gave a vehicle speed of 305 km/hour (190 miles/hour). This resulted in gas turbines being the most viable powerplant option. A swept-wing design, retractable landing gear, autopilot, and large ruggedized airframe



Fig. 2. *DV8R "unmanned microgravity flight platform."*

were selected on merit and budget, and aligned with ESA's recommendations. Ultimately, a TroyBuilt DV8R aircraft was selected and modified to accept an oversized KingTech K-170E gas turbine engine per the manufacturer's recommendation (figure 2). The aircraft has a wingspan of 210 cm (83 in.), length of 221 cm (87 in.), and a dry weight of 10 kg (22 lbs). The turbine weighs 1.6 kg (3.5 lbs) and produces 40 lbs of thrust at 123,000 rpm with an exhaust gas temperature of 700°C (1292°F). The engine runs on a mixture of Jet-A1 fuel and turbine oil.

Modifications

In addition to being modified to accept the larger turbine, several changes were made to the airframe. The landing gear hardpoints were reinforced to accept the heavier landing weights. All control surface hinges were reinforced and sealed to handle the expected high airspeeds. A more elaborate fuel delivery system was installed to deliver fuel to the turbine under microgravity conditions. A fully redundant flight control system was added to increase fault tolerance of the aircraft. Finally, the airframe was modified and aircraft systems were relocated to provide an internal volume



Fig. 3. *Payload module.*

Unmanned Microgravity Flight Program

continued

that could accept a payload module (figure 3). The payload module (approximately the size of a shoebox) carries with it a 1080p digital video camera and light-emitting diode light to film experiments. Future payload modules could be custom built per the investigator's needs.

Autopilot

The need for a custom autopilot was anticipated. To save on development labor, a commercial off-the-shelf, open-source autopilot was selected (figure 4). The existing software would be sufficient for early phases of operation, while the open-source software could freely be modified for follow-on phases. The autopilot collects data from accelerometers, gyroscopes, a barometric altimeter, Global Positioning System receiver, magnetometer, and pitot-static pressure sensor. A separate microprocessor with watchdog reboots the primary processor in error scenarios. Data from the array of sensors are downlinked on a 900-MHz telemetry radio to drive cockpit instruments (including a g-meter) on the ground. As an added benefit, the autopilot supports a hardware-in-the-loop computer simulation to support development and testing of flight algorithms prior to any flight tests.

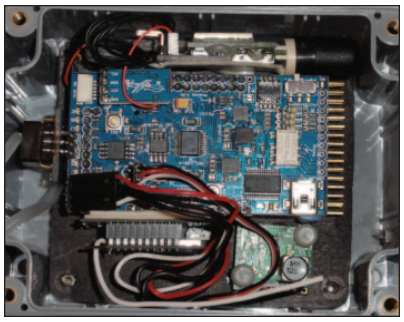


Fig. 4. *Autopilot/sensor suite.*

Phases of Operation

The flight test program is divided into three incremental phases of operation. In Phase I, the autopilot is downlinking telemetry, but it is not part of the flight control system. The aircraft is piloted manually according to flight instruments driven by downlink. A virtual cockpit with wraparound displays can give the pilot a point-of-view from the aircraft and display live flight instruments (figure 5). Phase II puts the autopilot in the flight control loops only for the roll and yaw axes to provide stability and to offload the pilot, allowing him or her to concentrate solely on flying the parabola via power and pitch modulation. Phase III gives the autopilot control of all axes while the pilot monitors, and can take control at any time. Phase III is expected to give the best results as the onboard autopilot will be able to compensate for local disturbances. Hardware simulations will be incorporated into all phases of operation.



Fig. 5. *Advanced Cockpit Evaluation System van wraparound display system.*

Flight Envelope Expansion

Because increasing microgravity time involves flying higher and faster, an incremental approach to increasing the safe flight envelope is desired. The versatility of the onboard computer makes it easy to add strain gauges to key aircraft components, such as the main wing spar, and downlink strain data live during flight. Such data could be compared to data from a failure-tested wing to determine definitive limits for speed and g-loading for this particular aircraft.

Conclusion

The aircraft is currently in the process of obtaining a flight clearance. Once granted, the plan is to progressively work through test Phases I, II, and III. This platform has interesting applications not only for science and engineering research, but also for public outreach and education. More experiments can be flown at a faster pace than with a human-rated aircraft. Less oversight is required for potentially dangerous payloads, such as those involving combustion. The aircraft is only limited by the size of the flight area and altitude, as determined by the parabola times needed. This opens up increased flight areas and flying out of remote venues can be considered.

Flammability and Explosive Technologies



New Ignition Mechanism in Oxygen-enriched Environment: Spontaneous Combustion

Joel M. Stoltzfus, *White Sands Test Facility*
Timothy D. Gallus, *White Sands Test Facility*

After a fire occurred overseas in an Expeditionary Deployable Oxygen Concentration System (EDOCS) unit used by the U.S. Air Force, the NASA Johnson Space Center's White Sands Test Facility (WSTF) Oxygen Group was requested to perform a failure analysis to determine the fire's cause. The EDOCS is a portable oxygen concentration system used to supply concentrated oxygen for medical purposes.

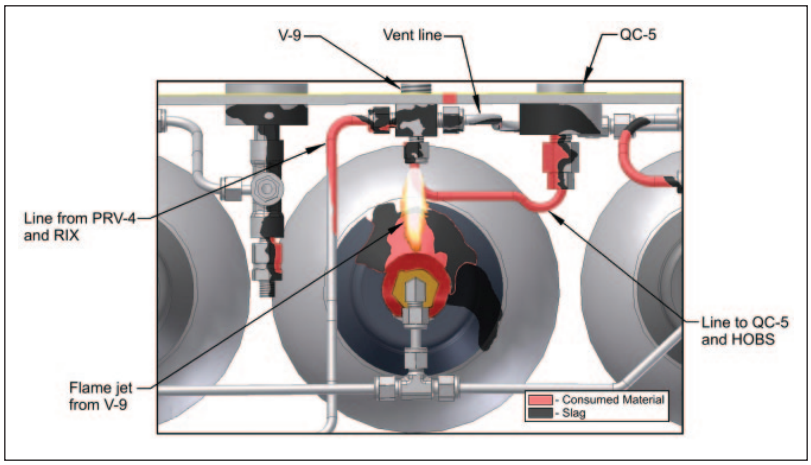


Fig. 1. *Flame jet from V-9 impinging on carbon steel cylinder u-bolt and cap.*

The failure analysis performed at WSTF ruled out all currently understood ignition methods as the cause of the fire. Instead, through inspection and analysis, the WSTF Oxygen Group determined a newly observed ignition mechanism most likely caused the fire event: spontaneous combustion. With results from the failure analysis, the group surmised that a leak of high-pressure, oxygen-enriched gas across the silicone-lubricated, polytetrafluoroethylene (PTFE)-encapsulated seat or ball of the V-9 (figure 1) valve was the initiating cause of the fire that subsequently burned through the downstream 90-deg bend in the 0.64-cm- (0.25-in.)-diameter stainless steel hardline. It was concluded that the fire jet from the burned hardline impinged the nearby cylinder containing oxygen-enriched gas near its top, igniting the carbon steel (figure 1). Oxygen rushing from the burned hardline fed the burning stainless steel until it failed, causing the release of its contents in a sudden, destructive flame jet that damaged many nearby components in the oxygen system.

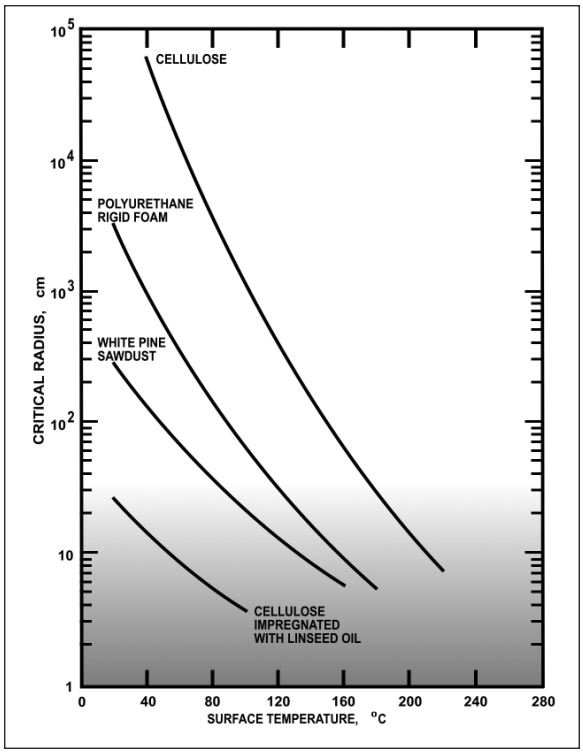


Fig. 2. *Critical radius of oil-soaked cellulose particles as a function of surface temperature in air.*

During the investigation, the group observed cellulose fibers in a 0.64-cm (0.25-in.) hardline in the system upstream of V-9. It was apparent that the hardline had not been properly de-burred during manufacture and that the cellulose fibers were snared in the stainless steel burrs formed during cutting of the tubing. It is surmised that cellulose particles accumulated near the leak path in V-9 between the PTFE capsule and ball, and were soaked with silicone-based lubricant. The result of accumulations of cellulose particle and fiber material being coated with silicone oil

New Ignition Mechanism in Oxygen-enriched Environment: Spontaneous Combustion

continued

in pressurized oxygen-enriched gas was to decrease their ignition temperature as the size of the accumulation grew. If the accumulation of silicone-soaked cellulose particles reached a critical diameter of 0.08 cm (0.32 in.), the particles could spontaneously ignite with no external energy input. If the accumulation were of a smaller diameter, then energy from one of the other heat sources present during system operation would be needed to raise the cellulose contaminant to its ignition temperature.

The autoignition temperature of an accumulation of cellulose fibers and particles is dramatically affected by the radius of the deposit of particles. Oil-impregnated cellulose will ignite in air at 100°C (212°F) if the radius of the accumulated deposit of particles reaches 4 cm (1.6 in.) (figure 2). If it is assumed that the critical diameter decreases directly as a function of the oxygen concentration, then the critical radius in 95% oxygen at 2200 psi would be [4 cm x (14.7 psi/2200 psi) x (21% oxygen/95% oxygen) =] 0.006 cm (0.002 in.). In addition, it is observed that if the diameter of the accumulated deposit of cellulose particles is increased to [27 cm x (14.7 psi/2200 psi) x (21% oxygen/95% oxygen) =] 0.04 cm (0.016 in.), then the autoignition temperature of the oil-soaked cellulose is 20°C (68°F).

In the EDOCS fire, it is surmised that cellulose particles accumulated between the PTFE seat capsule packing and the stainless steel seat or ball and reached the critical diameter that would cause spontaneous ignition of the particles. It is postulated that the burning cellulose particles ignited the PTFE seat packing and burned downstream to the edge of the stainless steel seat or ball. As the flame impinged the sharp corner of the stainless steel seat or ball, it was ignited (Location A in figure 3). The burning proceeded downstream, out of V-9, into the connecting stainless steel tube and out through the 90-deg bend, producing the flame jet seen in figure 1.

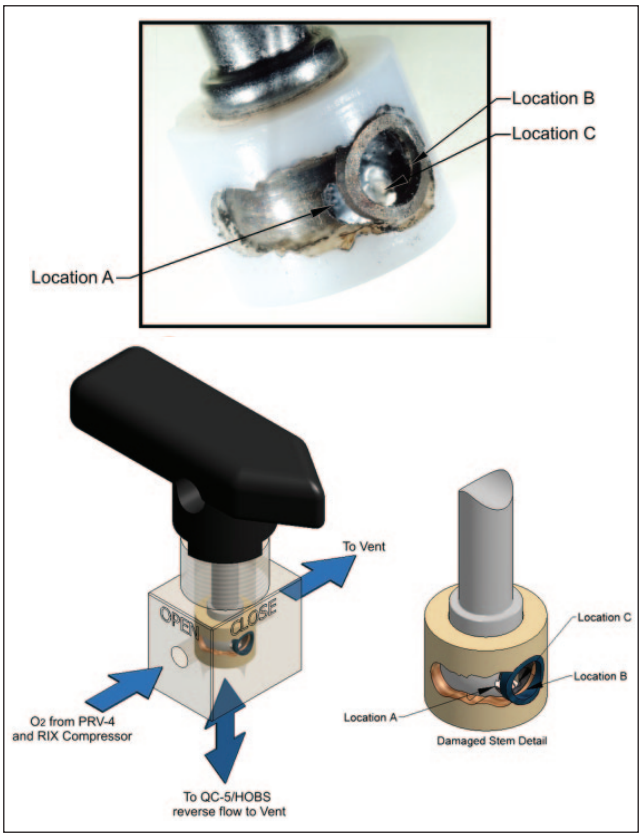


Fig. 3. *Damaged stainless steel valve stem/polytetraflourethylene capsule seat packing from V-9. (See Location A.)*

In conclusion, a previously unobserved ignition mechanism in oxygen-enriched environments has been postulated as the best explanation of a fire in a pressurized system. Of all the possible ignition mechanisms, spontaneous combustion of silicone oil-soaked cellulose particles in a leaking valve is the most likely to have caused the fire. As funding becomes available, the WSTF Oxygen Group will develop a test to recreate and validate this proposed ignition scenario. Data from this test will enhance designers' ability to control fire hazards in oxygen-enriched environments.

Novel Ignition Promoter for Investigation of the High-pressure Oxygen Generator Assembly Fire-containment Capability

Timothy D. Gallus, *White Sands Test Facility*
Dax L. Rios, *White Sands Test Facility*

The possibility of a fire within a high-pressure oxygen generator assembly (HPOGA) creates critical safety issues when the HPOGA is to be used on the International Space Station. An investigation was therefore needed to determine whether a properly designed, constructed, equipped, and aligned HPOGA could contain a fire indefinitely, preventing an over-board pressure release from endangering lives and causing catastrophic structural failure.

The HPOGA is a high differential pressure cell stack assembly consisting of a hydrogen end assembly, an oxygen end assembly, and alternating layers or bipolar plate assemblies as well as membrane and electrode assemblies sandwiched between a stack compression system. The stack compression system maintains sufficient compressive load on the cell stack hardware to ensure the mechanical and electrical integrity of the assembly is maintained up to the maximum design operating pressure of 3000 psig. Personnel at NASA's White Sands Test Facility constructed several mock-ups of varying fidelity, including a complete HPOGA, in order to study the ability of an HPOGA wall to contain a fire (figure 1). This would either validate or disprove the hypothesis that the oxygen inventory was sufficiently limited to ensure that a membrane breach-initiated fire would extinguish before a burnout could occur.

Arc starting is a convenient way to ignite metals because measurement of the deposited energy is simple and accurate. Two mock-up test articles were manufactured for the testing process to develop an appropriate electrical arc ignition method to initiate a fire at the pressure containment wall in high-pressure oxygen. The design allowed for electrical arc current to be delivered through a stainless steel probe with a niobium tip to the inner wall of the niobium foil laminate assembly shown as the porous plate frame in figure 1.

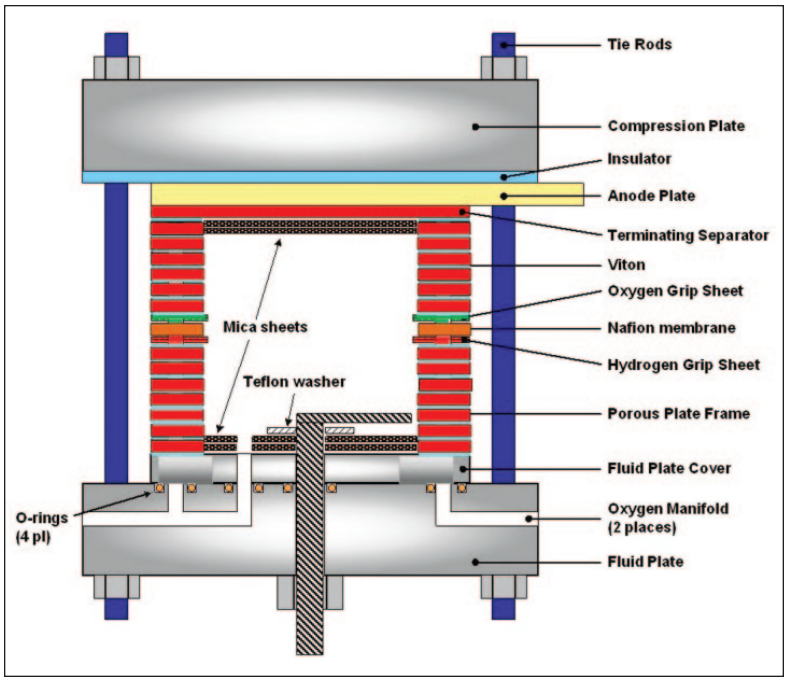


Fig. 1. *Test article to be ignited inside by welder arc.*

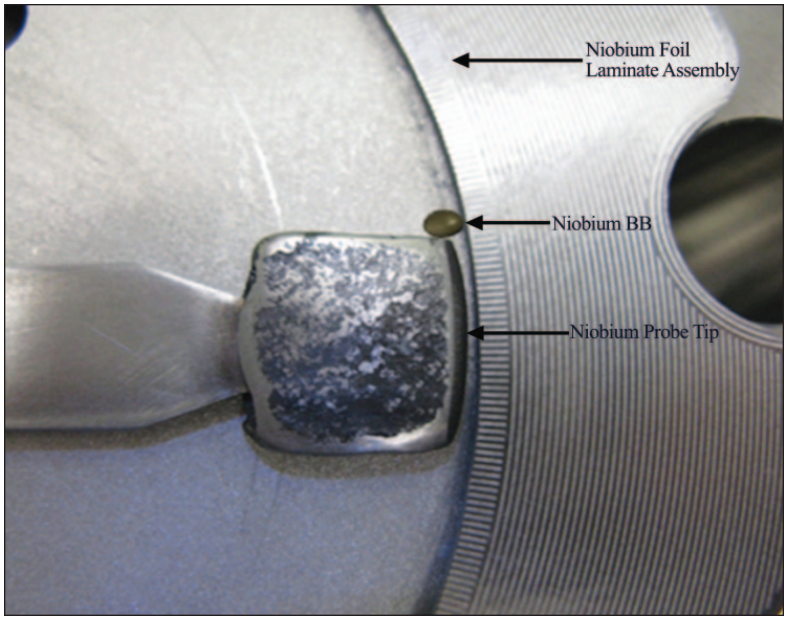


Fig. 2. *Niobium BBs added to bridge the arc gap.*

Novel Ignition Promoter for Investigation of the High-pressure Oxygen Generator Assembly Fire-containment Capability

continued

During checkout testing, researchers discovered that the insulating properties of high-pressure oxygen were greater than anticipated. While the high-frequency generator was able to pierce oxide coatings in 3000-psig oxygen, it was unable to produce a sufficient overvoltage to allow an arc to be established across the 1.5-mm gap to the laminate assembly. After numerous unsuccessful attempts to adjust the intensity of the high-frequency arc, oxygen pressure was reduced incrementally to determine the breakdown threshold. Arc initiation in oxygen occurred only below a pressure of 200 psig. Above 200 psig, the arc would not jump the gap. A solid niobium BB was applied to the test article to reduce the gap between the probe and the cell frames, but this proved inconsistent at establishing the electrical arc at the wall of the laminate assembly (figure 2). A BB-sized piece of fine niobium turnings was used next. That niobium wool was ignited and had the power to kindle to the niobium probe tip and the laminate assembly (figure 3).

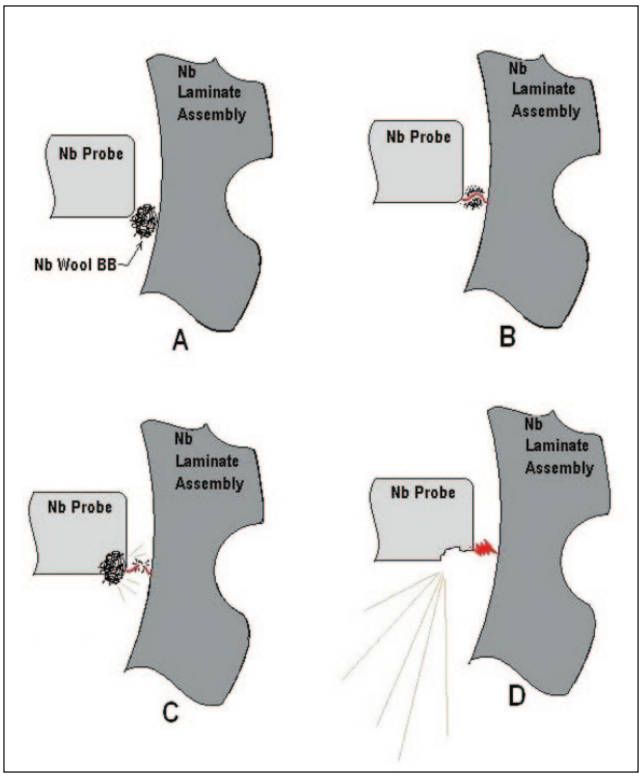


Fig. 3. *Sequence of fire propagation in test series.*

Conclusions

High-pressure oxygen is an efficient electrical insulator. When the oxygen pressure is more than 200 psig, arcs could not be initiated using a high-frequency arc starter alone. A combination of niobium wool and a high-frequency start was necessary to initiate a fire in the probe tip and laminate assembly.

The selection of niobium to make the wool did not change the combustion chemistry of the niobium probe tip or the laminate assembly.

The NASA Johnson Space Center's White Sands Test Facility mock-up provided a reasonable simulation of a fire in a real HPOGA unit because the niobium wool approximated the density of the porous niobium supports used in a true HPOGA.

Three-dimensional Modeling Assists in Investigation of Fires in Oxygen-enriched Environments

Dax L. Rios, *White Sands Test Facility*
Kyle M. Sparks, *White Sands Test Facility*
Stephen F. Peralta, *White Sands Test Facility*

After an Expeditionary Deployable Oxygen Concentration System (EDOCS) unit used by the U.S. Air Force experienced an oxygen fire on May 24, 2009, the NASA Johnson Space Center White Sands Test Facility (WSTF) was asked to perform a failure analysis to determine the cause of the fire. The EDOCS unit is a portable oxygen concentration system used to supply concentrated oxygen for medical purposes. The EDOCS module generates oxygen using vacuum swing adsorption technology. The EDOCS-120B concentrator generates 120 liters per minute at 551.6 kPa (80 psi). The oxygen can be delivered directly from the concentrator to the hospital distribution system at 551.6 kPa (80 psi) and/or supplied to the boost compressor. The built-in boost compresses the gas to 15 513.2 kPa (2250 psi) to allow for filling standard medical oxygen cylinders using a cylinder-filling manifold. A vacuum pump is included with the EDOCS to evacuate cylinders prior to filling.

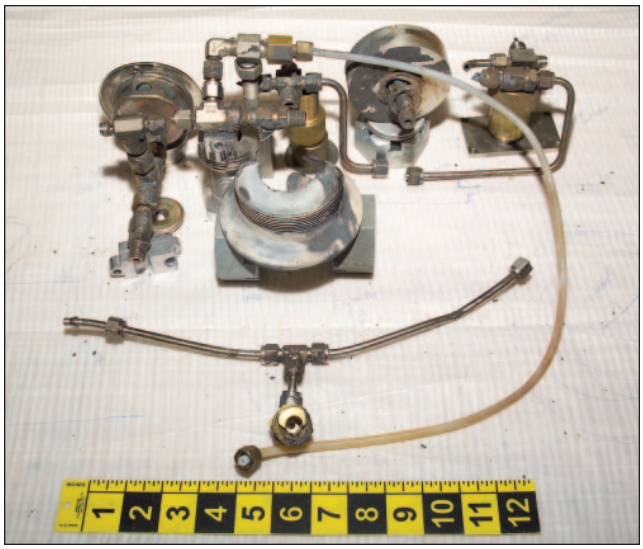


Fig. 1. *Damaged parts in pre-fire arrangement.*

Since the fire incident occurred overseas, only portions of the damaged EDOCS were shipped to WSTF. The WSTF Oxygen Group, using photographs and witness reports as guides, arranged the damaged parts from the system into the original configuration at the time of the fire (figure 1). When reconstructing damaged parts, clues to the cause of a fire are not always obvious, as was the case in the EDOCS failure investigation. After performing a detailed inspection and chemical analysis of the damaged EDOCS parts and evaluating every possible ignition mechanism that could have led to the fire, a model was needed to reconstruct the EDOCS system and compare the damaged system to that of the undamaged, pre-fire system. The fire scenario at this point in the failure investigation was still not clear. While significant damage on the neck of the M-Bottle drew a lot of attention, it lacked some of the characteristic elements for an ignition to occur at that location. Creating computer-aided three-dimensional (3-D) models allowed the WSTF Oxygen Group to compare the two models (pre- and post-fire) to investigate the failure and postulate the most probable ignition and burning scenario (figures 2 and 3). The 3-D models were created from measurements and photographs taken to estimate component sizes and locations. Modeling helps explain how the fire scenario was possible, telling the story of the fire by overlaying the damaged component with an undamaged component.

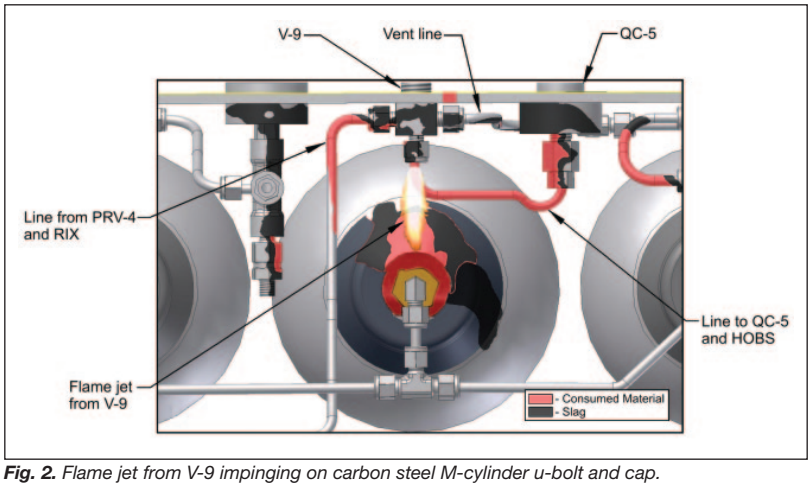


Fig. 2. *Flame jet from V-9 impinging on carbon steel M-cylinder u-bolt and cap.*

The WSTF Oxygen Group examined, in detail, all damaged components. The group concluded that while the components that did not contain high-pressure, oxygen-enriched gas at the time of the fire had been damaged in the fire, these components were not part of the causal

Three-dimensional Modeling Assists in Investigation of Fires in Oxygen-enriched Environments

continued

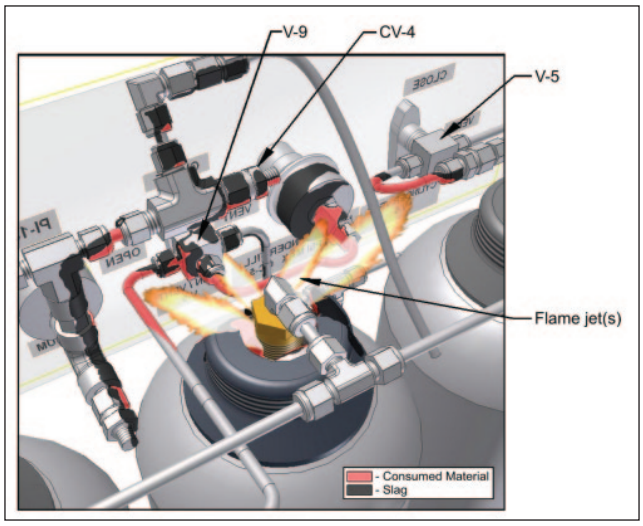


Fig. 3. *3-D illustration used to reconstruct fire scenario.*

chain. The components that had high pressure in them at the time of the fire included the inlet to V-9, which was pressurized at the inlet to 15 168.5 kPa (2200 psi). The V-9 was inspected visually using a 20´ power stereo microscope. Damage was observed both internally and externally. Disassembly of the valve revealed extensive internal damage to the valve-stem/capsule-seat assembly. Photographs demonstrated the fire damage, which could then be explained using the 3-D models (figure 4).

The modeling of V-9 told the fire scenario story by showing the flow paths through the damaged component. This V-9 model also led to the discovery that the valve was configured incorrectly, which made it more likely a leak across the seat had occurred and was a contributing factor to this incident.

Through inspection and analysis, the WSTF Oxygen Group determined a "most likely" cause of the EDOCS fire event. The group surmised that a leak of high-pressure, oxygen-enriched gas across the silicone-lubricated, polytetrafluoroethylene-encapsulated seat of V-9 was the initiating cause of the fire that subsequently burned through the downstream 90-deg bend in the 0.64-cm (0.25-in.)-diameter stainless-steel hardline. The group concluded that the fire jet from the burned hardline impinged the carbon steel M-cylinder near its top, igniting the carbon steel.

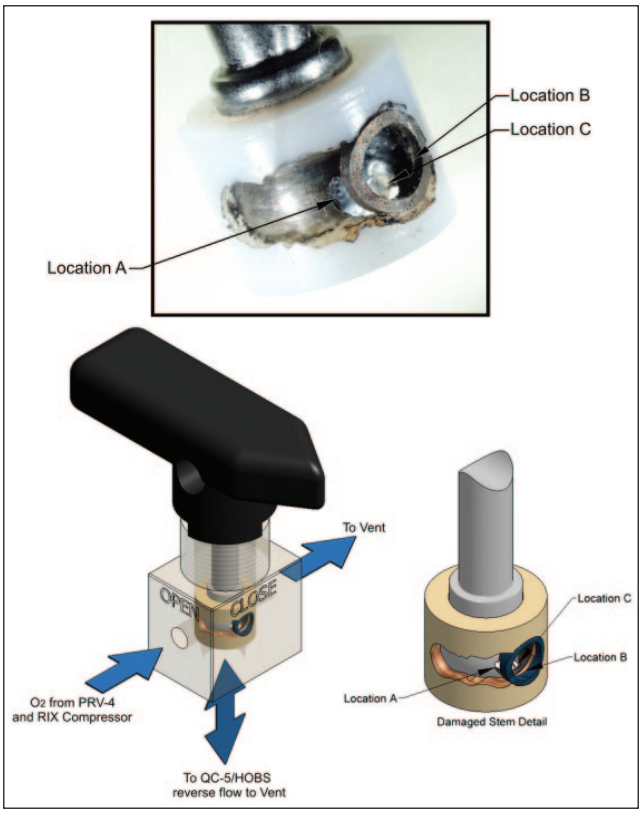


Fig. 4. *Fire damage evidence from photos explained through 3-D models.*

Oxygen rushing from the burned hardline fed the burning stainless steel until the stainless steel failed, causing the release of its contents in a sudden, destructive flame jet that damaged nearby low-pressure or unpressurized components in the oxygen system. A small flame jet from V-9 torched the M-Bottle, which, in turn, caused a lot more damage to the surrounding components.

This failure analysis was effective in determining the cause of the fire—in large part due to available 3-D modeling technology. Without modeling, the cause of the fire would probably have been undetermined, inconclusive, or possibly misidentified. But, because of the 3-D modeling, the most prevalent fire scenario stood out from the rest. As a result of the fire investigation findings, the WSTF Oxygen Group was able to make recommendations to prevent a similar fire from occurring in the future.

Spectroscopic Determination of Trace Contaminants in High-purity Oxygen

Steven D. Hornung, *White Sands Test Facility*

Oxygen used for extravehicular activities (EVAs) must be free of contaminants because a difference in a few tenths of a percent of argon or nitrogen content can significantly reduce available EVA time. These inert gases build up in the extravehicular mobility unit because the gases are not metabolized or scrubbed from the atmosphere. Measurement of oxygen purity above 99.5% is problematic; currently, only instruments such as gas chromatographs or mass spectrometers are used to make these determinations. Because liquid oxygen boil-off from the space shuttle will no longer be available to supply oxygen for EVA use, other concepts are being developed to produce and validate high-purity oxygen from cabin air onboard the International Space Station.

Personnel at NASA Johnson Space Center's White Sands Test Facility developed a prototype optical emission technique capable of detecting argon and nitrogen below 0.1% in oxygen. A glow discharge in reduced-pressure gas is used to produce atomic emission from the species present. Because the atomic emission lines from oxygen, nitrogen, and argon are discrete and, in many cases, well separated, trace amounts of argon and nitrogen can be detected in the ultraviolet and visible spectrum.

A glow discharge is plasma formed in a low-pressure (1- to 10-Torr) gas cell between two electrodes. Depending on the configuration, voltages ranging from 200 V and above are required to sustain the discharge. The gas is ionized in the discharge region, and a certain population is in the excited state. Light is produced by transitions from the excited states formed in the plasma to the ground state. The spectrum consists of discrete, narrow-emission lines for the atomic species and broader peaks that may appear as a manifold for molecular species such as oxygen and nitrogen, the wavelengths and intensities of which are a characteristic of each atom. Glow discharge spectra of oxygen, nitrogen, and argon are shown in figure 1. In a mixture of gases at a fixed pressure, the intensity of lines in the spectrum depends on the concentration of gas, total pressure of the system, and discharge current through the plasma.

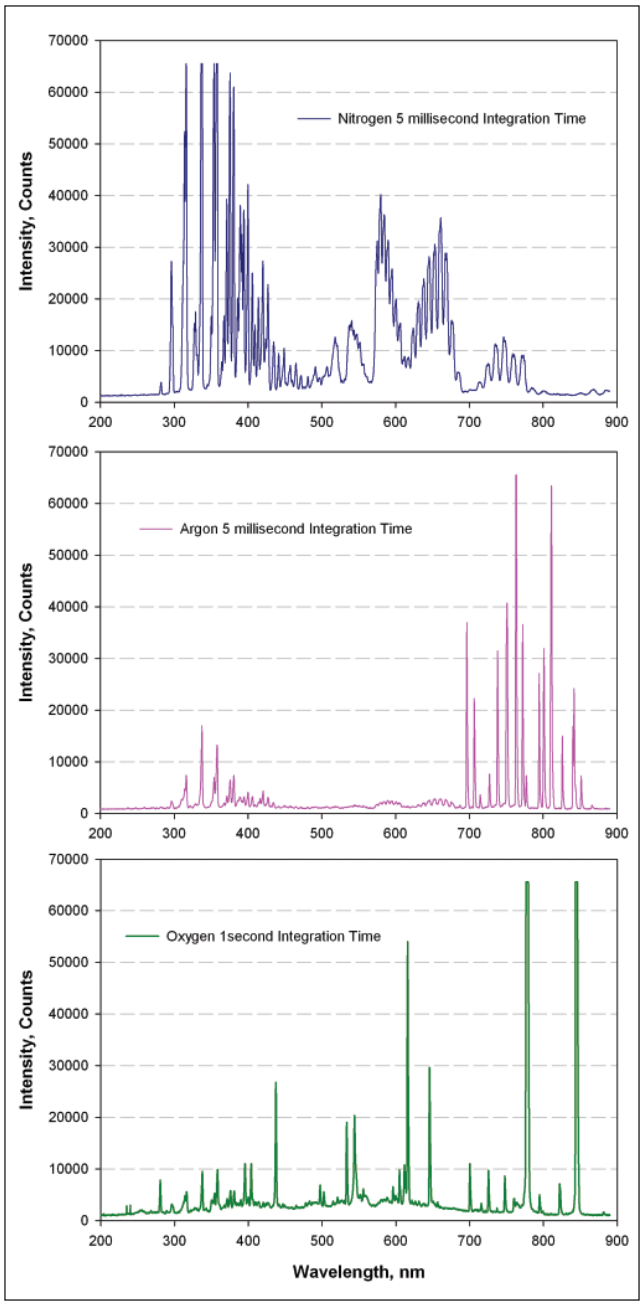


Fig. 1. *Reference glow discharge emission spectra for pure nitrogen, argon, and oxygen taken at 1.3 Torr.*

Spectroscopic Determination of Trace Contaminants in High-purity Oxygen

continued

The prototype optical emission system (figure 2) uses a quartz capillary tube with stainless-steel end fittings to form the glow discharge tube. The sample gas is introduced into the glow discharge cell using an adjustable vacuum leak valve. From the glow discharge cell, the sample gas passes a vacuum gauge, the downstream valve, and then the vacuum pump. During operation, the pressure in the glow discharge cell is maintained between 0.5 and 10 Torr using the adjustable leak valve and the downstream valve. In proof-of-concept testing, the discharge power was supplied by a 5-kV AC [alternating current], 10-mA power supply. Light from the discharge is collected by a lens and coupled to a ultraviolet-visible fiber-optic cable. This cable directs the light from the glow discharge into a spectrometer. The spectrometer detects in the 200- to 850-nm region with a spectral resolution of 1.5 nm using a 25-µm entrance slit. The spectrometer is connected to a data acquisition computer via a USB [Universal Serial Bus] cable.

This work represents a proof-of-concept investigation into using a glow discharge emission system to detect and quantify trace amounts of argon in pure oxygen. A similar analysis will need to be done for nitrogen. Straightforward, direct measurement of these target contaminants may lend itself to a device that is capable of on-orbit verification of oxygen purity.

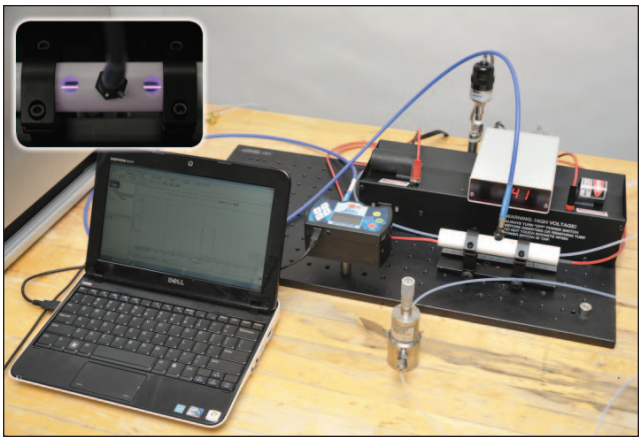


Fig. 2. *Prototype system with inset showing glow discharge region.*

Particle Impact Test Results on Stainless-Steel, High-Pressure Manual Valve

Keisa Rosales, *White Sands Test Facility*
Stephen F. Peralta, *White Sands Test Facility*
Joel M. Stoltzfus, *White Sands Test Facility*

An HiP® 20A-11HF9 valve failed in the closed position during oxygen venting and transfer operations, and a second valve of the same type had internal leakage. The Oxygen Compatibility Assessment (OCA) Team, at the request of the failure investigation team, assessed the oxygen compatibility of the valve components. The valves are within a 316 stainless-steel body and have a 17-4PH stainless-steel stem; 316 stainless steel is recognized as being flammable at pressures greater than 111 pounds per square inch absolute (psia), and 17-4PH stainless steel at pressures greater than 200 psia.

The OCA review concluded that particle impact was the only credible ignition mechanism for this valve. Particles entering the valve from the lower port would impact directly on the body first and then possibly the flat geometry of the stem. Particles entering the valve from the upper port would most likely impact the stem first but have a lower probability of igniting it due to the small location of 90-deg impact points. However, a particle, or particles, could miss the stem altogether and still impact the body of the valve. Therefore, particle impact is considered possible when the valve is constructed with a 316 stainless-steel body. The history of use is significant for normal operation at NASA Johnson Space Center's White Sands Test Facility (WSTF) in that no known particle impact ignitions of stainless-steel body valves have occurred. The reason that these valves have been used successfully is thought to be due to system cleanliness levels at WSTF.

Because of concerns, WSTF performed particle impact testing in 100% oxygen on identically constructed HiP 20A-11HF9 valves to determine whether there is a particle impact ignition hazard in these manual valves. Multiple series of particle impact tests were performed at 4000 pounds per square inch gauge (psig) with approximately 1400 psig backpressure in each flow direction using various sizes and amounts of iron powder particulate mixtures. Each particulate mixture consisted of 50% -50+100 mesh iron powder and 50% -60 mesh iron powder. No ignitions occurred during

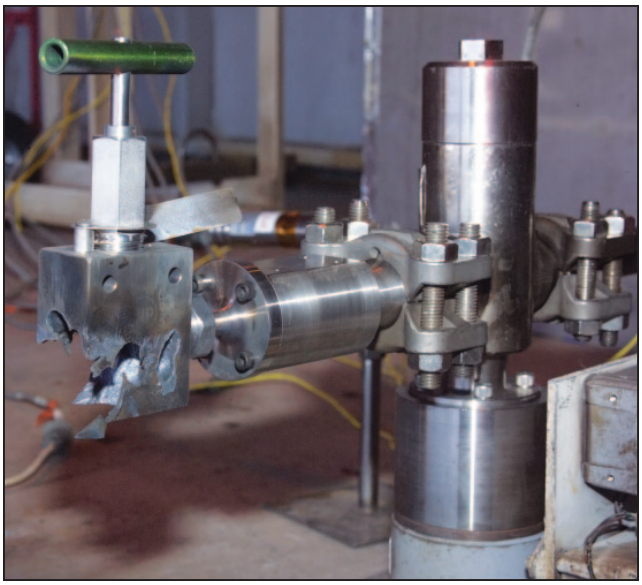


Fig. 1. *Outlet of valve impacted with 1000-mg iron powder.*

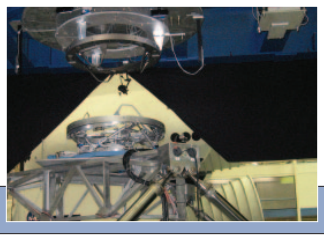


Fig. 2. *Inside of valve impacted with 500 mg iron powder.*

the first test series with 100 mg of iron powder, but ignitions occurred with greater amounts of particulate mixtures on the first impacts of both test series 2 (1000 mg) and 3 (500 mg). Figure 1 shows a valve after impact and ignition with 1000 mg of iron powder; figure 2 shows damage with 500 mg.

The results of the 250-mg iron powder testing were deemed invalid after attempts to duplicate the 500- and 1000-mg ignitions were unsuccessful. During disassembly of the valve, a difference in the internal valve configuration was discovered. The valve used for the 250-mg test had a tapered edge seat, but it is assumed that the valve used in the previous series had a sharp edge seat. When the 250-mg test series was repeated with the identical configuration (valve with sharp edge seat), no ignitions occurred in either direction. The valve exhibited no ignitions in 120 tests (60 in each flow direction) with the following particulate mixture: 125 mg of -50+100 mesh iron powder and 125 mg of -60 mesh iron powder, for a total of 250 mg per test.

It has been determined that HiP® model 20A-11HF9, stainless-steel body and 17-4PH stem valves do not pose a fire hazard when the design of the system and maintenance performed precludes the simultaneous impact of 250 mg or more of iron-containing particulate on any oxygen-wetted surface and as long as the inlet pressure to the valve is less than 4000 psig. If the inlet pressure is greater than 4000 psig, the particular application must be assessed to determine whether these data can be used to predict the risk of a particle impact ignition.



Space and Ground Operations

The Rapid Prototyping Laboratory: The Shortest Space-Time Between Dream and Reality

Lee Morin, *Johnson Space Center*
Patrick Henry, *Johnson Space Center*
Tim Verborgh, *Johnson Space Center*
Patrick Laport, *Johnson Space Center*
George Scheuch, *Johnson Space Center*

Prototyping is like evolution. Prototypes evolve because experienced engineers and users find some models are more fit than others to survive.

The Rapid Prototype Lab (RPL) is small team of developers led from within the Astronaut Office. The lab is located in Houston, Texas, at the Johnson Space Center (JSC) and is dedicated to providing quick and correct solutions to challenges in human space flight vehicle interfaces. This work has led to the development of the generic "glass cockpit."

The Glass Cockpit

Successive approximations to a safe and functionally correct glass cockpit require that the RPL prototype the hardware and software of an avionics suite for a spacecraft; drive the prototype cockpit with simulators and other mathematical models; fly the test bed in representative tasks from each phase of flight; evaluate displays, controls, and user interface elements; correct deficiencies; and repeat until the prototype is correct and complete.

The RPL, in conjunction with subject matter experts from all flight disciplines, is in the process of designing the complete suite of Orion displays and controls. Early conceptual design began in 2006. The design matured with the vehicle and by 2009 reached a state of maturity that enabled comprehensive evaluations. These evaluations began in 2010 and continue through 2011.

Proximity and access to flight crew permit the prototypes to be evaluated and validated by experienced operators—an essential ingredient of the RPL's effectiveness.

Orion will be the first spacecraft with a glass cockpit. Unlike previous spacecraft, the user interface will be almost entirely through graphics displays on console screens. These screens are Honeywell's DU 1310 glass, currently flown on the Boeing 787 (figure 1). Orion's systems will be operated by manipulating graphical screen objects, not by throwing physical switches or circuit breakers. While the shuttle employed approximately 2000 physical controls and 10 display screens, Orion will have about 50 physical controls and three DU 1310 screens.



Fig. 1. *Faux DU 1310 display units mounted in the low (top) and medium (bottom) fidelity mock-ups in Building 9 at Johnson Space Center. The low-fidelity console flew and was tested aboard the Reduced Gravity C-9 aircraft.*

The RPL is adept at using immediate feedback and close collaboration from a multidisciplinary JSC team (including Mission Operations, Human Factors, Engineering, and crew) to integrate conceptual designs and successfully apply the rapid prototyping model. This work allows the RPL to apply 40 years of JSC space flight knowledge and experience to operations in the next generation of spacecraft cockpits. Over the past decade, the RPL has prototyped, evaluated, and helped define glass cockpit hardware and software for the Shuttle Cockpit Avionics Upgrade, the X-38 Crew Return Vehicle, and Orion.

Orion Displays and Controls

Of course, a glass cockpit includes the physical display units and the edge keys and other devices used to manipulate them. But equally in need of evolution by prototype are abstractions, such as the design of data structures and of the images shown on the display units. Prototyping the glass cockpit for Orion involves mocking up display units, creating the data and flight formats shown on them, and providing navigation for cursor control and data entry. Physically, edge keys and a rotational tabber allow selection and data manipulation (figure 2).

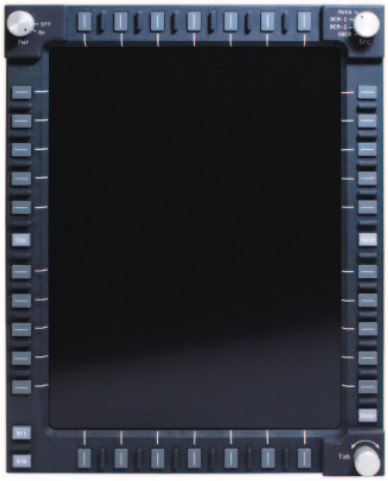


Fig. 2. *The Faux DU 1310 Mark 3 uses a Liquid Crystal Display panel with high viewing angles in all directions. The knob on the lower right is the tab control.*

When crew members are suited and restrained, such as during liftoff and landing, they cannot directly operate the display's switches and controls. A left-handed Cursor Control Device was prototyped to permit the crew to operate the spacecraft during these periods. A great deal of effort went into proving that the displays could be operated by this device by a crew member wearing a pressurized glove.

The Evolution of a Hand Controller

Designs for the left-handed Cursor Control Device evolved over time, guided by observations and comments by Astronaut Office participants in studies conducted by RPL and NASA's Human Research Program. The crude first approximation varied greatly in shape, construction, and functionality from subsequent iterations. The large foam core box quickly evolved into a "steam iron," which was electrically functional—the switches worked; it didn't iron cloths. The steam iron was better, but it was still unfit. An intermediate shape arose and was deemed adequate by the users, but the controls were still not right. Subsequently, various kinds, numbers, and locations of buttons were tried. Figure 3 shows the surface migrations of two rocker switches (green), and two castle switches (red). Ultimately, the testing led to consensus about the type, number, location, and function of the buttons.



Fig. 3. *The evolution of the Cursor Control Device included changes in form as well as in function. Rocker switches (green) and castle switches (red) changed positions, and jobs, several times before the final design was achieved.*



Fig. 4. *Electronic procedures weigh nothing and take up nothing but disk space, yet they provide far better insight into—and control of—spacecraft operations than their paper counterparts.*

Electronic Procedures

In previous spacecraft, hundreds of pounds of payload and several cubic feet of storage space were provided for paper documents. Electronic procedures (dubbed "eProcs") will eliminate this mass and storage requirement from future vehicles (figure 4). Not only that, eProc guides the crew by automatically locating and displaying essential information as it is needed. eProcs direct an operator's attention to critical items and actions. This reduces stimulus clutter, enhances situational awareness, and reduces task workload to help ensure safe, error-free flight.

The RPL strives to encapsulate glass cockpit concepts developed at JSC over the past decade in a way that they can be communicated and shared with NASA organizations and commercial partners under Space Act Agreements.

Reengineering the Mission Operations Directorate Flight Production Process

James Ruszkowski, *Johnson Space Center*

The Mission Operations Directorate (MOD) at NASA Johnson Space Center (JSC) is responsible for operating the NASA human flight programs. The MOD Mission Operations System (MOS) includes the infrastructure, people, and processes that are used to "plan, train, and fly" the corresponding space missions. The MOS has been refined over time, and the underlying know-how that allows the system to run smoothly is inherent in each of the system elements. Reengineering the MOS to meet the MOD goal to reduce sustaining costs by 50% as compared to space shuttle missions entails fully characterizing the MOS, understanding its strengths and limitations, identifying the gaps between its current capabilities and those required for meeting future program needs, and designing a feasible transition plan for reaching the desired end state.

The MOD Space Shuttle Program and International Space Station Program flight production processes (FPP) were not built as an integrated system. The separate and distinct production processes used for these two programs were instead built one piece at a time by each of the large functional areas within MOD. These processes have been streamlined and refined over time, but never engineered to maximize efficiencies. Today, MOD produces more than 600 products for each shuttle mission to the International Space Station. These products are manually integrated at a high level called the management level. While this high-level integration process allows MOD to meet its top-level product delivery requirements, it does not provide sufficient insight into the processes necessary to understand, integrate, or reengineer the detailed processes.

The FPP Reengineering Project has established a model-based systems engineering methodology and the technological infrastructure to design and develop a reference, product-line architecture as well as an integrated workflow model for the MOS for human space exploration missions. The design and architectural artifacts have been developed based on the expertise and knowledge of numerous subject matter experts. The technological infrastructure developed by the FPP Reengineering Project has enabled structured collection and integration of this knowledge and further provides simulation and analysis capabilities for optimization purposes. A key strength of this strategy has been the judicious combination of commercial off-the-shelf products with custom coding. This foundation is now being extended to include the breadth of the processes involved in the operation of human and robotics missions, and is being used to guide the redesign of the Mission Control Center.

Goals of the FPP Reengineering Project are achieved by using cutting-edge systems engineering techniques to model the processes involved in the development of flight products and finding an optimal strategy for allocating resources to each of these processes. Figure 1 shows a high-level architecture for the model that is being built. This architecture includes multiple layers. At the lowest level is the layer that includes the views generated based on the Department of Defense architecture framework. This layer is used to define and analyze the relationships between the key attributes of the system and their interfaces. On the right side is a database that includes the underlying data for the system; these underlying data in turn feed all of the layers. This database is updated as the system is designed, and will continue to be updated even after it operates and more data become available. The next layer includes executable models such as the discrete event simulations and risk models that are used to validate the end-to-end architecture of the system. The actual MOS depicted in this layer uses the data available in the database to run simulations and demonstrate system performance metrics such as the minimal cut-sets of the system, critical paths, and probability distribution function of the time to complete a full run. The MOS depicted is the actual system that is being designed during the design phase and will be used to perform operations. During the operations phase, the actual measures of system performance are produced by this layer and fed back into the database, as are other layers of the model as necessary for continuous improvement.

The topmost layer is the manage and control layer, which serves the function of orchestration and uncertainty management. The orchestrator is called the management-level network executive and uncertainty management is conducted by a replanning tool. The management-level network executive has a direct interface with components of the MOS and sends commands to them to automatically

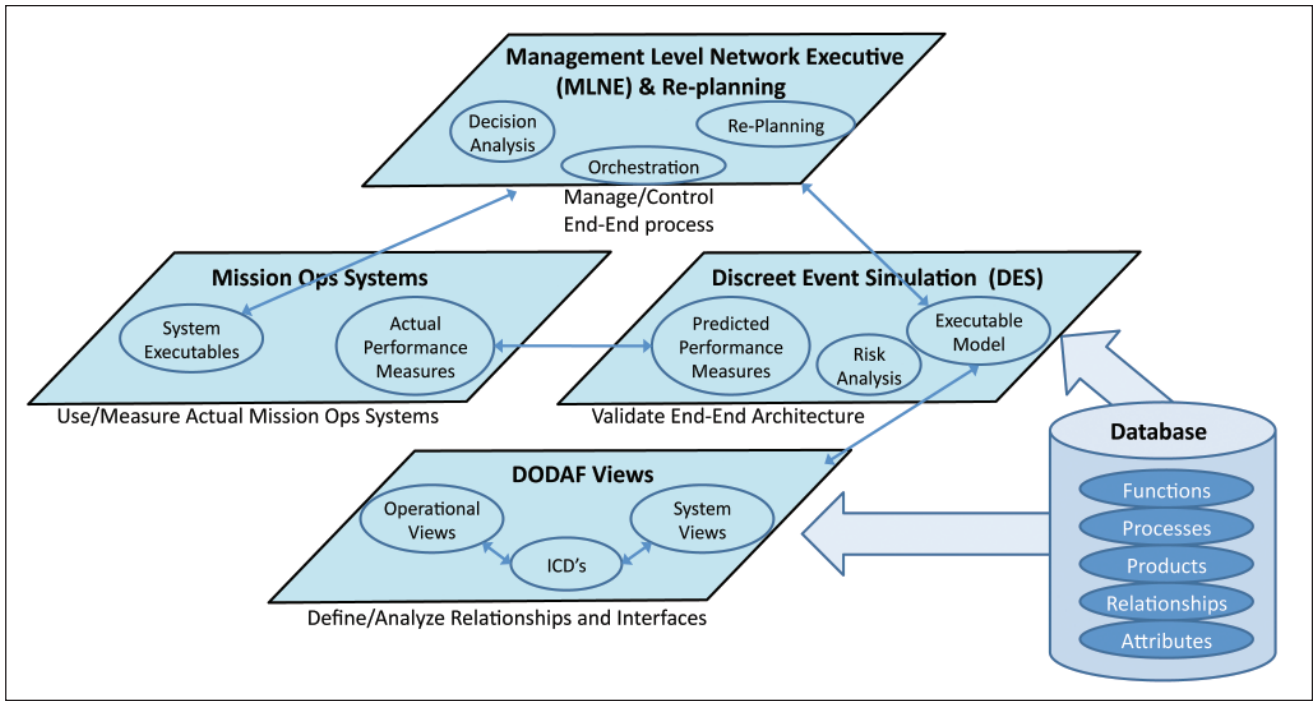


Fig. 1. *Multilayered architecture of the Mission Operations model.*

orchestrate the activities identified in the final system model, which is representative of the FPP design. The replanning entity allows for uncertainty management during operations. Such management might entail making changes to the original integrated workflow process as appropriate to address change requests that are either being produced externally or internally by the system based on the state of the system and its performance metrics. The re-planner does this dynamically and automatically.

Management interfaces with the manage/control layer to get the necessary information for making executive decisions. These decisions are then communicated with the operators and translated into commands for the flight system. Performance of the system is monitored, and the performance metrics are fed back into the database that in turn feeds the system models. The additional data are then used to update the existing data and make them more accurate.

Mission Evaluation Room Concept of Operations Evolution: Successful Merging of Technologies and Techniques

Thomas E. Diegelman, *Johnson Space Center*
Tony Sang, *Johnson Space Center*

The International Space Station (ISS) Mission Evaluation Room (MER) is a flight control facility used by Engineering Directorate personnel in support of ISS vehicle operations and science projects. The facility is staffed with engineers who possess in-depth knowledge of each of the ISS systems, and they provide real-time engineering support to the Mission Operations Directorate staff in the Flight Control Room.

Following the final space shuttle flight, the demand for real-time ISS MER support will decrease due to the absence of shuttle visits to the ISS. This will enable the ISS MER to transition to a lower-cost, remote, distributed support posture—i.e., a remote MER—while maintaining "essential support" such that the risk to crew and the ISS are not increased.

The existing ISS MER, shown in figure 1, will be abandoned by engineering personnel in a planned, stepwise fashion. Once the operation of the remote MER concept has had sufficient operational experience, the MER room will be repurposed for other customers. A new approach for providing MER personnel access to the voice, video, and data systems from remote locations would be required to accommodate this transition. Note, however, that the MER tool set—including the MCC Automation System tool set—will not be affected, thereby preserving the investment already made in the staff's training. The additional requirements were for secure remote access from office or off-site, and the need to use the training investment in the current tool set and its support environment.

The challenge was met; all associated risks were successfully managed. Specifically, the risk challenge was centered on the production of a service that cannot be interrupted, but that cannot be continued without significant changes to the Concept of Operations (Con Ops) currently being implemented. It required that new, different, and disruptive technologies be incorporated into the system, while incorporating the current, trained, skilled cadre of operations staff into a sufficiently familiar environment to avoid undue "learning curve" risk.

NASA selected an existing prototype of a virtualized MCC, called Mission Control Center Experimental (MCCx).

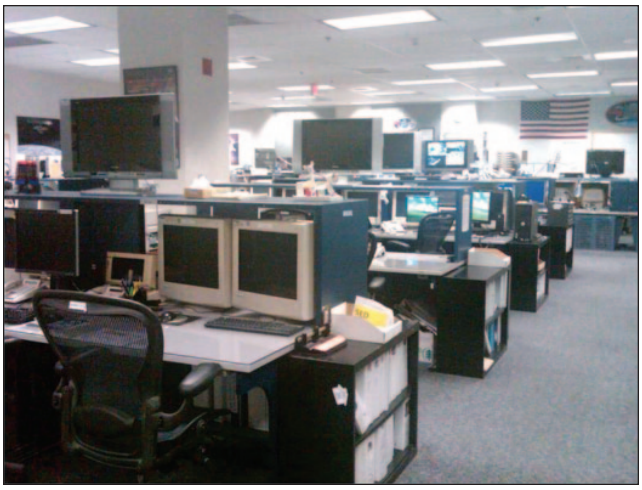


Fig.1. *International Space Station Mission Evaluation Room facility.*

This prototype used existing MER tools and the trained MER personnel. The solution was Internet Protocol (IP) based, and already had secure operations and remote access available. By combining the available Johnson Space Center (JSC) IP Television (IPTV) system for the monitoring of video and audio signals over IP, and a prototype Voice over IP (VoIP) system recently integrated by the Mission Operations Directorate, the combined data, voice, and video services could now all leverage existing IP infrastructure. This approach is referred to as "Everything Over Internet Protocol" and simplifies the deployments of these services to remote locations.

The confluence of activities, technologies, and requirements used to transition the MER operations defines a prescriptive methodology that can be repeated in the future within NASA and industry. Recall, the challenge is that production of an ongoing service cannot be interrupted, but yet it cannot be continued as configured without change. This is a "soft" technology called operations research— commonly referred to as Knowledge Capture in the Knowledge Management arena.

In project scenarios like this, the search for detailed requirements begins, and quickly mires down. The push to define the requirements usually consumes the team. Not so here. Since this transition of the MER to remote

operations was a partnership between the MER and the Mission Operations Facilities Division of the Mission Operations Directorate, that pitfall was avoided by directing the team energy on what was available as a system to interface to the MCC. This resulted in the definition of very high level "Mission Support Requirements," as shown in figure 2.

System Driver	Definition of Driver	Measure of Driver
Performance	Provide a usable system that is responsive and provides optimized utilization of hardware for the stakeholders	For remote access primary measurements of performance are responsiveness, throughput and utilization from the controlled portion of the system architecture
Scalability	Provide ability to expand utilization of provided services which may involve increasing the number of simultaneous users, increasing the volume of data, increasing the number of services provided, or increasing the number of remote access points	Scalability is defined as the maximum number of simultaneous users, maximum amount of simultaneous transmitted data, and the maximum number and location of remote connections.
Availability	Provide a system that meets the up-time needs of the stakeholders to support their operations concept	Measured using industry standard uptime metrics
Usability	Provide the users with the remote collaborative environment by enabling the operations scenario	Stakeholder demonstrations with feedback in regards to the ease of use of system, and refinement on system design when necessary
Security	Provide the infrastructure to allow for one-way push of data from a high security environment	IT security local to MOFD and FDOC will analyze intrusion detection, and implement designs that will allow for mitigations in the event of an intrusion

Fig. 2. *System performance requirements.*

To provide secure display information using ISS real-time data to remote locations, secure two-way voice loops to remote locations, and standard definition video channels to remote locations, the team developed and followed a process that defines the methodology for any system that must change while still in motion. First, a return on investment must be completed that indicates, to the first order of approximation, the goals and performance trades were made quantifiably, and show positive, or at least non-negative, return on investment. Second, tools are maintained in place to preserve the training and associated "sunk cost" of the current staff. Third, recognition of the impacts of a radical change in Con Ops (such as remote operations) on both the system and staff performance must be made. Fourth, to the extent practical, use commercial off-the-shelf products; there is no penalty in project time and money for switching if insurmountable problems are encountered. Fifth, leverage the prototype systems available to minimize risk to the total project, filling the commercial off-the-shelf gap. Sixth, run the new system with the current staff parallel to the old system prior to "lights out" on the old system as a risk control.

The demonstration of return-on-investment benefits of a Con Ops modification—employing prototype systems in an integrated fashion to build a new system—results in a Con Ops/system that is cost effective and risk bounded, and is completed in a relatively short time span. When repeated for future facility transitions, this Knowledge Capture will benefit not only JSC, but any critical real-time operation requiring seamless transition.

Next-Generation Spaceflight Training for Mission Operations

Valerie Gordon, *Johnson Space Center*
Leslie Court, *Johnson Space Center*

The Distance Learning team within the Mission Operations Directorate (MOD) Spaceflight Training Management Office is prototyping a next-generation online learning experience for a student population that includes astronauts, flight controllers, instructors, and other MOD personnel. Spaceflight training is a complex, heavily integrated activity, requiring efficiency in both planning and execution to meet flight dates and timely certification requirements for crew and MOD personnel. The goal of this project is to make a case for providing on-demand training that will meet these needs effectively and efficiently. Traditional classroom content is converted to a fully web-based environment, creating interactive, media-rich lectures and multimedia presentations available from any location with access to NASA's intranet. Students can easily access training content at any time to assist in gaining and maintaining proficiency of both technical and soft skills required for spacecraft mission operations.

Historically, MOD has used online training for additional review of content that had already been presented via more traditional methods (i.e., classrooms, mock-up trainers, etc.); however, this same online content has been used as a primary means of training for organizations external to MOD and other NASA centers that are unable to get this training in-house. The team is building on the successes and lessons learned from this previous implementation to develop a proof of concept for the next generation of online training to be implemented in a blended-learning approach, in conjunction with traditional spaceflight training media. Simultaneously, the team is addressing technological upgrades in these online prototypes due to the rapid growth of multiple browser and platform technologies and ensuring that MOD remains in sync with the latest developments in training technology.

The approach for developing and producing this next generation of online training includes identifying and selecting appropriate development and production software; choosing the appropriate training content; producing the online lesson prototypes; and, finally, implementing these lessons for proof of concept. The effectiveness of this technology for future implementation into formal MOD student training flows will be determined using both a qualitative and quantitative approach.

NASA initially investigated over 50 technological solutions, including both software and hardware, for this project. Selection criteria included the following:

- Low-cost solution for rapid development
- Design flexibility
- Ability to be customized and formatted to support the required training environment
- Compatibility with emerging mobile technology
- Capability for student interaction
- Support of animations in multiple formats
- Synchronization of audio, video, graphics, html, .pdf files, and PowerPoint files in a single template
- Compatibility with existing NASA web servers
- Sharable Content Object Reference Model specification compliance for testing, evaluation, and tracking, as well as for compatibility with other learning management systems, as needed
- Ease of updating final product

Ultimate selection was based on the ability to produce multiple types of lessons with increased student interaction, minimal resource utilization, and accessibility across platforms and browsers. NASA selected four key software technologies from this field—Accordent PresenterPlus, Articulate Studio Pro, TechSmith Camtasia, and Adobe E-Learning Suite. In combination, the various features provide the team with the means to create state-of-the-art e-learning technology.

Training content for the online lesson prototypes was selected based on the existing needs of the student community, the desire to showcase multiple types of online training, and the potential for highlighting increased student interactivity in an online format. Certain content lends itself to online training, such as high-

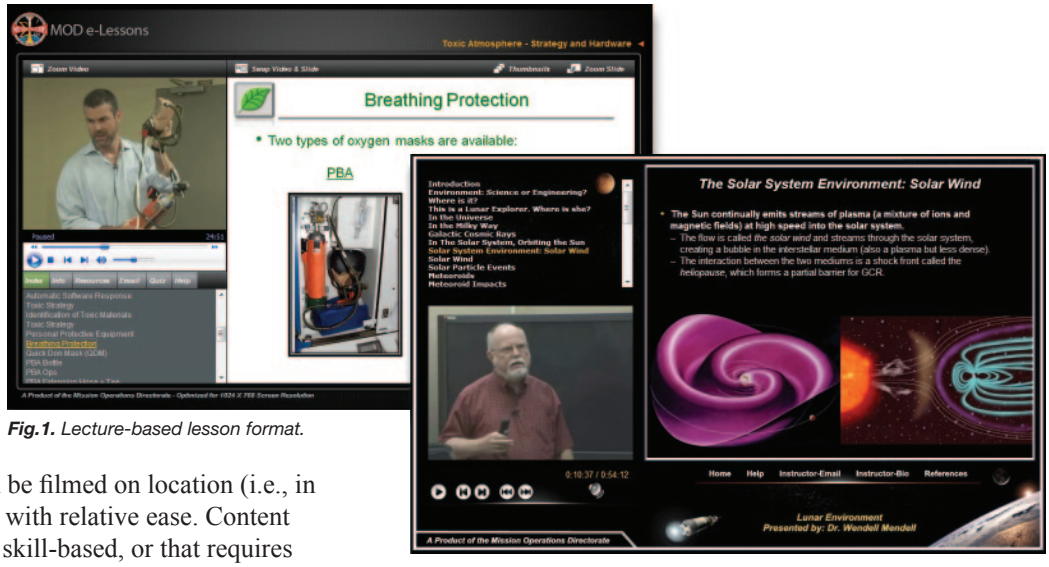


Fig.1. *Lecture-based lesson format.*

level overviews of technical information, information that is global to multiple or extensive student populations, introductory hardware or "show and tell" lessons, and simple training scenario lessons that can be filmed on location (i.e., in mock-ups or simulators) with relative ease. Content that is more specialized, skill-based, or that requires hands-on interaction will not lend itself as easily to online training technology. Since MOD training flows incorporate a mixture of content, the proof of concept relies on the integration of these online lesson prototypes with traditional training to result in a successful blended-learning approach.

The chosen content for the online training prototypes will be developed in two training flows. The first flow consists of a series of introductory emergency strategy and hardware lectures and emergency procedural scenarios, intended to be used for International Space Station international partners and flight controllers, with the potential for expansion to additional student populations. The second flow is a combination of introductory information regarding proper evaluation and feedback techniques, as well as self-guided content for introducing flight controller and instructor evaluation forms and terminology to certifying peer evaluators.

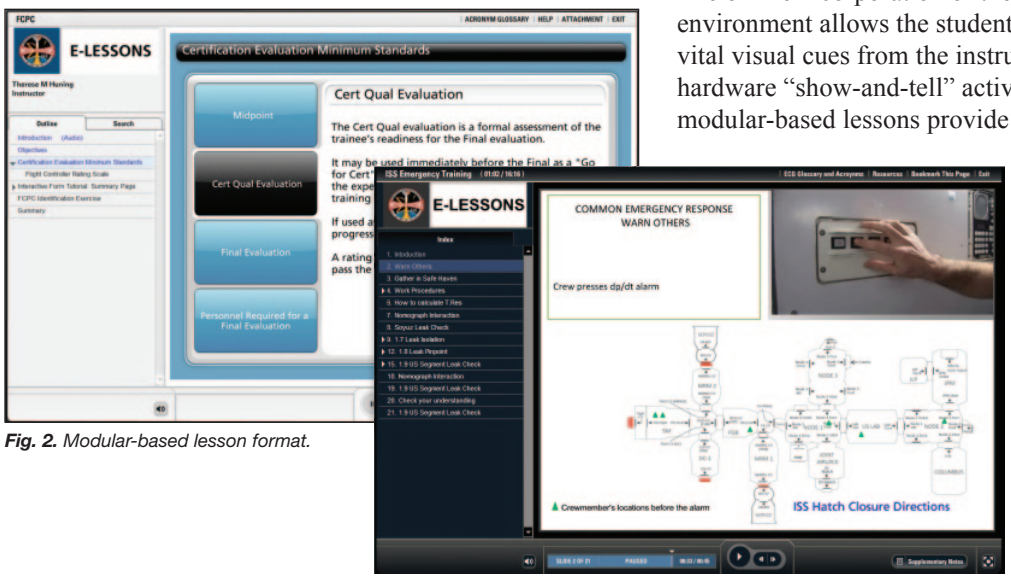


Fig. 2. *Modular-based lesson format.*

The training content is produced in two distinct types of online lesson prototypes: lecture-based and modular-based. The lecture-based lessons provide an online experience that allows the student to view the instructor and presentation material as if they were in the classroom. The online incorporation of the familiar instructional environment allows the student to feel at ease and offers vital visual cues from the instructor, as well as system hardware "show-and-tell" activities (figure 1). The modular-based lessons provide an opportunity for students to learn the content at their own pace, without requiring an instructor as a guide. These lessons emphasize student interaction and are also useful for presenting scenario-based content that may incorporate multiple elements (figure 2).

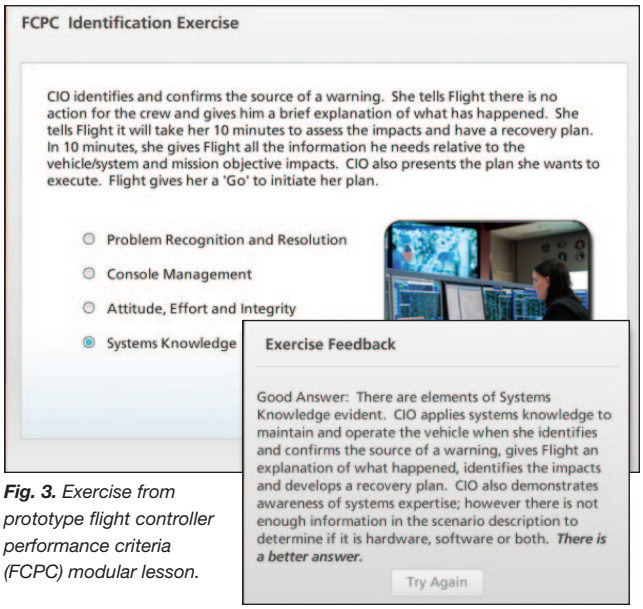


Fig. 3. *Exercise from prototype flight controller performance criteria (FCPC) modular lesson.*

Both types of lessons include interactive exercises and quizzes for increased student comprehension and retention, which is key to implementing this technology in MOD training flows, where crew and vehicle safety is paramount (figure 3). The lesson prototypes also feature the following: the capability to e-mail questions to the instructor or subject matter expert; an interactive table of contents to navigate to different sections of the lesson for review; reference material libraries; notes pages that can also serve as closed-captioning; and an interactive glossary of terms and acronyms. Efforts to produce bilingual online lessons have also been successful, and, although there are no bilingual lesson prototypes for this current proof of concept, the team expects to continue to carry this capability into the next generation of online training for the benefit of international partner training content.

Production of these lesson prototypes is currently ongoing. The team is taking a phased approach in implementing the online lessons. The first phase of implementation, in April 2011, included an initial set of lecture- and modular-based lessons from the evaluation training flow, which were provided to a relatively small audience for a preliminary review of the prototype formats in addition to new content. The majority of the emergency training flow is slated to be delivered in summer 2011, and will incorporate the lessons learned from the first implementation phase. This second phase will also include a sufficient mix of both lecture- and modular-based lessons delivered to a wider audience. The final phase will include remaining evaluator and emergency content. In this last phase of implementation, MOD flight controller and instructor students will have an opportunity to experience the fully developed, blended-learning training concept for the evaluator flow—a key step in the proof of concept. All phases of implementation incorporate student surveys to rate the effectiveness, ease of use, and the overall "likeability factor" of this prototype technology, and to request suggestions for improvement.

The success of this concept of training will be measured qualitatively via the student survey feedback and quantitatively by accounting for prototype production time and resource savings estimated from tracked lesson usage. Student comprehension, as measured informally by captured lesson quiz performance data, will also be factored. Based on the initial achievements in the first phase of implementation and the continued, measured advancement in the development of this next generation of training technology, the Distance Learning team is anticipating the launch of a new era of heightened convenience, efficiency, and efficacy in MOD spaceflight training.

Mission Systems Test Bed Project: The 21st Century Mission Control Center Environment

Lindolfo Martinez, *Johnson Space Center*
Anthony C. Bruins I, *Johnson Space Center*
Thomas E. Diegelman, *Johnson Space Center*

The Mission Control Center System (MCCS) is an institutional resource that, from the Gemini Program through the International Space Station (ISS), has supported human space flight operations at Johnson Space Center (JSC). Under the Mission Control Center 21ST Century (MCC-21) Project, the MCCS will be modified to support a broader array of space flight operations and mission classes, including flagship technology demonstrations, human precursor, robotic, and human-robotic missions. These missions include near-Earth objects, LaGrange points, lunar activities, science utilization of the ISS, as well as commercial crew and cargo missions to the ISS.

The Operations Technology Facility Mission Systems Test Bed (MSTB) Project is a Mission Operations Facility Division project implementing Information Technology (IT) infrastructure that prototypes, tests, and supports the development of key operational architecture concepts for MCC-21.

Mission Control Center System and Mission Control Center 21st Century Overview

The MCCS provides a set of functional capabilities for command, control, and support of space vehicles and their payload elements. From Gemini through the ISS—and with the strategic upgrades and the tactical equipment replacements—the MCCS has evolved to include elements that provide mission critical and mission support functions such as spacecraft command and control functions that reside in a "high security area." These functions include: acquisition, processing, distribution, and display of telemetry downlink data; initiation of uplink and verification of command uplink data; acquisition, processing, and distribution of network, trajectory, timing, voice, video, and ancillary data; recording, storage, retrieval, distribution, and playback of selected telemetry, command, trajectory, and voice data enabling remote access and use of all of this information on displays for the flight control team.

A "moderate security" area supports: preflight production, pre-mission planning, and real-time mission re-planning; spacecraft system modeling for monitoring, evaluation, and analysis; facilities for development, integration, and testing of new functionality; resolution of flight anomalies; and remote access for use of the capabilities.

The term "high security area" refers to a physically separated environment within MCCS for functions and capabilities that, by their nature, are required to ensure the safety of MCCS-controlled spacecraft and crew. The term "moderate security area" refers to MCCS mission support functions that reside on the institutional JSC campus network.

A conceptual depiction of the new MCC-21 architecture spanning these two security areas—high and moderate—is provided in figure 1. These areas will contain the functionality described above. The MCC Operations environment in the high security area provides capabilities for the command and control of spacecraft and payload elements, spacecraft trajectory evaluation, and "safe haven" operations for ensuring safety and mission success in the event the moderate security area is unavailable. Connectivity to the spacecraft will be solely through the MCC Operations environment. A new Mission System Development Environment will be created in the moderate security area that will support the development needs of both the high and the moderate environments. The Mission Support Environment in the moderate security area provides access to the command and control functions located in MCC Operations as well as a host of mission support functions including flight production, mission planning, analysis, trajectory design, procedures development, and spacecraft system modeling.

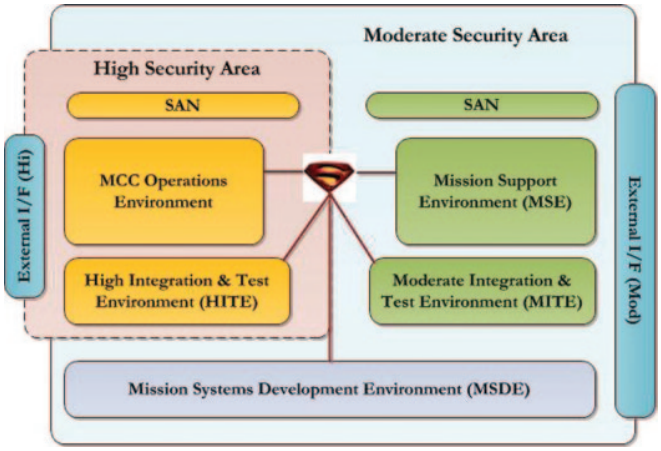


Fig. 1. *Mission Control Center 21st Century conceptual high-moderate dichotomy architecture.*

Integration and test environments are provided within each security area. The high integration & test (I&T) environment and moderate I&T environment facilitate development of capabilities and migration into operations. Each I&T environment is the functional equivalent of the operations environment that they support. These environments will provide an area external to operations for integration, testing, and introduction of new technology and capabilities, assuring minimal disruption to operations, while providing staging grounds for verification of operational concepts.

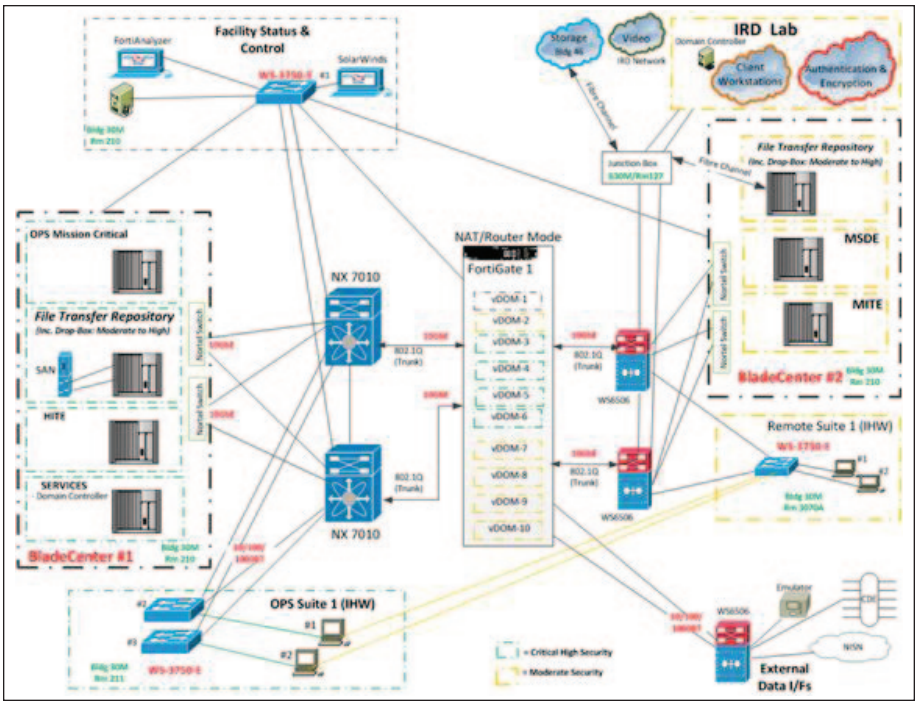


Fig. 2. *Mission systems test bed high-moderate dichotomy architecture.*

The significance of the MSTB Project is the risk and cost reductions for the MCC-21 Project through prototypes of the secure network and computation architectures, security and information assurance policies, and technical management of the IT infrastructure, culminating in a tested "secure network, systems architecture, and operations concept." The prototyping in the MSTB will provide in-depth understanding of the MCC-21 IT systems and refines the MCC-21 Systems Architecture and Operations Concept.

Given a tested MCC-21 Operations Concept, this then evolves the critical security policy configuration and deployment in a cross-domain environment (mission critical/high and moderate), with integrated secure network and computation architectures, into the MCC-21 environment, thus defining the cross-domain virtualization architecture for new secure local area network configurations, and its effect on system behavior, redundancy, and backup system capability. Utilization of the Operations Technology Facility and its state-of-the-art equipment, such as Nexus 7000, FortiGate, Blade Centers, and Storage, as an integrated platform for prototyping of a "MCCS Data Center" and secure network, are planned. As the MSTB Project evolves, additional equipment and software—guided by the functional requirements—will be added. Test case results and trade studies on these new technologies for potential infusion into the MCCS will be conducted here.

Figure 2 shows an intermediate stage of the MSTB as it is today. This depiction illustrates both the high critical environment and moderate support environment, as well as the "Sentinel" security gateway.

The MSTB is the showcase prototype and evaluation environment for the continued evolution and proving grounds for MCC-21 operational concepts. Given the rapidity of IT technology evolution, especially in the commercial commodity areas, the MSTB is a necessary part of the operational MCC-21 infrastructure that assures lower risk to operations, even when new, disruptive technologies are infused. Additionally, future architectures for the MCC-21 can be examined, refined, and enhanced—all with minimal risk and cost to critical mission and space operations.

MCCx Convergent Technologies: Bringing the Mission Control Center to Your Personal Computer

Keith Martin, *Johnson Space Center*
Jennifer Morehead, *Tietronix Software, Inc.*
Karun Sen-Roy, *Tietronix Software, Inc.*
Thomas E. Diegelman, *Johnson Space Center*

The current Mission Control Center (MCC) operates in a secure environment at Johnson Space Center (JSC). The center uses a distributed architecture that has been in operation since 1994, featuring separate hardware systems and networks for audio, video, voice, office personal computers (PCs), and flight control workstations. Each console contains Linux workstations for vehicle telemetry, monitoring, and control; a Windows PC for procedures, shift logs, and e-mail; a telephone; video channel monitoring capability; and a separate hardware voice communication system. The control center has evolved to be workstation hardware-agnostic and its distributed software architecture is adaptable to equipment and network modifications. As a consequence, equipment replacement tends to yield minimal operational cost reductions. The MCC system's robust, stable performance is reflected by the number of successful missions, but also by the challenge to reduce total cost of ownership. The MCC is, then, both a challenge and an opportunity.

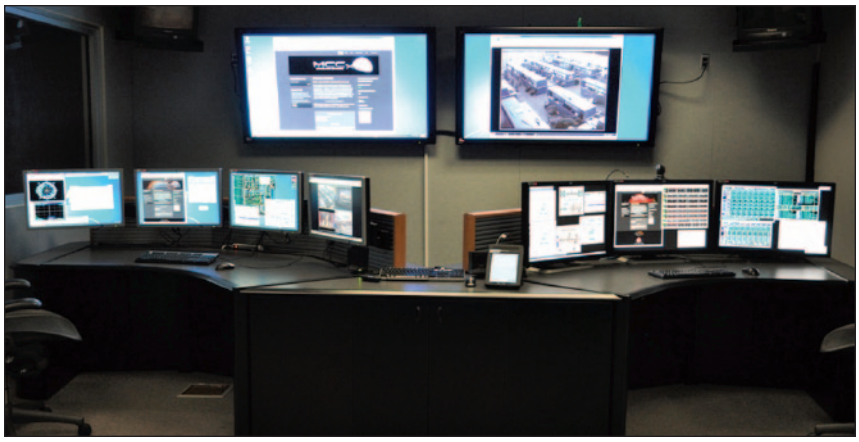


Fig. 1. *MCCx—a "virtualized replica" of Mission Control Center infrastructure.*

The drivers for lower MCC cost of ownership are a combination of budget challenges across NASA, the limited cost flexibility of the MCC hardware replacement cycle, and the new focus on commercial crew services. Collectively, this prompted the Mission Operations Facilities Division of JSC's Mission Operations Directorate to charter a development initiative to demonstrate an alternative set of IT technologies in a future MCC architecture concept. This initiative includes the goal of reducing the development, maintenance, and operations costs, while enabling a more extensible operations concept for human and robotic missions. Through product research and evaluation, the team developed a preproduction system that meets these goals while providing the MCC "as a service." This preproduction configuration, known as MCCx, is currently in use by several operations groups at JSC.

MCCx is a "virtualized replica" of the Mission Control Center infrastructure, as shown in figure 1.

MCCx provides real-time, situational awareness of the International Space Station (ISS) by supporting the majority of the standard MCC flight control applications and live mission data. MCCx is available to authorized users, securely, from any location around the globe. Users perceive very few differences between MCCx and the actual MCC. In fact, the "look and feel" of the MCC is enhanced by the new features such as the seamless integration of the Windows and Linux desktops on a single PC. Owing to the fact this is a "preproduction system" there are policy limits, such as prohibiting vehicle commanding from remote locations. In the context MCCx is operationally serving today, this is not an issue.

MCCx is an implementation of the "2-wire Flight Control Room (FCR)" concept, where power and Internet connectivity are the only services required for mission support other than a PC. The thin client approach integrates easily with technologies such as Voice Over Internet Protocol (VoIP) and Internet Protocol Television (IPTV). These replace the individual, non-integrated networks in the MCC video, audio, and voice solutions as well as the associated complexity, cost, and equipment footprint. The 2-wire FCR significantly increases extensibility, lowering the total cost of ownership, and making it possible for MCC functionality to become a commodity function.

The architecture of MCCx is based on a data center approach that minimizes the hardware system footprint. It leverages hardware virtualization allowing for MCC Linux

MCCx Convergent Technologies: Bringing the Mission Control Center to Your Personal Computer

continued

workstations to run in a virtual environment on blade servers, as shown in figure 2. The MCC software load and software architecture is installed into the MCCx system completely without modification.

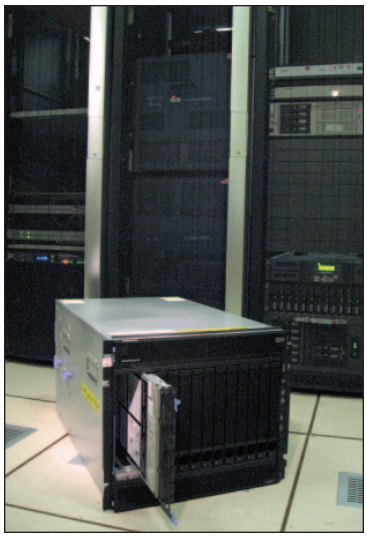


Fig. 2. *The architecture of MCCx minimizes the hardware system footprint.*

A consolidation ratio of 40 Linux virtual machines to one blade is easily achieved, even with very modest blade servers. Of note, the virtual machine runs Scientific Linux 4—a *free* distribution of Linux, instead of a purchased operating system as in the MCC. Therefore, MCCx introduced and validated the potential for significant cost savings on both the hardware platform count and the software required. A commercial off-the-shelf remote access tool, along with additional security layers, allows for secure, remote access to the Linux machines from any Windows or Linux PC. It creates a hybrid desktop for a flight controller. The desktop will run both the MCC Linux and the local Windows applications simultaneously on a single PC.

MCCx was first deployed in 2008, into the ISS System Integrated Simulation facility. Today, MCCx is an integral piece of the ISS training environment—one that enables a new, lower-cost training flow model for flight controllers. MCCx provides the MCC as a service to the ISS training facility, without use of the actual operational MCC. This implementation delivers substantial cost savings in flight control room implementation, hardware costs and configuration, and systems management and administration.

Over 500 members of the flight control community at JSC currently use MCCx for remote mission support from their office or home, and from JSC off-site locations. The Houston Support Group's Houston Support Room in Moscow, Russia, and the ISS Mission Evaluation Room have both adopted MCCx as the platform of choice for mission operations. The attractiveness of MCCx in these applications is enhanced productivity, and substantially lower costs than the remotely located native systems. The Mission Evaluation Room support, previously executed in the MCC, is now remote in the office, with VoIP (voice) and IPTV (video) available. In addition, the Goddard Space Flight Center and other NASA centers are using MCCx for payload mission situational awareness. MCCx services also extend to the software engineering community in the Operations Technology Facility through a "virtual development environment" capability, requiring nothing beyond the user's PC. The architecture of MCCx is flexible enough to support not only current ISS operations, but also those of prototype and future vehicles, including commercial crew. MCCx is currently collaborating with JSC's Engineering Directorate to host flight software displays and live vehicle telemetry from the Morpheus Lunar Lander prototype.

The virtualized environment that MCCx employs is a new operations concept for flight control at NASA, as well as a new architecture. By demonstrating remote operations faithful to MCC functionality, a significant step has been taken in the evolution and validation of design options for the future MCC. With remote, secure access, all NASA centers could be connected to the MCC data center. A robotic, human, or combined human-robotic mission can be executed and the tool set and the number of controllers is limited only on the number of blades in cabinets with identical software loads. In combination with the video and voice over IP, MCCx technologies open new opportunities for the next generation MCC—an MCC "without walls," capable of embracing any new mission NASA as an agency undertakes.

Next-Generation Mission Control Center Voice System: Extended Voice System

Eric R. Gallagher, *Johnson Space Center*
Thomas E. Diegelman, *Johnson Space Center*

Voice communication in the Mission Control Center (MCC) traditionally used physical keysets as the user interface. Controllers and engineers use the keysets to select "meet-me" conferences over which they communicate. Typically, more than one conference is selected simultaneously. The system "sums" the conferences and the audio sounds as if it were a single source.

In the late 1990s, the MCC voice keyset system was externalized to computer networks so that engineers located in office areas could monitor selected voice conferences using a custom software program installed on personal computers. A decade later, the components of the monitor-only system—or "MCC Audio"—were essentially obsolete. Concurrently, the Mission Evaluation Room engineering group and several operations groups at Johnson Space Center desired full office-based remote operations capability, where remote operations meant two-way selectable intercom communications outside the MCC. The keyset became an obvious impediment to implementation, unless the "keyset" were to become software on a personal computer. Requirements for the traditional fixed-location keyset-centric system, based on 30+ years experience in command and control operations, did not incorporate the lessons learned during the decade-long operation of the MCC Audio System, since that system was not an integrated part of the MCC Voice System.

A requirements synthesis effort captured the lessons learned. These requirements then became an integral part of the Extended Voice System (i.e., Evoice) requirements. At a summary level, the requirements can be rolled up to a table:

Evoice should provide communication for users located at any combination of the following locations: offices, off-site contractor facilities, and/or arbitrary off-site locations.
Evoice shall integrate, at reasonable cost, with the traditional, fixed location, high performance, core MCC voice system.
Evoice shall offer the user two modes of operation. In the primary mode of operation, Internet Protocol based networks shall be the primary transmission media for both audio and operator control commands.
In the backup mode of operation the system shall allow autonomous use of the world phone system as an audio transmission and receive device
Internet Protocol based communications shall be encrypted. Default encryption provides a reasonable assurance of confidentiality.
Evoice shall enable communication latency of less than 200 milliseconds independent of transmission media. Industry standard documents indicate that acceptable conversational dynamics begin to degrade if delays exceed 200 ms
Evoice shall offer the same basic functionality as the traditional core mission control center voice system.
Evoice should use connection oriented TCP/IP protocols for audio and control transport.
Evoice shall authenticate users against identities maintained within existing infrastructure. .
Access to conferences shall be controlled on a per user, per conference basis. Evoice should interface with a third party business process management tool to enable management of these permissions.
Evoice shall provide expandibility for later addition of recording devices.

Next-Generation Mission Control Center Voice System: Extended Voice System

continued

Based on these requirements, parametric cost models were developed when assessing Evoice design options. Figure 1 shows cost profiles associated with an off-the-shelf hardware-based Voice over Internet Protocol (VoIP system) (Option A), an off-the-shelf software-based and feature-rich VoIP system (Option B), and a less-mature off-the-shelf software-based VoIP system (Option C). Average per-user costs in software-based systems decrease with user count because no additional physical elements are added to the system. The selection has an obvious dependency on the number of simultaneous users in both the deployment costs and the total cost of ownership, or life-cycle cost.

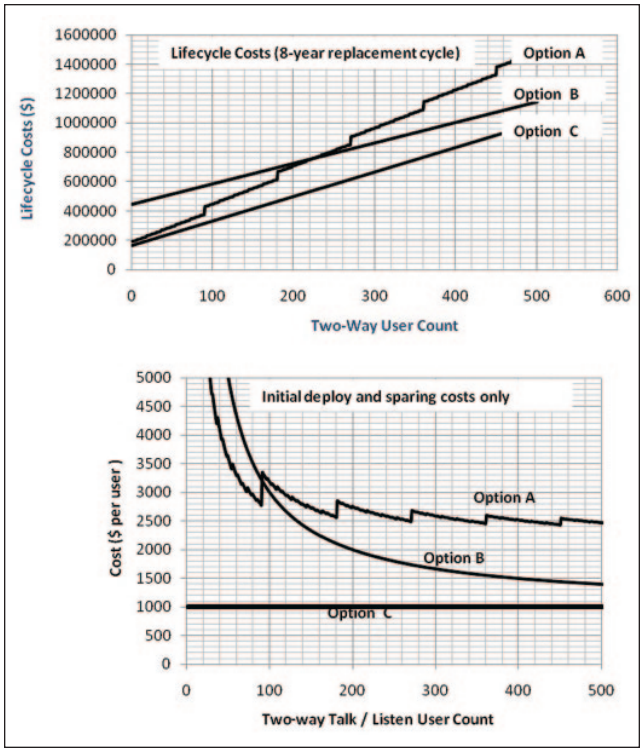


Fig. 1. *Cost estimates.*

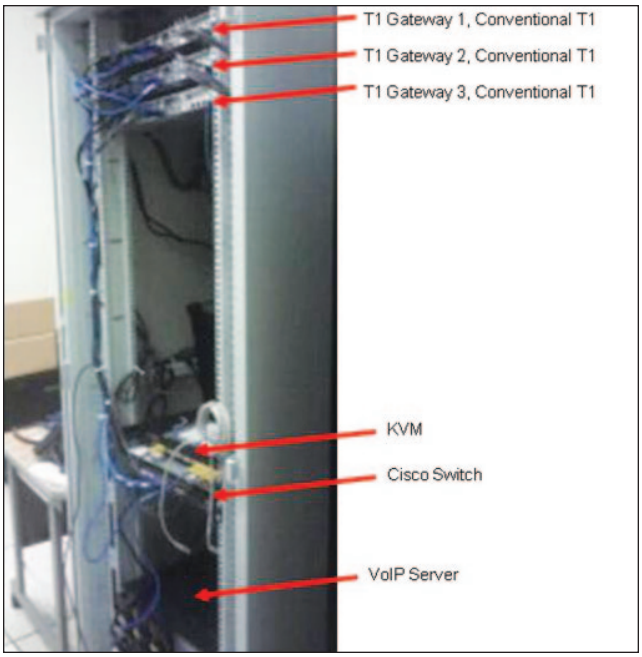


Fig. 2. *System deployment.*

Option B was selected to satisfy the Extended Voice System requirements. The Quintron DICES VoIP system was selected for deployment in the MCC for the reasons already mentioned, but also due to its synergy with the VoIP deployment at Marshall Space Flight Center. Future plans for VoIP site contingency operations, leveraging the analogous assets between Marshall Space Flight Center and Johnson Space Center, are forthcoming.

As configured, the Johnson Space Center system can support over 300 simultaneous users. The configuration, complete with support gear, is shown in figure 2.

The significance of this system is its ability to deliver two-way voice communications to flight controllers and engineers, wherever they are located. This is a significant enabling step toward the goal of providing lower cost, flexible mission support infrastructure for missions of today and the future.

Motion Imagery and Robotics Application Project: Standards Based Protocol

Thomas Diegelman, *Johnson Space Center*
Steve Lucord, *Lockheed Martin*
Lindolfo Martinez, *Lockheed Martin*

The current Mission Control Center (MCC) is dedicated to the execution of human space flight missions. As the future of NASA and human space flight evolves, it is clear that robotic artifacts will ultimately be integrated and immersed into the human mission as tools and even as assistants. To make the evolution and integration as technically capable at a constrained risk level and with reasonable cost, the robotic elements must adhere to standards that allow not only reuse of previous work, but that keep the interfaces stable and reusable. This experience has been seen already on the International Space Station (ISS) experiment packages and with the Robonaut robot.

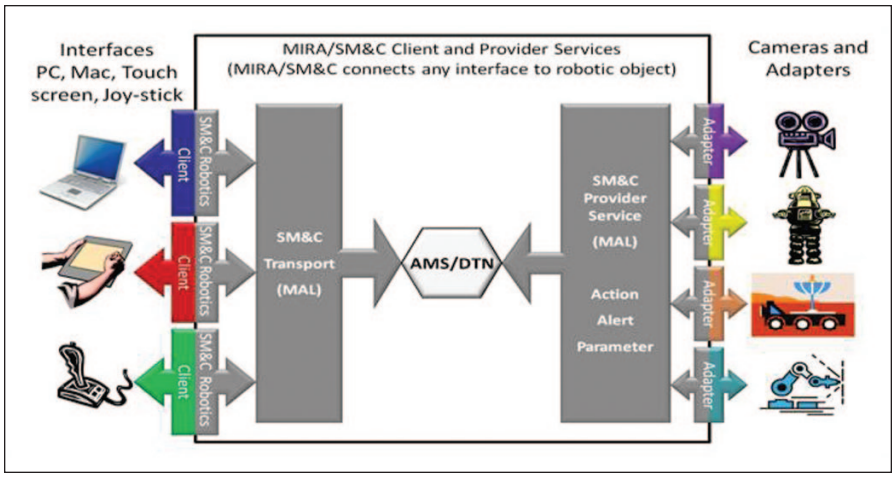


Fig. 1. *Spacecraft Monitor and Control architecture.*

The Motion Imagery and Robotics Application (MIRA) project—a collaborative effort among several NASA centers including Jet Propulsion Laboratory, Marshall Space Flight Center, and Johnson Space Center's (JSC's) Engineering and Mission Operations Directorates, as well as with the University of Colorado—was built to Consultative Committee for Space Data Standards (CCSDS) Spacecraft Monitor and Control (SM&C) and Asynchronous Message Service (AMS) and Delay Tolerant Networking (DTN) specifications. The "stacked protocol" provides standard-based methodology to control and status tele-robotic devices (figure 1), starting with a space-based robotic camera application. Largely developed with JSC inputs, SM&C is an application service that isolates many lower layer services by providing a consistent set of interfaces to mission development and operations teams.

The MIRA project integrates several tele-robotic functions into a powerful international standards-based tele-robotic service capable of running in an ISS payload computer. The MIRA goal is to mature, integrate, and demonstrate the MIRA, SM&C, AMS, and DTN approaches into an integrated system.

The ultimate goal of the MIRA project is to develop the application stack in figure 2 for all robotics—even complex ones. MIRA Phase 1 developed a new CCSDS state-based camera control service standard, with code, capable of controlling a robotic camera system remotely. MIRA Phase 2 will be capable of status and control of three different cameras on the exposed facility (the "porch") of the ISS Japanese Experiment Module, from MCC. Each successive phase will add incremental capabilities such as handling human factors and performance, automatic/semiautomatic change detection from imagery of space flight vehicles and equipment. In later project phases, ground control of robotic assets over Earth-moon-Mars time delays and remote sensing of planetary surfaces and surface navigation will be possible. Additional phases will add functionality to the robotic service until project completion with a demonstration of the Common Communication for Visiting Vehicle (C^2V^2) protocol using MIRA and SM&C services. The MIRA approach to robotic control is therefore applicable near Earth or to distant applications where the DTN provides the bridge across the time delay impacts.

Currently, there is no consensus between the MCC and international partners with respect to the use of standard protocols, ease of access, and robotic system control applications. For the MCC to continue to lead human space missions, it must not only support human missions, but integrate with robotic and human precursor mission

Motion Imagery and Robotics Application Project: Standards Based Protocol

continued

requirements. The state of the art for interoperability, via standards, is well established in the international partner community. This project seeks to develop a new standard for robotics such that interoperability with crewed as well as non-crewed elements is provided, assuring that cost-effective collaboration between NASA and the international space community is possible. In addition, the standard that is proposed to be developed will be extensible to support technology insertion into both crewed and non-crewed elements. The evolution of the proposed standard will be coordinated through the CCSDS international standards community. The confluence of the MIRA, SM&C/AMS /DTN standards, the robustness of DTN capability, and remote connectivity to ISS and ground assets (interoperability) will assure that JSC/MCC will be the hub of human, human precursor, and robotic missions where the mission components can be seamlessly integrated with other locations without excessive reconfiguration and integration costs that would render the MCC noncompetitive.

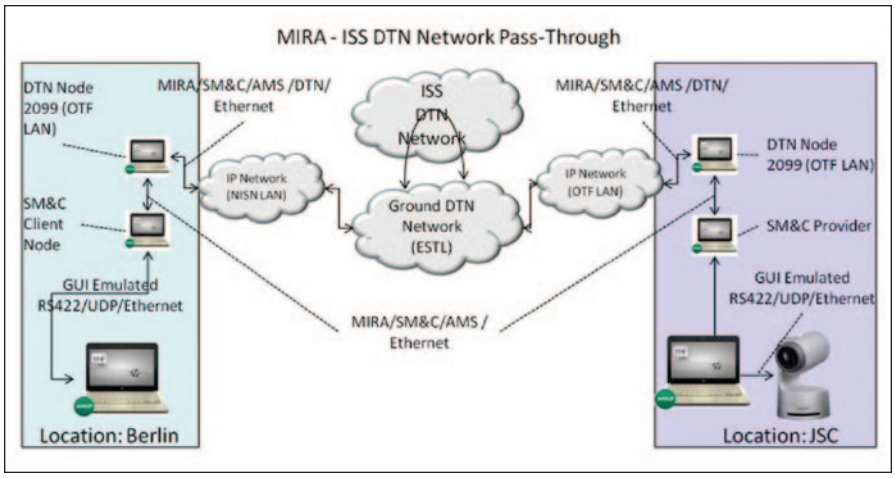


Fig. 2. *Motion Imagery and Robotics Application architecture.*

The results of the MIRA Phase 1 camera demonstration, referred to as Phase I, have demonstrated robotic camera control that is applicable near Earth or to distant applications where the DTN provides the bridge across the time delay impacts. The MIRA, SM&C/AMS/DTN standards-based status and control system software and protocol could be hardened, and expanded into the next-generation MCC protocol supporting human, robotic, and human-robotic missions. As such, this simple robotic camera prototype is a significant first step in the integration of robotic and human missions into true distant independent building blocks for future missions—the scope of which will dwarf the mission complexity of the last 50 years of human exploration.

Display Sharing Technology

Michael A. Brown, *Johnson Space Center*

As the Mission Operations Directorate (MOD) looks for innovative ways to reduce the sustaining cost of its facilities at Johnson Space Center, the directorate tasked MOD Operations Technology Facility personnel with studying the feasibility of alternative architectures for the video transport system. Most flight control data displays consist of text and graphics; however, motion imagery is also used. That imagery is delivered through the video transport system.

The current video transport system is a custom build of broadcast-quality hardware and video cabling, and requires specialized maintenance, sparing, and support. The system satisfies the MOD requirement that a given computer display can be shared to other displays, such as large projectors in the flight control rooms, or a picture-in-picture window within any console position workstation. Any alternative architecture for the video system must also satisfy this requirement. The system that was developed is called "display sharing."

The preliminary list of requirements for display sharing included: the ability to share a screen or application in a one-to-one, one-to-many, or many-to-many fashion; the ability to scale the image based on the target's screen resolution and size; the ability to easily configure and operate the display sharing system; and the ability to maintain an adequate performance margin and a high level of security.

Display sharing—while not intended to be an alternative to straight Internet Protocol (IP) video systems—delivers display sharing and video at a lower cost of sustaining and maintenance. There are definite advantages to the employment of this technology in the remote operations scenario because of the relatively significant lower bandwidth requirements.

The display sharing process is a means of actively sharing only the pixels that change from one viewing apparatus to another through a secure and robust IP infrastructure. This system delivers image sharing across the local area network while simultaneously managing bandwidth, supporting high-end U.S. government-accepted encryption, enabling recovery and resynchronization following a loss of signal, and minimizing latency, while being encompassed by an internal secure directory server that couples with local NASA Data Center credential authentication processes. Additional critical elements to be added include image scaling support, multi-sharing, ease of initial integration and configuration, integration with desktop window managers, collaboration tools, and host and recipient controls.

A tool developed by VSee Labs, Inc. (Sunnyvale, California), with inputs from MOD, is specifically designed to share data and imagery from a Microsoft Windows desktop by selecting a specific application or the entire desktop to another Microsoft Windows PC machine.

In compiling the proposed requirements for the display sharing tool, selected customer groups at Johnson Space Center were polled for input. Although there will be other interested customers, use of display sharing generally breaks down into three areas of interest: flight control rooms; conference room collaboration; and training and simulation.

Flight control room users require the ability to share any flight control discipline application to a variety of clients, including each other's workstations, the large projected screen, and via secure remote access to the office environment and remote users.

Conference room collaboration users require the ability to share any applications, most commonly the entire desktop, by pairing both subscription models ("push/share" and "pull/broadcast") in a quick, secure, and convenient way to share data over an existing network.

Training and simulation users require the ability to share any flight controller's application in an instructor-to-student-led training exercise over the network. Training and simulation functions encompass all flight control rooms sharing requirements with the addition of training-specific tasks. The instructor must be able to control imagery shared from their student's entire desktop without the student being aware of the instructor's actions. The instructor must be able to select particular monitors from the student's workstation to manage the training. Instructors may also require the use of recording and playback features to run simulations.

Display Sharing Technology

continued

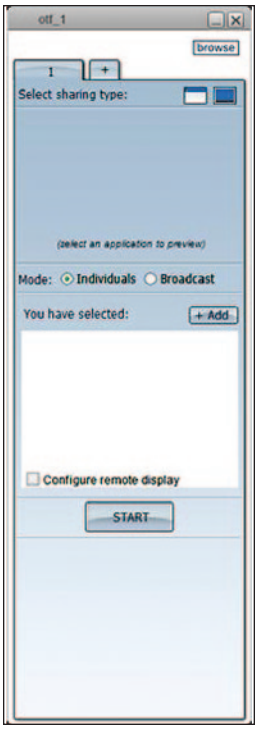


Fig. 1. *The VSee display sharing graphic user interface contains many functions of sharing including: the ability to automate the sign-on process using the existing Windows authentication from the Active Directory or Lightweight Directory Access Protocol; share up to 16 separate applications; share the entire desktop; or select multiple monitors or regions of the desktop.*

An individual can "push" their data to another individual (or set of individuals) without having to distinguish the different resolution factors from each shared personal computer.

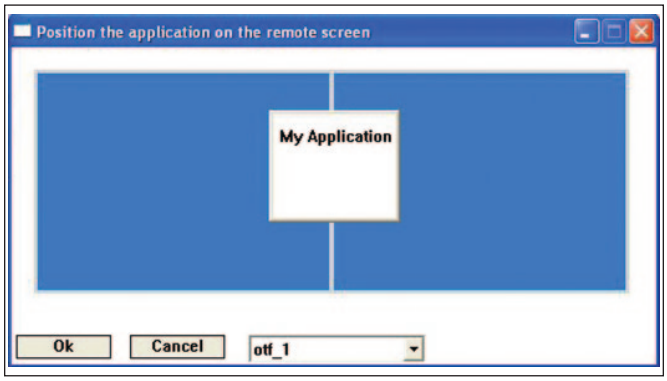


Fig. 2. *The data are displayed onto the existing destination monitors (i.e., two monitors in figure 2) and then resized and placed in a desired target location. Each shared space can be selectively chosen for a selected individual.*

An individual (or set of individuals) can "pull" existing shared data from a secured published broadcast of shared data.

The VSee display sharing graphic user interface, given in figure 1, shows a rather simple interface that has the ability to select specific members to visually collaborate.

The ability to collectively collaborate with the shared display includes "action" buttons that can intensify the visual conversation. This features a pen allocation for creative drawing, text annotation, color assignment, erasing previous annotations, and the ability to allow the remote control to another display.

Selected shared data for an individual can be managed through an "address book" that allows the individual to create specific groups of individuals, automatically accept display sharing calls, browse through a set of securely published data from broadcasted individuals, and acquire status activity from all registered members. This technology is significantly less resource-intensive than the existing non-commercial off-the-shelf implementation. This may be a first step toward the evolution of an enhanced commercial off-the-shelf desktop data sharing protocol through a pixel sharing image process in real time, thereby eliminating the need for large data handling bandwidth.

ISS*Live!* Translator: From NASA Operations Nomenclature to Everyday Language

Matthew D. Healy, *United Space Alliance*
Philip D. Harris, *Johnson Space Center*
Jesse B. Ehlinger, *United Space Alliance*
Katharine M. West, *Johnson Space Center*
Ahmed Khan, *United Space Alliance*
Jennifer B. Price, *Johnson Space Center*

Background: NASA Operations Nomenclature

ISS*Live!* is a software suite that allows the general public to view International Space Station (ISS) timelines (A. Khan, "ISS*Live!* Rich Internet Application Development for ISS Educational Outreach," Johnson Space Center Biennial Research and Technology Development Report 2011). A prime requirement for the display of ISS timelines is a translation of the short, highly abbreviated activity names used in the NASA operations environment, known as operations nomenclature, to something more public friendly. Ideally, the translated name is a phrase or short sentence that can be well understood by a middle school student without any unique knowledge. The ISS*Live!* Translator is a component of the software suite designed to perform the translations using a variety of techniques. It also performs two other essential functions in support of ISS*Live!*: protection of confidential, sensitive, or private data; and data conversion from ISS execution timelines to ISS*Live!* timelines.

Translation is possible because the timelines executed in support of the ISS use an activity naming scheme regulated by international agreements. The agreements specify the following: official names of hardware; verbs used for common actions, format, and word arrangement; and acceptable abbreviations. Activity names are further constrained to a maximum of 20 characters by the planning software used for timeline development. New activities are all assigned a unique name by their creator, adhering to the governing rules. Once created, the name is always the same whenever the activity is scheduled.

Translator Design

The ISS*Live!* translator uses a relational database to store translation rules. A rule is a one-to-one mapping of an operationally used character string to its translation. The rules are developed by users familiar with ISS operations and can be entered one at a time through an administrative interface or in bulk through a specially formatted file. Once the database is built, the translator application uses a series of logical branches, each of which applies one or more rules to build a complete translation of an activity. Depending on the activity in translation, the number of branches executed and rules applied vary. Once translation is complete, the new description is associated with the activity and a determination is made about the sensitivity of the data. Anything deemed sensitive will not be passed forward to the public front-end applications of ISS*Live!* Activity data that is operationally significant but of no use to the front-end application of ISS*Live!* is removed, and the whole output is reformatted to suit the needs of the ISS*Live!* front-end.

Process Description

The technique used to build a translation falls into one of three categories: direct translation; partial translation; or assembled translation. These techniques are mutually exclusive and are attempted in the order listed. The order is

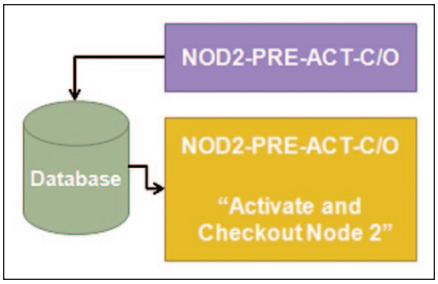


Fig. 1. Direct Translation: *The database contains a translation rule for the name NOD2-PRE-ACT-C/O. Since this rule uses the whole input, no other steps are needed to build a translation.*

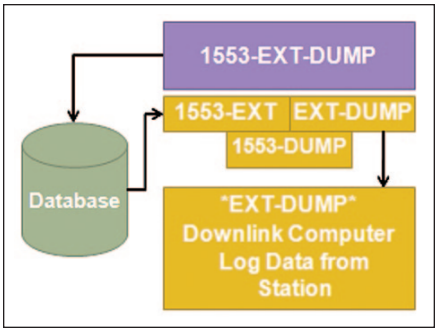


Fig. 2. Partial Translation: *The database does not contain a rule for 1553-EXT-DUMP; however, the partial name EXT-DUMP does have a rule, so the translation uses that rule.*

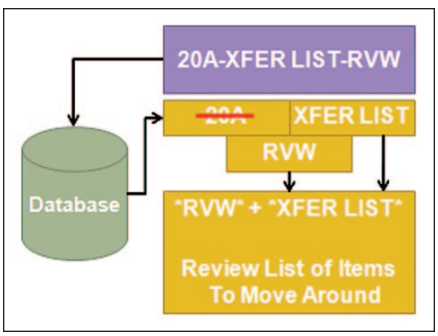


Fig. 3. Assembled Translation: *The name 20A-XFER LIST-RVW is decomposed using dashes as delimiters. Each fragment is translated separately, and a sentence is assembled from the translated fragments.*

based on a qualitative assessment of the overall suitability of the resulting translations. Figure 1 is an example of direct translation. In this technique, the database contains a rule that encompasses the whole input string, NOD2-PRE-ACT-C/O, so the translation is considered complete by the application of this single rule. In figure 2, the input string 1553-EXT-DUMP was not found in the database, so it is split into fragments using the dashes as delimiters. These fragments are then recombined into all possible combinations that maintain word order. As shown in figure 2, there are three such combinations for the input 1553-EXT-DUMP and one of the combinations, EXT-DUMP, is a rule so the translation is completed. In the final technique—assembled translation—the input is again decomposed using dashes as delimiters, but the fragments are translated individually and any that do not have a rule are ignored. Figure 3 uses the example input 20A-XFER LIST-RVW. 20A does not have a rule, but XFER LIST and RVW do have rules and can be translated individually. In an assembled translation, the rules are categorized and the final output is created by applying a scheme that places the individual translations in an order designed to enhance the readability of the translation. The order is: CONFERENCE – PERSON – VERB – OWNER – SYSTEM – EXPERIMENT – HARDWARE – GENERIC. Qualitative testing indicated this order often results in a sentence that meets a reasonable level of understanding. If an activity cannot be translated by one of the three techniques, it is left "as is."

Data Protection

In addition to translation, the rules also serve a secondary but essential function for ISS*Live!*—the protection of sensitive data. There are a variety of reasons why data may be sensitive. Protection of those data is accomplished by a database flag for each rule. By default, all translations are considered sensitive and can only be considered public if the translation was built using a rule that is specifically designated as public. For direct and partial translations, this concept is straightforward; the translation is public if the rule used is designated as such. Assembled translations are public if any of the individual fragments use a rule that is tagged as public. This also means that any unsuccessful translations will be automatically sensitive, since no rule was successfully applied to designate them as public.

Outputs

The ISS*Live!* translator does not pass all operational data to the front-end applications. Only data that suits the purpose of the ISS*Live!* timeline display and application programmer interface are forwarded, and some of those data are modified during the translation process. In this way, the translator acts as a filter that reduces the bulk of operational data to its bare essentials, and reformats that information in a manner acceptable to the front-end applications.

Future Work

The ISS*Live!* translator has successfully demonstrated a method to convert operational activities into descriptions designed for the public. The application is an essential component of the ISS*Live!* software suite and will support the release of ISS operational data to a public that currently enjoys only limited access to such data. The rules database is currently under construction by a dedicated group of experts at Johnson Space Center, and a sustaining plan to accommodate the evolving nature of ISS operation is in works. ISS*Live!* has been deployed to the NASA portal (www.nasa.gov).

Push Technology Approach to Information Streaming: ISS*Live!*

Bruce W. Hochstetler, *Tietronix Software Inc.*

ISS*Live!* is a Mission Operations Directorate project designed to deliver telemetry and timeline information in a rich content format to the public. This includes a website that hosts three-dimensional images that are fed with real-time telemetry from the Mission Control Center. In today's information technology (IT) environment, people use mobile devices such as iPads and mobile phones to access data and information content. ISS*Live!* provides this type of information from the International Space Station (ISS) to any platform suitably equipped. The ISS*Live!* project has developed a solution to the technical challenges to share ISS data with the public.

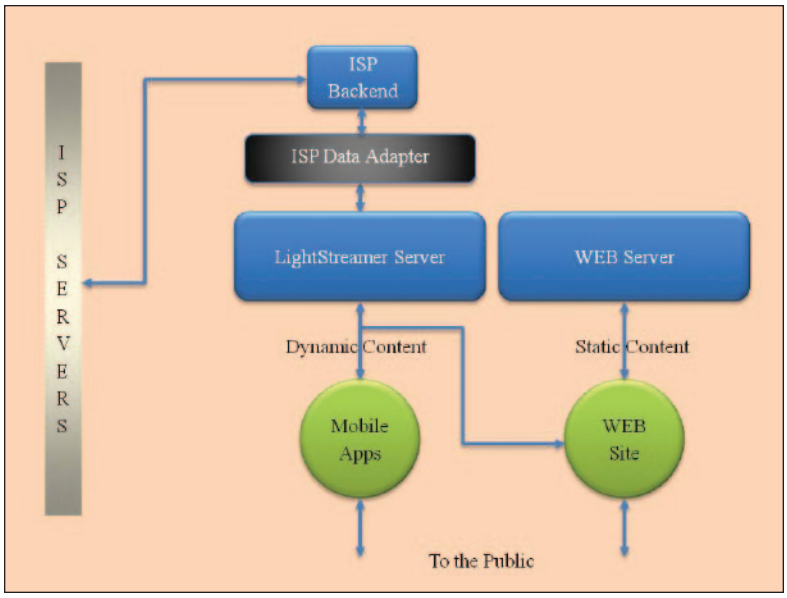


Fig. 1. *Telemetry topology.*

The classic approach fulfilling a client's content or information request uses what is known as "pull technology." With this technology, a client is required to poll a centralized server for the information on a periodic basis. The problem with this approach is that a heavy load is placed on both the server and connecting network. When multiple clients—thousands or perhaps millions of them—request information, the server must respond. In some cases, pull technology is a perfectly valid approach. For instance, when searching from a web browser, the search criteria is entered and the resultant information is returned for viewing. However, if constantly changing time-critical data are requested, this approach is not a good choice. The reason is that the client does not know when the data are new. If the polling interval is too short, the server is saturated with requests for data it does not have. If the interval is too long, the client will miss some data. It is nearly impossible to optimize the length of the poll interval.

On the other hand, "push technology" allows the server to send the data when they are ready for all interested parties. An example of push technology would be a graphical user interface that has a button. When the button is clicked, a notification is sent (i.e., pushed), indicating some action has occurred. In this scenario, a telemetry processor that delivers ISS data could also be pushed to different clients, such as web browsers, mobile devices, and desktop applications, with low overhead and significantly reduced resource requirements.

The Mission Control Center delivers telemetry using different approaches, which include both polling and pushing. The software, called the Information Sharing Protocol (ISP), uses push technology, but it does not provide a mechanism such as web browsers and mobile applications to deliver data to clients. A different solution that can leverage the ISP interface is required to accommodate these types of clients. Several commercial off-the-shelf solutions are available. Lightstreamer is one of these solutions. It was selected for its simple interface requirements, and it proved to be relatively easy to leverage the ISP interface as a data portal.

The static content of a website is delivered by the web server, while the dynamic content is sent from the push server. In this configuration, Lightstreamer can provide the push capability to different clients and avoid impacting the web server, as shown in figure 1.

Push Technology Approach to Information Streaming: ISS*Live!*

continued

While the ISP interface is efficient at processing and delivering data, it does not provide a web-based solution, nor does it provide a solution for mobile applications. ISP does have a well-defined application program interface that supports thick client development. At the time of development over 15 years ago, ISP predated the inception of mobile applications, and the world wide web was in its infancy. Consequently, ISP did not take into account these technologies. Since the delivery of the data uses the hypertext transfer protocol (http), the push server can be set up to use the secure http with the Secure Sockets Layer/Transport Layer Security. These are the same cryptographic protocols that provide communications security over the internet.

While the Lightstreamer server is primarily used for delivery of telemetry, it can be used to solve other problems that require low bandwidth with simple asyronchronous notification. For instance, most websites are backended by databases. In some cases, based on the business model, the web application may be waiting for a change to occur in the database before updating the view. The typical solution of course would be to poll the server for any changes. Consequently, this places undue loads on the database. A simpler solution would be to provide a "SqlDataAdapter" (Structured Query Language [SQL]) object that places a "SqlDependency object" on the database and the application—in this case, the data adapter. When a change is detected, the notification is sent to all interested parties. Other solutions might include the delivery of special data files (e.g., Extensible Markup Language) that an application may need to consume and process.

As NASA moves to the 21st century, the new emerging technologies are presenting new challenges and opportunities for more cost-effective system architectures. It is seen, in this example, that the push technology provides a flexible-yet-robust solution with less-intensive resource loading, hence cost savings. This architecture moves Johnson Space Center, the Mission Control Center, and NASA toward solutions that will allow the flight control team to work from anywhere, at anytime, without the geographic constraints of being physically located in the Mission Control Center. Moreover, because of the unique ability to isolate the data as one-way, this solution allows NASA, for the first time, to deliver real-time ISS telemetry to the real stakeholders and owners of the ISS—the American public.

International Space Station Power Planning and Analysis Tool

Molly Meyer-Allyn, *Johnson Space Center*
Dan Jackson, *Barrios Technology, Inc.*
Michael Genest, *United Space Alliance*
Thomas Miller, *Barrios Technology, Inc.*
Benjamin Chisholm, *United Space Alliance*
Aaron Allcorn, *Johnson Space Center*

The individuals supporting the International Space Station (ISS) from the Mission Control Center are known for their ability to manage complex systems, minimize error, and maximize success. Another innate ability that exists is to look for better, more innovative ways to accomplish day-to-day mission goals.

The Power Planning and Analysis Tool (PLATO) is one such innovation. PLATO is a single, integrated tool with a simple and intuitive user interface that will be used to perform analysis and planning of the generation, storage, and use of electrical power/energy onboard the ISS (figure 1). It will provide users with the ability to complete an end-to-end, 7-day International Space Station power analysis in 2 hours or less—a roughly five-fold decrease in the current time required. Its goals are to consolidate all current power planning tools under the PLATO umbrella; highly automate application setup, execution, and output display; simplify user interfaces; and simplify interfaces with providers of external inputs—the U.S. Operating Segment Systems, operations planners, payload planners, and international partners. Even as it makes ISS power planning much more expeditious, PLATO will maintain the same robust level of computational fidelity/accuracy as the current power analysis toolset.

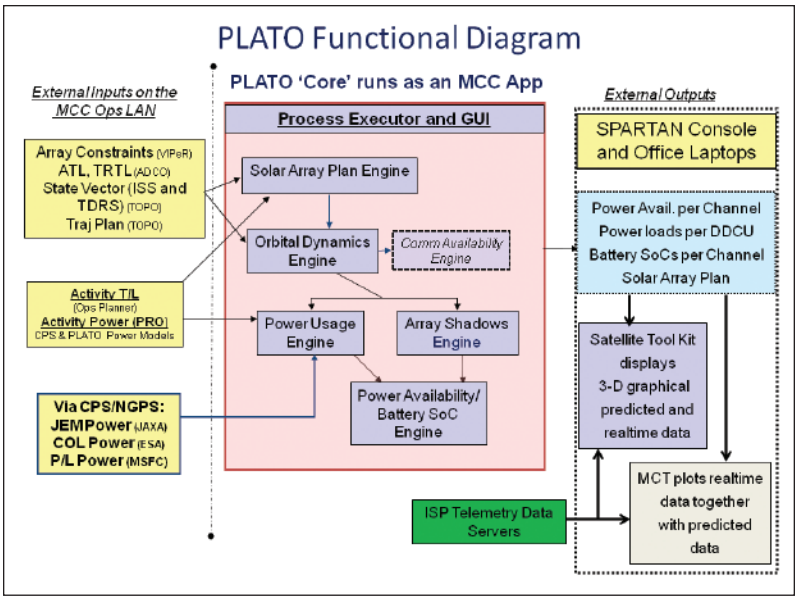


Fig. 1. *The Power Planning and Analysis Tool (PLATO) functional diagram.*

The power planning process that exists today uses nine separate applications involving an average of 20 hours of human interaction to complete a weekly plan. As a result of the efficiency to be provided by this tool, the ISS Power and External Thermal Systems Branch will be able to reduce its sustaining workforce by three people. This simplified and more automated process also mitigates the risk of human error that is present with the current, more manpower-intensive process.

The main internal components of PLATO consist of the following:

- ***Integrator/Graphic User Interface*** seamlessly integrates all the other components within the tool and eliminates or minimizes user involvement needed to complete end-to-end analysis after initial inputs have been made. It provides the user with an easy way to model complex operations and contingency scenarios and perform iterative "what-if" assessments for both. It also provides the user with a simple and fast way to define power downs and to determine the effects of power downs on channel/direct current to direct current converter unit power levels and battery states of charge (SoC).
- ***Solar Array Constraint Engine*** uses the attitude timeline, thruster configuration files, and ISS state vector to correlate mission timeline events with calculated array constraint matrices and constructs an optimized solar array plan that satisfies all solar array constraints while providing the optimal amount of power generation capability.

International Space Station Power Planning and Analysis Tool

continued

- ***Orbital Dynamics Engine*** propagates trajectory ephemeris from a state vector and trajectory plan, determines orbital sunrise/sunset times, calculates array pointing angles from the attitude timeline and solar array plan, and generates the integrated joint state file, which includes all the ISS solar array/sun angles as a function of time as well as other pertinent data files.
- ***Array Shadowing Engine*** uses satellite tool kit to process a three-dimensional graphical model of the ISS, orbital day/night data, and the integrated joint state file to determine shadow patterns on each solar array as a function of time. It then passes specific shadow pattern data for each solar array to the power availability engine.
- ***Power Usage Engine*** reads the appropriate ISS activity timeline from the ISS ops planner tools (Consolidated Planning System/ Next Generation Planning System), associated attitude, orbital beta angle, and sunrise/sunset data, Electrical Power System architecture configuration data, activity-specific power usage data, and inputs on power usage of the international partner modules and payloads, and then calculates total electrical loads as a function of time at various levels within the power distribution architecture.
- ***Power Availability/Battery SoC Engine*** calculates power availability and/or battery SoC as a function of time based on a defined power loads profile. In power availability mode, it calculates the total electrical load each channel can support given the amount of solar flux illuminating the solar arrays during insolation and the rate of discharge of the batteries during eclipse over each orbit in the analysis timeline without violating minimum operational SoC limit. In battery SoC mode, it determines the resultant battery SoC given the electrical loads per power channel, the amount of solar flux illuminating the arrays during insolation, and the rate of discharge of the batteries during eclipse for each orbit in the timeline.

Once operational, PLATO is expected to be equally accessible to users from multiple locations including the office environment, Mission Control Center/Mission Control-Houston, and all relevant training environments. Input and output data will flow freely between environments and platforms, including those associated with external sources of input data such as international partners and Marshall Space Flight Center/payloads.

In addition to its primary function as a power planning tool, PLATO will also have some capability to support real-time operations. It will be able to compare selected telemetry values pertinent to power resource management and to compare those values to the PLATO predictions. It will then notify the user—the SPARTAN flight controller—if there are significant deviations between actual and predicted values or developing trends that could lead to such a deviation.

Space Weather Monitoring Improves International Space Station Extravehicular Activity Safety and Operations

Steven L. Koontz, *Johnson Space Center*
Drew Hartman, *The Boeing Company*
Leonard Kramer, *The Boeing Company*
Danny Schmidl, *The Boeing Company*

The orbit of the International Space Station (ISS) causes the vehicle to pass through electrically conducting layers of the Earth's ionosphere. This environment, in combination with the 160-volt solar array power system on the ISS, facilitates an accumulation of varying electrical charge on the vehicle. The charge corresponds to an intrinsic electrical potential, posing a possibly catastrophic hazard to crew safety during extravehicular activity (EVA).

Recently, NASA—with support from Boeing (Houston, Texas)—has been engaged in studies of solar state and its effect on ionospheric conditions with the goal of providing operational constraint relief during EVA on the ISS.

Plasma contactor units (PCUs) operate during EVA to control the charging hazard. The corresponding electrical potential must be maintained to less than 40 volts between the ISS structure and the external ionospheric plasma. PCUs expel an artificially generated plasma, providing low resistance grounding path to bleed off any excess charge from the ISS. This achieves the specified hazard control.

There are two PCUs providing only two-fold redundancy and a third control is required according to NASA safety requirements for controlling possibly catastrophic hazards. This third control—invoked in the event that one PCU fails—is a carefully planned procedure consisting of an emergency shutdown of all eight ISS solar arrays to eliminate the immediate electrical hazard followed by a re-enabling of two arrays, thus permitting the EVA to go forward but with reduced power capability.

The careful planning of the emergency solar array shutdown is contingent on variables associated with the state of the ionopsheric plasma environment determined largely by preconditioning physical effects from the sun. The sun provides a highly variable ultraviolet flux that determines the plasma density (N_e) and the temperature of its electrons (T_e). The variability (N_e, T_e) plasma state is referred to as a space weather effect. Space weather along with the vehicle attitude directly determine the amount of electrical charge collected by the ISS. NASA's PCU failure contingency is planned according to the severity of worst-case attitude and plasma state scenarios determined though examination of historic records of ionosphere plasma conditions.

However, the worst-case conditions in the historic space weather climatology record place constraints on operations the can be relieved if real-time conditions can be monitored. As part of the ongoing process improvement activity, NASA, with the support of Boeing, is engaged in efforts to achieve this real-time space weather monitoring and, to the extent possible, relieve the constraints on mission power imposed by the existing PCU failure contingency.

There are resources available for monitoring and evaluating the plasma environment. NASA has developed a Floating Potential Measurement Unit (FPMU), which is a suite of instrumentation that provides diagnostic information originally deployed to validate the Plasma Interaction Model developed by Boeing for the purpose of understanding and controlling the charging properties of the ISS.

These tools are used for the contingency planning. Prior to any EVA, N_e, T_e, and floating potential (FP) are measured by the FPMU. These data are compared to the historic data set to determine whether the ionosphere is in a pre-established standard condition deemed sub-nominal (–2 Sigma), nominal (+/–1 Sigma), or active state (+2 Sigma). Figure 1 is a plot of N_e, T_e, and FP calculations given from the model for a pre-established environmental standard conditions.

The hazard condition usually occurs when the ISS emerges from eclipse. The data in figure 1 show that a –2 Sigma environment typically exhibits N_e below 1×10^{11} m^{-3} (per cubic meter). The nominal, +/–1 Sigma environment has a density about 5×10^{11} m^{-3} and the active environment; the +2 Sigma environment exhibits an enhanced density exceeding 10×10^{11} m^{-3}.

The calculated FP exemplifies the effect of plasma density on the electrical charging state of the vehicle. In the –2 Sigma state, FP ranges from about –8 to –25 volts. In the nominal case, FP ranges from –35 to –40 volts; in the active case, the FP is more negative than –40 volts. The active case violates operational hazard control

Space Weather Monitoring Improves International Space Station Extravehicular Activity Safety and Operations

continued

constraints whereas the nominal and sub-nominal cases are within safe limits.

The active ionospheric case must be protected against but is not uniformly present. Based on the historical space weather climatology, tables are prepared that specify the number of solar arrays that need to be pointed to wake during a PCU failure. This task is performed for each EVA.

Without real-time monitoring, the plan for PCU failure would continue the EVA with only two arrays active, which would impose severe restrictions on operational capability resulting from the lost electrical power and often leads to required termination of the EVA.

However, figure 2 illustrates the actual measured state (N_e, T_e, and FP) of the ionosphere for comparison with the model predictions based on historical climatology in figure 1. The actual floating potential experienced by the vehicle was much less severe than that predicted according to the worst-case planning. This is a result of lower-density plasma prevailing at times when worst-case planning predicted severe charging.

Figure 3 is a product produced to support EVA according to the improved process. This table shows that the largest FP at critical positions on the ISS structure for the range of Sigma state conditions.

Because it was determined that the environment in this example is in a sub-nominal state, only two of the eight arrays needed to be taken out of service. Previously it would have been necessary to shut down six arrays.

Work is continuing to streamline processes and to exploit other space weather forecasting metrics. Predicting the state of the ionosphere is challenging, owing to scientific uncertainty concerning the physics controlling solar activity

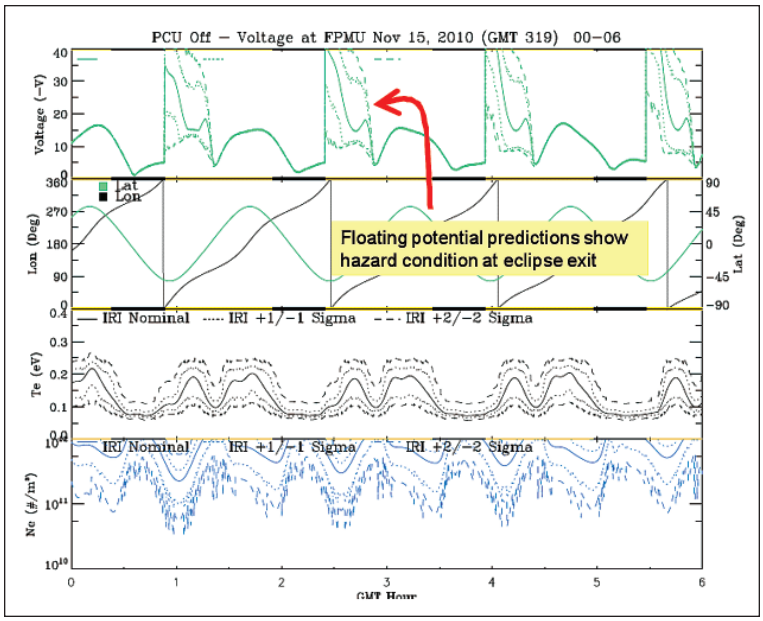


Fig. 1. *Plasma Interaction Model floating potential predictions for differing (including worst-case planning).*

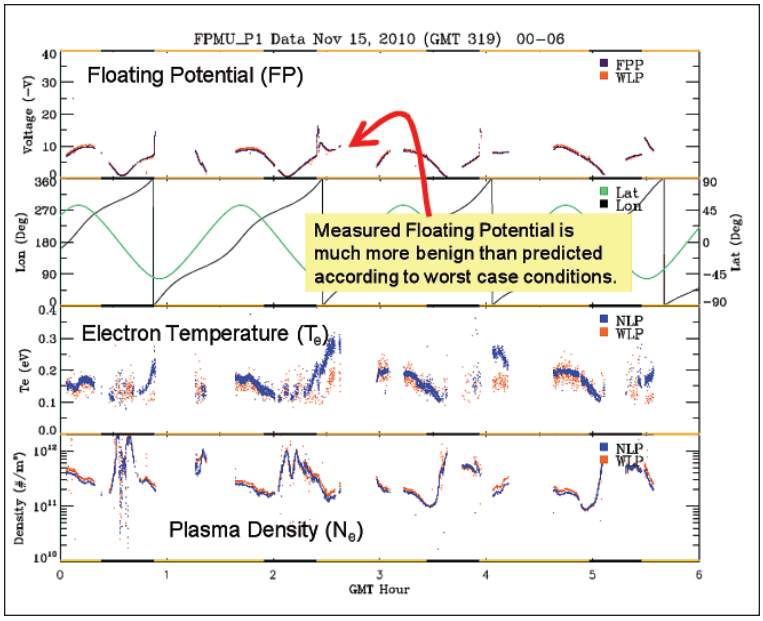


Fig. 2. *Floating Potential Measurement Unit observations show that the actual state of the ionosphere was much less severe than that predicted by worst-case conditions.*

				+2 Sigma					0 Sigma					-1 Sigma					-2 Sigma				
GMT Day	Shunt	Config	Attitude	Port Truss Tip	Stbd Truss Tip	Port SARJ	Stbd SARJ	center	Port Truss Tip	Stbd Truss Tip	Port SARJ	Stbd SARJ	center	Port Truss Tip	Stbd Truss Tip	Port SARJ	Stbd SARJ	center	Port Truss Tip	Stbd Truss Tip	Port SARJ	Stbd SARJ	cen
2010_319	All	Complete	XVV	-36.91	-32.27	-28.14	-24.60	-18.35	-36.99	-32.41	-28.21	-24.75	-18.42	-37.04	-32.39	-28.27	-24.72	-18.48	-37.05	-32.42	-28.28	-24.76	-18.
2010_319	S4,P4,P6	Complete	XVV	-39.00	-32.31	-30.22	-24.65	-20.44	-37.86	-32.40	-29.12	-24.74	-19.42	-37.60	-32.39	-28.82	-24.72	-19.05	-37.49	-32.39	-28.72	-24.73	-18.
2010_319	S4,P4,S6	Complete	XVV	-37.98	-32.31	-29.20	-24.65	-19.43	-37.40	-32.36	-28.63	-24.70	-18.87	-37.26	-32.40	-28.49	-24.74	-18.72	-37.28	-32.45	-28.51	-24.78	-18.
2010_319	P4,P6,S6	Complete	XVV	-38.85	-32.29	-30.08	-24.63	-20.32	-37.76	-32.41	-29.02	-24.74	-19.32	-37.49	-32.38	-28.72	-24.72	-18.95	-37.45	-32.40	-28.68	-24.74	-18.
2010_319	S4,P6,S6	Complete	XVV	-38.10	-32.30	-29.33	-24.64	-19.54	-37.48	-32.37	-28.70	-24.70	-18.91	-37.34	-32.38	-28.57	-24.72	-18.78	-37.32	-32.40	-28.55	-24.74	-18.
2010_319	S4,P4	Complete	XVV	-40.63	-32.29	-32.96	-24.62	-28.77	-38.46	-32.39	-29.72	-24.73	-25.16	-37.85	-32.41	-29.08	-24.75	-21.26	-37.71	-32.43	-28.94	-24.77	-19.
2010_319	P4,P6	Complete	XVV	-47.39	-32.28	-38.69	-27.50	-32.43	-38.99	-32.39	-33.13	-24.73	-28.64	-38.12	-32.39	-29.35	-24.73	-24.14	-37.94	-32.45	-29.17	-24.79	-19.
2010_319	S4,P6	Complete	XVV	-41.59	-32.30	-33.90	-25.10	-29.31	-38.57	-32.41	-29.98	-24.75	-25.67	-37.90	-32.40	-29.12	-24.73	-21.74	-37.76	-32.44	-28.99	-24.78	-19.
2010_319	P4,S6	Complete	XVV	-40.29	-32.29	-32.15	-24.62	-28.29	-38.38	-32.39	-29.64	-24.73	-24.64	-37.78	-32.37	-29.01	-24.71	-20.69	-37.65	-32.46	-28.88	-24.80	-19.
2010_319	S4,S6	Complete	XVV	-39.38	-32.25	-30.66	-24.59	-25.99	-37.90	-32.40	-29.14	-24.74	-22.37	-37.59	-32.37	-28.82	-24.70	-19.05	-37.47	-32.39	-28.70	-24.73	-18.
2010_319	P6,S6	Complete	XVV	-40.62	-32.28	-33.00	-24.62	-28.78	-38.50	-32.35	-29.76	-24.69	-25.12	-37.81	-32.43	-29.04	-24.77	-21.22	-37.72	-32.42	-28.95	-24.76	-19.
2010_319	P4	Complete	XVV	-55.68	-36.71	-48.76	-39.73	-43.99	-48.59	-32.36	-44.06	-35.14	-39.71	-42.05	-32.41	-38.16	-29.97	-34.79	-38.16	-32.43	-29.39	-24.77	-22.
2010_319	S4	Complete	XVV	-50.81	-34.91	-45.53	-37.78	-41.96	-45.68	-32.41	-41.22	-33.19	-37.56	-39.68	-32.37	-36.03	-28.00	-32.72	-37.97	-32.40	-29.19	-24.74	-20.
2010_319	P6	Complete	XVV	-56.80	-37.14	-49.51	-40.14	-44.49	-49.16	-32.44	-44.66	-35.57	-40.21	-42.57	-32.37	-38.60	-30.41	-35.27	-38.20	-32.46	-29.46	-24.80	-23.
2010_319	S6	Complete	XVV	-49.93	-34.51	-44.89	-37.35	-41.47	-45.01	-32.41	-40.62	-32.77	-37.13	-39.15	-32.41	-35.55	-27.59	-32.20	-37.92	-32.43	-29.15	-24.77	-20.
2010_319	None	Complete	XVV	-62.71	-45.72	-56.99	-48.69	-52.89	-56.69	-40.65	-52.23	-43.77	-48.25	-49.95	-34.98	-46.32	-38.15	-42.92	-38.55	-32.41	-33.17	-24.75	-29.

Fig. 3. *Real-time monitoring permits identification of benign International Space Station charging environmental conditions.*

and the ionosphere's response to it. For example, in recent years, the activity of the sun has been anomalously weak and this was not predicted by the scientific community.

The FPMU instrumentation was originally commissioned to validate Boeing modeling effort. However, its value to the ISS as a source of real-time data for the purpose of supporting EVA safety has become apparent. FPMU measurements are now a part of formal operational planning and its ground support equipment are being upgraded for long-term program use.

In summary, NASA, with Boeing's support, has been working toward real-time monitoring of the ionospheric environment associated with space weather influences for the purpose of relieving constraints on power availability in the event of PCU failure during an EVA. These efforts have yielded clear improvements that permit nearly normal operations during the majority of any EVA contingency involving PCU failure. The increased power availability has the effect of increasing productivity of the operations workforce at minimal cost without impacting safety.

Mission Control Technologies Project

Alan R. Crocker, *Johnson Space Center*

The Mission Control Technologies (MCT) project is a collaborative effort between NASA Johnson Space Center and NASA Ames Research Center to develop and deploy new user interface software to support real-time spacecraft mission operations. MCT provides a unique object-oriented method to manage data—vehicle telemetry, analysis data, archived information, and more—in an intuitive manner that increases the efficiency of the spacecraft operator. As compared to off-the-shelf tools, the MCT technique literally reverses the way in which operators interact with their tools, making the tools organize the data in the same way that the operator thinks of that data.

MCT provides users with the reusable building blocks necessary to assemble user interfaces in whatever form and organization they need (figures 1 and 2). A user can grasp the basic capabilities provided by MCT in minutes. MCT also provides industry standard plug-and-play interfaces that allow the software to be used in multiple facilities and by multiple organizations. The software components that make up MCT can be separately tested and certified without requiring costly recertification of entire applications. MCT's architecture allows both easy integration of data from multiple sources and a cost-effective means to update the ways in which users view that data. MCT components will support vehicle telemetry monitoring, spacecraft commanding, ground-based performance analysis, and other operations functions. Separate development projects can use MCT to build other capabilities such as electronic procedure authoring and execution tools, and facility operation user interfaces.

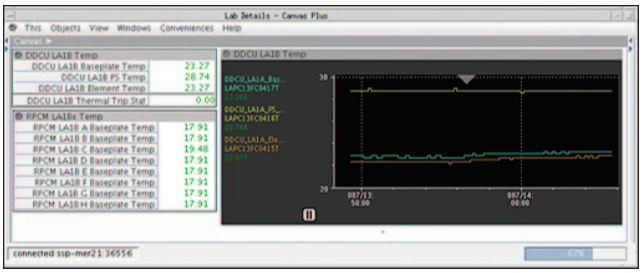


Fig. 2. *Viewing International Space Station data in Mission Control Technologies.*

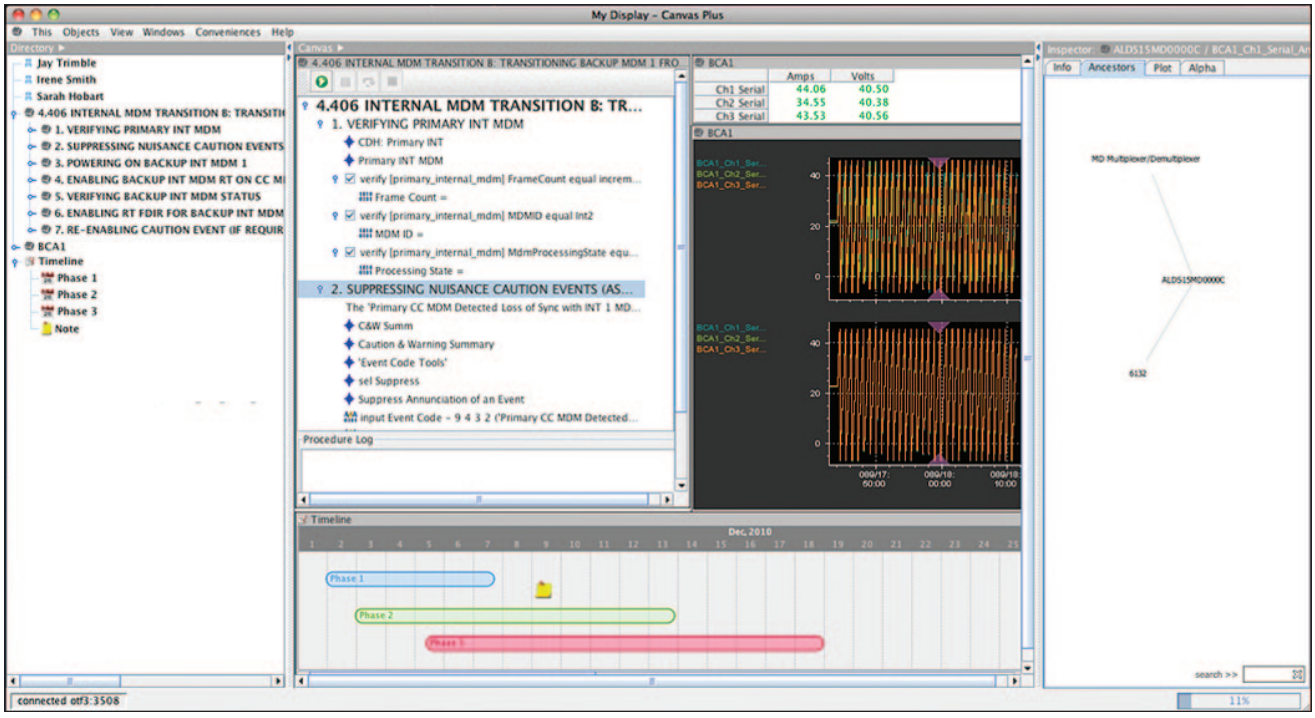


Fig. 1. *A variety of software components available in the Mission Control Technologies toolkit.*



Fig. 3. *Collaborative design of Mission Control Technologies capabilities.*

Since 2006, Johnson Space Center and Ames Research Center have worked together to define and develop this technology, teaming spacecraft operations personnel directly with user experience designers and software developers in a unique teamwork environment. To define the requirements and design for software deliveries, the team analyzes the processes through which users interact with their software tools and identifies the "pain points" and potential inefficiencies in those processes. From this research, the team first defines more efficient processes and then determines the requirements and design implementations necessary to support those processes (figure 3).

The first operational version of MCT is undergoing integration into the Mission Control Center, with future deliveries expanding MCT's capabilities. By the end of 2012, MCT will replace multiple legacy software tools with a more streamlined and extensible toolset supporting the International Space Station and future spacecraft operations. Other NASA centers are investigating use of MCT to meet their operational needs as well.

Development of the International Docking System Standard

Joe Anderson, *Johnson Space Center*
Tim Briscoe, *Johnson Space Center*
Monty Carroll, *Johnson Space Center*
Stan Donahoe, *Johnson Space Center*
Steve Gaylor, *Johnson Space Center*
Robert Grady, *Johnson Space Center*
Skip Hatfield, *Johnson Space Center*
Sean Kelly, *Johnson Space Center*
Thang Le, *Johnson Space Center*
James Lewis, *Johnson Space Center*
George Parma, *Johnson Space Center*
Ben Quasius, *Johnson Space Center*
Alexander Tabakman, *Johnson Space Center*

Improving the affordability of future space flight programs is one of the big challenges for NASA as budgets continue to decrease. As exemplified by the current International Space Station (ISS) Program, future large-scale space initiatives will be successful using collaborations with other nations to share the cost burden while achieving the long-term technical goals and benefits. As U.S. Governmental and Agency policies shepherd us toward more global cooperation via such programs, we will find that the development and standardization of space flight elements will enable nations and industries to focus their respective contributions toward a broader collective effort. One such standardization effort initiated, in December 2008, is the International Docking System Standard (IDSS), whose first product—the IDSS Interface Definition Document (IDD)—was initially released in September 2010. This document establishes a recommended standard docking interface to be used for joint collaborative endeavors while enabling potential rescue missions. The interface is based on both validated designs and new technologies.

The IDSS IDD was developed by NASA along with its International Space Station partners, the Canadian Space Agency, European Space Agency, Japanese Space Agency, and the Russian Space Agency. The IDD provides the basic geometry and design parameters that would allow developers to independently design compatible docking systems suitable to their own unique program and mission requirements. The IDSS is intended for crewed or autonomous space vehicle applications ranging from low-Earth orbit to deep-space exploration missions. Among these missions are ISS visitation, lunar exploration, crew rescue, and international cooperative missions.

Detailed physical geometry of the mating interface, along with some performance requirements—i.e., design loads for initial docking capture event and mated loads—have been defined. Adhering strictly to the geometric interface definition ensures physical mating compatibility while accommodating the documented performance requirements supports a broad set of design reference missions and



Fig. 1. *Androgynous Peripheral Assembly System.*

conditions, thus increasing the probability of successful docking between different spacecraft. Additionally, using this standard by future developers will provide easier program planning and integration of collaborative efforts of the future.

Achieving total agreement among the International Partners on a docking interface standard proved to be challenging. There is a long history of success with existing docking systems, like the Androgynous Peripheral Assembly System (APAS) built by Rocket Space Corporation-Energia, which has been used on the space shuttle orbiter and the ISS (figure 1). However, new docking system technology development efforts have been under way at NASA for many years and offer important benefits over existing technologies. The Low Impact Docking System (LIDS)/NASA Docking System (NDS) has been under development to specifically address docking challenges associated with a wide array of vehicles, ranging from ultra-light satellites to large space vehicles like the ISS (figure 2). As one can imagine, bringing these two technologies together as a standard created a number of technical challenges and resulted in the need for several key trades regarding standardization of the necessary geometric structures and performance

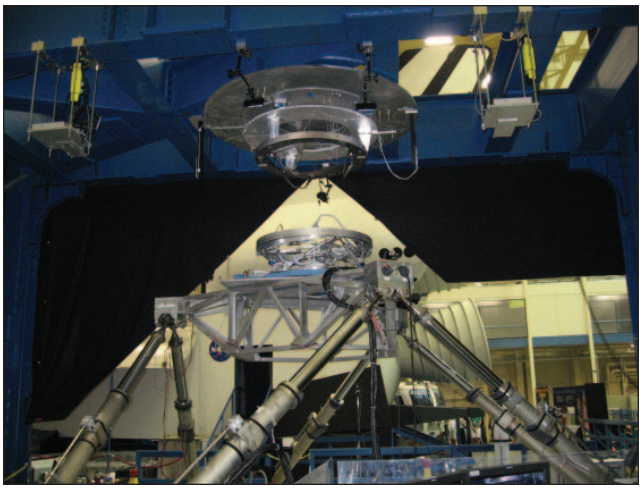


Fig. 2. *NASA Docking System soft capture system degree-of-freedom testing.*

capabilities. It was a goal of the IDSS team to find a way to blend the best of the legacy system (APAS passive mechanical design) with new technology (active force feedback system NDS design) designs to create an international standard.

A docking standard must define the basic geometry of both the capture system and the structural latching/hard docking system. Successes of the operation of the Apollo Soyuz Test Program and APAS docking mechanisms drove early decisions to standardize interface androgyny (meaning the interface configuration is capable of mating to an identical configuration) to enable crew rescue. As such, the characteristics of the APAS mechanism were used as the starting model, but because the new technology designs of NASA required a wider capture system ring than that of APAS, the wide ring soft capture interface became fundamental to the agreement for the docking standard. Another key decision was to maintain the structural latching interface/hard docking ring based on the APAS hard mate geometry. Maintaining the legacy geometry allowed the Russian Space Agency to continue with existing hard dock manufacturing lines and vehicle architectures, but resulted in a slightly reduced capture ring diameter that impacted the transfer tunnel dimensions and the capture performance envelope. These impacts required the team to perform capture system trade studies.

After an in-depth review of the resulting dimensions of the passageway and capture system performance capabilities, the team determined that the resulting specifications satisfied system performance requirements. In addition, implementing a petal design scheme with folding or removable capture system petals will enable a larger transfer passageway, if needed, in contingency scenarios. These decisions resulted in the definition of the basic geometry of the IDSS.

Trade-offs for other interface features of the capture system and the hard dock system were also studied in detail. For soft capture, it was decided to accommodate the features of both mechanical and magnetic capture latch passive systems. This would ensure that docking principles of different countries would be honored, while preserving a future goal toward commonality. The hard dock system features of fine alignment, seal placement and hooks were adopted from the APAS. For other features like separation systems and sensors, designated striker areas were allocated and standardized to allow some flexibility for implementation by developers (striker areas are defined, free areas for active components on one mating half to press against the opposite mating half during docking operations). Resource umbilicals were not standardized as deemed program unique, but future work may be organized to standardize designated areas for umbilical location. It is also a possibility in the future to agree on a specific umbilical standardization if determined beneficial by the IDSS team.

An April 2011 modification of the IDSS resulted in the successful combination of the legacy system hard dock features and dimensions of the APAS with new technology soft capture ring dimensions of the LIDS/NDS low impact system (figure 3). With this standard completed, developers around the world can use it as the basis for their future designs. While the NDS development activities are targeted toward completion and implementation of this standard on the ISS by 2014, other countries and industry are foreseen to take much longer. Having the IDSS available on the ISS is expected to provide the impetus for future ISS visiting vehicles to use the new standard and to establish an excellent test bed from which to gain operational experience.

Development of the International Docking System Standard

continued

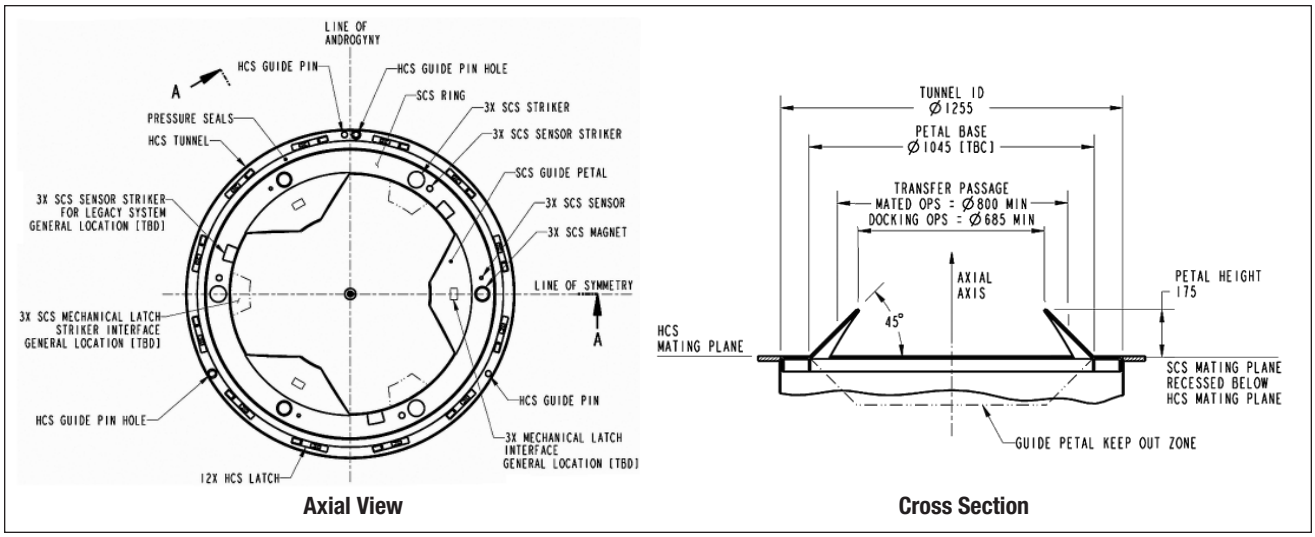


Fig. 3. *International Docking System standard interface.*

The website http://www.internationaldockingstandard.com was established to provide the global community access to the IDD. Plans are under way for further development of the IDSS standard website to include test and verification strategies, docking principles, information on compliant IDSS systems, etc. (figure 4). Collaboration between current IDSS partners will continue, and others are expected to join this technical community. As discussions continue, evolution of the IDSS is anticipated along with additional collaborations within the docking discipline.

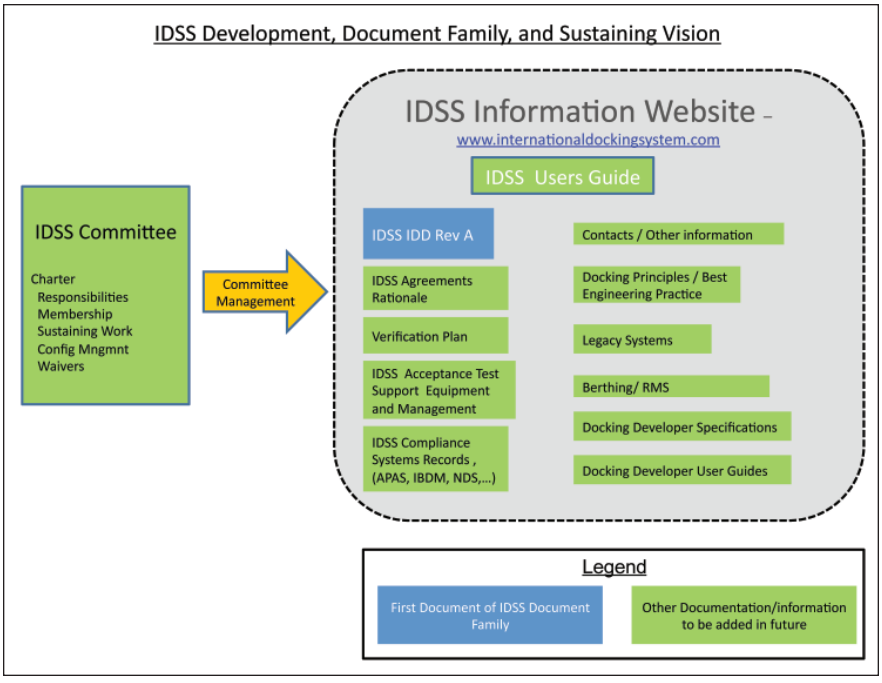


Fig. 4. *International Docking System Standard development, document family, and sustaining vision.*

Integrated Ultra-Wideband Tracking and Communication System

Jianjun (David) Ni, *Johnson Space Center*
Dickey Arndt, *Johnson Space Center*
Phong Ngo, *Johnson Space Center*
Chau Phan, *Johnson Space Center*
Kent Dekome, *Johnson Space Center*
John Dusl, *Johnson Space Center*

This report briefly discusses a design effort for a prototype Ultra-Wideband (UWB) Tracking and Communication System that is currently under development at NASA Johnson Space Center (JSC). The system is being designed to provide tracking and communication (audio/video) capabilities to the personnel working in and around the launch pad structures at Kennedy Space Center for safety enhancement. The UWB technology is exploited to implement this integrated tracking and communication system due to the technology's properties such as high data rate, fine time resolution, low power spectral density, and multipath immunity. The UWB Systems Group at JSC has developed a UWB two-cluster Angle of Arrival (AOA) Tracking Prototype System, which can provide long-range tracking capability. In this design effort, the communication functionalities (two-way voice and one-way video) are integrated into this tracking system. This report summarizes the development effort with system design configuration and field tests that validate the system's integrated tracking and communication capabilities.

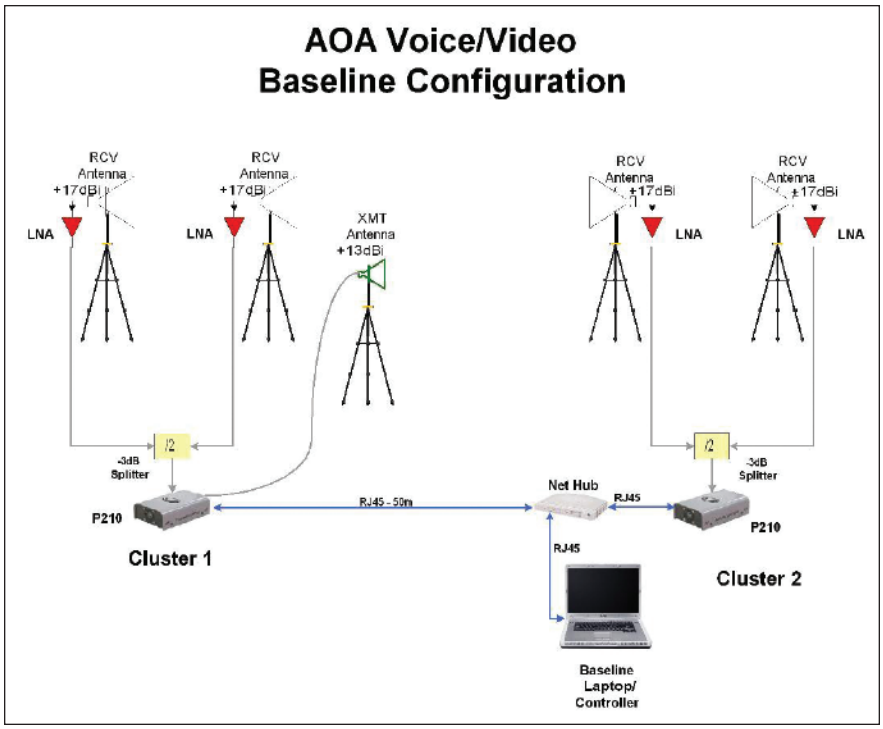


Fig 1. *Baseline configuration of integrated Ultra-Wideband Tracking and Communication System.*

System Design

The extremely high fidelity of the UWB timing circuitry permits precise measurements of propagation time while transmitting data. A key element of the tracking system design philosophy is to avoid introduction of system components or structure that would in any way degrade the fine time resolution of the UWB signal since it is critical for precise tracking. In keeping with this goal, the AOA technique using time-difference-of-arrival estimates is adopted for tracking to avoid the degradation in time resolution introduced by synchronization errors between the transmitter and receiver. A two-cluster prototype tracking system has been designed. This system connects two antennas through a power combiner to one UWB radio at each cluster using low-loss, phase-aligned interconnect cables with precisely calibrated delays. A two-way link is required for two-way voice/one-way video communication. An additional antenna is connected to the transmitting port of one cluster radio. Baseline configuration is illustrated in figure 1. Baseline consists of two clusters. Each cluster has one UWB radio with two receiving horn antennas (+17 decibels [dB]) connecting to its receiving port through low-noise amplifiers and power combiner. In cluster one, a transmitting horn antenna (+13 dB) is connected to the transmit port of the radio. Both radios are connected to the baseline control laptop through a hub. The configuration on the target side is illustrated in figure 2. The target carries a backpack with one UWB radio and power supply inside. The radio is connected to two omni-antennas for both transmitting and receiving. A netbook computer is connected to the radio for control and display. Headset, microphone, and web camera are all connected to the

Integrated Ultra-Wideband Tracking and Communication System

continued

netbook for audio and video communication. The AOA tracking software is developed in house. A commercial off-the-shelf application software VSee is used for audio and video communication.

Field Test

The test of the integrated UWB tracking and communication prototype system has been conducted at the antenna test range behind Building 14 at JSC. The test setup is shown in figure 3. On the baseline side, two clusters are set up with baseline size of 35 m (~115 ft) and antenna distance of 15 m (~49 ft) in each cluster. On the target side, the test personnel carry a backpack with a UWB radio and transmit/receive antennas mounted on a pole. He or she also carries a portable computer for control and display. A calibration point is set as (0, 303) m ([0, ~ 995] ft). The test shows that the system can track the moving target and maintain audio/video communication between target and baseline up to the range of 366 m (~ 1200 ft). The quality of two-way voice is very good and the quality of one-way video is good. The tracking data update rate is up to 10 hertz.

Conclusion

An integrated UWB tracking and communication system has been designed, implemented, tested, and proven feasible for tracking a moving target as well as communicating with the target through voice and video. These integrated capabilities can enhance the safety of the launch personnel at Kennedy Space Center. This system can also serve as a test bed for the lunar surface tracking and communication in the future. Future work includes expanding the system capability to track and communicate with multiple targets using the concept of reverse tracking.

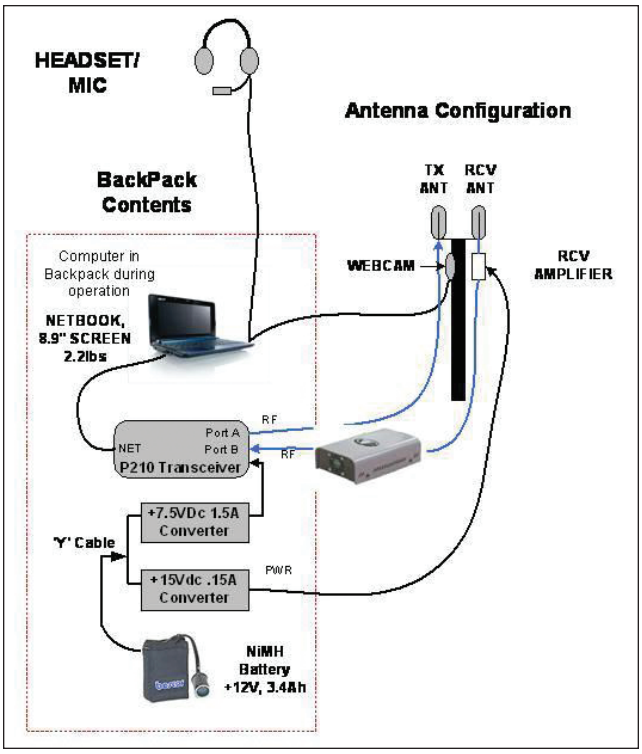


Fig 2. *Target configuration of integrated Ultra-Wideband Tracking and Communication System.*



Fig 3. *Integrated Ultra-Wideband Tracking and Communication System test setup (target and baseline).*

Ultra-Wideband Tracking System Design for Relative Navigation

Jianjun (David) Ni, *Johnson Space Center*
Dickey Arndt, *Johnson Space Center*
Phong Ngo, *Johnson Space Center*
Kent Dekome, *Johnson Space Center*
John Dusl, *Johnson Space Center*
Jodi Graf, *Johnson Space Center*

This report briefly discusses a design effort for a prototype Ultra-Wideband (UWB) Time-Difference-of-Arrival (TDOA) Tracking System that is currently under development at NASA Johnson Space Center (JSC). The system is being designed for use in localization and navigation of a rover in a Global Positioning System-deprived environment for surface missions. In one application enabled by the UWB tracking, a robotic vehicle carrying equipments can autonomously follow a crewed rover from work site to work site such that resources can be carried from one landing mission to the next, thereby saving up-mass. The UWB Systems Group at JSC has developed a UWB TDOA High-Resolution Proximity Tracking System that can achieve sub-inch tracking accuracy of a target within the radius of the tracking baseline. A tracking system is being designed and tested to enable relative navigation between two vehicles for surface missions by extending the tracking capability beyond the radius of the tracking baseline.



Fig. 1. *Ultra-Wideband Time-Difference-of-Arrival Tracking System configuration for relative navigation.*

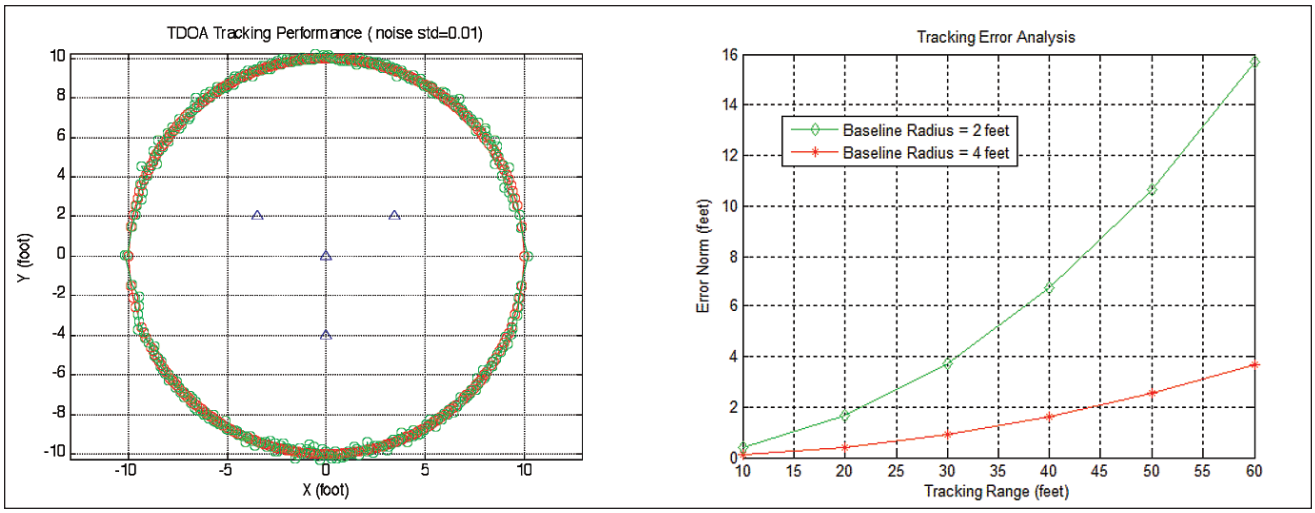
System Design

In a general mission operation scenario, the crewed rover is the leading vehicle and the robotic equipment rover is the following vehicle. To autonomously follow the leading vehicle, the following vehicle needs the accurate relative position information of the leading vehicle with an adequate update rate according to the relative velocity between two vehicles.

For this prototype design (figure 1), one UWB P210 transmitting radio with an omni antenna is mounted on the leading vehicle; a one-radio, four-antenna configuration is used on the following vehicle to eliminate the synchronization issue among receivers. Four receiving antennas are connected to one UWB radio receiver through a power combiner. A TDOA tracking algorithm is adopted to avoid the synchronization between transmitter and receiver. A signal processing technique—Cross-Correlation plus Peak-Detection—was developed to enable robust TDOA estimate in a noisy multipath environment. With received signals processed using the TDOA estimation algorithm, the position of the leading vehicle can be tracked. The tracking data are used by the following vehicle for autonomous control.

Performance Analysis

The UWB TDOA High-Resolution Proximity Tracking System can achieve sub-inch tracking accuracy of a target within the radius of the tracking baseline. To analyze the tracking error behavior and gain some insight regarding achievable tracking resolution when the target is outside of the baseline, the group performed simulations using the same TDOA tracking algorithm with tracking range greater than the baseline radius. The simulation results in figure 2 show that the TDOA tracking error is proportional to the square of the ratio (R/r), where "R" is the tracking range and "r" is the radius of baseline. By choosing the baseline radius of 1.2 m (4 ft), a tracking error about 1.16 m (~3.8 ft) can be achieved at range of 18 m (60 ft) while a tracking error about 0.03 m (~0.1 ft) can be achieved at range of 3 m (10 ft). Hence, this tracking performance behavior (more accurate when two vehicles get closer) is feasible for the application of vehicle following.



a. Tracking Scenario **b. Tracking Error Analysis**

Fig. 2. *Ultra-Wideband Time-Difference-of-Arrival Tracking System performance outside of baseline.*

Field Test

The field test of this tracking prototype system has been conducted at the antenna range behind Building 14 at JSC. The tests show that the UWB Tracking System at the following vehicle can track the leading vehicle in real time with a update rate of 1 Hertz (Hz) by running the experimental code. It is anticipated that the update rate can be improved greater than 5 Hz with immigrants to the application code.

Conclusion

A prototype UWB TDOA Tracking System has been designed, implemented, tested, and proven feasible for relative navigation of robotic vehicles. Future work includes testing the system with the application code to increase the tracking update rate, and evaluating the linear tracking baseline to improve the flexibility of antenna mounting on the following vehicle.

Ultra-Wideband Time-Difference-Of-Arrival Two-Point-Tracking System

Jianjun (David) Ni, *Johnson Space Center*
Dickey Arndt, *Johnson Space Center*
Phong Ngo, *Johnson Space Center*
Chau Phan, *Johnson Space Center*
Kent Dekome, *Johnson Space Center*
John Dusl, *Johnson Space Center*

This report briefly discusses a design effort for a prototype Ultra-Wideband (UWB) Time-Difference-of-Arrival (TDOA) Two-Point-Tracking System that is currently under development at NASA Johnson Space Center (JSC). The system is being designed for use in assisting a docking process in a two-dimensional (2-D) space; e.g., the lunar rover Chariot docking to its battery charging station. The UWB Systems Group at JSC has developed a UWB TDOA High-Resolution Proximity Tracking System, which can achieve sub-inch tracking accuracy of a target. A two-point-tracking system is designed to enable aligning a vehicle docking into its station in a 2-D space by using this high-resolution tracking capability.

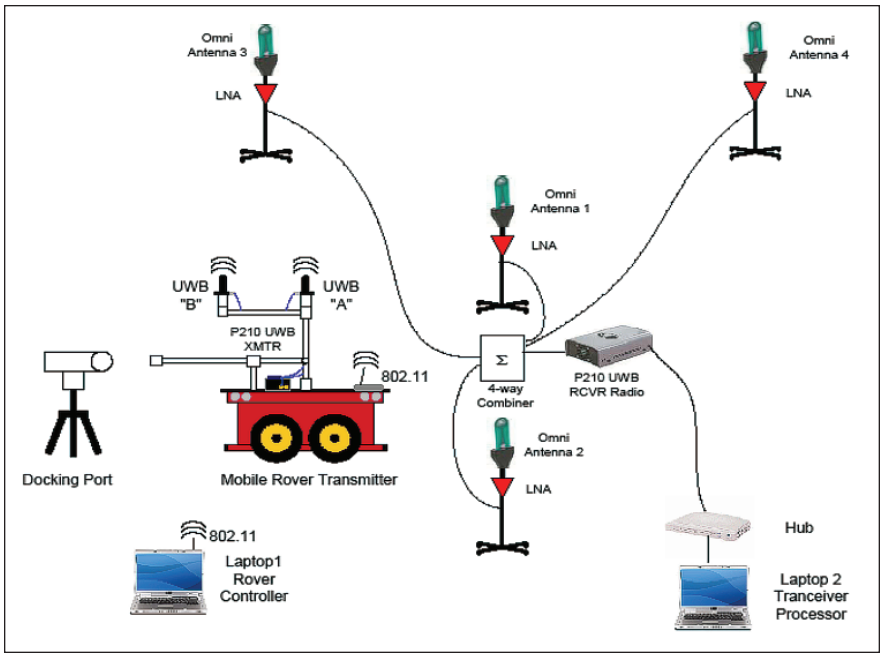


Fig 1. *Baseline configuration of integrated Ultra-Wideband Tracking and Communication System.*

System Design

To dock a vehicle in a 2-D space, the controller needs the location information of at least two points of the vehicle. With that two-point information, the vehicle can be aligned with the planned docking trajectory. For this prototype design, one point (Primary Point) is chosen at the center of the vehicle and another point (Secondary Point) is chosen 0.3 m (1 ft) apart from the center at the front of the vehicle. Primary Point aligns with Secondary Point along the center line. The system configuration is illustrated in figure 1. On the vehicle, one UWB P210 transmitting radio is connected with two antennas through a two-way power splitter. Antenna "A" represents Primary Point and antenna "B" represents Secondary Point. Antenna "B" has a cable delay of about 5 nanoseconds (ns) compared to antenna "A." The vehicle is controlled through an 802.11 wireless link. On the receiving side, a one-radio, four-antenna configuration is used to eliminate the synchronization issue among receivers. Four receiving antennas are connected to one UWB radio receiver through a power combiner.

Performance Analysis

When the transmitter radio on the vehicle transmits one signal, two versions of the same signal are transmitted through two transmitting antennas. Due to the cable delay added to Antenna "B" being greater than the spatial delay between Antenna "A" and Antenna "B," the received signal from Secondary Point is delayed (from 4 ns to 6 ns, depending on the vehicle orientation) and will show up after the Primary Point signal (figure 2). In one scan window, there are four pairs of signals (one pair consists of a Primary Point signal and a Secondary Point signal). A TDOA tracking algorithm is adopted to avoid the synchronization between transmitter and receiver. A signal processing technique—Cross-Correlation plus Peak-Detection—is developed to enable robust TDOA estimate in a noisy multipath environment. With some minor modification of this TDOA estimation algorithm, the positions of the Primary Point and the Secondary Point can be tracked within sub-inch accuracy.

Ultra-Wideband Time-Difference-Of-Arrival Two-Point-Tracking System

continued

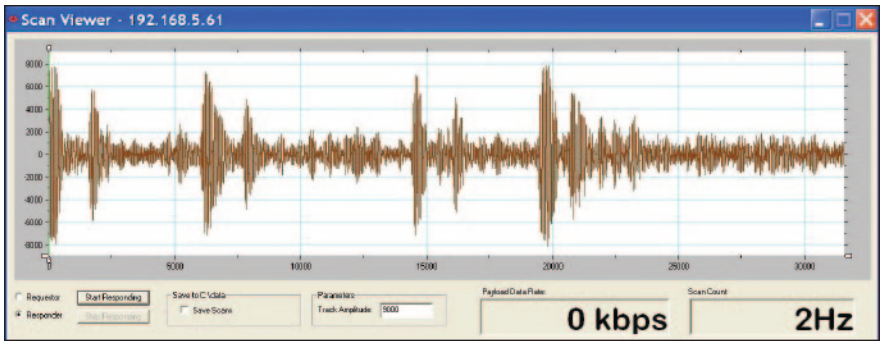


Fig. 2. *Four pairs of signals in one scan window.*

Laboratory Test

The test of the two-point-tracking prototype system has been conducted in the Building 14 High Bay area at JSC. The tests show that the system can track both the Primary Point and the Secondary Point of the vehicle accurately (errors are less than one inch). The controller can use this information to successfully guide the vehicle into its docking station (figure 3) in a 2-D space.

Conclusion

A prototype UWB TDOA two-point-tracking system has been designed, implemented, tested, and proven feasible for docking applications in a 2-D space. Future work includes expanding the tracking area to the size of Chariot docking site and testing the docking process with the actual dimension of the Chariot battery charging station.

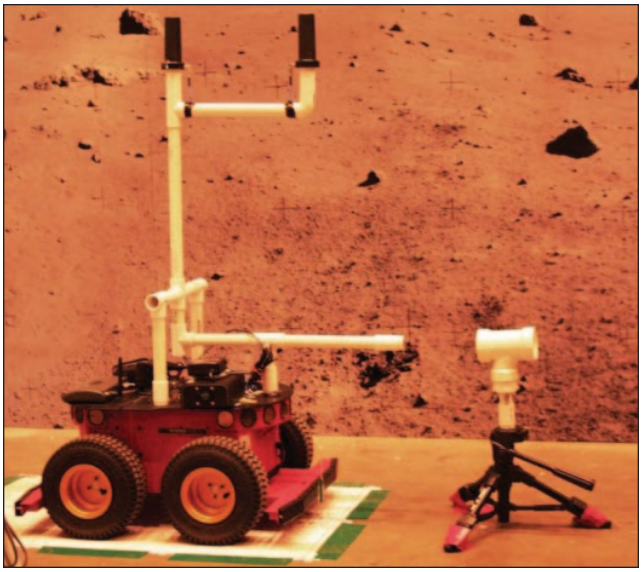


Fig. 3. *Docking process guided by two-point-tracking.*

Variable Bragg Peak Methodology for Testing Electronic Parts

Charles R. Bailey, *Johnson Space Center*
Patrick M. Oneill, *Johnson Space Center*

The Variable Bragg Peak Method (VBPM) is a new methodology for testing electronic parts for ionizing radiation susceptibility using the Brookhaven National Laboratory (BNL) (Upton, New York) cyclotron. Dr. Patrick Oneill, with collaboration from Dr. Charles Foster and the staff physicists at the BNL, developed the method. The new method uses the high-energy beam at BNL in a way that can characterize the electronic parts without having to de-lid the parts, and will also enable the characterization of thick electronic parts that have been difficult to characterize using other cyclotron sources. The method also enables testing of parts at the board level, although the development of the procedures for this are ongoing.

The specifics of the methodology involved the degradation of a high-energy beam to control the position in space of the Bragg peak. The degradation of the beam is accomplished by a series of plastic masks of varying depths that are controlled by the user (figure 1). Significant modeling of the high-energy heavy ion beam through this material was required to determine the exact nature of the beam contacting the electronic part. As the beam passes through each layer of plastic, the speed (energy) of the beam is diminished and the Bragg peak and consequent linear energy transfer is moved along the x-axis. The Bragg peak is moved through the part until the sensitive volume is characterized. Figure 2 shows a representation of the Bragg peak movement.

This method will make the characterization of some part package types available for the first time while making the characterization process cheaper and more reliable due to not having to de-lid a part for this test.

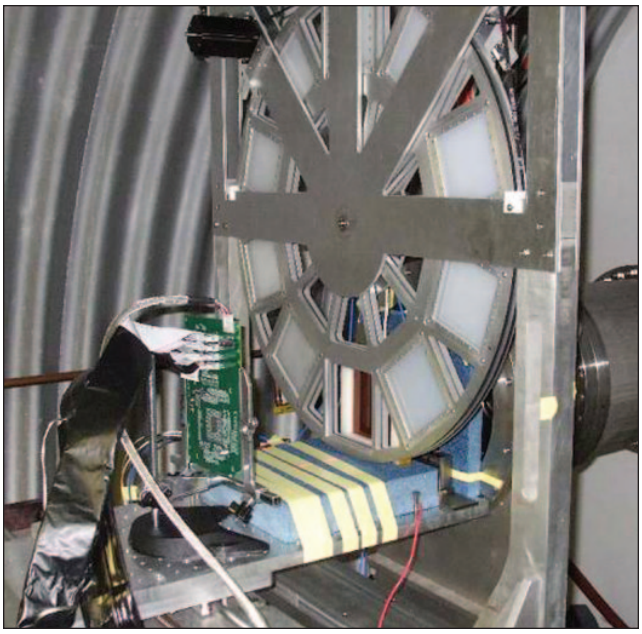


Fig. 1. *Degradation of the high-energy beam is accomplished by a series of plastic masks.*

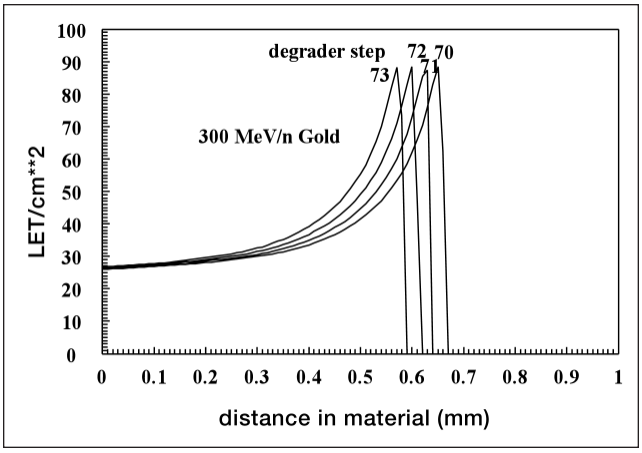


Fig. 2. *Representation of Bragg peak movement.*

Standards-Based Wireless Sensor Networks and Modular Instrumentation for Space Flight Applications

Raymond S. Wagner, *Jacobs Technology*
Richard J. Barton, *Johnson Space Center*
Patrick Fink, *Johnson Space Center*
Phong Ngo, *Johnson Space Center*

Wireless instrumentation provides a powerful new data-gathering paradigm for space flight applications. Outfitting sensors with radios to form nodes in a wireless sensor network (WSN) opens a new range of possibilities in measurement and monitoring. Eliminating wire runs and their associated harnesses and connectors can substantially reduce vehicle launch weight—a principle advantage of WSNs. Freeing sensors from wires also allows sensors to be added to a vehicle or relocated during a vehicle's operational phase, well after its initial design and construction period. This allows unprecedented flexibility in increasing situational awareness as lessons are learned and sensing needs that were initially unanticipated become apparent. Wireless sensors can also be used to augment a vehicle's permanent sensing suite during its initial checkout, only to be easily removed once the vehicle becomes operational. Finally, WSN nodes can be reused between vehicles on orbit. For example, a node can be relocated from a spent vehicle, such as a supply vehicle, to one currently in service, such as an International Space Station module or cislunar/near-Earth-object cycler. This transfer of hardware augments the operational capabilities of the in-service vehicle using equipment that would otherwise be a loss once the spent vehicle is discarded.

Cutting a sensor's wires—for both communication and power—is not without its perils. To conserve onboard power resources (e.g., battery power), a wireless sensor node must sparingly communicate using a low-power radio. This requirement renders WSNs especially prone to interference from a variety of sources. Time-varying multipath interference can induce local signal fades, which are difficult to overcome. Other, more powerful wireless systems operating in the same frequency band (e.g., Wi-Fi) can monopolize access to the wireless channel. Crew members and equipment moving in microgravity can create unpredictable physical barriers to radio frequency (RF) communication, and wideband noise from equipment such as pumps and fans can also generate RF interference.

Fortunately, a number of wireless communication standards aimed at mission-critical monitoring and control applications in the terrestrial world have arisen in the last decade. These technologies, such as Institute of Electrical and Electronics Engineers (IEEE) 802.15.4 and its derivatives—International Society of Automation (ISA) 100.11a and ZigBee standard—show great promise in being applicable to the unique needs of both space flight applications and ground-based spacecraft testing and launch processing. The Johnson Space Center (JSC) team created a program to study these and similar technologies in the laboratory and field environments in pursuit of standardized NASA approaches to wireless instrumentation. The team employs the Consultative Committee for Space Data Systems approach: adopt existing technologies when possible, adapt them as needed, and develop new technologies from scratch only if necessary. The key to this effort is evaluation of all candidate technologies in controlled laboratory environments as well as real-world field environments. This allows the team to determine its strengths and shortcomings in relevant aerospace applications and propose, implement, and evaluate modifications as necessary.

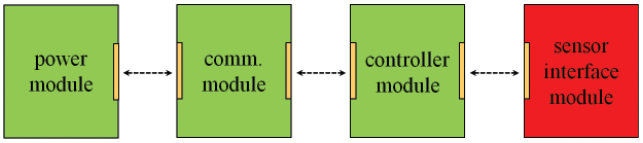


Fig. 1. *Modular Instrumentation composed of stock (green) and mission-specific (red) components.*

To enable this approach, the team developed a suite of modular instrumentation components that allow it to mix and match stock modules with custom sensor interfaces to form integrated, wireless sensor nodes (figure 1). Development of modular instrumentation begins with the definition of generic classes of modular components and the interfaces between them. A processor (e.g., a microcontroller or single-board computer) anchors the design and manages the data acquisition, processing, and transport. Depending on the processor's native capabilities and the application requirements, it may interface with an analog-to-digital conversion module, a memory module, a data-processing module (such as a digital signal processing chip), etc. A communication module (IEEE 802.15.4, ISA 100.11a, ZigBee, etc.) provides a path for data out of the network, and a power module sized appropriately to the application requirements and resources (e.g., mains, battery, or power-harvesting) rounds out the set of stock

components. Only the sensor interface specific to a particular application needs to be designed from scratch.

The benefits of this approach are twofold. First, laboratory studies can be accomplished merely using the control, radio, and power modules. The team generated synthetic data in software on the controller module, allowing it to characterize the performance of each radio in representative environments (figure 2) while carefully regulating the type and level of interference (e.g., competing 802.11 Wi-Fi traffic). Guided by these laboratory studies, the team can then quickly infuse the new radio modules (and their interface software) into the field for real-world trials by incorporating them into the modular instrumentation suite.



Fig. 2. *Johnson Space Center wireless habitat test bed.*

Second, this approach allows the JSC team maximum reusability across applications. The team developed a communication infrastructure, identifying a set of well-understood, open standards suited to a particular set of requirements (power consumption, reliability, cost, etc.), which can apply across multiple distributed sensing applications. Pairing the stock control, radio, and power modules with an application-specific sensor interface allows for quick assembly of modular, add-on instrumentation units capable of addressing a wide variety of sensing applications as they arise. Importantly, it reduces the frequency of "square peg, round hole" difficulties encountered when applying monolithic add-on instrumentation systems to measurement tasks for which they were not specifically designed.

In combination, these activities are allowing the JSC team to study and apply commercial WSN standards to real NASA operational requirements, with a quick and cost-efficient path from the lab to the field and beyond.

Effect of Space Vehicle Structure Vibration on Control Moment Gyroscope Dynamics

Tatiana Dobrinskaya, *Johnson Space Center*

Control Moment Gyroscopes (CMGs) are used for non-propulsive attitude control of satellites and space stations, including the International Space Station (ISS). A CMG is a mechanical device that has a spinning wheel and one or two gimbals used to change the position of the spin axis. When the spin axis is moving, the CMG angular momentum is changing, thus providing a torque for space vehicle attitude control.

CMG performance is critical for operation of a vehicle since CMG failures or degraded performance limit vehicle attitude control capabilities. CMGs could be essential for future long-duration space missions due to the fact that they help to save propellant. CMGs were successfully tested on the ground for many years, and have been successfully used on satellites. However, after a little more than a year of operation on the ISS, the first CMG had failed. The CMG failure resulted in the limitation of the attitude control capabilities, increased propellant consumption, and additional operational issues. About 4 years later, periods of higher-than-nominal CMG vibrations triggered a second CMG problem on the ISS. As a result, another CMG was shut down and returned to Earth. The question was raised: why is the CMG service life on the ISS significantly shorter than the predicted service life of 15 years? Since the dynamic environment of the ISS differs greatly from the nominal environment of satellites, it was important to analyze how operations specific to the ISS (dockings and undockings, solar array motion, crew exercise, robotic operations, etc.) affect CMG performance. The goal of this work was to analyze the CMG dynamics in the ISS environment, to suggest explanations to the observed CMG telemetry, and to find ways to increase the CMG service life onboard the ISS. In this work, the equations describing the coupling of CMG dynamics with the vehicle structure vibrations were derived. The equations were obtained for the unbalanced gimbals to match the CMG configuration on ISS. The analysis shows that at a certain frequency of ISS structure oscillations, CMG vibrations are significantly increased. This result reveals the resonance in the system due to coupling of external vibrations with the CMG motion in case of unbalanced gimbals. It was found that the effect of the vehicle structure vibration depends on the magnitude of gimbal imbalance, the direction of vehicle structure vibration, and the gimbal friction. Computer modeling results show that nominal CMG dynamics coupled with external vibration of the vehicle structure can cause off-nominal CMG vibration spikes similar to the spikes, observed on the ISS.

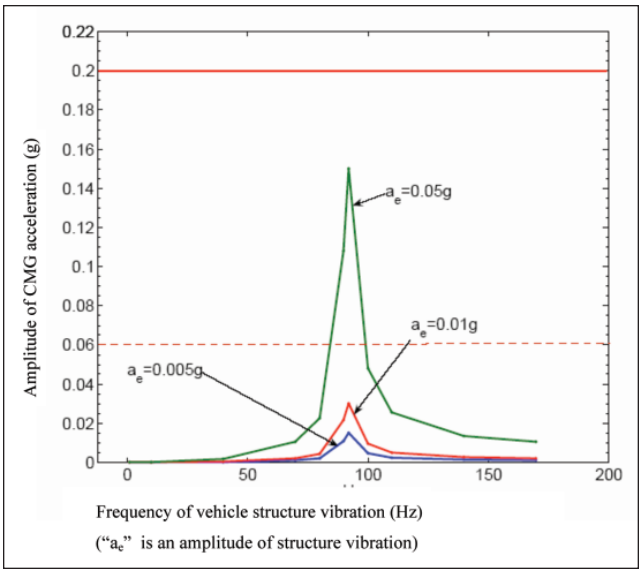


Fig. 1. *Amplitude of Control Moment Gyroscope acceleration (g) vs. frequency of vehicle structure vibration (Hz).*

Figure 1 shows the computation results: the dependence of CMG accelerations on the frequency and amplitude of external vibration. Calculations show that the nominal value of the CMG acceleration amplitude is in the range of 0.005g to 0.02g. This value is of the order of the CMG vibration measurements on the ISS. For the typically observed vehicle structure vibrations, the magnitude of computed spikes at resonance is in the nominal range (below the dotted line in figure 1). However, computations with decreased gimbal friction or increased magnitude of external vibration resulted in off-nominal resonance

spikes. Based on the equations and computation results, the resonance effect is more noticeable if:

1. The magnitude of structure vibrations is higher than usual (crew exercises, robotic operations, thruster firings, etc.).
2. The gimbal friction is lower than usual. (This may occur when gimbal rates are high since gimbal friction decreases with the increase of gimbal rate.)

Both of these conclusions match the onboard observations on the ISS. First, most of the spikes seen onboard were correlated with increased dynamic activities. In addition, the second conclusion suggests the possible explanation for the onboard telemetry observations: it explains why the CMG vibration spikes were, in most cases, correlated with high gimbal rates. Figure 2 shows gimbal rates and an off-nominal vibration spike. This case was recorded during a Russian segment extravehicular activity. A command to position gimbals, which caused the gimbal rates to increase, triggered this event. In 2008, the problem with CMG vibration spikes was supposedly fixed by limiting the CMG gimbal rates, after which no spikes were observed onboard.

The results of this work show that the vehicle structure vibrations coupled with CMG motion can increase CMG accelerations (even to the off-nominal levels), thus increasing loads and possibly decreasing the CMG service life. The effect of a single CMG vibration spike at resonance may not be enough to cause a CMG failure. However, since the external vibrations are constantly applied to CMGs, they may have a noticeable accumulated effect on the CMG service life similar to the effect of small wheel unbalance loads. There are several ways to reduce the CMG vibrations due to vehicle structure oscillations:

1. Balancing CMG gimbals can decrease the CMG vibrations since it eliminates the coupling terms in the equations of motion.
2. A proper selection of gimbal friction (not too low) can adjust the CMG accelerations to suitable levels.

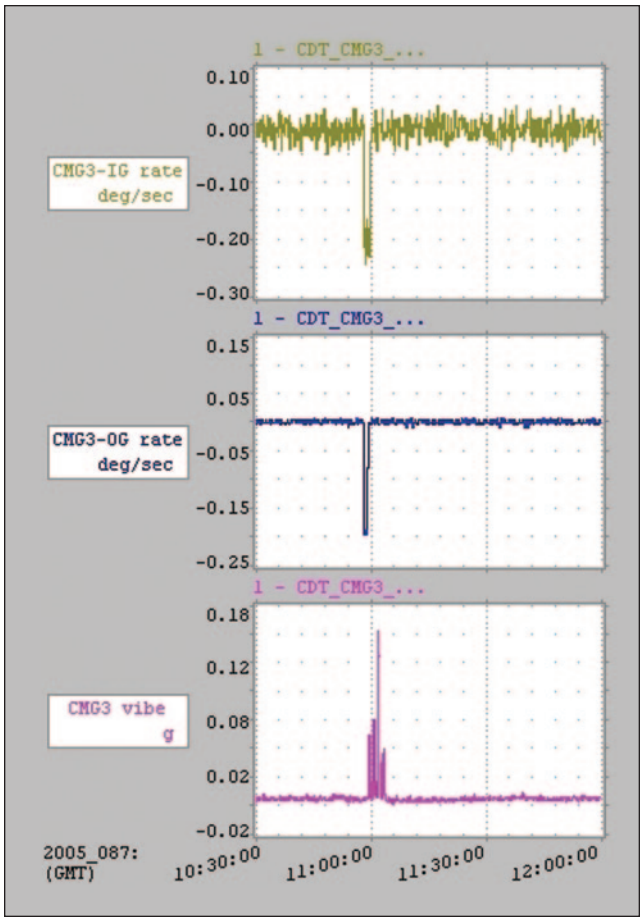


Fig. 2. *Control Moment Gyroscope gimbal rates and vibrations as functions of time.*

The suggested modifications could increase the CMG service life beyond the current expectations and might allow the use of higher gimbal rates (as was initially designed), thus improving vehicle attitude control capability.

Transfer Impedance Measurement of Flexible Printed Wiring Board Cable Shields for Use in Crewed Space Flight

Robert C. Scully, *Johnson Space Center*
Charles W. Roberts, *MEI Technologies Inc.*
Xiang Ni, *Jacobs Technology*

Over the years, materials and processes for manufacturing flexible printed wiring board (PWB) cable assemblies have improved to such a state as to make them attractive candidates for use in crewed space flight. The reliability, low mass, and producibility of flexible PWB cables in lengths up to 2 m (7 ft) make the design an ideal candidate choice. However, there are additional requirements for the wiring of crewed spacecraft, and among these is the transfer impedance of the shields of interconnecting cables and harnesses. NASA's International Low Impact Docking System (iLIDS) project team has taken the lead in attempting to qualify flexible PWB cable designs for critical space flight systems in an effort to reduce overall mass. As part of the qualification process, an effort was undertaken to measure the transfer impedance of representative cables. The team tested two different flexible PWB cable designs. Both cables were identical in construction except for the shield designs, which differed only by the addition of stitching vias along the edges of one of the cables. The team used a triaxial apparatus to measure each of the two cables. The length of RG-58 coaxial cable was also measured using the same triaxial apparatus, so as to obtain data for comparison with published results from independent testing of the same cable type. By so doing, the accuracy of the test apparatus setup and measurement technique would be established.

Cable and Fixture Design, and Test Setup

Flexible Printed Wiring Board Cable Construction and Shield Design

The flexible PWB cables were constructed using a rigid-flex laminate process. A rectangular area at either end of the cable, fabricated using a rigid PWB process, provided structural support for mounting connectors terminating the cable shields to special fixture plates and backshells. The remaining length of the cable was fabricated using a flexible PWB process, allowing the cable to be formed into place on installation. Pioneer Circuits (Santa Ana, California) provided technical assistance and design of the layer stack-up for the rigid-flex construction.

Inner-layer conductors and outer-layer shielding were formed by copper foil laminates having thicknesses of 0.0014 in., with a 0.001-in.-thick Kapton® interlayer between conductors. The shield layers formed the outer most copper layers in the stack-up. Further shielding of inner layer conductors was provided by perimeter guard traces, 0.030 in. in width and placed along the cable edges. Both cable shield designs incorporated these features. Vias, 0.02 in. in diameter with 0.04-in. center spacing, were placed along the entire length of both edges of one of the cables to be measured. The vias were positioned to provide an electrical connection between the top, bottom, and guard trace shields, thus providing shielding with much smaller apertures to electromagnetic fields.

The shielded conductors were brought out through press-fit socket contacts installed in the rigid PWB portion of the cable. This allowed for connection to specially designed plates with which to drive and measure signals in the conductors of the flexible PWB cable. The flexible PWB cables used in the measurements were approximately 31 in. long and 0.8 in. wide, the length being decided prior to the design and fabrication of the transfer impedance fixture hardware.

Test Fixture

A cylindrical test fixture, based on the triaxial measuring setup of International Electrotechnical Commission (IEC) standard 62153-4-4, was fabricated from a 3-in. inner diameter schedule 40 copper pipe, wall thickness approximately 0.24 in., made of Electrolytic Tough Pitch (ETP) 110 copper. End plates and intermediate mounting plates of varying thicknesses were fabricated from flat stock ETP 110 copper and nylon material. Figure 1, taken from IEC 62153-4-4, illustrates the electrical schematic of the triaxial fixture.

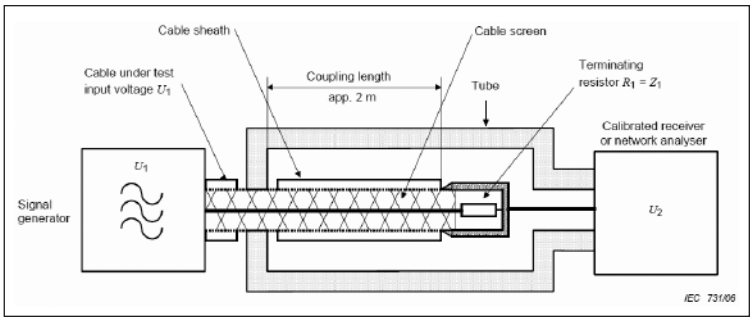


Fig. 1. *Electrical schematic diagram.*

Test Setup

Primary measurement equipment consisted of a vector network analyzer (VNA) with a scattering parameters test set, and an impedance adapter for the cables under test. A secondary setup using a signal generator, a spectrum analyzer, and an automated software controller, was used for comparison measurements, and to provide confidence that the data collected and displayed by the network analyzer were accurately processed.

Setup calibration, impedance matching, and measurement procedures using the VNA were in accordance with IEC 62153-4-4. Setup calibration, impedance matching, and measurement procedures using the spectrum analyzer (SA) and signal generator (SG) were in accordance with standard laboratory practice.

Data Collection and Review

Data collection was straightforward for both setups. In the case of the VNA, no further effort was required other than to set up the instrument using a standard, short, open, and loaded dual-port calibration. The setup using the SA and the SG was a bit more complex, requiring some minor programming to the computer controller to run the SG and collect the data from the SA. The data from the VNA were presented and taken from the instrument. The data from the SA/SG setup were taken from the computer controller after some minor interface processing. The data were available in both cases as a XXX.CSV file, as well as a XXX.BMP file.

As a means of calibrating the system to a known result, a length of RG-58 cable was introduced into the fixture and measured from 10 kilohertz to 1 gigahertz. The data were then plotted and, as shown in figure 2, independently collected data for RG-58 transfer impedance was laid over the resulting curve for direct comparison. The black straight line and the x's are from the independent data source. Examination of this comparison yields good comparison, and establishes confidence in the ensuing results for the flexible PWB cable measurements. The iLIDS baseline curve is the solid blue line, and the measured data are represented by the green line.

With the fixture thus calibrated, data were then collected for the flexible PWB cables using both measurements setups. Figure 3 plots the data from both sets of

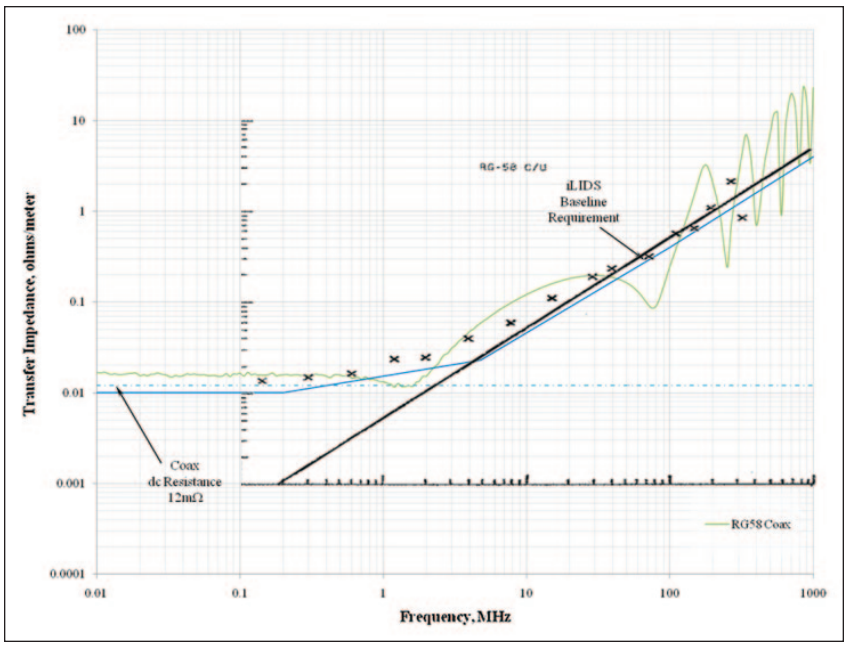


Fig. 2. *RG-58 data compared to independent data.*

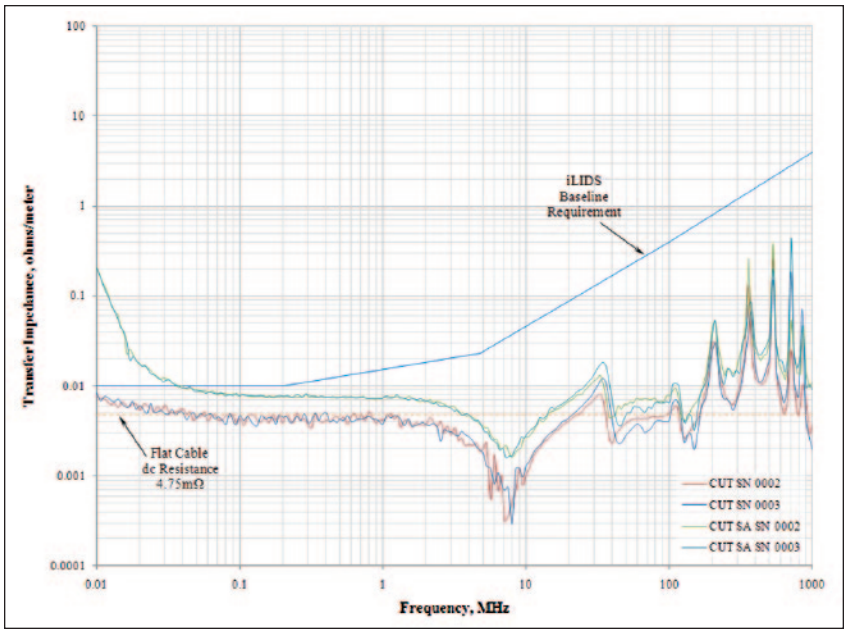


Fig. 3. *Comparison of vector network analyzer data to spectrum analyzer/signal generator data.*

Transfer Impedance Measurement of Flexible Printed Wiring Board Cable Shields for Use in Crewed Space Flight

continued

measurements for review. Examination of these data show good agreement between the two techniques in terms of frequency behavior, but the magnitude of the data collected using the SA/SG setup appears to be slightly high. The data in the lower frequency range should be close to the direct-current resistance of the cable. The data collected using the VNA do show excellent agreement with the direct-current resistance value. For this reason, the VNA data are considered to be the most accurate representation of the flexible PWB cable transfer impedance. Again, note the solid blue iLIDS baseline requirement.

Finally, the VNA data are plotted in figure 4 against the RG-58 data and the iLIDS baseline for direct performance comparison.

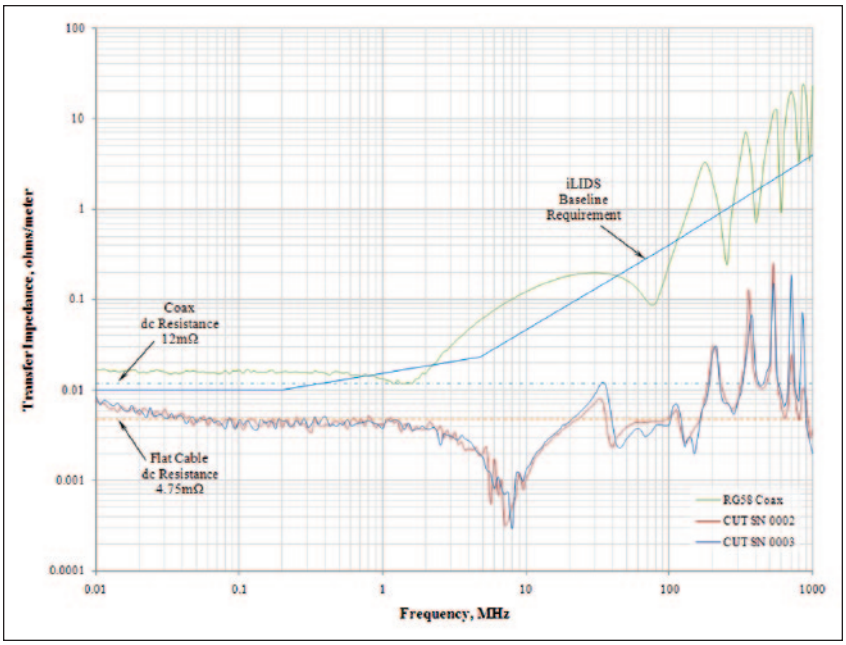


Fig. 4. *Comparison of RG-58 data to flexible printed wiring board cables.*

Conclusion

The transfer impedance of the integral shields of two flexible PWB cable designs was measured and shown to be superior to the baseline requirement, thus paving the way for future integration of this type of cable in the iLIDS project, and potentially in other space vehicle projects as well.

Shuttle Radiator Protection Helps Prevent Mission Loss from Micrometeoroid and Orbital Debris

Eric Christiansen, *Johnson Space Center*
Dana Lear, *Johnson Space Center*
Eugene Stansbery, *Johnson Space Center*

NASA's Hypervelocity Impact Technology team, located at Johnson Space Center, routinely inspects the space shuttle vehicle after each mission for micrometeoroid and orbital debris (MMOD) damage. During the post-flight inspection after the Space Transportation System (STS)-128 flight of *Discovery*, NASA found 14 MMOD impacts on the crew cabin windows, 16 impacts on the wing leading edge and nose cap, and 21 impacts on the payload bay cooling radiators. Of these, one is perhaps the most important because it highlights a success story over 10 years in the making (figure 1).

Although the impact crater was not the largest damage found on the radiators, the crater was strategically placed directly over one of the cooling tubes bonded to the backside of the radiator face sheet. The impact crater is important because, if not for decisions to "harden" the shuttle fleet to the increasing orbital debris environment in the late 1990s, the impact would have breached the Freon cooling loop and, by flight rule, would have resulted in a leak rate high enough to result in an early mission termination (i.e., loss of mission).

The space shuttle was designed in the 1970s, before the risk from human-made orbital debris was widely recognized. The vehicle was originally designed with requirements for protection against only the micrometeoroid environment. Almost immediately, damage from orbital debris started showing up. The first significant impact was a 0.2-mm-sized paint chip that damaged a window during the STS-7 mission and required the window to be replaced prior to re-flight.

In the early 1990s, NASA applied the BUMPER code— a NASA MMOD risk analysis software—to predict the risk of damage to different surfaces of the spacecraft given their orbit, orientation, and the MMOD environment. Analysis showed that the shuttle risk was highly dependent on its flight attitude or orientation. The highest vulnerability to loss of mission was penetration of the cooling loop bonded to the inside surface of the radiator face sheet (figure 2a).

During this time, the on-orbit heat rejection system in the shuttle vehicle consisted of two Freon coolant loops routed through the radiator panels attached to the payload bay doors and accumulator tanks. There was no provision

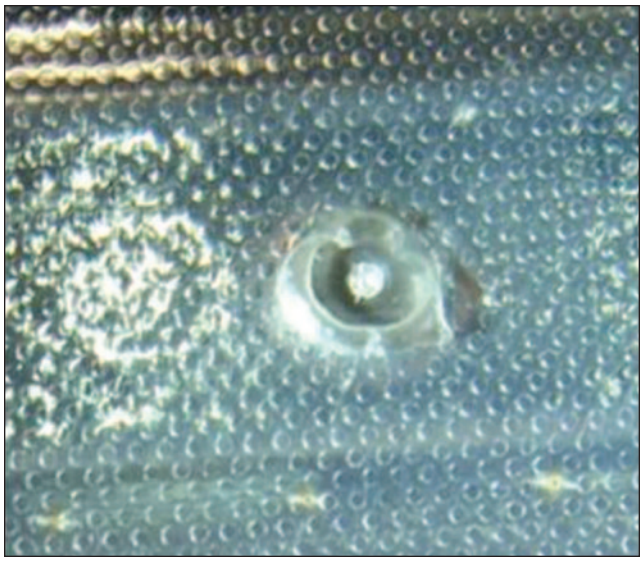


Fig. 1. *Impact crater on the radiator located on the interior of the shuttle payload bay doors. The impact was on an aluminum "doubler" directly over the tube carrying Freon coolant used to cool electronic equipment and avionics in the shuttle.*

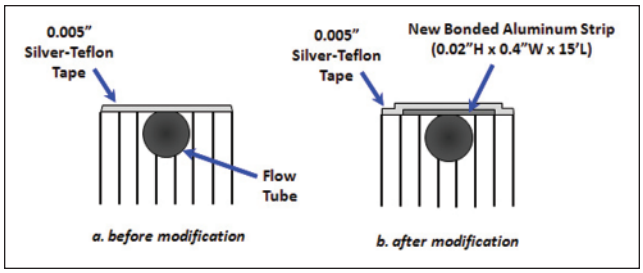


Fig. 2. *The shuttle radiators are curved panels, located on the inside of the payload bay door, that are exposed to space when the doors are open. The panels are a honeycomb structure sandwiched between a face sheet and a back sheet with a total thickness of either 12.7 or 22.9 mm. Aluminum tubes are bonded to the backside of the 0.28-mm-thick face sheet at intervals. This figure shows a cross-section of the honeycomb radiator revealing the configuration before and after the addition of the 0.5-mm aluminum "doubler."*

for isolating a leak in the system. Puncture of a tube by MMOD would totally deplete the coolant in one of the two loops, necessitating that approximately half of the heat sources (such as avionics in the crew cabin) be switched off. Flight rules under this situation required a next primary landing site abort; i.e., that the shuttle mission be aborted

Shuttle Radiator Protection Helps Prevent Mission Loss from Micrometeoroid and Orbital Debris

continued

immediately and preparations made to land at the next available primary landing site. Because coolant is lost quickly from the pumped flow system in the event of a leak, some of the avionics would be turned off during reentry and landing, decreasing the ability to recover from some other anomaly that could occur during this critical mission phase (due to loss of redundancy in the avionics systems).

The BUMPER predictions were put to the test during the first flight of the U.S. Microgravity Laboratory during STS-50. One of the experiments required that the shuttle fly nose up, payload bay into the velocity vector for 10 days of the 14-day mission. After much discussion with shuttle managers and impact tests on various spacecraft components that were contained in the payload bay of the orbiter, it was decided to fly the mission as planned. Fortunately, no MMOD impact breached the Freon cooling loop. However, post-flight inspection of the radiators showed that the number of impact features closely matched the preflight BUMPER predictions and were much higher than typical for shuttle missions flown with the payload bay facing Earth.

After STS-50, new flight rules were implemented that required the shuttle to fly with the payload bay to the Earth and the tail toward the velocity vector "unless payload or orbiter requirements dictate otherwise." This procedure worked well while the shuttle flew independently. Flights to the Russian space station Mir and later to the International Space Station, once again exposed the cooling loops to higher risk of MMOD impact for long periods while docked.

In 1997, modifications were approved by the Space Shuttle Program to "harden" the orbiters from the increasing orbital debris environment. Three of these modifications involved the Freon cooling system, two of which would prove critical for STS-128. First, an extra layer of 0.5-mm-thick aluminum (aluminum doubler) was bonded to the radiator face sheet directly over the cooling tubes (figure 2b). Automatic isolation valves were added to each coolant loop that could isolate a leak in a radiator panel from the rest of the Freon system (accumulator and pumps) so that sufficient Freon remained to activate the cooling system for all electronics during reentry, when heat is rejected to the flash evaporator system. If sufficient coolant was saved, the need for a next primary landing site abort was alleviated.

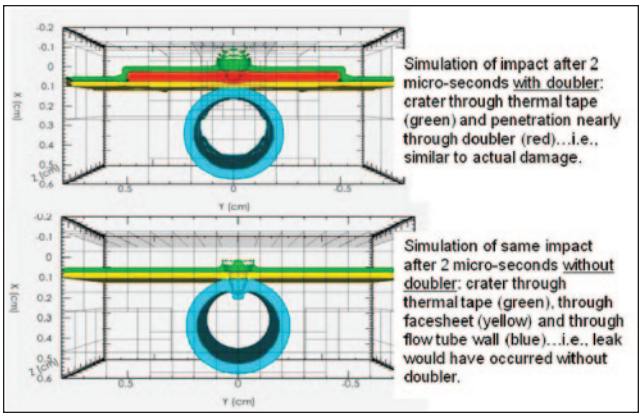


Fig. 3. *Hydrocode simulation of the impact with and without the aluminum "doubler." Without the doubler, the Freon cooling loop would have been breached.*

The modifications were incorporated into the shuttle fleet during routine maintenance between 1998 and 1999. These modifications, made 11 years prior to the STS-128 mission, saved the mission from early termination.

During the STS-128 mission, an orbital debris particle impacted the aluminum doubler directly above the Freon tube. Simulations show that had the doubler not been in place, the Freon tube would have been breached (figure 3). Without the second modification isolating the leak to the radiator panels, all of the Freon (which is under pressure) would have leaked from the system, requiring the shuttle to land within 24 hours and with reduced avionics.

This success story is a tribute to the entire NASA Hypervelocity Impact Technology, Orbital Debris and Space Shuttle management team. The Orbital Debris Program Office created the debris environment flux models that were based on solid science and measurement data. The Hypervelocity Impact Technology team applied the BUMPER code, which demonstrated the vulnerability of the Freon cooling system and its impact to overall mission risk, as well as evaluating risk mitigation techniques, such as the addition of aluminum doublers (which was eventually selected). Then, the Space Shuttle Program management made critical decisions in tight economic conditions to enhance the safety to the orbiters from the MMOD threat. A decade later, their hard work and tough decisions paid off.

Shielding Against Micrometeoroid and Orbital Debris Impact with Metallic Foams

Shannon Ryan, *Johnson Space Center Postdoctoral Fellow*
Eric Christiansen, *Johnson Space Center*
Dana Lear, *Johnson Space Center*

For the past 50 years, the protection of manned spacecraft against micrometeoroids and orbital debris (MMOD) has, for the most part, been performed by the Whipple shield or derivatives thereof. Although highly capable, the installation of Whipple-based shielding configurations requires a significant amount of non-ballistic mass for installation (e.g., stiffeners, fasteners, etc.), that can consume up to 35% of the total shielding mass. As NASA's vehicle design focus shifts from large pressurized modules operating for extended durations in relatively debris-polluted low-Earth orbits, to small-volume lower-duration craft, new protective concepts are being designed and evaluated to address the new threats.

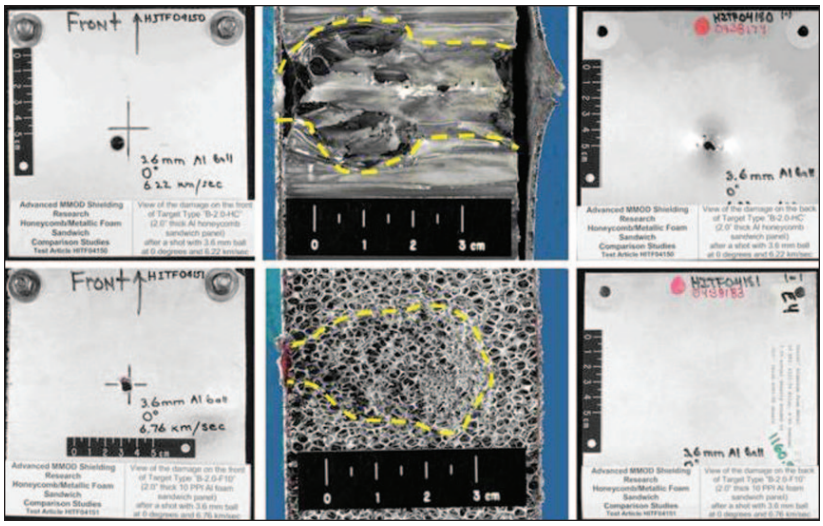


Fig. 1. *Comparison of damages in a honeycomb core (top) and open-cell foam core (bottom) sandwich panel impacted by 3.6-mm-diameter aluminum spheres at 6.22 km/s (honeycomb) and 6.76 km/s (foam) with normal incidence (0°). From left to right: bumper (front view); core cross-section (emphasis added); and rear wall (rear view).*

One possible solution involves the use of structural components that have intrinsic shielding capability. Traditional primary structures such as honeycomb sandwich panels are unsuited for use in manned vehicles due to their poor shielding performance. Metallic foams, however, are a relatively new material with low density and novel physical, thermal, electrical, and acoustic properties that offer a promising alternative for MMOD protective systems. There are two competing types of metallic foam: open cell and closed cell. Although closed-cell foams are capable of retaining some residual atmosphere, which may aid in the deceleration of penetrating fragments via drag, open-cell foams are considered the more promising technology due to their lower weight and higher degree of homogeneity. Preliminary investigations have demonstrated the potential of open-cell foam core structures, as shown in figure 1, compared to a traditional honeycomb core sandwich structure.

Researchers at Johnson Space Center's Hypervelocity Impact Technology Facility performed the following experimental investigations to comprehensively evaluate the performance of open-cell foams during hypervelocity impact: a fundamental study to investigate penetration and failure mechanisms in open-cell metallic foam structures; an application study evaluating the performance effect of modifying International Space Station-representative shields with open-cell metallic foams, and; a study comparing the performance of open-cell foams of varying materials with alternate MMOD shielding materials and structures.

Hypervelocity Impact Performance of Open-Cell Foams

An advantageous property of open-cell metallic foams, in terms of MMOD shielding, is their periodic structure of small diameter, low mass pores. During a hypervelocity impact event, the isentropic (constant value of entropy) shock and non-isentropic release process acts to raise the thermal state (internal energy) of the impacting particle. As a projectile penetrates through an open-cell foam structure, repeated impacts on individual foam cell ligaments induce multiple shock and release events, resulting in the fragmentation, melt, and vaporization of meteoroid or debris particles at impact velocities significantly lower than with traditional shields. The multi-shock shield used a similar concept, demonstrating potential weight savings of 30% to 40% over traditional Whipple shields for equal levels of protection. Although enhanced fragmentation and melting was clearly observed in experiments on foam

core sandwich panels, rear facesheet failure was almost exclusively caused by the penetration of individual solid (or molten) fragments, even at impact velocities above 7 kilometers per second (km/s). Given the non-homogeneity of the foam structure on a micro scale, it is considered that these individual fragments have propagated through the foam core with minimal secondary impacts. Subsequently, the degree of experimental scatter for these structure types may be greater than that of traditional configurations.

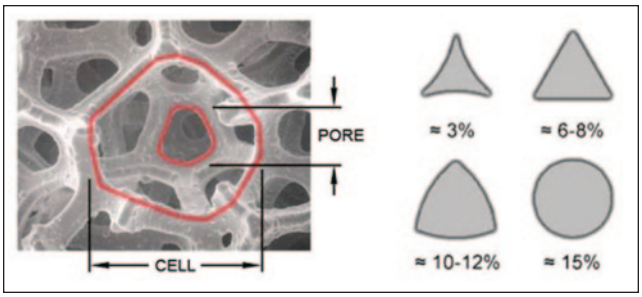


Fig. 2. *Foam pore size, cell size, and ligament cross-section (variation with relative density). © ERG Aerospace*

The number and size of foam ligaments is a function of material pore density (i.e., pores per linear inch [PPI]), which is specified in the manufacturing process. Additionally, the relative density of the foam (also adjustable during manufacturing) controls both the panel weight and the cross-sectional form of the foam ligaments (figure 2). It was found that increased pore density led to minor improvements in protective capability. For instance, 40 PPI foam core sandwich panels were found to be approximately 5% more capable than 10 PPI configurations. The effect of ligament shape was found to be minimal, with 3% to 5% (nominal) relative density cores providing equal levels of protection as heavier 6% to 8% (nominal) panels.

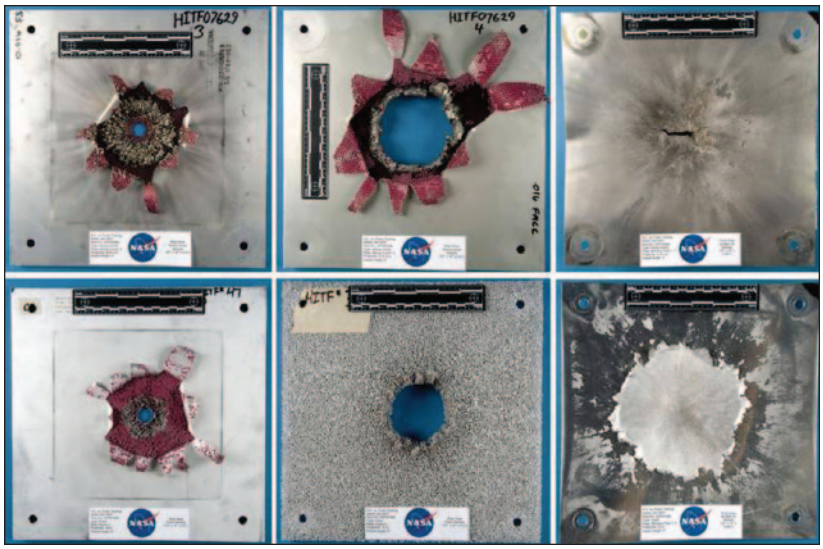


Fig. 3. *Comparison of impact damages induced by impact of 0.833-cm-diameter Aluminum spheres at approx. 6.9 km/s (0°) on the double layer honeycomb (top) and foam (bottom) targets. From left to right: outer sandwich panel (rear view); second panel (rear view); and rear wall (front view).*

Improved Shielding Performance Through use of Metallic Foam

Metallic open-cell foams provide comparable mechanical and thermal performance to honeycomb structures, without the MMOD shielding detrimental through-thickness channeling cells. A double-layer honeycomb sandwich panel shield, with a mesh outer layer and monolithic aluminum rear wall was modified to include aluminum open-cell foam, and thus evaluate the effect on shielding performance. The aluminum honeycomb core of the outer sandwich panel was replaced with 10 PPI foam, while the second honeycomb sandwich panel was replaced with an equal thickness foam panel (no facesheets), maintaining approximate totals for shield standoff and weight. The foam modified shield was found to provide a 3% to 15% increase in critical diameter for impacts normal to the target surface (0°). For oblique impacts, the performance gain was more substantial, particularly at low velocities. A comparison between impact damages induced by 0.833-cm-diameter Al2017-T4 (aluminum) spheres at approximately 6.9 km/s with normal incidence is shown in figure 3. In addition to reduced rear wall damage, clear evidence of enhanced fragment melting is visible on the foam-modified target.

Evaluation of Advanced Shielding Materials and Structures

The performance of aluminum, titanium, copper, stainless steel, nickel, nickel/chromium, reticulated vitreous carbon, silver, and ceramic open-cell foams was evaluated in an extensive experimental impact campaign. Configured in single-, double-, and triple-bumper shields, their protective capability was assessed against metal plates, meshes, and various flexible fabrics via a figure of merit based on cratering and impulsive failure modes. Further ballistic limit-based evaluations were performed, in which the advanced shield configurations were compared against equivalent weight all-aluminum shields. The top performing configurations were found to generally include monolithic aluminum outer bumper plates, with metallic foam and/or Kevlar® fabric inner bumper plates. Of the various foam types investigated, copper was found to provide the best protection, with reticulated vitreous carbon providing the worst.

The generation of ejecta during MMOD impact on a shield outer bumper is of concern due to the danger of secondary impacts, and the general pollution of the orbital environment. For impact on common shielding materials (i.e., aluminum, carbon-fiber reinforced plastic), ejecta can constitute up to 30% of the total expelled mass (ejecta + fragment cloud). Impact on foams, meshes, and fabrics was found to generate almost no ejecta of any significance, providing a substantial reduction in ejecta mass over monolithic structures (figure 4).

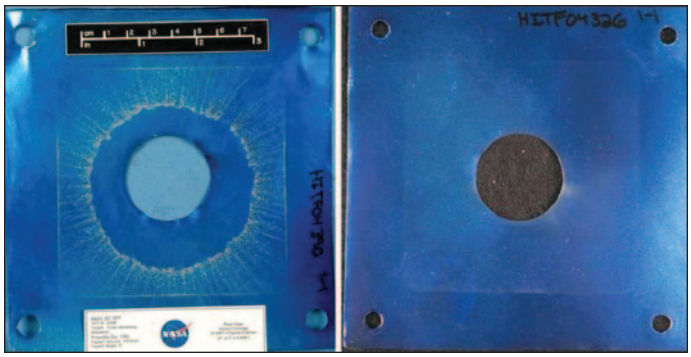


Fig. 4. *Comparison of ejecta plate damages following impact of 0.3175-cm-diameter aluminum spheres on a monolithic aluminum outer bumper (left) and stainless steel foam outer bumper (right) at hypervelocity (approximately 6.8 km/s).*

International Space Station Solar Array Guide Wire Micrometeoroid and Orbital Debris Damage

Daniel Kent Ross, *Johnson Space Center*
Eric Christiansen, *Johnson Space Center*
Dana Lear, *Johnson Space Center*

During the STS-120 mission in 2007, astronauts moved the International Space Station's (ISS's) Port 6 (P6) solar photovoltaic power module from its original location on the Z1 truss, where it generated power for almost 7 years, to its permanent location on the port outboard truss. P6 contains two solar array wings (SAWs), referred to as SAW 2B and SAW 4B. The P6 transfer operation consisted of first retracting each SAW, then moving the P6 module from Z1 and reinstalling it at its permanent location, and finally having to redeploy the solar array wings to generate power. During the SAW 4B deployment operation, the solar array began to tear in two places, and deployment was halted at about 90% deployment. The STS-120 crew and ground control determined that a guide wire had frayed and snagged on a grommet, causing tears that measured 1 foot and almost 3 feet in the solar array (figure 1). During extravehicular activity (EVA) #4, astronaut Scott Parazynski cut the snagged wire from the 4B SAW. The EVA crew also installed reinforcing straps and fully extended the solar array. The piece of guide wire that was removed was returned to the ground for analysis.

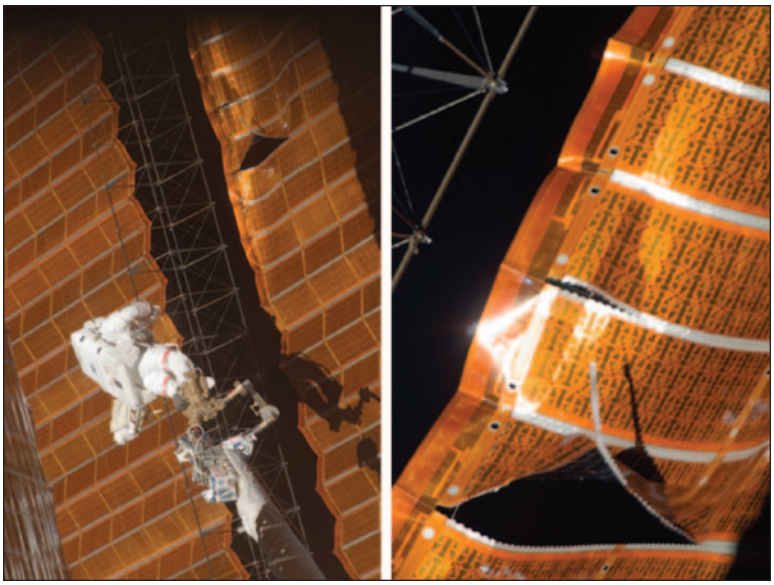


Fig. 1. *Tears in the International Space Station Port 6 solar array wing 4B after attempt at redeployment during the STS-120 mission.*

Personnel of the Hypervelocity Impact Technology Team examined the frayed end of the guide wire by using scanning electron microscopes at Johnson Space Center's Astromaterials Research and Exploration Science

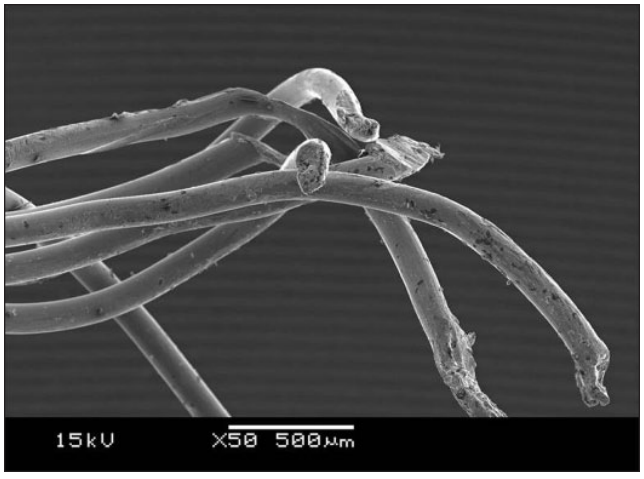


Fig. 2. *Frayed end of 4B solar array wing guide wire. Wires at bottom and in lower right-hand corner exhibited melt near ends.*



Fig. 3. *Three wires exhibiting melt.*

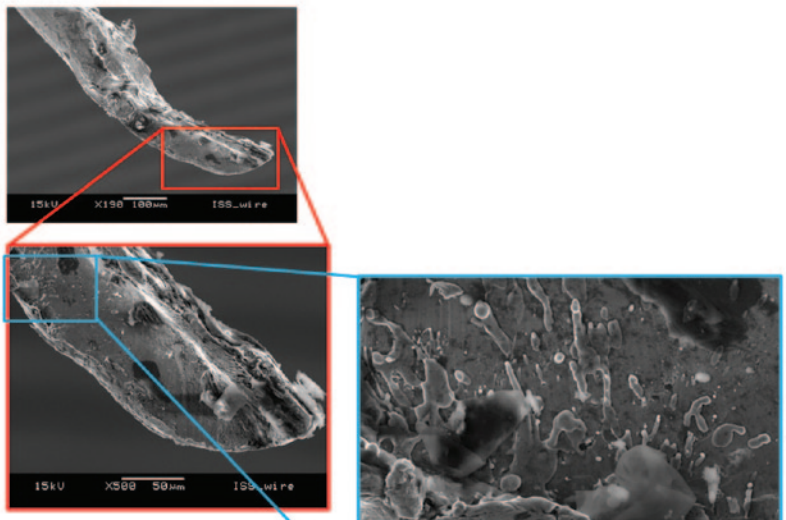


Fig. 4. Evidence of melting.

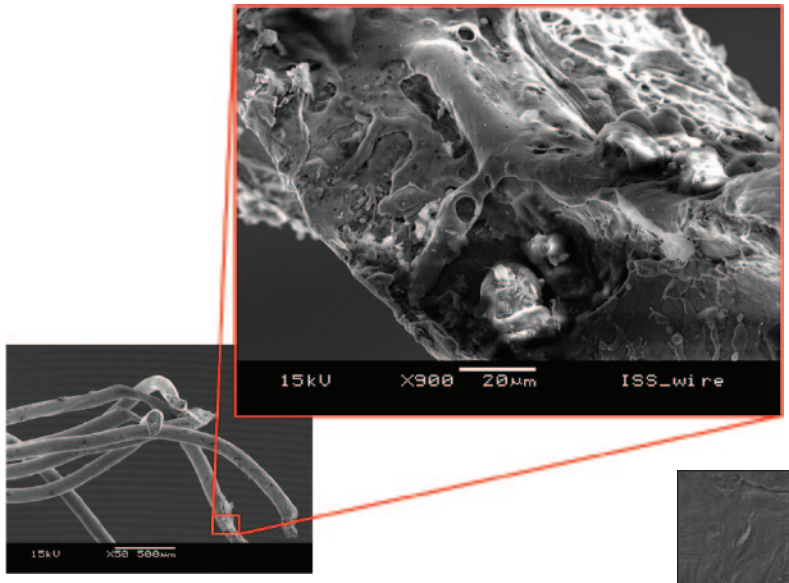


Fig. 5. Additional evidence of melting.

Directorate. Seven individual wires had been broken at the frayed end (figures 2 and 3). The microscopes' examination revealed that, on three of those wires, a large amount of material appeared to have been melted at one time near the broken ends (figures 4 through 6).

Micrometeoroid and orbital debris (MMOD) particles typically impact at high speed and release a large amount of energy, resulting in the displacement of target material with a mass 10 to 100 times the projectile mass due to melting and plastic flow local to the impact site. The presence of melt is a clear indication that the damage to these three wires was caused by MMOD impact. Other wires in the bundle appear to have been broken by mechanical action. A likely scenario that explains the observed damage to the guide wire is that MMOD impact damaged and broke a few of the wires, which allowed the guide wire to snag in a SAW grommet during deployment. Subsequently, as the process of deployment continued with a snagged guide wire, additional wires in the guide wire were sheared as they were pulled against the grommet.

An effort was made to identify the source of the impact damage. The scanning electron microscope is equipped with a narrow focus electron microprobe and an energy dispersive X-ray spectrometer to detect elemental composition of materials found in the impact zone. Several foreign particles with composition differing from the stainless steel wire material were detected in the area

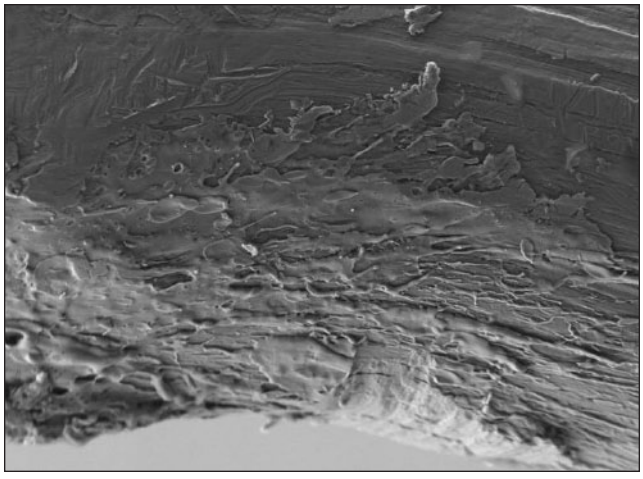


Fig. 6. More evidence of melting.

of the wires that had considerable melt. The composition of these particles suggest the possibility that an orbital debris impact was responsible for breaking wires within the guide wire bundle. Bismuth metal, gold-copper-sulfur, gold-silver-copper, lanthanum-cerium, antimony-sulfur, and tungsten-sulfur bearing particles were identified (figures 7 through 9). No evidence of micrometeoroid impact was identified. The wire is composed of iron-chromium-nickel (FeCrNi)-rich stainless steel, and these elements are present in all spectra. Also, carbon-rich particles are abundant on all of the wires, likely from the plastic bag containing the sample (i.e., contamination).

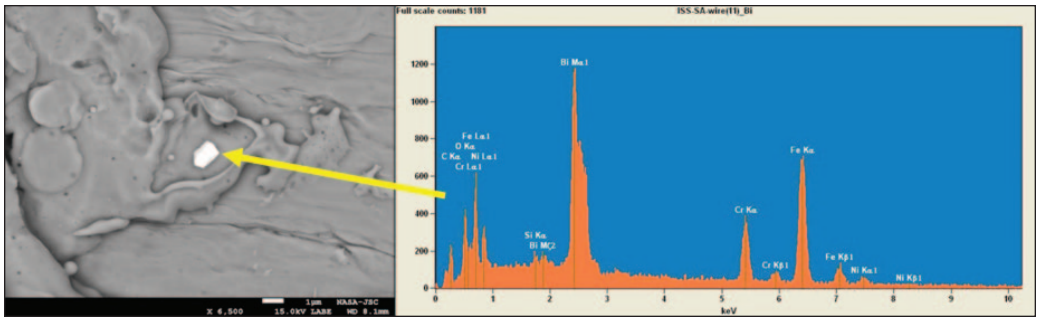


Fig. 7. *Bismuth-rich particle on melted zone on steel wire. Iron, chromium, and nickel peaks are from underlying wire.*

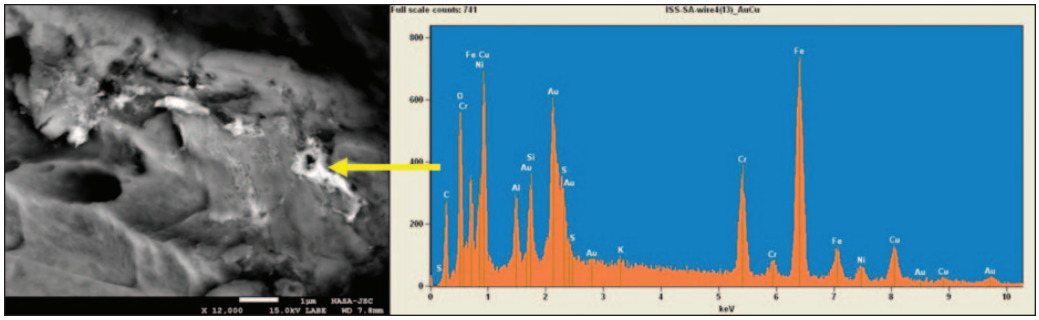


Fig. 8. *Gold-rich particles.*

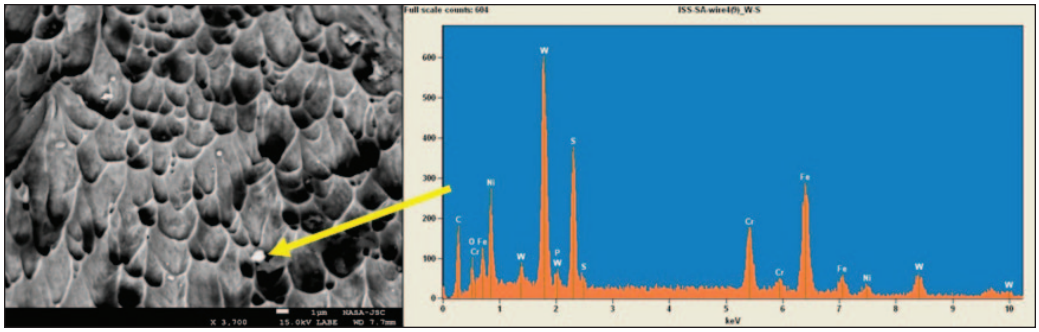


Fig. 9. *Tungsten-sulfur particle on damaged steel wire.*

Low-Earth Orbit Environment Remediation with Active Debris Removal

J.-C. Liou, *Johnson Space Center*

The catastrophic collision between Cosmos 2251 (a defunct Russian communications satellite) and the operational Iridium 33 (a United States commercial communications satellite) in 2009 signaled a potential onset of the "Kessler Syndrome" in the environment, predicted by Donald J. Kessler and Burton G. Cour-Palais in 1978. This event also supports the conclusion of several recent modeling studies: even with a good implementation of the commonly adopted mitigation measures, the debris population in low-Earth orbit (LEO)—the region below 2000-kilometer (km) altitude—will continue to increase. The population growth is driven by fragments generated via accidental collisions among existing satellites. Therefore, active debris removal should be considered to remediate the environment. The need for active debris removal is also highlighted in the National Space Policy of the United States released in June 2010 where, under the Section of "Preserve the Space Environment," NASA and the Department of Defense are directed to pursue research and development of technologies and techniques to remove on-orbit debris.

There are many technical and nontechnical challenges for active debris removal. If the objective is to remediate the environment, then the most effective approach is to target the root cause of the problem—objects that have the greatest potential of generating the highest amount of fragments in the future. These are objects with the highest mass and collision probability products. Figure 1 shows the mass distribution in LEO. It is obvious that the major mass reservoirs are located around 600-, 800-, and 1000-km altitudes. The 600-km region is dominated by spacecraft while the other two regions are dominated by spent rocket bodies. Note the operational spacecraft accounts for only approximately 10% of the mass in LEO. Since the 800- to 1000-km region also has the highest spatial density in LEO, it is expected that many of the potential active debris removal targets will be rocket bodies in that region.

A key element for any active debris removal planning is the ability to quantify the requirements of the operations and the benefits to the environment. Figure 2 shows the latest results from the NASA Orbital Debris Program Office on LEO environment remediation.

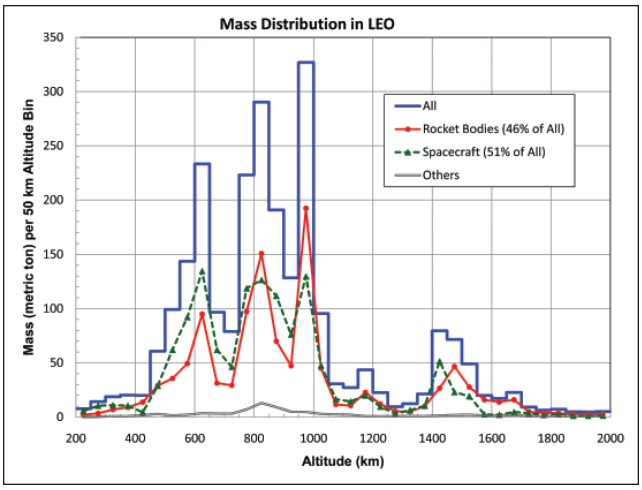


Fig. 1. *Mass distribution in low-Earth orbit. The three major peaks are dominated by rocket bodies and spacecraft.*

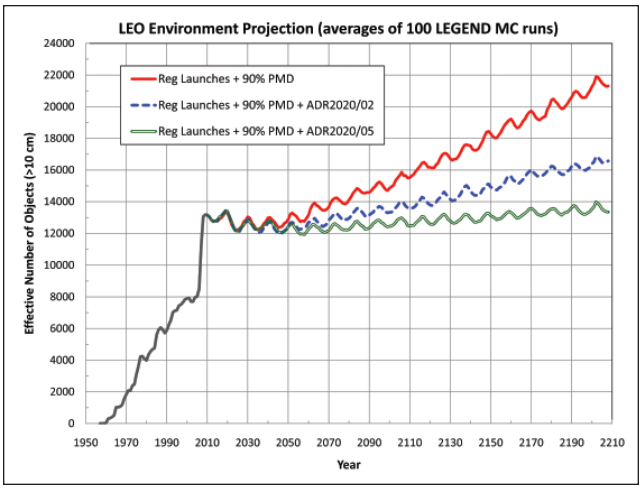


Fig. 2. *Simulated low-Earth orbit (LEO) population growth as a function of time. To maintain the future LEO population at the current level requires a good implementation of the mitigation measures and an active debris removal rate of about five objects per year, starting from the year 2020.*

Simulations were carried out with the NASA long-term debris evolutionary model, LEGEND. The future projection part of the top curve assumes a nominal launch cycle and a 90% compliance of the post-mission disposal measures (e.g., the 25-year rule). The average of 100

Low-Earth Orbit Environment Remediation with Active Debris Removal

continued

Monte Carlo LEGEND runs indicates that the LEO population will continue a steady increase in the next 200 years. With the addition of active debris removal operations of two objects per year, starting from the year 2020 (the middle curve), the population growth is approximately reduced by half. If the active debris removal rate is increased to five objects per year, then the LEO population in the next 200 years can be maintained at a level similar to the current environment (bottom curve). However, if the objective is to restore the environment back to the level prior to January 1, 2007, (before the Chinese anti-satellite test), then a removal rate of more than five objects per year must be implemented.

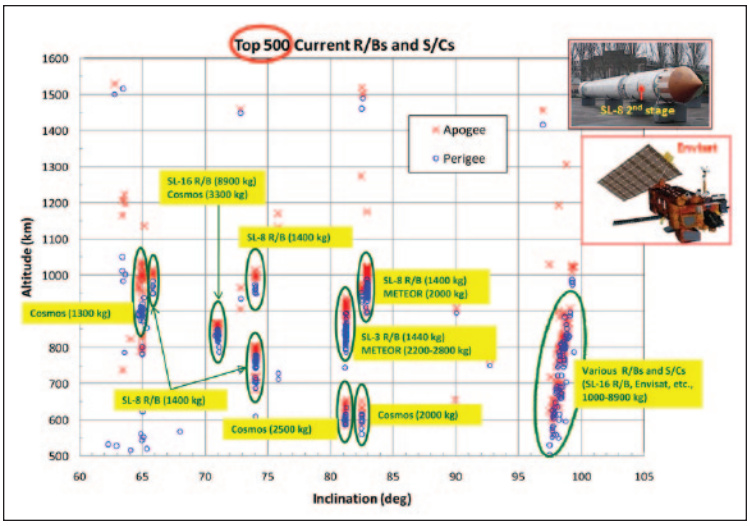


Fig. 3. *Apogee altitude (crosses) and perigee altitude (open circles) versus inclination distributions of the existing low-Earth orbit rocket bodies and spacecraft that have the highest mass and collision probability products. Only the top 500 are shown. These are potential targets for active debris removal.*

The active debris removal target selection criterion used in the LEGEND simulations was the [mass × collision probability] value of each object. This criterion can be applied to objects in the current environment to identify potential targets for removal in the near future. The altitude-versus-inclination distribution of the top 500 objects identified via this selection criterion is shown in figure 3. The prograde group is dominated by several well-known classes of vehicles: SL-3 rocket bodies (Vostok second stages; 2.6 meter [m] diameter by 3.8 m length; 1440 kilogram [kg] dry mass), SL-8 rocket bodies (Kosmos 3M second stages; 2.4 m diameter by 6 m length; 1400 kg dry mass), SL-16 rocket bodies (Zenit second stages, 4 m diameter by 12 m length; 8900 kg dry mass), and various Meteor-series (Russian meteorological satellites) and Cosmos spacecraft (masses ranging from 1300 to 2800 kg). Below 1100-km altitude, the total mass of all SL-3, SL-8, and SL-16 rocket bodies is about 500 tons, which accounts for close to 20% of the total mass in LEO. Objects in the retrograde region are more diverse. They include, for example, Ariane rocket bodies (1700 kg dry mass), CZ-series rocket bodies (1700 to 3400 kg dry mass), H-2 rocket bodies (3000 kg dry mass), SL-16 rocket bodies and spacecraft such as Envisat (8000 kg) and meteorological satellites from various countries.

If active debris removal is to be conducted in the near future, objects in figure 3 should be high on the target list for removal. In general, rocket bodies ought to be considered first because they have simple shapes and structures, and belong to only a few classes. However, some of the rocket bodies may carry leftover propellant in pressurized containers. Any capture operations of those rocket bodies will have to be carefully conducted. A potential problem to capture and remove objects shown in figure 3 is the nontrivial tumble rates of the targets. New ground-based observations on those objects are needed in the near future to identify their tumble states. As the international community gradually reaches a consensus on the need for active debris removal, the focus will shift from environment modeling to technology development, engineering, and operations. It is clear that major cooperation, collaboration, and contributions at the national and international levels will be needed to move forward to implement active debris removal for environment remediation.

Habitat Particle Impact Monitoring System

J.-C. Liou, *Johnson Space Center*
John Opiela, *Johnson Space Center*

Johnson Space Center's (JSC's) Habitat Demonstration Unit (HDU) is a large-scale test bed designed for the testing and demonstration of technologies, processes, and operations that would be needed to support the future human exploration missions to the International Space Station, near-Earth asteroids, the moon, or Mars. The 2010 configuration of the HDU included a Pressurized Excursion Module (PEM) that measures approximately 6 meters (m) in diameter and 4 m in height), and an airlock (figure 1). NASA is planning to install a multilayer inflatable loft on top of PEM in late 2011. The construction of the HDU was completed at JSC in the summer of 2010. After a brief dry run at a JSC rock yard facility, the unit was shipped to the SP Mountain—approximately 40 miles north of Flagstaff, Arizona—and participated in a successful NASA Desert Research and Technology Studies (DRATS) campaign for 3 weeks in late August 2010.



Fig. 1. *The Habitat Demonstration Unit in front of the SP Mountain. The large module in the center is the Pressurized Excursion Module; the smaller structure to the left is the airlock.*

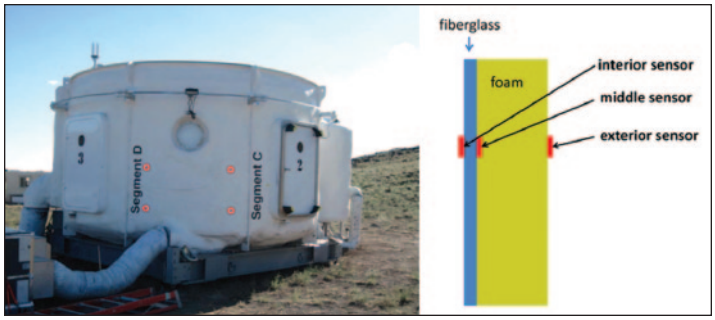


Fig. 2. *Left: the red circles indicate the locations of the sensors. Right: an illustration of the cross-section of the Pressurized Excursion Module wall structure.*

A key requirement to improve the safety of long-term habitat operations is the capability to monitor potentially damaging particle impacts on the structure. Sources of the impacting particles include orbital debris and micrometeoroids in the near-Earth environment, micrometeoroids and lunar secondary ejecta on the surface of the moon, and micrometeoroids in interplanetary space. NASA's Orbital Debris Program Office at JSC initiated an effort, with collaboration from the Naval Research Lab and Virginia Polytechnic Institute and State University, to develop the Habitat Particle Impact Monitoring System (HIMS) for the HDU in April 2009. Twelve space-qualified acoustic impact sensors were installed at four different locations and three layers on the wall of Section D of the PEM. The four locations are indicated by the red circles in the left portion of figure 2. The wall of the PEM consists of a fiberglass hard shell with a thickness of about 1 centimeter (cm) and an exterior layer of 10-cm-thick foam insulation. Sensors were attached both to the inside and outside of the PEM, and between the fiberglass shell and foam insulation (right portion of figure 2). The objective of the project in 2009-2010 was to demonstrate the HIMS capability of detecting particle impact location and the degree of impact penetration. The former is achieved by triangulation analysis using signals received by sensors at different locations. The latter is achieved by analyzing signal strength from sensors located at different layers.

Habitat Particle Impact Monitoring System

continued

The space-qualified HIMS sensors have been tested on different materials (aluminum plate, Kevlar®, multilayer insulation, etc.) subjected to hypervelocity impacts up to 7 kilometers per second (km/sec). For demonstration purposes during the DRATS campaign, however, hypervelocity impacts on the HDU were not possible. Instead, a 10-pump air rifle was used to simulate particle impacts. The degree of projectile penetration was controlled by varying the number of pumps of the air rifle. The speed of the projectile was also measured using a ballistic chronometer. It ranged from about 30 meters per second (m/sec) for one pump to 150 m/sec for 10 pumps. The transition from partial to full penetration through the foam insulation of the structure occurred around 130 m/sec.

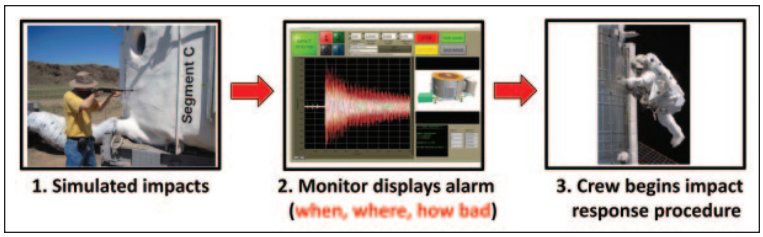


Fig. 3. *The goal of the Habitat Particle Impact Monitoring System project is to demonstrate the fully automated end-to-end capability, from simulated particle impacts to crew response based on processed impact information, during the 2011 Desert Research and Technology Studies campaign.*

HIMS team members conducted a successful impact test series during the 2010 DRATS campaign. The team collected a total of 113 air rifle shots and more than 20 hours of the HDU background acoustics data. Team members analyzed the data to optimize the HIMS parameters and developed a triangulation algorithm to identify each impact location. Key objectives for the project in 2010-2011 were to develop a three-dimensional graphical console to display impact time/location/penetration information in real time, to develop an impact response procedure for crew members in preparation for the integrated 2011 DRATS campaign, and to fully integrate the HIMS hardware and software into the existing infrastructure of the PEM. The aim for the 2011 DRATS campaign will be to test the end-to-end detection capability of the system (figure 3), and to demonstrate the potential applications of this low-cost, low-mass, low-power-consumption, easy-to-install system to other habitat structures, such as a multilayer inflatable, for future mission opportunities.

Orion On-Orbit Inspection Capability Study

Michael Rollins, *Johnson Space Center*

NASA has been directed to build a Multipurpose Crew Vehicle capable of carrying humans beyond low-Earth orbit and conducting operations in low-Earth orbit. The Orion spacecraft development is anticipated to have high applicability to this project. Service in low-Earth orbit may require the vehicle to be docked to the International Space Station (ISS) for several weeks. During this time, it will be exposed to micrometeoroids and orbital debris (MMOD), which can potentially cause critical damage to the vehicle with respect to reentry heating. Understanding the criticality of damage will depend on effective on-orbit inspection of the vehicle. In 2008, the Orion Project tasked Johnson Space Center's Image Science and Analysis Laboratory (ISAL) to study the ability to inspect the Orion thermal protection system while docked to the ISS. The findings of the study will have direct applicability to the Multipurpose Crew Vehicle.

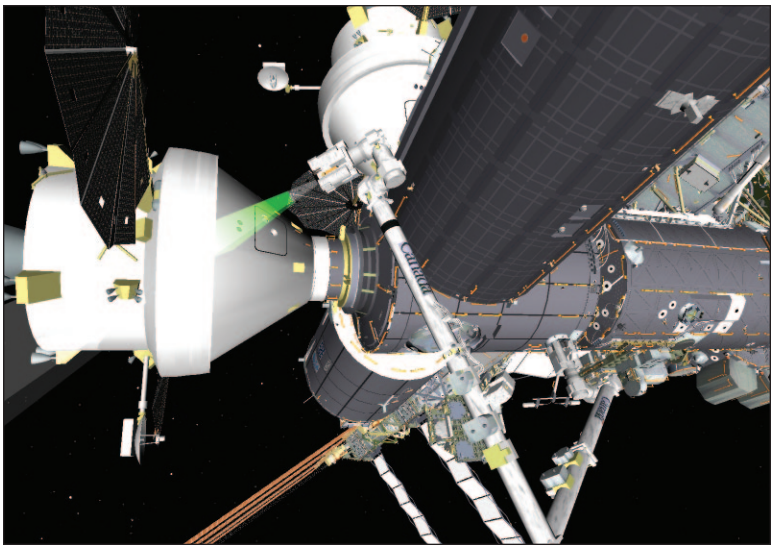


Fig. 1. *Snapshot of full-surface survey of the Orion Crew Module docked at International Space Station Node 2 Forward using Space Station Remote Manipulator System Latching End Effector camera.*

Specifically, ISAL was directed to explore the effectiveness of currently space-qualified sensors as inspection sensors for Orion docked to the ISS. At the same time, as part of their risk analyses, Orion Project personnel estimated the likelihood of critical MMOD strikes to the vehicle and has assumed that on-orbit inspections can be 95% effective in finding and determining the criticality of any such MMOD damage. For an Orion spacecraft, the surfaces of particular interest are the backshell and forward bay cover, due to their representing large components in the overall MMOD-based risk to crew safety and mission success. These surfaces are composed of tiles that are similar to the black thermal protection system tiles on the space shuttle. Critical damage to such tiles from MMOD strikes can result in damage cavities whose observable entry holes are as small as a quarter inch in diameter.

While NASA has placed a major emphasis on examining the utility of existing space-qualified sensors in the detection and characterization of MMOD damage cavities within thermal protection system tiles, the space agency has examined other sensors as well. All of the sensors examined by ISAL as candidates for on-orbit thermal protection system inspection have been non-penetrating two-dimensional (2-D) sensors (i.e., various cameras) and inherently three-dimensional (3-D) sensors (e.g., the Laser Camera System—currently space-qualified—and the Mold Impression Laser Tool). Other organizations have collected data from penetrating sensors, especially x-ray and millimeter-wave, but such sensing technology

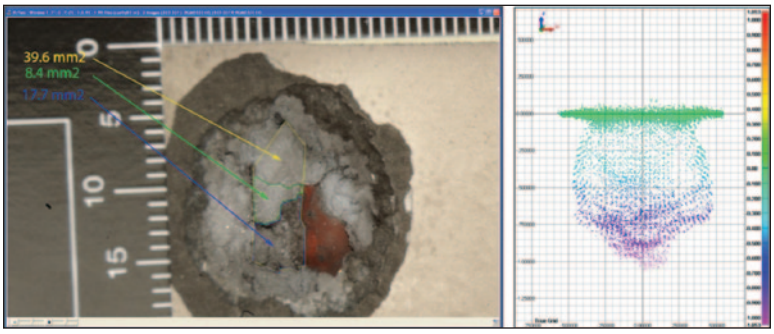


Fig. 2. *High-resolution digital image from stereo pair (left) and Laser Camera System three-dimensional point cloud elevation view (right) of hypervelocity impacted Orion thermal protection system tile are examples of potential focused-inspection sensor products.*

Orion On-Orbit Inspection Capability Study

continued

has been outside the area of expertise for ISAL to date. Non-penetrating sensors have the advantage of high resolution and strong surface contrast as compared to penetrating sensors. The latter have the advantage of not requiring unobstructed lines of sight to structural damage. The attractiveness of space-qualified sensors is that they are known to be robust to launch acceleration and vibration, space radiation, and poor cooling from the lack of atmospheric convection. Space-qualified hardware generally has also (but not always) been the product of assembling reliable, high-quality components for which an expectation for long on-orbit operating life is justified.

Based on extensive experience with space shuttle on-orbit inspections, ISAL assumed that Orion inspections would consist of two major operations—the initial full-surface survey (figure 1) and close-range focused inspection (figure 2) for any suspected damage found during the initial survey. The full-surface survey is expected to be accomplished using a camera positioned by the ISS Space Station Remote Manipulator System over comprehensive scan trajectories. The focused inspections are expected to require both cameras and 3-D sensors as well as visible-band and, possibly, ultraviolet illumination, which has been seen to cause fluorescence in material underlying the tile, greatly enhancing the possibility of determining full tile penetration (figure 3). Focused inspections may also benefit later from penetrating sensors as technology allows. The survey cameras may be the Mobile Servicing System cameras already at each end of the Space Station Remote Manipulator System (and also positioned on a robotic attachment called Dextre), or another camera with greater resolution and/or greater robustness to varied lighting such as the Laser Dynamic Range Imager, a survey-type sensor used in space shuttle inspections. Focused-inspection sensors may require six degrees of freedom in positioning to ensure needed proximity and view angles, and will most likely need to be attachable to the "arms" of Dextre (shown in figure 4).

ISAL conducted various subjective tests using data collected by cameras and 3-D sensors to try to estimate inspection effectiveness using that hardware. The testing was designed to represent both an initial survey and focused inspection as described above. Probability of

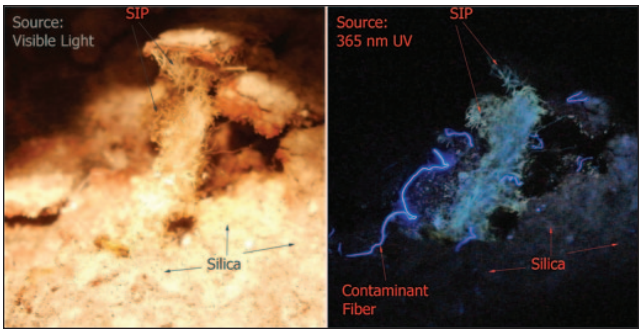


Fig. 3. *High-resolution digital image pair showing enhanced detectability of strain isolation pad material under ultraviolet illumination (right) as compared to visible-band illumination (left). Detection of exposed strain isolation pad (which will underlie tile on the Multipurpose Crew Vehicle) is an excellent indicator of full-tile penetration.*

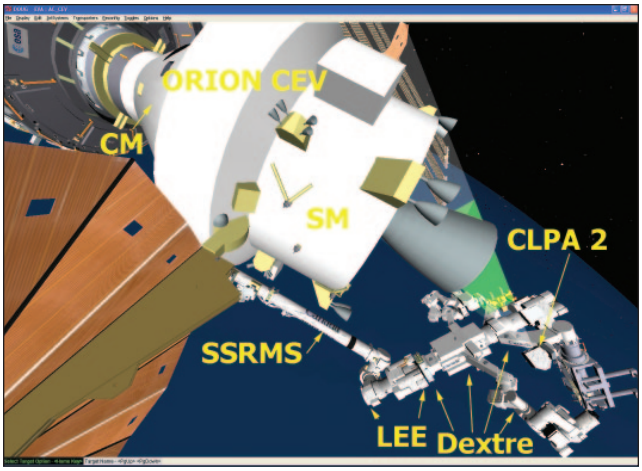


Fig. 4. *Dextre, on the Space Station Remote Manipulator System, provides additional reach and potential sensor positioning capability.*

detection for the survey portion of the inspection has been estimated to exceed 95%, especially if redundant screening teams are employed. Although results using 2-D and 3-D non-penetrating sensors are encouraging, further testing will be required to determine focused-inspection effectiveness—and therefore overall inspection effectiveness—and whether penetrating sensors will also be needed. Testing to date shows that focused-inspection effectiveness will not only be dependent on sensors selection and deployment, but also on a ground process that draws on the discernment of structural experts.

Development and Application of Space Flight Performance Shaping Factors for Human Reliability Analysis

Roger Boyer, *Johnson Space Center*
Teri Hamlin, *Johnson Space Center*
Richard Heydorn, *Johnson Space Center*
Jennifer Mindock, *University of Colorado*

A human space system must provide two primary functions with respect to its crew: protect the crew members; and use the crew members' capabilities. These are fundamental tenets of human rating a space vehicle, and designers must consider these functions in their candidate designs. They must manage both the risks that may cause harm to the crew members and the risks that may negatively impact crew members' abilities to perform their tasks.

The importance of crew performance during space missions is widely recognized, as the human ability to respond to new and dynamic situations depends on effective performance capabilities. This motivates the need to understand factors that influence performance so that factors with positive influences can be enhanced, and factors with negative influences can be minimized. Analysis of these factors and resulting performance within operational scenarios can lead to insights for improving current environmental conditions or future designs of mission elements such as the spacecraft and operations approach.

Methods exist for analyzing the reliability of human performance within the context of operational scenarios, and they are appropriately called Human Reliability Analysis methods. Most of the existing methods have their roots in nuclear power plant operations. While perhaps similar, the factors influencing performance used in these methods do not take into account the unique conditions of space flight. Therefore, this research identified factors that influence human performance of tasks during space missions and organized them into a functional hierarchy. Example factors include how a crew member's presence in microgravity causes physiological changes to occur, such as reduced aerobic capacity and bone strength. These changes can in turn alter the capability to perform a given task. Psychological and cognitive factors are also introduced from living in an isolated and confined environment, vehicle habitability factors, and high public interest and visibility. Research is aimed at incorporating these factors into a Human Reliability Analysis method, which can subsequently be included in a Probabilistic Risk Assessment for analyzing human space missions. This research is investigating approaches for quantifying the effects of these factors on reliability using existing human performance data from space and ground studies to inform the statistics. The ensuing analysis techniques can also help to define risk mitigation strategies, such as biomedical countermeasures, operational procedures, and crew training. The resultant design and/or operational solutions may then be considered for inclusion in the system.



Fig. 1. *Crew members perform tasks on the International Space Station.*

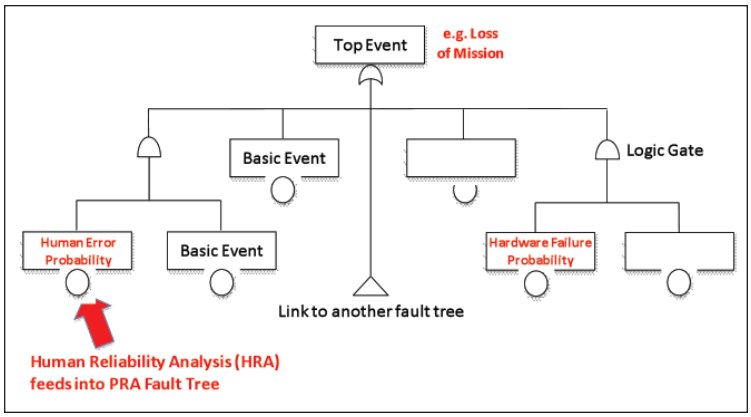


Fig. 2. *Human Reliability Analysis results inform Probabilistic Risk Assessment efforts.*

Development of a Cursor Control Device for Space Flight Operations

Kritina L. Holden, *Lockheed Martin*
Shelby G. Thompson, *Lockheed Martin*
Anikó Sándor, *Lockheed Martin*
John W. Pace, *Lockheed Martin*

Future spacecrafts will be primarily controlled through "glass cockpits" with software displays rather than hardware switches and buttons. Human factors researchers at NASA Johnson Space Center have worked for a number of years in research and development to determine the best cursor control device (CCD) for space flight operations. The device must work under vibration and acceleration, in microgravity, and ungloved and gloved (with and without pressure). Crew performance will depend greatly on the intuitiveness and ease of use of the CCD selected/designed for future missions.

Past Work

During the early 1990s, NASA conducted several CCD evaluations in the laboratory, on the KC-135 reduced-gravity aircraft, and during space shuttle missions STS-29 and STS-41. The goal was to gather data to determine the best CCD design characteristics for use in microgravity. These results ultimately serve as a starting point for future research with the Constellation Program. Standard devices such as a trackball and mouse, as well as a variety of other commercial and prototype devices, were tested using custom experimental software that recorded response times and errors. An optical mouse proved to be the fastest device in a variety of environments, but it was not a good choice for the microgravity environment due to the number of separate components. The trackball provided good performance, and had the advantage of being a fixed, one-piece design that did not require a work surface.

Constellation and the Orion Crew Exploration Vehicle

As the Constellation Program began, there was renewed interest in developing a CCD for space flight. Starting with design characteristics determined from the earlier CCD work and the knowledge that any new design had to accommodate the 1st- to 99th-percentile hand breadth and length, researchers began testing commercially available devices using a CCD test battery developed through Human Research Program funding. The CCD test battery employed cursor control tasks described in the ISO [International Standards Organization] 9241-9 standard, as well as tasks from previous studies conducted in microgravity.

In 2007, a laboratory study compared performance of nine commercial and proprietary devices with and without extravehicular activity gloves. In general, the trackball devices showed the best performance, and data were used to down-select devices for future studies. Since pressurized gloves impact gripping ability and tactility, an early concern was performance in a pressurized spacesuit. Thus, an engineering test was performed in a pressurized glove



Fig. 1. *Cursor control device prototypes.*

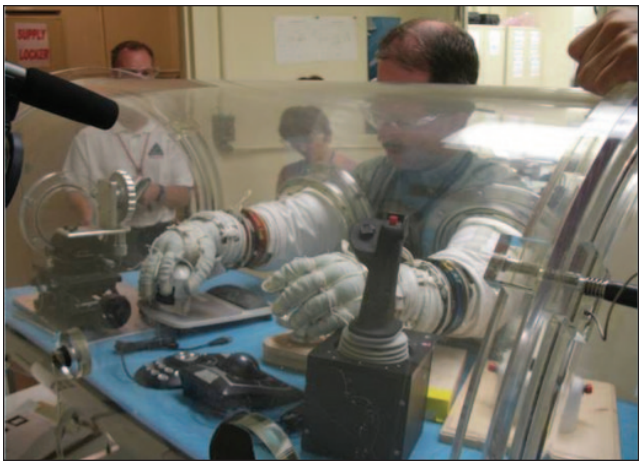


Fig. 2. *Pressurized glovebox study.*

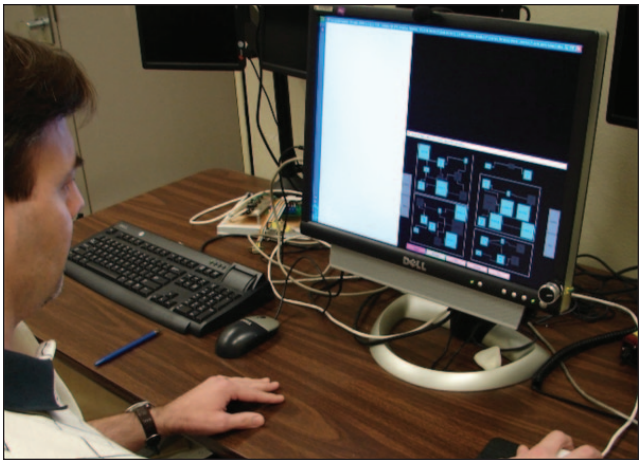


Fig. 3. *Laboratory study.*

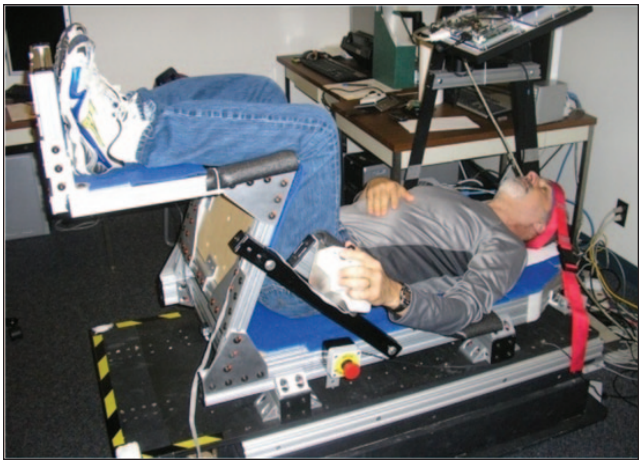


Fig. 4. *Vibration study.*

box to identify basic types of hand and finger positions as well as motions that worked best under pressure. Device components that were problematic with pressurized gloves were dropped from further consideration.

A 2008 laboratory study examined the type of cursor movement (continuous vs. discrete) and experimentally compared a trackball, cursor knob, castle switch, and scroll wheel. All devices were operated with the participant's left hand (Orion requirement) while wearing an unpressurized glove (without a thermal micrometeoroid garment). Participants performed best with the trackball in continuous mode and castle switch in four-way discrete mode in terms of movement time and accuracy.

The trackball and castle switch were then tested in 2009 with two new device prototypes: (1) a large, continuous, castle-type switch that was modeled after an F-18 aircraft control; and (2) a rocker switch. The trackball, castle switch, and F-18 device were tested in two- and four-way discrete modes; the rocker switch could only operate in two-way discrete mode. Results indicated that participants had the best performance with the rocker switch, the trackball in four-way mode, and the castle switch in four-way mode in terms of response times, with the castle switch having the lowest error rate. Results of these studies were used by the Cockpit Working Group to make design decisions about the CCD for Orion. See figures 1 and 2.

Testing Under Extreme Conditions

Some concerns were expressed about the use of the CCD under vibration, such as during launch, in the course of its development. Accordingly, in 2010 NASA performed a study in the Ames Research Center Vibration Facility to determine characteristics of CCDs that perform well or are problematic under different levels of vibration. The vibration platform provided one axis of vibration (X axis/chest to spine) at various amplitudes and frequencies. Displays for the CCD tasks were shown on a monitor mounted in a fixed position at viewing distance above the participant's head; the monitor did not vibrate. CCDs were mounted on the chair for left-handed use as planned for Orion.

The trackball was tested in continuous and four-way discrete mode, the castle in two- and four-way discrete mode, and the rocker switch in two-way discrete mode. For all devices, the vibration conditions with higher amplitudes (3 Hz 0.17g, 6 Hz 0.35g and 12 Hz 0.70g) affected performance; lower amplitude vibrations did not cause a significant decrement in performance as compared to performance with no vibration. Response times for the two-way devices were negatively impacted by vibration, while four-way and continuous modes were not. Further research is warranted to confirm/clarify these results. See figures 3 and 4.

Conclusions

A CCD for the space environment must be accurate and efficient under a variety of challenging environmental conditions. The described body of research suggests the following: when high accuracy is required (e.g., vehicle commanding), consider CCD solutions such as the castle switch and rocker switch with a discrete cursor movement type, and the trackball for applications in which errors do not have a serious safety consequence (e.g., standard computer use in a vehicle or space-based habitat).

Development of a Composite Overwrapped Pressure Vessel Profilometry and Eddy Current Scanning System to Meet Manufacturing and Analytical Needs

Regor L. Saulsberry, *White Sands Test Facility*
Charles T. Nichols, *White Sands Test Facility*

Composite overwrapped pressure vessels (COPVs) are used extensively in spacecraft and other applications because they offer significant weight savings over metal vessels. However, even though a great deal of effort has been expended to ensure consistency of manufacturing processes and materials, variability has been higher with COPVs than with metal vessels. Samples from a recent batch of COPVs built for stress rupture testing resulted in T1000 vessel burst pressures that varied by 5%, and IM7 vessel burst pressures that varied by 8.5%, even though they were wound on computer-controlled equipment and were made from the same lots of fiber. This type of inconsistency necessitates an increase in safety factor to cover the scatter unless the lower-performance vessels can be identified and removed from the population. Additionally, issues have occurred due to liner flaws that were not detected prior to wrapping. Most COPV manufacturers apply fluorescent dye penetrant for external liner flaw detection while video scope inspections evaluate interior surfaces for defects; however, these inspections sometimes miss the presence of defects and mild ripples or buckles that result from liner anomalies.

Johnson Space Center's White Sands Test Facility (WSTF) and the NASA Nondestructive Evaluation (NDE) Working Group (NNWG) recently developed an NDE system to inspect COPVs and provide an analytical tool to understand mechanical responses of the vessels. The system consists of an internal and external laser profilometer and eddy current (EC) scanner, and can be used both during the manufacturing process and as a part of test programs. The basic COPV scanning station was originally built as shown in figure 1. The station consisted of several positioning stages, a vessel centering guide, and a calibration fixture traceable to the National Institute of Standards and Technology.

The NDE system was recently modified to retain the internal profilometry capability, but also to allow it to be reconfigured for either external profilometry or EC scanning. The rotating interior sensor probe is easily removed and replaced with offset external probes (figure 2). A rotational stage is used to spin the bottles or liners for EC and external profilometry. The system is operated by a modern LP4000 data acquisition, control, and display system, and a motor controller. This makes the system uniquely applicable to in-process manufacturing support since it has the ability to scan vessel liners and ensure that

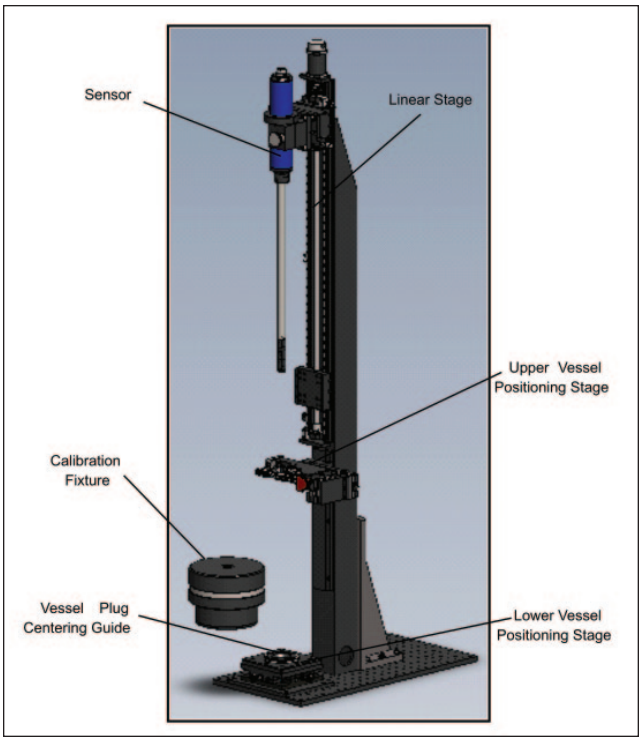


Fig. 1. *White Sands Test Facility cylindrical composite overwrapped pressure vessel mapping system.*

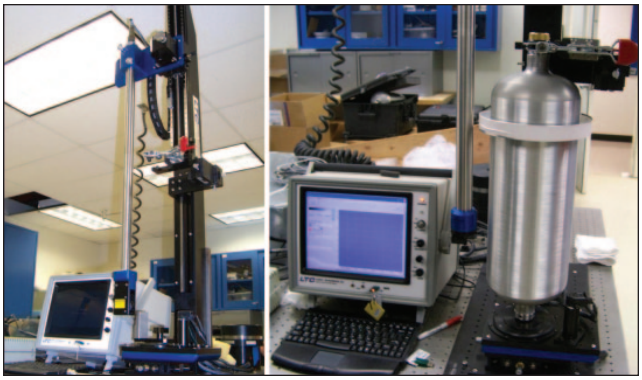


Fig. 2. *External scanner calibration using NIST-traceable standard (left) and scan of liner defect standard (right).*

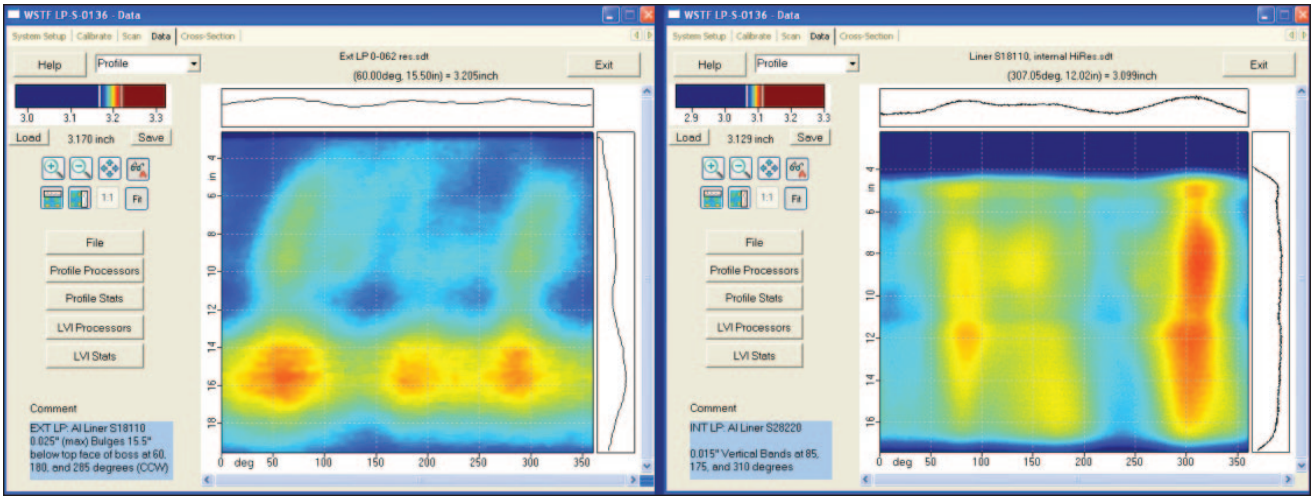


Fig. 3. *Internal cylindrical scan (left) and external scan of the same vessel (right).*

critical cracks and other EC-detectable defects do not exist, and then provide an accurate profile map of the interior and exterior (figure 3) after wrapping and testing.

The internal and external scanning system is designed to provide data accurate to +/- 0.001 of an inch (in.), which allows an accurate evaluation of any pits, bulges, and distortion, and evaluation of the amplitude and periodicity of any liner buckles or anomalies. These data provide engineering information used to see if specifications are met, and for calculation of resulting allowable cycles. These data can also support rationale to continue using COPVs with minor defects rather than replacing them. The EC system has detected surface defects approximately 0.001 in. deep in aluminum liners. A current project is under way to add sensors to evaluate for internal cracks as well as for liner crack though the composite after wrapping. The flaw detection sensitivity will be less in the new modes and will be quantified using physical standards.

The system has been used for many COPV applications at White Sands Test Facility and vendor facilities. It was shipped and used at General Dynamics (Falls Church, Virginia) to evaluate changes that occurred as the liners were wrapped and then autofrettaged to help produce optimum vessels to use for stress rupture testing. This helped identify vessels that indicated "out-of-family" deformations after autofrettage. The system was also used in a NASA Engineering and Safety Center study that characterized the response of T1000 and IM7 vessels to autofrettage. Additionally, it was used by the NNWG to evaluate bulging and other distortions that occurred as 60 vessels were incrementally strained to stress rupture

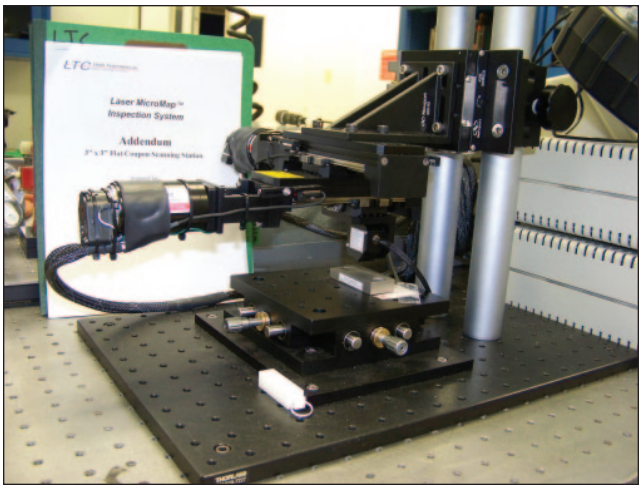


Fig. 4. *X-Y scanner, shown with NIST-traceable calibrations standard.*

failure (visit *http://nnwg.org/current/WSTF/composite.html* for more information).

An add-on to the system is an X-Y scanner for measurement of small features and defects. This can be configured as a coupon scanner (figure 4) or with legs to sit on a surface being evaluated to accurately measure and map defects, such as those resulting from impacts. This system is engineered for a shorter range and greater accuracy of 0.0002 in.

More information is available on the NNWG website (*http://nnwg.org/current/WSTF/copv.html*) or by contacting the authors.

High-Speed Measurements Provide Key Information on Events Inside a Pyrovalve

Stephen H. McDougle, *White Sands Test Facility*
Regor L. Saulsberry, *White Sands Test Facility*

In 2008, the NASA Engineering & Safety Center (NESC) conducted an assessment of four spacecraft propulsion system pyrovalve anomalies that occurred during ground testing. In all four cases, a common aluminum (Al) primer chamber assembly (PCA) was used with dual NASA Standard Initiators (NSIs) and the nearly simultaneous (separated by less than 80 microseconds [µs]) firing of both initiators failed to ignite the booster charge.

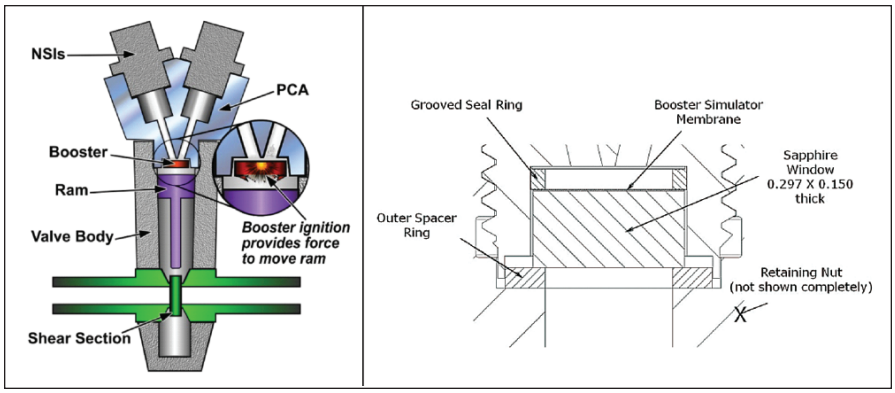


Fig. 1. *Typical stainless steel V-PCA pyrovalve and sapphire window assembly.*

As a result of the assessment's work, and because the Mars Science Laboratory (MSL) spacecraft planned to use pyrovalves with similar features, the MSL project team made changes to the PCA. The material for the PCA body was changed from aluminum to stainless steel to avoid melting and distortion of the NSI flow passages. The flow passages, which were interconnected in a Y-shaped configuration (Y-PCA), were separated into a V-shaped configuration (V-PCA). The V-shape was used to more efficiently transfer energy from the NSIs to the booster (figure 1). Development and qualification testing of the new design clearly demonstrated improved performance in terms of shorter booster ignition delays and greater margin for booster ignition.

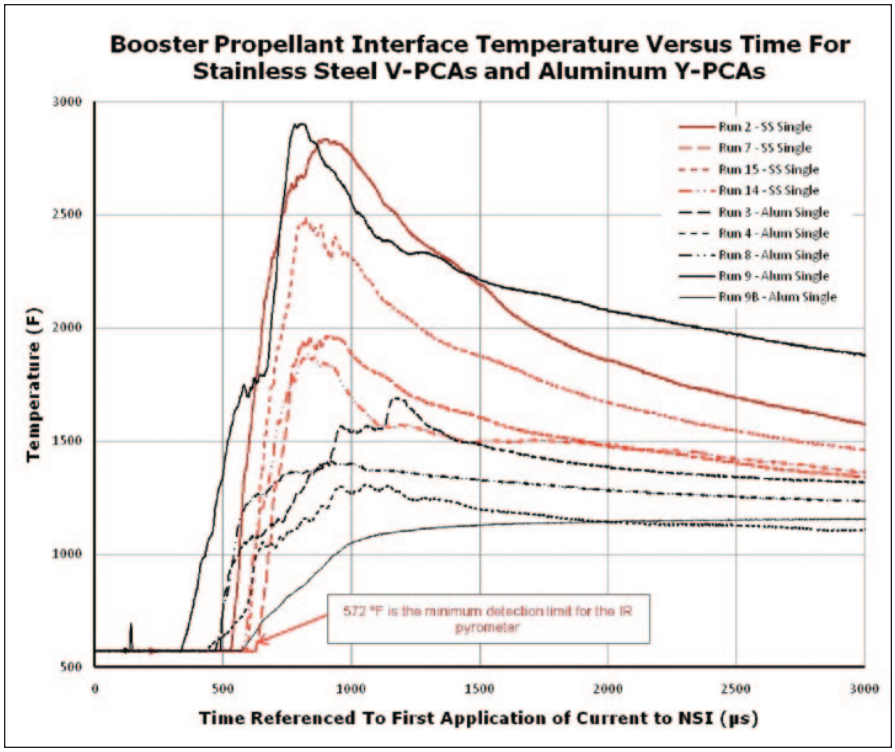


Fig. 2. *Stainless steel V-PCAs (red lines) produce much higher temps than aluminum Y-PCAs (black line).*

However, the final NESC assessment report recommended that the stainless steel V-PCA be experimentally characterized and quantitatively compared to the aluminum Y-PCA design. In addition to benefitting MSL, these data would help future NASA projects to properly evaluate the selection and use of the stainless steel V-PCA vs. the aluminum Y-PCA.

In the first phase of this new assessment, the team performed single and dual simultaneous firings of the NSIs in both PCA types to measure the peak temperature delivered to the booster propellant. This required the measurement of temperatures as high as 1649°C (3000°F) and pressures as high as 25,000 pounds per square inch gauge (psig) within time periods measured in microseconds. To accomplish this, a 0.003-in.-thick disk of booster cover stainless steel was installed where the top of the booster would normally be. A grooved seal ring, sapphire window, and retaining nut were manufactured and installed to provide a sealing arrangement that passed hydrotesting to 30,000 psig without leakage (figure 1).

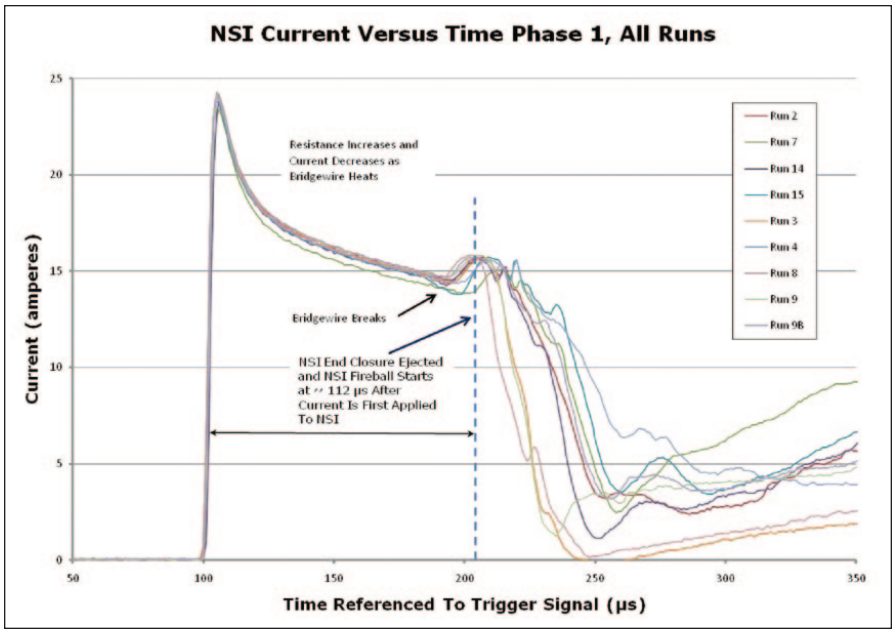


Fig. 3. *NASA Standard Initiator (NSI) current provides insights on timing of events within the primer chamber assembly.*

With such a small test article, it was important to measure temperature without adding any additional mass that would cause an unwanted heat sink. Temperature was measured with an infrared pyrometer with response time of 6 µs and a range of 300°C to 2000°C (572°F to 3632°F). The effects on the booster simulator membrane were recorded with a high-speed video camera aimed through the sapphire window at the underside of the membrane and operating at 20,000 frames per second. Special firing circuitry provided variable timing such that one or both NSIs could be fired with a precision of ±2 µs. To minimize small variations in firing times, the firing circuitry provided current of 22 to 24 amps vs. the normal NSI firing current of about 3 to 5 amps (figure 3). Data were acquired at 1 to 2 megahertz (MHz) for 20 to 40 milliseconds (ms), depending on test requirements. The data acquisition system is capable of 60 MHz. The team paid special attention to eliminate ground loops or other interferences that could compromise the data.

Testing showed the stainless steel V-PCA units delivered an average booster/propellant interface temperature much greater than that delivered by the aluminum Y-PCA units. Although the aluminum Y-PCAs ignited the booster propellant reliably, the stainless steel V-PCAs provided extra margin and produced maximum temperature in half the time. The stainless steel V-PCA units also produced pressures in the NSI cavity that were several thousand psi greater than the aluminum Y-PCA units produced (figure 2).

Dual, simultaneous (within 20 µs) firing of the redundant NSIs was shown to significantly reduce the performance of either PCA design to the point where it is doubtful the booster charge would be reliably ignited. This is consistent with findings from previous NESC assessments. The booster interface temperature needed to ignite the titanium hydride/potassium perchlorate booster charge is approximately 538°C (~1000°F). In the dual, simultaneous test firings, the maximum temperature observed was several hundred degrees below this threshold.

The second phase of the assessment evaluated the effects of various NSI ignition delays (skews) and NSI flow passages of greater cross-sectional areas with only the stainless

High-Speed Measurements Provide Key Information on Events Inside a Pyrovalve

continued

steel V-PCAs. The stainless steel V-PCAs were modified to have NSI flow passages with cross-sectional areas two and four times larger than the original design. The second phase tests showed that even with flow paths having four times the original cross-sectional area, dual, simultaneous (within 20 µs) firings of the redundant NSIs significantly reduced performance to the point the booster charge would not be reliably ignited.

The high-speed data acquisition during these tests allowed characterization of events early in the firing of an NSI (figure 4).

The assessment successfully characterized the greater margin for booster ignition provided by the stainless steel V-PCA design over the heritage aluminum Y-PCA design. Designers of spacecraft and pyrovalves now have additional information to make informed decisions regarding the trade-off between the greater weight and improved performance of the stainless steel V-PCA.

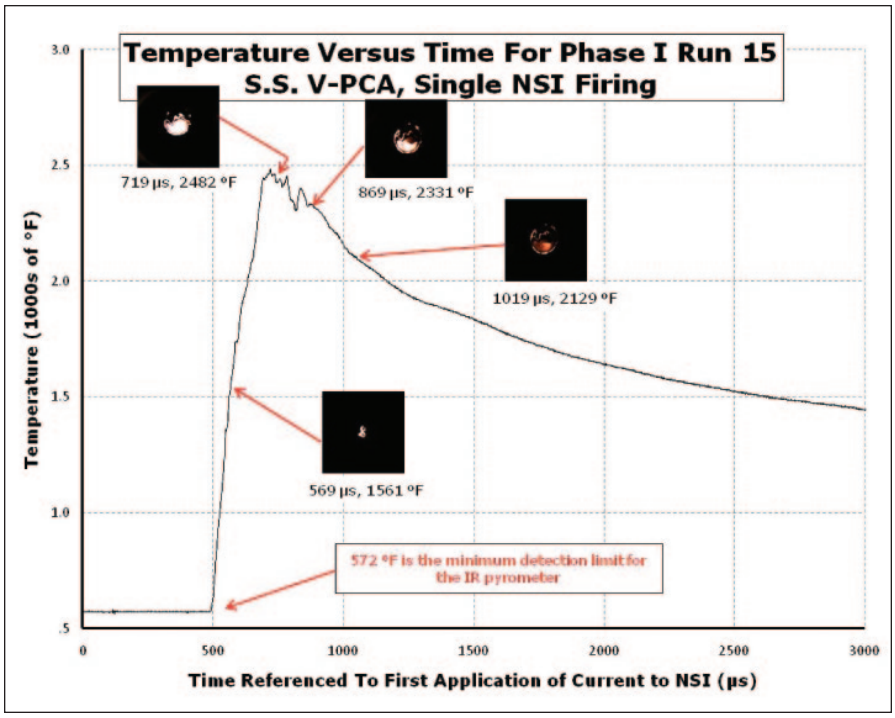


Fig. 4. *High-speed video evidence of diaphragm burn-through and correlation with pyrometer temp measurements.*

Stress Rupture Nondestructive Evaluation of Composite Overwrapped Pressure Vessels

Regor L. Saulsberry, *White Sands Test Facility*
Nathanael J. Greene, *White Sands Test Facility*
Luis Hernandez, *White Sands Test Facility*

A team of nondestructive evaluation (NDE) experts was assembled to develop and demonstrate NDE techniques capable of assessing stress rupture-related strength degradation for carbon composite overwrapped pressure vessels (COPVs), either in a structural health monitoring (SHM) or periodic inspection mode. The team was composed of individuals from the NASA NDE Working Group (NNWG), the NASA Engineering and Safety Center, academia, and industry.

The team approach was to build a versatile NDE test bed for real-time monitoring of the carbon composite vessels as they progressed under stress toward failure. To accomplish this, a 20-station test system, referred to as the NNWG Carbon Stress Rupture Test System (CSRTS), was fabricated at NASA Johnson Space Center's White Sands Test Facility (WSTF) (figure 1). The CSRTS provides a test bed for NDE and SHM development and verifications. The system design is unique because it uses a technique called "active pressure management," which uses computer control to maintain the bottle pressure within ±2 pounds per square inch (psi) regardless of temperature variation without the use of accumulators. The COPVs are housed in a protective polycarbonate enclosure so that visual inspection can be performed while vessels maintain full test pressure. In addition, pressure vessels are automatically isolated as they rupture, so adjacent vessels remain in test. The state-of-the-art facility offers extensive data acquisition and real-time NDE capability to validate sensors and NDE for spacecraft applications.

T1000 and IM7 carbon fiber bottles were wrapped and stress rupture aged in lots of 20. The team selected these two fiber types to represent current and future carbon COPV designs. During stress rupture progression testing that started in 2008, NDE and SHM data were correlated with real-time instrumentation (pressure, strain gauges and belly bands, and temperature) to evaluate and demonstrate potentially effective spacecraft applications. Creep was monitored during progression to failure for the accelerated 6- to 8-week tests. Data from fiber Bragg grating sensors (surface mount and embedded) (figure 2), conventional and fiber-based acoustic emission sensors, wireless distributive impact detection systems, and phased array



Fig. 1. *Reviewing data from carbon vessels and real-time nondestructive evaluation in test bed.*

acoustic emission were collected for comparison. A new felicity ratio method for COPVs developed by WSTF has shown promise, and in limited testing has predicted failure within 2%. WSTF personnel are creating real-time analysis software to further refine predictions and modularize the system for flight applications.

The test system is offered as a test bed to evaluate other SHM systems being developed by Small Business Innovation Research and Small Business Technology Transfer programs. As long as NNWG testing continues,

these SHM systems can be added to COPVs as they become available. Without testing of these SHM systems on COPVs, their performance is subjective and not well evaluated. Current plans call for application of various in-situ fiber-based methods, the WSTF-developed felicity ratio acoustic emission method, as well as passive wireless (strain and temperature measurement) and eddy current strain sensors orientated to measure strain in specific wrap angles. These new methods are to be added during testing planned from 2012 through 2014 as a close simulation of future flight applications. In testing to date, pretest NDE (shearography, thermography, and internal profilometry) has been performed on vessels prior to installation in the test system. The NDE response has been compared to physical standards to better quantify results and evaluate manufacturing consistency. After pretest NDE, the vessels have been instrumented in lots of 20 and installed in the test system. Once the test is started, the vessels are initially pressurized to approximately 90% of their design burst pressure. If no failure occurs after 2 weeks, the pressure is increased by approximately 100 psi and held at this pressure for another 2 weeks before implementing the next pressure step. The process continues until four or five of the vessels fail, then the system pressure is dropped to ambient and the remaining vessels are removed for NDE evaluation. Correlations are made between pretest, real-time, and posttest data. Posttest NDE is being performed at NASA centers (Marshall Space Flight Center, Langley Research Center, and Glenn Research Center [GRC]), in academia, and at industry sites best suited to apply the various techniques.

Once posttest evaluation is complete, vessels are returned to WSTF for further stress rupture aging and monitoring. The posttest NDE is then repeated to provide at least two levels of stress rupture aging data for NDE response comparison. Posttest NDE methods have included Raman spectroscopy scanning, phased array ultrasonic testing (UT), immersion UT scanning, other UT-guided wave techniques to evaluate modulus change and distributed damage, and profilometry to map and measure bulging, distortions, and growth that have occurred. Deformation is evaluated by internal laser profilometry and other techniques such as shearography, UT, and line scan



Fig. 2. *Conventional strain gauges installed near fiber Bragg gratings, relative to laser profilometry map.*

thermography, which is used to evaluate distributed damage accumulation. The UT techniques have shown the greatest promise for physical property evaluation, such as modulus, which may be correlated to loss of integrity.

In addition to evaluating the progression toward stress rupture failure by NDE, WSTF has partnered with GRC for performing destructive analysis of failed and virgin vessels to further evaluate physical property and microstructural changes. Data from this analysis may be useful in selecting additional NDE techniques to measure these changes.

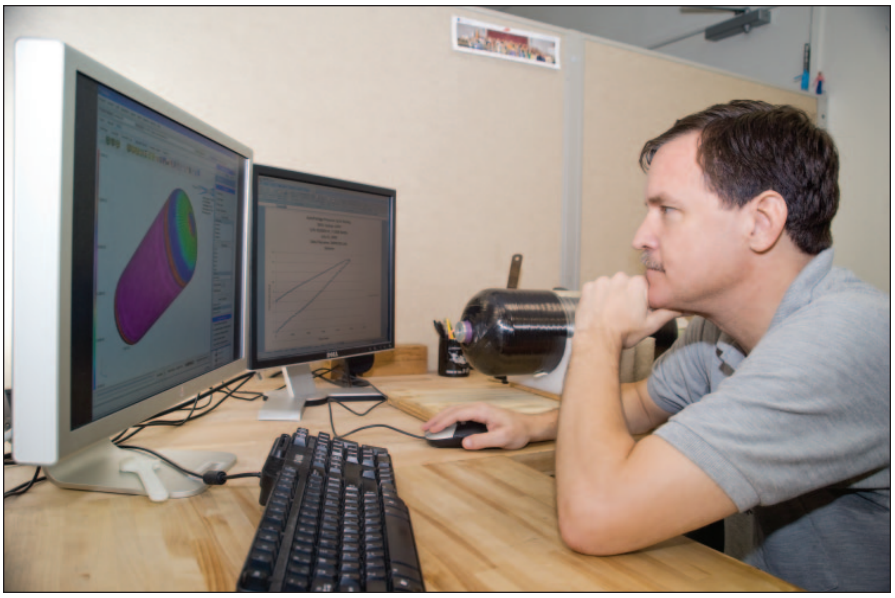


Fig. 3. *Comparing vessel test data to a composite overwrapped pressure vessel model.*

Understanding the physical and chemical property changes associated with stress rupture progression, and development of fundamental methods for stress rupture aging evaluation and vessel health monitoring can help ensure mission success and safe COPV use. This will benefit NASA spaceflight programs, Department of Defense, Department of Transportation, Department of Energy, and commercial aerospace companies that are developing NDE and SHM technology. Data from the program also serve to enhance the carbon stress rupture database, housed at WSTF, as well as increase the technical communities' understanding of vessel mechanical response as compared to modeling effort results (figure 3) being worked at WSTF and GRC and supported by the NASA Engineering and Safety Center Composite Pressure Vessel Working Group.

Acoustic Emission and Development of Accept-Reject Criteria for Assessing Progressive Damage in Composite Materials

Jess M. Waller, *White Sands Test Facility*
Charles T. Nichols, *White Sands Test Facility*
Regor L. Saulsberry, *White Sands Test Facility*

NASA has been faced with recertification and life extension issues for epoxy-impregnated Kevlar® 49 (K/Ep) (E.I. du Pont de Nemours and Company, Wilmington, Delaware) and carbon (C/Ep) composite overwrapped pressure vessels (COPVs) used in various systems on the space shuttle and International Space Station, respectively. Each COPV has varying criticality, damage and repair histories, time at pressure, and pressure cycles. COPVs are of particular concern due to the insidious and catastrophic burst-before-leak failure mode caused by stress rupture of the composite overwrap. Stress rupture life has been defined as "the minimum time during which the composite maintains structural integrity considering the combined effects of stress level(s), time at stress level(s), and associated environment." Stress rupture has none of the features of predictability associated with metal pressure vessels, such as crack geometry, growth rate and size, or other features that lend themselves to nondestructive evaluation (NDE). In essence, the variability or "surprise factor" associated with stress rupture cannot be eliminated. Consequently, NASA has devoted much effort to develop NDE methods that can be used during post-manufacture qualification, in-service inspection, and structural health monitoring of COPVs. One of the more promising NDE methods for detecting and monitoring actively growing flaws and defects in composite materials is acoustic emission (AE). It is hoped the AE procedures being developed will lay the groundwork for establishing quantitative accept-reject criteria of composite materials and components such as COPVs so that precautionary or preemptive engineering steps can be implemented to minimize or obviate the risk of stress rupture.

Experimental

Testing was performed at NASA Johnson Space Center's White Sands Test Facility. Unidirectional 4560 denier Kevlar® 49 composite strands (manufactured in 1987 and prepared per American Society for Testing and Materials [ASTM] D 2343) had an ultimate tensile strength of 3.74 ± 0.19 gigapascal (GPa) (542 ± 28 kilopound per square inch [ksi]); the epoxy matrix was LRF-092 resin. Unidirectional 3817 denier T1000 and 3775 denier IM7 12,000-filament composite tows had an ultimate tensile strength of 6.81 ± 0.37 GPa (988 ± 53 ksi) and 3.96 ± 0.31 GPa (575 ± 45 ksi), respectively; the epoxy matrix was UF3323-102 resin from TCR Composites (Ogden, UT). Each tow specimen had 25 × 51-mm (1 × 2-in.) cardboard end tabs with spacers on the outside edge (figure 1, left). Tow ends were secured inside the end tabs with a fast-setting epoxy. This tabbing procedure reduced the amount of tow pullout and crushing (fewer grip failures) and reduced grip noise. IM7 unidirectional composite tow results were then compared to a 15.7-cm- (6.2 in.)-diameter cylindrical IM7 COPV with an aluminum liner, manufactured from the same IM7 material-of-construction (same carbon fiber spools, epoxy matrix, cure cycle, and fiber volume fraction).

AE measurements were taken using a DWC FM-1 system (Digital Wave Corp., Centennial, Colorado). Each channel was connected to a DWC PA-0, 0 dB gain preamplifier. Tabbed specimens were configured with four DWC B1080 piezoelectric sensors (50 kilohertz [kHz] to 1.5 megahertz [MHz] frequency range) positioned approximately 4 cm (~ 1.6 in.) apart (figure 1, right).

Intermittent load hold (ILH) tensile stress profiles (figure 2) based on the pressure tank examination procedure described in ASTM E 1067 (also referred to as the manufacturer's qualification test in ASTM E 1118) were applied. Accumulated composite damage was monitored by the decrease in the Felicity ratio (*FR*), given by:

$$FR = \frac{load\ at\ onset\ of\ significant\ AE}{previous\ maximum\ load}$$

Fast Fourier transforms (FFTs) were obtained using DWC WaveExplorer™ software. FFTs were exported to Microsoft Excel® (Microsoft Corporation, Redmond, Washington), and the area under the frequency curve was calculated using a right Riemann sum and a step size equal to the default interval between frequencies (0.49 kHz). Frequency ranges were assigned to micromechanical damage mechanisms per de Groot's "Real-time Frequency Determination of Acoustic Emission for Different Fracture Mechanisms in Carbon/Epoxy Composites" as follows: matrix cracking, 90 to 190 kHz; fiber pullout and debonding, 190 to 300 kHz, and fiber breakage, > 300 kHz.

Results and Discussion

The most significant finding was the observation of linear decreases in the *FR* with increasing load during ILH testing. While acceptable linearity ($R^2 > 0.9$) was obtained on K/Ep tow by using the first significant AE event to determine onset of significant AE, acceptable linearity could only be obtained on C/Ep tow using the first five or more significant events. All K/Ep, all C/Ep IM7, and most (four of six) C/Ep T1000 tow specimens failed explosively. A new parameter, referred to as the critical Felicity ratio (*FR**), was developed, and is simply the extrapolated value of *FR* at failure. K/Ep tow gave an *FR** close to 0.88 (scatter not determined). Both IM7 and T1000 gave an FR* near 0.96 with an observed scatter between 1.2% and 1.4%. Based on the rate of progressive damage accumulation, T1000 was found to be more damage tolerant than IM7, and C/Ep (T1000 or IM7) was found to be more damage tolerant than K/Ep (figure 3).

By comparison, IM7 and T1000 gave an ultimate tensile strength with an observed scatter between 5.3% (T1000) and 7.9% (IM7), indicating that *FR* behaves more like a universal damage parameter, while the tensile strength is more sensitive to surface flaws and strength variation over the cross-sectional area. By analogy, COPV burst pressure would be expected to be more scattered than the *FR** for a given COPV population. For example, taking *FR* = 1 as the threshold for significant accumulated damage, a damage threshold of 743 newtons (N) (167 pounds force [lb_f]) was obtained for IM7, and 939 N (211 lb_f) for T1000. Similarly, the slope of the *FR* vs. load ratio (*LR*) line was flatter for T1000 than for IM7 (figure 3). K/Ep, although quieter than C/Ep, undergoes a steeper and more dramatic drop in *FR* upon loading and therefore is less damage tolerant. This seems counterintuitive (quieter = lower damage tolerance) until it is realized that the

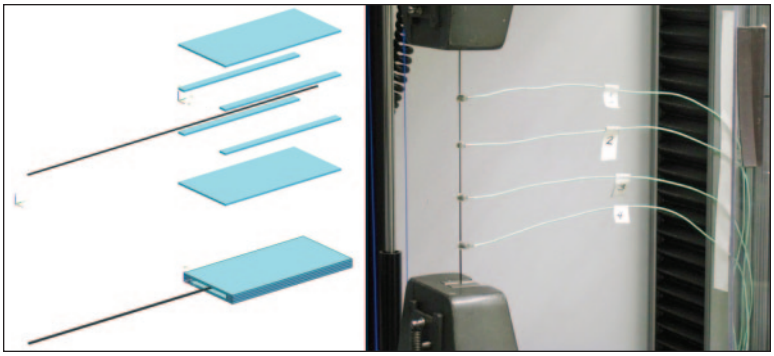


Fig. 1. *Cardboard end tabs and a mounted carbon epoxy tow specimen showing four B1080 acoustic emission sensors.*

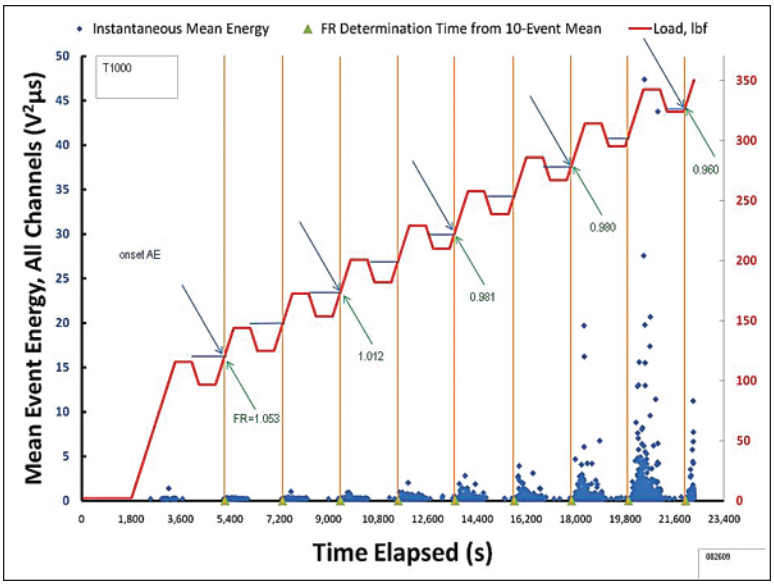


Fig. 2. *Representative intermittent load hold stress schedule used for T1000 carbon epoxy tow. Right y-axis units are in lbf.*

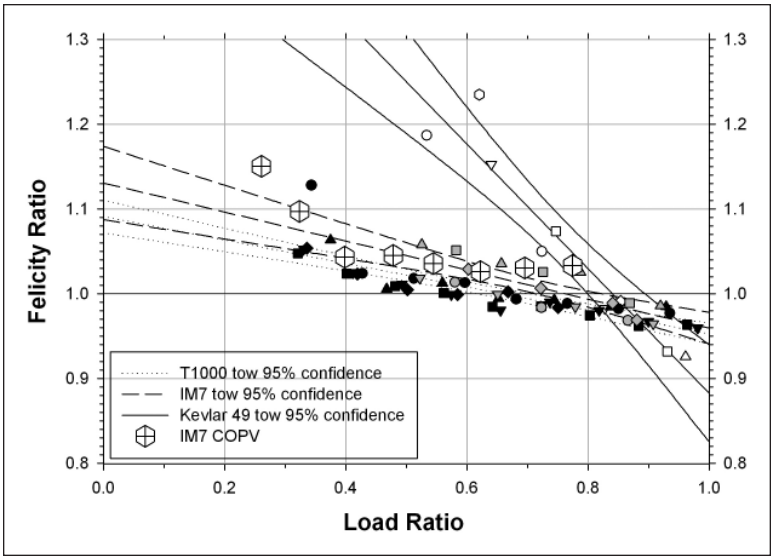


Fig. 3. *Least squares fits and 95% confidence intervals.*

AE events associated with K/Ep damage, while fewer, tended to be more energetic than those associated with C/Ep damage.

IM7 COPV data acquired using the same ILH profile as used in the above unidirectional tow tests were found to overlap IM7 tow data (figure 3) (Note: *FR*s were calculated the same way; i.e., the first 15 events were averaged). This overlap suggests that the IM7 COPV was trending toward failure in much the same way the IM7 tows were proven true in a subsequent two-part ILH test to burst (Nichols et al., this publication).

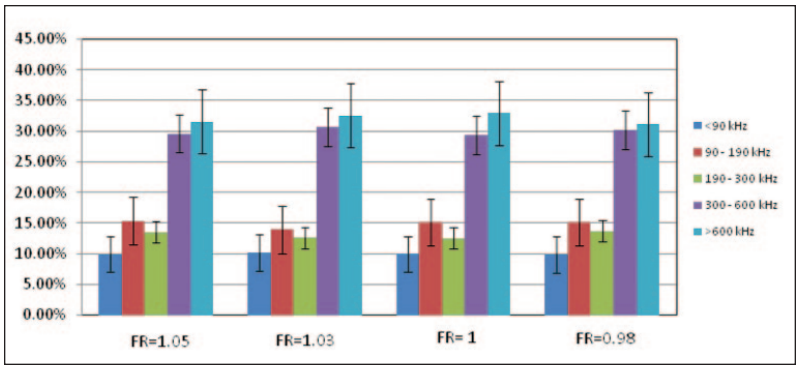


Fig. 4. *Fast Fourier transform frequency distributions for IM7 Felicity ratio events at increasing levels of accumulated damage.*

Waveform and Fast Fourier Transform Analysis

Three characteristic waveforms were identified in the C/Ep tow tests, each differentiated on the basis of amplitude, duration, and frequency: low amplitude signals with lower frequencies and short durations attributed to matrix cracking; moderate amplitudes with high frequencies and short durations attributed to fiber breakage; and high amplitudes with a wide range of frequencies and long durations attributed to concerted failure including all modes of micromechanical damage (most common).

In the case of uniaxial loading parallel to the fiber axis, microdamage attributable to tranverse matrix cracking would not be expected to be as relevant as microdamage attributable to fiber breakage. C/Ep FFT data show this is exactly what occurred in IM7 and T1000 tow specimens. More specifically, FFT analysis of the *FR* events responsible for the onset of significant AE (due to creation of new damage sites or growth of existing ones) during the ILH up ramps revealed that the frequency distribution for these events was invariant with respect to applied load (figure 4). Also, the frequency distribution noted for T1000 (data not shown) was essentially the same as for IM7. For example, fiber breakage (> 300 kHz) was the most predominant failure mode for both IM7 and T1000 at all applied loads. Lastly, T1000 had slightly more low-frequency (90-190 kHz) damage associated with matrix cracking than IM7, perhaps due to the higher fiber strengh of the T1000, thus causing stresses to be localized more within the matrix at equivalent loads.

Summary

Linear decreases in *FR* were observed with increasing stress during ILH testing of K/Ep tow, C/Ep T1000 and IM7 tow, and an IM7 COPV. Tests on C/Ep tow further showed that *FR** behaves like a universal damage parameter that exhibits less scatter than the tensile strength or, analogously in the case of a COPV, the burst pressure. An FFT analysis of the *FR* events responsible for the onset of significant AE revealed that the frequency distribution was invariant with respect to applied load, hence the amount of accumulated damage. These observations lay the groundwork for using both the *FR* and accumulated amount of composite damage (e.g., fiber damage) determined from FFTs as analytical accept-reject criteria for composite materials and components subjected to periodic stress over their service lifetime (e.g., cyclic loading for structural composites, or refill cycles for COPVs).

Optimized Software Approaches to Predict Rupture in Fracture-critical Composites and Implications for Structural Health Monitoring

Charles T. Nichols, *White Sands Test Facility*
Jess M. Waller, *White Sands Test Facility*
Regor L. Saulsberry, *White Sands Test Facility*
Kenneth L. Johnson, *NASA Engineering and Safety Center*
Douglas E. Weathers, *Intern, New Mexico State University*
Jonathan M. Tylka, *Intern, University of Missouri*

The NASA Johnson Space Center (JSC) White Sands Test Facility (WSTF) has been active in testing and evaluating composite overwrapped pressure vessels (COPVs) since the 1970s, including that of the first flight-rated vessel test program for the JSC Crew and Thermal Systems Division. More recently, WSTF has been investigating COPV catastrophic failure modes. The highly energetic and unpredictable burst-before-leak failure mode is especially worrisome.

Current empirical and modeling approaches to evaluate COPV performance and reliability are either not practical, cost effective, or sufficiently accurate (e.g., conventional remove-and-inspect strategies cannot be employed on International Space Station COPVs). Stochastic failure prediction models that assess reliability risk factors are often based on data acquired on older designs and do not bracket newer designs and materials. Reduced lifetime or premature rupture due to impacts from handling or micrometeorite orbital debris must be taken into account for carbon-epoxy (C/Ep) COPVs. Together, these factors contribute to uncertainty concerning the remaining life in a COPV, thus tipping the balance toward overdesign to increase the margin of safety and resulting in loss of payload.

No integrated nondestructive evaluation (NDE) plan currently exists by which to baseline defect levels in fleet COPVs, or to perform life-cycle maintenance inspections either in a traditional remove-and-inspect mode or in a more modern in-situ structural health monitoring (SHM) mode. Lastly, quantitative NDE accept-reject criteria have not been developed to assess mechanical damage in COPVs. Work at WSTF has identified acoustic emission (AE) as a promising tool for quantitative accept-reject criteria of composite strand specimens (see Waller et al., Acoustic Emission and Development of Accept-Reject Criteria for Assessing Progressive Damage in Composite Materials, in this 2011 JSC Biennial Research and Technology Development Report publication). This paper discusses application of that AE method to flight-like C/Ep COPVs.

Individualized lifetime prediction is especially important for COPVs due to their varying criticalities, usage, damage, and repair histories. For the AE approach to be applicable, the composite test material must be subjected to thermal or mechanical stresses that can cause new flaw sites to be created or preexisting ones to grow, thus producing measurable AE. The stresses must be applied in a controlled, reproducible manner so the trends in the generated AE response can be examined analytically and in such a way as to determine how much the Kaiser effect is being violated. The Kaiser effect is violated when AE activity is observed below a previous highest stress (or, in the case of a COPV, pressure) due to increasing levels of accumulated damage in the composite. Failure can then be predicted by determining analytically how close a composite is to a critical threshold of damage where failure is known to occur.

Experimental

A periodic intermittent load hold pressure profile that is based on the pressure tank examination procedure described in American Society for Testing and Materials (ASTM) E 1067 (referred to as the manufacturer qualification test in ASTM E 1118) was applied to an IM7 COPV using a high-pressure hydraulic pump. The COPV was pressurized at approximately 10 pounds per square inch per second (psi/sec). Depressurization rates were controlled manually. The pressurant media was a 95% water and 5% soluble oil solution. Pressure was measured using two pressure transducers located upstream of the COPV. Temperature, which remained relatively constant, was monitored upstream of the COPV and in the Lexan® (SABIC Innovative Plastics [formerly General Electric Plastics], Pittsfield, Massachusetts) blast-containment area. In-house software capable of remotely monitoring and controlling the pressure profile was used to ensure safety. Personnel access was strictly controlled during tests.

The IM7 COPV consisted of a cylindrically shaped 6061-T6 aluminum alloy liner wrapped with IM7 pre-preg strands of the same lot used in analogous composite strand tests (Waller et al., this publication). The COPV had a nominal outer diameter of 16.0 cm (6.3 in.), length of 50.0 cm (19.8 in.), and a minimum wall thickness of 2.0 mm (0.080 in.). The wrap pattern was 3H/15C. Helical (H) wraps consisted of 2 plies oriented at ± 13.8 and ± 17.1 deg with an average angle of 14.9 deg relative to the axial direction of the vessel. The cirque (C) or "hoop" wrap consisted of 1 ply. Hydroburst tests on two vessels of identical construction gave a burst pressure of 51.91 ± 1.01 MPa (7529 ± 147 psi).

Optimized Software Approaches to Predict Rupture in Fracture-critical Composites and Implications for Structural Health Monitoring

continued

The COPV was instrumented with six broadband B1025 piezoelectric sensors spaced acceptably for picking up high-frequency (> 300 kHz) AE caused by fiber breakage. The corresponding AE data were used to calculate changes in Felicity ratio (FR) (Waller et al., this publication, for details pertaining to AE).

Predicting Composite Overwrapped Pressure Vessel Burst Pressure

Predicting COPV burst pressure, P^*, is difficult given the wide Weibull variability exhibited by composites. However, C/Ep composite strand data suggest that *FR* behaves like a universal damage parameter and should therefore exhibit much less scatter than P^* (Waller et al., this publication). This opens up the possibility of predicting the P^* of an unknown COPV by comparing its initial *FR* behavior to that of a population of identical COPVs (or identical composite strands). Implicit in this approach is the notion that as one approaches P^* with more *FR* data points, the accuracy of the predicted P^* will increase.

The *FR* dependence was determined for an "unknown" IM7 COPV subjected to a two-part intermittent load hold pressure profile to its burst pressure as a proof of concept. If the *FR* has a good or better linear dependence on load ratio with an $R^2 > 0.8$, the expected FR^* for the family of identical COPVs or strands can be used to predict the burst pressure with reasonable accuracy using Eq (1):

$$P^* = \left(\frac{FR^* - b}{m}\right)[1 \pm (1 - R^2)^2] \qquad (1)$$

where, based on the linear least-squares fit, m is the slope and b is the hypothetical zero load *FR*. Assuming that COPV FR^*s exhibit the same scatter as composite strand FR^*s (1.2% to 1.4%), the *FR* method should be able to predict the burst pressure with similar accuracy. Application of Eq(1) verified this, giving a predicted P^* of 54.3 ± 1.0 MPa (7870 ± 144 psi), with a 1.8% error, which was virtually identical to the observed P^* of 54.25 MPa (7869 psi) (figure 1).

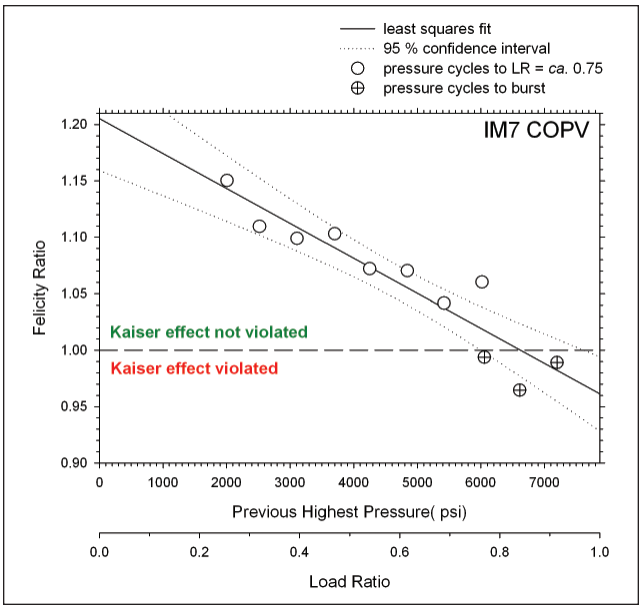


Fig. 1. *Felicity ratio results for an IM7 composite overwrapped pressure vessel pressurized to 6800 psi and then to burst at 6870 psi.*

Optimized Software Approaches

Analyzing AE data without the aid of sophisticated software is time consuming and occasionally introduces human error due to the complexities involved. To circumvent these issues, an algorithm was developed to reduce the AE data and automatically predict the critical rupture point. An extensive validation process has been undertaken to increase the versatility and accuracy of the algorithm. A graphical user interface is also being developed to allow real-time analysis of pressurized (stressed) systems.

Specific features of the algorithm include automatic AE data filtering and synchronization of the AE and pressure data. This algorithm also checks the linearity of the *FR* vs. previous highest-pressure data using several different averaging methods for determining the onset of significant AE (*FR* nominator), selecting the best (optimal) averaging method to use for the existing AE data set. Four averaging methods are considered: (1) n method: n^{th} AE event = onset; (2) $\bar{n}$ method: mean of the first n AE events = onset; (3) $n\%$ method: the AE event n% into all of the AE events for that ramp = onset; and (4) $\bar{n}\%$ method: mean of the first n% of the AE events for that ramp = onset. A Ramer-Douglas-Peucker subroutine is used to determine the previous maximum load (*FR* denominator). To assess the goodness of fit of the generated FR data, both coefficient of

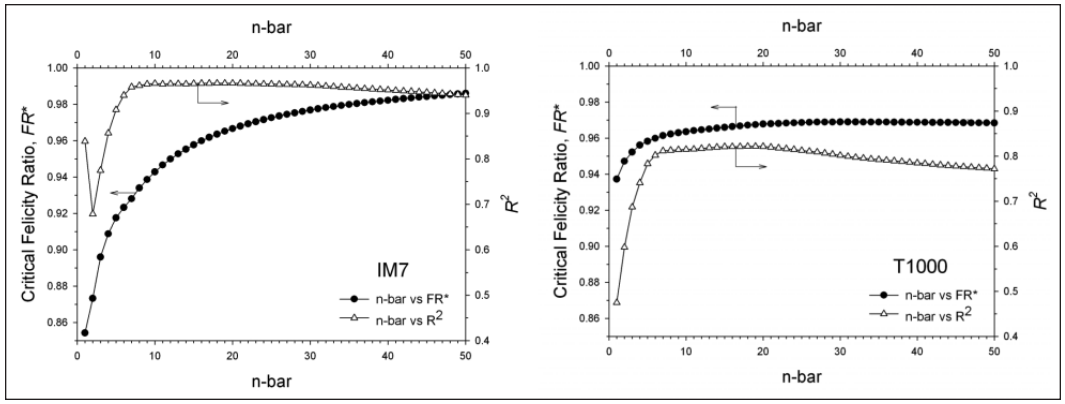


Fig. 2. *Dependence of R^2 and FR* with mean of acoustic emission events to determine onset of significant acoustic emission.*

determination, R^2, and least absolute residual approaches are used, eliminating outliers when necessary. Data output consists of R^2 vs. *FR* plots for each averaging method (figure 2). Data suggest that by developing a master *FR* curve for a family of identical composite materials, a rapid assessment of in-family or out-of-family performance can be made solely on the basis of comparing the initial *FR* vs. *P* curve. It is intended that future revisions of the algorithm will include this feature.

More elaborate statistical analyses of AE test results are being performed, in collaboration with the NASA Engineering and Safety Center, to determine the minimum *FR* data/pressure ramps that need to be collected to predict burst pressure accurately (e.g., with 95% confidence). The output of these analyses will be a response surface (figure 3) determined by multiple regression of the difference between the actual and the predicted failure pressures plotted against the number of initial *FR* data points (or pressure ramps) for a given *FR* significance method.

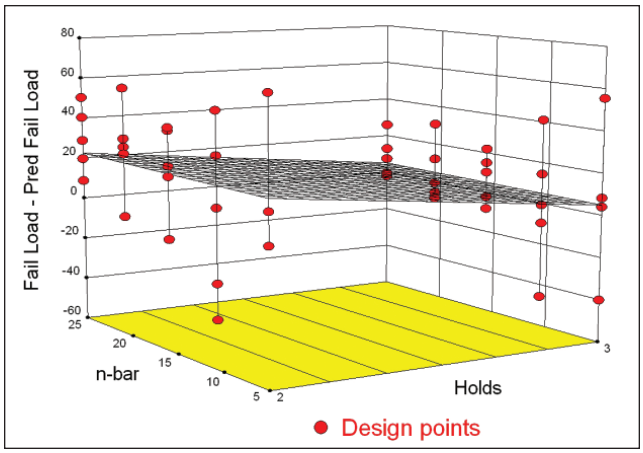


Fig. 3. *IM7 response surface showing actual and predicted failure load (z), FR (y), n̄ method (x).*

Future Applications

While individualized lifetime prediction is especially important for COPVs, the same can be said for fracture-critical structural composites used in commercial airplanes, bridges, and pipelines subjected to periodic or fixed loading. Another ideal candidate would be compressed natural gas energy storage devices used in automobiles.

To provide greater benefit to NASA spacecraft applications, the software must be further developed into a fully automated, real-time AE SHM system. This tool would then undergo application refinement and ruggedization tailored to the qualification requirements of specific spacecraft programs. Prototype executable software is being prepared for distribution to NDE departments at other NASA centers for evaluation, which should reduce AE data-reduction labor requirements. WSTF is also considering developing a "black box" system for real-time SHM of COPVs and other amenable fracture-critical composite components (in which periodic controlled loading can be applied) on crewed and crewless NASA platforms. These systems, once developed, will represent a unique stand-alone capability not present elsewhere in NASA or industry, and may have cross-cutting implications extending into the SHM of COPVs used in the transportation industries as well.

Space Environments and Thermal Vacuum Effects on Composite Overwrapped Pressure Vessels

Nathanael Greene, *White Sands Test Facility*
Christopher Keddy, *White Sands Test Facility*
Ralph E. Lucero, *White Sands Test Facility*
Joshua D. Tamminga, *White Sands Test Facility*

Since 1978, the NASA Johnson Space Center White Sands Test Facility (WSTF) has been active in testing and evaluating composite overwrapped pressure vessels (COPVs) in support of NASA human space exploration missions. WSTF has developed new approaches for test and evaluation of COPVs in simulated space flight environments of thermal vacuum. Specifically, COPVs are being evaluated to determine the effect of vacuum, shelf life, and thermal effects on cycle, stress rupture, and residual static strength.

Partnerships

Several NASA organizations are contributing funding and support to this project. The partnership includes:

- NASA Headquarters Safety and Mission Assurance, which has provided overall guidance
- The In-Space Propulsion Program, which has donated test articles
- The NASA Engineering Safety Center (NESC) Composite Pressure Vessel Working Group (CPVWG), which has provided technical support for development of finite element analysis (FEA) models at WSTF
- The NASA Jet Propulsion Laboratory, which has provided guidance on experiment planning
- Lawrence Livermore National Laboratories, which has provided technical support and composite coupon-level vacuum environment test data

Test System

The test chamber (figure 1), located in the WSTF Laboratories Building, has been uniquely designed to perform long-term durability components and materials testing using parallel vacuum systems. During testing, one vacuum system can be isolated and maintained with the other system in operation, which allows testing of components and materials that continuously outgas for multiyear durations. Typical test chambers lose high vacuum as soon as out-gassed products contaminate vacuum equipment, resulting in loss of test integrity.

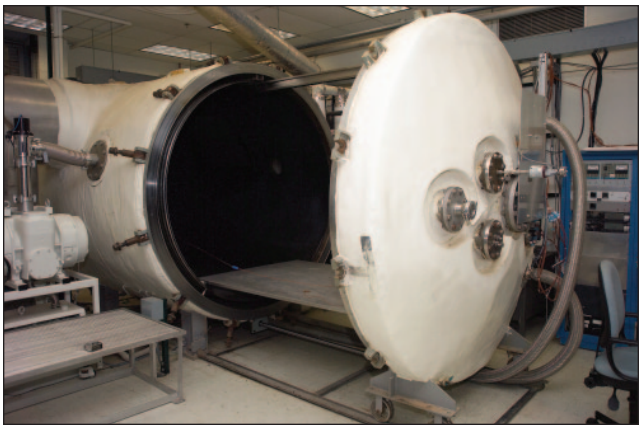


Fig. 1. *White Sands Test Facility thermal vacuum cycle and stress rupture test chamber.*

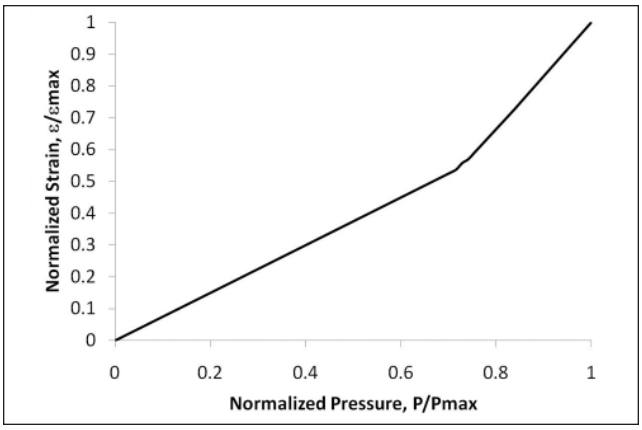


Fig. 2. *White Sands Test Facility finite element model of composite overwrapped pressure vessel strain and pressure.*

Results

WSTF has developed FEA models of test articles using GENOA-PFA (AlphaSTAR Corporation, Long Beach, California) software. Stress ratios have been established for the vessels (figure 2). The vacuum chamber and the blast enclosure with COPVs have been validated to achieve stabilized vacuum levels of 10^{-7} Torr with 18 vessels (figure 3). Visual inspection and flash thermography inspections (figure 4) have been performed on COPVs to establish the as-manufactured condition.

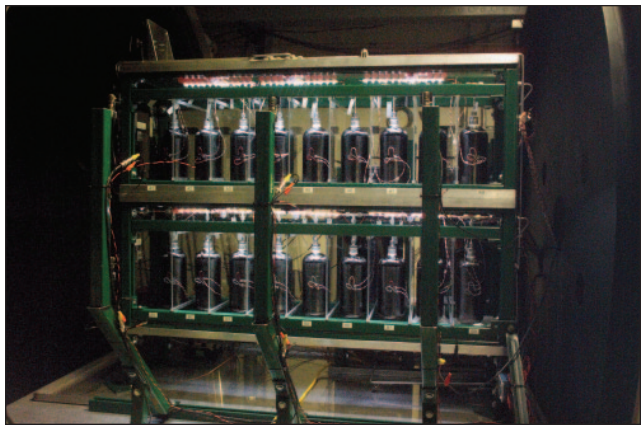


Fig. 3. *Blast enclosure with 18 composite overwrapped pressure vessels installed.*

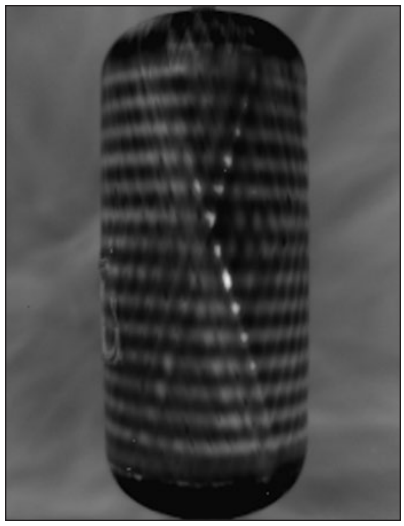


Fig. 4. *Flash thermography image of composite overwrapped pressure vessel.*

Testing in vacuum has been conducted to check out strain, pressure, and temperature instrumentation at vacuum levels between 10^{-7} to 10^{-9} Torr. Also, the chamber heating capability has been exercised from 21 to 49°C (70 to 120°F), and baseline strain, pressure, and temperature data have been collected.

Findings

Several findings were made about the structural response of COPVs in a simulated space vacuum environment during system validation. These findings have affected the methodology NASA applies in testing vessels for determination of long-term durability. Findings include the following:

- The first measured creep response of COPVs during autofrettage, resulting in new understanding of proof strain offset and vessel stress ratio
- The first measured carbon COPV fiber creep strain data to failure, thus allowing for a new carbon creep-life model to be developed and a new method to measure vessel health (strain/pounds per square inch) that is now used by NASA and was implemented in the NESC and the Space Shuttle Orbiter Program to assess space shuttle Kevlar® (E. I. du Pont de Nemours and Company, Wilmington, Delaware) COPV health beyond the manufacturer certification
- The first measurement of COPV vessel-to-vessel variability in stress ratio affecting reliability assessment approach and accuracy
- The first carbon COPV stress rupture structural response data, used in analysis by NESC CPVWG to compare current COPV FEA modeling approaches
- New baseline information for testing COPVs, including fixtures, barriers, pressurization capability, and instrumentation requirements

Ongoing and Future Work

Testing is being performed at on-orbit simulated thermal (-60 to 200°F [-51 to 93°C]) and vacuum (10^{-7} Torr) conditions on COPVs. Results will provide data on long-term durability of COPVs, and will involve cycle, stress rupture, and static strength burst testing.

Correlating Composite Vessel Shearography Nondestructive Evaluation Response to Impact Damage and Associated Burst Pressure Reductions

Charles T. Nichols, *White Sands Test Facility*
Regor L. Saulsberry, *White Sands Test Facility*
Tommy B. Yoder, *White Sands Test Facility*
Ralph E. Lucero, *White Sands Test Facility*

The NASA Johnson Space Center White Sands Test Facility (WSTF) has used laser shearography (LS) for several years to inspect and test composite overwrapped pressure vessels (COPVs). Shearography provides full-field, non-contact nondestructive testing for rapid wide-field inspection of composites, bonded structures, and other advanced materials. Shearography is an optical video strain gauge that uses appropriately applied stress to locate strain concentrations caused by internal defects. WSTF has worked closely with Laser Technology Inc. (Centennial, Colorado) to refine the LS inspection methods used for quality control by NASA and COPV manufacturers. Various types of COPVs were custom wrapped with carefully placed defects to provide reference standards (figure 1) and accomplish blind tests in which LS was compared against thermographic, ultrasonic, and other nondestructive evaluation (NDE) methods. A series of tests correlated the response of the different methods to varying amounts of impact damage and evaluated the resulting reduction in burst pressure. Shearography was identified as the most effective method of locating and quantifying defects within the carbon overwrap of COPVs. WSTF acquired a new high-definition LS system with thermal excitation to achieve greater scan versatility.

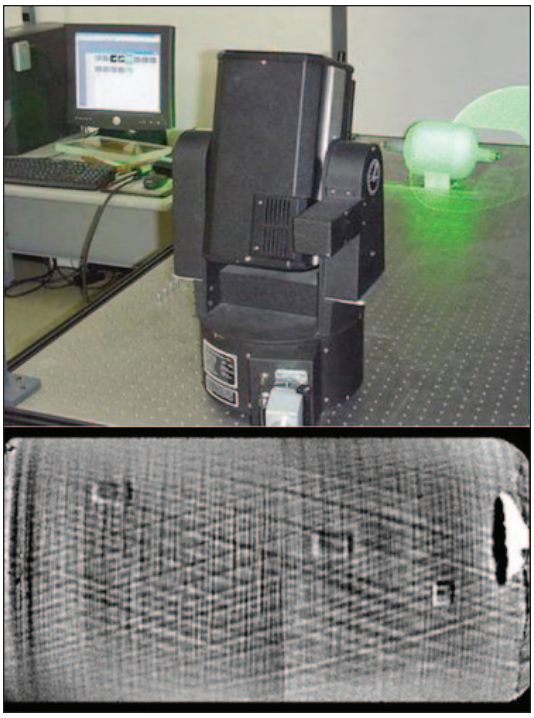


Fig. 1. *Composite overwrapped pressure vessel inspection (top) and thermal shearograph of a vessel with delaminations and a void (bottom).*

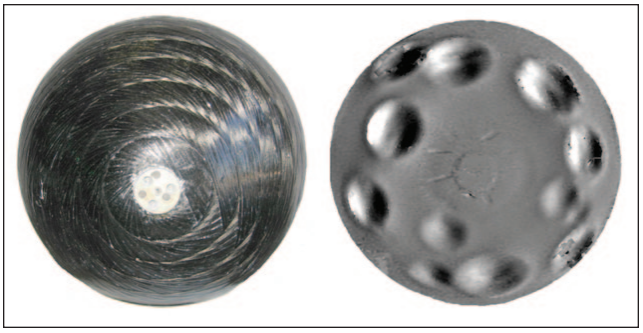


Fig. 2. *Spherical composite overwrapped pressure vessel with visible 0.15-in.-dia. dent and shearograph showing 0.75- to 2.3-in.-dia. damage.*

Shearography uses a laser-based imaging interferometer to detect, measure, and analyze surface and subsurface anomalies in structures. This is achieved by imaging slightly out-of-plane changes to a test article surface when an appropriate stress is applied or removed. The stress can result from excitation of pressure/vacuum, thermal, and/or acoustic sources, for example. Similar shearography systems are used by NASA and the aerospace industry for rapid, near-real-time evaluation of critical structures. Inspections of composite structures such as the space shuttle external tank, solid rocket booster heater cable and joint ablators, aircraft control surfaces, flight leading edges, carbon nozzle exit cones, helicopter blades, concrete bridges, radomes (radar dome), and many other components also rely heavily on laser shearography for quality control inspections and structural health monitoring.

As an NDE technique widely used as a component screening tool, LS is capable of detecting defects on composite structures such as mechanical damage (figure 2), disbonds, delaminations, near-surface porosity, wrinkled fibers, fiber bridging, foreign objects, and cracks. Thermal, mechanical, and a combination of the two methods provided optimized results depending on the indication.

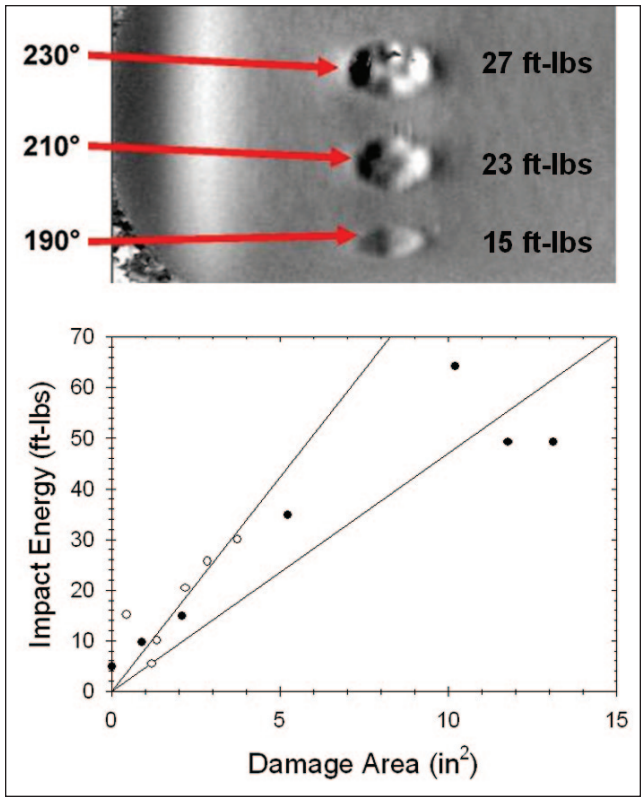


Fig. 3. *Damage area increases in composite overwrapped pressure vessels with impact energy.*

WSTF's LTI-5100HD Advanced Shearography System, equipped with a TES-200 thermal excitation unit, has greatly improved the ability to baseline the received stress state and monitor and identify visually undetectable subsurface impact damage. This capability provides support for inspection standard development efforts within NASA, manufacturing partners, and the American Society for Testing and Materials (ASTM). In fact, WSTF worked with ASTM to produce an NDE standard: ASTM E 258107, *Standard Practice for Shearography of Polymer Matrix Composites, Sandwich Core Materials, and Filament-Wound Pressure Vessels in Aerospace Applications*. Testing confirmed that the subsurface damage area, which was frequently below the visual detection threshold, increased with impact energy (figure 3) and was much more extensive than was visually evident.

Visual indications of composite damage range from severe fracturing at the impact site to a small crack or dimple, but shearography uncovers the visually undetectable damage.

Impact energy tests were performed on 43 426-cm^3 (2650-in^3), 17-cm × 56-cm (6.6-in. × 22-in.) cylindrical and 8194-cm^3 (500-in^3), 26-cm (10.25-in.) spherical COPVs to determine the reduction in residual strength as a consequence of impact energy (figure 3). Test results suggest impact energy greater than 13.6 Newton-meters (10 ft-lbs) (a 13-cm^2 [2-in^2] damage area) causes significant burst after impact pressure decreases for composite pressure vessels. An impact damage threshold was suggested to define the acceptable level of damage for a given impact subsequently. These findings can be directly applied to present and future aerospace systems of similar graphite composite construction, including commercial and military applications. Commercial applications can also be realized for compressed-gas storage systems including natural and hydrogen gas-powered vehicles.

Shearography inspection of COPVs for impact damage and other anomalies has been demonstrated to have a lower detection limit than most other NDE methods, but the technology still requires more work to develop the capability of directly correlating burst pressure reductions to impact energy. Future work will add more data and complete this analysis for a more effective impact standard. Since the sensors used for acoustic emission NDE respond to fluctuations in out-of-plane strain measurements, it is suspected that, after factoring in acoustic emission attenuation effects, a relationship would exist between impact damage energy and acoustic emission event energy. Furthermore, acoustic emission may be capable of locating and tracking the formation and growth of micromechanical flaws detected using LS. Additional instrumentation and high-pressure testing are planned to investigate the link between these measurements and impact damage.

NASA White Sands Test Facility Valve Repair Facility Helps Resolve Relief Valve Issues

Christina Y. Piña Arpin, *White Sands Test Facility*
Richard McCarson, *White Sands Test Facility*

Disassembly, cleaning, maintenance, reassembly, and testing of pressure relief and pressure safety valves is performed at the NASA Johnson Space Center White Sands Test Facility (WSTF) in compliance with American National Standards Institute [ANSI] National Board Inspection Code (NBIC)/NB-23. The WSTF cleaning process is approved for oxygen service, International Space Station, and space shuttle support.

Background

WSTF, a human space flight test facility since the 1960s, has a requirement for items used in site test systems to be precision cleaned. Because of the possibility that contaminants could adversely affect the performance of test articles and test systems, components in hypergolic propellant, oxygen, and other fluid systems must be safely decontaminated and precision cleaned. After an "as-received" inspection, including review of the manufacturer drawings and specifications, the item is disassembled for cleaning. Precision cleaning combines chemical, mechanical, and ultrasonic cleaning. Procedures have been developed to safely clean various metals, elastomers, and composites. Item reassembly is performed in a clean room. Once the item has been reassembled, it is subjected to various checks and tests to ensure that it is operating as the manufacturer designed.

A component, to be properly cleaned, must be fully disassembled before each piece is partly cleaned, reassembled, and functionally tested. This became a problem when the standard for NASA ground-based pressure systems required that pressure systems be NBIC-compliant and all relief valves in a code application meet NBIC requirements. Not only do the valves have to be manufactured according to NBIC code, but the code must be maintained by an NBIC-approved valve repair facility. Code valves have a tamper-proof seal; if the seal is broken, the valve is no longer code compliant. WSTF faced conflicting requirements as there was no NBIC-approved valve repair (VR) facility that could maintain the required cleanliness level during testing. It was a vicious cycle because if WSTF cleaned a code valve, the valve would be out of compliance. To make the valve code compliant again, it would have to be sent to an NBIC-approved VR facility, which would then contaminate the valve because cleanliness could not be maintained.

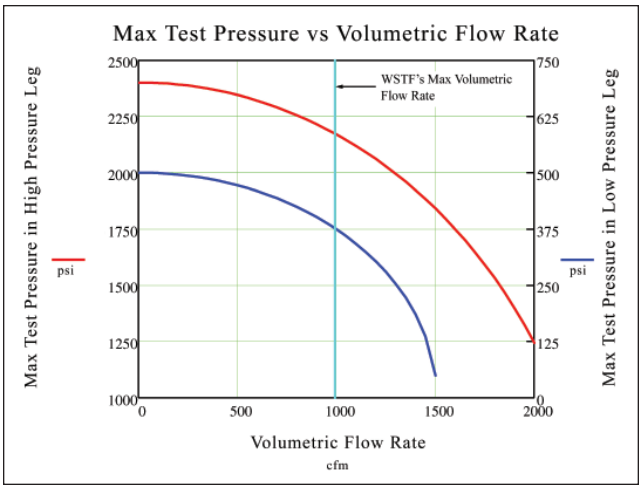


Fig. 1. *Flow and pressure rating of the White Sands Test Facility flow facility.*

To solve this code-compliance problem, WSTF applied for and received the "VR" stamp from the National Board of Boiler and Pressure Vessel Inspectors in February 2010. Now, WSTF can repair relief valves in a Class 100 clean room that meets the requirements of the National Board. Only facilities certified by the NBIC can perform relief valve refurbishment and retain the valve code stamp. Unique to WSTF, and to NASA, is receiving "authorization of use" of the "VR" stamp from the National Board. In support of the VR capability, WSTF also built a relief valve flow facility in the Class 100 clean room to verify that the valve meets the flow requirements as approved by the National Board.

The VR facility ensures that relief valves are operating within manufacturer specifications and to customer expectations. The facility is capable of verifying flow capacities of pressure relief valves up to 1000 scfm, and pressures not to exceed 2800 psig, using clean gaseous nitrogen (figure 1). Because assembly and testing of the relief valves is performed in a Class 100 clean room environment, WSTF is the only known clean flow test facility in North America (figure 2).

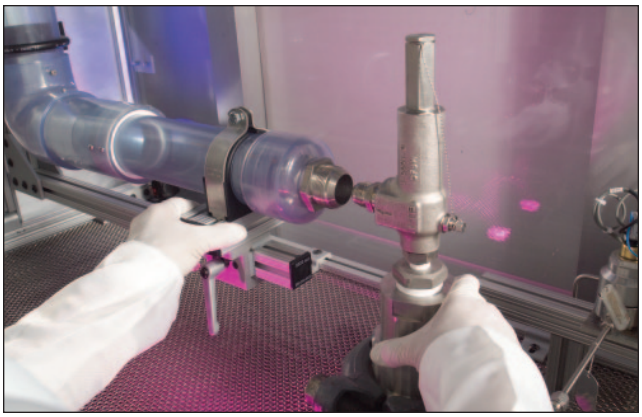


Fig. 2. *Relief valve to be tested is being connected to the GN2 exhaust system.*

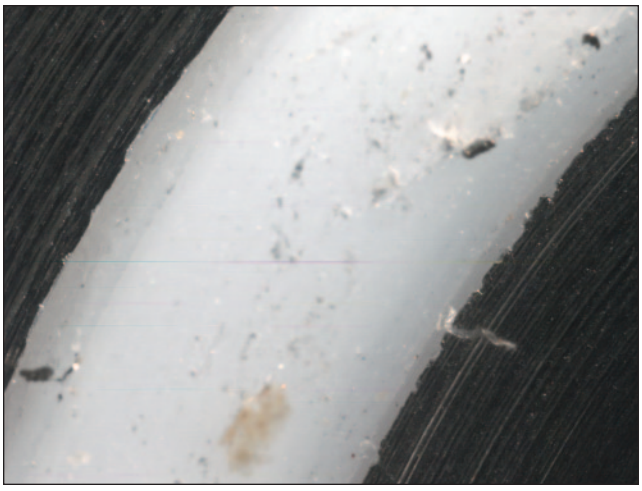


Fig. 3. *Softgoods contamination.*

Working with Manufacturers

Due to the hazardous fluids that flow through many of the valves at WSTF, even more stringent leak tests are needed than are required by NBIC. During routine leak tests, the VR facility found several valves that leaked prematurely at the crack pressure. Since these particular valves were low-pressure valves, it was initially thought the seating problems were caused by the design of the polytetrafluoroethylene (PTFE) seats. After inspection, however, embedded metal particles were found in the soft goods received from the manufacturer (figure 3), which caused the leakage and released loose particles of metal into the pressure system. WSTF began working with the manufacturer to remedy the problem of foreign particles embedded in the soft goods of the valve repair kit. To improve the leak tightness of the low-pressure valves, the manufacturer is working with WSTF in redesigning the shape of the soft goods to promote cold flow of the PTFE soft goods.

Another area in which WSTF has been working with manufacturers is in valve spring selection. Every valve received at WSTF is disassembled before cleaning, reassembly, and functional testing. Although not required by NBIC, WSTF flow tests each valve before returning it to the customer as part of WSTF quality control process to ensure the valve flow capacity is the same as stated in its specifications. During flow testing, some valves flowed significantly lower than the specified capacity. After investigating, it was discovered that the incorrect spring had been inserted at the manufacturing facility. In this case, the valve specifications called for a 60-psi-rated spring, while the actual spring in the valve was rated for 150 psi. Compression tests on the same valves using other springs determined that the springs were mislabeled. WSTF is working with the manufacturer to remedy this, and has added spring compression tests as well as flow testing to its processes.

Replacement Parts

The VR facility also provides replacement parts control. This ensures that parts being used for relief valve repair are replacement parts from the original manufacturer, or from a vendor approved by the National Board to make replacement parts that meet original manufacturer specifications. WSTF maintains traceability for parts and testing on code and non-code applications. All inspection measurement and test equipment used to support the VR facility is calibrated at WSTF and is traceable to National Institute of Standards and Technology or other internationally agreeable intrinsic standards.

By exceeding industry standards for superior precision cleaning and component refurbishment, the WSTF VR facility satisfies customer needs for the highest-quality products possible. With WSTF identifying issues with both code and non-code valves and working with various manufacturers to mitigate these problems, a better product is produced—not just for WSTF, but for all customers of the manufacturer.

Hardware Odor Containment Validation Methodology Development Using Gas Analysis and Controlled Human Evaluation Methods

Thomas B. Handley, *White Sands Test Facility*
Susana A. Harper, *White Sands Test Facility*

Odor Containment Evaluation Methodology

The issues associated with the control of odor on spacecraft have been mitigated by screening materials, processing wastes, and/or segregating wastes. The spacecraft designs for the Orion Program make the processing of wastes impossible and the segregation of wastes very difficult. This issue was identified early during the design of the spacecraft, thus a requirement for the odor containment of waste odors was developed. The requirement is for odor containment hardware to contain the odors for the potential maximum duration of the missions—i.e., 90 days. The program funded the development of hardware to contain the odors and development of a methodology to validate this hardware. While developing the methodology for evaluation of odor containment, NASA addressed the following technical issues: use-scenario packaging and conditioning; gas analysis; control comparisons; waste volume to spacecraft free volume simulation; and a controlled human evaluation.

Use-Scenario Simulation

To accurately evaluate the odor containment properties of the hardware, testing must closely simulate the actual use conditions. The use-scenario packaging and conditioning were scrutinized such that the configuration and the amounts of wastes could be simulated to obtain results that are as close to representing the actual mission as possible. The use-scenario packaging and conditioning included the odor containment hardware, waste identity, waste quantity, waste preparation, waste packages, waste prepackaging, and environmental conditions. The odor containment hardware evaluated must be in the end-use configuration and contain all of the materials that the end-use hardware will contain. The identity and quantity of the waste to be contained in the hardware must be known and duplicated. The quantity of waste used in the evaluation should be the maximum anticipated quantity to be generated such that the worst-case scenario is represented. If the waste will be prepared in any way, these procedures must be known and duplicated. The way that any packages will be opened, used, and then configured and sealed prior to being placed into the hardware must be known and duplicated.

It is possible to be interested in testing an entire odor containment system. This could include various types of waste, primary containment, secondary containment, and, finally, final containment. In this case, the waste must be controlled inside of the hardware in such a way that it simulates multiple disposal activities. Simulation must incorporate all final waste conditions from the initiation of test. Configuration must ensure that primary and potential secondary containment of deposited waste simulates use conditions inside of final containment vessel. The evaluation of both primary and final containment will be evaluated as a whole in this system test. Rigor of primary containment seals and potential failure during additional disposal activities should be considered as a risk to containment system. The entire test configuration will be encapsulated in a non-permeable chamber in which any permeated volatiles can be fully contained and analyzed (see figure 1).

The environmental conditions in the spacecraft—in particular, temperature and relative humidity—must be known. The set conditions for evaluation of the hardware should use the worst case. Temperature is a strong driver for diffusion with worst cases being defined as the hottest the temperature could be. Relative humidity also can affect material barrier qualities with the worst-case condition being defined as the most humidity that could be present. Selected worst-case conditions are simulated and maintained inside of non-permeable vessel containing waste test configuration.

Odor Breakthrough Determination, Part 1: Gas Analysis

The toxicity of the test atmosphere generated and the determination of the odor breakthrough time must be predicted by gas analysis of the test atmosphere. To determine the odor breakthrough time, it is necessary to monitor the test atmosphere using an analysis method. The analysis methods were selected such that any potential volatile organic or inorganic chemical present in the test atmosphere could be identified and quantified in the presence of a complex matrix. The analysis method to determine the odor breakthrough time was selected such that small amounts of chemicals being released into the test atmosphere could be separated and quantified quickly. The identities and quantities of the chemicals being evolved from the waste were also determined to have significant importance for the characterization of the chemicals responsible for the odors, and how the chemical

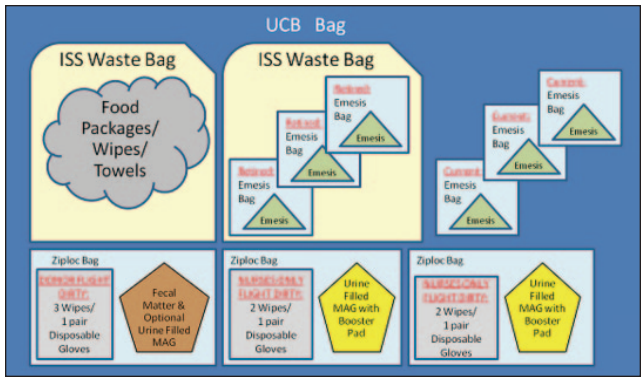


Fig. 1. *Urine containment bag Block0 waste bag configurations.*

composition and odor changed over time. The analysis data must be rigorous enough to be used to evaluate toxicity of the test atmosphere accurately such that they meet the requirements detailed in 21 Code of Federal Regulations Part 50-Protection of Human Subjects.

Odor Breakthrough Determination, Part 2: Control Comparisons

The use of control comparisons was identified as a crucial part of the evaluation. The identification of the odor breakthrough time must be predicted as a result-evident increase in volatiles in chamber indicating breakthrough identified by gas analysis and then confirmed through human evaluation. Nonetheless, most nonmetallic materials off-gas chemicals into their environment, thus the gas analysis must be able to discriminate between chemicals that are off-gassing from the containment hardware itself from the chemicals from waste odor chemicals permeating through the packaging and indicating breakthrough. To make the odor breakthrough determination from the analysis results, a comparison sample containing all the clean and empty hardware and all primary and secondary containment material must be evaluated in parallel schedule and conditioning to the hardware with the waste. The comparison sample must also have the same configurations of the hardware and prepackaging materials, and must be environmentally conditioned in the same fashion as the hardware with the waste. This can be termed the "control configuration." The general value to use as a guideline in determining odor breakthrough is when the difference in total hydrocarbons between the control and waste configurations is greater than or equal to 2 parts per million (ppm).

Waste Volume to Spacecraft Free Volume Simulation

The waste volume to spacecraft free volume governs the concentration of the chemicals being evolved from the waste and eventually released into the breathing zone of the crew. If the odor breakthrough time will be representative of the actual use conditions, this parameter must be simulated so that the controlled human evaluation is evaluating what the spacecraft crew will be experiencing. The simulation of the waste volume to spacecraft free volume is accomplished by determining the craft free volume, waste volume, and available test chamber volumes. The test chamber volume is selected such that the ratio of the waste volume to container volume is the same or greater than the ratio of the waste volume to spacecraft free volume. The result of the ratio for the waste volume to test chamber volume being greater than the ratio of the waste volume to spacecraft free volume is that the simulation will have greater concentrations of chemicals in the test atmosphere than would be anticipated for the spacecraft atmosphere. The greater concentrations in the test atmosphere allow for the test atmosphere to be diluted to the anticipated concentration for the spacecraft prior to being provided to the controlled human evaluation.

Odor Breakthrough Validation and Assessment; Controlled Human Evaluation

The controlled human evaluation was determined to be of significant importance due to the inability of any analysis method to rate a test atmosphere according to the quality of the odor. Odor is an ability of living organisms and the quality of an odor is a subjective and individual experience that cannot be duplicated by analysis or algorithm. Special considerations must be implemented when using human subjects to obtain information. The population of human subjects used must be great enough to allow for statistical comparisons and is typically randomly selected; a baseline odor sensitivity test is conducted to ensure that the subject has sufficient sensitivity to a range of smells.

The strategies used to obtain information from the individual human subjects are also of significant importance. The human subjects must not be allowed to influence each other, so they are exposed and questioned privately and then requested to not discuss the experience. The way that the questions are asked and how rating scales are presented are of significant importance. Semantic differential research methodologies were used to develop a semantic differential scale (figure 2).

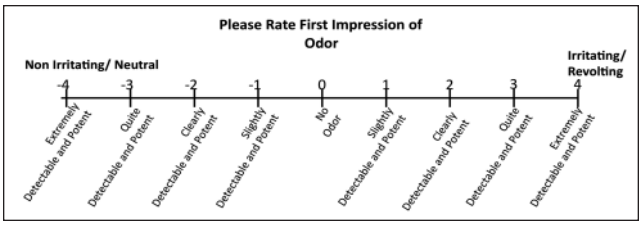


Fig. 2. *Odor containment semantic differential scale.*

The validation and assessment of the odor breakthrough time uses five human subjects. This number is sufficient to have confidence that the odor from the waste is being

Hardware Odor Containment Validation Methodology Development Using Gas Analysis and Controlled Human Evaluation Methods

continued

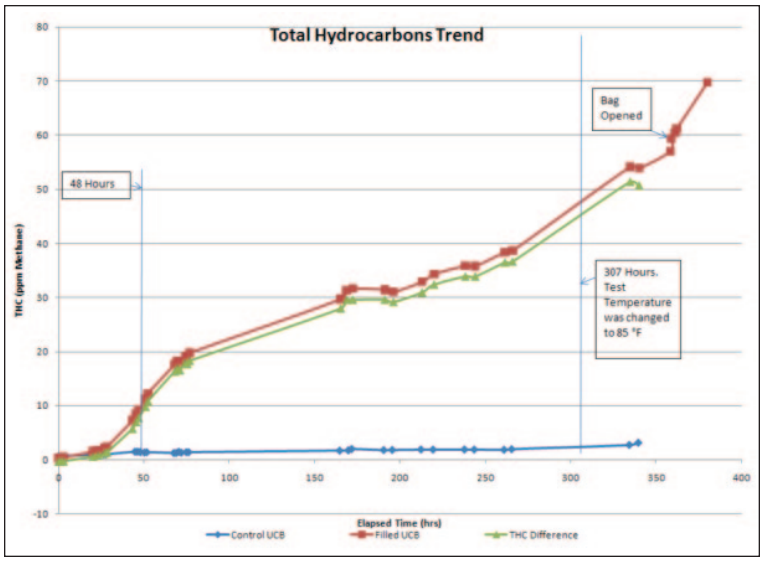


Fig. 3. Total hydrocarbon content analysis results.

detected or not detected by the human subjects. The potential validation and confirmation of odor breakthrough is based on exposure to, and comparison between, the control configuration and the waste configuration. Human panel members compare odors and confirm that an odor difference is detected as described above. When the quality of the odor and assessment of potency in the test atmosphere over time after breakthrough is desired, continued evaluation at strategic time intervals is recommended to account for individual differences from human subject to human subject. A larger group of evaluators is recommended for post-breakthrough odor potency monitoring and evaluation. It was determined that six to 10 human subjects would supply enough information such that the quality of the odor could be confidently described as time passed after breakthrough. The methodology is designed to determine the maximum amount of time a device will contain odor in a desired configuration. The odor acceptability will be determined by human test subjects at intervals and is recommended to be monitored for the length of time simulating the duration of the mission. The test, however, can be halted at the point the system owners feel that odor potency is not acceptable. The test results from developed methodologies are summarized in the following section.

Odor Containment Evaluation Methodology Conclusions

The total hydrocarbon content analyses on the filled urine containment bag and control urine containment bag test atmospheres show divergence of the content of the two test atmospheres, indicating odor breakthrough (figure 3). Rigorous chemical analyses performed for toxicity evaluation supports the total hydrocarbon content results.

The human panel evaluation unanimously confirms that the chemical analyses were in fact detecting odor breakthrough at the 2 ppm delta (figure 4). Data validated that the developed methodology produces the desired information. The rigorous chemical analysis reveals much about the odors. Comparisons of the description of the odors to the chemical analyses that correspond to the times of the human panel evaluation clearly show the detection of many chemicals that are known to have strong odors. The challenges associated with the Orion Program and future programs are not insurmountable. With a proven methodology to evaluate odor containment properties of materials and components, the hardware can be challenged, developed, and eventually perfected.

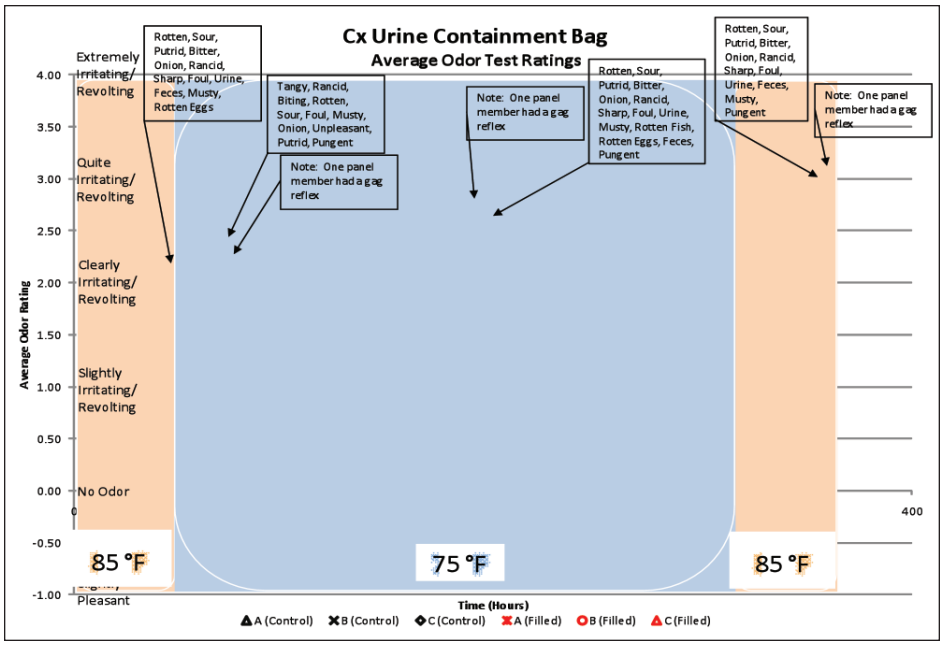


Fig. 4. Odor assessment results for control and filled urine containment bags.

Image Science Support to Commercial Development

Tracy Calhoun, *Johnson Space Center*

The Image Science and Analysis Laboratory (ISAL) at Johnson Space Center is continually building, honing, and adapting its image science capabilities to provide optimum support to NASA customers. Often this evolution is driven by the pace of imaging technology, but sometimes the evolution results from new space policy. NASA's effort to commercialize space transportation to and from the International Space Station is a recent example of an agency goal spurring lab evolution.

Under Commercial Orbital Transportation Services (COTS), NASA awarded Space Act Agreements to Space Exploration Technologies (SpaceX, Hawthorne, California) and Orbital Sciences Corporation (Dulles, Virginia) to develop systems that can provide cargo to the International Space Station after the space shuttle retirement. COTS partners will fly demonstration missions of these systems, culminating in each demonstrating a mission that berths with the space station. Under COTS, NASA provides requirements, funding, and high-level oversight, and the companies provide vehicle design, construction, and operation.

To support oversight, NASA secured the services of the ISAL, one of the first Johnson Space Center teams to support commercialization. The traditional model for ISAL support to a program is to partner with a NASA customer on every step of the image science process—from the design of imagery acquisition, through the meticulous screening of mission imagery, and ending with the application of image analysis techniques to investigate significant findings derived from the screening. But now, with the agency removed from day-to-day mission development, the ISAL was tasked to help NASA design an engineering imagery plan that could provide a feel for overall performance but, in the event of a mishap, would be adequate to support an accident investigation. The latter is an important element considering that it is fiscally impractical for commercial partners to acquire imaging resources comparable to those already in place at NASA's Kennedy Space Center.

The first mission that ISAL supported was SpaceX's Falcon maiden flight in June 2010 from launch complex



Fig. 1. *The SpaceX Falcon 9 with the Dragon vehicle demonstration flight on December 8, 2010. (Photo courtesy of SpaceX.)*

40 at the Cape Canaveral Air Force Station. The ISAL worked with NASA managers to establish vehicle events and features of interest. The ISAL then coordinated with Kennedy Space Center imagery teams to design a camera

Image Science Support to Commercial Development

continued

complement, imagery acquisition plan, distribution plan, and schedule. This included the acquisition of high-quality still images to document the preflight condition of the vehicle and ground structures. This vehicle configuration imagery is essential to the imagery screening process and to any subsequent image analysis.

During and after the launch, the ISAL screened each piece of imagery with an experienced eye from their support to numerous NASA launches. They also leveraged Kennedy Space Center launch experts to screen the same imagery set. Launch findings were documented in a custom database with access limited to key NASA and SpaceX personnel, due to the proprietary nature of the imagery. NASA managers used the database to identify events of interest, but they also provided the database to SpaceX to offer insight into things that cannot be monitored or detected in telemetry. Additionally, a courtesy copy of the NASA imagery was supplied to SpaceX via portable hard drives, delivered by overnight mail.

On December 8, 2010, SpaceX launched a second Falcon from Cape Canaveral Air Force Station with their Dragon capsule as an official demonstration flight for the NASA COTS program designated as "C1." That mission was again supported by the ISAL (figure 1). In late 2011, the ISAL will support SpaceX's C2 launch and a maiden launch of Orbital Sciences Corporation's Taurus 2 rocket. In 2012, ISAL will support the second Taurus 2 launch—the official demonstration flight for NASA COTS—and possibly a C3 SpaceX demonstration mission. The Orbital Sciences Corporation missions will launch from Virginia's Mid-Atlantic Regional Spaceport, adjacent to the Wallops Flight Facility.

Spacecraft Flight Operability Assessment Technique

Alan R. Crocker, *Johnson Space Center*

The design of a human-rated spacecraft is a complex and costly process requiring the integrated assessment of many considerations. Historically, it has been difficult to include, in that integrated assessment, the design's full impact on the flight operations community. The unique "operability" requirements have not been well understood, nor has there been a well-defined set of criteria for assessing operability. As programs approach their operational phases, program managers and flight operations organizations alike are often surprised when faced with difficult and costly operations implementations. A formal means of forecasting operability issues during the development phases of a program is therefore necessary to reduce operations phase costs.

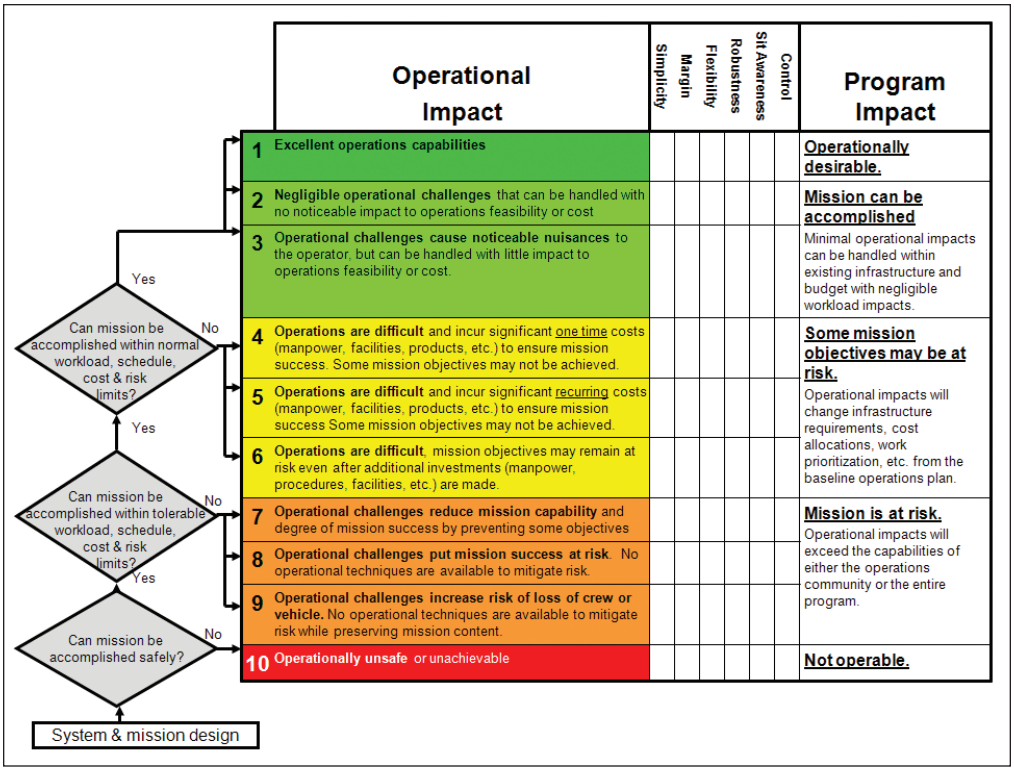


Fig. 1. *Flight operability assessment technique.*

The challenge in addressing flight operability needs for a new program is threefold: (1) there is no accepted universal definition of flight operability; (2) there is no clear mapping of flight operability needs to program and vehicle requirements; and (3) there is no formal method to assess flight operability characteristics given a spacecraft design and mission definition. These challenges are similar to those faced by the aircraft flight test community in the 1950s and 1960s. Over the course of years, a technique for the characterization of an aircraft's handling techniques—as assessed by the pilot operating the aircraft—was developed by George Cooper and Robert Harper and has long stood as the standard tool for aircraft handling assessment. Modified versions of this scale are employed widely in the assessment of crew equipment and interfaces for NASA human-rated spacecraft.

In response to these challenges, the Mission Operations Directorate at Johnson Space Center established a formal method for the evaluation and communication of a spacecraft system design's operational characteristics. The spacecraft flight operability assessment method is born of the need to identify the operations systems' drivers and critical requirements that are a significant influence on operations cost, schedule, performance, and risk. This process is not intended to replace or replicate other critical assessments such as risk, reliability, or safety assessments. Instead, this new technique adds to a program's assessment toolset a means to address the concerns and potential cost drivers that are unique to the operational phase of a program and the flight operations community.

Spacecraft Flight Operability Assessment Technique

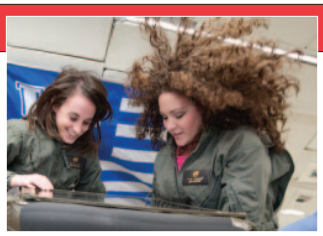
continued

The scale incorporates three basic elements: a set of operability themes to be evaluated; criteria with which to evaluate each characteristic; and a grading scale to normalize the results. The operability themes correspond to six operability themes—simplicity, margin, flexibility, robustness, situation awareness, and control. Flight operability criteria are imposed to categorize assessments of each operability theme: "Can the mission be accomplished?"; "Can it be accomplished within tolerable limits (workload, cost, risk)?"; "Can it be accomplished within normal limits?"; and "To what degree?". These four questions guide the assessor in determining which color-coded range within the possible 10 scores should be assigned for an operability theme (figure 1).

Formal flight operability assessment practices may be applied to both development and operational programs. For development programs, the Spacecraft Flight Operability Assessment Scale can and should be employed in generating inputs at formal design reviews (Subsystem Design Review, Preliminary Design Review, Critical Design Review) in less-formal design team forums, and in the assessment of formal change requests. For operational programs, the scale may be applied to proposed incremental vehicle changes such as hardware upgrades and flight software updates.

The Mission Operations Directorate began using this scale as a tool both for operational vehicles such as the space shuttle and for new vehicle designs such as those developed under the Constellation Program. Initial use of this scale has yielded encouraging results. Evaluators find the scale easy to use, and the resulting evaluations quickly identify and isolate operability issues within specific subsystems and scenarios.

Inspiring Future Generations: Education and Outreach



Systems Engineering Education Discovery Program: NASA Utilization of Undergraduates to Conduct Reduced Gravity Flight Research

Sara W. Malloy, *Johnson Space Center*

Each year, teams of undergraduate students from across the country converge at NASA's Johnson Space Center (JSC) for the unique opportunity to conduct scientific research in a reduced gravity environment. As participants of the Reduced Gravity Education Flight Program, these teams spend approximately 4 to 6 months prior to their arrival at JSC designing and testing their experiments at their home institutions. Once they arrive for their flight week, they undergo physiological training, hardware inspections, and flight-readiness orientations before they are allowed to accompany their experiments onboard a modified Boeing 727 aircraft. During flight, the students conduct their experiments and gather data while the aircraft completes 30 parabolic maneuvers over the Gulf of Mexico. Each parabolic pattern provides roughly 18 to 25 seconds of microgravity (figures 1 and 2).



Fig. 1. *Student teams conduct research during a reduced-gravity flight.*

This innovative program has had a clear impact on student participants. By supplementing traditional undergraduate coursework with an exciting field experience, the Reduced Gravity Education Flight Program exposes students to real-world applications, research experience, and career possibilities. Consequently, student participants have reported a renewed passion for the study of science and technology, an enhanced dedication to pursuing a career in science and technology, and a stronger motivation to acquire an advanced degree.

In 2008, program managers for the Reduced Gravity Education Flight Program recognized the potential to expand this innovative program beyond a student outreach opportunity and partnered with the Systems Engineering Education Discovery (SEED) Program to make this happen. Unlike the original undergraduate student program in which student teams devise a research project of their own choosing, the SEED Program pairs student teams with a NASA engineer to work on a research topic of immediate relevance to NASA. The NASA engineer acts as the research lead and mentor, guiding the students remotely until they arrive at JSC for their flight week. This program's design continues to provide all of the benefits to student participants of the original undergraduate student program, while advancing NASA's mission and goals through the completion of needed research. In 2010, the SEED Program received applications from 23 institutions and ultimately selected 13 student teams to collaborate with a NASA engineer on a research project. Because the focus of SEED is on increasing student awareness and competencies in systems engineering, all research projects were selected based on their efficacy in teaching systems engineering concepts. Examples of assigned research

Systems Engineering Education Discovery Program: NASA Utilization of Undergraduates to Conduct Reduced Gravity Flight Research

continued

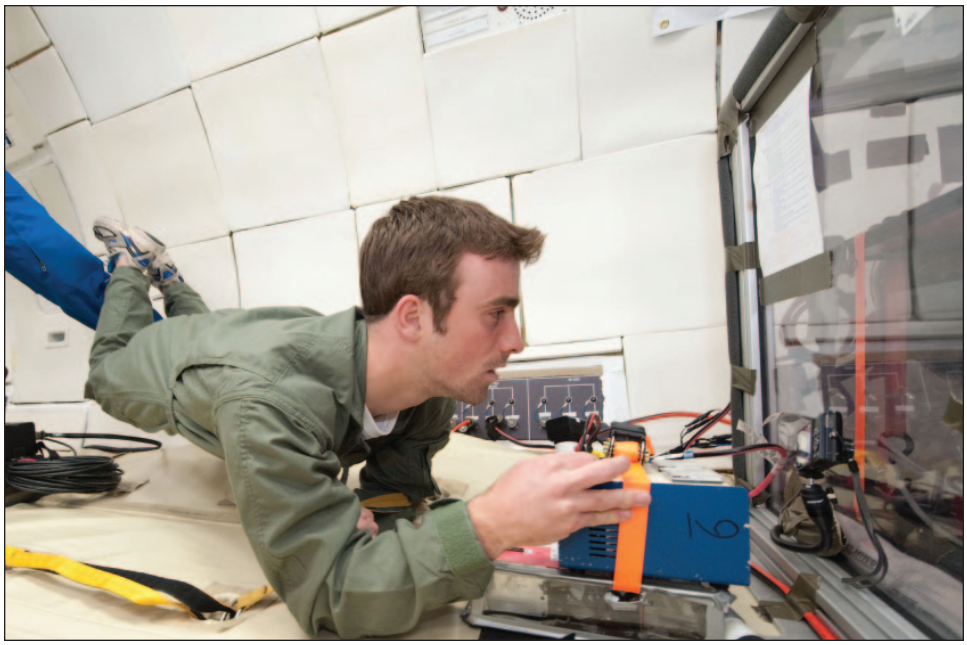


Fig. 2. *A student conducts research during a reduced-gravity flight.*

topics included: measuring the dielectric properties of lunar regolith; dynamic wheel traction concepts in lunar gravity; investigation of propellant sloshing and zero-gravity equilibrium for the Orion Service Module propellant tanks; and Human Research Program subjects such as a bubble-free injection syringe and effective sharps containment in space environments.

Regarding the success of the SEED Program and its contribution to NASA research, one former NASA SEED project lead/mentor stated: "It took some effort to start, since we had to bring [the students] up to speed about the project, but they have understood the application well and have taken it farther than what we expected. We are very impressed with some of the ideas that the students have conceived. In fact, they are most likely going to get us more data than what we anticipated in the beginning. We are grateful that we will be able to collect data for our project in microgravity. The fact that we will have experimental data collected in microgravity will strengthen our argument and validate our design."

Successful Recruitment Strategy for Student Programs: Using the Example of the Undergraduate Student Research Program

J. Anthony Zippay, *Johnson Space Center*

In 2010, the NASA Undergraduate Student Research Program (USRP) received 4,700 submitted applications from qualified undergraduate science, technology, engineering, and mathematics (STEM) students from across the nation, increasing five-fold the amount of interest and awareness for the NASA internship program over the 3 years that Johnson Space Center (JSC), in collaboration with Universities Space Research Association (USRA), has managed the project. This figure indicates an immense increase in applications received for the program, and demonstrates the success of the USRP communications and recruitment campaign. USRP has achieved something unique in creating a high level of interest from undergraduate students. The lessons learned in this achievement can be applied to other student programs.

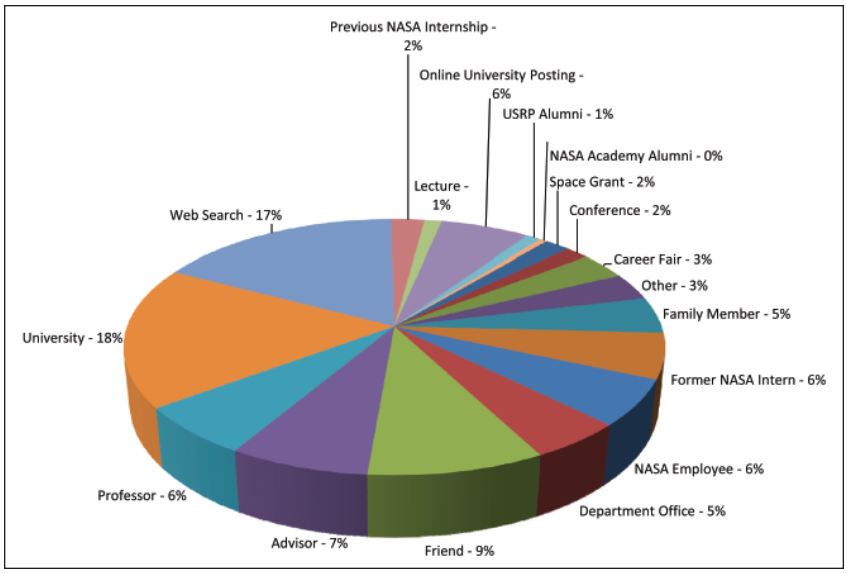


Fig. 1. *How applicants find out about the Undergraduate Student Research Program.*

Fundamental to the successful generation of a large and diverse pool of applicants is developing a comprehensive user-friendly database and reporting system. Marketing research enhances the effectiveness of project personnel in making critical decisions about the recruiting plan. Having a reliable data set that answers important timely questions is essential to determining the effectiveness of the communications plan at any given time. Having the ability to understand the effectiveness of a campaign with up-to-the-minute results, and knowing the exact media source that is working successfully, is priceless. The USRP Connect database and application tool provide up-to-the-minute and reliable information on the USRP student core audience. For example, figure 1 indicates the primary way in which students first learned about the USRP internship program. The chart indicates that applicants primarily learned about the program from their university and from the web. Knowing that, researchers understood that the university was a prime influencer in determining whether the student would apply for the program.

Based on these data, researchers were able to refocus their efforts toward the professors and other university personnel who have the most influence on potential student applicants (total 48%).

For example, conventional recruiting practice calls for a physical presence at university career fairs and conferences. However, based on the data shown in figure 1, only 5% of applicants learned about USRP through career fairs and conferences. Therefore, USRP decided to focus efforts primarily on the online university communications resources, and through key influencers of potential student applicants (i.e., professors, department heads, and other university personnel) to reach its target audience. The five-fold increase in qualified applications demonstrated that the results were effective.

At the core of the USRP communication and recruiting strategy was JSC's mission to do the following: develop an internship program that provided degree-related, hands-on internships for talented undergraduate students pursuing STEM degrees that align with NASA's critical workforce competency needs; provide a high-quality, nationwide undergraduate hands-on experiential program in a technical environment; to attract and stimulate a diverse group of highly qualified undergraduate students from a wide array of academic institutions; and coordinate undergraduate research internships at NASA field centers

under the guidance of NASA scientists and engineers. To accomplish this mission, a strategic communications and marketing effort is essential in creating an educational program that will sustain and thrive for years to come. Figure 2 shows the ways in which USRP distributed its communication messages across the nation. USRP recruiting efforts focused heavily on university and online resources. By focusing on online resources, the communication messages filtered down through the necessary stakeholders within the universities, thus creating the word of mouth necessary to get the message to the intended student target audience. Many students also indicated that they learned about the program through a professor, peer, or academic advisor. Therefore, the indication is that the strategy achieved effective word of mouth by means of viral communications through the web.

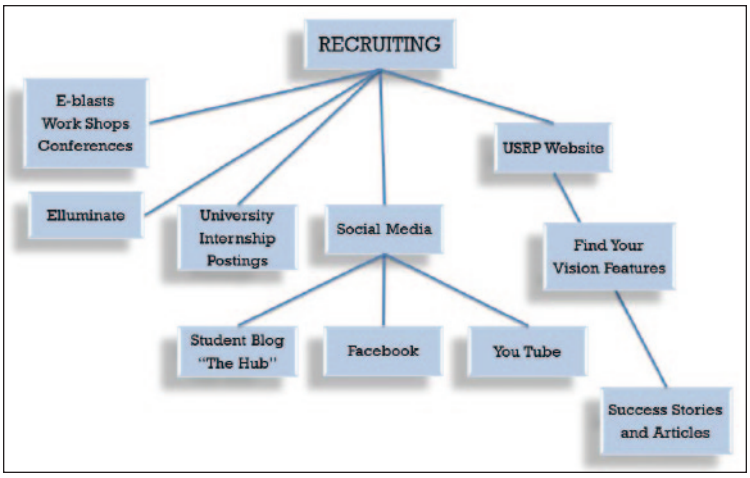


Fig. 2. *Communication strategy.*

In recruiting efforts, researchers sought ways in which they could show the connection between USRP and the latest exciting NASA research that interns have the opportunity to work on every day. The result aligned USRP among its core target audiences of prospective student interns and NASA mentors as NASA's premier internship program. Based on research to date, students are searching for a way to be a part of the NASA mission. They are unaware of educational programs and are confused by the NASA workforce structure and research opportunities. Students who participate in USRP learn quickly the nature and scope of their mentor organizations' mission and focus, and how these missions fit in with NASA's "big picture." USRP wanted to give undergraduate students across the nation a new level of awareness about the opportunities at NASA, as well as excite students about the possibilities that await them.



Fig. 3. *Undergraduate Student Research Program website.*

To see how our communication and recruitment efforts have evolved, and to learn more about the USRP program, go to *http://usrp.usra.edu* (figure 3).

Undergraduate Student Research Project Social Networking and Student Stories Initiative

Heather L. Ogletree, *Universities Space Research Association*

Student Stories Initiative

The Undergraduate Student Research Project (USRP) entered the news business in May 2009. Since the Public Affairs Office has limited coverage of the Education Department, USRP took on the task of creating its own stories, capturing intern experiences through the Student Stories Initiative (SSI). The process takes approximately 3 weeks to complete. First, interns are chosen based on the quality of their work and the newsworthiness of their project. In the journalistic community, a story is newsworthy if it contains the following news values:

- Impact—how many people does the event/project affect?
- Timeliness—how recently did the event occur?
- Prominence—how well-known are the people involved in the event?
- Uniqueness—how distinctive and rare is the event or project?
- Currency—is the event related to some topic people are talking about or interested in?
- Balance—do stories encompass a diverse representation of students, NASA centers, and projects?

SSI is a voluntary effort, and the process begins when students are asked if they would like to participate. Students are asked a series of 10 routine questions to provide an overview of their entire experience, from garnering the internship award to the completion of their projects. They are given a week to respond. Once USRP receives their answers, the research phase begins. Research for articles includes examining each student's application and project description, and conducting online research to gain a better grasp of each project (figure 1).

Prior to being published, USRP stories follow a rigorous approval process. Each story goes through the intern and through the mentor or the mentor's technical organization to ensure the technical accuracy and nonsensitive nature of the data presented in the story. Each story also goes through the USRP administrator for final approval.

A new student story goes on the USRP website and Facebook page each week to consistently provide the public and USRP's stakeholders with new, in-depth, qualitative data about USRP internship experiences.



Fig. 1. *Intern Cody Ensley with the focus of his work—Robonaut 2.*

OUTSIDE PUBLICATIONS	
NASA	17
Student University	2
Local Newspaper	2

Since the summer of 2010, USRP has increased its scope to publish in venues internal and external to NASA. Student stories have been published on the NASA Higher Education website, on psychorg.com, at student universities, and in student hometown local newspapers. This effort generates awareness to NASA research, USRP opportunities, and student achievements while serving as a great recruiting tool for future science, technology, engineering, and math (STEM) candidates. USRP was also featured in *Forbes* magazine online and on internships.com.

Special Interest Stories

In the fall of 2010, USRP began publishing special interest stories to cover a broader spectrum of topics, such as prior-service interns, interviews with African-American interns for Black History Month, coordinator interviews for Women's History Month, intern conference attendance, and "STEM Pipeline" successes. USRP also uses the SSI to document programmatic activities, such as center visits, volunteer activities like Space Day, and recruiting activities that include the University of Texas at El Paso Leadership Conference (figure 2).

Undergraduate Student Research Project
Social Networking and Student Stories Initiative
continued

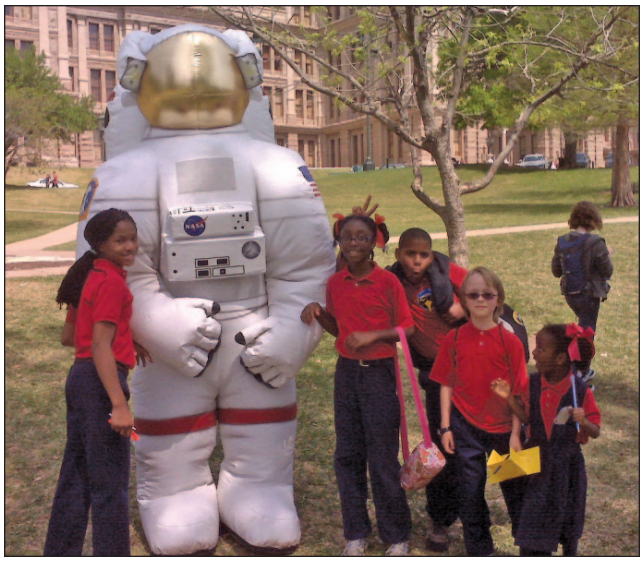


Fig. 2. *The author inspiring elementary students at Space Day.*



Fig. 3. *Student stories and videos can be found at http://usrp.usra.edu*

With the addition of special interest stories, the USRP website and Facebook page now have two to three new stories online each week. To date, USRP has published 78 stories and plans to publish 32 spring student stories over the summer—more than three times as many stories as USRP published for the summer of 2010.

Social Networking

USRP created a Facebook account in August 2009. In December 2010, USRP increased its friend count from 300 to around 1,900 friends, which represents over a 500% increase. They accomplished this by inviting the applicant pool to be friends. By asking interns to tag photos each semester, USRP increased its number of photos from 20 to more than 600—a 2,900% increase.

USRP uses Facebook as another venue to publish student stories, which generates more interest in the program by tagging the student covered by each story and by friends reposting stories. USRP also uses its page to give program updates and to recruit (figure 3).

In the spring of 2011, USRP created a group solely for USRP interns. This group can be used to send out opportunities for paper competitions, scholarships, and conferences. Currently, over half of USRP alumni and current interns belong to this intern group.

ISS*Live!* A Rich Internet Application Development for International Space Station Educational Outreach

Ahmed Khan, *United Space Alliance*
Jennifer B. Price, *Johnson Space Center*
Matthew D. Healy, *United Space Alliance*
Philip D. Harris, *Johnson Space Center*
Katharine M. West, *Johnson Space Center*
Jesse B. Ehlinger, *United Space Alliance*

Safely and Securely Putting Informative, Live Internal International Space Station Data for Use on the Web

The International Space Station (ISS) uses numerous internal computer networks to handle downlinked telemetry, operational timelines and procedures, and activities in day-to-day operations on the ground and for the onboard crew. The ISS and its control centers around the globe use a web-based intranet to handle some of this important, non-critical mission data in a read-only format. In addition, web-based software links to Mission Control Information Sharing Protocol Servers allow for some select mission control telemetry data to be made available in a viewable format, identical to existing flight controller displays inside the Mission Control Center. This existing system, which lets external users access displays on the web, is part of the Mission Control Center Data Portal System and uses a Java-based web technology called MSKWin.

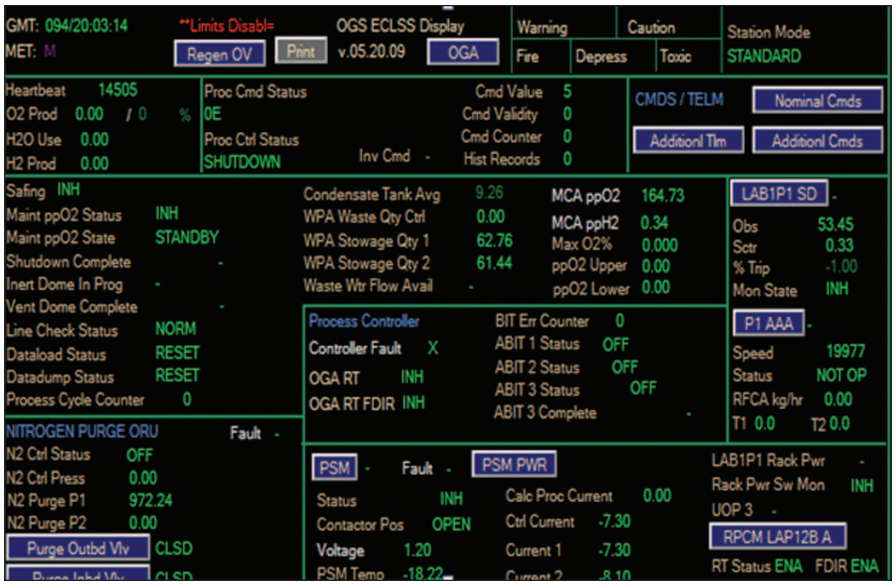


Fig 1. MSKWin web view of a sample International Space Station Environmental Telemetry Display.

To advance this technology further, a new "push" technology server was added to this network. This server, which uses a .NET interface and Asynchronous JavaScript, and XML streaming called "Lightstreamer," will allow for continuous lightweight streaming of telemetry data in a web-friendly JavaScript/html form. This allows for configurable and lightweight MSKWin-type displays (figure 1) to be generated on the web without having to use any heavy client-dependant plug-ins or Java applets. This technology makes these displays and telemetry portable enough for use on mobile devices and smartphones like the Apple iPad and iPhone, and on Google Android devices.

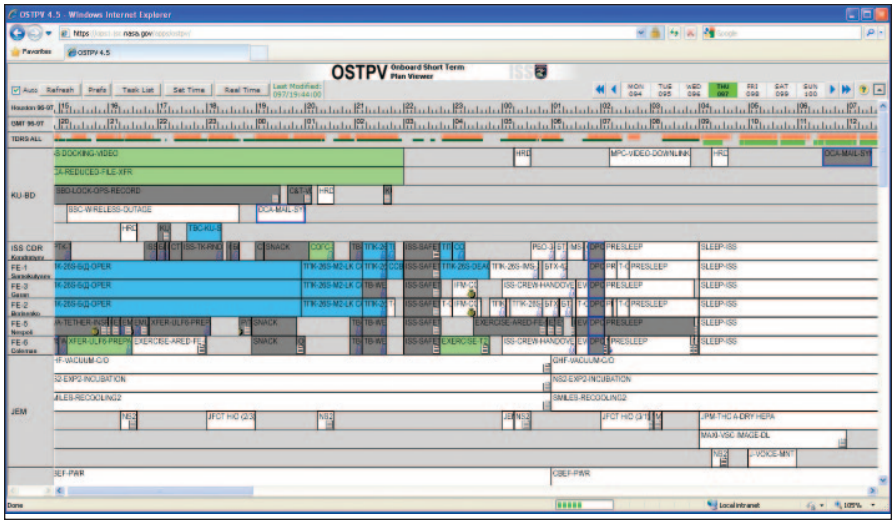


Fig 2. Onboard Short-Term Plan Viewer timeline viewer.

In addition, the Mission Control Center Web Tools team and Johnson Space Center's (JSC's) Mission Operations Directorate's Flight Planning Branch currently produce a web-based crew timeline called the Onboard Short-Term Plan Viewer (OSTPV) (figure 2). This JSC award-winning software is a *"TV Guide-like"* view of daily activities used

ISS*Live!* A Rich Internet Application Development for International Space Station Educational Outreach

continued

by both the ground and the crew in day-to-day operations of the station. Every event that goes on, related to any Mission Control Center or onboard the station, is scheduled and viewable on this web-based viewer. As such, OSTPV is a vital, internal situational awareness resource for the ISS community and onboard the station.

ISS*Live!*: International Space Station Mission Control in Your Pocket

ISS*Live!* is a software suite that combines and uses the availability of these two internal data sources through web services and a dedicated external server, into a new, public-friendly web content delivery source for NASA ISS Educational Outreach (figure 3).

ISS*Live!* will include websites and mobile applications that tie ISS telemetry and operational timelines into one "Rich Internet Application" experience, made public off of the NASA portal (www.nasa.gov) as well as on commercial "app" stores such as the Apple App store (see ISS*Live!* prototype views: iPad in figure 4; and iPhone in figure 5). The applications will offer data on real-time parameters such as station position, internal environment, altitude, payload rack science activities, and other interesting data and crew activities. ISS*Live!* will tie this data into an interactive application that will include the latest social media feeds relevant to the ISS, including astronaut Twitter feeds, image of the day, and real-time mission video.

ISS*Live!* will contain a scrollable timeline with a "public-friendly" view of crew and payload activities. As a website, it will use some of the latest interactive web content technologies, including creating three-dimensional interactive virtual views of the Mission Control Center and ISS. The intention is to have ISS*Live!* be a "one-stop shop" for ISS data, letting users in on the fascinating activities that happen daily onboard the ISS.

Working in conjunction with the NASA Education Office, ISS*Live!* content will serve as the basis for development of interactive lessons in the science, technology, engineering, and math fields. ISS*Live!* will also be a resource for the space enthusiast and the life-long learner to participate in the mission of the ISS.

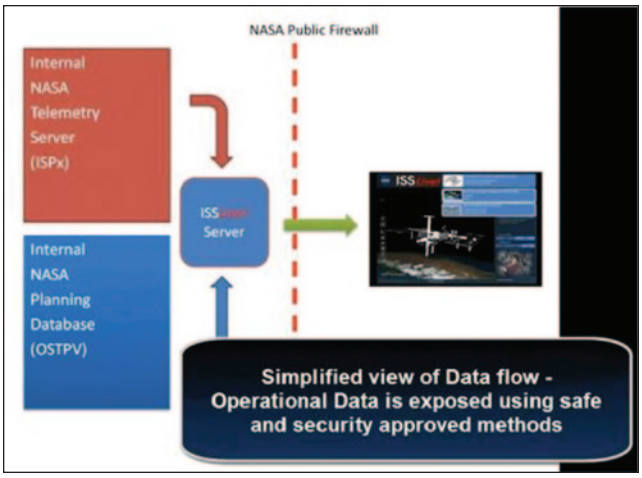


Fig 3. *ISS*Live! *simplified dataflow architecture.*



Fig 4. *iPad interactive view of ISS*Live! *(prototype).*

ISS*Live!*: A Mobile and Interaction Design Challenge

ISS*Live!* developers are currently partnering with Human Computer Interface Design Students at top-ranked Carnegie Mellon University to create application prototypes and interfaces to display ISS*Live!* data for the public. ISS*Live!* will also include an activity translator (also see the article titled "ISS*Live!* Translator: From NASA Operations Nomenclature to Every Day Language," in this Johnson Space Center Biennial Research and

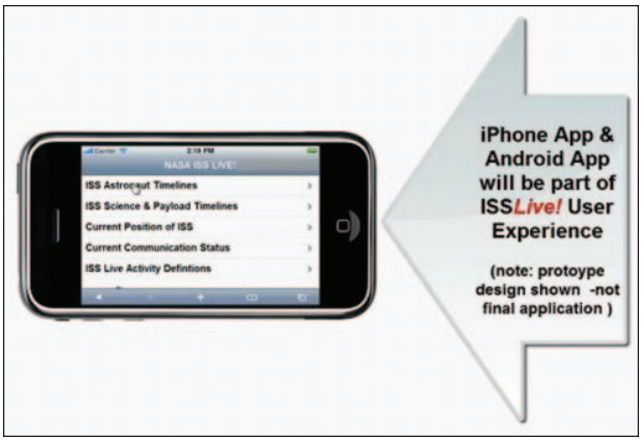


Fig 5. *Smartphone view of ISS*Live! *(prototype).*

Technology Development Report 2011). ISS*Live!* will further make an application programming interface available as a web service for external developers to take ISS data and put those data into their own websites and mobile applications.

ISS*Live!*: In Summary

Working with mission control operators, educators, and developers, ISS*Live!* will strive to develop innovative user interface designs and implement them in code to provide a Rich Internet Application experience for overall ISS educational outreach. ISS*Live!* has been deployed to the NASA portal (www.nasa.gov).

Astronaut Earth Observations—Earth's Dynamic Events and Twitpics

Justin Wilkinson, *Johnson Space Center*
Sue Runco, *Johnson Space Center*
Kim Willis, *Johnson Space Center*
William L. Stefanov, *Johnson Space Center*
Mike Trenchard, *Johnson Space Center*



Fig. 1. *View from the International Space Station cupola centered at 34°N 77°W of the mid-Atlantic coast of the United States, with Cape Lookout included as the cape on the right.*



Fig. 2. *Eruption of Sarychev Volcano, Kuril Islands, northeast of Japan, in June 2010.*



Fig. 3. *Hurricane Earl, Atlantic Ocean, on August 27, 2010—5 days after it formed in the Eastern Atlantic—approaching the Caribbean Islands.*

Almost every week, images of some "dynamic event" are requested from orbiting International Space Station (ISS) crews. Dynamic events include hurricanes, floods, tsunami damage, volcanic eruptions, and forest/bush fires. When immediacy is important, NASA can get an image from the astronaut camera to a public website in less than 24 hours. Dynamic and other images are made available on the Crew Earth Observations website, *http://eol.jsc.nasa.gov/*, which is known as the Gateway to Astronaut Photography of Earth.

Other "tools" for quick viewing of dynamic events from orbit include the use of social media in the form of the first Twitter feeds from the ISS, and the installation of the cupola on the ISS in 2010, with its 360-degree viewing capability. Figure 1 is a "fish-eye" view, acquired from the cupola, of the mid-Atlantic coast of the United States.

Volcanoes

Amazing as it may seem, astronauts have sometimes been close to volcanoes at the moment of the first major explosive activity. Astronaut Jeffrey Williams captured the first explosion of Cleveland Volcano in the Aleutian Islands before the science world was even aware of the incident (*http://earthobservatory.nasa.gov/IOTD/view.php?id=6592*). Crews on board ISS Expedition 20 captured an even more amazing plume of ash rising from Sarychev Volcano, Kuril Islands, northeast of Japan. The image is cataloged at *http://earthobservatory.nasa.gov/IOTD/view.php?id=38985* and illustrated in figure 2. The upward

blast incorporates a white, strikingly bulbous pileus cloud that may be water condensing as air is forced to rise in the plume, and ground-hugging ash, known as a pyroclastic flow, streams down the hillside to the lower right. The origin of the circular, cloud-free zone around the island raised interesting questions in the science community and were discussed at the catalog link. Through a computerized smoothing of a sequence of still images, the movement of the astronaut as well as the billowing plume as it surges upward is illustrated, thereby allowing a desk-bound observer to experience both of these movements. This sequence can be found at: *http://earthobservatory.nasa.gov/images/imagerecords/38000/38985/sarychev_oblique_final_H264.mov*.



Fig. 4. *The Arnica fire in Yellowstone National Park, September 2009. Other fires are visible near Jackson Lake (left) and on the flanks of the Grand Tetons Mountains (top center). NASA ID no. ISS20-E-43017.*

Hurricanes

Major storms last for many days, and their cloud bands rise up to the top of the troposphere—the weather layer of the atmosphere. The storms are therefore easily photographed and usually evoke much public interest. Images of any hurricane that approaches land are candidates for fast downlink so the public can see the views from space. Hurricane Earl (figure 3) was a long-lived, powerful storm that formed on August 25, 2010, and finally dissipated 10 days later. Interestingly, Hurricane Earl interacted with Hurricane Danielle, which crossed the Atlantic Ocean behind Earl. Traveling just off the East Coast of the United States, Earl was blamed for six fatalities, and became the first major hurricane to threaten New England since Hurricane Bob in 1991. Earl caused power outages for hundreds of thousands of people in Nova Scotia, Canada.

Fires

The Arnica fire in the Yellowstone National Park (figure 4) was imaged on September 24, 2009—the day after the fire began—when it grew to 101 acres in area (*http://earthobservatory.nasa.gov/IOTD/view.php?id=40681*). Astronauts have observed even small fires giving rise to enormous smoke palls. Here, smoke can be seen streaming southwest toward the Grand Tetons Mountain Range. Oblique images such as this give a powerful sense of three dimensions to fire images and many other phenomena: the smoke rises over Yellowstone Lake, casting an orange reflection in the lake and dark shadows on West Thumb embayment of the lake.

Social Media

Social media have promoted the immediacy of astronaut photography, sometimes with images of dynamic events. Astronaut Soichi Noguchi was the first to downlink Twitpics on a regular basis. An example of one of his dynamic Twitpic images include the May 2010 floods in Central Poland. Figure 5 compares one of Soichi Noguchi's images of the Vistula River floods in Poland with a Landsat image of the same region in 2011. The entire area of low country where the Vistula River meets a major tributary is inundated by brown muddy water.

Another example of social media used to share dynamic events observed from the ISS is Soichi Noguchi's Twitpic posting of the Gulf of Mexico following the Deepwater Horizon oil rig disaster on April 20, 2010. Figure 6 captures sun glint patterns of oil on the surface of the Gulf of Mexico on May 4, 2010, several days after the start of the disaster (*http://earthobservatory.nasa.gov/IOTD/view.php?id=43897*).



Fig. 5. *Flooded Vistula River valley, Poland, (left) as captured by Astronaut Soichi Noguchi in May 2010 and centered at 50.6N 21.8E as compared to Landsat image (right) of the same area in 2011.*

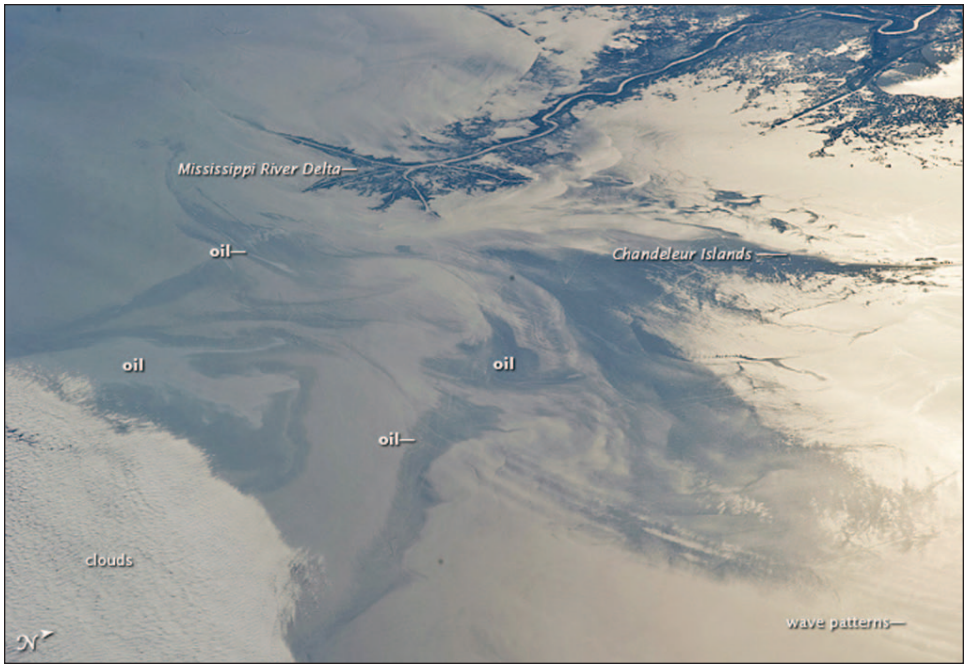


Fig. 6. *Deepwater Horizon oil spill in the Gulf of Mexico, as captured by International Space Station astronauts on May 4, 2010, and subsequently shared with the public via Twitpic posting.*

Capturing Immediate Learning Outcomes of Undergraduate Internships

Bryan E. Dansberry, *Johnson Space Center*

When viewed from the broadest employer perspective, student programs such as internships or co-op generate positive outcomes in three general areas:

1. Student competencies (learning)
2. Useful productivity (task completion)
3. Retention into the workforce (graduation, advanced degrees, employment)

Traditionally, metrics collected for NASA internships focused solely on retention outcomes. While important, retention outcomes require years to emerge as students complete their undergraduate degrees, decide whether to pursue graduate programs, and finally enter the workforce. Because of this long time lag between participation in the experiential program and the eventual hiring into the workforce, retention data can be a poor tool for managers looking to implement continuous improvements to their programs in the short term.

Outcomes in the areas of student learning and productivity hold the promise of providing more immediate information to program managers in monitoring the rigor and challenge of student experiences, maximizing the quality of the selection process, and capturing student growth in areas directly related to the Accrediting Body for Engineering and Technology demonstrated abilities criteria (ABET a-k criteria). Additionally, data gathered in the area of productivity can be used to estimate the value of the work produced by students to the organization—a metric that can carry significant weight in defending student program budgets during difficult economic times.

In 2008, managers of NASA's Undergraduate Student Research Program (USRP) instituted new end-of-internship surveys for both students and mentors. These surveys were designed to better capture outcomes generated in the areas of student learning and productivity.

The data presented here are derived from 724 student surveys and 517 mentor surveys collected from spring 2008 through fall 2010. The data represents internships at all NASA centers, and in spring, summer, and fall sessions.

Student Learning: Cognitive Skills

Table 1 shows the percentage of USRP interns who indicated their experience provided them growth opportunities in areas closely aligned to ABET a-k criteria. These are areas deemed critical to career success in engineering and technology careers. Overall, these data indicate that USRP internship experiences are appropriately rigorous and challenging, providing students ample opportunity to grow in many of the areas considered critical in producing a highly qualified pool of future engineers and scientists for the nation's technical workforce.

Table 1. *Percentage of Undergraduate Student Research Program Interns, Indicating Growth in Key Skill Areas*

Professional/Technical Communication	98%
Conceptual/Analytical Ability	99%
Learning/Applying Knowledge	99%
Professional Qualities	98%
Teamwork	93%
Leadership	88%
Technology	97%
Work Culture	99%
Organization/Planning	97%

Student Learning: Attitudinal Change

USRP interns were asked a series of questions designed to determine how their USRP experience affected their commitment and attitude in regard to their current career path. Table 2 shows the student responses to these questions. The percentage given represents the number of interns who expressed agreement with the statement. Considering that about 50% of USRP interns are seniors, the results are another indication of the strong impact that hands-on experiential opportunities have on student development.

Capturing Immediate Learning Outcomes of Undergraduate Internships

continued

Table 2. *Student Responses to Affective Questions in Undergraduate Student Research Program Survey*

This experience helped me determine my own strengths and weaknesses	96%
This experience increased my professional self-confidence	98%
This experience increased my academic motivation	96%
This experience increased my understanding of my chosen profession	95%
This experience helped me to clarify my career plans and options	97%
This experience helped prepare me to achieve my career goals	98%

Student Productivity

Another outcome of internships and co-op that has not been captured previously is useful technical productivity. These data are captured for USRP by asking mentors to compare the output of their student intern to a typical fresh-out new hire in their organization. While this opinion can only lead to an approximation of the actual value, results have remained consistent across the nine sessions for which these data have been captured. The following equation is used to generate a dollar value:

Productivity ($$) = mentor rating x ave. starting salary+benefits x total length of USRP internships

Using this equation and the average mentor ratings of their students, USRP interns have generated approximately $20.8 million in useful technical work, which helps to further NASA's technical missions. This represents a positive return on investment of approximately $2.1 for each dollar spent to fund USRP internships.

The Value of Student Learning

In an attempt to create a value metric for student learning similar to that for student productivity, USRP project managers asked the following question on student surveys:

"Please relate the total value (educational learning, professional growth, etc...) of your internship experience to the value you get from a typical semester (or quarter) at your institution. Please quantify your answer in terms of credit hours."

The average response to this question was 13.7 credit hours. Applying this value to all internships resulted in an estimated quantity of learning generated by USRP internships equivalent to 13,000 credit hours over the 3-year span for which data were collected. Converting this figure to a dollar amount was somewhat more complex than the conversion for productivity. Depending on whether a strict cost per credit hour national average was applied, or the total average cost for a semester of school was reviewed, the dollar value equivalent could range widely. However, when using a $10,000 per semester figure and 12 credit hours as a full load, this figure converted to approximately $11 million.

The Value of Immediate Outcomes for Internships and Co-op

USRP internships generate approximately $3.1 in immediate student learning and useful technical productivity for each dollar invested, based on 3 years of data collected across every NASA center. The capture of these outcomes provides strong evidence for the observed connection between healthy student programs and a healthy organization seen in science, technology, engineering, and math employers in both the private sector and government.

Space Life Sciences Directorate Innovation and Collaboration for Education and Outreach

Tacey Baker, *Johnson Space Center*

Johnson Space Center's (JSC's) Space Life Sciences Directorate has initiated the Student Teacher Outreach Mentorship Program (STOMP) as a collaborative and innovative approach to achieving its education and outreach goals. STOMP will contribute to sustaining and enhancing Space Life Sciences core competencies and inspiring the next generation to pursue science, technology, engineering, and mathematics (STEM) careers.

The Tufts University STOMP is an engineering education and outreach program that began in 2001, implemented through the Center for Engineering Education Outreach at Tufts University. In August 2009, Tufts University staff met with representatives from JSC Space Life Sciences and Engineering directorates to discuss partnership and collaboration potential in the area of education and outreach.

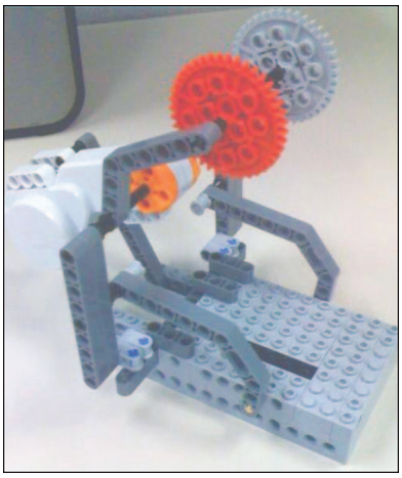


Fig. 1. *Example of LEGO ARED.*

The collaboration of JSC and Tufts STOMP is aimed at developing activities that are appropriate for STOMP outreach based on NASA Space Life Sciences content using the LEGO® MINDSTORM® robots (figures 1 and 2); developing and implementing a STOMP outreach program at JSC that places employees in local K-12 classrooms; and engaging STOMP students in NASA Space Life Sciences research.

The first phase of the pilot was completed during the summer of 2010 and included hosting a Tufts University student within the JSC Space Life Sciences Directorate to develop a unit of lessons equivalent to 6 to 8 hours of classroom time. Space Life Sciences research topics and related countermeasures are included in this set of lessons and were pilot tested in STOMP fifth-grade classrooms in the Boston, Massachusetts, area. The results of the pilot test will be used to refine the lessons into a final product, and are part of the second phase to begin in the summer of 2011 and carry through the fall.



Fig. 2. *Example of LEGO Treadmill.*

Pilot testing in Houston, Texas, elementary schools is planned during the second phase. This testing will be planned and accomplished through collaborations with other education and outreach discipline experts within NASA and external parties. Existing surveys developed by the Tufts' program will be used to determine the volunteers', teachers', and students' assessments of the program.

Tufts University is a member of the Massachusetts Space Grant Consortium, which was a recipient of the Summer of Innovation 2010 awards issued by the NASA Office of Education. The experience and lessons learned will be leveraged in developing and implementing the long-term goal of establishing a JSC STOMP effort that engages employees to volunteer for this outreach activity with students.

Space Life Sciences Academy and the NASA Science and Technology Institute

Pamela Denkins, *Johnson Space Center*
Karla S. Marriott, *Savannah State University*
Alamelu Sundaresan, *Texas Southern University*
Jinghe Mao, *Tougaloo College*
Shakhawat Bhuiyan, *Jarvis Christian College*
Jacqueline Madry-Taylor,
United Negro College Fund-Special Programs

Overview

The NASA Human Health and Performance Center/Space Life Sciences Academy is partnered with the agency's Office of Education and the United Negro College Fund-Special Programs in support of the NASA Science and Technology Institute (NSTI) whose purpose is to create a consortium of minority institutions that participate in cutting-edge research in collaboration with NASA, other government agencies, private organizations, majority institutions, and research and technical organizations. The specific goals of the NSTI program include the establishment of research and development partnerships and the development of comprehensive strategies that provide faculty and students with a year-round NASA research experience, and that increase the interest and number of academically talented students pursuing careers in science, technology, engineering, and mathematics (STEM) disciplines. Faculty and student participation in the NASA centers' research further enhance the capacity of minority-serving institutions to conduct cutting-edge research.

The Space Life Sciences Academy serves as the Johnson Space Center (JSC) lead science organization with oversight and guidance of the research activities of the United Negro College Fund-Special Programs Mission Enabling Technology (UNIMET) Cluster whose long-term research objectives are: the synthesis of agents for the evaluation of the pathophysiological function of cannabinoid receptors in immune system disorders (CB_2 receptors); and contribution to the development of a therapeutic pharmacophore for the treatment of autoimmune diseases associated with long-term space flight.

Research Synopses

In long-term space flights, crew members are exposed to deep-space radiation, microgravity, and infectious agents from other crew members and microbial contamination—all of which have a significant impact on the body's immune system and may contribute to the development of autoimmune diseases or allergic reactions. Collectively, these contributing factors create a significant imbalance in the body's immunomodulatory system, affecting cells such as CD4+ (helper) T cells, B cells, monocytes/macrophages/dendritic cells, natural killer cells, hematopoietic stem cells, and cytokine networks. The CB_2 cannabinoid receptor—located almost exclusively in tissues of the immune system, spleen, tonsils, and lymph nodes—is highly suggestive of a CB_2 receptor mediated immunomodulatory effect.



Fig. 1. *NSTI UNIMET Researcher (TSU) and Summer 2011 Interns from Tugaloo and Jarvis Christian Colleges.*

Cannabinoids reportedly possess antitumor and immune-enhancing properties. UNIMET research professors from Jarvis Christian College (Hawkins, Texas) and Texas Southern University (Houston, Texas), and three of its students including the post-doctoral student, will engage in research during the summer of 2011 at JSC and Texas Southern University to further assess these properties. Analyses will be conducted on the lymphocyte function and cytokine expression of human lymphocytes exposed to: simulated microgravity using the bioreactor (at Texas Southern University); and radiation (at Texas A&M University [College Station, Texas]); and then to cannabinoid receptors.

Additional faculty research opportunities are planned with the Space Radiation Branch on the effects of radiation exposure to the signal transduction pathway on mitogen-activated protein kinases that regulate various cellular activities and, in parallel, on the cannabinoid receptors (CB_1 and CB_2) that are involved in the control of cell proliferation by stimulating mitogen-activated protein kinases.

Value of the Research

Scientific merit. Successful long-duration exploration is critical to the understanding of the fundamental cellular processes that are affected by microgravity and radiation. The results of the NSTI investigation will advance the understanding of the signal transduction events that are sensitive to changes in gravity and as a result of radiation exposure. Additionally, the ability to ameliorate the defects and/or damages may offer the prospect of identifying alternate and co-stimulatory pathways that lead to cell activation and locomotion.

Education and Outreach. Overall, the NSTI program offers its participants numerous opportunities, which include: conducting new research; accessing NASA's internal and informal networks; acquisition/expansion of knowledge of NASA's technical and scientific needs; sharing information about the capabilities and technologies of the respective applicant minority institutions; competing for research awards; interfacing with high-level NASA and other government officials; participating in research and development programs from NASA and related science and technology communities to learn about innovative scientific and engineering research methods; participating in discussions on the pedagogy of STEM disciplines; enhancement of research and management capabilities of minority-serving institutions in science and technology areas of interest including the entire aerospace industry; engaging in professional development geared toward managerial development, and research marketing skills; networking and establishing long-lasting relationships with STEM colleagues throughout the country; enhancing undergraduate and graduate research; and building entrepreneurial, scholarly publication and intellectual property protection skills.

Specifically, for the UNIMET Cluster, the outcomes include student training in state-of-the-art laboratory techniques, modeled microgravity and radiation exposure; an understanding of the complexities of the space environment, immunology, and biotechnology; increased and enhanced STEM awareness; exposure to the NASA environment and opportunities; and curriculum



Fig. 2. *UNIMET Faculty researcher and undergraduate at Jarvis Christian College*

enhancement in biology and engineering. The synergism between Texas Southern University, NASA Education, and Space Life Sciences will broaden participation in these areas and serve overall and specific NSTI goals with possible publications and intellectual property.

Students are required to engage in an education and outreach activity during the summer. The activity may include speaking to elementary, middle school, or high school students regarding their interest in STEM or their experience in the NASA internship program, and/or assisting with ongoing education and outreach tasks within the Space Life Sciences Directorate such as website suggestions for the Space Life Sciences Academy.

The UNIMET Cluster is in its third year of research. The universities represented are Savannah State University (Georgia), Tougaloo College (Mississippi), Jarvis Christian College, and Texas Southern University. (Figures 1, 2, and 3.)

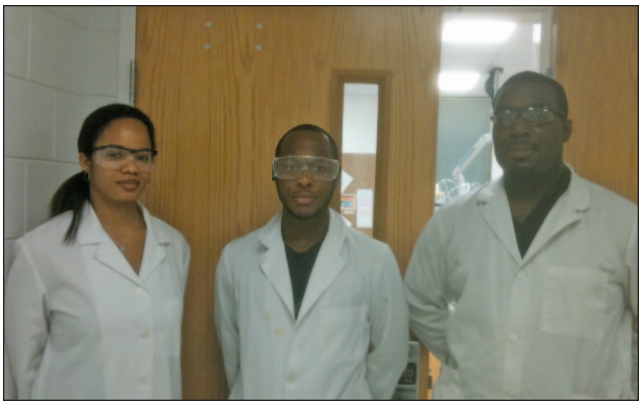


Fig. 3. *The UNIMET Undergraduate Research Group at Savannah State.*

Research for Space Colonization: NASA Ralph Steckler/Space Grant Space Colonization Research and Technology Development Opportunity

Frank Prochaska, *Johnson Space Center*

The late Ralph Steckler, a successful assistant film director and photographer from Southern California, maintained a lifelong interest in space colonization. Mr. Steckler left the significant remainder of his estate to NASA "for the colonization of space because [he believed] this is for the betterment of mankind." NASA accepted the gift under the National Space Grant College and Fellowship Act, and established the program to implement Mr. Steckler's testamentary direction. For purposes of this endeavor, space colonization is understood to be the establishment of a broad range of human activity in space that, for the most part, is not reliant on Earth's resources.

The NASA Office of Education invited proposals for the NASA Ralph Steckler/Space Grant Space Colonization Research and Technology Development Opportunity (hereafter "Steckler/Space Grant Opportunity"). Each funded awardee addressed innovative, meaningful, and enduring research and technology development activities, aligned to a NASA research agenda that could enable space colonization or space settlement by providing a sustained human presence on the moon as a stepping-stone to future exploration of Mars.

The processes of innovation, research, and technology development frequently happen incrementally; therefore, the Steckler/Space Grant Opportunity provides implementation through three funding and development phases. Below are the number of awardees and monetary amounts with each phase.

Phase 1—Awarded January 2010
Number of awardees: 18
Award maximum: $70,000
Duration: 9 months

Phase II—Awarded January 2011
Number of awardees: 5
Award maximum: $250,000
Duration: 24 months

Phase III:
Number of awardees: 2
Award maximum: $275,000
Duration: 24 months

Below are project descriptions for (Ralph Steckler/ Space Grant Space Colonization Research and Technology Development Opportunity) Phase II awardees.

Title:
Flywheel Storage for Lunar Colonization
Technical Monitor:
Raymond Beach, Glenn Research Center
Principal Investigator:
David Atkinson, Idaho Space Grant Consortium

Project Description
Energy available on demand is absolutely necessary for long-term exploration and colonization of the moon. Energy generation is likely to be dominated by capture of solar energy and by nuclear energy sources. These and other sources of energy require storage to enable them to meet demand that varies with time of day and level of activity. Flywheels provide a reliable, efficient, and low-maintenance way to obtain continuous energy on demand. They have minimal shielding and require lighter payload for installation than batteries (NASA's current alternative) in the atmospheric vacuum, extreme temperature, and lunar surface's moderately elevated radiation levels. This project seeks to establish the scientific and technical merit and feasibility of using flywheel energy storage systems in support of human long-term exploration and colonization of the lunar surface. The project focuses on developing, verifying, and determining the characteristics of an idling iron energy loss reduction algorithm applied to an integrated hubless flywheel and motor generator design.

Title:
Acquisition of Planetary Samples During Human Surface Activities on the Moon and Beyond
Technical Monitor:
Jacob Bleacher, Goddard Space Flight Center
Principal Investigator:
Patricia Hynes, New Mexico Space Grant Consortium

Project Description
One of the crowning achievements of the Apollo Program was the return of approximately 382 kg (842 lbs.) of



Fig. 1. *Acquisition of planetary samples during human surface activities on the moon and beyond.*



Fig. 2. *Lunar greenhouse.*

lunar material to Earth during six human missions. These samples provided a fundamental understanding of the origin and evolution of the Earth-moon system and the history of the early solar system. One of the major scientific activities that will occur during the future exploration of the moon and other planetary bodies (Mars, near-Earth objects) will be the acquisition of samples by humans. Past designs for exploration architectures (i.e., Constellation) had the capability for accommodating upwards of 100 kg (220 lbs.) of returned material, although increasing the capability for returning between 250 to 300 kg (551 to 387 lbs.) of material is scientifically valuable and have been investigated. Based on the Apollo 17 model, future sortie missions to the lunar surface have the capability of collecting 800 kg (1764 lbs.) of samples and lunar outpost activities will collect even more. This is significantly more than all proposed exploration architecture can return to Earth. Further, these sampling activities will acquire materials that are sensitive to both changes in environment and the techniques used in sampling and storage. Phase I of this study defined measurements and instrumentation required to enable humans to carefully select and "high-grade" scientifically important samples within the context of both sortie- and outpost-style surface activities and identified and demonstrate protocols and technologies necessary to preserve the integrity of environmentally sensitive and fragile samples. In Phase II, NASA will do the following: design, develop, and test a combined hand-held X-ray diffraction/X-ray fluorescence instrument that could be used for human "high-grading" of samples (in addition to robotic exploration of planetary surfaces); and establish a consortium to study material collected in Apollo-era sample containers. The former will increase the efficiency of human surface activities, whereas the latter will lead to improvements in the design of containers for environmentally sensitive samples (figure 1).

Title:

Lunar Greenhouse Prototype for Bio-regenerative Life Support Systems

Technical Monitor:

Raymond M. Wheeler, Kennedy Space Center

Principal Investigator:

Michael J. Drake, Arizona Space Grant Consortium

Project Description

Bioregenerative Life Support Systems (BLSS) are architected to revitalize the lunar habitat's atmosphere, recycle the crew's water, and generate a portion of the crew caloric intake and reduce resupply requirements. One component of the BLSS is the greenhouse subsystem. The Lunar Greenhouse (LGH) Prototype at the Controlled Environment Agriculture Center on the University of Arizona (UA) campus is comprised of a single modular deployable structure equipped with artificial lighting and growing system where plants grow in plastic envelops suspended from each end with nutrient solution flowing to the roots with very limited substrate.

The NASA Ralph Steckler Phase 1 funding focused on collecting data and understanding the LHG performance for BLSS of future lunar outposts with specific goals to demonstrate the polyculture growing systems, to determine the food production capability, the water, the carbon, energy balances, and to document the capabilities and weaknesses.

Phase II expands and enhances the UA-LGH facility to improve recycling capabilities of the gaseous, liquid, and solid phases of the system, increase food production efficiency (kg/unit time/resource input), and increase system fidelity. The objectives are to expand the number of LGH units to a maximum of no greater than 89.7 m^3 volume and 189 m^2 of growing area; enclose the interconnecting hallway so that the LGH units can provide

for combinations of NASA food crops; incorporate water recycling, and evaluate the potential for solid waste recycling/composting; redesign the LGH1 plant microclimate to improve uniformity of its atmospheric aerodynamics; improve the monitoring, feedback control with additional non-contact sensing, and telepresence within a decision support system; and develop international cooperation by including faculty and students sponsored by foreign space agencies (i.e., Agencia Spatiale Italiano). See figure 2.

Title:
Nuclear Power for Space Colonization Research and Technology Development—Phase II

Technical Monitor:
Al Juhasz, Glenn Research Center

Principal Investigator:
Tom Blue and Gary Slater, Ohio Space Grant Consortium

Project Description
This project proposes to continue development of the Space Molten Salt Reactor that started in Phase I of the Ralph Steckler/Space Grant Space Colonization Research and Technology Development Opportunity with specific mission analysis, preliminary experimental verification, and rigorous computational models.

The Space Molten Salt Reactor will be developed primarily as an advanced nuclear surface power system for a space colony or scientific outpost. Specifically, development will be focused on electrical outpost above 100k to meet power needs associated with in-situ resource utilization and closed-loop life support. Meeting these power demands is essential to establishing a sustained human presence on the moon and eventually Mars.

To a lesser extent, the Space Molten Salt Reactor will be developed as an energy source for nuclear electric propulsion. Nuclear electric propulsion and nuclear surface power have similar design requirements, and nuclear electric propulsion supplements a colonization research agenda by assisting in crewed travel beyond near-Earth space.

Title:
Safety, Reliability and Reproducibility of Microbial Systems for Space Colonization

Technical Monitor:
John Hogan, NASA Ames Research Center

Principal Investigator:
Christopher House, Pennsylvania Space Grant Consortium

Project Description
Microbial reactors for waste treatment and food production are important parts of future life support systems. In Phase I research, the team verified the utility of three microbial components for inclusion in a life support system: a novel packed-bed, fixed-film anaerobic digester, a methantrophic co-culture for food production, and the novel Halomonas strain SP1 for secondary waste treatment at alkaline pH. In Phase II, the team will determine the safety, reliability, and reproducibility of these components to ensure predictable operation as part of a life support system. In Section 1 of the Phase II research, the team will construct small-scale anaerobic digesters and determine the reproducibility of biofilm community changes in response to operational stresses. The team will also examine methods of preserving biofilm for rapid start-up of a new anaerobic digester. Section 2 test will determine the reproducibility of the methanotrophic biomass as a food source, and experiment with a new type of bioreactor as well as various solid substrates as a way to improve growth rate and biomass density. In Section 3, the team will analyze the utility of strain SP1 for secondary waste treatment and possibly as an additional food source. Section 4 tests will be conducted to address safety of the system components by tracking the flow of proxy organisms for pathogens through each microbial reactor. In Phase III, the team will link the individual microbial reactors together into a continuously operated system to determine system losses and efficiency.

Minority University Research and Education Program at Johnson Space Center

Jennifer Scott Williams, *Johnson Space Center*

Since October 2005, the Johnson Space Center (JSC) Office of Education has worked through the Minority University Research and Education Program (MUREP) to strengthen its relationship with Minority-Serving Institutions of higher education to ensure that NASA can meet future workforce needs in science, technology, engineering, and mathematics (STEM) fields. MUREP was created to increase the agency's responsiveness to three federal mandates related to Minority-Serving Institutions:

- Executive Order 13532: Historically Black Colleges and Universities (Dated Feb. 26, 2010)
- Executive Order 13555: Educational Excellence for Hispanics (Dated Oct. 19, 2010)
- Executive Order 13270: Tribal Colleges and Universities (Dated July 3, 2002)

MUREP engages underrepresented populations through a wide variety of STEM initiatives. During 2010 and 2011, JSC actively recruited and employed approximately 45 students during the summer of 2010 through summer internship opportunities, and 50 students during the summer of 2011 through various MUREP-related programs and projects.

MUREP is comprised of eight different projects:

- University Research Center (URC)
- NASA Science and Technology Institute (NSTI)
- MUREP Small Projects (MSP)
- Motivating Undergraduates in Science and Technology (MUST)
- Curriculum Improvements Partnership Award for the Integration of Research (CiPAIR)
- Tribal Colleges and Universities Project (TCUP)
- NASA Innovations in Climate Education (NICE)
- Harriet B. Jenkins Pre-doctoral Fellowship Program (Jenkins)

Assigned to JSC are two of 13 URCs (URC is a multiyear grant up to 1 million dollars a year)—one to Prairie View A&M University, and one to The University of Texas at El Paso. The grants are designed to assist faculty and students in research of pertinent missions in radiobiology, propulsion, and space radiation. More than 20 students from both URCs participated in summer internships during 2010 and 2011.

NSTI currently host three cluster grants at three NASA centers. One of these cluster grants—the Mission Enabling Technology Cluster—is assigned to JSC and is comprised of Texas Southern University, Savannah State University, Tougaloo College, and Jarvis Christian College. Seven students were engaged through the NSTI project where interns and researchers conducted pertinent research in the Space and Life Sciences organization. The Harriet B. Jenkins Pre-doctoral Fellowship Program is a graduate student program for underrepresented and underserved populations in STEM. JSC hosted one fellow who conducted research on anti-fog coating for space visors. Three new Jenkins fellows were selected for JSC for the 2011 incoming cohort of students.

Through MSP, the Achieving Competence in Computing, Engineering and Space Science (ACCESS) is a program designed for students with disabilities. During 2010 and 2011, four students successfully completed work in the ACCESS program through projects in aerospace, mechanical engineering, and physical science.

The MUST project is comprised of scholarships and internships, and currently hosts 115 scholars who are placed in internships across the agency. During 2010 and 2011, JSC hosted nearly 30 MUST scholars who engaged in various engineering, science, and mathematics projects. Through CiPAIR, JSC was able to host eight students and two faculty members selected for research opportunities.

The Pre-Service Teacher Institute (PSTI) is a summer residential workshop targeted for Minority-Serving Institutions' early childhood and elementary education majors preparing to teach in an elementary or middle

Minority University Research and Education Program at Johnson Space Center

continued

school (K-8). In 2010, JSC was able to host one 2-week session. In 2011, JSC hosted two 1-week sessions of PSTI workshops where college students from diverse backgrounds were exposed to the aerospace community through STEM inquiry-based learning activities. Nearly 90 students were involved in this program. PSTI participants were able to actively put into action the newly learned lessons through an outreach to more than 400 students in partnership with the JSC Visitor Center, Space Center Houston, and a local Young Men's Christian Association.

JSC's Office of Education, in collaboration with the Integrated Project Office, Public Affairs Office, and Space and Life Sciences, Astromaterials, and Engineering Directorates, supported the Hispanic Engineering, Science, and Technology (HESTEC) Conference 2010 in Edinburg, Texas. HESTEC is a partnership with the University of Texas-Pan American and Congressman Rubén Hinojosa's office. NASA exhibited activities to expose and inspire underserved minority middle school students to become scientists, mathematicians, and engineers, which supports the goals of the NASA Summer of Innovation initiative.

Overall, JSC MUREP has taken strides to engage students from Minority-Serving Institutions and underrepresented populations with quality research experiences as well as valuable skills that will lead to future success in the classroom, graduate school, post-doctorate work, as well as the STEM workforce.

International Humans in Space Symposium Youth Art Competition

Jancy C. McPhee, *Johnson Space Center*
S. Douglas Holland, *Johnson Space Center*

Emerging efforts and studies demonstrate that art plays a critical role in enhancing science, technology, engineering, and math (STEM) education, an important NASA and U.S. goal of great importance, given that current U.S. youth lag far behind other industrialized countries in math and science skills. Partnering science with art also encourages the development of creative and critical thinking, problem solving, and communication skills. These abilities are becoming increasingly necessary to ensure high performance in a rapidly changing global society. Thus, educational approaches combining space science topics with art could provide an effective method to inspire youth to seek education and careers in STEM-requiring fields, and to approach them innovatively and creatively.

In addition, the integration of science with art can provide a more effective outreach tool for youth and adults than using science alone. Prompting artistic expression with information about our current knowledge of human space exploration has the potential to reach a wide audience of youth. The resulting artwork can then be used as a communication tool to inspire even more people of all ages, enhancing awareness, interest, and support for human space flight. The artwork can also provide new ideas or renewed inspiration to those already working in the space industry. In the past, many of our science programs in human space exploration have been inspired by the works of artists.

An opportunity to test these education and outreach ideas arose in 2009 during the local planning for the 18th International Academy of Astronautics (IAA) Humans in Space Symposium, which was to be held in Houston in 2011. The theme of the Symposium was "Integration and Cooperation in the Next Golden Age of Human Space Flight." The symposium organizing committee reasoned that while the current adult generation would do much of the planning for this golden age, the next generation would do much of the implementation. Thus, youth ought to be involved in the planning. To allow for this



Fig. 1. *Visual Artwork, ages 10-13: a) Moonworkers, by Albert Choi, U.S; b) B.E.A.M. Base Exploration Aboard Moon, by Emily Miedema and Abby Bull, Canada; c) Look at our New World, by Chi Yin Yu, China. (Images courtesy of authors.)*

International Humans in Space Symposium Youth Art Competition

continued

involvement, a Humans in Space Symposium Youth Art Competition was designed to engage young people from around the world in *thinking* about the future of human space flight, and to provide a means for them to *creatively communicate* their ideas to the symposium attendees. "Be Inspired, Be Creative and Be Heard" was the adopted tagline of the art competition, stressing the three main intentions of the activity.

The online international art competition invited youth, ranging in age from 10 to 17 years, to submit visual, literary, musical, and video art expressing "What is the future of human space exploration and why is it important?" The response by youth to the call for artwork was enormous: 550 art entries were received from 22 countries, distributed across five continents. (See examples of literary and visual artwork in figures 1-3.) An international panel of 71 judges—including artists, scientists, teachers, engineers, astronauts, and others—evaluated the art and provided scores and comments used to award prizes and certificates of recognition.

To ensure that adult symposium attendees were exposed to the creativity and messages of the youth artists, the best artwork was woven into a multimedia live performance using artwork of each submitted type. Together, four performance sets cohesively displayed how the youth artists addressed four questions: What is the future of human space exploration?; Why is it important?; How will it happen?; and Who will carry it out? In addition, the art was displayed throughout the week of the symposium, allowing adult attendees to continuously view the artwork. A few top winning artists from around the world were also invited to visit at the symposium and discuss with the attendees, in person, their vision for our future in space. After viewing the artwork, attendees said that they were deeply influenced by the thoughts, beauty, and intensity of the youth artwork. The hope is that this influence will be long lasting, and that the youth ideas may have a role in developing strategies for human space flight, giving



Fig. 2. *Visual Artwork, ages 14-17:*
a) Cradle of Cosmos, by Anastasia Pronina, Russian Federation;
b) Future City in Space, by Man Wai Leung, China;
c) What's Your Horizon, by Mayisha Nakib, U.S.
(Images courtesy of authors.)

planners fresh ideas and new energy while helping them to learn what the next generation—the implementers of the future—believes is important for human space exploration.

The current intent is to use the artwork displays and performance products further as educational and outreach tools by exhibiting them at various venues, including classrooms, museums, space industry conferences, and NASA centers. The winning artwork is also displayed and viewable worldwide in an online gallery at *http://www.dsls.usra.edu/meetings/IAA/artContest/*. Placing the artwork online provides another means for the ideas and creativity of the youth to continue to inspire both generations of space explorers as they plan and carry out the future of human space flight.

The success of the youth art competition required the bridging of people from different generations, skill bases, and national affiliations. The project was performed as a partnership between the IAA, the NASA Human Research Program, the NASA Johnson Space Center Engineering Directorate, the Universities Space Research Association, and the University of Houston. Advertising, awards funding, and judging drew in additional partners from the commercial and educational sectors (including the International Association of Educators for World Peace, associated with the United Nations, the artistic and scientific disciplines, the space community worldwide, and more).

The art competition engaged many youth in a fun and absorbing manner to learn about past human space flight, and to think about the future of human space exploration. Products from the competition will become lasting educational and outreach tools that can be used continually to stimulate youth and adult interest and involvement in space science. Future projects that blend art and science should be created to promote youth education, original thinking, and communication of ideas, as well as outreach to multiple generations.

The Glorious Cavern

The cavernous darkness abounds,
Rich with twinkling stars,
Like tiny pearls in an ocean of black.

Riddled with stars,
Dotted with planets,
Shrouded in mystery…

The depths of space never end,
Like an endless shawl studded with pearls
Wrapped around planets.

The layman stares,
The astronaut observes,
The child delights.

All with awe,
At the majesty,
And the mystery.

Nothing has intrigued man more than this
Black envelope
Addressed to all who wish to explore its mysteries.

From the exploits of Apollo 11,
To the ambitions of space agencies,
To the gleaming rockets probing the frontiers of the world.

The silvery craft nears the planet,
The astronauts breathless
With excitement and awe.

The ship breaks through the atmosphere,
Like a silver arrow piercing a membrane
And the humans are speechless.

The rocky landscape glows in the setting sun,
And the humans disembark,
Feeling more excited than they've ever had.

The sense of adventure,
To wonderful new realms…
Strange new planets.

Even as the fragile Earth,
Struggles from pollution,
We probe the universe…

For a new planet,
A new galaxy,
A new universe…A new home, a brand-new life.

Fig. 3. *The Glorious Cavern, Prannoiy Chandran, age 14, Singapore.*

REPORT DOCUMENTATION PAGE

Form Approved
OMB No. 0704-0188

Public reporting burden for this collection of information is estimated to average 1 hour per response, including the time for reviewing instructions, searching existing data sources, gathering and maintaining the data needed, and completing and reviewing the collection of information. Send comments regarding this burden estimate or any other aspect of this collection of information, including suggestions for reducing this burden, to Washington Headquarters Services, Directorate for Information Operations and Reports, 1215 Jefferson Davis Highway, Suite 1204, Arlington, VA 22202-4302, and to the Office of Management and Budget, Paperwork Reduction Project (0704-0188), Washington, DC 20503.

1. AGENCY USE ONLY *(Leave Blank)*	2. REPORT DATE	3. REPORT TYPE AND DATES COVERED
	December 2011	NASA Technical Memorandum

4. TITLE AND SUBTITLE
Biennial Research and Technology Development Report

5. FUNDING NUMBERS

6. AUTHOR(S)
Kamlesh P. Lulla

7. PERFORMING ORGANIZATION NAME(S) AND ADDRESS(ES)
Lyndon B. Johnson Space Center
Houston, Texas 77058

8. PERFORMING ORGANIZATION REPORT NUMBERS
S-1110

9. SPONSORING/MONITORING AGENCY NAME(S) AND ADDRESS(ES)
National Aeronautics and Space Administration
Washington, DC 20546-0001

10. SPONSORING/MONITORING AGENCY REPORT NUMBER
TM-2011-216163

11. SUPPLEMENTARY NOTES

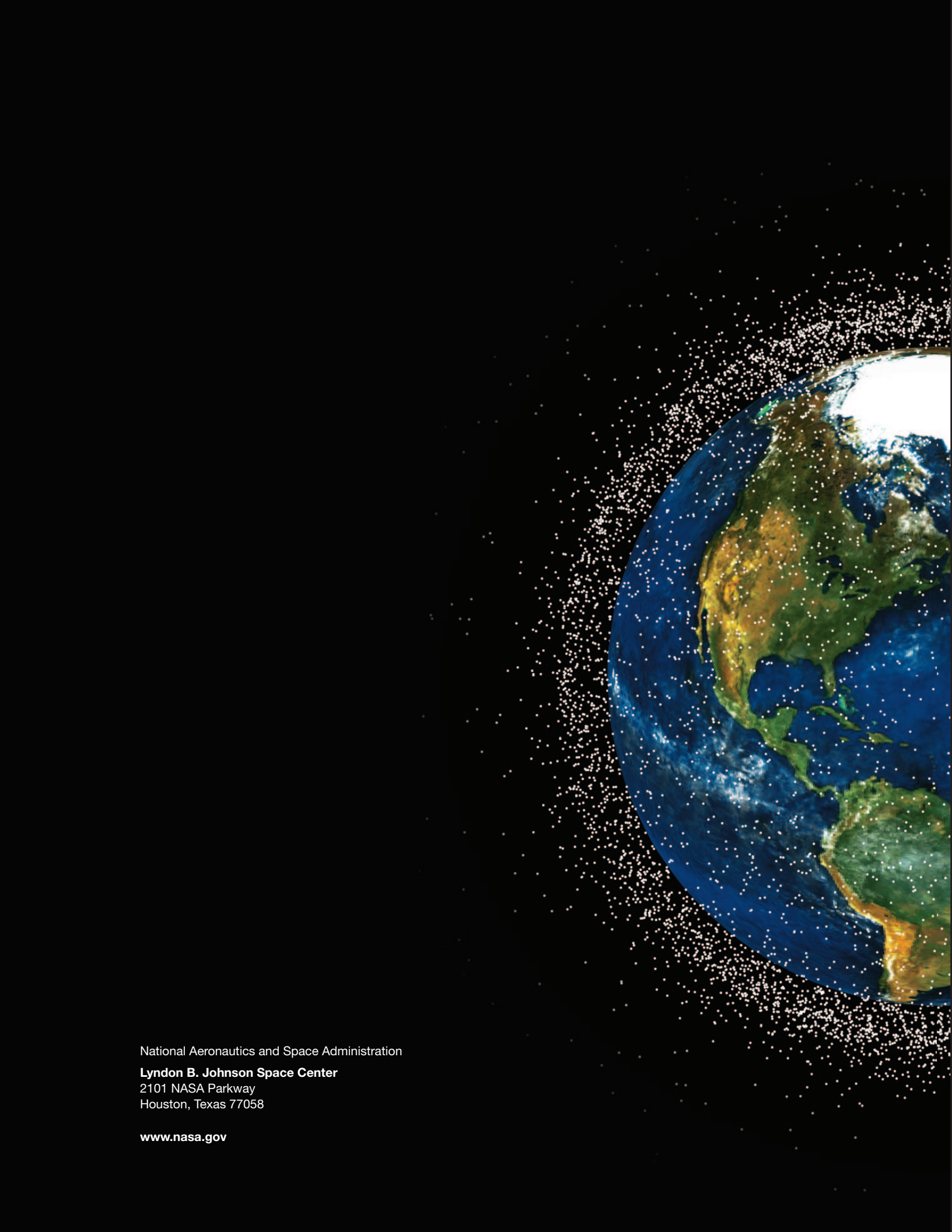
12a. DISTRIBUTION/AVAILABILITY STATEMENT
Unclassified/Unlimited
Available from the NASA Center for AeroSpace Information (CASI)
7115 Standard
Hanover, MD 21076-1320 Category: 99

12b. DISTRIBUTION CODE

13. ABSTRACT *(Maximum 200 words)*
The Biennial Research and Technology Development Report is a compilation of advances in research and technology accomplished by Johnson Space Center (JSC) engineers and scientists. The articles contained within this report further JSC's and NASA's historical tradition of working with colleges and universities, industry, federal laboratories, and other research and technology development organizations for the betterment of humankind. This report is organized into10 broad categories: Human Health, Life Support and Habitation Systems, and Space Medicine; Human Exploration Systems, Technologies for Extravehicular Activity and Harsh Environments; Environmental Technologies; Materials, Structures, Development and Testing; Space Power, Energy Storage, and Propulsion; Robotics, Tele-Robotics, Autonomous Systems, and Software; Exploration, Planetary Science, and Sensor Systems; Flammability and Explosive Technologies; Space and Ground Operations; and Education and Outreach.

14. SUBJECT TERMS	15. NUMBER OF PAGES	16. PRICE CODE
aerospace enivironments, life support systems, aerospace medicine, robotics, telerobotics, space exploration, extravehicular activity, propulsion, flammability	370	

17. SECURITY CLASSIFICATION OF REPORT	18. SECURITY CLASSIFICATION OF THIS PAGE	19. SECURITY CLASSIFICATION OF ABSTRACT	20. LIMITATION OF ABSTRACT
Unclassified	Unclassified	Unclassified	Unlimited



National Aeronautics and Space Administration

Lyndon B. Johnson Space Center
2101 NASA Parkway
Houston, Texas 77058

www.nasa.gov